



UNIVERSITY OF  
BIRMINGHAM

**Synthesis and Application of Nitrogen Containing  
Heterocycles**

by

**Matthew George Wakeling**

A thesis submitted to The University of Birmingham

for the degree of DOCTOR OF PHILOSOPHY

School of Chemistry

College of Engineering and Physical Sciences

University of Birmingham

September 2020

UNIVERSITY OF  
BIRMINGHAM

**University of Birmingham Research Archive**

**e-theses repository**

This unpublished thesis/dissertation is copyright of the author and/or third parties. The intellectual property rights of the author or third parties in respect of this work are as defined by The Copyright Designs and Patents Act 1988 or as modified by any successor legislation.

Any use made of information contained in this thesis/dissertation must be in accordance with that legislation and must be properly acknowledged. Further distribution or reproduction in any format is prohibited without the permission of the copyright holder.



# Abstract

This thesis describes the exploration of trisubstituted oxazoles as building blocks in the synthesis of complex nitrogen containing heterocycles for medicinally relevant polycyclic piperidines and novel annulated nucleophilic heterocyclic carbene ligands.

The research presented discusses advancements made in a gold-catalysed cascading cycloaddition process that delivers epoxy-bridged piperidine fused polycycles through intramolecular Diels-Alder cyclisations of 4-amidooxazoles. A complementary cobalt-catalysed approach is then presented that accesses regioisomeric piperidine fused heterocycles *via* 5-amidooxazoles utilising chemically related catalysis precursors. The subsequent reactivity of a range of previously unknown structures is then discussed, offering rapid access into a host of diverse  $sp^3$ -rich architectures including polycyclic 1,3-aminoalcohols,  $\delta$ -lactams and functionalised piperidine motifs.

The gold-catalysed formal [3+2] dipolar cycloaddition is then presented as a key step in the construction of a series of oxazole annulated imidazolium salts as precursors to nucleophilic heterocyclic carbene ligands. Building on key concepts from this series, a second ligand design is then presented and realised that incorporates pyrimidine annulated imidazolium salts. Finally, the coordination chemistry of these salts to transition metals is discussed alongside analysis of the steric impact of the ligands in Au(I) complexes.



# Acknowledgements

As eight years in Birmingham come to an end, I have many people to thank for their support and encouragement throughout my studies. I am fortunate enough to have been surrounded by a fantastic cohort of scientists who have pushed me to be the best that I can be.

First and foremost, I would like to thank my supervisor Dr Paul Davies for his mentorship and guidance throughout my PhD studies. His extensive scientific knowledge, combined with his excitement for scientific discovery, continually challenged me to keep learning and improving as a scientist.

Thank you Josh, Matt, Miguel, Ana, Paige, Laura, Alessandro and all others who have spent time in the Davies research group. It has been a pleasure to work alongside you all. There are too many names from the extended Haworth family to mention, however I'd like to say a special thank you to: Nick, Russel, Edd, Sajni, Izzy, Glenn, Dan, Kesar, Connor, Danni and Sam, with whom I have many fond memories in Staff House and the Goose.

I would also like to give my gratitude to the technical staff in the School of Chemistry. Cecile, Louise, Chi and Chris I could not have done this without your many hours of support.

To my friends and family outside of university life, thanks for all your help, love and support. Finally, thank you Elsa. You have enabled me to become the person I am today through your unrelenting support and inspiration, and I am extremely grateful.

# Contents

Chapter 1: Targeting sp <sup>3</sup> -rich scaffolds for natural product-like drug discovery .....	- 1 -
1.1 Fused piperidines for potential drug discovery.....	- 1 -
1.2 Drug discovery guidelines and metrics.....	- 4 -
1.3 Approaches to drug discovery library design .....	- 7 -
1.4 Diels-Alder reactions of oxazoles to build molecular complexity.....	- 11 -
1.5 Aims and objectives.....	- 18 -
Chapter 2: Polycyclisation methods to rapidly assemble molecular complexity.....	- 20 -
2.1 Gold-catalysed cascading cycloaddition reactions .....	- 20 -
2.1.1 Gold-catalysed cycloaddition reaction to access 4-aminooxazoles .....	- 20 -
2.1.2 Synthesis of cyclisation precursors .....	- 22 -
2.1.3 Diels-Alder studies with dienophile tethered <i>N</i> -acyl pyridinium ylides .....	- 30 -
2.1.4 Diels-Alder studies with dienophile tethered ennamides .....	- 36 -
2.1.5 Formation of macrocycle <i>via</i> ring closing metathesis.....	- 44 -
2.2 Cobalt-catalysed polycyclisation reactions.....	- 48 -
2.2.1 Cobalt-catalysed oxazole formation and potential polycyclisation method.....	- 48 -
2.2.2 Initial development of the methodology .....	- 49 -
2.2.3 Synthesis of catalysis precursors .....	- 51 -
2.2.4 Polycyclisations with alkene tethered <i>N</i> -(pivaloyloxy)amides .....	- 55 -
2.2.5 Polycyclisations with 1,6- and 1,7-enamides .....	- 64 -
2.3 Summarising the gold- and cobalt- catalysed polycyclisation processes .....	- 66 -
Chapter 3: Post catalysis reactions: polycycles for potential library synthesis.....	- 69 -
3.1 Reduction at the amidine to deliver fused piperidines.....	- 69 -
3.1.1 Reduction to fused piperidin-3-ols.....	- 69 -
3.1.2 Reduction selectivity model.....	- 74 -
3.1.3 Thioketal reductions.....	- 77 -
3.2 Activation with Brønsted and Lewis acids .....	- 80 -
3.2.1 TsOH mediated hydrolysis.....	- 80 -
3.2.2 Acyl iminium activation.....	- 83 -
3.2.3 Rearrangement reactions .....	- 85 -

3.3 Functional group manipulation .....	- 87 -
3.4 Initial attempts at framework elaboration of polycycles accessed through cobalt catalysis.....	- 88 -
3.5 Analysis of polycycles for potential use as scaffolds in library synthesis .....	- 92 -
3.6 Outlook and future work.....	- 95 -
Chapter 4: Nucleophilic heterocyclic carbenes and their development in organometallic chemistry	- 97 -
4.1 Nucleophilic heterocyclic carbenes .....	- 97 -
4.2 Synthesis routes to access imidazolium motifs.....	- 99 -
4.3 Coordination to transition metals.....	- 104 -
4.4 Analysis of nucleophilic heterocyclic carbene ligands .....	- 107 -
4.4.1 Measuring electronic parameters .....	- 107 -
4.4.2 Measuring the steric impact of NHC ligands .....	- 110 -
4.5 Ligand development and reactivity.....	- 112 -
4.5.1 Increasing the steric impact of NHC ligands .....	- 112 -
4.5.2 Annulated imidazolylidenes as alternative ligand backbones.....	- 114 -
4.5.3 SMART ligands that impact catalytic activity .....	- 116 -
4.6 Conclusion .....	- 122 -
Chapter 5: Novel strategies to access heterocyclic fused imidazolium salts .....	- 123 -
5.1 Aims, objectives and ligand design .....	- 123 -
5.2 Oxazole annulated imidazolium salt synthesis .....	- 125 -
5.3 Pyrimidine annulated imidazolium salt synthesis.....	- 131 -
5.3.1 Design of the synthesis route .....	- 131 -
5.3.2 Condensation reactions to access functionalised pyrimidines .....	- 133 -
5.3.3 Synthesis of imidazolium salts.....	- 139 -
5.4 Conclusion .....	- 147 -
Chapter 6: NHC transition metal complexes.....	- 149 -
6.1 Synthesis of transition metal complexes.....	- 149 -
6.2 Analysis of NHC ligands .....	- 157 -
6.3 Preliminary catalyst activity study.....	- 163 -
6.4 Conclusion .....	- 165 -

Chapter 7: Supporting information .....	- 167 -
General Experimental .....	- 167 -
Formation of precursors to ynamides .....	- 170 -
Formation of ynamides .....	- 180 -
Formation of <i>N</i> -acyl pyridinium ylide and <i>N</i> -(pivaloyloxy)amide precursors .....	- 195 -
Formation of <i>N</i> -(pivaloyloxy)amides.....	- 203 -
Formation of <i>N</i> -acyl pyridinium ylides.....	- 203 -
Polycyclisation catalysis products .....	- 224 -
Gold-catalysed polycyclisation products .....	- 224 -
Products derived from alkene tethered <i>N</i> -acyl pyridinium ylides (Chapter 2.1.3).....	- 224 -
Products derived from enynamides (Chapter 2.1.4).....	- 233 -
Cobalt-catalysed polycyclisation products.....	- 248 -
Products derived from alkene tethered <i>N</i> -(pivaloyloxy)amides (Chapter 2.2.4) .....	- 248 -
Products derived from enynamides (Chapter 2.2.5).....	- 268 -
Post catalysis transformations.....	- 271 -
Formation of aminoalcohol derivatives .....	- 271 -
Products derived from reduction of thioketals .....	- 282 -
Products derived from treatment with Brønsted and Lewis acids.....	- 287 -
Products derived from functional group manipulation .....	- 292 -
Formation of oxazole annulated imidazolium salts .....	- 295 -
Formation of pyrimidines annulated imidazolium salts .....	- 304 -
Condensation reactions to access functionalised pyrimidines (Chapter 5.3.1 .....	- 304 -
Products derived from $S_NAr$ reactions .....	- 310 -
Products derived from the synthesis of imidazolium salts (Chapter 5.3.3).....	- 313 -
Formation of transition metal complexes (Chapter 6) .....	- 324 -
Chapter 8: X-Ray data.....	- 339 -
8.1 Macrocycle 95.....	- 339 -
8.2 Polycycle 105a .....	- 344 -
8.3 Formamide 343a .....	- 350 -
8.4 Imidazolium 355•HCl .....	- 356 -
8.5 353aAgCl.....	- 361 -

8.6 353cAgCl.....	- 367 -
8.7 353aAuCl.....	- 373 -
8.8 353bAuCl.....	- 379 -
8.9 353cAuCl.....	- 387 -
8.10 353dAuCl.....	- 393 -
3.11 354aAuCl.....	- 400 -
3.12 355AuCl.....	- 408 -
Chapter 9: References .....	- 414 -

# Abbreviations

<b>%V<sub>bur</sub></b>	percentage buried volume	<b>DME</b>	dimethoxyethane
<b>Å</b>	Ångström(s)	<b>DMF</b>	dimethylformamide
<b>Ac</b>	acetyl	<b>DMP</b>	Dess-Martin periodinane
<b>Ad</b>	adamantyl	<b>DMSO</b>	dimethylsulfoxide
<b>alloc</b>	allyloxycarbonyl	<b>eq.</b>	equivalent(s)
<b>Ar</b>	aryl	<b>ES</b>	electrospray
<b>Bn</b>	benzyl	<b>Et</b>	ethyl
<b>Boc</b>	<i>tert</i> -butoxycarbonyl	<b>EWG</b>	electron-withdrawing group
<b>Bu</b>	butyl	<b>g</b>	gram(s)
<b>C</b>	Celsius	<b>h</b>	hour(s)
<b>calcd</b>	calculated	<b>HMBC</b>	heteronuclear multiple bond correlation
<b>Cbz</b>	carboxybenzyl	<b>HMDS</b>	hexamethyldisilazane
<b>cod</b>	cyclooctadiene	<b>HP</b>	hotplate
<b>COSY</b>	correlation spectroscopy	<b>HRMS</b>	high resolution mass spectrometry
<b>Cp</b>	cyclopentadienyl	<b>HSQC</b>	heteronuclear single quantum coherence
<b>Cp*</b>	pentamethylcyclopentadienyl	<b>HTS</b>	high-throughput screening
<b>CPME</b>	cyclopentyl methyl ether	<b>i</b>	<i>iso</i>
<b>Cy</b>	cyclohexyl	<b>IR</b>	infrared
<b>d.r.</b>	diastereomeric ratio	<b>J</b>	coupling constant
<b>DBU</b>	1,8-diazabicyclo[5.4.0]undec-7-ene	<b>K</b>	Kelvin
<b>DCB</b>	dichlorobenzene	<b>L</b>	litre
<b>dec.</b>	decomposed	<b>LA</b>	Lewis acid
<b>DCE</b>	dichloroethane	<b>LG</b>	leaving group
<b>DIAD</b>	diisopropyl azodicarboxylate	<b>M</b>	molar
<b>DIPEA</b>	diisopropylethylamine	<b>m/z</b>	mass/charge
<b>DIPP</b>	2,6-diisopropylphenyl	<b>Me</b>	methyl
<b>DMA</b>	dimethylacetamide		
<b>DMAP</b>	dimethylaminopyridine		

<b>Mes</b>	mesitylene	<b>ppm</b>	parts per million
<b>min</b>	minutes	<b>Pr</b>	propyl
<b>mol</b>	moles	<b>r.t.</b>	room temperature
<b>MMP</b>	<i>meta</i> -methoxyphenyl	<b>RO5</b>	rule of 5
<b>mp</b>	melting point	<b>SMART</b>	Switchable, Multifunctional, Adaptable oR Tuneable
<b>Ms</b>	methanesulfonyl	<b><i>t</i></b>	tertiary
<b>MS</b>	molecular sieves	<b>TEP</b>	Tolman's electronic parameter
<b>MW</b>	molecular weight	<b>Tf</b>	trifluoromethanesulfonyl
<b>MW</b>	microwave	<b>TFA</b>	trifluoroacetic acid
<b>NBS</b>	<i>N</i> -bromosuccinimide	<b>TFE</b>	2,2,2-trifluoroethanol
<b>NHC</b>	nucleophilic heterocyclic carbene	<b>THF</b>	tetrahydrofuran
<b>NMM</b>	<i>N</i> -methylmorpholine	<b>TIPS</b>	triisopropylsilyl
<b>NMR</b>	nuclear magnetic resonance	<b>TLC</b>	thin layer chromatography
<b>Ns</b>	4-nitrobenzenesulfonyl	<b>TM</b>	transition metal
<b>PG</b>	protecting group	<b>TMS</b>	trimethylsilyl
<b>Ph</b>	phenyl	<b>TOF</b>	time of flight
<b>Pic</b>	pyridinecarboxylato	<b>TPSA</b>	topological polar surface area
<b>PIFA</b>	phenyliodine bis(trifluoroacetate)	<b>Ts</b>	4-methylbenzenesulfonyl
<b>Piv</b>	pivaloyl	<b>u</b>	amu
<b>PMB</b>	<i>para</i> -methoxybenzyl	<b>UV</b>	ultraviolet
<b>PMP</b>	<i>para</i> -methoxyphenyl	<b>v</b>	wavenumber
		<b>XRD</b>	X-Ray diffraction

# Chapter 1: Targeting $sp^3$ -rich scaffolds for natural product-like drug discovery

## 1.1 Fused piperidines for potential drug discovery

Natural products have been used as attractive starting points in drug discovery programmes due to their complex  $sp^3$ -rich architecture and compelling bioactivity. Amongst all anti-tumour drugs approved worldwide between 1981 and 2014, 36% were either natural product mimics, derivatives or synthetic drugs containing a natural product pharmacophore.<sup>1,2</sup>

Fused piperidines are frequently found in a range of alkaloid motifs with potent bioactivity, making them excellent candidates for drug discovery (Figure 1). A broad range of connectivity was observed amongst the bioactive molecules, containing an array of fused rings for several unique target scaffolds. However, the synthesis of natural products is often complex and cannot be produced from natural sources in sufficient quantities for library synthesis and testing. To overcome these limitations, natural product-like scaffolds that are inspired from a biologically active compound are often targeted by synthetic chemists.<sup>3</sup>

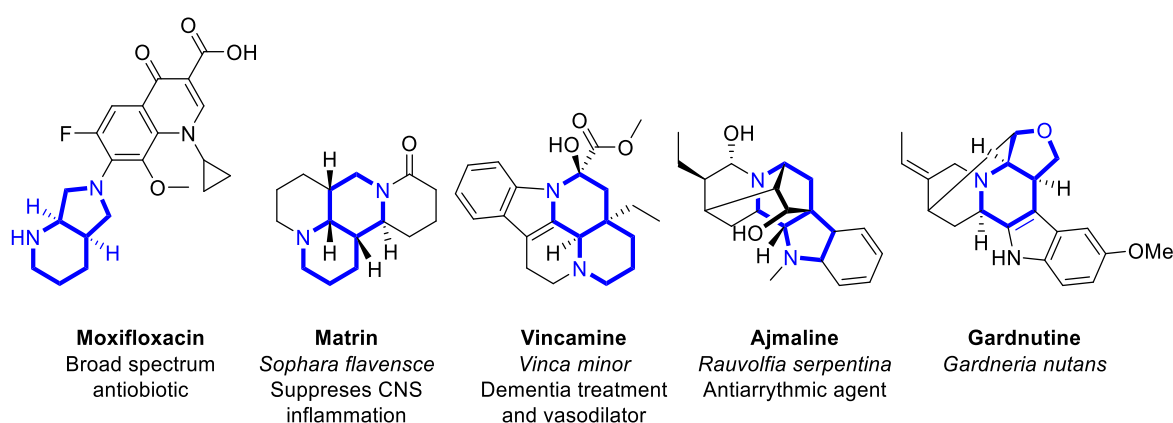
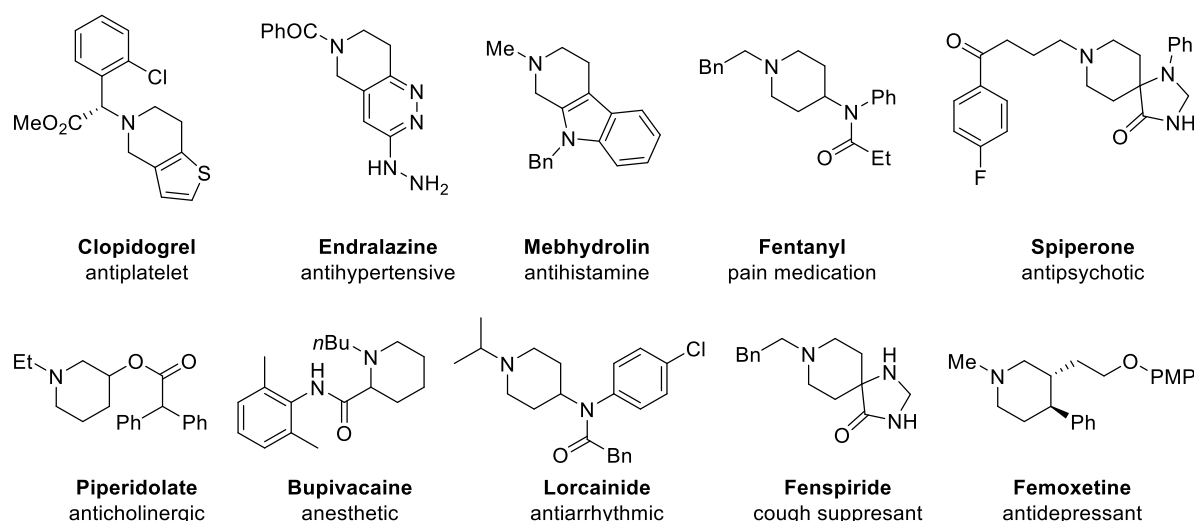


Figure 1: Fused piperidine alkaloid structures from natural products, with targeted frameworks highlighted.



Alongside the prevalence of piperidine analogues in nature, Njardarson reported that of 1086 FDA approved small molecule pharmaceuticals as of 2014, 59% contained a nitrogen heterocycle and 89% contain at least one nitrogen atom.<sup>4</sup> Of the 640 nitrogen containing heterocycles, the most common was piperidine, followed by pyridine, piperazine and pyrrolidine. The vast biological activity of piperidine containing molecules was captured in an extensive review of piperidine-based drug discovery by Vardanyan in 2017, with examples shown in Figure 2.<sup>5</sup>



**Figure 2: Marketed drugs containing piperidines and their pharmacological action.**

Various strategies have been developed to prepare functionalised piperidines (Figure 3). Hydrogenation of pyridines under rhodium,<sup>6</sup> nickel,<sup>7</sup> ruthenium,<sup>8</sup> palladium,<sup>9</sup> and platinum<sup>10</sup> catalysis is well established, with recent advances expanding asymmetric hydrogenation methods to deliver **3** and **4**.<sup>11,12</sup> Intramolecular Michael addition reactions provided access to **6**, which was subsequently used in the synthesis of alkaloid motifs,<sup>13</sup> whilst tandem intra- and intermolecular Michael reactions have been developed for the construction of pyrrolidines and piperidines such as **7**.<sup>14</sup> Several variations of the aza-Diels-Alder reaction, with the nitrogen installed in diene **8** or dienophile **9**, have been developed to deliver heterocycles such as **10**'

from cyclobutane diene precursor **10**.<sup>15</sup> Metathesis strategies including ring-closing metathesis of non-natural amino acids<sup>16</sup> to access **12** and the ring rearrangement of cyclopentene derivatives to access (-)-halosaline from **13** offered additional approaches from bis-alkene tethered amines.<sup>17</sup> Finally, intramolecular substitution reactions of amine nucleophiles with groups such as triflate<sup>18</sup> as for **15** or chlorides as for **16**, generated through the chlorination of amino alcohols,<sup>19</sup> offered an approach from amines tethered with a suitably placed leaving group.

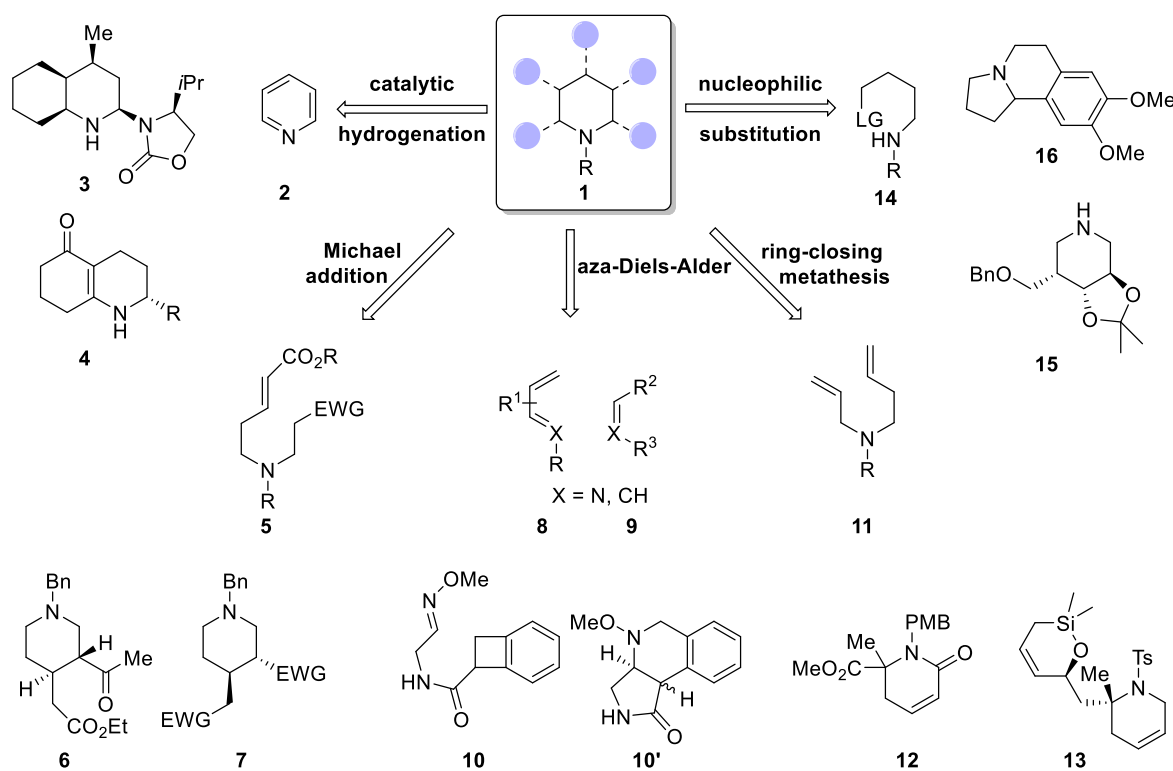


**Figure 3: Overview of common strategies to prepare piperidines, alongside representative examples of molecules accessed through these methods. **3**,<sup>11</sup> **4**,<sup>12</sup> **6**,<sup>13</sup> **7**,<sup>14</sup> **10**,<sup>15</sup> **12**,<sup>16</sup> **13**,<sup>17</sup> **15**,<sup>18</sup> **16**,<sup>19</sup>**

Whilst the current methods available to prepare piperidines are vast, a method that provided divergent access to numerous fused piperidine motifs would add considerable value. Importantly, the ability to use a single approach whilst varying the core polycyclic framework and functional groups installed was desired. With these targets in mind, a modular and flexible

synthesis route that would allow access to a variety of fused piperidines was required. An approach that aligned with common strategies used in drug discovery was considered necessary to maximise the potential of any methodologies developed.

## **1.2 Drug discovery guidelines and metrics**

Medicinal chemists have looked to improve their ability to successfully navigate the drug development process, from identifying initial lead compounds through to drug approval. With a dramatic shift towards large library synthesis and new high throughput screening (HTS) processes in the early 1990s, many compounds were being prepared and screened independently across industrial and academic laboratories.<sup>20</sup> At the turn of the 21<sup>st</sup> century a number of fundamental ideologies were published from a variety of academic and industrial sources that looked to enhance the efficiency and success of future drug discovery efforts that evolved from the decades of prior research.

In 1996 Murcko analysed the Comprehensive Medicinal Chemistry database to analyse the properties of known drugs and identify common structural motifs.<sup>21</sup> The analysis identified ring systems, linkers, side chains and frameworks across a series of 5120 compounds. The term ‘Murcko framework’ is widely used to this day and refers to the core structure of a compound with its sidechains removed. This early example of drug database mining emphasised the huge number of resources at the disposal of computational researchers to guide medicinal chemists in the generation of new compound libraries.

Developments in HTS approaches allowed much larger screening programmes to be run. DMSO stock solutions were used that removed the aqueous solubility factor of the drug candidates. A critical factor in many failed drug candidates then became poor bioavailability of

the identified drug targets when examined under physiological conditions.<sup>20</sup> Through the analysis of 2245 phase II candidates, Lipinski identified 5 key characteristics of small molecule drugs that could be utilised to infer the oral bioavailability of novel drug candidates.<sup>20</sup> Lipinski's guidelines are often referred to as the 'rule of 5' (RO5) and are comprised of the following parameters: molecular weight <500, hydrogen bond donors  $\leq 5$ , hydrogen bond acceptors  $\leq 10$  and  $\text{LogP} \leq 5$ . Whilst these factors have heavily influenced rational drug design, it is worth noting they are only guidelines and successful drug candidates falling outside of these ranges have been taken to market.

In 2000 Selzer then provided a new fragment based approach for calculating Topological Polar Surface Area (TPSA) from the molecular topology, and demonstrated the ability of TPSA to predict bioavailability, allowing rapid screening of virtual libraries.<sup>22</sup> Suggested limits for TPSA values depend on the target within the body: blood brain barrier <90 Å<sup>2</sup>,<sup>23</sup> central nervous system <70 Å<sup>2</sup>,<sup>24</sup> and intestinal <140 Å<sup>2</sup>.<sup>25</sup> Martin developed this into a bioavailability score by considering the charges of drug compounds at physiological pH, formulating the probability of containing >10% bioavailability in rat or measurable Caco-2 permeability.<sup>26</sup>

This was followed by a rotatable bond<sup>a</sup> property introduced by Veber in 2002 that, alongside polar surface area, was able to provide an effective predictive tool: an increase in molecular rigidity, as determined by the rotatable bond count, and a low polar surface area was observed to improve oral bioavailability.<sup>27</sup> Their suggested criteria for increased permeation was for a target compound to contain  $\leq 10$  rotatable bonds. Further observations from this study

---

<sup>a</sup> Rotatable bonds were defined as any single bond, not in a ring, bound to an internal heavy (i.e. non-hydrogen) atom. Amide C-N bonds were excluded from the count because of their high rotational energy barrier

recognised that the poorer bioavailability of high molecular weight drug targets could be linked to the increased molecular flexibility and TPSA values.

Another metric, fraction of  $sp^3$ -rich carbons ( $F_{sp^3}$ ), was introduced by Lovering in 2009 as a measure of structural complexity (Eq. 1).<sup>28</sup> A clear trend was observed with higher  $F_{sp^3}$  values correlating well with improved aqueous solubility. Analysis of small molecules (MW <1000 u) with data from phase I through to approval established that higher  $F_{sp^3}$  values correlated with improved success through discovery to drugs. Mean molecular weights saw a clear decrease from discovery (436 u) through to approved drugs (360 u) and a higher  $F_{sp^3}$  ratio (36 to 47). The overarching theme linked increased saturation with architecturally more complex molecules, resulting in the exploration of more diverse chemical space, without increasing molecular weight. This was followed up in 2013 by Lovering when showing the reduced promiscuity observed in molecules with higher  $F_{sp^3}$  values, in turn reducing the toxicity through greater selectivity and specificity characteristics.<sup>29</sup>

$$\text{Eq. 1: } F_{sp^3} = \frac{\text{number of } sp^3 \text{ hybridised carbons}}{\text{total carbon count}}$$

These non-exhaustive predictive tools of molecular properties allow for analysis of potential target libraries and offer a good starting point to maximise physiological properties for drug design. Modern day drug library molecular properties are often evaluated and visualised using principal component analysis, comparing against known drug and natural product molecules, to assess their pharmacokinetic profiles.

One such tool that allows synthetic chemists to calculate and visualise the predicted pharmacokinetic profiles of a potential drug discovery scaffold is the Lead Likeness And Molecular Analysis (LLAMA) software launched in 2016.<sup>30</sup> As well as calculating the

predicted molecular properties of the defined scaffolds uploaded by the user, LLAMA is able to auto-generate derivations of the defined scaffolds with a suite of medically-relevant chemical transformations with either the standard chemical reagent library contained within the software or unique inventories uploaded by the user. Lead-likeness penalty scoring of the decorated molecules (through LogP, heavy atom count, aromatic ring count and ‘bad functional groups’) is plotted alongside molecular weight and ALogP to indicate how closely a lead compound fits into lead-like space. The graphical outputs from this software are displayed when analysing the scaffolds generated in this thesis in Chapter 3.5.

### 1.3 Approaches to drug discovery library design

Alongside the guidelines discussed, an emphasis on preparing diverse libraries of lead-like molecules has been promoted. Schreiber first introduced the term diversity oriented synthesis in 2000, calling for a change in strategy when preparing new drug libraries.<sup>31</sup> Previously, target oriented synthesis was the main approach utilised in drug discovery; this typically involved the identification of a potential candidate, retrosynthetic analysis and then ultimately library preparation. Diversity oriented synthesis called for the preparation of structurally complex and diverse frameworks, with a focus on developing divergent synthesis routes to access a wide range of Murkco frameworks. A follow-up review by Schreiber in 2004 described a *build, couple, pair* procedure: synthesise molecular building blocks; couple them through a developed method; pair them with intermolecular coupling reactions that diversify the structures.

This aligned with the lead-like combinatorial library approach discussed by Oprea.<sup>32</sup> Analysis of the common sources of leads in drug discovery produced three categories: high affinity leads, lead-like leads and drug-like leads. High affinity leads were often peptidic or based on natural

products and contained heavily functionalised molecules that suffered during attempts to retain sufficient potency whilst improving the pharmacokinetic profile. Drug-like leads containing molecular weights of 350 – 500 u and LogP values of 3 – 5 rarely gave potent results as the specificity of the decorated molecules gave poor affinities in the screening assays and left little room for modification without inadvertently reducing the drug-like properties. Lead-like compounds on the other hand contained lower molecular weights (<350 u) and LogP values (<3) and were more easily elaborated into drugs with the required physical properties. A recent review on lead-like drugs from Bhattacharya surveyed FDA drug approvals and the top 200 prescribed drugs from 2011 – 2017 and found that the molecular weight of final drug compounds were often very similar to the lead-like target, suggesting an increased focus on lead-like starting points in screening libraries could deliver higher success rates.<sup>33</sup>

These approaches have overlapping principles and can be summarised as preparing a range of molecular frameworks *via* a diversity-oriented synthesis approach and identifying the lead-like hits at the couple stage. An emphasis of both approaches is to prepare a diverse range of molecular frameworks that occupy a wide variety of chemical space, as opposed to a large library of compounds with similar three dimensional characteristics and small chemical changes. These can then be modified (paired) to improve the pharmacokinetic properties through strategically placed reactive functional groups. While these guidelines and approaches are far from exhaustive, they highlight the changes in approach towards building successful small molecule drug discovery programmes.

Small molecule libraries are often inspired from biologically active alkaloids due to their structural complexity and sp<sup>3</sup>-rich nature. An elegant combination of the discussed approaches is exemplified by Aube *et al.* in the preparation of a large library derived from four naturally

occurring compounds (Figure 4).<sup>34</sup> Accessible primary and secondary scaffolds **17-20** were identified from four natural product families and these scaffolds were utilised to access a library of 686 new compounds. Primary scaffolds were derived directly from the natural product framework, whilst secondary scaffolds were obtained through modification of the connectivity or functional groups.

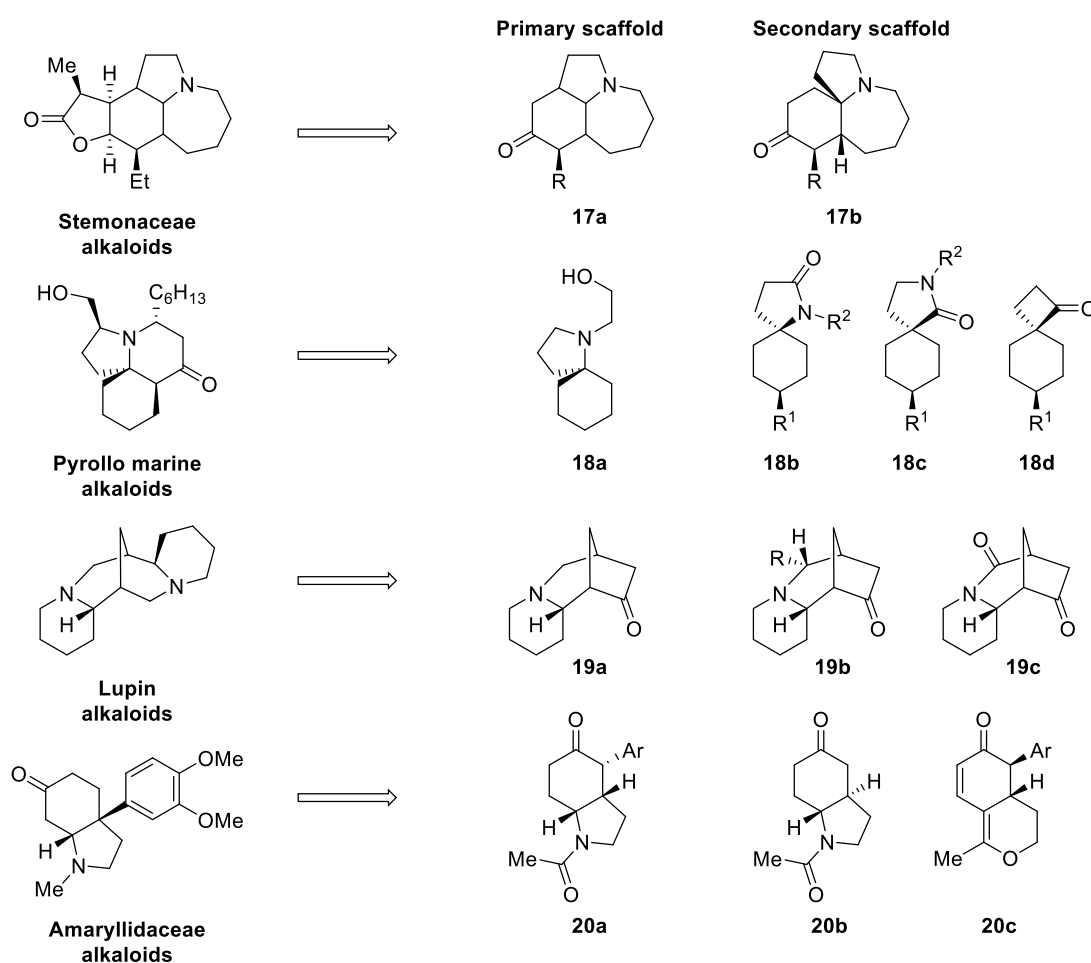


**Figure 4: Alkaloid inspired libraries for probing molecular space by Aube *et al.***

The generated library was highly Lipinski RO5 compliant and contained good bioavailability when calculated computationally. Cheminformatic analysis of the molecular properties and chemical descriptors using principal component analysis revealed significant overlap of the alkaloid inspired libraries with both alkaloid natural products and approved drug molecules.



A similarly powerful example from Oguri used a common intermediate approach to access five unique molecular scaffolds, again derived from alkaloid motifs (Figure 5).<sup>35</sup> This remarkable example of molecular diversity, achieved by harnessing the versatile reactivity of **22**, exemplifies the potential of carefully planned methodologies to provide divergent access to a wide range of chemical space.

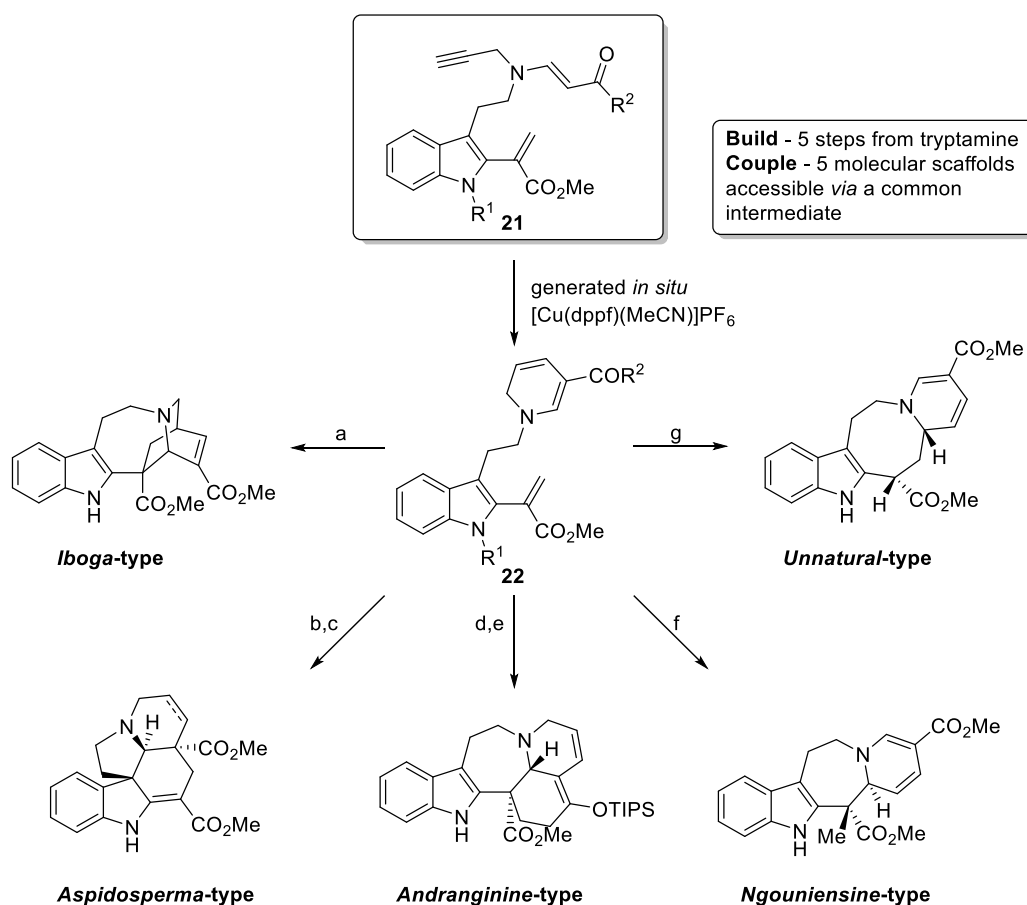


**Figure 5:** Synthesis of 5 alkaloid scaffolds from a common intermediate by Oguri. <sup>a</sup>  $\text{ClCH}_2\text{CH}_2\text{Cl}$ , 60 °C. <sup>b</sup>  $\text{Pd/C}$ ,  $\text{H}_2$ ,  $\text{MeOH}$ . <sup>c</sup> hydroquinone,  $\text{NEt}_3$ , hydroquinone,  $\text{PhMe/ClCH}_2\text{CH}_2\text{Cl}$ , 180 °C. <sup>d</sup> TBAF, THF, r.t. <sup>e</sup> TIPSOTf,  $i\text{Pr}_2\text{NEt}$ ,  $\text{ClCH}_2\text{CH}_2\text{Cl}$ , r.t. <sup>f</sup>  $\text{ClCH}_2\text{CH}_2\text{Cl}$ , 120 °C. <sup>g</sup>  $[\text{Ru}(\text{bpy})_3](\text{BF}_4)_2$ ,  $\text{CH}_2\text{Cl}_2/\text{MeNO}_2$ , r.t.

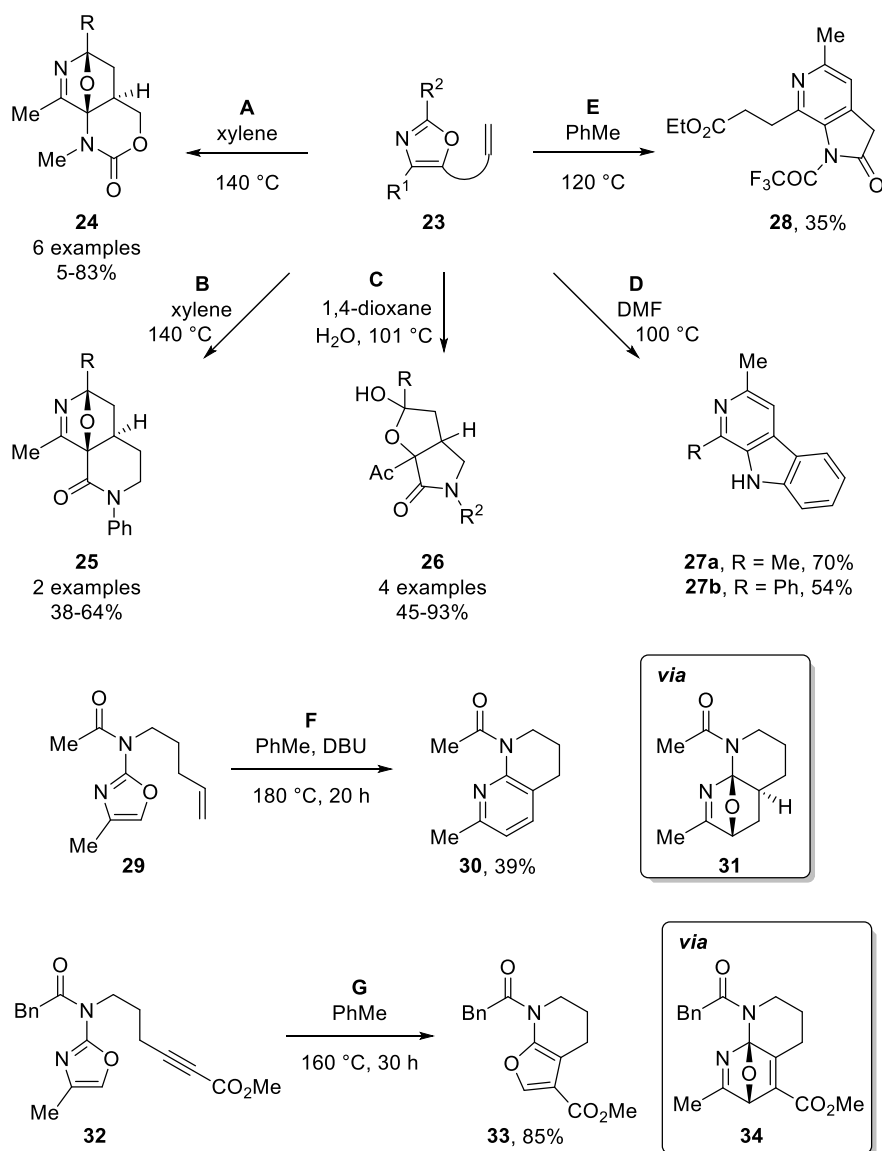
Our approach looked to utilise chemically related building blocks to access an array of Murcko frameworks that are commonly found in alkaloid motifs, alongside novel derivatives, providing lead-like molecules with multiple points of diversity for elaboration. A viable pathway to achieve this was through the intramolecular Diels-Alder reactions of oxazoles.

## 1.4 Diels-Alder reactions of oxazoles to build molecular complexity

Since its discovery, the Diels-Alder reaction has become a widely used transformation that can convert simple precursors into  $sp^3$ -rich polycyclic scaffolds, rapidly building molecular complexity. Since Kondrat'eva's seminal synthesis of pyridines in 1957,<sup>36</sup> the Diels-Alder reactions of oxazoles have been extensively studied with inter- and intramolecular reactions. Alkenes, allenes and alkynes have been utilised to access a variety of fused pyridines, furans, naphthyridines and polycyclic scaffolds.<sup>37,38</sup> As these areas have been extensively reviewed in the literature<sup>37</sup> and by previous members of the Davies' group,<sup>39,40</sup> the scope of this introduction will primarily focus on intramolecular reactions and amino- and ethoxy- substituted oxazoles.

The first example of an intramolecular oxazole Diels-Alder reaction was published by Shimada in 1983, utilising C5 tethered carboxamide and carbamate dienophiles (Scheme 1, A, B and C).<sup>41</sup> Whilst **24** and **25** were isolable, spontaneous hydrolysis was observed to give the tetrahydrofuran motifs in the case of **26**. Developed for application in the total synthesis of Haplophytine, Padwa then reported the synthesis of azacarbazole **27** and azaindole **28** through dehydration of the Diels-Alder products (Scheme 1, D and E).<sup>42</sup>

Whilst describing the total synthesis of Hippadine and various substituted indolines and tetrahydroquinolines, Padwa also demonstrated 2-amidooxazole **29** underwent an intramolecular Diels-Alder reaction (Scheme 1, F).<sup>43</sup> The forcing reaction temperature and presence of DBU favoured spontaneous dehydration of **31** to pyridine **30**, as DBU is often employed in Kondrat'eva's synthesis of pyridines. Using **32**, with an alkyne in place of the alkene, resulted in isolation of the subsequent furan motif **33** via a *retro*-Diels-Alder process and elimination of acetonitrile (Scheme 1, G).

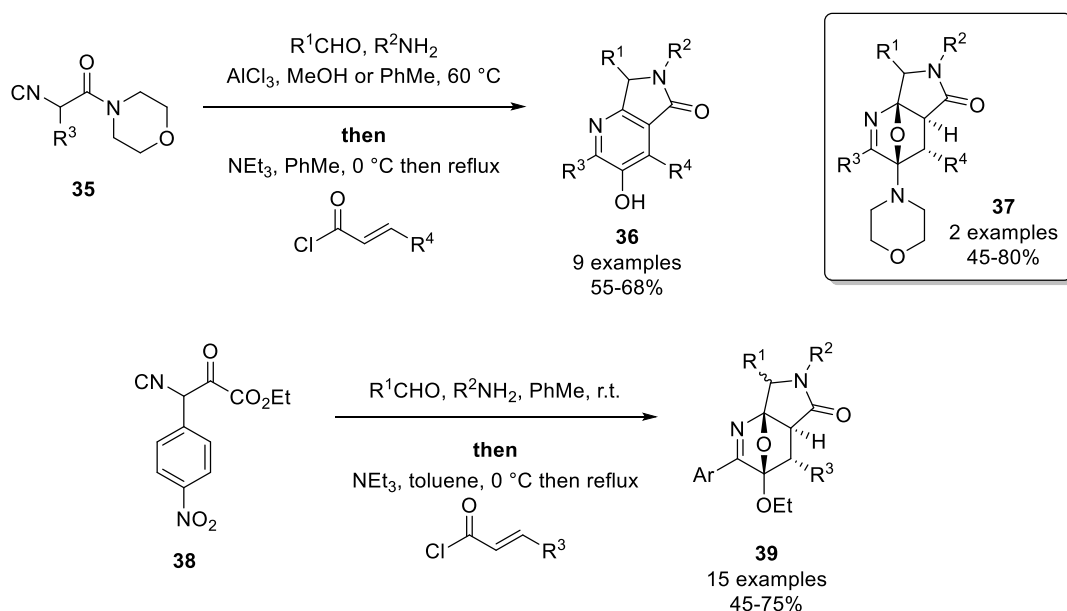


**Scheme 1: Examples of intramolecular Diels-Alder reactions of alkene tethered oxazoles.**

These syntheses relied on the alkylation of prebuilt oxazoles, limiting the modular nature in which they could be selectively functionalised at different positions. In all cases, an unactivated dienophile was shown to undergo Diels-Alder cycloaddition at elevated temperatures (>100 °C).

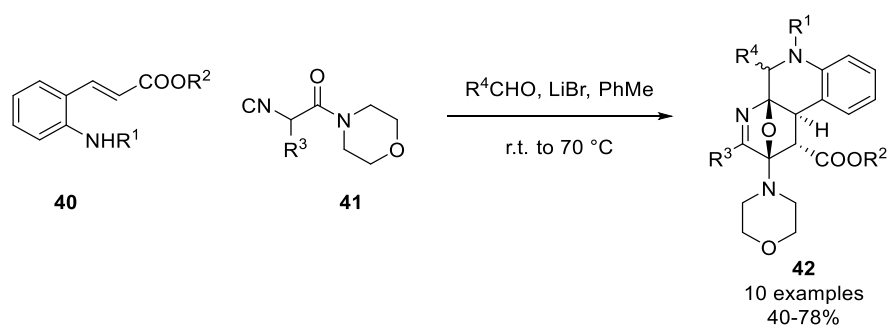
Zhu's group instead developed multicomponent reactions to access the intermediate 5-amino<sup>44</sup> or 5-alkoxy oxazoles,<sup>45</sup> which subsequently underwent Diels-Alder cyclisation from an

appended alkene (Scheme 2). Using  $\alpha$ -iso-cyanoacetamides **35** provided access to pyrrollopyridinones **36** *via* deamination of the morpholine moiety, although polycycle **37** could be isolated when the reaction was performed at room temperature. By employing  $\alpha$ -iso-cyanoacetates **38**, alkoxy polycycles **39** were isolated as a mixture of diastereomers, with no fragmentation observed. A short reaction time of just 20 minutes at reflux demonstrated the reactivity of the intermediate oxazoles towards Diels-Alder cyclisation when pairing electron deficient dienophiles with electron rich oxazoles. An enantioselective version was later developed using a chiral phosphoric acid catalyst.<sup>46</sup>



**Scheme 2: Zhu's multicomponent reaction to access polycyclic scaffolds.**

The same approach was used with vinyl aniline **40** to access naphthyridine derivatives **42** as diastereotopic mixtures (Scheme 3). Moderate reaction temperatures afforded the desired polycyclic scaffolds with no dehydration observed. Tetrahydrofuropyridines were accessed when an alkyne tether was used *via* a retro-Diels-Alder reaction and expulsion of benzonitrile.<sup>47</sup>



**Scheme 3: Zhu's multicomponent reaction to access polycyclic hexahydronaphthyridines derivatives.**

These select examples demonstrate the rich potential of intramolecular oxazole Diels-Alder reactions to rapidly build molecular complexity in a selective manner. Literature precedence indicates that electron-rich oxazoles undergo rapid Diels-Alder cyclisation with electron deficient dienophiles, with low reaction times or temperatures.<sup>37</sup> Similarly, 5- and 2- amido oxazoles have been shown to react with un-activated dienophiles, however require high reaction temperatures. Multiple displays of one-pot approaches validate that the Diels-Alder process is amenable to developing cascade procedures, with no additional reagents required once the alkene tethered oxazole has been generated *in situ*.

Several frameworks have been accessed, with dehydration and deamination processes presenting themselves as obvious choices for diversification studies. The ability to develop a robust and practical methodology to access a range of Diels-Alder products with a modular synthesis route whilst controlling dehydration pathways and substitution patterns would give access to a considerable number of Murcko frameworks with potential as lead-like compounds for use in drug discovery library synthesis.

One such method developed recently within the Davies group employs a gold-catalysed [3+2] dipolar cycloaddition to access 2,4,5-substituted oxazoles. By appropriate design of an *N*-acyl pyridinium ylide **43** or enynamide **48**, the resulting oxazoles **45** and **49** generated from the gold-

catalysed cycloaddition reaction can contain an appended alkene at either the C2 or C5 position of the oxazole, which undergo a [4+2] Diels-Alder reaction to give polycycles **46** and **50** as racemic mixtures of single diastereomers (Figure 6). The cascade process forms four new bonds, introduces three stereocentres, selectively provides *trans* ring junctions and accesses an amidine functionality that provides opportunity for later elaboration.

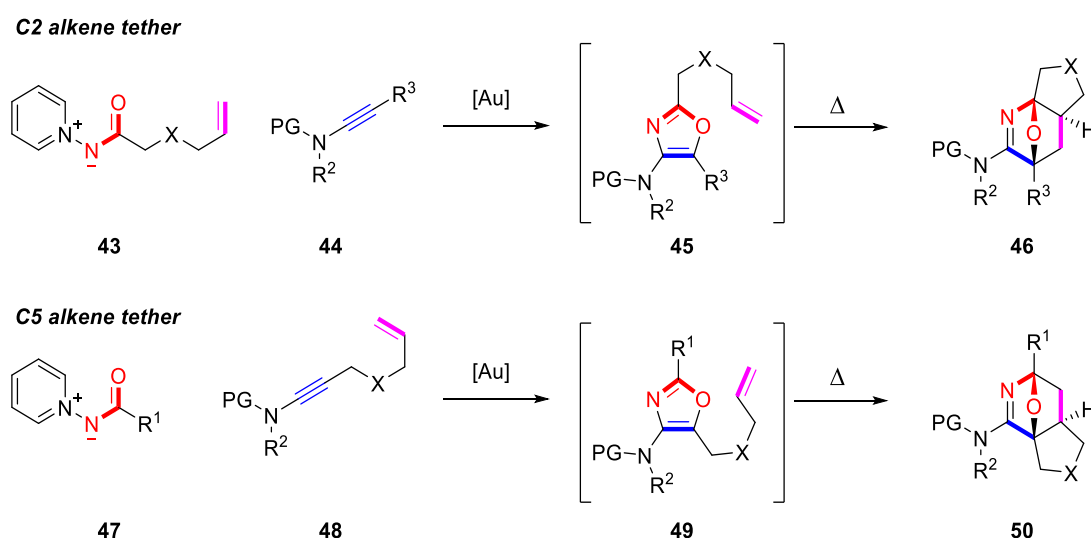


**Figure 6: Overview of new gold-catalysed cycloaddition cascade process developed within the Davies group.**

The protocol was developed and an initial substrate scope for the C2 series was prepared (Figure 7). The scope of the reaction to access hexahydropyrollopyridines **46** proved general, with a variety of functionality tolerated at the C-terminus of the ynamide. The nitrogen tethered alkene primarily utilised tosyl as the protecting group, due to the simple preparation of the corresponding ylide, however mesyl and Cbz were also employed.

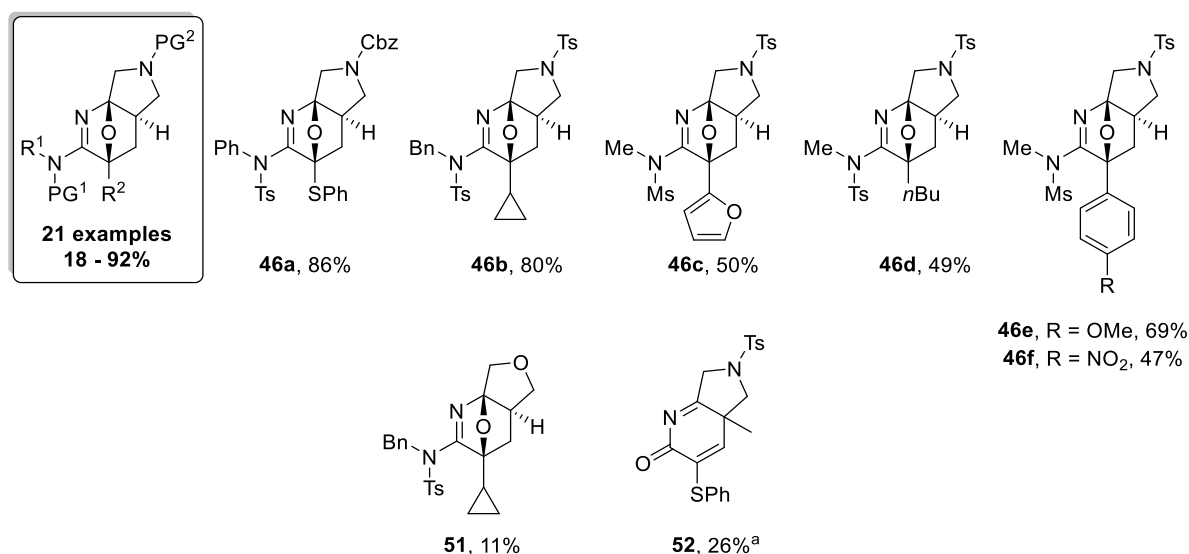


**Figure 7:** Selected examples of substrate scope for 6,5-C2 Diels-Alder reaction prepared by MPB and ADG. Standard reaction conditions: Ynamide (1.0 eq.), ylide (1.2 eq.), [Au-III] 5 mol%, PhMe, 1 – 2 h 90 °C, 65 – 72 h 110 °C. <sup>a</sup> 1,2-DCB, 1 h 90 °C, 64 h 125 °C.

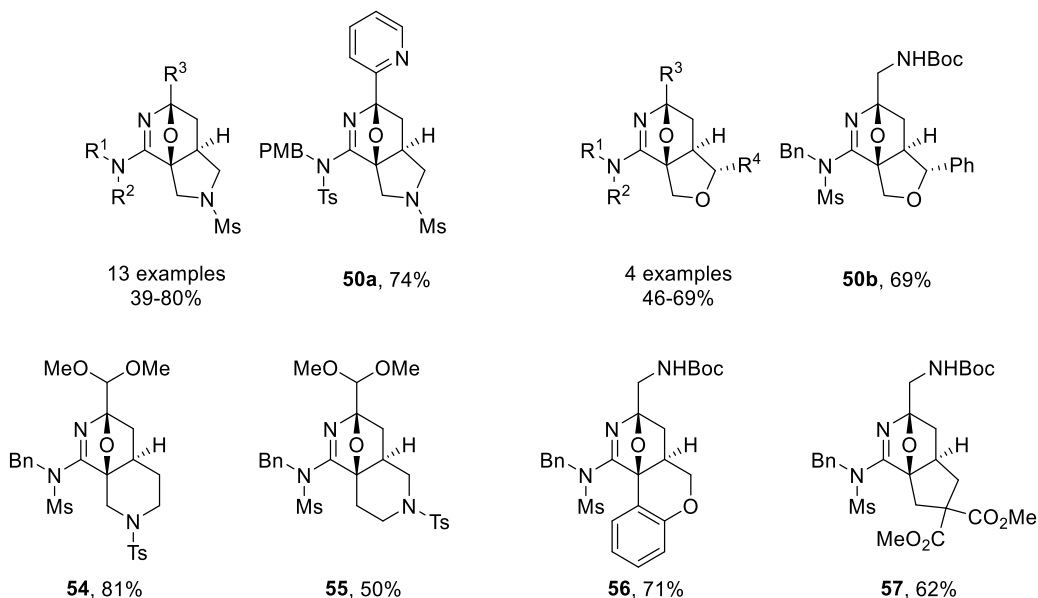
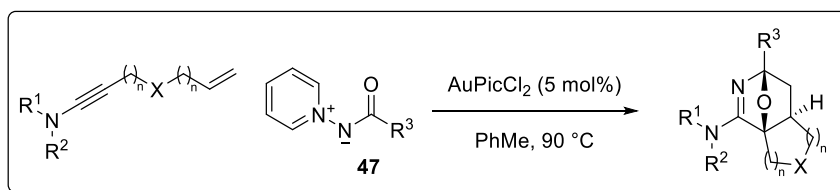
Thio- and cyclopropyl- functionalised ynamides were noted to give increased conversion to polycycles **46a-b**. Furan and alkyl polycycles **46c-d** demonstrated the capability of heterocyclic and alkyl ynamides to undergo the desired cascade reaction. Electron-rich methoxy substituted polycycle **46e** was isolated in higher yield than the electron-poor nitro polycycle **46f**.

Hexahydrofuronopyridine **51** was obtained in a low yield, *via* an oxygen tethered alkene, yet emphasised that a range of polycyclic scaffolds could be accessed using this methodology. Finally, tetrahydropyrrolopyridinone **52** was obtained through hydrolysis of the amidine motif and ring opening of the cyclic ether bridge. This stand-alone example was the only occasion in which hydrolysis or dehydration was observed.

The method was extended using homoallyl tethered ylides to provide access to 6,6-polycycles **53** (Figure 8), albeit with lower conversions from the corresponding oxazole. This was attributed to the increased flexibility and degrees of freedom in the longer alkene tether which







**Scheme 4:** Selected examples from MPB studies on scope of the C5 Diels-Alder cascade process.

This process was extended to use oxygen tethered alkenes to access furan derivatives such as **50b** as single diastereomers and benzopyran derivative **56** in excellent yields. The formation of a single diastereomer of **50b** presents an opportunity for an enantioselective methodology by utilising single enantiomers of the starting ynamide – however this remained yet to be investigated. Finally, an all carbon tether proved successful, albeit activated by diester functionality, in accessing polycycle **57**.

## 1.5 Aims and objectives

With a gold-catalysed cascade protocol in hand to access complex  $sp^3$ -rich polycycles, a novel cobalt-catalysed polycyclisation was envisaged to provide a regiodivergent methodology (*vide infra*). This work aimed to deliver two complementary methodologies to access a wide range

of polycyclic scaffolds from chemically related building blocks (Figure 9). To achieve this, the approach looked to: provide modular, robust, and scalable synthetic procedures; install reactive sites for post catalysis modifications; and show broad functional group compatibility (Chapter 2). Modification of the catalysis precursors through changing the heteroatom linker, the length of the tether, and the position of the heteroatom would also provide access to additional polycyclic frameworks.

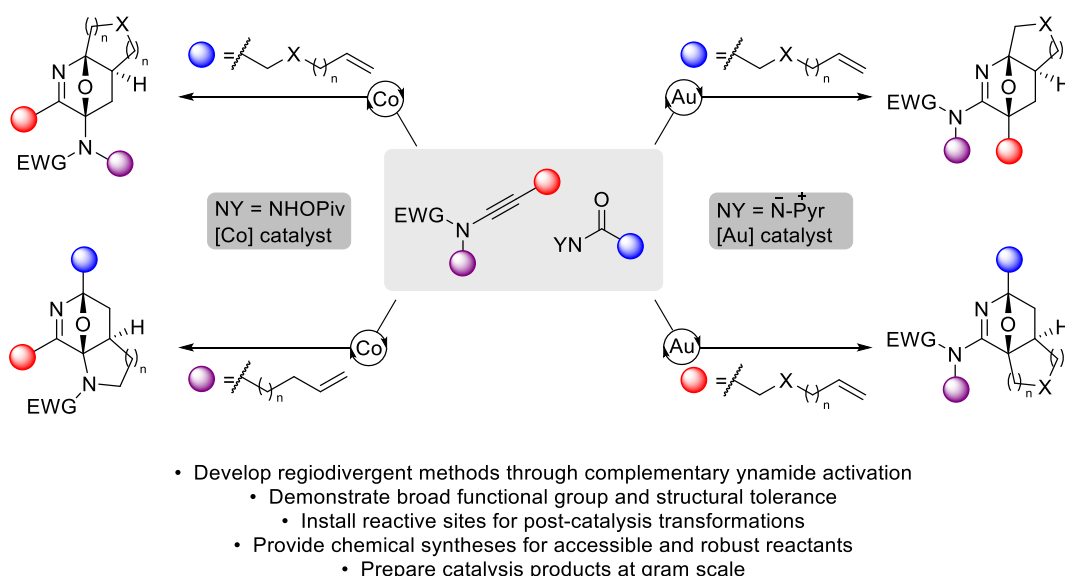


**Figure 9: Schematic representation for the aims of the investigation into complementary gold- and cobalt-catalysed polycyclisation reactions.**

The objective then became to demonstrate the potential of the catalysis products as a good basis for drug discovery library synthesis. To achieve this, the investigations looked to develop robust strategies to manipulate the inherent functionality generated during the polycyclisation processes to provide access to polycyclic piperidine motifs containing reactive sites for library generation. Amine, amide, alcohol and ketone reactive sites were targeted due to their extensive use in drug discovery library synthesis. Finally, the polycycles produced from these transformations should contain desirable pharmacology scores for predicted bioavailability, bioactivity and specificity (Chapter 3).

## Chapter 2: Polycyclisation methods to rapidly assemble molecular complexity

In this chapter new or improved syntheses of the cyclisation precursors were developed. Novel oxygen- and nitrogen- tethered en-ylides and en-ynamides were prepared that increased the range of Murcko frameworks accessible through the gold-catalysed cascade protocol. A complementary cobalt-catalysed polycyclisation was developed that provided access to regioisomeric polycyclic piperidines, delivering additional Murcko frameworks with distinct connectivity. A range of novel *N*-(pivalolyloxy)amides were prepared and a substrate scope was performed to assess the generality of the process.

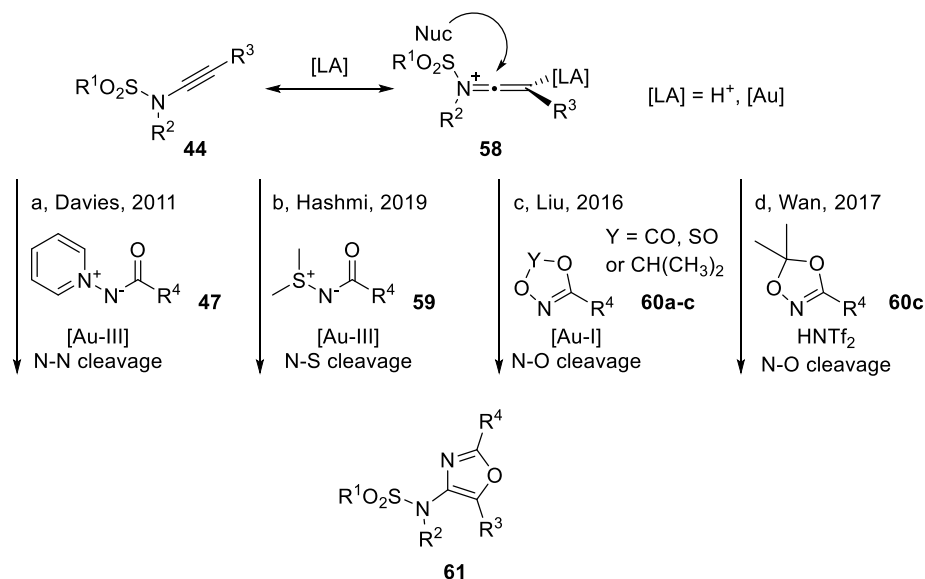
Functional groups that were desirable in drug discovery and readily cleavable protecting groups were installed. Both polycyclisation protocols were used at gram scale to demonstrate their robustness and prepare material for further synthetic manipulations discussed in chapter 3.

### 2.1 Gold-catalysed cascading cycloaddition reactions

#### 2.1.1 Gold-catalysed cycloaddition reaction to access 4-aminooxazoles

In 2011 the Davies group developed a novel methodology to access 4-aminooxazoles **61** *via* a gold-catalysed formal [3+2] dipolar cycloaddition between ynamides **44** and *N*-acyl pyridinium ylides **47** (Scheme 5a).<sup>48–50</sup> The key intermediate that furnishes the oxazoles in a regioselective manner can be visualised as gold keteniminium **58**, which highlights the electronic bias of the alkyne *via* the appended nitrogen. This underlying reactivity using ynamides has subsequently been achieved by a number of groups in combination with a range of different nucleophilic nitrenoid equivalents, including *N*-acyl sulfilimines **59** (Scheme 5b),<sup>51</sup> dioxazolones,

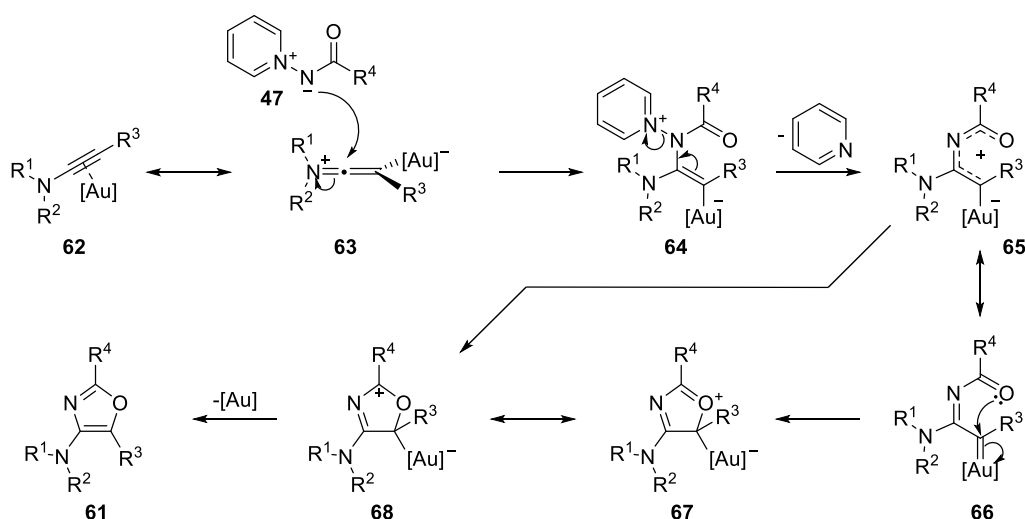
dioxathiazoles and dioxazoles **60** (Scheme 5c).<sup>52</sup> Activation by HNTf<sub>2</sub> has also been demonstrated in the case of dioxazoles **60c** (Scheme 5d).<sup>53</sup>



**Scheme 5: Routes to access 4-aminooxazoles from ynamides and nucleophilic nitrenoid equivalents.**

The work discussed in this thesis uses *N*-acyl pyridinium ylides **47** in the cycloaddition reaction, due in part to their simple preparation from the corresponding ester derivatives, themselves accessed from glycine methyl ester hydrochloride, and the excellent functional group compatibility displayed throughout previous studies.<sup>48,49</sup> In contrast, the dioxazoles and dioxazolone derivatives are accessed *via* the hydroxamic acid, prepared from the corresponding acid chloride or carboxylic acid. Access to the sulfilimines would require conversion of an ester functionality into a primary amide. For the catalysis precursors used in this process, all of these requirements would result in an increase in linear synthesis steps and a decrease in the efficiency. Furthermore, the use of dioxazoles, dioxazolones and dioxathiazoles employs DCE as the reaction solvent in both the  $[Au-I]$  and HNTf<sub>2</sub> methods, which limits the temperature accessible and is a known carcinogen.

The mechanism for this transformation is shown in Scheme 6. Activation of the ynamide  $\pi$ -system by the gold catalyst proceeds with electronic bias from the nitrogen causing slippage to gold keteniminium **63**, which ylide **47** then attacks in a regioselective manner to provide **64**. Gold-stabilised carbocation **65** is generated through elimination of the pyridine, which then undergoes cyclisation through either a  $4\pi$  electrocyclisation or by capture of the electrophilic carbon in carbenoid **66** by the acyl oxygen to generate **68**. Deauration then provides aromatisation to oxazole **61**, regenerating the gold catalyst.



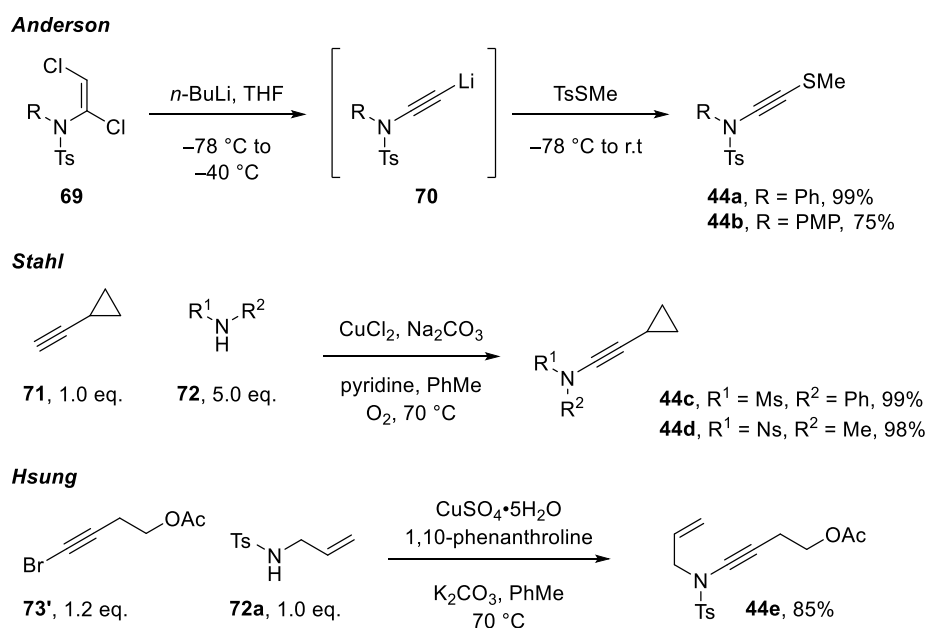
Scheme 6: Mechanism of gold catalysed oxazole formation between ynamides and N-acylopyridinium ylides

## 2.1.2 Synthesis of cyclisation precursors

### 2.1.2.1 Preparation of ynamides

A variety of ynamides were prepared to supplement those available within the Davies lab for these studies *via* the Hsung,<sup>54</sup> Stahl<sup>55</sup> and Anderson<sup>56</sup> methods. For the C2 Diels-Alder series, ynamides **44a-d** were selected due to previous observations that thio- and cyclopropyl-functionalised ynamides provided higher yields in the cascade sequence. Homopropargylacetate derivative **44e** was prepared as a desirable alkyl motif containing a

reactive handle for later modification (Scheme 7). During scaffold elaboration work (see Chapter 3) the sulfonamide is typically eliminated *via* reactions at the amidine motif, therefore the choice of sulfonamide at the ynamide was based on ease of handling<sup>c</sup> and potential visualisation of the ynamide and polycyclic products.<sup>d</sup>



**Scheme 7: Synthesis of ynamides used in the C2 Diels-Alder reaction study.**

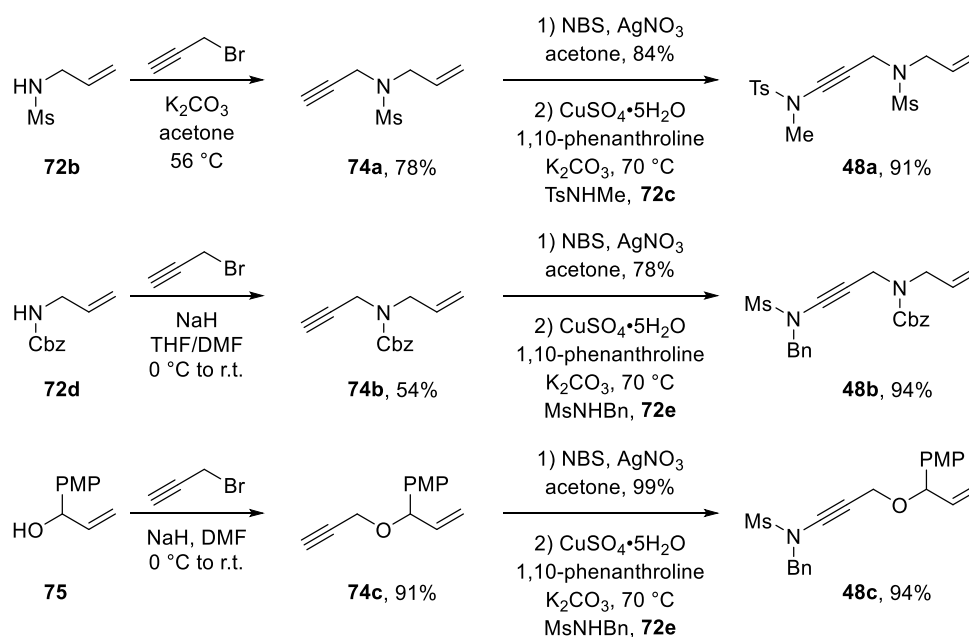
Unfortunately, previous attempts at removing tosyl protecting groups from the fused ring framework proved unsuccessful, with a wide range of conditions attempted and either no reaction or decomposition observed. For the continuation of this project, new sulfonyl groups that offered desirable functionality to be viewed as part of the final products instead of as protecting groups were used alongside readily cleavable carbamate groups.

The low molecular weight of mesyl sulfonamides and the catalytic hydrogenation of Cbz carbamates met these requirements. Therefore 1,6-enynes **74** were prepared *via* alkylation of

<sup>c</sup> Sulfonamides likely to produce solid ynamides and ease of separation during purification of the ynamide from the remaining sulfonamide and alkyne were the main considerations.

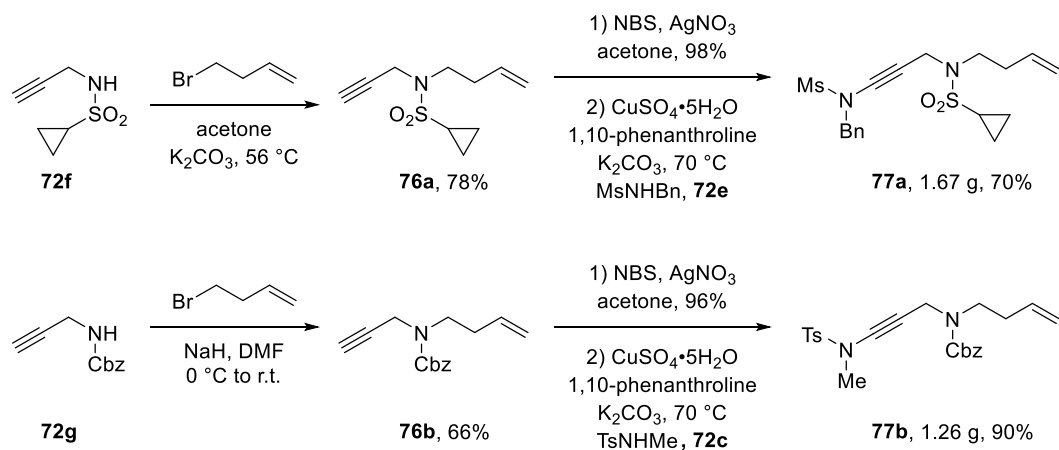
<sup>d</sup> Sulfonamides that are strongly UV active or oxidise strongly with KMnO<sub>4</sub> were preferred.

the respective allyl amine derivatives **72** for use in the C5 Diels-Alder protocol (Scheme 8). Allylic alcohol **75** was prepared by addition of vinyl magnesium bromide into *p*-anisaldehyde and subsequently alkylated with propargyl bromide. Employing the Hsung methodology provided 1,6-enyamines **48** *via* the bromoalkynes.<sup>54</sup>



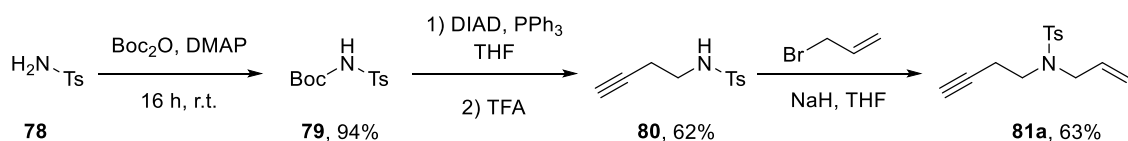
**Scheme 8: Synthesis of 1,6 enyamines *via* alkylation and copper-catalysed ynamide formation.**

Focus was then turned to increasing the scope of the 6,6-ring systems accessible *via* the C5 Diels-Alder methodology. A desirable sulfonyl group in drug discovery that would remain a part of the final molecule was targeted: cyclopropyl sulfonamide **72f** was therefore prepared (Scheme 9). Alkylation with homoallyl bromide afforded 1,7-enyne **76a**, which was converted into corresponding 1,7-enyamine **77a** using the Hsung methodology.<sup>54</sup> The same route was used to access Cbz derivative **77b**.



**Scheme 9: Synthesis of 1,7-enamides *via* alkylation and copper-catalysed ynamide formation.**

Attention was then turned to the improved synthesis of 1,7-enyne **81a**. Homopropargyl enynes would provide another Murcko framework when used in the tandem process. Previous attempts at preparing the required enyne in the Davies group had eventually led to a route *via* a Mitsunobu reaction and subsequent allylation (Scheme 10).



**Scheme 10: Synthesis route to homopropargyl 1,7-enynes used by MPB.**

The preliminary result obtained using the corresponding 1,7-enynamide to access **55** was encouraging (Scheme 4). However, the synthetic flexibility of the catalysis precursors was limited by this route. As octahydronaphthyridine motifs are commonly found in nature (Figure 10), the ability to deprotect and functionalise the alkyl nitrogen was of interest. Although there are strategies to selectively deprotect a single Boc group from di-*tert*-butyl-iminodicarboxylate derivatives of **79**, alkylation of the corresponding carbamates has proven low yielding throughout these studies and a more atom efficient process was desirable.



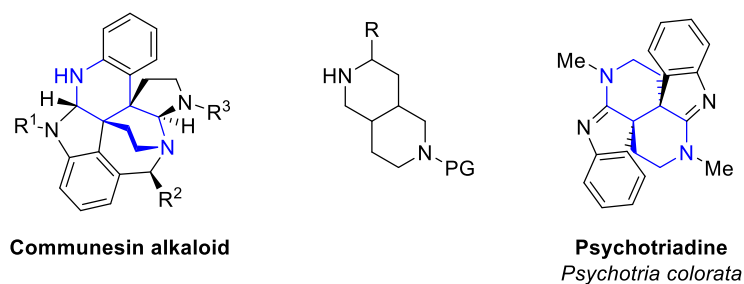
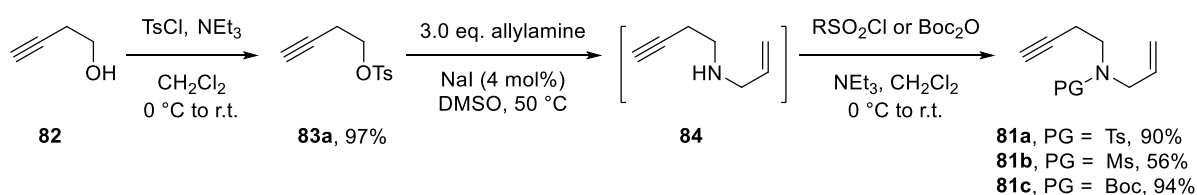


**Figure 10:** Octahydronaphthyridine scaffold in nature. Communesin and Psychotriadine alkaloids reproduced from ref. [57] and ref. [58].

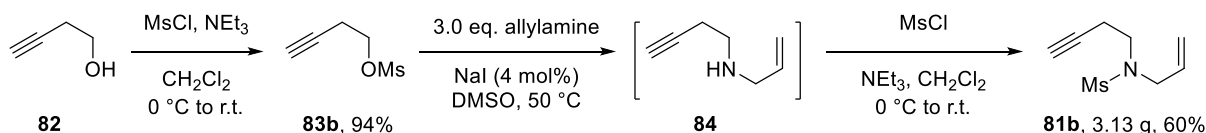
Homopropargyl alcohol is readily available and low cost compared to homopropargyl bromide (£3.40/g vs £11.80/g).<sup>e</sup> Tosylation of alcohol **82** gave access to sulfonate **83a** which would serve as an appropriate substrate for S<sub>N</sub>2 alkylation. Initial alkylation strategies using protected amine derivatives proved fruitless, however when treated with an excess of allylamine and NaI, secondary amine **84** was generated and the crude material used to access enynes **81** (Scheme 11).



**Scheme 11:** Improved synthesis of homopropargyl 1,7-enynes.

Further improvements to the efficiency of the process were made by switching to methanesulfonate **83b** (Scheme 12). Not only did this reduce the carbon count of the by-products, the higher reactivity of excess MsCl produced water soluble MsOH during quenching, providing **83b** pure from aqueous work up. This process was used again when protecting **84** to access 3.13 g of **81b** pure from aqueous work up, with no chromatography required across the synthesis.

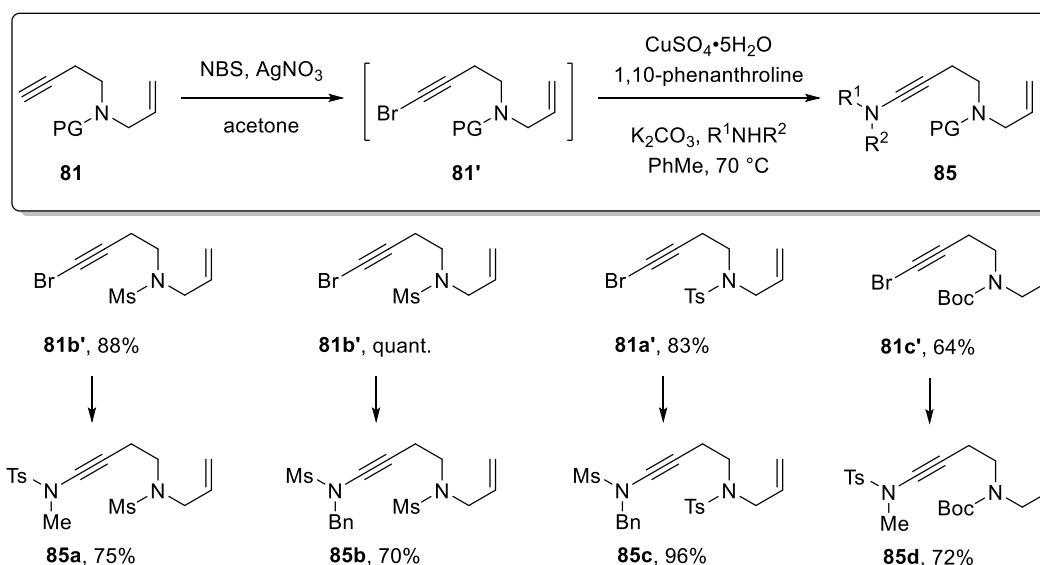
<sup>e</sup> Prices provided from Sigma Aldrich website, accessed 29/04/20



Scheme 12: Further improvements to the synthesis of enyne **81b**.

Overall, a 4-step synthesis requiring 3 individual purifications, with a significant number of by-products and poor atom economy, was reduced to a 3-step synthesis with no purifications required.

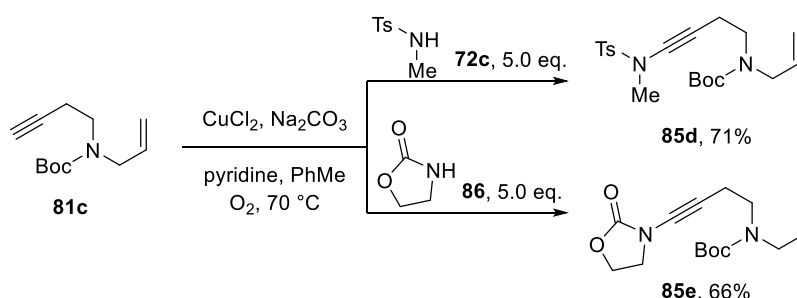
Enynes **81** were then coupled with sulfonamides to give the subsequent ynamides *via* the Hsung method (Scheme 13). As the choice of sulfonamide seemingly had little effect on the result of the cascade cycloaddition, TsNHMe was preferred due to its UV active nature resulting in facile reaction monitoring.



Scheme 13: Synthesis of homopropargyl 1,7-enynamides *via* copper catalysis.

The importance of freshly recrystallised NBS became apparent when attempting to prepare bromoalkyne **81c'** (Scheme 13). When an off-white NBS powder was used, Boc removal was observed in the reaction mixture. In contrast, when using freshly recrystallised NBS (from

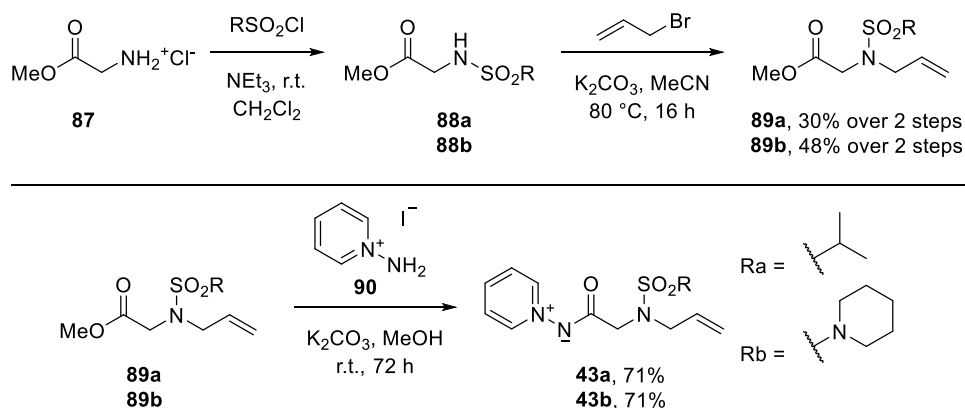
PhMe) bromoalkyne **81c'** was obtained, albeit with a diminished yield compared to the sulfonyl equivalents. Although ynamide **85d** was found in moderate yield (46% over 2 steps), in this case an improved yield of 71% was obtained using the Stahl method (Scheme 14).<sup>55</sup> This approach was also used to prepare oxazolidinone derivative **85e**, which provided an alternative to sulfonamides as the protecting group of the ynamide nitrogen, with a range of cleavage and ring opening procedures possible due to their extensive use as Evans auxiliaries.



Scheme 14: Synthesis of homopropargyl 1,7-enamides through the Stahl method.

#### 2.1.2.2 Preparation of *N*-acyl pyridinium ylides

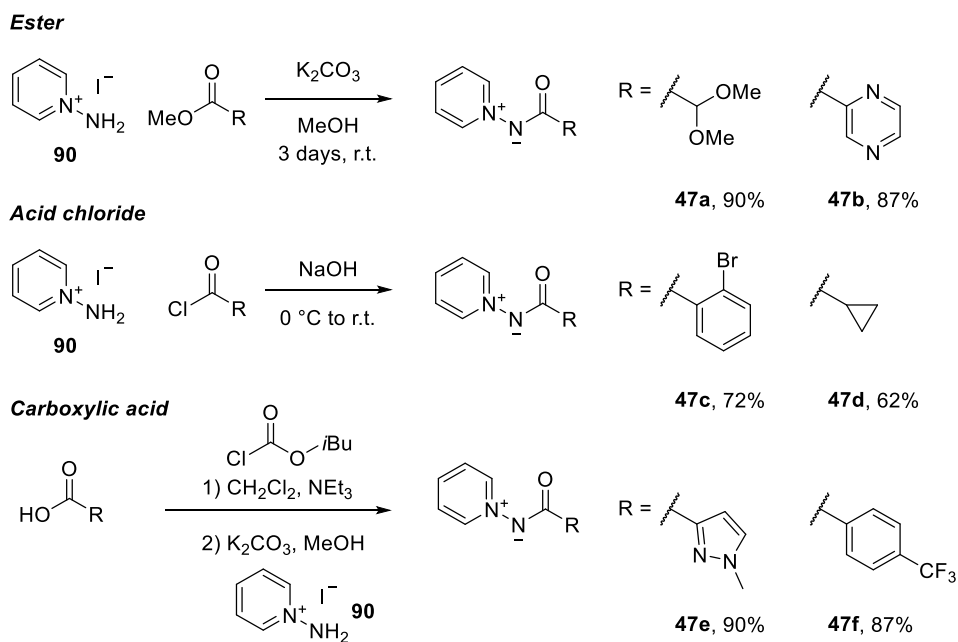
A range of *N*-acyl pyridinium ylides were then prepared. For studying the C2 Diels-Alder series, isopropyl- and piperidine- sulfonyl chlorides were selected to install desirable functional groups for drug discovery purposes and to investigate their compatibility with the cascade process. To this end, glycine methyl ester hydrochloride was treated with NEt<sub>3</sub> and the respective sulfonyl chloride in CH<sub>2</sub>Cl<sub>2</sub> to access isopropyl- and piperidine- sulfonamides **88** (Scheme 15). Low purity of the sulfonyl chlorides led to poor conversion in the protection of glycine ester **87**. Alkylation of the crude material through treatment with allyl bromide and K<sub>2</sub>CO<sub>3</sub> in refluxing MeCN furnished esters **89**. Treatment of esters **89** with *N*-aminopyridinium iodide **90** provided ylides **43** in good yields in only three steps.



**Scheme 15: Synthesis of allyl tethered ylides used in C2 Diels-Alder substrate scope.**

In the C5 Diels-Alder series, dimethyl acetal ylide **47a** has proven to be one of the best in the cascade reaction and provides a versatile handle for further reactivity (Scheme 16). Pyrazine and pyrazole ylides **47b** and **47e** offered desirable heteroaromatic functional groups, contain Lewis basic sites and score well in drug discovery prediction tools. 2-Bromo and 4-trifluoromethyl ylides **47c** and **47f** offer an insight into the steric and electronic impact of the substituents at the C2 position of the oxazole. Finally, cyclopropyl ylide **47d** was prepared to access an electron-rich alkyl group whilst limiting the overall molecular weight of the catalysis products.

The *N*-acyl pyridinium ylides were prepared according to literature procedures from the reaction of either acid chlorides, carboxylic acids or methyl ester precursors with *N*-aminopyridinium iodide **90** (Scheme 16), highlighting the multifaceted approaches available when preparing *N*-acyl pyridinium ylides.

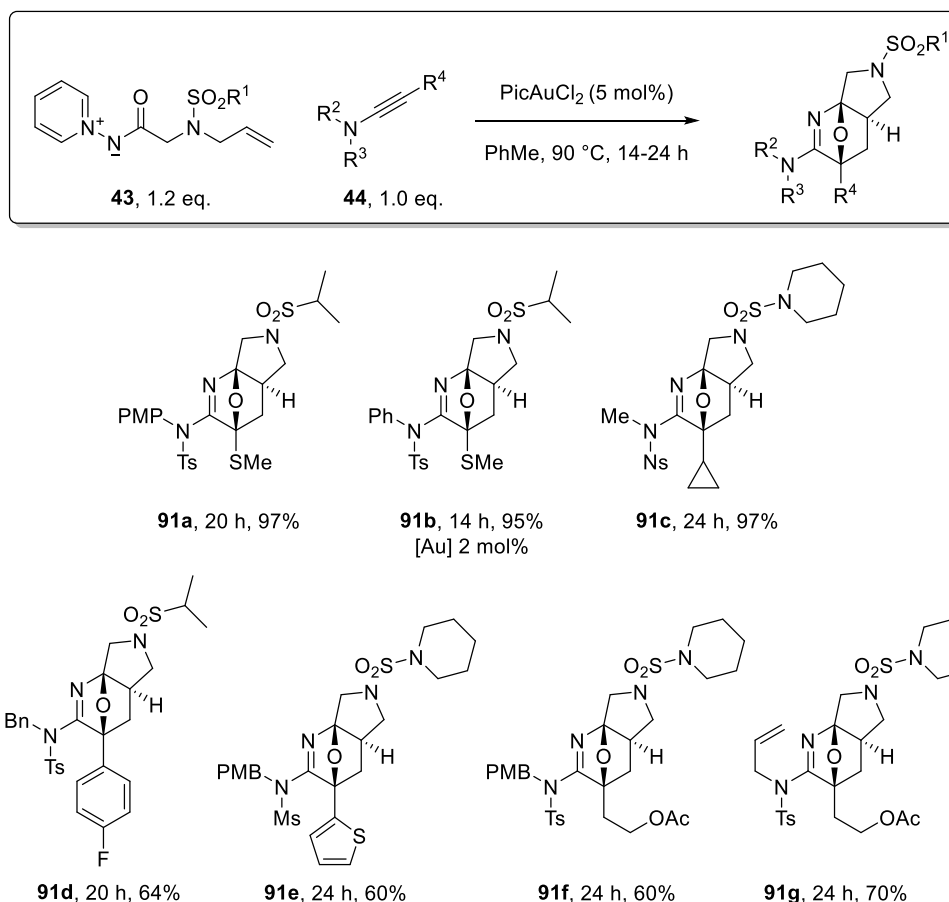


**Scheme 16: Synthesis of *N*-acyl pyridinium ylides used in the C5 Diels-Alder study.**

As the compounds employed in this study overlap with a range of previous and ongoing projects in the Davies group, a number of *N*-acyl pyridinium ylides and ynamides were donated from the Davies group members who are acknowledged in the experimental section (Chapter 7).

### 2.1.3 Diels-Alder studies with dienophile tethered *N*-acyl pyridinium ylides

Having prepared a range of catalysis precursors, their proficiency in the cascade protocol was examined. Ylides **43a-b** were tested in the cascade reaction with a variety of ynamides **44** to increase the substrate scope of the ynamide substituents (Scheme 17). The results from these reactions clearly demonstrate that the isopropyl and piperidine sulfonyl groups did not diminish Diels-Alder reactivity, with good to excellent yields across the series after 14 – 24 h at 90 °C.



**Scheme 17: Hexahydropyrollopyridines accessed from novel ylides 43a-b.<sup>f</sup>**

In all cases consumption of the ynamide was complete within 2 h, as monitored by TLC analysis. Examining the TLC and  $^1\text{H-NMR}$  spectra of the crude reaction mixtures suggested that the bulk of the material was a combination of the oxazole and Diels-Alder products, with minor impurities. Purification by flash column chromatography proved capable of separating the catalysis polycycles, although where oxazole remained its isolation proved challenging due to similar retention times.

<sup>f</sup> Throughout this thesis general structures are shown where appropriate to optimise scheme presentation as the ynamide and *N*-acylpyridinium ylides can be derived from the catalysis products. Further details of the cyclisation precursors can be found in the ESI.

An increase in Diels-Alder conversion was observed with thioynamides, compared to non-sulfur terminated ynamides, to give thioketals **91a-b** in near quantitative conversion. The catalyst loading could be reduced to 2 mol% with no impact on conversion to **91b**, once again highlighting the proficiency of the oxazole formation. Similarly, when a cyclopropyl ynamide was employed, polycycle **91c** was obtained in excellent yield with no remaining oxazole observed.

4-Fluorophenyl and thiophene substituted polycycles **91d-e** were isolated with lower yields due to incomplete Diels-Alder cyclisation, nevertheless these examples further demonstrate the ability of aromatic and heteroaromatic ynamides to undergo the desired cascade reaction.

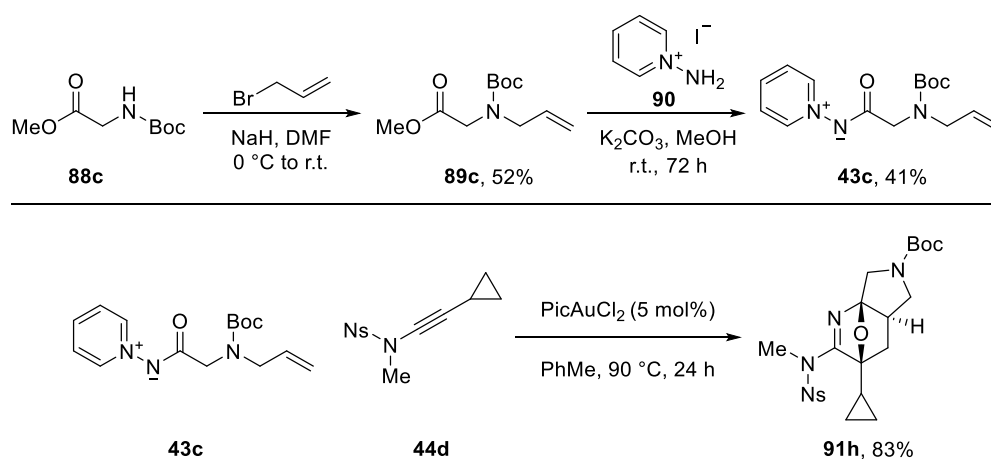
Ethyl acetate derivative **91f** proved difficult to separate from its corresponding oxazole resulting in a reduced yield, however this issue was overcome by changing the sulfonamide of the ynamide, highlighted when **91g** was isolated with comparative ease due to the larger difference in retention time on silica gel. This observation that some polycycles were significantly more polar than the respective oxazole whilst others had similar retention times held true throughout the studies on gold-catalysed cycloadditions, indicating that selection of the sulfonamide functionality at the ynamide should be considered before scaling synthesis reactions up to simplify purification, although no trends were observed to identify an optimal sulfonamide.

Following on from this, the use of a removal protecting group was explored. Boc-protected ester **89c** was prepared *via* alkylation of **88c** using NaH in place of K<sub>2</sub>CO<sub>3</sub>, due to the higher pK<sub>a</sub> of carbamates,<sup>g</sup> albeit in a moderate yield. Treatment with **90** afforded ylide **43c** which was utilised in the cascade reaction with ynamide **44d** to furnish polycycle **91h** (Scheme 18).

---

<sup>g</sup> pK<sub>a</sub>: EtOOCNH<sub>2</sub> = 24.2;<sup>59</sup> MeSO<sub>2</sub>NH<sub>2</sub> = 17.5;<sup>60</sup> PhSO<sub>2</sub>NH<sub>2</sub> = 16.1.<sup>61</sup> All measured in DMSO solutions

An excellent yield was obtained, with a slight decrease in conversion when compared to sulfonyl derivative **91c** (Scheme 17). Complete consumption of the ynamide was observed within two hours, with the oxazole remaining in the crude reaction mixture making up the remaining mass balance.

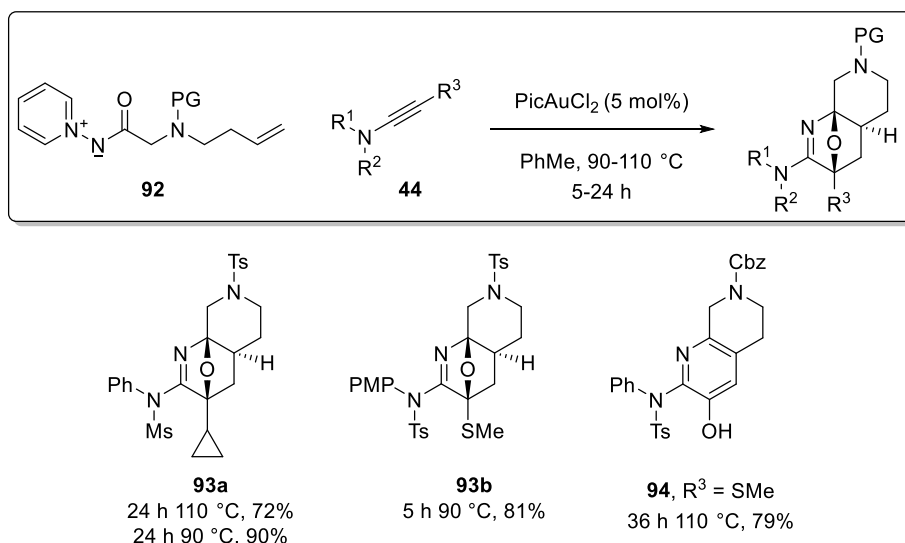


Scheme 18: Synthesis of a Boc-protected hexahydropyrrolopyridine.

Polycycle **91h** contained two orthogonal protecting groups: Boc deprotection under acidic conditions; *para*-nosyl removal through thiolate mediated  $\text{S}_{\text{N}}\text{Ar}$ . An increase in reactive sites for future elaboration, alongside the opportunity for selective deprotection, was a core objective during the development of this project.

To further examine the capability to access these octahydronaphthyridine motifs, homoallyl ylides **92** were tested in the cascade reaction with the most reactive ynamides from the earlier study (Scheme 19).





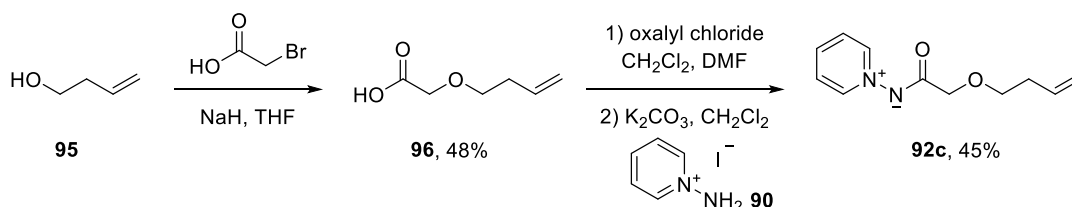
**Scheme 19: Catalysis results obtained using homoallyl tethered ylides.**

When cyclopropyl ynamide **44c** was used, consumption of the ynamide was complete and evidence of Diels-Alder cyclisation was observed *via* TLC analysis after 1 h at  $90\text{ }^\circ\text{C}$ . Upon heating to  $110\text{ }^\circ\text{C}$  for 24 h polycycle **93a** was obtained, alongside significant side products that appeared overnight. When repeated and left to stir at  $90\text{ }^\circ\text{C}$  for 24 h, a much cleaner reaction afforded a higher isolated yield of **93a**. Similarly, thioynamide **44b** only required 5 h at  $90\text{ }^\circ\text{C}$  for all traces of oxazole to be consumed *via* TLC analysis, although a small amount was observed in the  $^1\text{H}$ -NMR spectrum of the crude reaction mixture. The lower reaction temperatures highlight the superior reactivity of the methylthio- and cyclopropyl-functionalised ynamides in the cascade process.

When Cbz-protected ylide **92b** was employed, a higher temperature was required for conversion from the corresponding oxazole. The reaction was stirred at  $110\text{ }^\circ\text{C}$  for 36 h and hydroxypyridine **94** was isolated *via* sulfide expulsion and aromatisation. This result is the only polycycle so far obtained through this methodology to undergo spontaneous fragmentation to the pyridine.

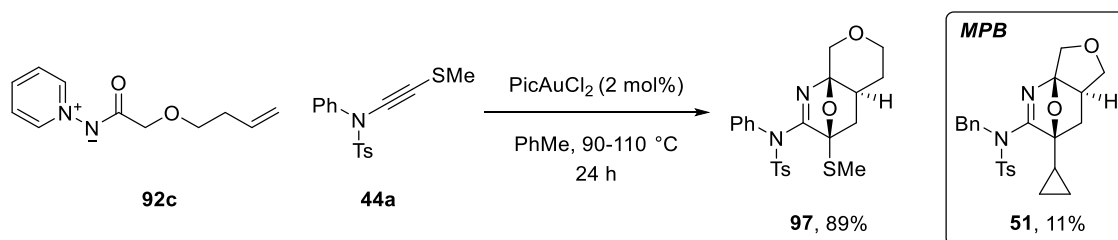
The successful synthesis of Boc-derivative **91h** (Scheme 18) and Cbz-protected **94** (Scheme 19) validated that carbamate protecting groups are compatible with the methodology, although higher temperatures may be required for optimal Diels-Alder cyclisation.

Another objective at the outset of this project was to change the heteroatom linker used in the ylide. To this end, homoallyl alcohol was alkylated with bromoacetic acid to give **96**. A one pot conversion to ylide **92c** *via* the acid chloride was preferred to esterification due to the low boiling point of the corresponding methyl ester (Scheme 20).



Scheme 20: Synthesis of an oxygen tethered homoallyl ylide.

Ylide **92c** was then employed with thioynamide **44a** and octahydropyranopyridine **97** was isolated in excellent yield (Scheme 21). Conversion to the Diels-Alder adduct was only observed when heated to 110 °C, however the reaction remained clean and no decomposition was observed. This was a remarkable improvement from the only previous C2 oxygen tethered example obtained previously, where **51** had been isolated in just 11%.



Scheme 21: Catalysis result using an oxygen tethered homoallyl ylide.

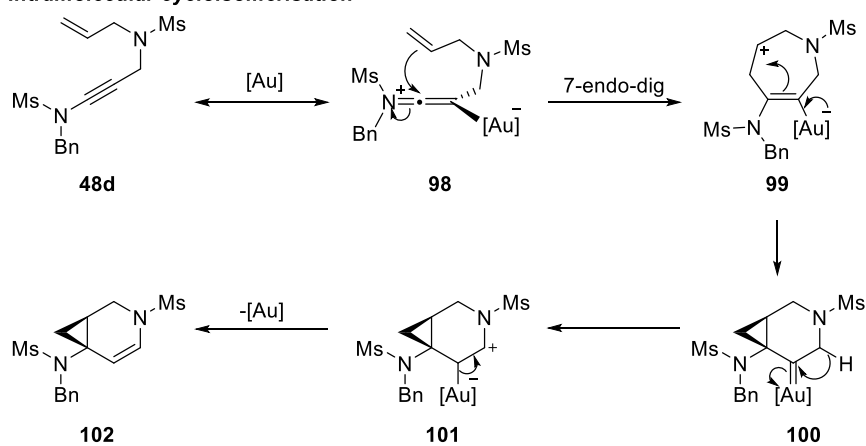
With a significant amount of material for post catalysis transformations (discussed in Chapter 3), attention was turned to the C5 Diels-Alder study.

#### 2.1.4 Diels-Alder studies with dienophile tethered enynamides

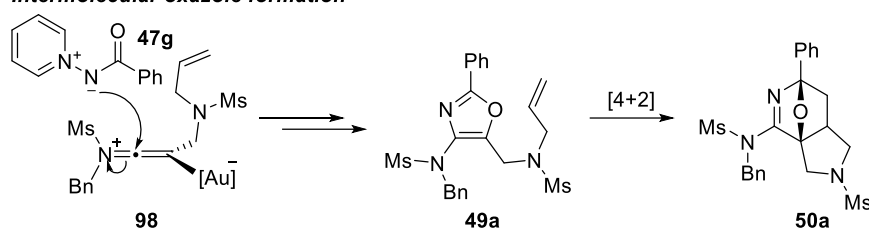
Before expanding the substrate scope of the 6,5-polycycles accessed by the C5 Diels-Alder process, the competing cycloisomerisation pathway was investigated. 1,6-Enynes undergo rapid enyne cycloisomerisation upon activation with a gold catalyst. 1,6-Enynamides have previously been shown to undergo cycloisomerisation through rhodium catalysis, and preceding observations during the substrate scope performed by MPB indicated that aryl and sterically demanding ylides gave rise to higher quantities of cycloisomerisation, whereas alkyl, in particular  $\alpha$ -heteroatom substituted, ylides showed minimal cycloisomerisation.

Gold-catalysed enyne cycloisomerisation is a well-established field<sup>62</sup> with silver-,<sup>63</sup> palladium- and ruthenium-<sup>64</sup> catalysed enynamide cycloisomerisation reactions having been developed. However, to the best of our knowledge a gold-catalysed approach with the connectivity observed in **48** has not been developed outside of the Davies research group. The reaction is believed to proceed *via* a 7-endo-dig cyclisation resulting from attack of the alkene onto gold activated ynamide, (Scheme 22), again with the regiocontrol provided by the nitrogen and visualised as gold keteniminium **98**. The resulting carbocation is trapped through the formation of gold carbene **100**, which undergoes a 1,2-hydride shift to **101**. Deauration then provides **102**.

**Intramolecular cycloisomerisation**



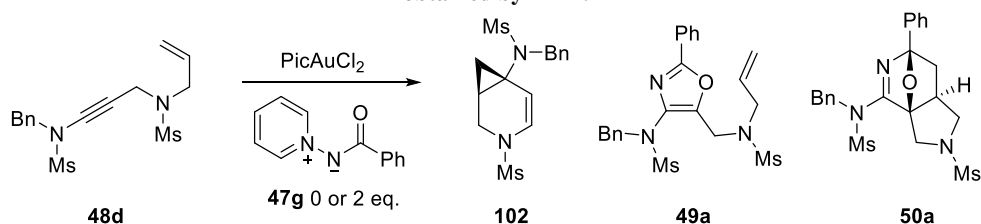
**Intermolecular oxazole formation**



**Scheme 22: Top: Mechanism of competing gold-catalysed 1,6-enynamide cycloisomerisation. Bottom: Intermolecular attack of **47g** onto gold keteniminium **98**.**

Both the intramolecular enynamide cycloisomerisation (Scheme 22, top) and the intermolecular oxazole formation (Scheme 22, bottom) proceed *via* gold keteniminium **98**. To gain an insight into the competing cycloisomerisation under gold catalysis conditions in the presence of ylide **47g**, a brief experimental study with 1,6-enynamide **48d** was performed (Table 1).

**Table 1: Investigation into enyne cycloisomerisation inhibition through an ylide  $[Au]$  interaction. Entries 3 and 4 obtained by MPB.**



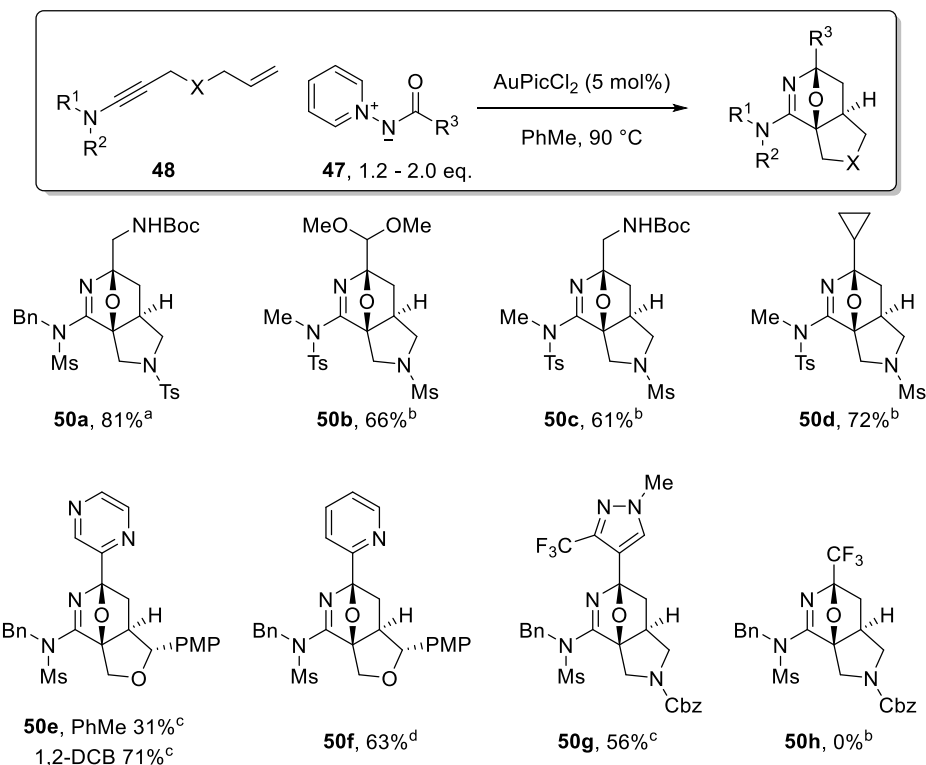
Entry	Solvent	<b>47g</b>	T (°C)	<b>102</b> (%)	<b>49a</b> (%)	<b>50a</b> (%)
1	CH <sub>2</sub> Cl <sub>2</sub>	0 eq.	r.t.	quant.	-	-
2	CH <sub>2</sub> Cl <sub>2</sub>	2 eq.	r.t.	0	0	0
3	PhMe	0 eq.	90	80	-	-
4	PhMe	2 eq.	90	N/A	42	15

Under standard gold-catalysed enyne cycloisomerisation conditions (Table 1, entry 1) quantitative conversion to enamine **102** was observed in just 1 h. In contrast, when the reaction mixture was doped with 2 eq. of ylide **47g**, no conversion was observed at r.t. (Table 1, entry 2), showing complete inhibition of the intramolecular pathway. When **48d** was treated with PicAuCl<sub>2</sub> in PhMe cycloisomerisation occurred to deliver **102** (Table 1, entry 3). Finally, when doped with ylide **47g** (Table 1, entry 4), inhibition of the intramolecular pathway resulted in oxazole **49a** and polycycle **50a** being isolated. Although the amount of cycloisomerisation was not quantified, a combined 57% of **49a** and **50a** displayed the ability of the desired intermolecular oxazole formation to outcompete the intramolecular cycloisomerisation.<sup>h</sup>

The 1,6-enynamides prepared in Chapter 2.1.2 were then used in the gold-catalysed cascade reaction with a variety of functionalised ylides to access the desired polycycles in good to excellent yields (Scheme 23).

---

<sup>h</sup> Complementary NMR and mass spectrometry studies performed by MPB indicated that pre-coordination of the ylide and gold catalyst may occur, prepositioning the ylide to attack the gold keteniminium species and favouring intermolecular attack over intramolecular isomerisation. MPB postulated that  $\alpha$ -heteroatom substituted ylides can undergo ligand exchange with the picolinate ligand.



**Scheme 23:** Cascade catalysis results using novel 1,6-enynamides. Equivalents of ylide: <sup>a</sup>1.3, <sup>b</sup>1.2, <sup>c</sup>1.5, <sup>d</sup>2.0.

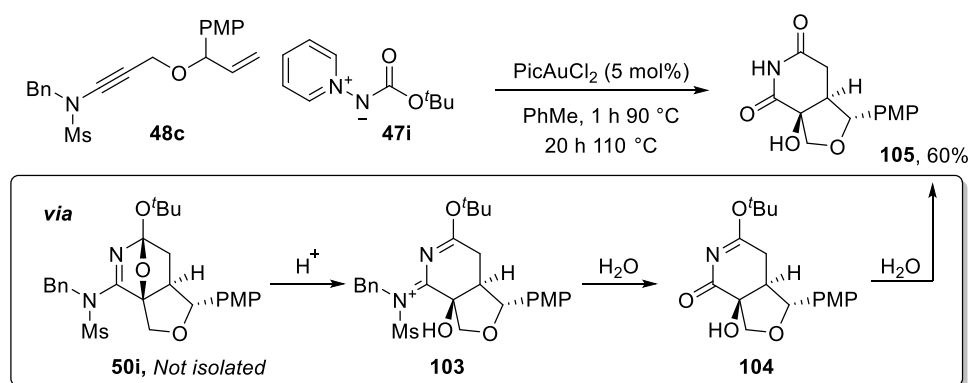
When alkyl substituted ylides were used, minimal cycloisomerisation was observed and polycycles **50a-d** were obtained as the major products from the crude reaction mixtures. Isolation of **50a** from a 0.40 mmol scale reaction proved simple due to polarity difference from its parent oxazole. For **50b-d**, performed at a 1.50 mmol scale, small amounts of remaining oxazole and impurities rendered purifications more challenging, and saw a minor compromise in yield due to coelution.

When utilising heteroaromatic functionalised *N*-acyl pyridinium ylides to access **50e-g**, an increase in cycloisomerisation was observed. This could be limited by adding a larger excess of ylides **47**. In all cases, cycloisomerisation was observed, although the amounts could not be quantified when analysing the <sup>1</sup>H-NMR spectra of the crude reaction mixtures due to overlap.

Pyrazine polycycle **50e** was obtained in just 31% yield under the standard cascade conditions, with the major product being identified as the cycloisomerisation adduct. It was hypothesised the low yield was the result of poor solubility of ylide **47b**, so the reaction was repeated in 1,2-DCB leading to an improved isolated yield of 71%. All three of these examples have additional basic sites within the ylide and yet do not prevent the gold catalyst from activating the ynamide, underlining the excellent functional group tolerance displayed within this methodology.

When trifluoromethyl ylide **47h**, derived from trifluoroacetic anhydride, was used a gold mirror was observed after 5 minutes. Despite this apparent reduction of the gold catalyst the ynamide was consumed, however the major product identified was impure cycloisomerisation.

In an attempt to access an electron rich oxazole and a polycycle with the oxidation state of an amide at the C2 position, *tert*-butyl ylide **47i** was used in the cascade process (Scheme 24).



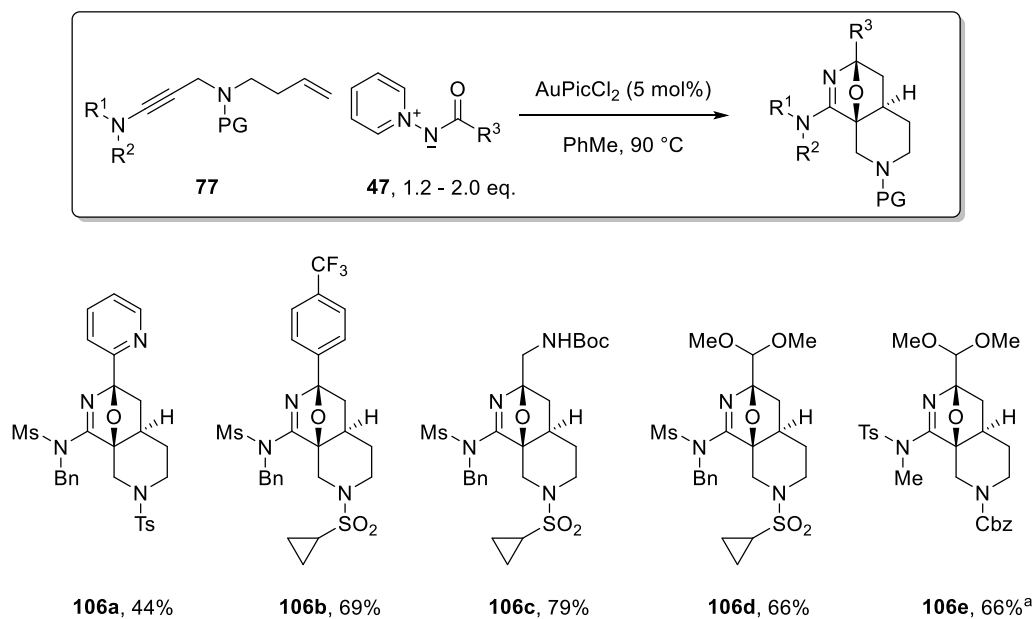
**Scheme 24: Imide formation through epoxy-bridge ring opening.**

Analysis of the  $^1\text{H}$ -NMR spectrum of the crude reaction mixture indicated two major products, neither of which contained a *tert*-butyl group. Purification by flash column chromatography resulted in 75% isolated yield of  $\text{MsNHBn}$  and 60% of what appeared to be imide **105**.<sup>i</sup> Initial

<sup>i</sup> Full characterisation was not obtained. The isolated compound had decomposed after 24 h in an NMR tube and the reaction was not repeated.

conversion to desired polycycle **50i** followed by cleavage of the cyclic ether bridge with conjugative assistance from the sulfonamide would yield **103**. Subsequent hydrolysis of both the amidine and the hemiaminal would deliver imide **105**.

1,7-Enynamides **77** were then utilised in the cascade reaction (Scheme 25). In all cases, the 1,7-enynamides underwent the desired cascade reaction, with no 1,7-enyne cycloisomerisation observed. Numerous metal catalysed 1,7-enyne<sup>65–67</sup> and 1,7-enynamide<sup>64,68–72</sup> cycloisomerisation methodologies can be found within the literature, however all enynamide substrates have the alkene appended to the ynamide nitrogen as opposed to the *C*-terminus. Although 7-exo-dig cyclisations are favoured according to Baldwin's rules, neither 7-exo-dig or 8-endo-dig isomerisation was observed by TLC or <sup>1</sup>H-NMR analysis.



Scheme 25: Catalysis results using 1,7-enynamides. <sup>a</sup> 1 h at 90 °C, 24 h at 110 °C.

In all cases conversion to the oxazole progressed smoothly. Diels-Alder cyclisation of the intermediate oxazole was observed at 90 °C in all cases except for Cbz derivative **106e** that required heating to 110 °C. The <sup>1</sup>H-NMR spectra of the crude reaction mixtures revealed



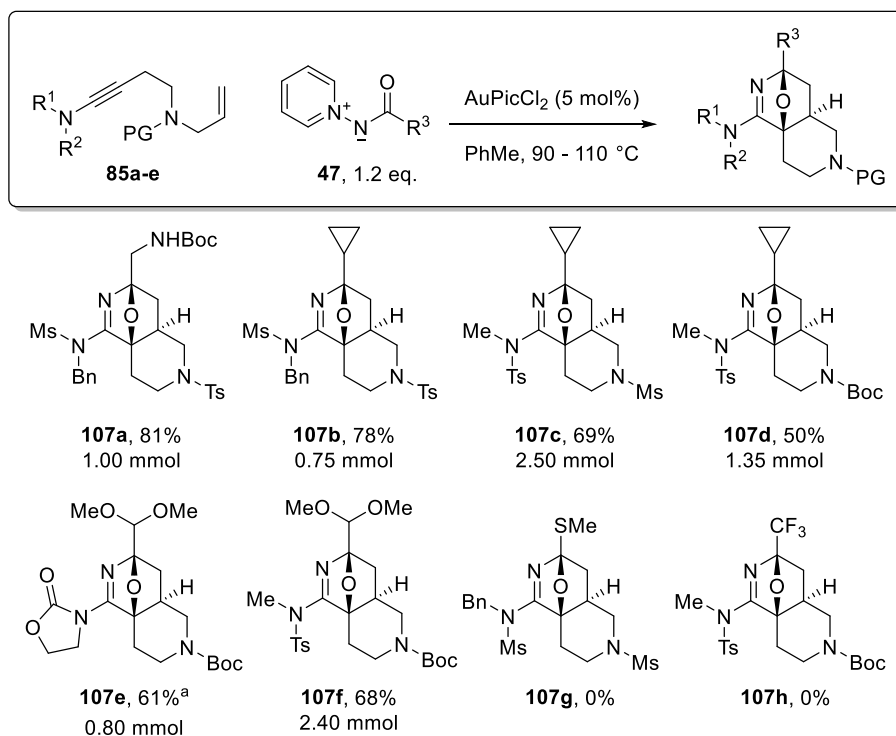
incomplete Diels-Alder cyclisation of the oxazole, although overlapping resonances made it challenging to determine reliable quantification.

Approximation from  $^1\text{H}$ -NMR analysis of the crude reaction mixture indicated that pyridine derivative **106a** was in a 2:1 ratio with the intermediate oxazole, which accounts for only 65% of the mass balance. The lower conversion is curious as the pyridine functionality has previously given excellent Diels-Alder conversion (Scheme 4).

NHBoc and dimethyl acetal derivatives **106c** and **106d** showed ratios of 4:1 and 3:1 of the desired polycycle and oxazole respectively, which accounted for the remaining material. Although isolation of the oxazole and subjection to heating in PhMe could provide further equivalents of the desired polycycle, the oxazoles tended to elute with minor impurities from the reaction and this action was not taken. If considering significant scaling up of this process, the remaining oxazole present could be isolated as the reactions did not suffer from extensive degradation.

Without a competing cycloisomerisation reaction, trifluoromethylphenyl ylide **47f** also proved compatible, even with sparing solubility in PhMe at 90 °C, to deliver **106b**. Cbz-analogue **106e** was isolated in comparable yield to **106d**, showing that in this case, an increase in temperature was enough to overcome the lower level of Diels-Alder reactivity when using carbamates.

1,7-Enynamides **85** were then tested in the cascade reaction to access octahydronaphthyridines (Scheme 26). In most cases, raising the temperature to 110 °C upon consumption of the ynamide was required for Diels-Alder reaction to occur. Initial reactivity appeared promising when **107a** was isolated in an excellent yield at 1.00 mmol scale, therefore the series was tested at a minimum of 0.80 mmol.



**Scheme 26:** Cascade catalysis products from novel 1,7-enynamides. <sup>a</sup>22 h at 90 °C.

Pleasingly the yields obtained across the series were again comparable to those obtained through the 6,5-polycycles (Scheme 23) and the propargyl linked 6,6-polycycles (Scheme 25). Higher temperatures were required - likely due to the additional flexibility in the alkene tether from repositioning the heteroatom linker - but did not result in decomposition.

Boc protected glycine ylide **47j** once again proved the best of those tested at promoting Diels-Alder cyclisation, with polycycle **107a** obtained in a remarkable 81% yield. Cyclopropyl derivatives **107b-d** were also accessed in high yield and proved a useful comparative tool across the protecting groups. Again, the change in sulfonamide for reaction tracking means that direct comparison was unavailable, though the slight reduction in yield for mesyl and Boc polycycles **107c-d** was tentatively attributed to the mesyl group and carbamates affecting the amount of reactive conformer available for the Diels-Alder reaction. Nonetheless, good yields were obtained that incorporated medically relevant sulfonamides and removable protecting groups.

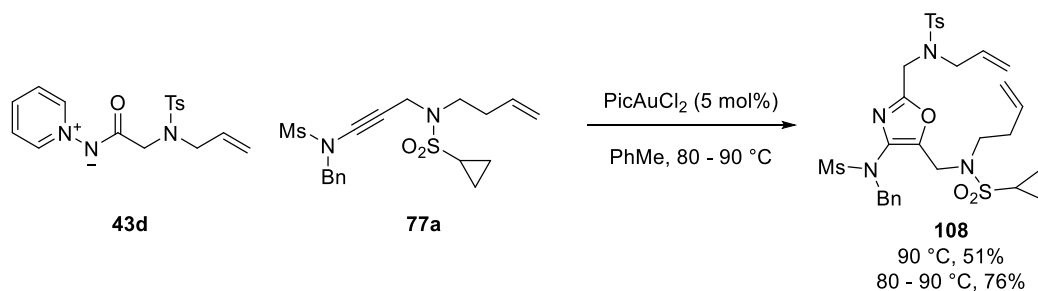
Ynamides **85d-e** were then utilised with ylide **47d** for a direct evaluation of oxazolidinone versus a sulfonamide at the ynamide nitrogen. Due to excessive line broadening caused by the presence of carbamate rotamers, quantification of the crude material by analysing the  $^1\text{H}$ -NMR spectrum was unfeasible. The isolated yields showed a small difference in overall efficiency, with oxazolidinone being marginally inferior at a smaller reaction scale. Nevertheless, the different reactivity accessible through the cyclic carbamate and the low molecular weight were attractive features.

An initial small-scale test reaction to access thioether **107g** showed promising results, as approximately 53% was isolated at around 85% purity. The purification proved difficult as the oxazole, ynamide and desired product all had near identical retention times on silica gel. In attempting to isolate pure material the reaction was repeated twice on larger scales, however purification was once again an issue and evidence of some sulfonamide cleavage was observed, suggesting similar susceptibility to sulfonamide expulsion as **50i** (Scheme 24).

When trifluoromethyl ylide **47f** was tested in a reaction with a 1,7-enynamide in an attempt to isolate **107h**, whilst avoiding the competing cycloisomerisation issue observed previously, again a gold mirror was produced within 5 minutes. Analysis of the  $^1\text{H}$ -NMR spectrum of the crude reaction mixture revealed only starting material recovery.

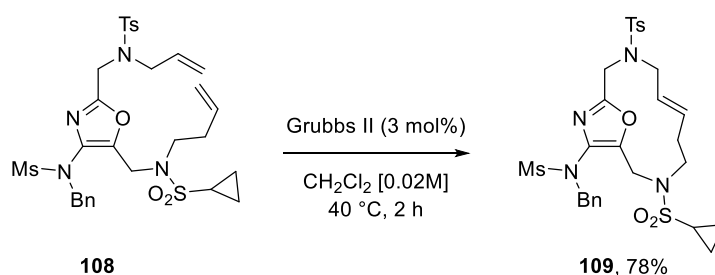
### 2.1.5 Formation of macrocycle *via* ring closing metathesis

Finally, an approach to access fused tetracycles *via* a ring closing metathesis reaction was explored. 1,7-Enynamide **77a** and allyl tethered ylide **43d** were subjected to gold-catalysed oxazole formation conditions (Scheme 27).



**Scheme 27: Synthesis of a bis-alkene tethered oxazole.**

An initial attempt showed some undesired Diels-Alder conversion after just 2 h at 90 °C. In a bid to hamper the Diels-Alder pathway the reaction was repeated at 80 °C for the first hour, although for consumption of ynamide **77a** the temperature was raised to 90 °C for the second hour. This resulted in an increase isolated yield of **108**, which was then treated with Grubbs 2<sup>nd</sup> generation catalyst (Scheme 28). The reaction was performed in CH<sub>2</sub>Cl<sub>2</sub> at relatively high dilutions to minimise cross metathesis and dimerisation.



**Scheme 28: Synthesis of a 12 membered macrocycle.**

Monitoring of the reaction by TLC revealed a new product with similar retention time to the starting oxazole. Ultimately purification by filtration through a pad of silica followed by hot recrystallisation from EtOH provided **109** in excellent yield. The bulk of the remaining mass balance was seemingly made up by dimerisation products. The <sup>1</sup>H-NMR spectrum showed significant line-broadening, presumably due to restricted rotation within the macrocycle. The product was assigned by one of the alkene CH resonances [ $\delta$  = 5.15 (dt,  $J$  = 14.3, 6.6 Hz, 1H) ppm] which contained typical coupling values for a *trans*-alkene (Figure 12, entry 1). This was

later confirmed by single crystal XRD analysis (Figure 11). The remaining alkene CH observed a significant upfield shift in the  $^1\text{H}$  NMR spectrum, assigned to potential interaction with the  $\pi$ -system of the oxazole ring.

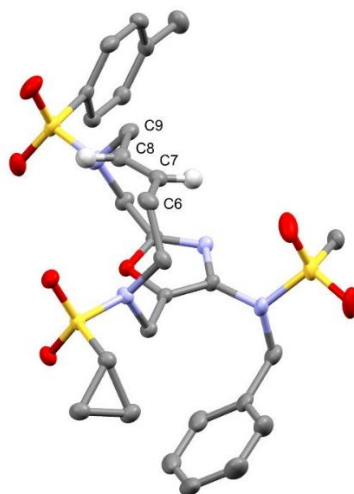
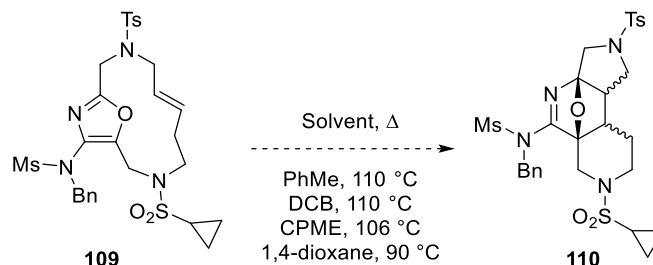


**Figure 11:** Crystal structure of macrocycle **109**. Ellipsoids at 50% probability, hydrogens omitted except at the alkene for clarity. X-ray data was obtained and solved with assistance from Dr Louise Male.

As the macrocycle appeared to place the alkene above or below the oxazole in its lowest energy crystal conformation, it was anticipated that Diels-Alder cycloaddition was a feasible outcome, with questions on the stereoselectivity of the two ring junctions, as a *cis*- and a *trans*- ring junction would be predicted. Macrocycle **109** was heated in a variety of solvents in an attempt to isolate polycycle **110** (Scheme 29).



**Scheme 29:** Attempted Diels-Alder reaction with macrocycle **109**.

When PhMe was employed at 90 °C, only starting material was observed. Upon heating in other solvents at increased temperatures new products were observed. Examining the  $^1\text{H}$ -NMR spectra of the reaction mixtures indicated the alkene resonance disappeared and was replaced by complex alkyl resonances (Figure 12). Although both PhMe and 1,2-DCB appeared to show potential Diels-Alder adducts, no products could be isolated pure through either flash column chromatography or recrystallisation. Disappearance of the distinctive alkene resonance at 5.15 ppm and the extensive range of new alkyl peaks suggested Diels-Alder cyclisation may occur, however conversion into a single major product is unlikely. With further optimisation this offers an attractive route into tetracyclic scaffolds.

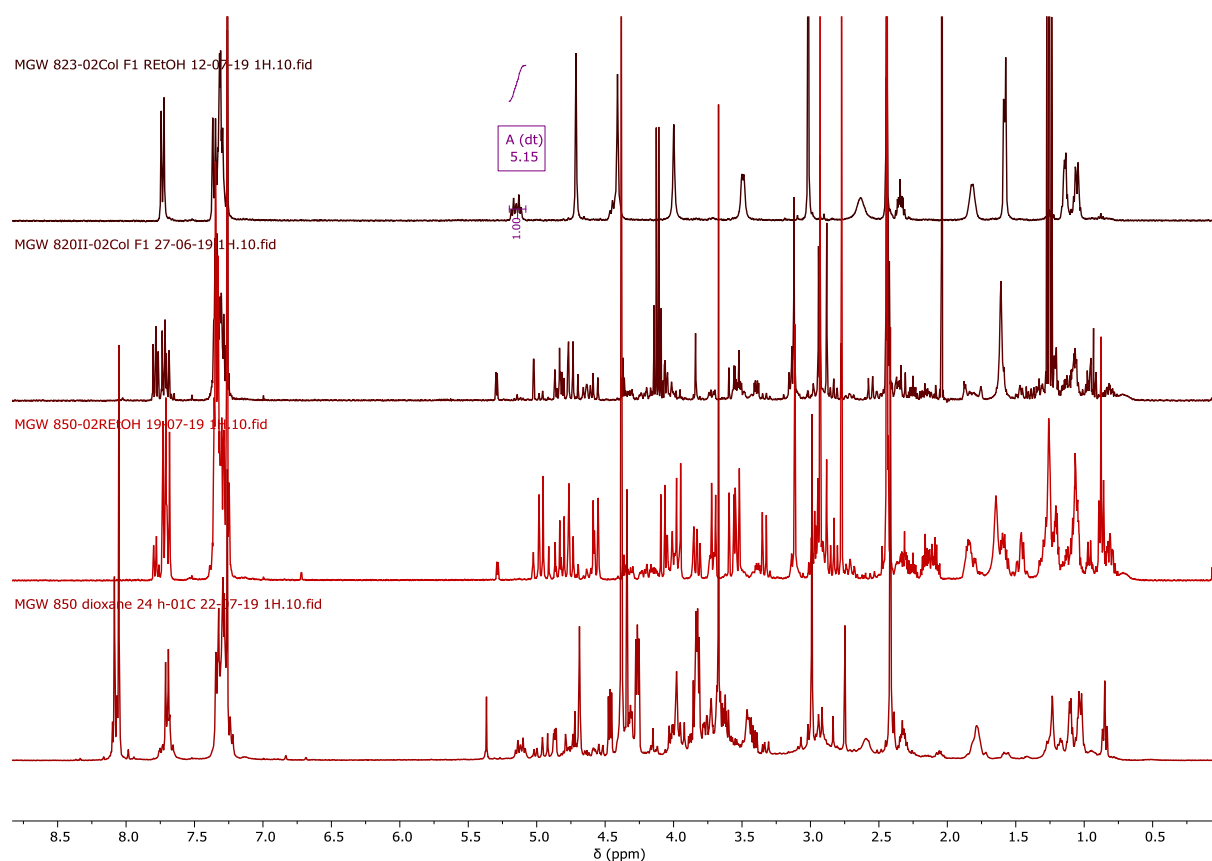
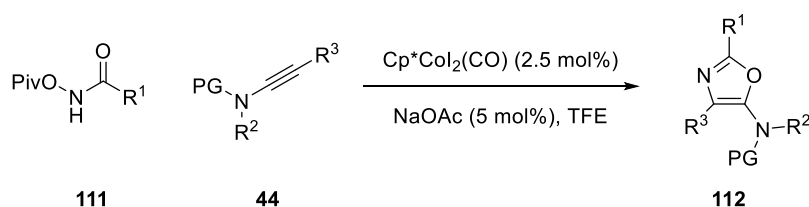


**Figure 12: Stacked spectra showing attempts at Diels-Alder reaction of macrocycle 109. 1) purified 109, with alkene resonance at 5.15 displayed. 2) PhMe 110 °C, post column. 3) 1,2-DCB 110 °C, post recrystallisation. 4) 1,4-dioxane 90 °C, crude reaction mixture.**

## 2.2 Cobalt-catalysed polycyclisation reactions

### 2.2.1 Cobalt-catalysed oxazole formation and potential polycyclisation method

Recent developments in cobalt-catalysed formal [3+2] cycloadditions have provided a new route to oxazoles, combining *N*-(pivaloyloxy)amides **111** with ynamides **44**<sup>73</sup> or alkynes<sup>74</sup> in a regioselective manner. The transformation that uses ynamides achieves the regioisomeric outcome of the Au(III)<sup>48,49,52</sup> and Tf<sub>2</sub>NH<sup>53</sup> promoted routes (Scheme 5), accessing 5-aminooxazoles **112** (Scheme 30).



**Scheme 30:** Cobalt-catalysed [3+2] cycloaddition reaction between *N*-(pivaloyloxy)amides and ynamides to access 5-aminooxazoles.

With *N*-(pivaloyloxy)amides recent popularity in a range of rhodium-catalysed reactions<sup>75–81</sup> and the practicality and flexibility of (en)ynamide preparations already highlighted previously,<sup>54–56,82,83</sup> the synthetic toolbox for making these materials is diverse and tolerates a wide range of functionality. Although in its infancy, cobalt-catalysed cycloadditions to form oxazoles have demonstrated reasonable functional group tolerance,<sup>73,74</sup> showing the potential for future advancements of this chemistry to build diverse libraries.

With prior examples of 5-amido activated oxazoles undergoing Diels-Alder reactions (Scheme 1), combination of the cobalt-catalysed process with an intramolecular Diels-Alder reaction was considered to provide a similarly modular and flexible synthetic methodology to access sp<sup>3</sup>-rich polycycles. The work herein describes an evolution of the cobalt-catalysed [3+2] cycloaddition process by exploiting an intramolecular [4+2] Diels-Alder reaction through an

appended alkene on either of the catalysis precursors to access hexahydropyrrolopyridines and derivatives **114** (Figure 13). The effect of a 5-amido functional group on the subsequent Diels-Alder transformation and the stability of the products towards spontaneous dehydration was of particular interest.

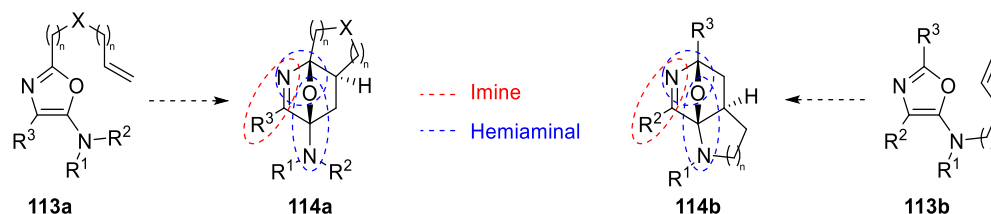
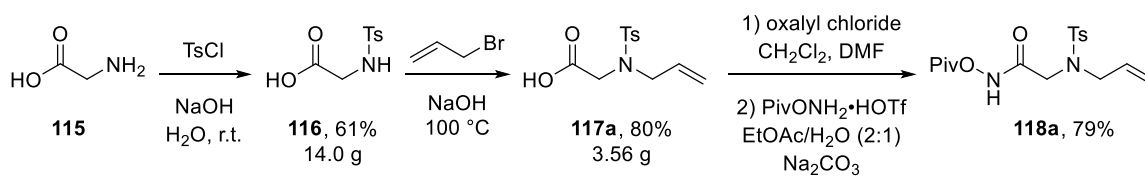


Figure 13: Molecular scaffolds accessible through intended cobalt-catalysed polycyclisation process.

This process was analogous to the gold-catalysed transformation discussed in chapter 2.1, providing different reactivity handles for future elaboration *via* the generation of imine and hemiaminal functional groups.

## 2.2.2 Initial development of the methodology

Preliminary efforts began by preparing alkene tethered carboxylic acid **117a**, prepared from glycine *via* tosyl protection and subsequent allylation (Scheme 31). Conversion to *N*-(pivaloyloxy)amide **118a** was achieved *via* generation of the acid chloride and treatment with PivONH<sub>2</sub>•HOTf under Schotten-Baumann conditions.

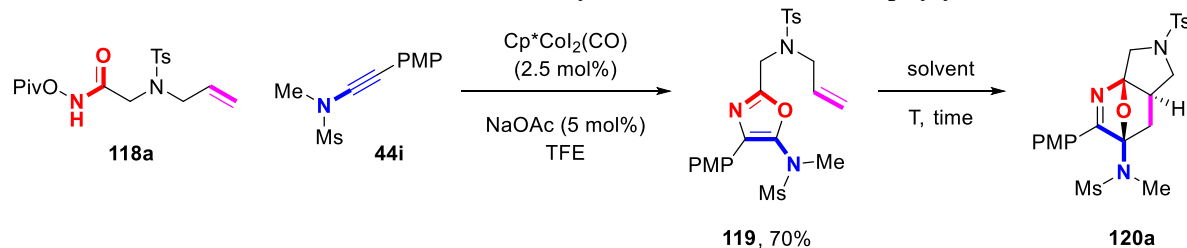


Scheme 31: Synthesis of allylated glycine derived *N*-(pivaloyloxy)amide **118a**.



Initially the reaction of *N*-(pivaloyloxy)amide **118a** with ynamide **44i** was studied. Under the previously optimised oxazole formation conditions,<sup>73</sup> oxazole **119** was isolated and a solvent screen performed for the Diels-Alder cycloaddition (Table 2).

**Table 2: Solvent screen for Diels-Alder cyclisation from oxazole **119** to polycycle **120a**.**

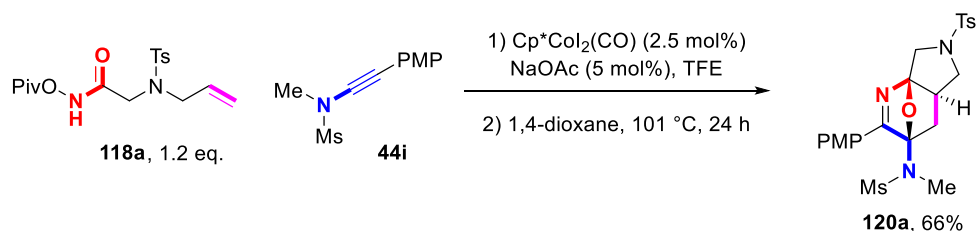


Entry	Solvent	Time (h)	T (°C)	119:120a
1	TFE	2	100 <sup>a</sup>	4.3:1.0
2	TFE/H <sub>2</sub> O	2	140 <sup>a</sup>	1.2:1.0
3	MeCN	4	150 <sup>a</sup>	4.6:1.0
4	1,4-dioxane	10	reflux	1.0:2.8
5	1,4-dioxane	24	reflux	1.0:5.8
6	CPME	24	reflux	1.0:1.2
7	PhMe	24	reflux	1.0:1.1

<sup>a</sup> Reaction performed with microwave heating. Reaction conditions: oxazole **119** (0.20 mmol) was heated to the indicated temperature in solvent (0.1 M) for the specified time. NMR ratios were calculated from the <sup>1</sup>H-NMR spectrum of the crude reaction mixture.

When a poor conversion to Diels-Alder adduct **120a** was observed when heating in TFE (Table 2, entry 1), it was clear that a solvent exchange was required. After a brief screening of solvents, it became apparent that 1,4-dioxane gave superior conversion among the solvents tested (Table 2, entries 4 and 5), with 24 h required for improved conversion.

When the oxazole formation was attempted in 1,4-dioxane to allow a one-pot procedure, the solvent switch proved detrimental and the desired oxazole was not observed. Pleasingly, performing the oxazole formation in TFE, followed by a filtration through silica and then a solvent exchange, without purification of the crude oxazole, led to isolation of **120a** in 66% (Scheme 32).



**Scheme 32: Optimised procedure to access Diels-Alder polycycle 120a through a solvent exchange.**

An excess of *N*-(pivaloyloxy)amide **118a** was required for consumption of ynamide **44i**, with trace amounts of the intermediate oxazole remaining after 24 h at reflux. No dehydration to the corresponding pyridine was observed throughout the screening, with the sulfonamide able to accommodate cyclisation without facilitating dehydration and aromatisation. Subsequent single crystal XRD analysis of **120a** confirmed the regioselectivity of the oxazole formation and the stereochemistry of the ring junction as *trans* (Figure 14).

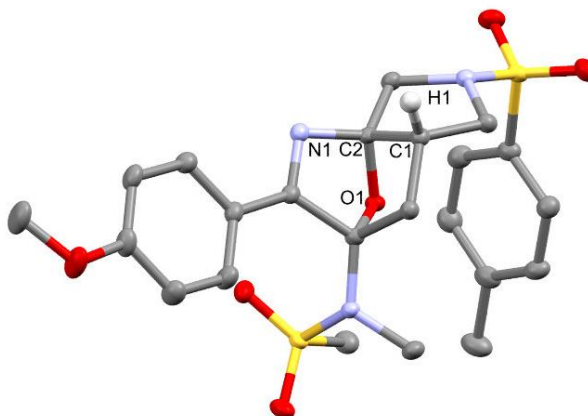
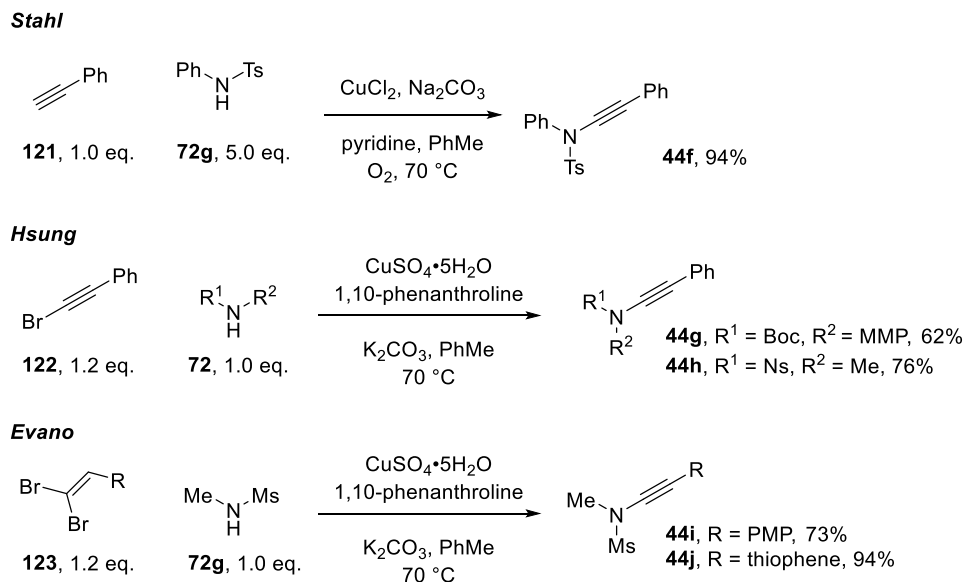


**Figure 14: X-ray structure of 120a. Ellipsoids at 50% probability, hydrogens omitted except at the *trans*-ring junction for clarity. X-ray data obtained and solved with assistance from Dr Louise Male.**

### 2.2.3 Synthesis of catalysis precursors

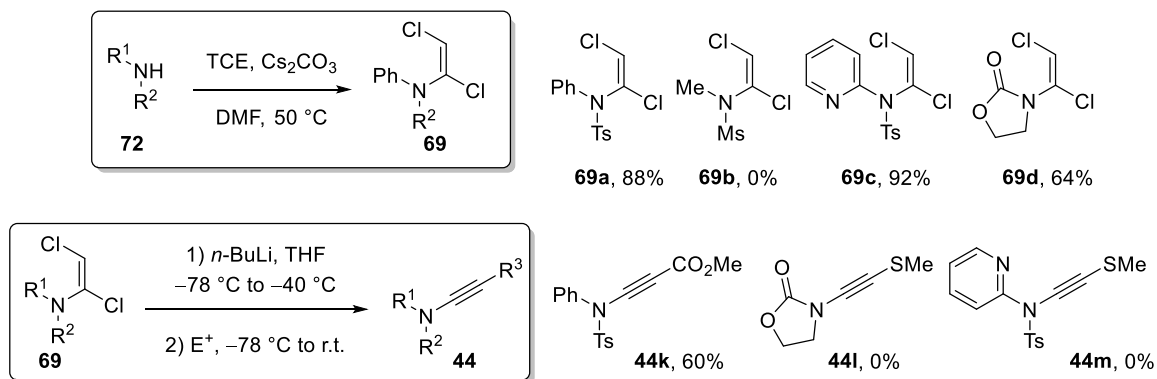
A range of *N*-(pivaloyloxy)amides and ynamides were prepared to complement materials described previously (Scheme 7) and available in the Davies lab. A variety of ynamides were

selected to probe the initial functional group compatibility of the process and prepared using the Stahl,<sup>55</sup> Hsung<sup>54</sup> and Evano<sup>82</sup> methods (Scheme 33).



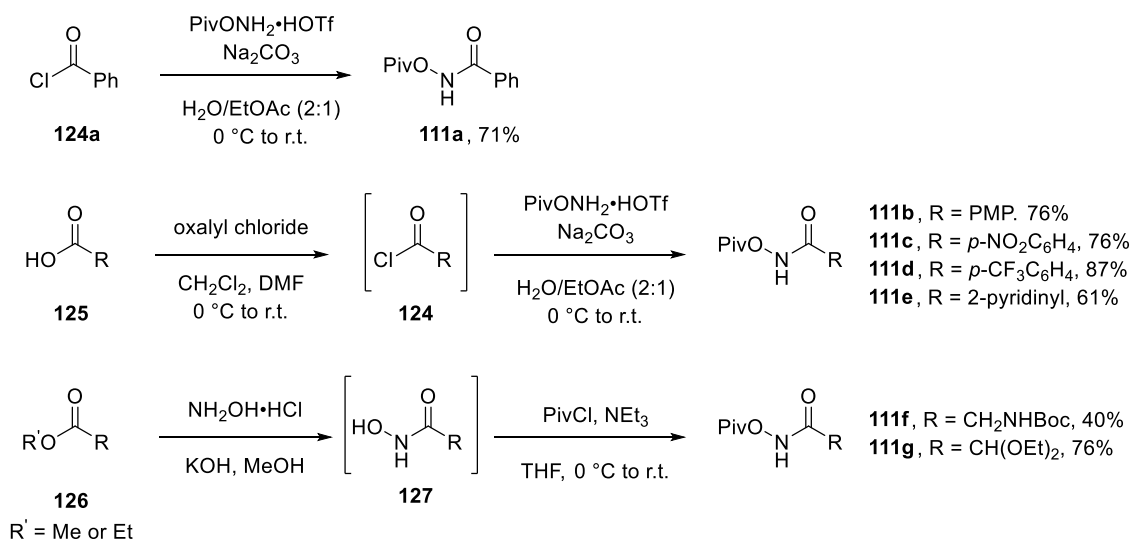
**Scheme 33:** Synthesis of a variety of ynamides for use in cobalt-catalysed polycyclisation reactions.

In an attempt to prepare a range of ynamides *via* the Anderson method, dichloroenamides **69** were prepared (Scheme 34).<sup>56</sup> 2-Pyridinyl sulfonamide **69c** was targeted to study the effect of a strongly electron withdrawing group on the ynamide nitrogen. **69b** was selected for a reduced steric impact and low molecular weight and oxazolidinone **69d** for alternative deprotection strategies. Unfortunately, **69b** gave an intractable mixture upon work up in the dichloroenamide formation, and only **69a** produced isolable products from the lithiation reaction to give **44k**.



**Scheme 34: Attempted synthesis of functionalised ynamides from dichloroenamides.**

A series of *N*-(pivaloyloxy)amides were also prepared from procedures described in the literature and newly developed procedures within the Davies group (Scheme 35). A variety of functionalised aromatic, heteroaromatic and alkyl substituted targets were identified and prepared from acid chloride **124** and carboxylic acids **125**.

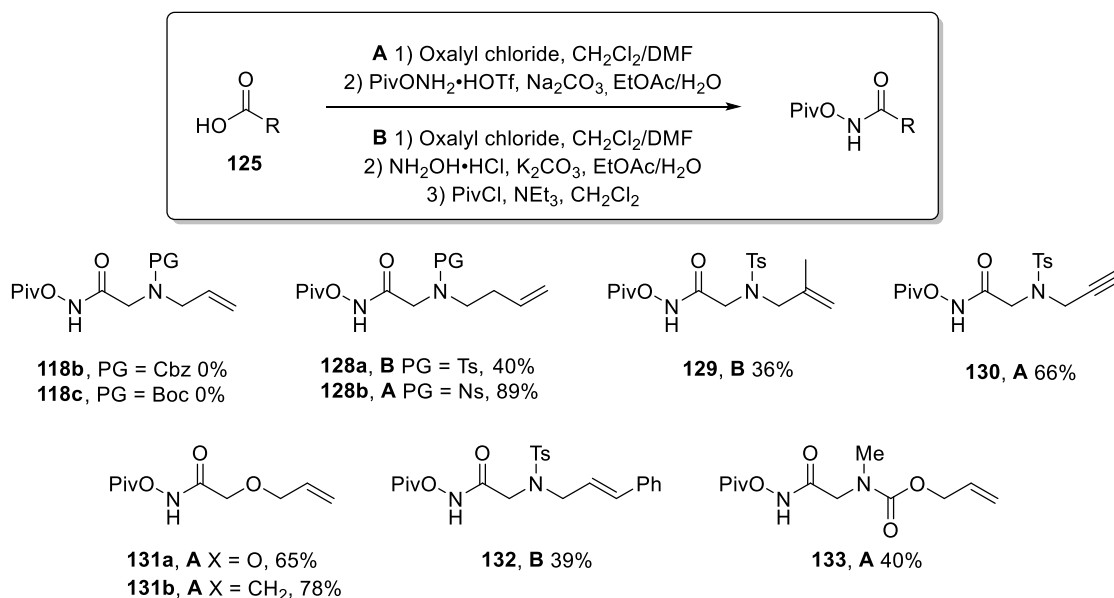


**Scheme 35: Synthesis of a diverse selection of *N*-(pivaloyloxy)amides.**

With established routes to access the desired *N*-(pivaloyloxy)amides from acid chloride and carboxylic acid derivatives, a direct method from esters was desired. A route was then developed through addition of functionalised esters **126** into a basic solution of NH<sub>2</sub>OH<sub>2</sub>·HCl in MeOH, generating hydroxamic acid derivatives **127**. After collecting the crude material

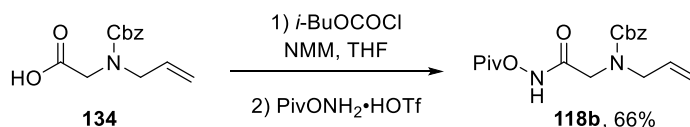
through an aqueous work up, treatment with PivCl and NEt<sub>3</sub> afforded **111f-g**. An acid wash during the extraction resulted in significant loss of the NHBoc hydroxamic acid, lowering the yield. Nevertheless, this synthetic pathway provided direct access into *N*-(pivaloyloxy)amides from the ester derivatives and added another option to the toolbox for their syntheses.

With these results in hand, focus was turned to modifying the heteroatom within the alkene tethered *N*-(pivaloyloxy)amides. A range of alkene containing glycine derivatives were prepared and converted into the corresponding *N*-(pivaloyloxy)amides **128-129** and **132-133**, in addition to propargyl, alkoxyallyl, and alkyl derivatives **130** and **131** (Scheme 36).



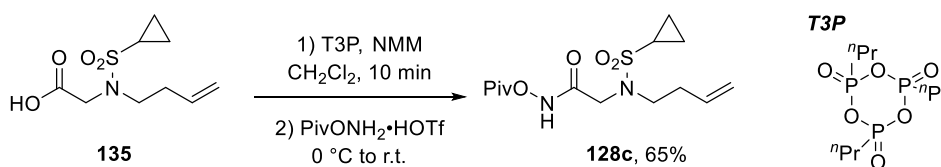
**Scheme 36: Synthesis of various alkene and alkyne tethered *N*-(pivaloyloxy)amides.**

An alternative route was required for carbamate protected carboxylic acids **134** due to their incompatibility with oxalyl chloride mediated acid chloride formation. Formation of the acyl carbonate followed by treatment with PivONH<sub>2</sub>•HOTf gave access to **118b** (Scheme 37).



**Scheme 37:** Synthesis of a carbamate protected *N*-(pivaloyloxy)amide *via* an acyl carbonate.

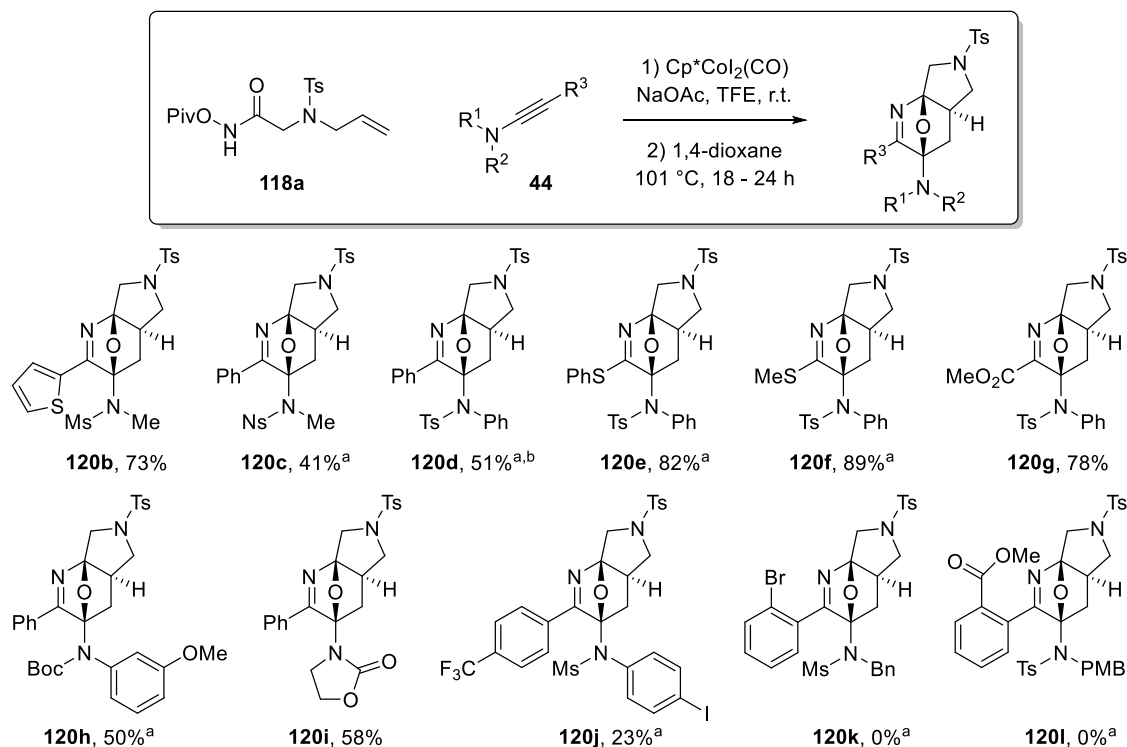
While this methodology provided access to the desired amide, a side product from the reaction included unreacted acyl carbonate. As these have similar polarities, separation of these compounds *via* flash column chromatography proved challenging, and a separate method was desired. To this end, an amide coupling reaction was envisaged to be successful, due to the more polar intermediates generated throughout the reaction pathway. Acid **135** was activated with **T3P** and treated with PivONH<sub>2</sub>•HOTf, yielding **128c** with no impurities of similar polarities (Scheme 38).



**Scheme 38:** T3P mediated synthesis of *N*-(pivaloyloxy)amide **128c**.

## 2.2.4 Polycyclisations with alkene tethered *N*-(pivaloyloxy)amides

With optimised conditions in hand, *N*-(pivaloyloxy) amide **118a** was tested across a selection of ynamides (Scheme 39). As the oxazole formation reaction was performed in TFE, solubility of the more apolar ynamides at room temperature was poor, however this issue was overcome by heating the reaction to 50 °C. All reactions were monitored for consumption of the ynamide *via* TLC analysis, after which the solvent was exchanged for 1,4-dioxane. Conversion of the intermediate oxazole into the Diels-Alder product could also be monitored by TLC.



**Scheme 39: Substrate scope of cobalt-catalysed polycyclisation with amide **118a**.** <sup>a</sup>Oxazole formation performed at 50 °C due to solubility of ynamide in TFE. <sup>b</sup>72 h at 101 °C.

Thiophene derivative **120b** showed excellent conversion, indicating that *N*-methylmesyl sulfonamide was a suitable choice for use in the ynamide synthesis. When *p*-nosyl ynamide **44n** was tested, poor solubility of the ynamide was compounded by reduced Diels-Alder conversion, with approximately 33% of the corresponding oxazole remaining. Polycycle **120d**, containing a more sterically demanding sulfonamide, was isolated in a moderate yield. Broadening of the NMR spectra resonances indicated that the bulky sulfonamide substituents observed restricted rotation. Methyl ester derivative **120g** was also obtained in high yield as the electron withdrawing effect of the ester, in conjugation with the sulfonamide, did not hamper reactivity. Thioynamides proved to be the most efficient ynamides in the polycyclisation, with only trace amounts of oxazole remaining. Of note is that **120f** was obtained in 89% yield after hot recrystallisation of the crude reaction mixture when performed at a 2.00 mmol scale with no

need for further purification. The product of these reactions have imidothioate functionality, which have been used as cross coupling partners,<sup>84,85</sup> can undergo hydrolysis<sup>86,87</sup> and contain an inherent sulfide handle. The excellent yields attained show that although the products are sterically congested when employing sulfonamide **72f**, it is not detrimental to the efficiency of the process. A variable temperature <sup>1</sup>H-NMR study of **120f** revealed that reversible resolution of the peak broadening occurs between 343 – 353 K (Figure 15).

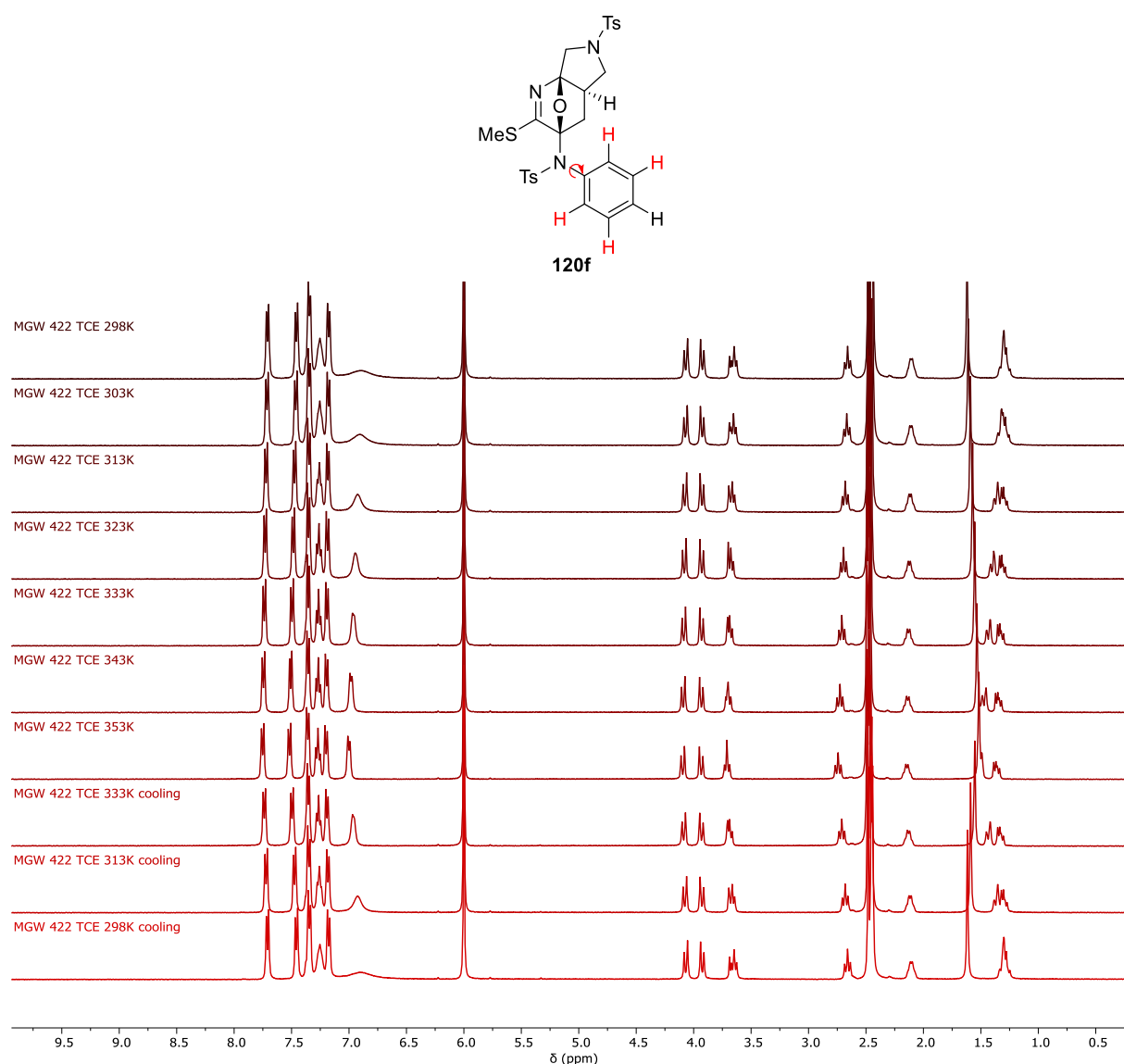


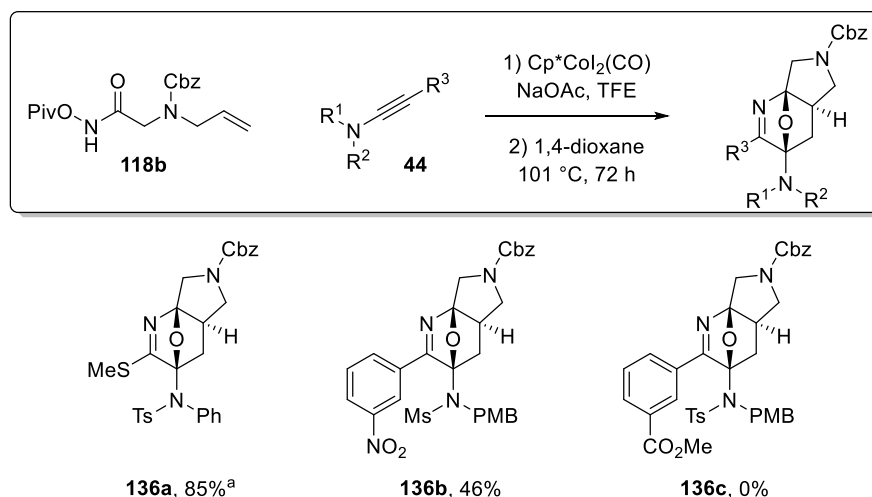
**Figure 15: Top: Structure of 120f showing restricted bond rotation and hydrogens affected. Bottom: Variable temperature <sup>1</sup>H-NMR study of 120f showing reversible resolution of line broadening due to restricted rotation at 70 °C.**



Alternatives to sulfonyl protecting groups were then accessed in the form of Boc and oxazolidinone derivatives **120h** and **120i**. Both were isolated in similar yields to sterically hindered **120d**, with **120i** showing a modest increase. Although ynamide **44o** was not fully consumed, complete conversion of the intermediate oxazole into **120i** was observed. The compatibility of carbamate protecting groups on the nitrogen increased the scope for post catalysis deprotections when considering further elaboration of the catalysis products.

Heterocycle **120j** was obtained in a low yield with remaining ynamide and oxazole present in the crude reaction mixture. A potential reason for the poor yield was the poor solubility of the ynamide in TFE, even at elevated temperatures. The increased steric impact of the 4-iodo substituent relative to an unsubstituted phenyl ring may also result in a reduced rate of Diels-Alder conversion. Ynamides **44p** and **44q**, containing PMB and benzyl groups, were cleanly converted to the respective oxazoles within 4 h at r.t., however minimal Diels-Alder cyclisation to **120k** and **120l** was observed even after 72 h at reflux.

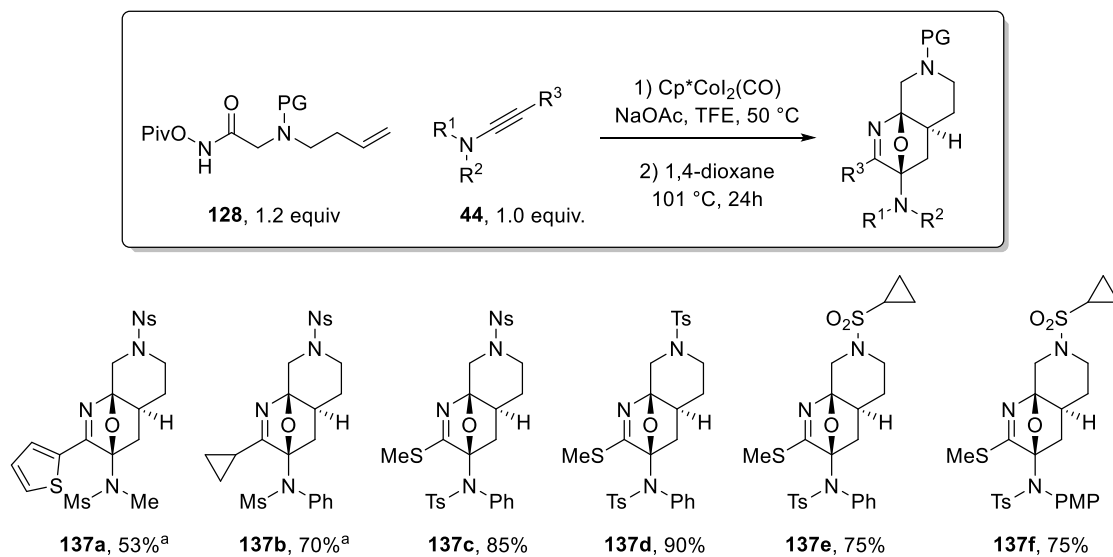
Cbz-protected amide **118b** was then reacted with a number of ynamides to assess the impact of carbamate protecting groups on the polycyclisation process (Scheme 40).



**Scheme 40: Synthesis of Cbz-protected hexahydropyrollopyridines.** <sup>a</sup> 24 h at 101 °C.

Pleasingly heterocycle **136a** was obtained in an excellent yield, with only a slight drop in conversion compared to tosyl derivative **120f**. Further attempts at using ynamides containing PMB functionality yielded **136b**, albeit in a moderate yield. When the polycyclisation was attempted with *meta*-methoxybenyl benzoate ynamide **44r**, **136c** was not observed. It appeared that employing ynamides containing a benzyl or PMB group, desirable for their potential cleavage under acidic or hydrogenative conditions, severely hindered conversion from the oxazole to the Diels-Alder adduct. Whilst not as sterically demanding as a phenyl group at the sulfonamide nitrogen, the increased flexibility introduced by the CH<sub>2</sub> linker may allow the aromatic ring to effectively block the alkene from approaching one face of the oxazole, therefore being more sterically demanding at the diene and hindering the Diels-Alder reaction.

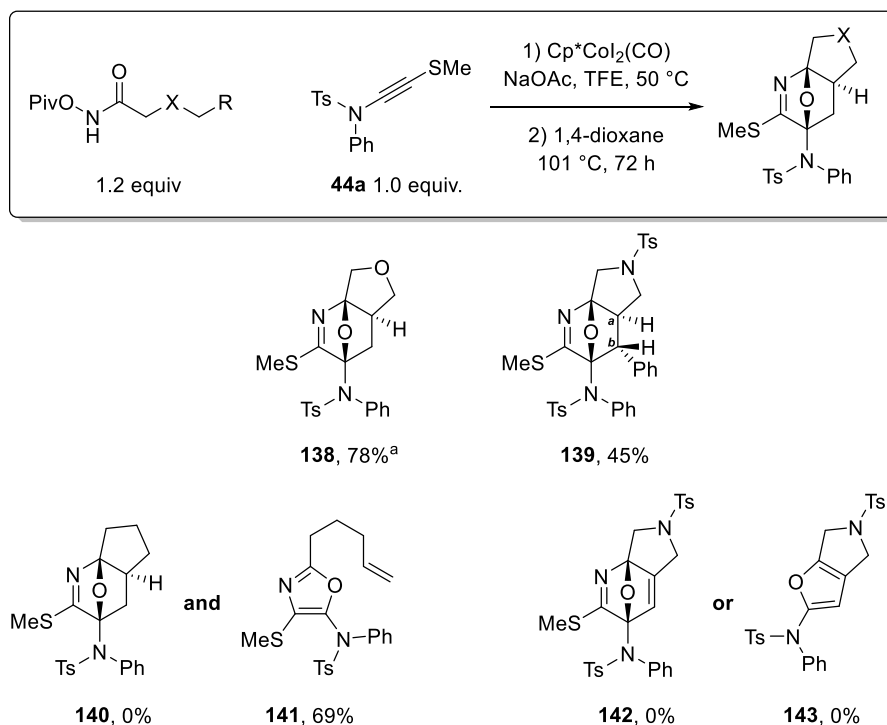
The capability to access octahydronaphthyridines was then investigated with sulfonyl protected *N*-(pivaloyloxy)amides **128a-c** (Scheme 41). The well documented cleavage of *p*-nosyl groups made this protecting group more desirable over the potentially more challenging tosyl group deprotections; cyclopropyl sulfonamides, on the other hand, offered a more attractive sulfonyl functionality for pharmacological properties without the need for removal.



**Scheme 41: Synthesis of 1,8 octahydronaphthyridines. <sup>a</sup>36 h at 101 °C.**

Suppression of Diels-Alder cyclisation to access thiophene derivative **137a** was observed relative to hexahydropyrrolopyridine **120b** (Scheme 39), requiring longer reaction times. This inhibition was not observed when thioamides **44a-b** were used, with excellent yields obtained for **137c-d**. A minor drop in efficiency was observed when isolating cyclopropylsulfonamides **137e-f**, with the intermediate oxazoles remaining in the crude reaction mixture. No effect was detected when an electron donating group was appended to the nitrogen at the C5 position in **137f**. It is hypothesised that the sulfonamide lies out of plane with respect to the oxazole which would severely hamper any electronic effects possible through conjugation.

Attempts to change the nature of the dienophile by changing the heteroatom linker, employing a substituted alkene and using a terminal alkyne were then performed to increase the molecular frameworks accessible through the methodology (Scheme 42). Longer reaction times were used in an attempt to isolate the desired polycycles.



**Scheme 42:** Results from modifying the nature of the alkene tether. <sup>a</sup> 24 h at 101 °C.

Replacing the heteroatom with oxygen yielded tetrahydrofuran derivative **138** in an excellent yield, although when the heteroatom was removed and aliphatic amide **131b** (Scheme 36) used, only oxazole **141** was isolated. This suggests a heteroatom, or another form of electronic influence, is required in the dienophile tether to promote subsequent Diels-Alder cyclisation. When propargyl tethered amide **130** (Scheme 36) was utilised, no conversion to **142** or the corresponding furan derivative **143** via a retro [4+2] Diels-Alder reaction was detected, with primarily degradation products observed after 72 h heating at reflux.

Cinnamyl derived amide **132** (Scheme 36) provided **139** in a modest yield as a single diastereomer. As the stereochemistry of the alkene is set as *trans*, this would result in an endo addition with respect to the oxygen bridge and Ph substituent. This was confirmed *via* the <sup>3</sup>*J* vicinal coupling constant of around 3.3 Hz between H<sub>a</sub> and H<sub>b</sub>: applying the Karplus equation,

the coupling constant is typical for a dihedral angle of 120 ° (Figure 16), evidencing an *anticlinal* relationship between the two protons.

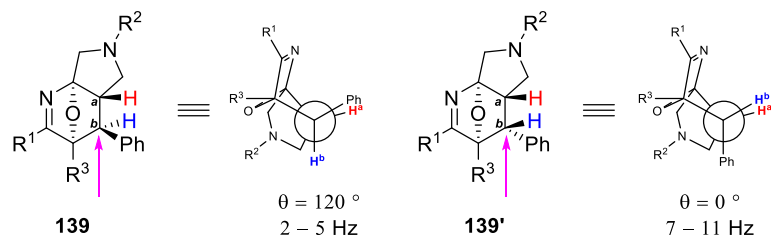
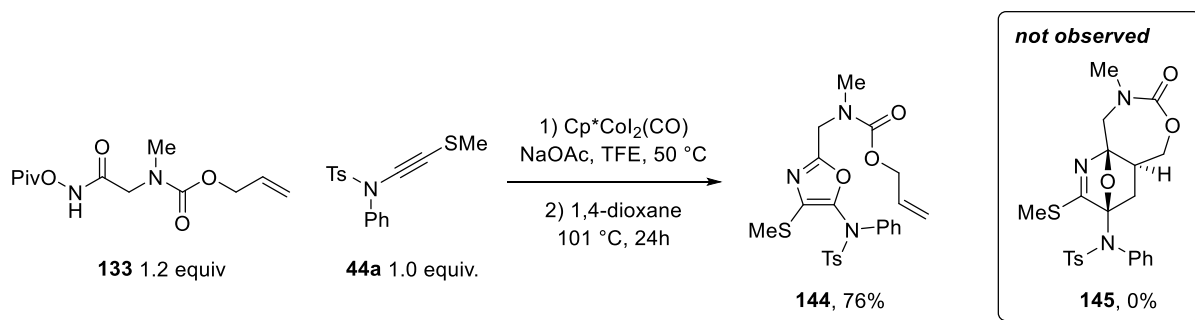


**Figure 16:** Newman projections used in stereochemical assignment of **139**. **139** is represented as its enantiomer due to modelling based on the crystal structure of **120a** (Figure 14).

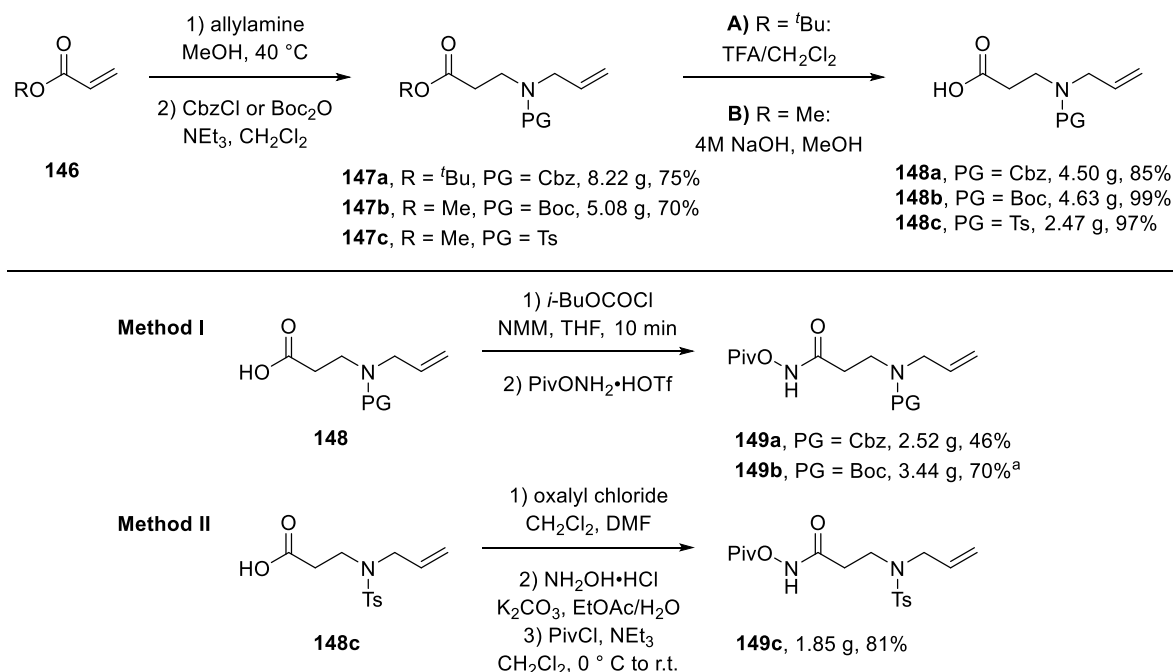
Alloc-glycine derivative **133** was then tested to determine whether larger ring systems could be accessed, whilst also containing a potential site for ring opening reactions that would provide densely functionalised piperidine scaffolds (Scheme 43). Unfortunately, when tested in the cascade process with thioynamide **44a** only oxazole **144** was isolated. As 4-thioxazoles proved the most reactive towards Diels-Alder cyclisation in our previous studies, no other ynamides were tested.



**Scheme 43:** Attempted synthesis of a 7,6-fused polycycle.

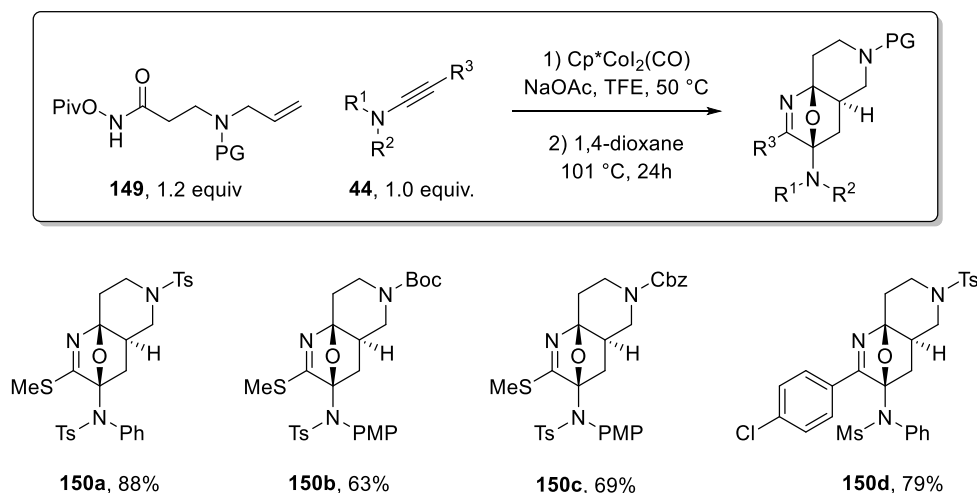
Following the successful use of  $\alpha$ -amino acid derived amides (Scheme 41), a general route to access  $\beta$ -amino acid analogues was desired. Adapting a literature produce,<sup>88</sup> acrylate derivatives were treated with allylamine and the crude material protected as the Cbz- and Boc- carbamates

in a two-step procedure (Scheme 44). The reactions were run at multigram scale, with acid or base catalysed ester hydrolysis delivering carboxylic acids **148**.



**Scheme 44:** Synthesis of  $\beta$ -amino acid derivatives. <sup>a</sup>Reaction heated to 50 °C upon addition of PivONH<sub>2</sub>·HOTf.

Access to *N*-(pivaloyloxy)amides **149a-c** was achieved *via* the acyl carbonate (method I) and acid chloride (method II) routes discussed beforehand. Unreacted acyl carbonate accounted for the reduced yield of **149a**, therefore the temperature was elevated to 50 °C in the case of **149b**, leading to an increased conversion and yield. **149a-c** were then tested in the polycyclisation process to assess their reactivity (Scheme 45).



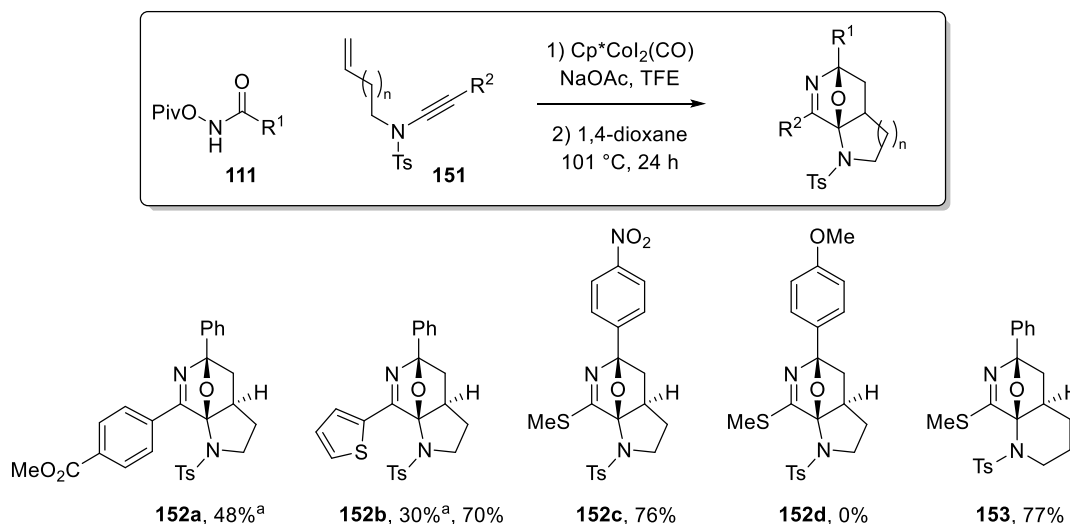
Scheme 45: Synthesis of 1,7 octahydronaphthyridines.

Pleasingly heterocycle **150a** was isolated in an excellent yield, comparable to  $\alpha$ -amino acid derivatives **120f** and **137d** (Scheme 39, Scheme 41). Carbamate amides proved less reactive with thioynamides when accessing **150b-c**, potentially due to the same reactive rotamer effect observed in the gold-catalysed process. Nevertheless, the ability to incorporate easily removable protecting groups was an important feature when considering the effectiveness of the polycyclisation process to install reactive sites for further elaboration. Finally, non-sulfur terminated ynamide delivered **150d** in an excellent yield.

### 2.2.5 Polycyclisations with 1,6- and 1,7-enynamides

A brief study introducing the dienophile tether onto the ynamide nitrogen was then performed. By attaching 3-buten- or 4-penten- alkene tethers to the ynamide nitrogen, it was believed that the corresponding oxazole would undergo the same [4+2] Diels-Alder cycloaddition reaction.

Pleasingly, when 3-buten- tethered ynamides **151a-b** were tested under unoptimized conditions with *N*-(pivaloyloxy)amide **111a**, aza-indole derivatives **152a** and **152b** were isolated in moderate yields with the remaining oxazole accounting for the mass balance (Scheme 46).



**Scheme 46:** Synthesis of sp<sup>3</sup>-rich azaindole and azaquinoline heterocycles. <sup>a</sup> Heated at reflux in PhMe for 24 h.

After optimisation of the reaction protocol with **120a** (Table 2, *Vida Supra*), thiophene heterocycle **152b** was obtained with an increased yield under the new protocol. Thioynamides again proved superior at accommodating Diels-Alder reactivity, with **152c** isolated in an excellent yield.

Intriguingly a strongly electron-withdrawing group in the C2 position of the oxazole did not hinder reactivity or promote any decomposition pathways. On the other hand, when PMP *N*-(pivaloyloxy)amide **111b** was tested, **152d** was not isolated. Conversion to the oxazole was complete within 2 h, however when heated to reflux consumption of the oxazole was immediately followed by degradation into a mixture of products. Strong electron-donors at R<sup>1</sup> are suitably positioned to break open the oxygen bridge, encouraging potential dehydration or hydrolysis, however the resulting products from these pathways were not isolable.

The reaction could also be used to access octahydroazaquinoline **153** in excellent yield from 4-penten-tethered ynamide **151d**. This reflected a significant addition to the methodology,



displaying the modular nature in which selection of an appropriate enynamide can deliver novel Murcko frameworks.

### **2.3 Summarising the gold- and cobalt- catalysed polycyclisation processes**

Building on the work of past Davies group members, an additional 30 examples have been prepared using the gold-catalysed cascade protocol that extends the full scope to 78 of the oxo-bridged polycycles.

Thio- and cyclopropyl- substituted ynamides were confirmed to show the highest conversion to the corresponding Diels-Alder products, providing the highest yields and cleanest reactions. Thioynamides proved proficient with more challenging substrates that previously showed limited reactivity, accessing an octahydropyranopyridine motif. A single example of sulfide extrusion also demonstrated access to a hydroxypyridine motif.

6,6-Polycycles accessed through the C5 cascade were shown to be as efficient as the 6,5-counterparts, with no competing enynamide cycloisomerisation. An improved synthesis of homopropargyl 1,7-enynes was developed, with increased atom economy and flexibility in choosing the nitrogen protecting group.

When investigating access to higher oxidation states at the C2 position with O'Bu and SMe functionalised ylides, abstraction of the sulfonamide was observed and the possible products were postulated to contain imide functionality through double hydrolysis. Control of this fragmentation *via* addition of an external nucleophile could be an interesting diversification route for future elaborations of this work.

Finally, the synthesis of a 12-membered oxazole tethered macrocycle containing a *trans*-alkene was demonstrated with an excellent yield. Subsequent Diels-Alder cycloaddition was observed but no pure products were obtained.

Simultaneously a novel cobalt-catalysed polycyclisation process has been developed, evolved from recent discoveries into cobalt-catalysed [3+2] cycloaddition reactions. Preliminary studies have focused on nitrogen linked dienophiles to access 27 novel polycycles that contain frameworks commonly found in nature. The ring size and nitrogen position can be controlled *via* judicious choice of the *N*-(pivaloyloxy)amide or ynamide building blocks.

A number of routes to access *N*-(pivaloyloxy)amides were developed to complement literature procedures, providing divergent access to a library of novel building blocks from carboxylic acid or ester derivatives.

A range of functionality was tolerated across the ynamides, with 4-thiooxazoles proving superior at promoting Diels-Alder cyclisation. Heteroaromatic, functionalised aromatic and alkyl substituents were tolerated at the *C*-terminus of ynamides, with sulfonamides and carbamates utilised as the protecting groups in the polycyclisation reaction. Benzyl derivatives at the ynamide nitrogen hindered the Diels-Alder pathway, with a single example undergoing cycloaddition. Alkyl and aryl substituents on the other hand did not hinder the desired reaction pathway. The scope of the transformation was extended with an oxygen tethered dienophile, although an all carbon linked alkene did not undergo the desired Diels-Alder cycloaddition. Preliminary results demonstrated the ability of 1,3- and 1,4- enynamides to undergo the desired polycyclisation.

In total, 13 unique Murcko frameworks have been accessed containing nitrogen, oxygen and all carbon alkene tethers *via* the developed tandem cycloaddition processes (Figure 17).

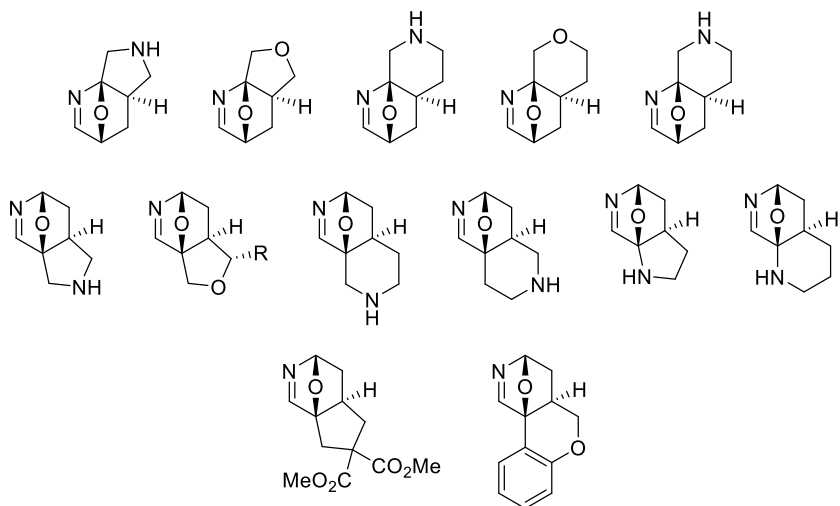


**Figure 17: Murcko frameworks accessible through novel polycyclisation reactions.**

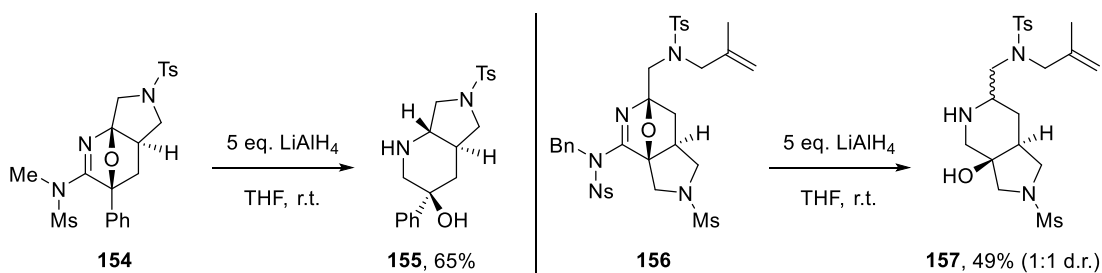
## Chapter 3: Post catalysis reactions: polycycles for potential library synthesis

With a diverse range of polycycles in hand, how the inherent functionality installed in the gold- and cobalt-catalysed transformations could be exploited to access complex alkaloid like structures was investigated. The majority of the transformations described in this chapter utilised polycycles accessed through the gold cascade process, with an initial venture into the cobalt polycycles discussed at the end of the chapter.

### 3.1 Reduction at the amidine to deliver fused piperidines

#### 3.1.1 Reduction to fused piperidin-3-ols

Previous results from the Davies group demonstrated the reactivity of the amidine functionality towards a three-step reduction procedure with  $\text{LiAlH}_4$  to access **155** and **157** (Scheme 47). Although reduction of sulfonyl amidine motifs exist in the literature,<sup>89,90</sup> there are few examples of cyclic variants<sup>91</sup> and to the best of our knowledge none containing a cyclic ether bridge.



Scheme 47:  $\text{LiAlH}_4$  reduction of polycycles performed by MPB and ADG.

With these preliminary results in hand, further exploration of the process was undertaken to examine its functional- and protecting- group compatibility, diastereoselectivity and the impact of changing the polycyclic framework (Figure 18). This transformation directly provides a

secondary amine and tertiary alcohol that are useful as reactive points of diversity. Moreover, the ability to tolerate desirable functionality and additional reactive sites, such as protected amines, aldehydes or alcohols, would increase the value of the products for use in potential library synthesis. Expansion of the scope to access various Murcko frameworks, with different ring sizes, heteroatoms and heteroatom positions, would significantly improve the scope of the transformation.

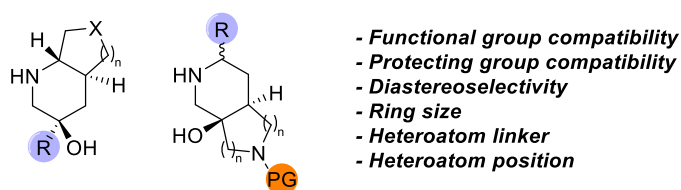
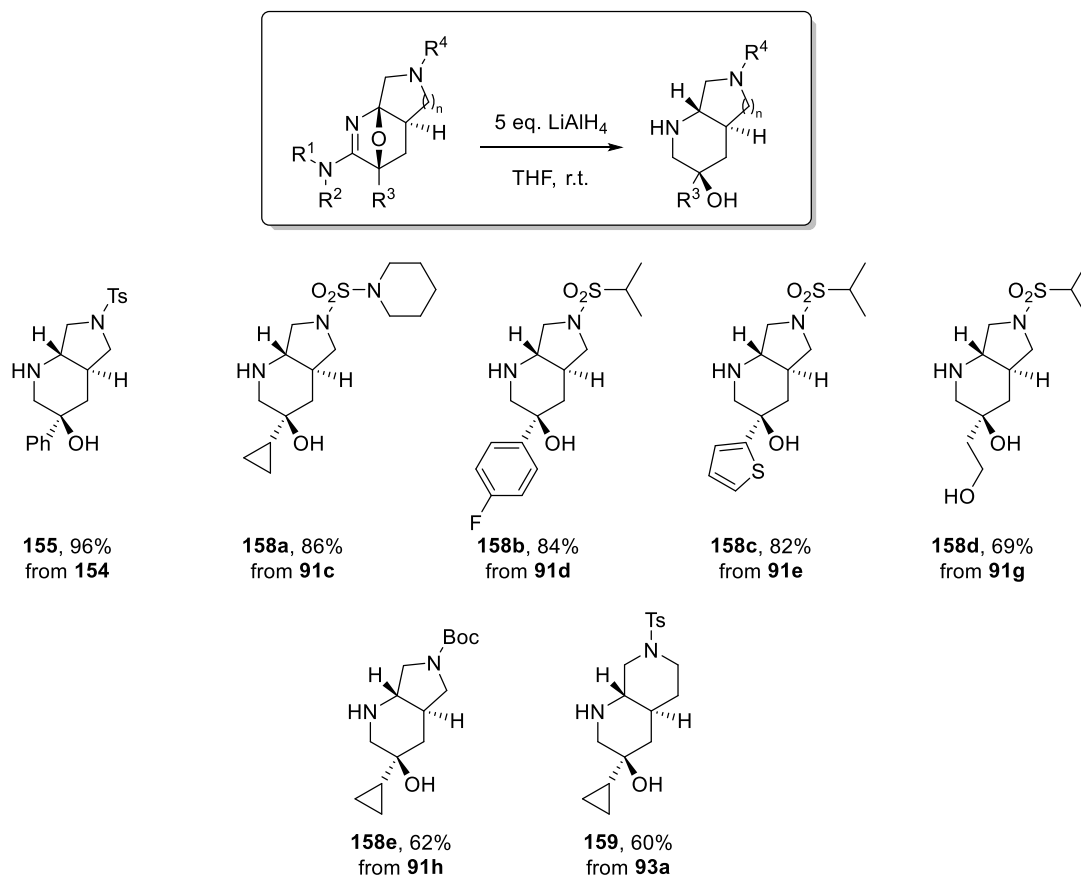


**Figure 18:** Targeted areas of exploration during the synthesis of polycyclic piperidin-ols.

An initial study looked to use the same substrate to try and achieve improved yields by refining the protocol used previously within our group when accessing **155** (Scheme 48). This was accomplished by modification of the aqueous work up procedure: extraction with a 3:1 mixture of  $\text{CHCl}_3/i\text{PrOH}$  in place of  $\text{CH}_2\text{Cl}_2$  resulted in superior mass recovery and subsequently an increased yield of 96% from 65%. The scope of this process was expanded to deliver a variety of 6,5- and 6,6- fused 1,3-aminoalcohols in good to excellent yields as single diastereomers, retaining the *trans*-fused ring junction in a diastereoselective process.



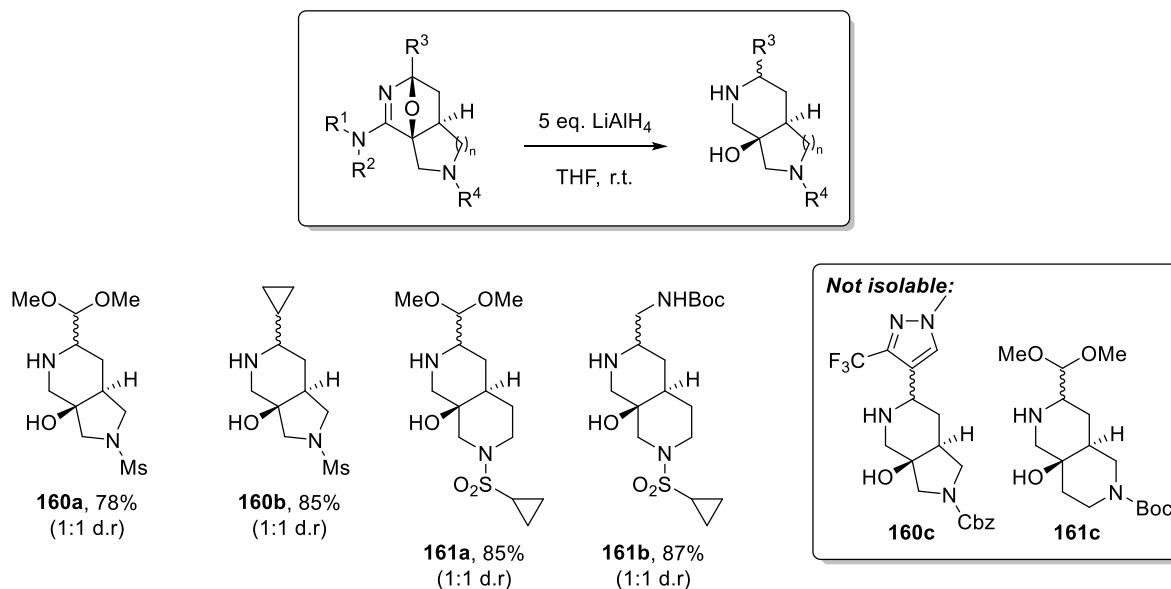
**Scheme 48: Diastereoselective LiAlH<sub>4</sub> reductions to access 1,3-aminoalcohols.**

Pleasingly, a variety of functionality was again tolerated at the bridgehead position, affording alkyl-, substituted aryl- and heteroaromatic- functionalised piperidine motifs **158a-c** in excellent yields. Diol **158d** was obtained from alkyl acetate derivative **91g** *via* ester reduction.

The reaction also worked well to deliver Boc-protected **158e**, despite the potential reactivity of carbamates towards reduction and the large excess of reductant, presenting another reactive site for further functionalisation once deprotected. Finally, **159** delivered a 6,6-bicyclic 1,3-amino alcohol in which the same stereochemical preference for a *trans* ring junction was observed.

The same conditions were applied to representative examples from the gold-catalysed C5 series (Scheme 49). The transformation again proved general for accessing fused piperidinols with

varying ring sizes. A range of functional groups were compatible at R<sup>3</sup>, including acid sensitive functionality such as acetals **160a** and **161a** and Boc-carbamate **161b**, offering opportunities to access aldehydes and primary amines for further manipulation.



**Scheme 49: Synthesis of diastereoisomeric polycyclic 1,3-aminoalcohols.**

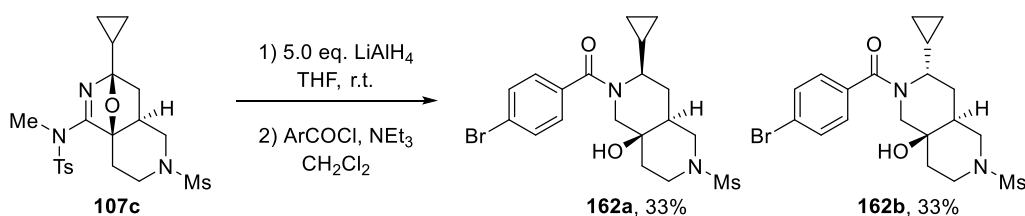
No diastereoselectivity was observed in the reductions, providing the amino alcohols as a 1:1 mixture of diastereomers in excellent yields. Whilst the diastereomers of dimethyl acetal derivatives **160a** and **161a** were separable by normal phase flash column chromatography, **160b** and **161b** were isolated as mixtures of diastereomers.

Frustratingly, consistent reactivity was not observed when carbamate protecting groups were used on the heteroatom linker within the polycyclic framework. Mass recovery of the crude material from the extraction protocol was generally poor in these cases, even when extracting with a 3:1 mixture of CHCl<sub>3</sub>/*i*PrOH. <sup>1</sup>H-NMR analysis of the crude reaction mixtures revealed partial or full reduction of the Boc protecting group. In the case of Cbz carbamate groups, the protecting group appeared to remain partially intact. This inconsistent stability of the carbamate

protecting groups towards  $\text{LiAlH}_4$  reduction was observed across multiple attempts, including when the reactions were performed at temperatures ranging from 0 °C (to limit reduction) and 66 °C (to encourage reduction).

The difficulty in separation of the diastereomers from the reduction protocol stemmed from the polarity of the amino alcohols, as the C5 products required more polar eluent systems to elute from normal phase silica gel. Non-aromatic protecting groups were chosen for their more desirable impact on predicted molecular properties when analysing this approach to ultimately prepare lead-like molecules. This resulted in compounds that were challenging to visualise at a level that allowed suitable distinction between diastereomers *via* TLC analysis. Visualisation was achieved by developing the TLC plates with  $\text{KMnO}_4$ , however minor coelution was observed in the NMR whilst appearing pure during TLC analysis. TLC development was also attempted with Dragendorff, vanillin, anisaldehyde, phosphomolybdic acid and ninhydrin.

As the secondary amine provided from this protocol was a point of diversity, an immediate reaction of the crude reaction material was envisaged to deliver a desirable derivative that would reduce the polarity of the molecule. To this end, **107c** was reduced and the crude material from the extraction was treated with an acid chloride to provide amides **162a** and **162b** in a combined 66% yield (Scheme 50).



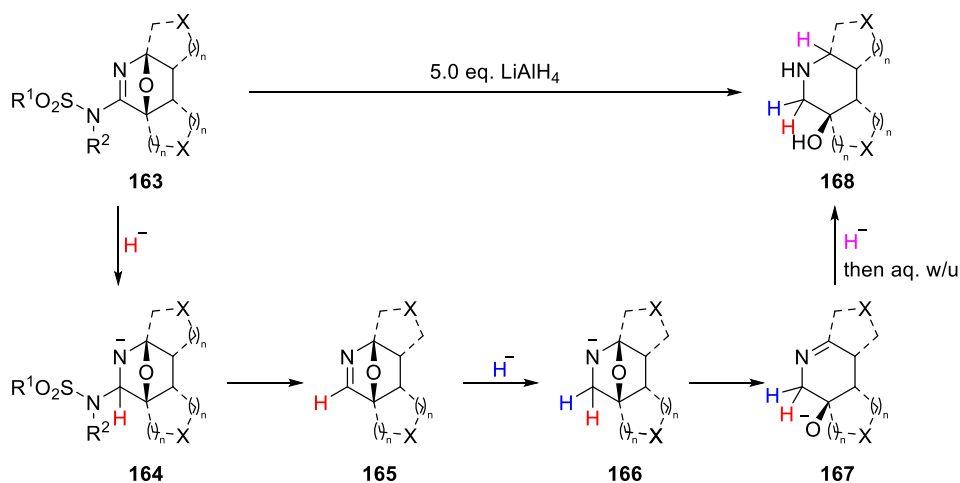
**Scheme 50: Formation of separable 1,3-amidoalcohols through reduction and subsequent amide formation.**



The reduced polarity of the reaction products allowed isolation of the distinct diastereomers, demonstrating that the challenging separation of the diastereomers can be overcome by purification at a later stage, with diversification possible using the crude reaction mixture.

### 3.1.2 Reduction selectivity model

The selectivity observed in these reactions was rationalised by the mechanism shown in Scheme 51, where an initial hydride addition is proposed to occur at the amidine of **163** to give **164**. This could then evolve by cleavage of the ether bridge, or elimination of the sulfonamide motif, to deliver imine **165**. Subsequent reduction of imine **165** then leaves charged hemiaminal **166**, which would cleave the cyclic ether bridge to give imine **167**, the key intermediate for the diastereoselectivity of this process. Hydride addition into **167** then controls the stereochemical outcome, *via* an S<sub>N</sub>1' type reaction, with aqueous work up completing the reaction pathway to deliver **168**.



Scheme 51: Plausible reaction pathway for multistep reduction.

Whether the sulfonamide is expelled before the cyclic ether bridge is cleaved is at this point unknown, however as no by-products containing partial reduction with the sulfonamide in place have been observed, it was postulated that sulfonamide elimination proceeds first. It was

hypothesised that for both the C5 and C2 Diels-Alder polycycles imine **167** is generated in a half chair conformation when the cyclic ether bridge is broken, and that is where the stereoselectivity is derived from.

For the C5 series, imine **169** is reduced with no facial selectivity to give **170** as a mixture of diastereomers (Figure 19). Although a systematic study on the effect of changing the R group has not yet been performed, in all examples assessed currently a 1:1 mixture of diastereomers was observed.

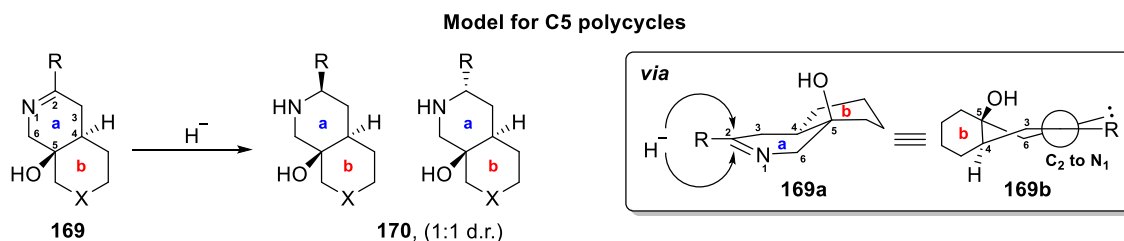


**Figure 19: Three-dimensional model for reduction of C5 polycycles. 154b looking down C<sub>2</sub>N<sub>1</sub> double bond.**

Structural minimisation<sup>j</sup> of imine **169** supported a half chair conformation of ring a, visualised best as **169a** with C<sub>2</sub>C<sub>3</sub>C<sub>6</sub> and N<sub>1</sub> in plane, whilst ring b adopts a twist boat conformation. Newman projection **169b** (C<sub>2</sub>→N<sub>1</sub>) enforces the lack of steric interactions available to bias the facial selectivity of the incoming hydride into the imine.

In contrast, hydride reduction of the C2 polycycle is completely diastereoselective. Through energy minimisation of the crucial half-chair conformation of imine **171** (Figure 20), it is hypothesised that this is due to the respective energies of the conformations obtained through the hydride addition where the ring junction incurs a significant impact on the energies of the respective reduction products and provides kinetic control.

<sup>j</sup> Minimization calculation performed with MM2 and MMFF94 in Chem3D v. 17.0.

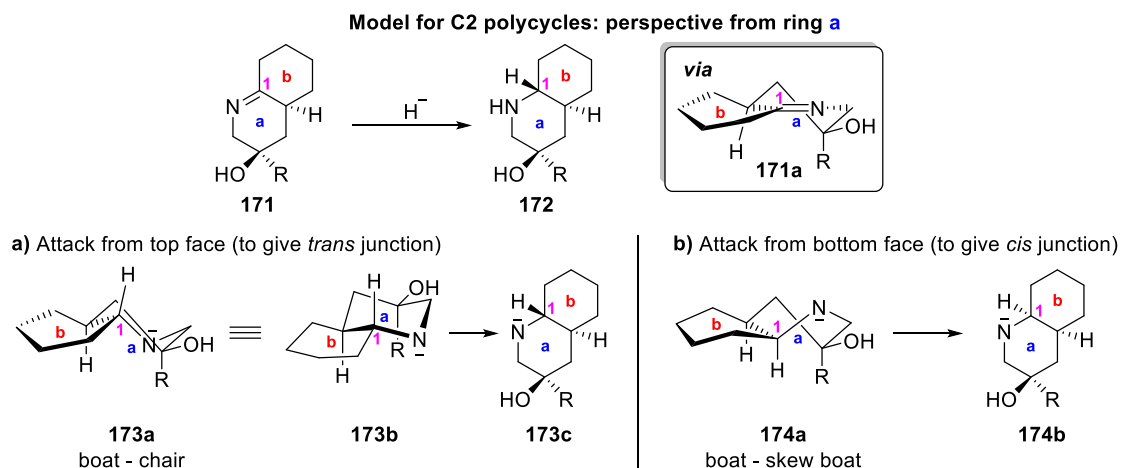
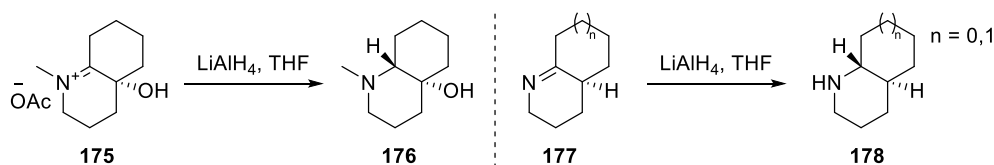


**Figure 20: Three-dimensional model for diastereoselective reduction of C2 polycycles.**

Imine **171** adopts half chair and twist-boat conformations for ring a and b respectively, represented by **171a**. Hydride addition to the top face results in boat-chair conformation **173a** as C<sub>1</sub> shifts to accommodate a tetrahedral geometry (Figure 20a). In contrast, hydride addition to the bottom face results in energetically unfavourable boat-skew boat conformation **174a** (Figure 20b). As no evidence of a *cis* ring junction was detected across the scope of these studies, the energy differences between conformations **173a** and **174a** appears to provide complete stereocontrol.

Related examples in the literature corroborate our observations, accessing *trans* ring junctions when reducing bicyclic imines **175**<sup>92</sup> and **177**<sup>93</sup> to the corresponding saturated amines (Scheme 52).

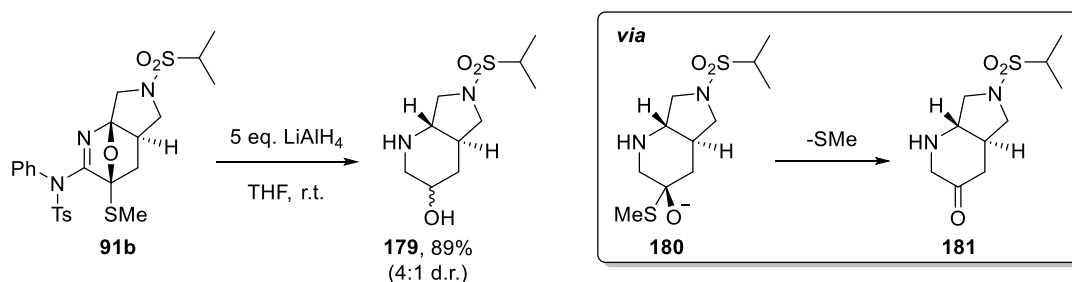


**Scheme 52: Thomas's and Lawesson's studies on imine reductions to *trans* fused bicycles.**

Lawesson<sup>93</sup> used the principle of torsion angle notation, developed by Toromanoff in 1980,<sup>94</sup> to determine that the least torsional distortion upon hydride reduction of **177** results in the *trans* selectivity, aligning with conclusions made in our conformational analysis.

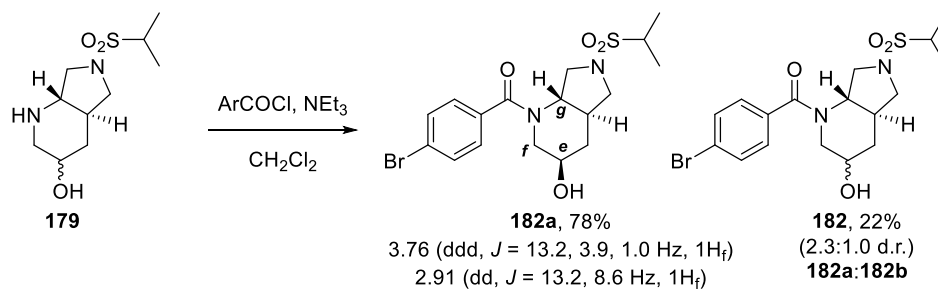
### 3.1.3 Thioketal reductions

When thioketal polycycle **91b** was subjected to the same reduction conditions, a diastereomeric mixture of amino alcohol **179** was isolated (Scheme 53). *In situ* expulsion of the methylsulfide group gave rise to aminoketone **181**, which was subsequently reduced by the excess LiAlH<sub>4</sub>. The process showed some stereoselectivity, with an approximate 4:1 ratio of diastereomers isolated.



Scheme 53: Initial reduction attempts upon thioketal **91b**.

Attempts to isolate the major diastereomer proved challenging by flash column chromatography or recrystallization of the diastereomeric mixture. Aminoalcohol **179** was therefore treated with 4-bromobenzoyl chloride to give diastereomeric amides **182**, from which major diastereomer **182a** was isolable *via* flash column chromatography, alongside a mixed fraction of **182a-b** (Scheme 54).

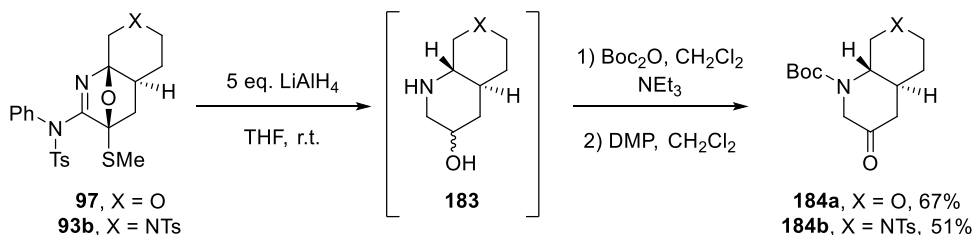


**Scheme 54: Determination of stereochemistry through amide protection and purification.**

Analysing the  $^1\text{H}$ -NMR of the major product from this reaction revealed **182a** to be the major product, with the alcohol *syn* to  $\text{H}_g$ . This conclusion was made due to the coupling constants: the two  $\text{H}_f$  protons observed values typical of  $\theta = 60^\circ$  and  $\theta = 180^\circ$  (3.9 and 8.6 Hz), consistent with **182a**; whereas **182b** would contain two  $J$  values of similar magnitude in the range of 2 – 5 Hz from dihedral angles of  $\theta = 60^\circ$ .

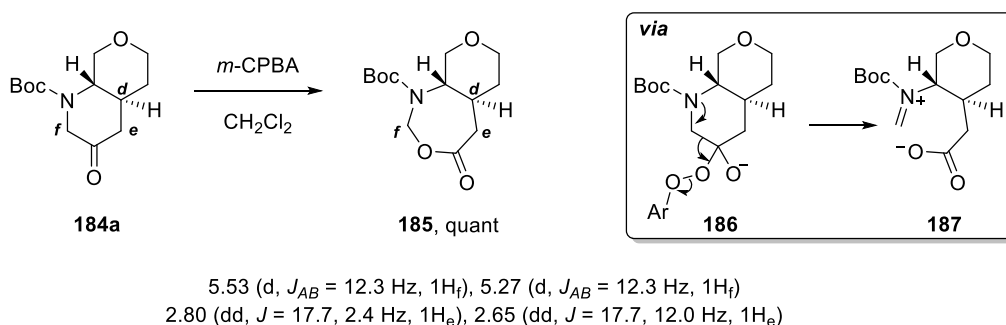
The facial selectivity of hydride reductions of cyclic ketones is well-established,<sup>95</sup> where the use of a bulky nucleophile can reverse the axial face selectivity observed with smaller nucleophiles. Attempts at inverting the stereoselectivity of the process by utilising a range of reducing agents proved unsuccessful: DIBAL-H and SuperHydride<sup>®</sup> proved unreactive towards reducing the amidine motif, with recovery of starting material. Red-Al facilitated the reduction pathway, however proved less selective than  $\text{LiAlH}_4$ , providing an approximate 1:2 ratio without reversing the diastereoselectivity.

A different approach that removed the need for separation of the diastereomers was then sought after, with modified reactivity for future elaboration. To this end, Boc protected 1,3-amino ketone derivatives **184** were prepared in a three-step procedure (Scheme 55). Attempts to perform the oxidation without the protection of the secondary amine provided intractable reaction mixtures.



Scheme 55: Formation of 1,3-amino ketone derivatives.

This process could be completed with a single purification after all three steps and offers stereoselective access to a range of fused bicyclic scaffolds. Most importantly, **184a-b** contain up to 3 sites for further diversification *via* the amine, alcohol, and ketone functionality. To test their reactivity towards elaboration, ketone **184a** was subjected to Baeyer-Villiger oxidation conditions to access ester **185** as a single regioisomer in excellent yield, providing access to yet another framework with unique connectivity and reactivity (Scheme 56).



Scheme 56: Baeyer-Villiger oxidation reaction for ring expansion.

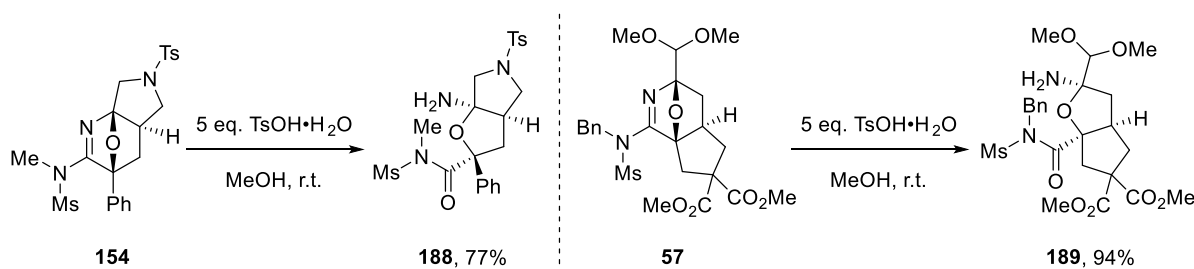
The regioselectivity of the process was determined when analysing the  $^1\text{H}$ -NMR spectrum of **185** as protons  $H_e$  contained  $J_{AB}$  splitting of 17.0 Hz, consisted with neighbouring a carbonyl functional group, and coupled to  $H_d$  in the COSY experiment. Additionally, the  $H_f$  proton resonances were shifted downfield from 4.42 and 3.49 ppm in **184a** to 5.53 and 5.27 ppm in **185**, indicative of the two flanking heteroatoms, whilst the  $H_e$  protons underwent a less significant downfield shift from 2.40 and 2.21 ppm in **184a** to 2.80 and 2.65 ppm in **185**. Literature precedent would indicate the regioselective bias of the oxidation comes from an

electronic influence from the nitrogen that can undergo ring opening to form **187** during the rearrangement process.<sup>96</sup>

## 3.2 Activation with Brønsted and Lewis acids

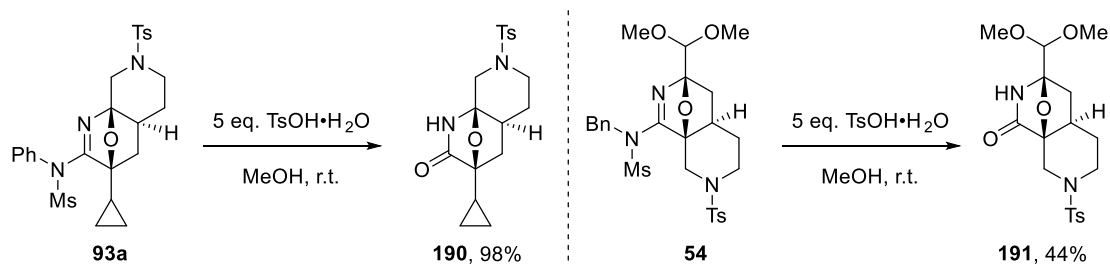
### 3.2.1 TsOH mediated hydrolysis

Another scaffold elaboration process utilising the amidine motif was discovered when treating the polycycles obtained under the gold-catalysed cascade procedure with TsOH (Scheme 57). This transformation was a simple hydrolysis reaction under acidic conditions yet furnished densely functionalised tetrahydrofuran motifs with a primary, albeit sterically hindered, amine and *cis* ring junctions. Remarkably the dimethyl acetal in **189** survived under hydrolysis conditions and remained stable in the product alongside the hemiaminal.



Scheme 57: Synthesis of heavily functionalised tetrahydrofurans by ADG and MPB.

Looking to expand the scope of this transformation and investigate the potential reduction of the sulfonyl amide motif, 6,6-polycycles **93a** and **54** were treated under the same acidic conditions with THF as a co-solvent due to poor solubility in MeOH (Scheme 58). To our surprise, lactams **190** and **191** were isolated *via* expulsion of the sulfonamide. Once again, the dimethyl acetal functionality survived the acidic conditions, and the cyclic ether bridge remained unaffected.



**Scheme 58: Synthesis of 6,6-polycyclic lactams via TsOH mediated hydrolysis.**

This change in reactivity must occur from the same reaction pathway, with initial acid catalysed attack of water onto the amidine to give **192** and **193** (Figure 21). From this point, either the protonated amine acts as the leaving group in the formation of THF **188**, or the protonated sulfonamide is expunged to give lactam **190**.

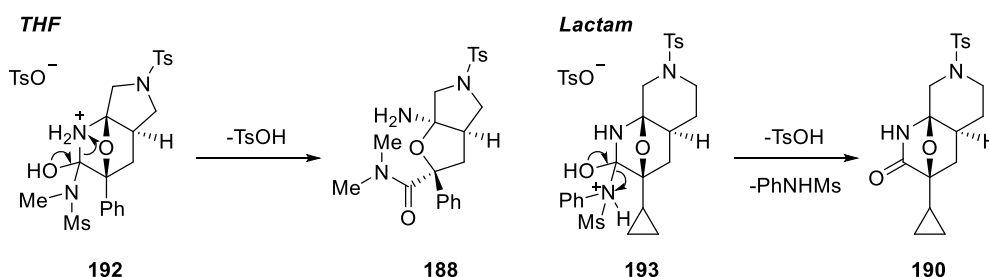
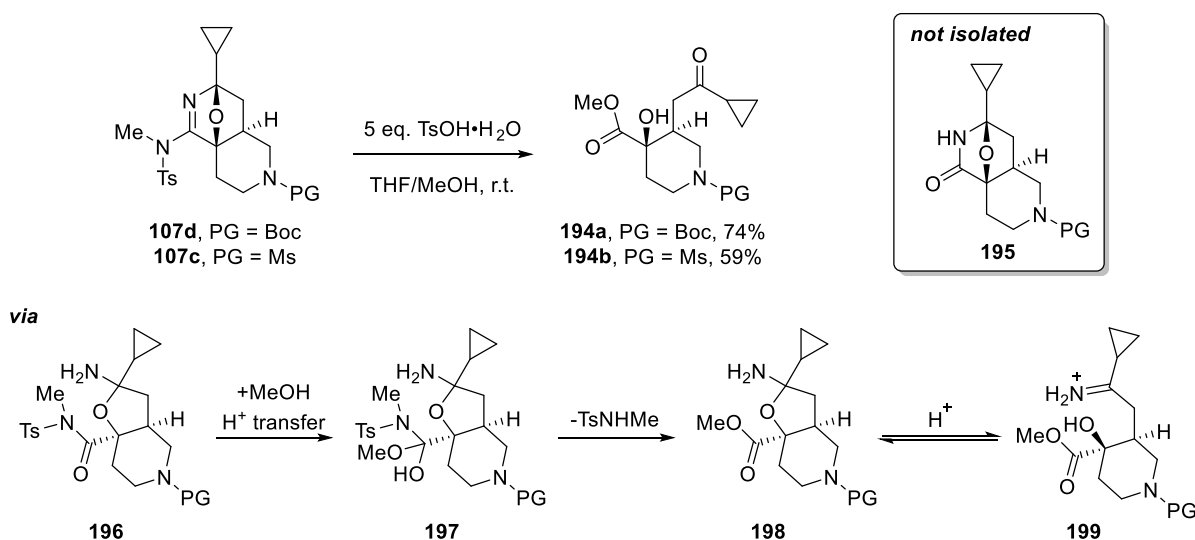


**Figure 21: Reaction pathways for THF and Lactam synthesis.**

Precedent within the literature suggests that sulfonyl amidine hydrolysis is often observed alongside expulsion of the amino functionality.<sup>90,97</sup> Further literature examples have demonstrated the ability of sulfonyl amidines to undergo substitution with various nucleophiles under basic conditions with the expulsion of the sulfonamide.<sup>98–100</sup> Rationalisations for the divergent pathways could include the leaving group ability of the sulfonamide and the differing ring strain of the 6,5- and 6,6- fused ring systems. As the same sulfonamide was employed in **57** and **54** (Scheme 57, Scheme 58), the dominating factor was presumed to be the ring strain in the different systems.



Cyclopropyl derivatives **107** were then tested under the same reaction conditions to test whether the reduced yield of **191** was due to the potentially acid sensitive dimethylacetal functionality (Scheme 59). When Boc protected polycycle **107d** was tested and consumed, only a small amount of desired lactam **195** was isolated as an impure mixture alongside near quantitative recovery of the sulfonamide. When repeated, visualisation of a TLC of the crude material with anisaldehyde revealed another product that was not observed previously. After isolating the by-product,  $^1\text{H}$ -NMR analysis revealed that the material was distinct from lactam **195** and that the sulfonamide group had been cleaved. To avoid the line broadening in the  $^1\text{H}$ -NMR caused by the Boc-carbamate, Ms-protected variant **107c** was subjected to identical conditions and **194b** was isolated as the major product. This allowed identification of **194a**, with the IR peaks of the ester and alcohol shifted through intramolecular hydrogen bonding. The structure was also confirmed by single crystal XRD analysis of **194b**.



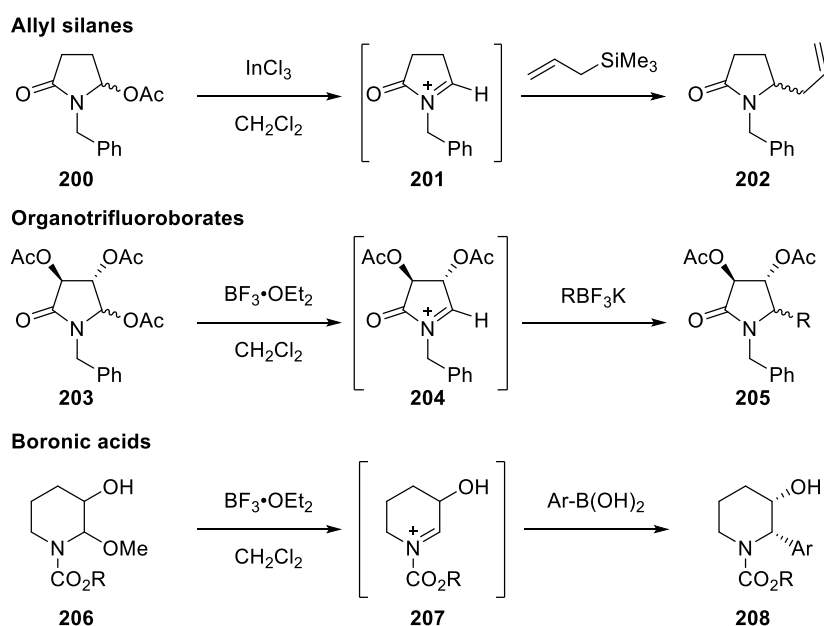
**Scheme 59:** Unexpected ring opening reaction to access functionalised piperidines.

The process was proposed to proceed *via* THF-intermediate **196**, where the sulfonyl amide generated *in-situ* is hydrolysed with MeOH to ester **197**. Subsequent ring opening of the THF

and hydrolysis of iminium **199** upon aqueous work-up afforded piperidine **194** in a stereospecific manner. With more time to study this reaction, an optimisation to selectively produce the three scaffolds accessed *via* this hydrolysis strategy would be a priority.

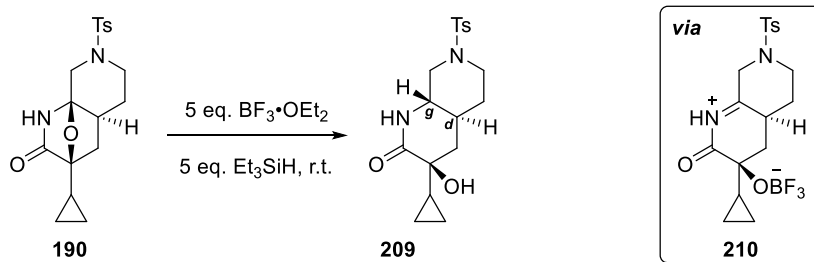
### 3.2.2 Acyl iminium activation

Lactams **190** and **191** were especially exciting outcomes as the functional groups installed in these compounds are precursors to acyliminium formation upon treatment with a Lewis acid. Acyliminium reactivity has been utilised in a wide range of inter- and intramolecular reactions to develop a diverse range of scaffolds,<sup>101–103</sup> with an array of addition reactions developed including allyl silanes,<sup>104</sup> organotrifluoroborates<sup>105</sup> and boronic acids (Scheme 60).<sup>106</sup>



**Scheme 60:** Selected examples of nucleophilic addition to acyliminium species.

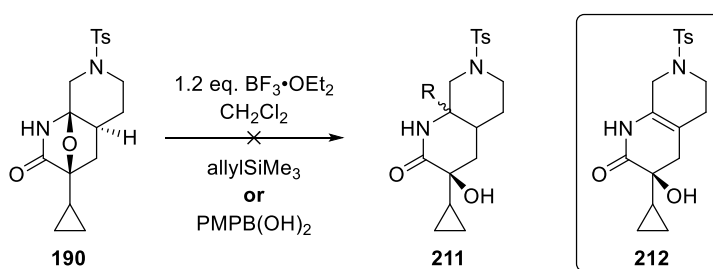
A reductive process was first studied to assess whether acyliminium **210** could be generated upon treatment with a suitable Lewis acid. To this end, lactam **190** was treated with triethylsilane in the presence of  $\text{BF}_3 \cdot \text{OEt}_2$  (Scheme 61). Pleasingly a single diastereomer of **209** was isolated in excellent yield.



**Scheme 61: Reduction of lactam through acyliminium activation.**

The ring junction was again identified as *trans* through analysis of the  $^1\text{H}$ -NMR spectrum: the vicinal  $\text{H}_g$ - $\text{H}_d$  coupling constant was measured at 10.0 Hz, which is consistent with a dihedral angle of  $180^\circ$ . Acyliminium **210** was predicted to favour an analogous conformation to imine **171** (Figure 20), generated in the  $\text{LiAlH}_4$  reduction process, and the same conformational analysis used to explain the *trans*-stereoselectivity.

The addition of alternative nucleophiles was then tested. Lactam **190** was treated independently with allylsilane and paramethoxyphenyl boronic acid in the presence of  $\text{BF}_3 \cdot \text{OEt}_2$  (Scheme 62). TLC analysis revealed starting material consumption after 3 h in both cases, however analysis of the  $^1\text{H}$ -NMR of the crude reaction mixtures revealed that no incorporation of either nucleophile had occurred.

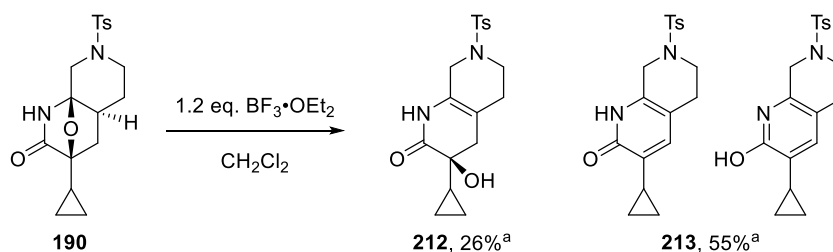


**Scheme 62: Attempted allylation and arylation of lactam 190.**

Isolation of a pure compound proved challenging due to the instability of the main product from this reaction, although a speculative assignment of the product was made as enamide **212**. This was achieved through single crystal XRD analysis from a crystal of **212** obtained through slow

crystallisation of an impure sample of **212** in an NMR tube. When steric hindrance prevents intermolecular reaction, loss of a proton from acyliminium **210** to form **212** is possible, with literature precedent for the formation of enamides *via* this pathway.<sup>107</sup>

In an attempt to isolate **212** the reaction was repeated under rigorously dry conditions in the presence of only  $\text{BF}_3 \cdot \text{OEt}_2$  (Scheme 63). In this case, a second major product was formed and identified as hydroxypyridine and pyridinone tautomers **213**. In the absence of an additive and water, it appeared the dehydration process was favoured.



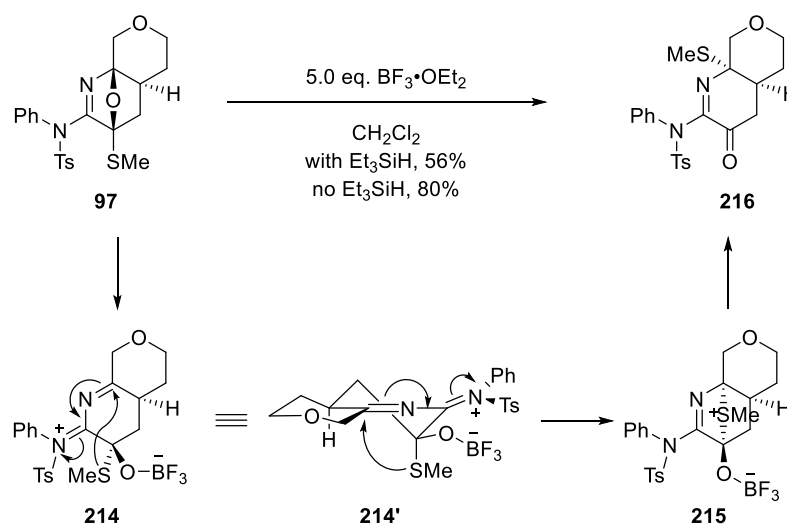
**Scheme 63:** Enamide and dehydration products from lactam **190**. <sup>a</sup>Yields given are approximates as pure material could not be isolated.

These examples, although proving complex, demonstrate the rich potential of the lactams towards elaboration *via* Lewis acid activation. Reduction to **209** and formation of enamide **212** evidenced that an acyl iminium intermediate is likely generated upon activation with  $\text{BF}_3 \cdot \text{OEt}_2$ . The potential for nucleophilic addition at the ring junction adds an excellent point of diversity, and if **212** can be isolated then Pt-catalysed hydrogenation may provide access to *cis* fused ring junctions. Hydroxypyridines and pyridinones are also valuable synthetic targets in medicinal chemistry.

### 3.2.3 Rearrangement reactions

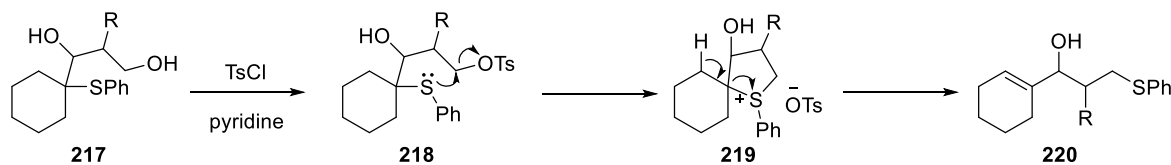
Another question posed was whether the amidine motif could activate the cyclic ether bridge through an analogous process, where the sulfonamide of the amidine provides conjugative

assistance. An initial attempt to react polycycle **97** with  $\text{BF}_3 \cdot \text{OEt}_2$  in the presence of triethylsilane produced an instant colour change to yellow and consumption of the starting material within 4 h (Scheme 64). The isolated product was identified as rearrangement product **216**, with migration of the sulfide group and formation of an iminone containing a *cis* ring junction. After conjugative assistance from the amidine to break the cyclic ether bridge and provide **214**, the sulfur can attack the electrophilic site and form sulfonium intermediate **215** in a stereospecific manner. Once migration product **216** was identified, the reaction was repeated without triethylsilane and the efficacy improved to an excellent 80% yield.



Scheme 64: Unexpected 1,4-rearrangement of polycycle **97** through treatment with  $\text{BF}_3 \cdot \text{OEt}_2$ .

This type of 1,4-sulfide migration had literature precedent: phenylthio- substituted diols **217** have been shown to undergo rearrangements under acidic conditions *via* formation of sulfonium intermediate **219** (Scheme 65).<sup>108,109</sup>



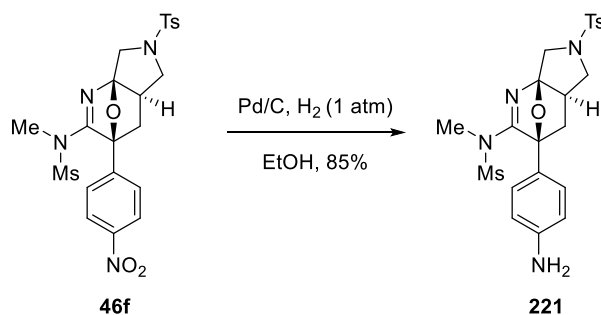
Scheme 65: Warren's intramolecular 1,4-sulfide migration.

This result revealed that the polycycles may be amenable to functionalisation strategies by nucleophilic attack from suitable nucleophiles in the presence of a Lewis acid catalyst and the absence of a migratory group. The potential to access *cis* ring junctions also increases the chemical space accessible through this methodology, as the three-dimensional shape of these polycycles will differ significantly to the *trans* equivalent.

### 3.3 Functional group manipulation

The flexible functional group compatibility afforded through both the gold- and cobalt-catalysed processes also allowed installation of a variety of different reactive functional groups for manipulation post polycyclisation.

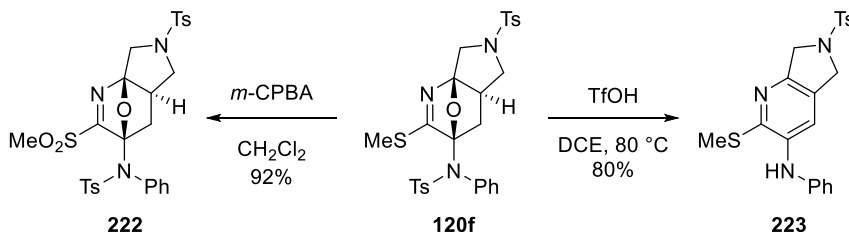
Hydrogenation of *para*-nitrobenzene derivative **46f** with Pd/C gave access to aniline derivative **221** (Scheme 66). Pleasingly the product remained stable towards silica gel chromatography, even with electron-rich aniline functionality, and no dehydration through to the pyridine was observed.



Scheme 66: Hydrogenation of nitrobenzene derivative **46f**.

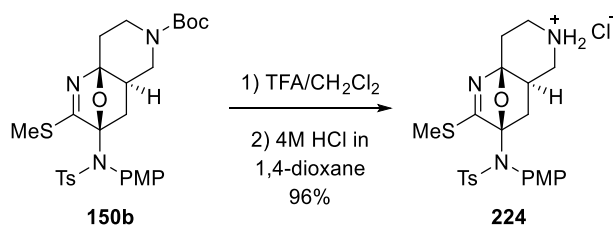
Modification of polycycles obtained under the cobalt protocol was then performed (Scheme 67). Oxidation of sulfide **120f** with *m*-CPBA cleanly afforded sulfone **222**, providing an electron deficient imine that offers opportunity for nucleophilic substitution. A chemoselective

TfOH mediated tosyl deprotection, followed by dehydration and aromatisation, afforded tetrahydropyrrolopyridine **223** in an excellent yield.<sup>110</sup>



**Scheme 67: Sulfide oxidation and tosyl deprotection of 120f.**

Boc deprotection could be achieved by treating **150b** with TFA without promoting dehydration, demonstrating the relative stability of the bridged ether (Scheme 68). As the free amine rapidly discoloured in air (from colourless to orange), HCl salt **224** was prepared from a solution of HCl in 1,4-dioxane.



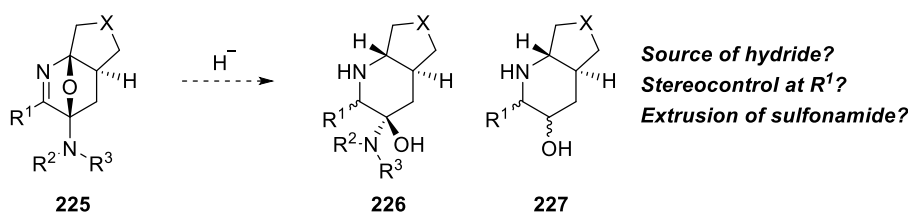
**Scheme 68: Boc deprotection to access secondary amine reactive sites.**

### 3.4 Initial attempts at framework elaboration of polycycles accessed through cobalt catalysis

Several early experiments to utilise the imine and protected hemiaminal functionalities installed in the cobalt-catalysed polycyclisation process were also attempted as avenues for post catalysis transformations.

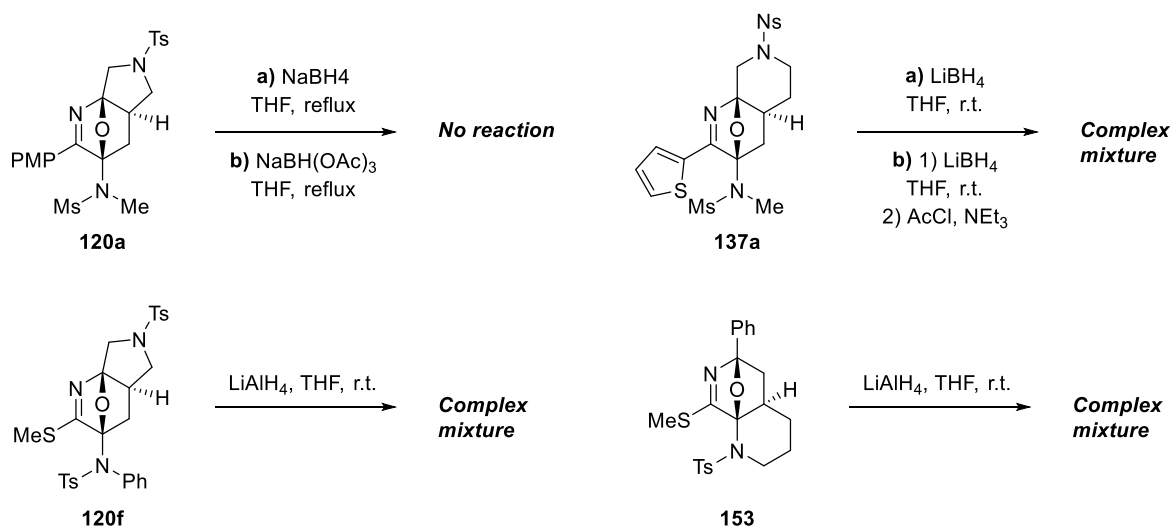
With the knowledge gained from  $\text{LiAlH}_4$  reductions of the polycycles accessed under the gold-catalysed method (Chapter 3.1), it was hypothesised that a similar transformation could deliver

a range of 1,3-aminoalcohols. As the amidine has been replaced with an imine there were three major components to be addressed: an additional point of stereoselectivity would have to be considered; whether or not the sulfonamide would be extruded *via* formation of the ketone; and the optimal choice of reducing agent (Scheme 69).



**Scheme 69:** Initial considerations for reduction process of polycycles accessed from cobalt-catalysed polycyclisation.

A selection of reducing agents of varying strengths were screened with a range of polycycles to assess the reactivity of the scaffolds towards reduction (Scheme 70). As the non-sulfur substituted polycycles contained imine functionality, NaBH(OAc)<sub>3</sub> and NaBH<sub>4</sub> were tested initially.



**Scheme 70:** Summary of reduction conditions tested.

When **120a** was treated with either of the sodium-based hydride reagents, no reaction occurred with complete recovery of the starting material following aqueous work up. Despite the reduced



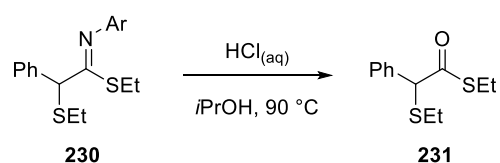
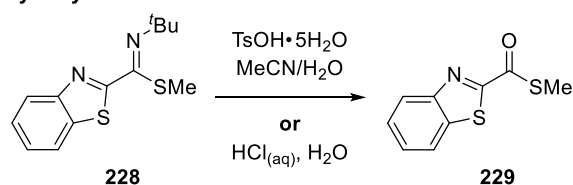
electrophilicity of the imine, afforded by the electron donating ability of the PMP group, the lack of reactivity was surprising. Polycycle **120a** had been selected due to the presence of a less sterically demanding sulfonamide moiety. With this in mind, polycycle **137a** was selected as a more suitable candidate and the reducing agent exchanged for LiBH<sub>4</sub> (Scheme 70). In this case, complete consumption of **137a** was observed and two major products were visible *via* TLC analysis. Upon purification by flash column chromatography a complex mixture was observed. Acetylation of the crude reaction mixture when repeated did not allow for isolation of pure material, nevertheless revealed that the sulfonamide remained intact. It was postulated that the remaining alcohol could be the cause of degradation between aqueous work-up and purification through potential dehydration pathways.

With the knowledge that both sulfonamide and sulfide expulsion occurred in the LiAlH<sub>4</sub> reduction of thioketal derivatives (Chapter 3.1.3), **120f** was selected as loss of the sulfide would remove a diastereoselectivity issue. Under the same reduction conditions used previously (Scheme 53), **120f** was consumed and purification led to a mixture of products that could not be separated. Intriguingly the sulfonamide was again present in the products, with only minor evidence of TsNHPPh extrusion observed in the crude reaction mixture. Due to the complexity of the crude material, analysis of the <sup>1</sup>H-NMR of the mixture made true quantification of the amount of sulfonamide unfeasible. A final attempt was performed on C5 polycycle **153**, however a poor mass recovery compounded with the complexity of the <sup>1</sup>H-NMR of the crude material meant no significant result was obtained.

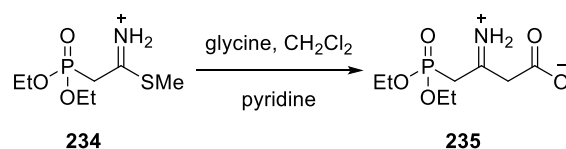
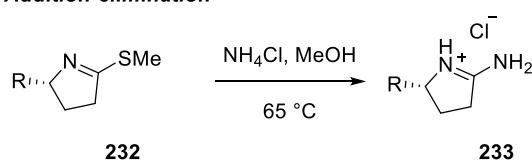
Attention was then turned to exploiting the thioimide functionality installed through the use of thioynamides. Literature precedent for the reactivity of thioimides included: hydrolysis reactions to access thioester **229** and **231**,<sup>111,112</sup> substitution reactions with ammonium

chloride<sup>113</sup> and glycine<sup>114</sup> to prepare amidine **233** and amino acid **235**, and cross coupling reactions to deliver **237** (Scheme 71).<sup>115</sup> Thioimide *N*-oxides have also been shown to undergo Stille and Suzuki-type cross-coupling reactions in the synthesis of **239** and **240**.<sup>116</sup> These examples demonstrate the diversity of potential reactivity accessible through the thioimide motif installed in the synthesised polycycles.

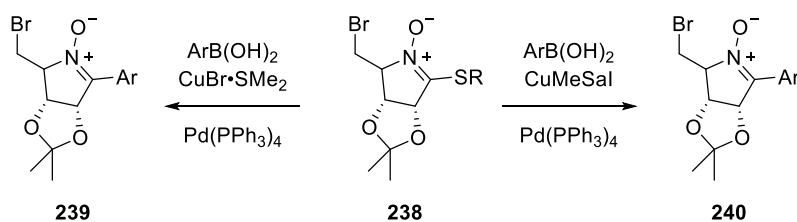
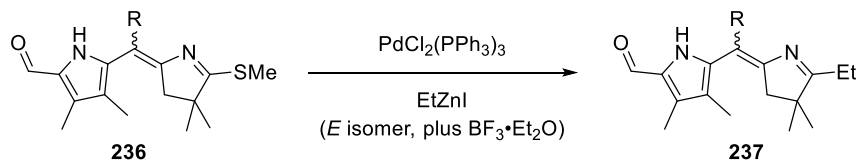
#### Hydrolysis



#### Addition-elimination

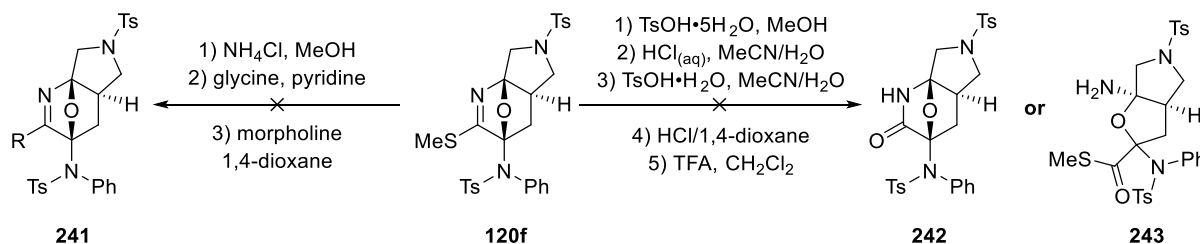


#### Cross coupling



Scheme 71: Literature precedent for reactions with thioimides.

In an attempt to exploit the thioimide motif's susceptibility to nucleophilic attack, **120f** was treated with a range of nitrogen based nucleophiles and a variety of hydrolysis conditions (Scheme 72).



**Scheme 72: Attempts to exploit the thioimide reactivity to perform nucleophilic substitution and hydrolysis.**

Surprisingly no reactivity was observed under any of the conditions attempted, as starting material was recovered in every case. Minor evidence of sulfonamide loss was observed *via* TLC analysis, due to its highly UV active nature, however in all cases over 90% of **120f** was recovered. In retrospect, the restricted rotation observed in the  $^1\text{H}$ - and  $^{13}\text{C}$ - NMR of **120f** would suggest that the  $\pi^*$  orbital of the C-N bond has a significantly hindered approach trajectory and may be the cause of the low reactivity. Regardless, the remarkable stability of the hemiaminal and ether bridge towards acidic conditions reinforces the durability of the polycycles accessed through the cobalt-catalysed process.

### 3.5 Analysis of polycycles for potential use as scaffolds in library synthesis

With a range of novel polycycles in hand, their predicted molecular properties and potential as lead-like scaffolds for drug discovery was assessed. Seven unique systems were selected with a range of ring connectivity, sulfonyl protecting groups and heteroatom linkers (Figure 22). Where polycycles containing Boc carbamates were selected, the corresponding free amine was analysed.

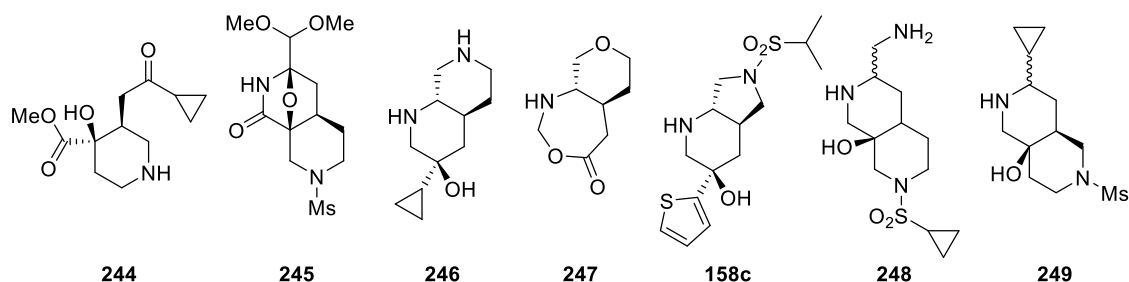


**Figure 22: Selected scaffolds for predicted molecular properties analysis.**

These scaffolds were then analysed using online software Molinspiration: the common metrics for drug discovery were calculated and compared against guideline values from the literature (Table 3).<sup>117</sup> As shown throughout the analysis, the scaffolds are highly ‘rule of 5’ compliant and contain desirable TPSA values for good bioavailability predictions. Complexity of the scaffolds also remains high, demonstrated by the low number of rotatable bonds and high Fsp<sup>3</sup> values.

**Table 3: Predicted molecular properties of selected scaffolds alongside drug discovery guidelines. <sup>a</sup> miLogP is a method for LogP prediction developed by Molinspiration.<sup>117</sup>**

Polycycle	MW (u)	miLogP <sup>a</sup>	H bond donors	H bond acceptors	No. of rot. bonds	TPSA (Å <sup>2</sup> )	Fsp <sup>3</sup>
<b>Guidelines</b>	<500 <sup>20</sup>	≤5 <sup>20</sup>	≤5 <sup>20</sup>	≤10 <sup>20</sup>	≤10 <sup>27</sup>	≤140 <sup>25,27</sup>	N/A
<b>244</b>	241.3	-0.15	2	5	5	75.6	0.83
<b>245</b>	320.4	-0.65	1	8	4	94.2	0.92
<b>246</b>	196.3	0.45	3	3	1	44.3	1.0
<b>247</b>	171.2	0.24	1	4	0	47.6	0.88
<b>158c</b>	330.5	1.51	2	5	3	69.6	0.71
<b>248</b>	249.3	-1.92	4	6	2	95.7	1.0
<b>249</b>	274.4	0.42	2	5	2	69.6	1.0

This represented the lead-like nature of the generated scaffolds, aligning with the lead-likeness guidelines proposed by Churcher in 2012,<sup>118</sup> with amine, alcohol and ketone functional groups available for further decoration during potential library generation and screening processes.

To further demonstrate the lead-likeness of our compounds prepared throughout these studies, a selection were analysed using the web-based Lead Likeness And Molecular Analysis (LLAMA) software (Figure 23, top).<sup>30</sup> The standard library reagent list was used for the decoration of the selected compounds with cleavable protecting groups removed for additional decorations – as recommended by the software developers.

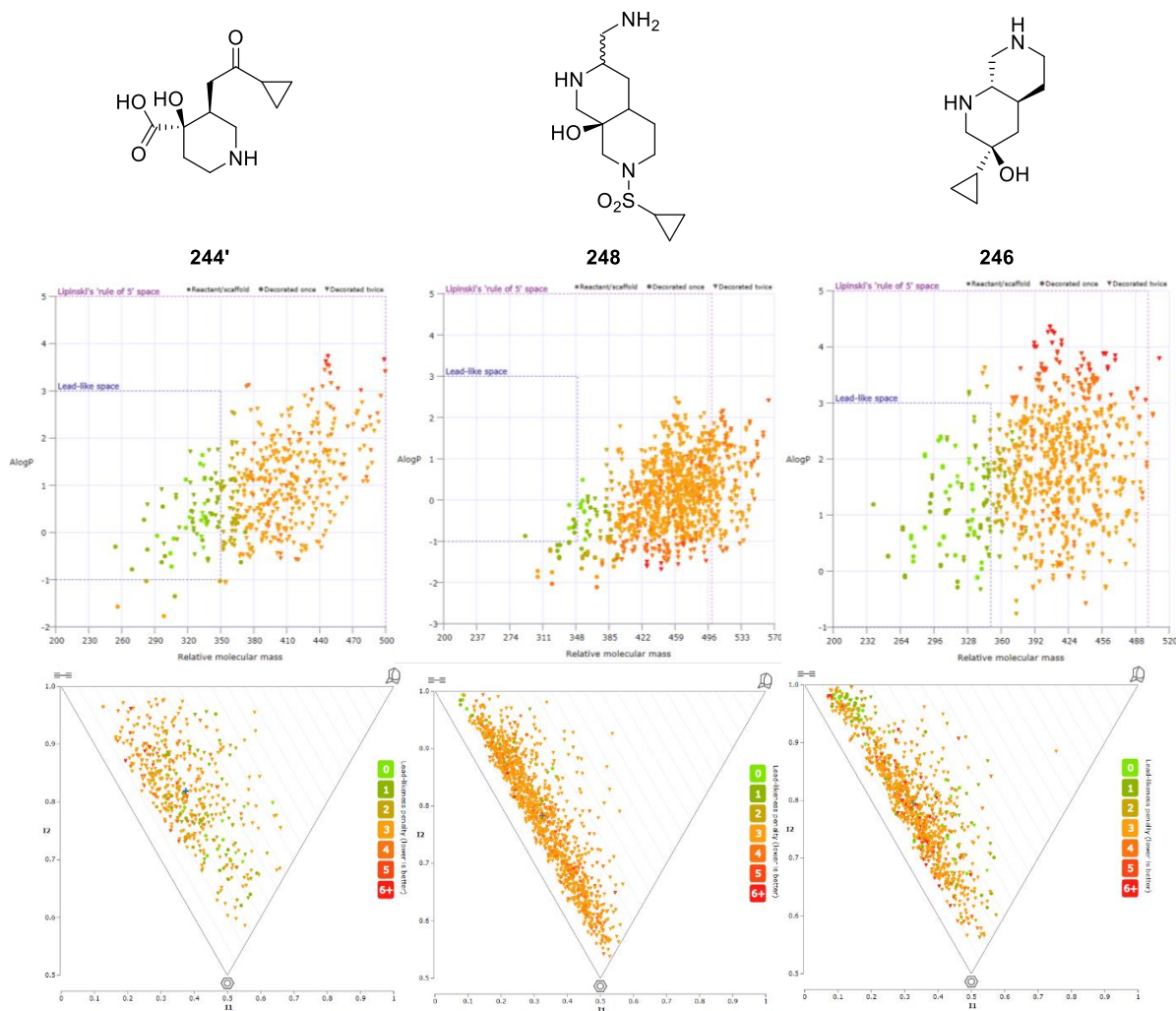


**Figure 23: Top: Lead-likeness plots of products derived from 244', 248 and 246. Bottom: Principal moments of inertia plots of products from virtual library generation. Plots produced using online LLAMA software.<sup>30</sup>**

The results showed promising trends: single decorations often fell into 'Lead-like space'; double decorations were highly 'rule of 5' compliant; there was a low lead-likeness penalty distribution, often derived from the reactants (heavy atom count and installation of aromatic

rings). Principal moments of inertia plots also indicated reasonable deviation, varying from linear to flat to spherical (Figure 23, bottom). Fsp<sup>3</sup> fraction distribution ranged from 0.3-1.0, with the majority falling within 0.5-0.7. These computational results indicate that libraries prepared from these scaffolds should contain reasonable bioavailability and have the potential for excellent specificity, aligning with the principle of lead-orientated synthesis.<sup>118</sup>

### 3.6 Outlook and future work

Through the combined efforts within our lab, a gold-catalysed cascade process has been developed to access a wide range of scaffolds. The cascading cycloaddition proceeds with excellent functional group compatibility, allowing for a number of scaffold elaboration methods to gain access to a diverse range of scaffolds (Figure 24).

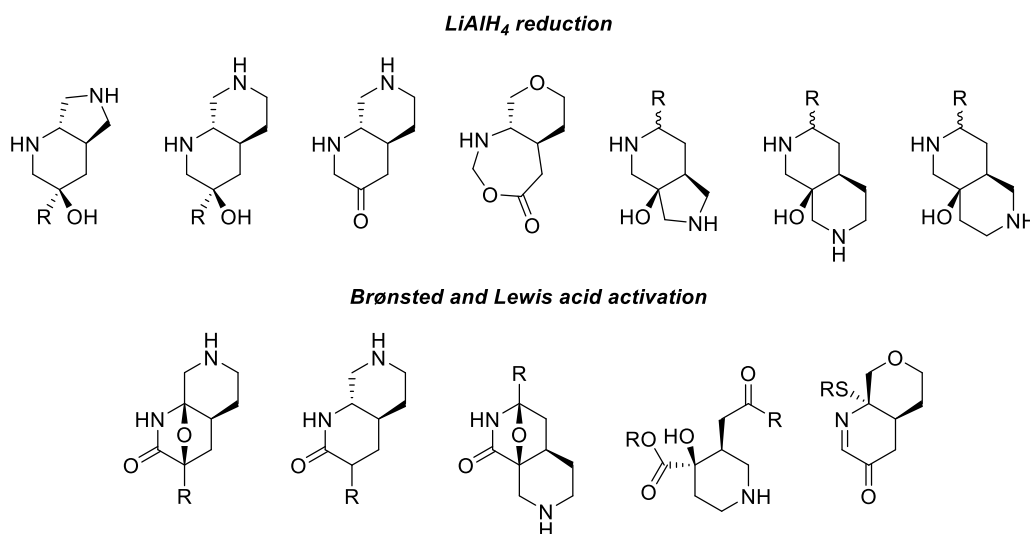


**Figure 24: Scaffolds accessed through scaffold elaboration of polycycles obtained under gold-catalysed protocol.**

Initial focus expanded on the two examples of LiAlH<sub>4</sub> reduction, extending the methodology to access 6,5- and 6,6- fused 1,3-aminoalcohols in moderate to excellent yields with an array of functionality tolerated for both the C2 and C5 series. Thioynamides have been shown as

superior at accommodating the desired Diels-Alder process and provide a thioketal handle for access to aminoketone derivatives.

Whilst not as conclusive as the reduction studies, Brønsted- and Lewis- acid activation also proved an exciting tool for diversification, providing tetrahydrofurans, lactams and piperidines in a divergent manner (Chapter 3.2.1). The ability to control the acid catalysed method has not yet been achieved and would be a priority in future work. Activation of the lactam motif *via* the acyl iminium demonstrated the rich potential of these scaffolds for further elaboration (Chapter 3.2.2), with the area of acyl iminium a well-developed field within the scientific community. Finally, Lewis acid catalysed access to a *cis* fused polycycle *via* a 1,4-rearrangement represents another avenue to explore through nucleophilic additions, reductions and the use of other migratory groups. With these results in hand, the further potential of these divergent transformations and a series of libraries are being prepared in collaboration with Mercachem (Alessandro Balella).

Alongside these discoveries, a new cobalt-catalysed method has been realised that provides complementary access to a range of 5-amido polycycles, although preliminary scaffold elaboration of the substrate scope has proven challenging. Initial reactivity towards hydride reductions have established that the lithium analogues are required for a reaction to occur, and the outcome of the reduction process has not yet become clear. The use of a suitably strong and bulky hydride source may allow for more control over the outcome. The surprising stability of the scaffolds towards dehydration under acidic conditions offers opportunity for diversification whilst maintaining the  $sp^3$  rich core.

## **Chapter 4: Nucleophilic heterocyclic carbenes and their development in organometallic chemistry**

Having established the utility of the gold catalysed [3+2] dipolar cycloaddition to access 4-amidooxazoles that were subsequently useful in the synthesis of medically relevant piperidines, interest was turned to further exploiting the power of this method for the generation of nucleophilic heterocyclic carbenes.

The following chapter discusses literature approaches for imidazolium salt synthesis that were of interest to this project, leading into the common parameters used for analysis and comparison of NHC ligands. Key areas in ligand design are then highlighted through the incorporation of additional steric bulk, fused imidazolylidene backbones, and bifunctional NHC ligands, including their effect on reactivity in transitional metal catalysis.

### **4.1 Nucleophilic heterocyclic carbenes**

Since the isolation of a phosphinocarbene by Bertrand<sup>119</sup> and an imidazole carbene by Arduengo,<sup>120</sup> research into Nucleophilic Heterocyclic Carbenes (NHCs) has received significant interest in the fields of transition metal (TM) catalysis. Whilst a variety of heterocyclic scaffolds have been identified (Figure 25), the following discussion will predominately focus on imidazolylidene derived NHCs.



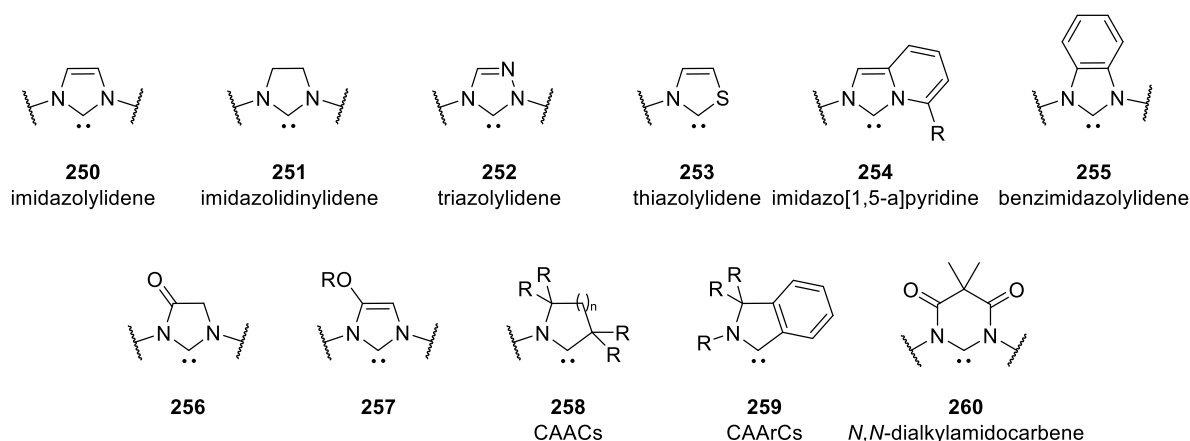


**Figure 25: Common heterocyclic frameworks of NHC ligands.**

Azolium NHCs exist in the singlet carbene form, with mesomeric stabilisation afforded by the neighbouring nitrogen lone pairs and an inductive electron-withdrawing effect from the neighbouring heteroatoms favouring the singlet over triplet state (Figure 26).<sup>121</sup> The pair of electrons occupying the  $sp^2$  orbital provide a strong  $\sigma$  donor for coordination to transition metals, with NHC ligands proving more electron donating than their phosphine counterparts.<sup>122</sup> Additional  $\pi$ -backbonding interactions from the metal centre to the empty  $p_z$  orbital also increases the ligands coordination ability in transition metal complexes. These characteristics allow NHCs to stabilise highly reactive organometallic species, providing vast opportunities for metal-mediated organic transformations.

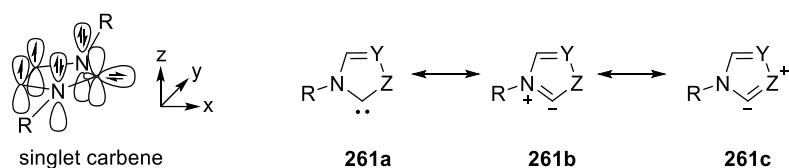


**Figure 26: Orbital representation of singlet state carbene and extreme resonance forms that underpin stability.**

NHCs are often compared to tertiary phosphine ligands due to the similar mode of bonding interaction. Developments in the early 2000s revealed NHC-TM complexes to be more stable than tertiary phosphine-TM complexes, and highly reactive for transition metal mediated

transformations. This resulted in NHC-TM complexes that were shown to be active where the phosphine counterparts were susceptible to degradation or were ineffective.<sup>123</sup> Across the two classes of ligands, modification of the appendages and skeletal ring structure has allowed extraordinary improvements in reaction control and methodology development.

## 4.2 Synthesis routes to access imidazolium motifs

Imidazolylidenes **250** are predominately accessed from their imidazolium salts **262**. As interest in NHC ligands grew exponentially, four main strategies to deliver imidazolium salts have been developed from a wide variety of bis-amine derivatives at varying oxidation states (Figure 27).

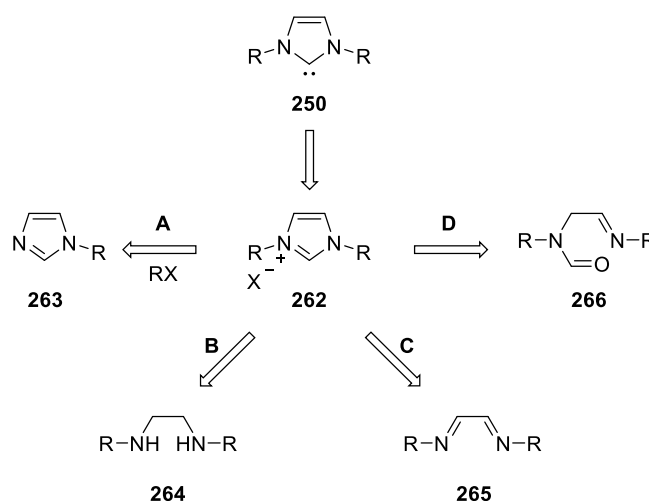
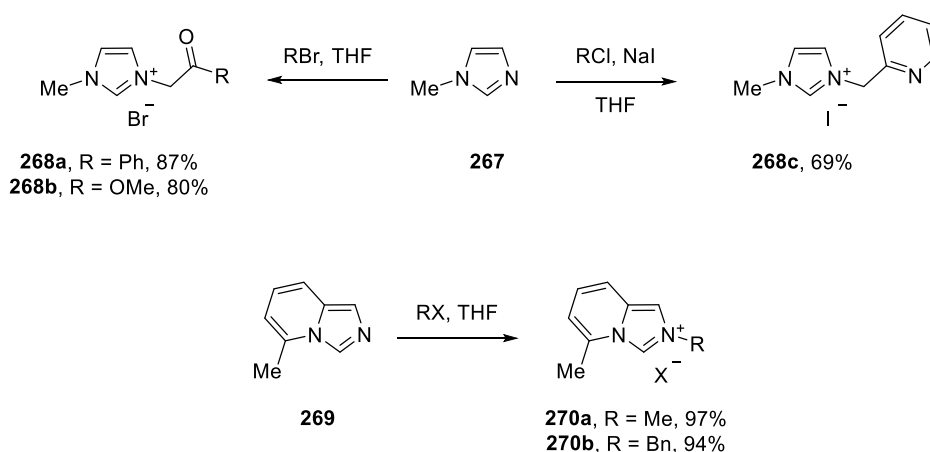


Figure 27: Overview of synthetic strategies to access imidazolylidene precursors.

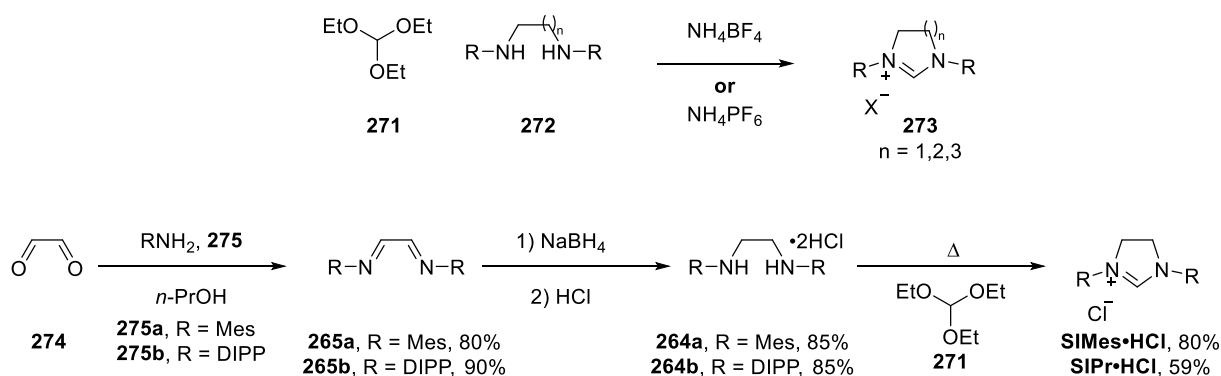
A straightforward alkylation approach with *N*-substituted imidazoles **263** offered access to imidazolium salts (route **A**). The remaining strategies relied upon building a bis-amine backbone and performing a cyclisation to build the imidazolium. Installation of the precarbene unit during this cyclisation step are the most widely employed approaches (routes **B** and **C**). Ring closure of the amino functionality with a preassembled pre-carbenic unit (route **D**) offered a complementary approach.

Cavell described the preparation of donor functionalised **268** derivatives through alkylation of 1-methylimidazole **267**,<sup>124</sup> whilst Lassaletta used this route in the synthesis of pyridine annulated **270** (Scheme 73).<sup>125</sup> Whilst simple and efficient, this route relied on quaternisation of a prebuilt imidazole structure and failed with aryl and secondary alkyl halides, limiting the scope of accessible NHC precursors.



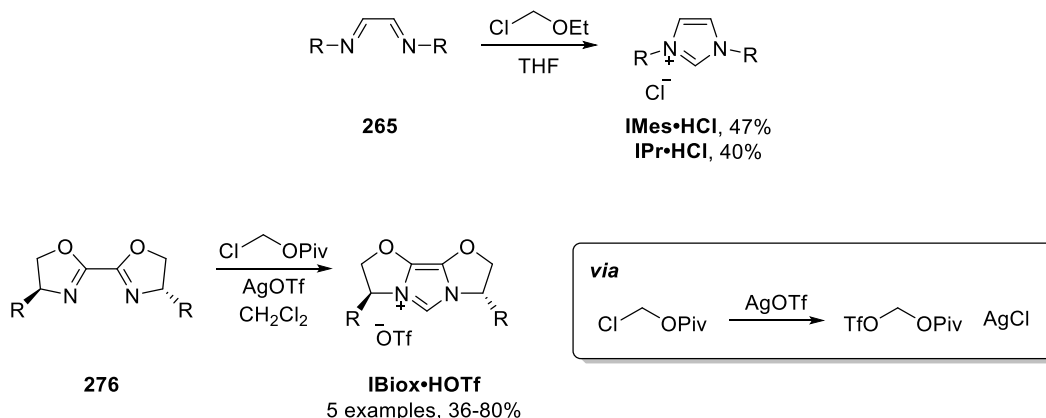
**Scheme 73: Top: Alkylations of 1-methylimidazole from Cavell. Bottom: Alkylation of imidazo[1,5-a]pyridine derivatives from Lassaletta.**

Saba and Kaloustian first described the reaction of orthoester **271** with diamines **272** in the presence of HBF<sub>4</sub> or HPF<sub>6</sub> to deliver dihydroimidazolium, tetrahydropyrimidinium and tetrahydrodiazepinium salts **273** (Scheme 74).<sup>126</sup> Arduengo used this route in the synthesis of **SIMes•HCl** and **SIPr•HCl**, preparing glyoxal diimines **265** *via* a condensation reaction followed by reduction to access diamines **264** (Scheme 73).<sup>127</sup>



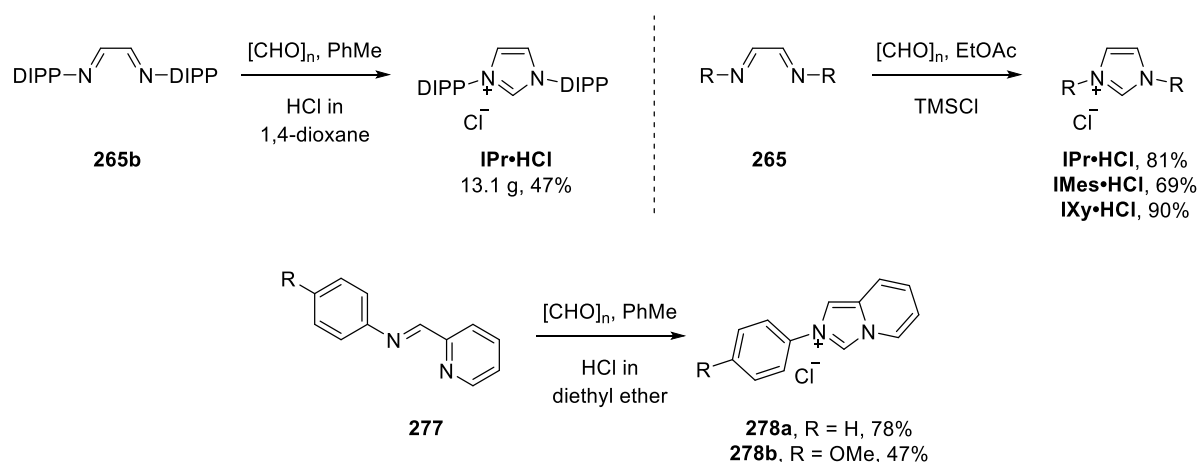
**Scheme 74:** Top: One-pot synthesis of amidinium salts from diamines using orthoester **254**. Bottom: Arduengo's synthesis of **IMes•HCl** and **IMes•HCl**.

In the same report, Arduengo reported that treating diimines **265** with chloromethyl ether provided access to the unsaturated analogues **IMes•HCl** and **IPr•HCl** without the need for a reduction process (Scheme 75).<sup>127</sup> Conveniently, the cyclisation proceeded with precipitation of the desired salts from the reaction mixture, negating any challenging purification steps. When developing oxazoline annulated **IBiox** ligand precursors, Glorius noted that the oxazoline backbone was sensitive towards ring opening by the chloride counterion generated *in situ*.<sup>128</sup> This issue was overcome by using chloromethyl pivalate in combination with silver triflate, where the resulting triflate counterion is unreactive towards oxazoline ring opening (Scheme 75).



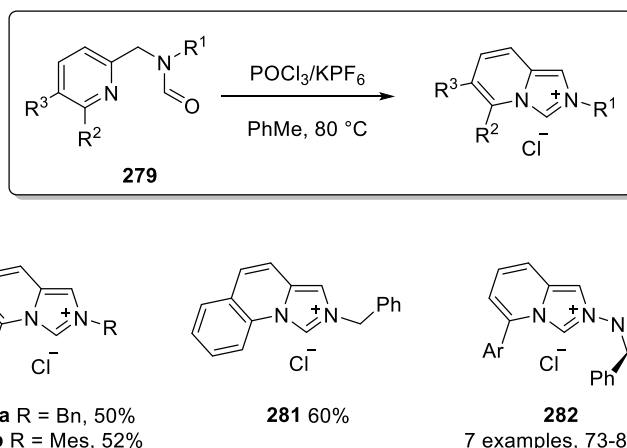
**Scheme 75:** Top: Arduengo's chloromethyl ether synthesis of imidazolium salts. Bottom: Glorius's synthesis of **IBiox•HCl** derivatives using **AgOTf**.

In 2000 Nolan demonstrated the use of paraformaldehyde as the precarbene unit, preparing **IPr•HCl** from diimine **265b** on large scale (Scheme 76).<sup>129,130</sup> This procedure was adapted by Hintermann, who replaced HCl in 1,4-dioxane with TMSCl for its comparatively simpler measuring, handling and lower cost.<sup>131</sup> By performing the reaction in EtOAc, pure imidazolium salts precipitated from the reaction mixture. Iminopyridine derivatives were also compatible with this method, accessing imidazo[1,5-*a*]pyridines **278**.<sup>132</sup>



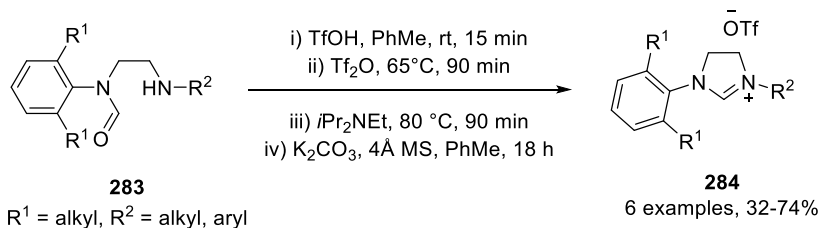
**Scheme 76: LHS: Nolan's paraformaldehyde route to IPr•HCl. RHS: Improved procedure employing TMSCl. Bottom: Compatibility with iminopyridines.**

The final approach exploited the cyclisation of formamide derivatives **279**. Lassaletta's group showed that a POCl<sub>3</sub> mediated cyclisation could access *N*-alkyl/aryl imidazo[1,5-*a*]pyridinium salts **280-281** via a modified Vilsmeier-Haack reaction (Scheme 77).<sup>125</sup> This method was also used to access fused heterobiaryl ligands **282** containing a chiral pendant group.<sup>133,134</sup>



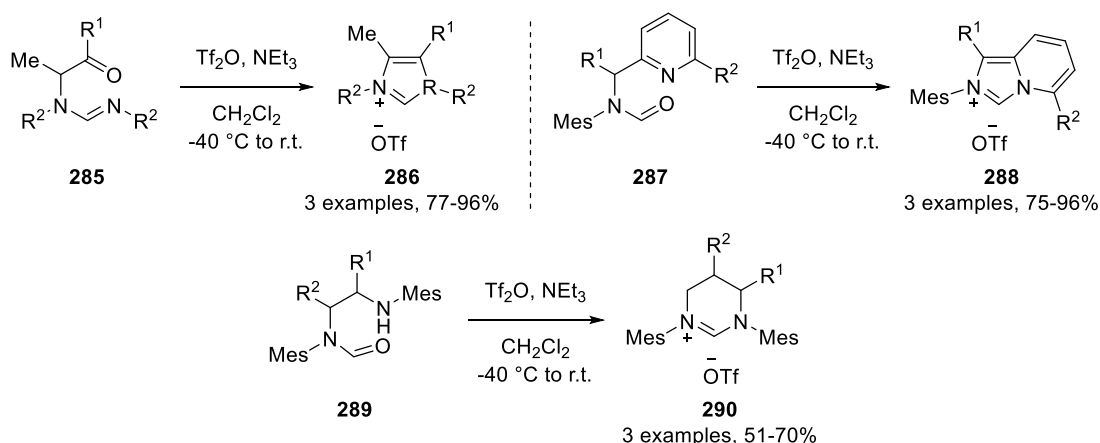
**Scheme 77: Lassaletta's POCl<sub>3</sub> mediated synthesis of imidazo[1,5-*a*]pyridinium salts.**

Noting that this method was only successful in examples where the nitrogen nucleophile was sp<sup>2</sup>-hybridised and the corresponding product an aromatic imidazolium ring, Organ's group showed that by treating formamide **283** with Tf<sub>2</sub>O, imidazolinium salts **284** could be isolated (Scheme 78).<sup>135</sup> Pre-treatment with TfOH to sequester the lone pair of the free amine was found to be crucial, subsequently requiring a base to free up the amine for the subsequent nucleophilic attack of the triflylimminium triflate.



**Scheme 78: Organ's imidazolinium construction through activation of formamides.**

Zhang's group then demonstrated that treatment of formamidine derived ketones **285** with Tf<sub>2</sub>O and NEt<sub>3</sub> gave the corresponding imidazolium salts **286**; further investigations demonstrated the same reaction occurred with pyridine-derived formamides **287** (Scheme 79). Saturated tetrahydropyrimidinium salts **290** were also accessible from formamides **289**.



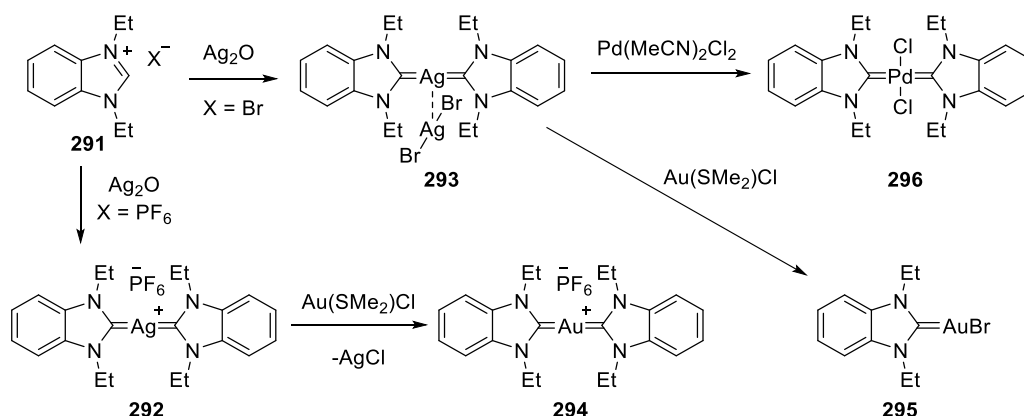
**Scheme 79:** Zhang's Tf<sub>2</sub>O mediated synthesis of imidazolium, imidazopyridine and tetrahydropyrimidinium salts.

Whilst these examples give an insight into the many established methods to access NHC precursors, it does not provide a comprehensive view of the field. A review by César and co-workers captured the broad range of methodologies available to synthesis NHC precursors.<sup>136</sup>

### 4.3 Coordination to transition metals

Early syntheses of transition metal complexes involved using a strong bases, such as NaH or KHMDS, alongside high reaction temperatures to deprotonate the imidazolium and form the free carbene, prior to coordination to transition metals.<sup>120,123,137</sup>

The use of Ag<sub>2</sub>O was then introduced for facile formation of NHC-Ag(I) complexes by Lin, with H<sub>2</sub>O the sole by-product from the reaction (Scheme 80).<sup>138</sup> Switching the counterion yielded different TM-NHC complexes: **291**•HPF<sub>6</sub> yielded **292**, stabilised by a PF<sub>6</sub><sup>-</sup> counterion, whereas **291**•HBr provided **293**, stabilised by a complexed [AgBr<sub>2</sub>]<sup>-</sup> counterion. The subsequent reactivity of **292** and **293** proved unique, providing cationic complex **294** and **295** respectively. Transmetalation from **293** to transition metals including palladium, copper, iridium, rhodium, gold, and ruthenium highlighted the versatility of this process.<sup>139</sup>



**Scheme 80:** Lin's counterion dependent Ag(I)NHC synthesis and subsequent transmetalation.

Since then, it has been shown that there are up to seven types of silver complexes formed depending on both the counterion and the type of NHC ligand (Figure 28).<sup>139</sup> The non-halide imidazolium salts are generally found to produce type 4 bis-NHC complexes, whereas most *N,N*-dialkyl, *N,N*-diaryl, *N*-alkyl, and *N'*-aryl imidazolium halide salts formed the type-1 ionic or type-2 neutral complexes. Type 2 mono-substituted NHC-Ag complexes were more desirable as they led to more accessible metal centres for catalysis reactions. This resulted in a drive for azolium salts containing halide counterions where possible for the preparation of reactive TM-NHC complexes *via* transmetalation approaches. More recently, Cazin's group showed a similar method employing  $\text{Cu}_2\text{O}$ , successfully performing the carbene exchange with both gold and palladium in high yields.<sup>140</sup>  $\text{Cu}_2\text{O}$  is a much cheaper alternative to  $\text{Ag}_2\text{O}$ , and silver NHC-complexes are often light sensitive.



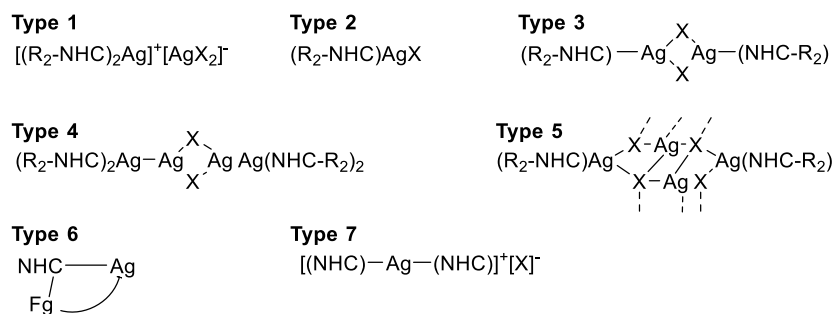
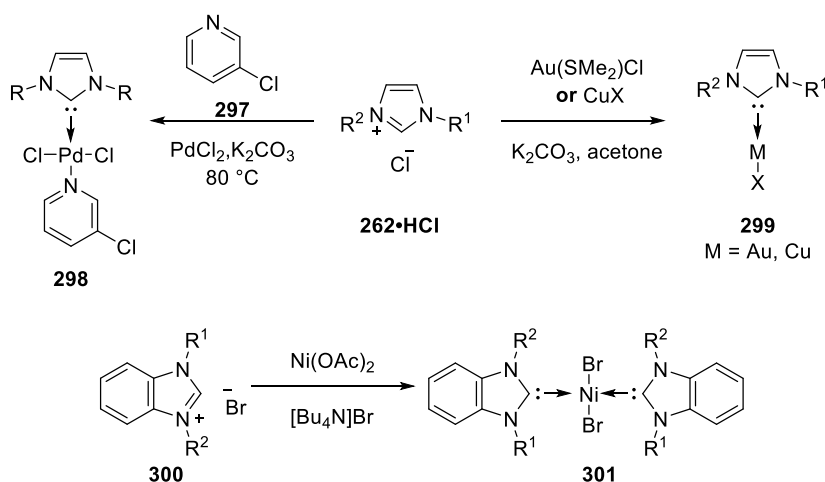


**Figure 28:** Types of silver NHC complexes formed through treatment with  $Ag_2O$ .

Direct complexation methods have also been developed. Organ demonstrated the synthesis of PEPPSI complexes **298** by refluxing **262•HCl** in 3-chloropyridine in the presence of  $PdCl_2$  (Scheme 81).<sup>141</sup> Access to gold and copper NHC complexes **299** was achieved by Nolan through treatment of **262•HCl** with  $K_2CO_3$  and  $CuX$  or  $Au(SMe_2)Cl$  in acetone under air.<sup>142,143</sup> Nickel complexes **301** were also prepared under related procedures with  $NiCl_2$  or  $Ni(OAc)_2$ .<sup>144,145</sup>



**Scheme 81:** Methods for direct coordination to transition metals.

The introduction of carbene transfer and direct coordination methods largely negated the need for *in situ* generation of sensitive free carbenes, although the free carbene route is still regularly performed during the synthesis of iridium and ruthenium complexes. The coordination of NHC

ligands to P-block elements has been reviewed by Tamm,<sup>146</sup> and copper, nickel and cobalt by Braunstein and co-workers.<sup>147</sup>

## 4.4 Analysis of nucleophilic heterocyclic carbene ligands

### 4.4.1 Measuring electronic parameters

With the synthesis of NHCs the focus of a large amount of research worldwide, metrics to characterise and compare the different NHC systems and their effects on metals have been introduced and adopted. The various methods introduced for measuring electronic impact of NHC ligands have been comprehensively reviewed by Nelson and Nolan,<sup>122</sup> and since updated by Huynh.<sup>148</sup>

Due to the reactive nature of NHCs, storage as their bench stable salt precursors is an attractive approach in the use of NHCs for organocatalysis reactions. Subsequently, the pK<sub>a</sub> of the azolium salts was of interest, informing solvent and base selections for organocatalysis reactions. Trends on the effect on pK<sub>a</sub> from the substitution pattern of azolium salts have been reported by several groups, alongside experimental routes to calculate these pK<sub>a</sub>s.<sup>149–153</sup> Acidity trends were then calculated for azolium salts (Figure 29).<sup>122</sup>

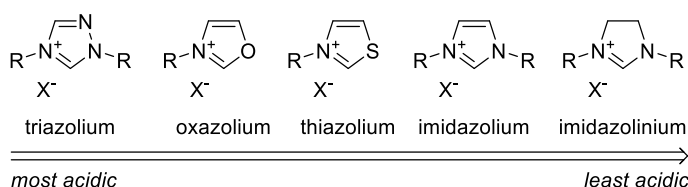
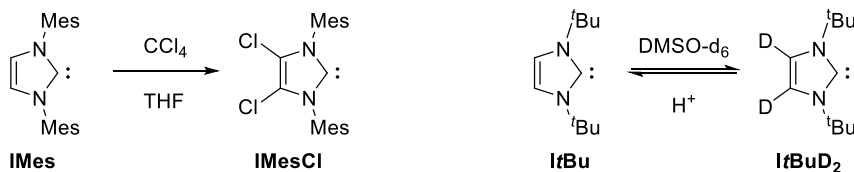


**Figure 29: Acidity trends of azolium salts.**

During initial pK<sub>a</sub> studies it was also shown that several NHCs were reactive towards halogenated solvents and DMSO. Substitution at C<sub>4</sub> and C<sub>5</sub> with Cl<sup>-</sup> to form **IMesCl** and D<sup>+</sup> to form **ItBuD<sub>2</sub>** as seen when treated with CCl<sub>4</sub> or DMSO-d<sub>6</sub> (Scheme 82).<sup>154–156</sup> The addition of

halogens to the NHC backbone renders it more electron deficient, with this discovery being utilised in the synthesis of a range of chloride bearing NHC ligand backbones.



**Scheme 82: LHS: Reaction of imidazolyliene backbone with  $\text{CCl}_4$ . RHS: Equilibrium observed in pKa studies performed in  $\text{DMSO-d}_6$ .**

Tolman's Electronic Parameter (TEP) is an established method for analysing the electron donor capability of NHCs. TEP studies require synthesis of either *cis*-[IrCl(CO)<sub>2</sub>(NHC)], *cis*-[RhCl<sub>2</sub>(CO)<sub>2</sub>(NHC)] or [Ni(CO)<sub>3</sub>(NHC)] complexes, with libraries of comparable values accessible (Figure 30). The vibrational wavelength of the A<sub>1</sub> CO stretch in transition metal NHC complexes is used to calculate TEP allows for to comparison of the electron donating ability of NHC ligands. Based on work studying the  $\sigma$ -donation of phosphorus ligands by Tolman,<sup>157</sup> the IR frequency belonging to the CO stretch is dependent on the electron density at the metal centre, as  $\pi$  back-bonding with the  $\pi^*$  orbital of the carbon monoxide ligand will affect its frequency. Whilst the original work was based on [Ni(CO)<sub>3</sub>(L)] complexes, where L = phosphine ligands, and the NHC TEP values were compared after extrapolation, libraries of NHC complexes have now been synthesized and analysed. This allowed for refined correlation equations between the possible nickel-, iridium- and rhodium- complexes.<sup>122,158,159</sup>

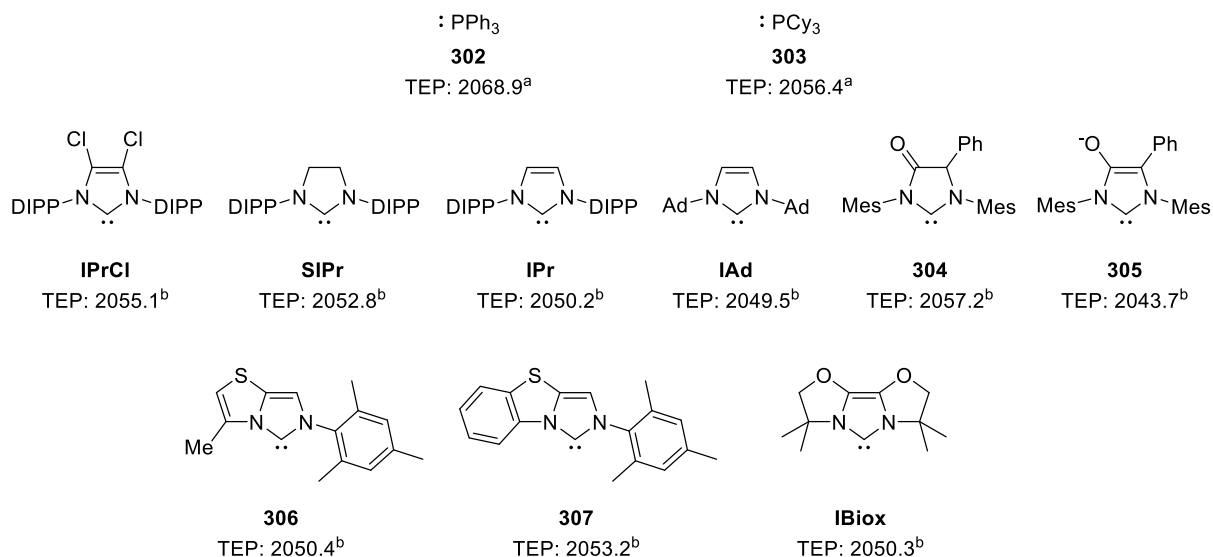


**Figure 30: TEP values (cm<sup>-1</sup>) for common phosphine and NHC ligands used in catalysis. <sup>a</sup>Reproduced from ref<sup>[159]</sup>. <sup>b</sup>Reproduced from ref<sup>[122]</sup>.**

Lower TEP values indicate more electron density at the metal centre through weakening of the carbon monoxide  $\pi$ -bond, allowing the  $\sigma$ -donor ability of ligands to be compared. Even electron deficient NHCs **IPrCl** and **304** offer similar  $\sigma$ -donation to **PCy<sub>3</sub>**, one of the most electron-rich simple phosphines, demonstrating their increased electron-donating abilities. Impact of modifications on the ligand backbone can also be visualised, as **IPrCl** shows poorer donation than **IPr** and **SIPr**. Reactive ligand backbones can be utilised to modify ligand properties, as highlighted by the significant difference between **304** and **305**. An extended conjugated  $\pi$ -system reduce the donor ability of **307** compared to **306**.

Whilst these values can be useful for comparison, secondary orbital interactions and steric interactions between the NHC, CO ligands and metal centre can result in inaccurate representations of the carbene-metal interaction.<sup>160</sup> Approaches to overcome the secondary interactions that limit accuracy of TEP measurements include the use of quantum chemical calculations that account for these shortcomings.<sup>161–163</sup>

More recently,  $^{13}\text{C}$ -NMR analysis has been used in combination with computational calculations to probe the strength of  $\sigma$ -donation from carbenes in palladium and gold complexes.<sup>164,165</sup> These results were extended into information on the ligand trans effect and the basicity of the resulting complexes. These methods contain superior sensitivity due to the margin of error within  $^{13}\text{C}$ -NMR being much lower than in solution state IR spectroscopy. Not only does this provide more insight into the electronic structure of these complexes, it also provides an alternative to the TEP values normally used, avoiding the synthesis of iridium-, rhodium- or nickel- complexes required for the TEP calculations.

#### 4.4.2 Measuring the steric impact of NHC ligands

In the search for a measurable steric factor to be used alongside TEP, percentage buried volume ( $\%V_{\text{bur}}$ ) has led the field. Phosphorus based ligands adopt a trigonal pyramidal shape, with the Tolman cone angle effectively describing the steric impact of these ligands (Figure 31), although it is not suitable for biaryl systems such as Buchwald phosphines.<sup>157,166</sup> NHC ligands instead adopt a  $C_2$  type symmetric shape.  $\%V_{\text{bur}}$  accounts for the total volume a ligand occupies in a predefined sphere around the metal, and was proposed by Nolan and Cavallo as a substitute to the Tolman cone angle.<sup>167</sup>

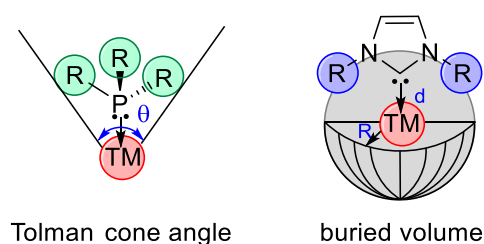


**Figure 31: Representation of the Tolman cone angle and buried volume steric descriptors used for phosphorus and NHC ligands respectively.**

Crystallographic data is used in combination with SambVca software, developed by Cavallo,<sup>168</sup> to calculate  $\%V_{\text{bur}}$ . Nolan recorded one of the highest value  $\%V_{\text{bur}}$  for  $\text{NHCAuCl}$  complexes

when preparing **IDIPP-TropAuCl** in 2015 (Figure 32).<sup>169</sup> By utilising a dibenzyltropyl group, the steric bulk was significantly increased compared to its parent **IPrAuCl**. Interestingly, %  $V_{\text{bur}}$  decreased in value for **IAd-TropAuCl**, suggesting a less sterically hindered metal centre. Whether this is an artefact of the parameters put in place during calculation or an actual consequence of the use of two bulky *N*-substituents, it highlights the potential limitations of the parameter subjective nature beyond initial NHC catalyst designs.

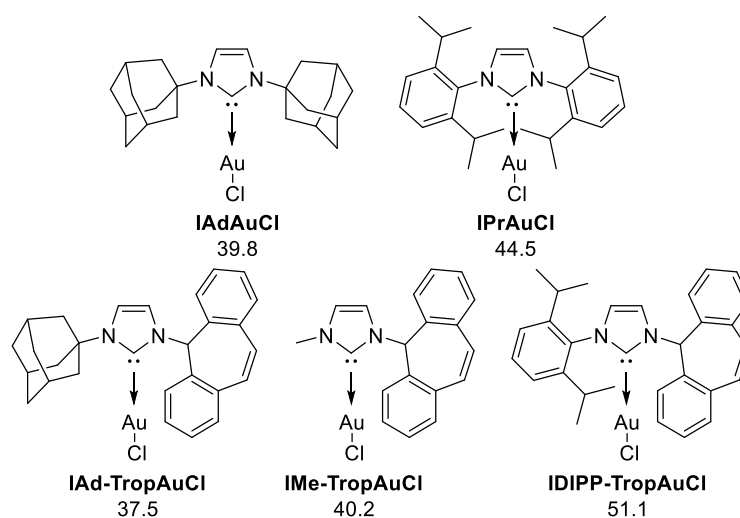


**Figure 32:** %  $V_{\text{bur}}$  figures for two common NHC catalysts and the dibenzotropyliene substituted NHC catalysts developed by Nolan. <sup>a</sup>Reproduced from ref<sup>[169]</sup>.

When considering ligand design, a high %  $V_{\text{bur}}$  is often desirable due to the increased stabilisation of low valent, active catalyst species and the increased affinity towards reductive elimination in cross coupling reactions. However, as ligand design becomes more complex, consideration of the parameters used for the calculations is important, as functionality outside of the 3.5 Å sphere may infer unexpected reactivity when %  $V_{\text{bur}}$  alone is accounted for.

In 2016 Cavallo developed SambVca 2.0, an online web tool that allowed users to calculate topographic steric maps from crystallographic data.<sup>170</sup> These maps allow three dimensional visualisation of the ligand impact on the coordination sphere of transition metal complexes,

subsequently offering a quantitative description of the catalytic pockets. Justification of regioselectivity inversion in Mizoroki-Heck reaction,<sup>171</sup> *cis/trans* selectivity in ruthenium-catalysed epoxidations<sup>172</sup> and even stereoselectivity in organocatalysed Michael additions<sup>173</sup> highlight the utility of these analyses. Discussion, examples, and analysis of topological graphs is discussed *vide infra*.

## 4.5 Ligand development and reactivity

### 4.5.1 Increasing the steric impact of NHC ligands

Ligand modification to improve catalytic activity has taken many approaches. Several of the most successful developments have stemmed from increasing the steric bulk of imidazolydene ligands. Initial research utilised **IPr** and variants for reaction discovery, once coordinated to transition metals, and their widespread use continues to this day (Figure 33). The topology of imidazolydene scaffolds places the pendant groups within the coordination sphere of TM complexes (Figure 33). Modification of the appended groups therefore resulted in significant changes in reactivity and stability when coordinated to transition metals.

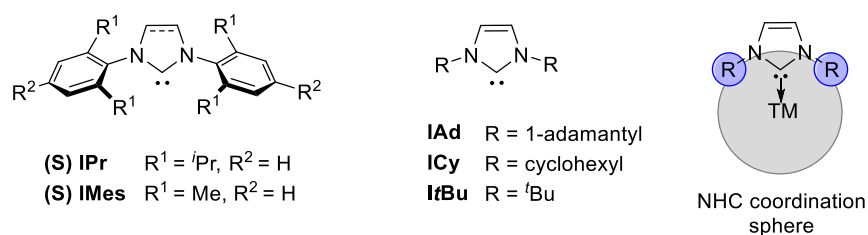
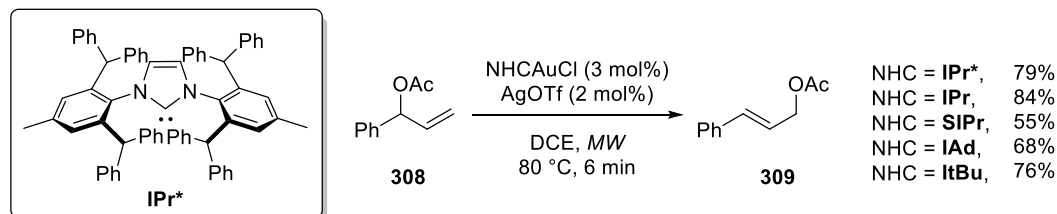


**Figure 33: LHS: Simple and common NHCs used during early discovery stages. (S) represents the saturated backbone. RHS: Coordination sphere for NHC TM complexes.**

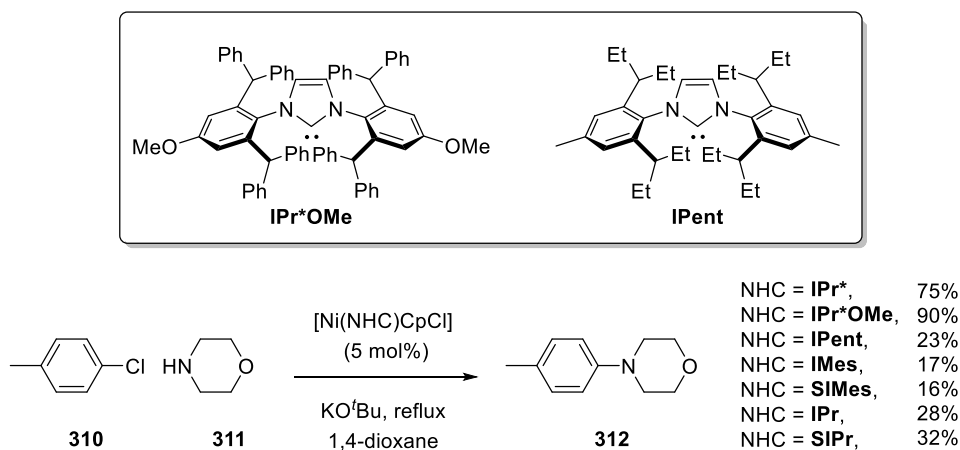
Enhancements in reactivity have been demonstrated by increasing the steric bulk of the ligands, enabling increased stabilisation of reactive organometallic species. In 2010 Markó published the first synthesis of **IPr\***, replacing the *i*Pr groups of **IPr** with diphenylmethyl groups (Scheme

83).<sup>174</sup> Nolan then prepared **IPr\*****AuCl**, which exhibited similar catalytic activity to **IPrAuCl** and its derivatives in the rearrangements of allylic acetate **308**.<sup>175</sup>



**Scheme 83:** Bulky **IPr\*** ligand prepared by Markó.<sup>174</sup> Screening **IPr\*****AuCl** against **IPr** derivatives in gold-catalysed allylic rearrangements.<sup>175</sup>

Further variations in **IPr\*OMe** and **IPent** were prepared and shown to promote enhanced conversion during the nickel-catalysed Buchwald-Hartwig amination reaction between **310** and **311** (Scheme 84).<sup>176</sup> Nolan hypothesised that dual activation occurs *via* increased disassociation of the Cp ligand and improved stabilisation of the active  $[\text{Ni}^0\text{NHC}]$  organometallic complex required for catalytic activity due to the sizable steric bulk of the **IPr\*** ligand derivatives.



**Scheme 84:** Novel **IPr\*OMe** and **IPent** NHCs. Screening of ligands in a nickel-catalysed Buchwald-Hartwig amination

This increase in efficacy was also observed in palladium-catalysed Suzuki-Miyaura<sup>177–179</sup> and Buchwald-Hartwig<sup>179</sup> cross-coupling reactions, nickel-catalysed carboxylation of organoboronates<sup>180</sup> and ruthenium-catalysed olefin metathesis.<sup>181,182</sup> **IPr\*** delivered depressed



yields in comparison to **IPr** and **SIPr** in various gold-catalysed transformations, such as alkyne nitrile hydrations and Meyer-Schuster and allylic acetate rearrangements, demonstrating that excessive steric bulk can be detrimental to reactivity in some cases.<sup>183,184</sup>

#### 4.5.2 Annulated imidazolyidenes as alternative ligand backbones

Ligand properties can also be changed by fusing the imidazolylidene with a second heterocycle. This offered pathways to alter ligand properties, changing the electronic backbone of the NHC and offering sites for installation of functional groups within the coordination sphere.

Glorius prepared a range of **IBiox** ligands that utilised a bioxazoline-fused imidazolium core (Figure 34).<sup>128,185,186</sup> Preliminary studies showed the cyclic rings to be conformationally flexible, with preference for **IBiox6i**. Although this flexibility reduced the impact of the cycloalkyl rings on the coordination sphere, they proved adept at catalysing sterically demanding Suzuki-Miyaura cross-couplings.<sup>185,186</sup>

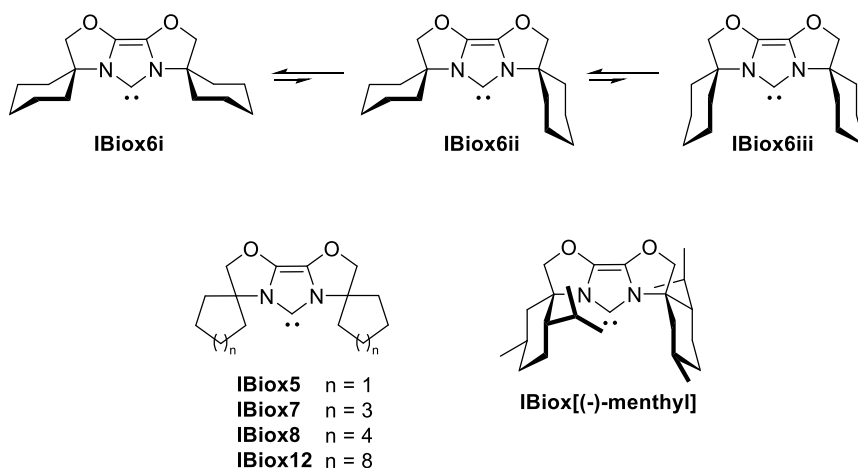


Figure 34: Top: Conformational equilibria in IBiox ligands, demonstrated with IBiox6. Bottom: IBiox derivatives.

To overcome this conformational freedom, **IBiox[(-)-menthyl]** was prepared from (-)-Menthone (Figure 34).<sup>187</sup> The additional substituents on the cyclohexyl ring caused the equilibrium to favour the most sterically demanding conformation, providing a chiral ligand

with significant steric bulk. **IBiox[(-)-menthyl]** exhibited significant enantioselectivity in the palladium-catalysed intramolecular  $\alpha$ -arylation of amides, including challenging aryl chloride substrates.

**ImPy** are another popular class of NHC ligands (Figure 35). First prepared by Lassaletta<sup>125</sup> and Glorius independently,<sup>188</sup> they contain rigid bicyclic backbones that facilitate unique steric environments within the coordination sphere from substitution at R<sup>2</sup>. Glorius utilised bromopyridine **315** as a divergent precursor to access **316**, which showed increased reactivity in Suzuki-Miyaura cross-coupling reactions of sterically hindered aryl chlorides compared to its unsubstituted counterpart (R=H).

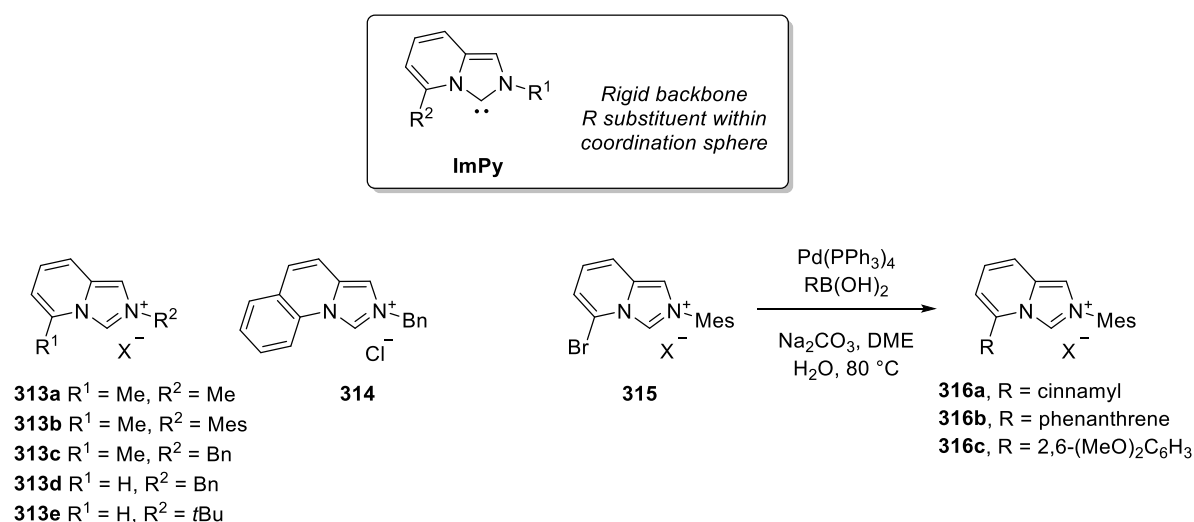
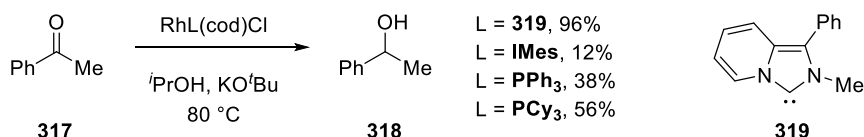


Figure 35: Imidazo[1,5-*a*]pyridine ligand derivatives prepared by Lassaletta (**313-314**)<sup>125</sup> and Glorius (**315-316**).<sup>188</sup>

Murai reported that **ImPy** NHCs observed significantly increased  $\pi$ -acceptor abilities than imidazolylidene equivalents due to overlap of the vacant  $p_z$  orbital within the carbene and the  $\pi^*$ -orbitals from the annulated pyridine, without the loss of  $\sigma$ -donor abilities.<sup>189</sup> This enhancement allowed for improved conversion and catalyst activity in the transfer hydrogenation of acetophenone with **319** (Scheme 85).<sup>190</sup>

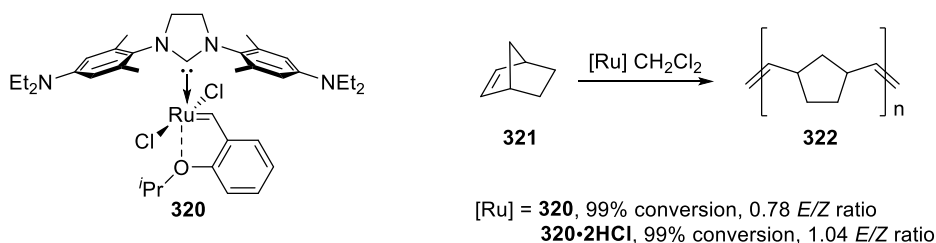


**Scheme 85: Rhodium-catalysed transfer hydrogenation of acetophenone.**

#### 4.5.3 SMART ligands that impact catalytic activity

With a huge variety of ligand backbones presented in the literature (Figure 30),<sup>122,148,191–194</sup> ligands that provide more than a sterically demanding pocket or variations of the electronic environment at the metal centre were sought after. An extensive review published in 2017 captured examples of Switchable, Multifunctional, Adaptable oR Tuneable (SMART) NHC ligands that modify their steric or electronic properties to facilitate catalytic processes.<sup>195</sup>

Schanz described the first proton responsive NHC complex when preparing diamino-tethered **320** (Scheme 86).<sup>196</sup> Disappointingly the metathesis reactivity of complex **320** under acidic conditions was poor, attributed to the reduced carbene  $\sigma$ -donor ability. Catalyst degradation was also observed under aqueous conditions. In a separate study, complex **320** was used to provide switchable stereocontrol in ring opening metathesis polymerisation.<sup>197</sup> Protonation of the tethered diamino groups led to a significant shift in the *E/Z* ratio of the resulting polynorbornene. This switch in selectivity was derived from the reduced electron donating ability of the protonated complex.



**Scheme 86: Proton responsive ruthenium complex and the effect of protonation on the *E/Z* ratio of ring opening metathesis polymerisation with norbornene.**

Choudhury developed stimuli-controlled reversible coordination and protonation processes when studying pyridyl complex **323** (Figure 36).<sup>198</sup> Treatment of bimetallic species **323** with PPh<sub>3</sub> resulted in decooordination of the second metal at the pyridyl moiety. Subsequent treatment of **324** with acid yielded **325**, which could be reverted to **323** *via* treatment with base followed by addition of a suitable metal dimer. Both bimetallic complex **323** and charged complex **325** observed significant reduction in electron density at the rhodium centre. Albrecht observed reversible coordination of a carboxylate wingtip in complex **326** upon treatment with acid or base.<sup>199</sup> Complementary catalytic activity was observed as tridentate complex **327** proved superior in Mizori-Heck cross coupling reactions, whilst being outperformed by **326** in Suzuki-Miyaura couplings.

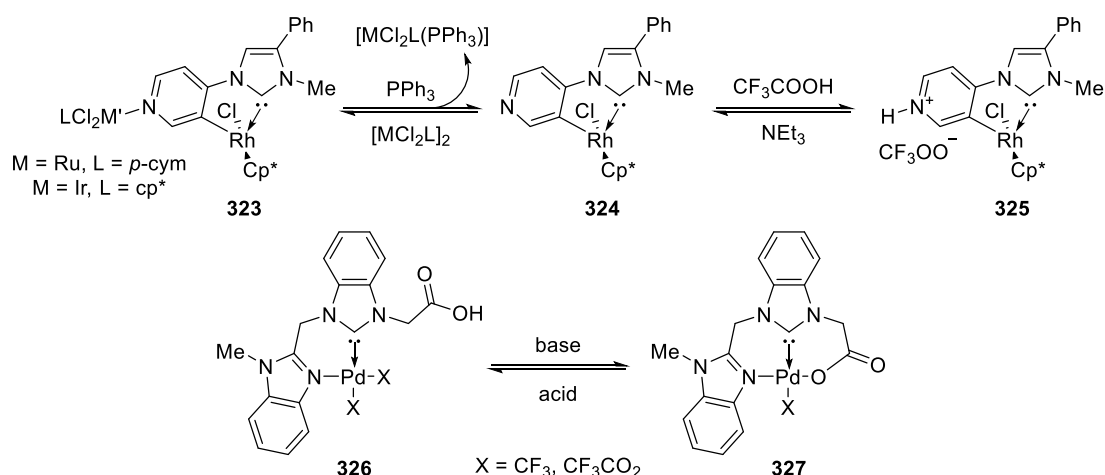
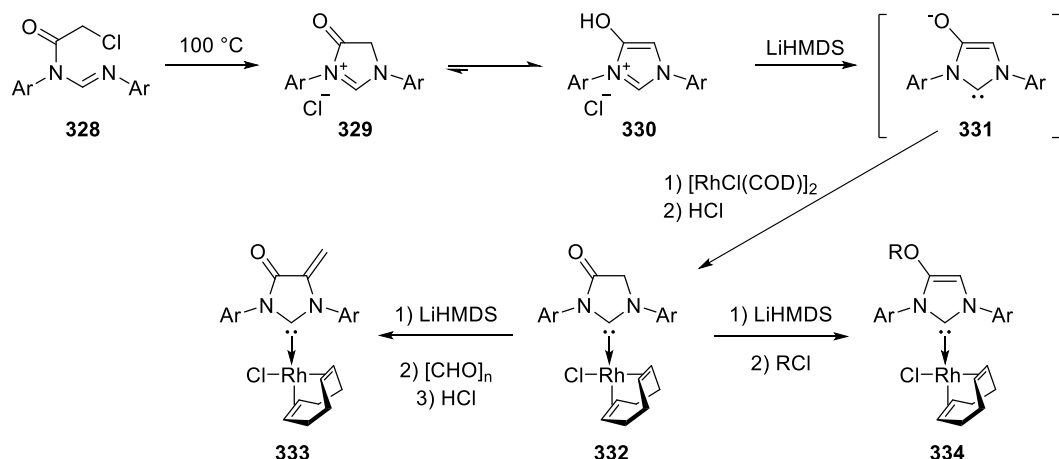


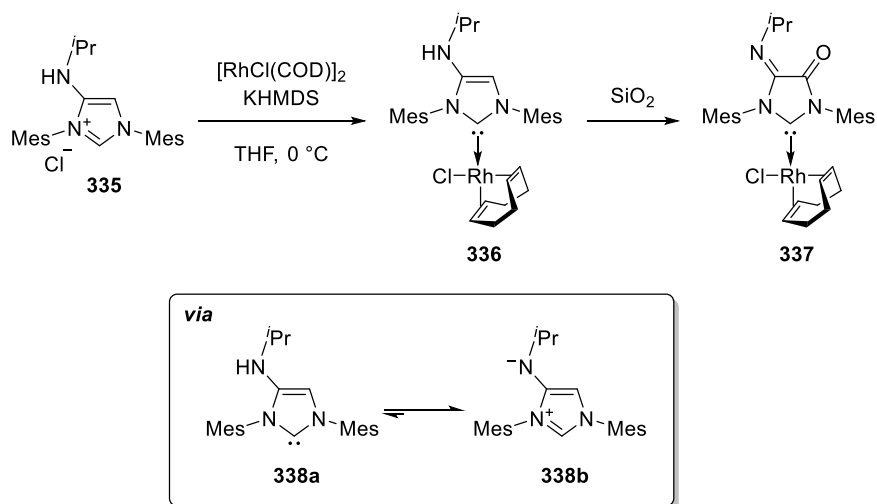
**Figure 36: Top: Postulated reversible *in situ* coordination and protonation processes of pyridinyl containing NHC ligands. Bottom: Reversible carboxylate coordination.**

Lavigne investigated the incorporation of reactive functionality within the ligand backbone by preparing hydroxyimidazolium **330** *via* the synthesis and tautomerisation of **329** (Scheme 87).<sup>200,201</sup> Carbene formation generated anionic NHC **331**, which was subsequently trapped with rhodium and protonated to give **332**. *O*- and *C*- functionalisation of the ligand backbone was achieved *via* enolate formation and trapping with a subsequent nucleophile.



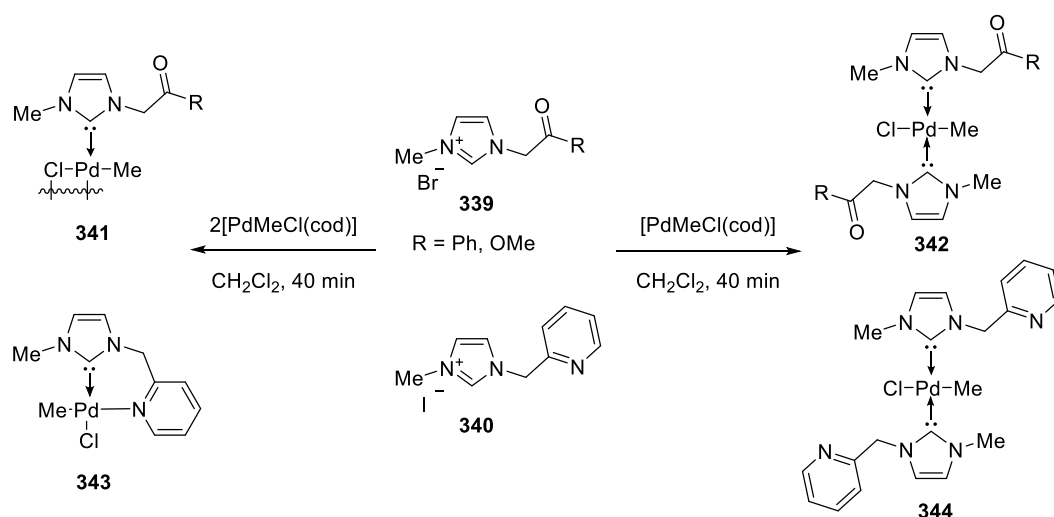
Scheme 87: Synthesis and functionalisation of reactive ligand backbones by Lavigne.

Lavigne then prepared secondary amine derivative **335** (Scheme 88).<sup>202</sup> Again, **335** underwent tautomerization upon deprotonation to isolable mesoionic species **338b**. Trapping of carbene tautomer **338a** with rhodium provided **336**, confirming the masked carbene character of **338b**. Treatment with SiO<sub>2</sub> gel under air caused a rapid four electron oxidation to amido-amidino complex **337**. Analysis of the TEP values revealed a 12.8 cm<sup>-1</sup> difference between **336** and **337**, highlighting the significantly reduced  $\sigma$ -donor ability of **337**.



Scheme 88: Tautomerization of amine functionalised carbene **338a** and subsequent trapping with rhodium.

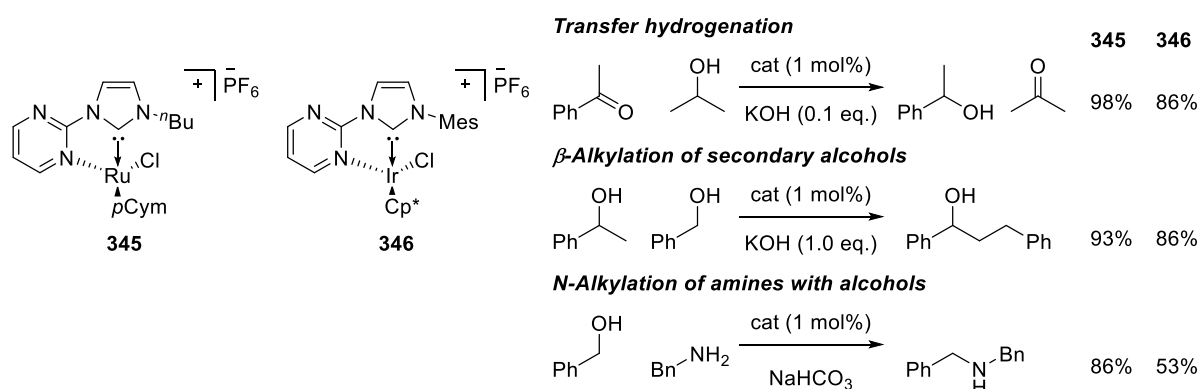
Numerous hemilabile NHC ligands contain secondary coordination sites that provide additional stability in saturated metal complexes whilst reversibly dissociating in solution to generate free coordination sites for catalysis reactions. Cavell produced several of the first examples when preparing **339-340**, a series of donor functionalised NHC precursors (Scheme 89).<sup>124</sup> Carbonyl derivatives **339** provided dimeric and monodentate complexes **341-342**, whereas pyridinyl functionalised **340** delivered both chelating and monodentate complexes **343-344**. When tested in Heck and Suzuki-Miyaura cross-coupling reactions, **343** and **344** provided excellent conversion and some of the highest turnover numbers reported at the time.



**Scheme 89: Donor functionalised NHC ligands and chelation in palladium complexes.**

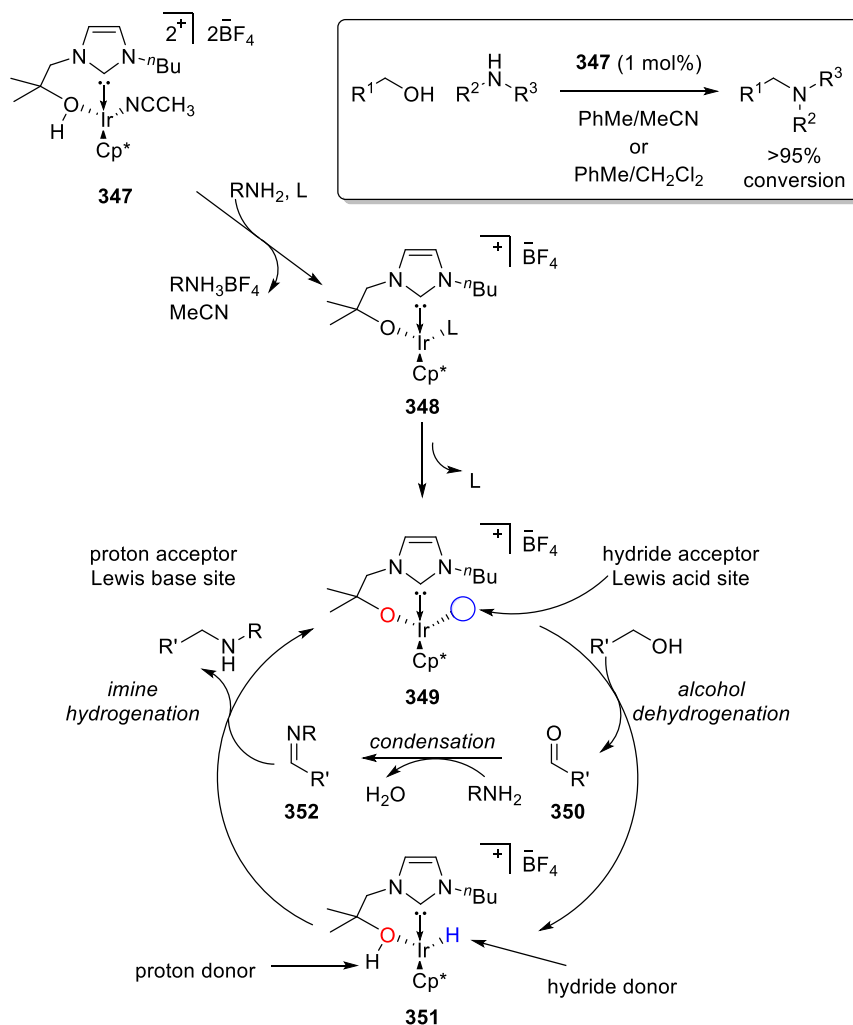
A wide variety of *N*-,<sup>195</sup> *O*-,<sup>191</sup> and *S*-<sup>193</sup> functionalised donor ligands have been investigated. The bulk of these examples employed the secondary coordination site for stabilisation of the electrophilic metal centre, from which dissociation provided an accessible coordination site for catalytic pathways. Often these chelating abilities provided positive impacts upon the catalytic processes, improving conversion and turnover rates of the catalysts.

Bifunctional NHC ligands influence catalytic processes through substrate interaction. Often this coincides with hemilabile ligand characteristics. Crabtree utilised pyrimidyl complexes **345**-**346** to perform hydrogen borrowing processes, allowing transfer hydrogenation,  $\beta$ -alkylation of secondary alcohols and *N*-alkylation of amines (Scheme 90).<sup>203</sup> The pyrimidyl unit acted as an internal base in the amine alkylation process, allowing for mild base NaHCO<sub>3</sub> to be used in place of strong bases such as KOH that were used previously.



**Scheme 90: Novel chelating pyrimidine NHC ligands that improve catalytic activity.**

Martin-Matute subsequently prepared **347**, the first alcohol chelated bifunctional system capable of catalysing hydrogenations, alongside various alkoxide derivatives (Scheme 91).<sup>204</sup> After demonstrating a range of *N*-alkylations of primary and secondary amines with primary alcohols, it was postulated that this transformation proceeds *via* a hydrogen borrowing mechanism. The dehydrogenation-hydrogenation process is facilitated by the bifunctional ligand, by generation of proton and hydride acceptor and donor sites. In the absence of the NHC ligand, only 12% conversion was observed. Computational and experimental evidence supported this mechanism, revealing the rate-determining step to be the addition of iminium hydride **351** to imine **352**.<sup>205</sup>



**Scheme 91: Hydrogen borrowing process during amine alkylations with primary alcohols. Reproduced from ref [204].**

A final application of NHC ligands that has recently gained increased attention is their interaction with metal surfaces.<sup>206–208</sup> In particular, their ability to form well defined transition metal nanoparticles in a controlled manner that exhibit excellent stability and limit aggregation. Their potential in transition metal catalysis and the effects of modifying the NHC ligands has been discussed in recent reviews that cover their synthesis, reactivity and application across a range of transition metals.<sup>206–208</sup>



## 4.6 Conclusion

Development of NHC ligands has grown exponentially over the last 20 years, providing significant improvements in transition metal catalysis. A wide variety of flexible and rigid NHC backbones have been developed, offering unique electronic and steric impacts. The introduction of bulky substituents into the coordination sphere of transition metal complexes has been shown to stabilise reactive organometallic intermediates and improve catalytic processes. Hemilabile tethers have provided additional stability to transition metal pre-catalysts, from which flexible decoordination resulted in improved catalyst activity and durability.

Exploration of SMART NHC ligands, particularly through bifunctional catalysis, is of great interest when designing novel catalyst systems. The following results and discussion chapters describe the preparation of novel annulated imidazolylidene precursors that contain modifiable functionality and their coordination to transition metals.

# Chapter 5: Novel strategies to access heterocyclic fused imidazolium salts

## 5.1 Aims, objectives and ligand design

The aim of the following work was to synthesise a range of annulated imidazolium salts for use as NHC precursors. Oxazole-fused system **353** had been identified as a suitable NHC precursor within our research group. The heterocyclic framework was attractive due to the untapped potential of heterocycle fused imidazolylienes with a pendant nitrogen group close to the metal centre (Figure 37). This then led to the design of pyrimidine annulated heterocycles **354** and **355** that incorporated secondary amine and guanidine residues within the ligand. Each framework presented a novel and unique fused backbone, with their impact on the donor ability of the subsequent carbene of interest.

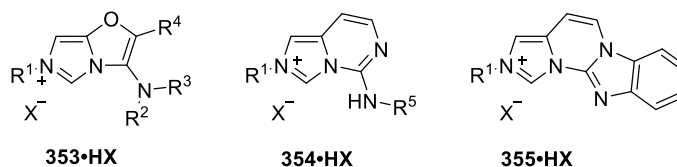
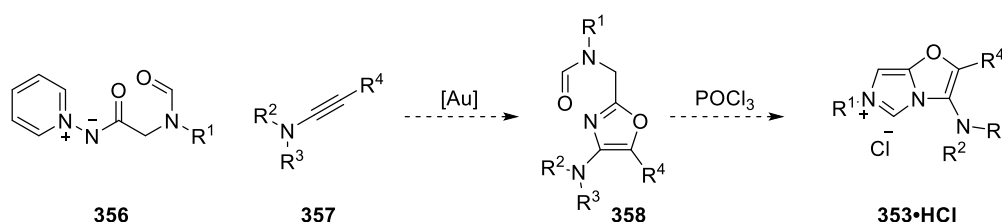


Figure 37: NHC precursors targeted during ligand design.

Additionally, each scaffold contained a nitrogen located near the carbenic carbon, such that when coordinated to a TM, there was potential for interaction through either the appended functionality (**353**), the NH (**354**) or the nitrogen lone pair (**355**). The ability to install various functional groups at this nitrogen in a modular fashion for NHC precursors **353** and **354** also presented an opportunity for crowding the coordination sphere of TM complexes, increasing the shielding of reactive organometallic species and introducing pathways for asymmetric induction with chiral ligands.

The synthetic route for oxazole-imidazolium **353** stemmed from previous work using the gold-catalysed oxazole formation developed within the Davies group (Scheme 92).<sup>48–50</sup> With flexibility in the choice of ynamide **357** used, a synthetic route that allowed rapid access to a library of oxazole-fused imidazolium salts was proposed. This ability to introduce a variety of different functionalities *via* the ynamide substituents presented an excellent opportunity to tune the steric environment around the TM centre.



**Scheme 92:** Planned synthesis route for oxazole imidazolium salts, building on the work of ADG.

The remaining frameworks contained a pyrimidine-imidazole fused NHC core. Whilst there are examples in the literature of a pyrimidine ring attached to the imidazolium through the imidazole nitrogen (Scheme 90),<sup>209–211</sup> this would represent the first example of a pyrimidine annulated imidazolium.

Interest in these systems was threefold (Figure 38). Firstly, the fused pyrimidine ring was in conjugation with the imidazolylidene, and therefore had the potential to influence the electronic properties of the carbene interaction with TMs when complexed. Reversible protonation of **359** to **360** at the pyrimidine nitrogen would reduce the electron density within the  $\pi$ -system, resulting in a more electron-deficient metal centre. This introduced the potential for switchable reactivity under protic conditions. Secondly, aniline **361** and guanidine **362** residues offer sites for secondary coordination from the ligand backbone. Direct coordination of either group would offer stabilisation of reactive TM complexes with vacant coordination sites, aiding oxidative

addition processes. Finally, the same reactive site offers the potential for substrate interaction and the opportunity for synergistic activation of both the electrophilic and nucleophilic reaction sites.

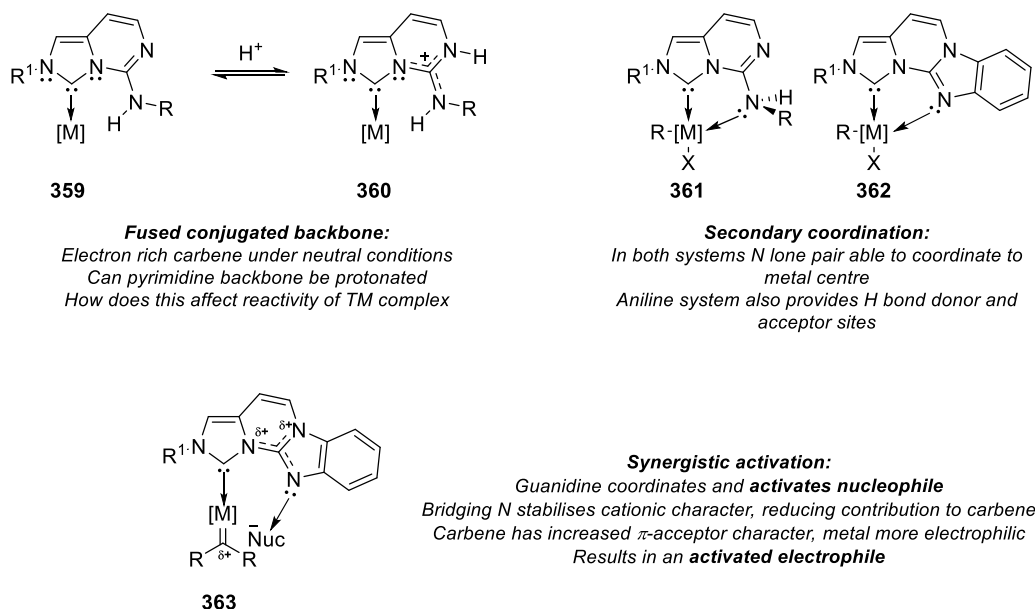


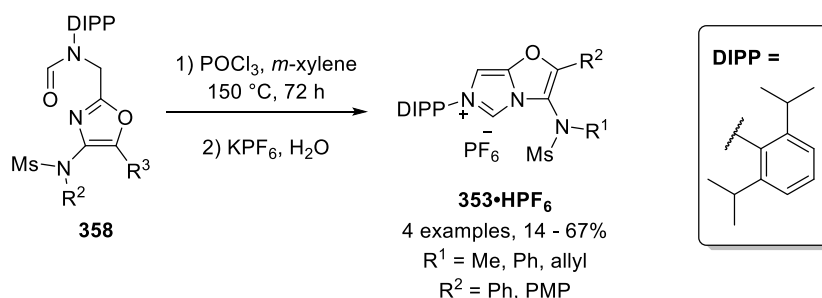
Figure 38: Design features in pyrimidine annulated imidazolylidenes.

With these exciting ligand designs in mind, modular and scalable synthesis routes that would provide access to a unique range of NHC precursors were desired.

## 5.2 Oxazole annulated imidazolium salt synthesis

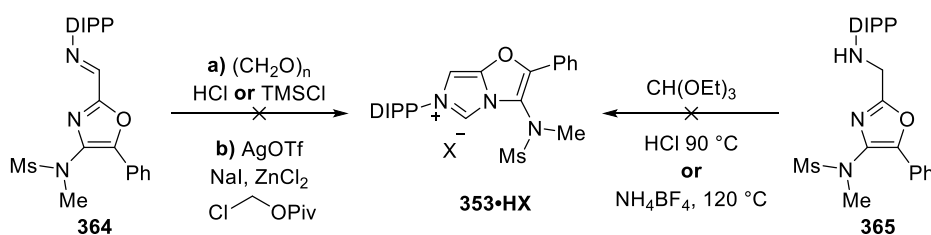
Building on the broad functional group tolerance facilitated by the gold-catalysed [3+2] dipolar cycloaddition, previous investigations within the Davies group had identified 4-aminoxazole **358** as a suitable precursor to imidazolium salts **353**•HPF<sub>6</sub>. Exploration of ring-closing reaction conditions had demonstrated that the desired imidazolium salts **353** were only formed when treating formamide **358** with POCl<sub>3</sub> at high temperatures (Scheme 93). Due to phosphorus-based impurities being present in the <sup>31</sup>P-NMR after purification, salt metathesis was performed to isolate the HPF<sub>6</sub> salts. While this provided clean samples, solubility of the imidazolium salts

in H<sub>2</sub>O was sparing due to the bulk of the ligand being hydrophobic resulting in diminished yields. In addition to the solubility issues, NHC precursors bearing [PF<sub>6</sub>]<sup>−</sup> counterions could not be used in silver trans-metalation routes without providing bis-NHC silver complexes.



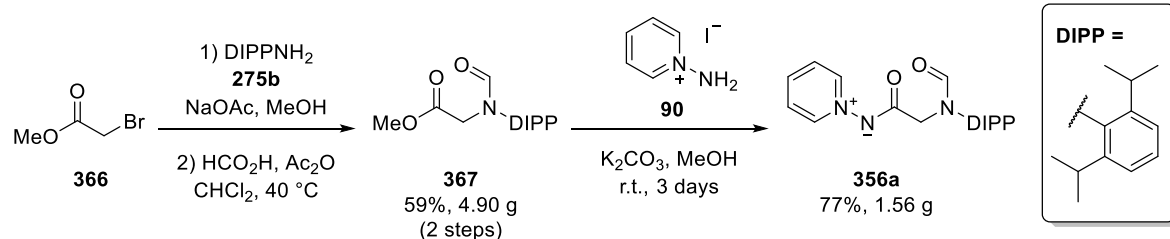
**Scheme 93:** POCl<sub>3</sub> mediated ring closure and salt metathesis developed by ADG.

Whilst imine and secondary amine motifs **364** and **365** have been readily accessed, the corresponding cyclisation conditions to access **353•HX** proved to be ineffective for the oxazole substrates (Scheme 94).



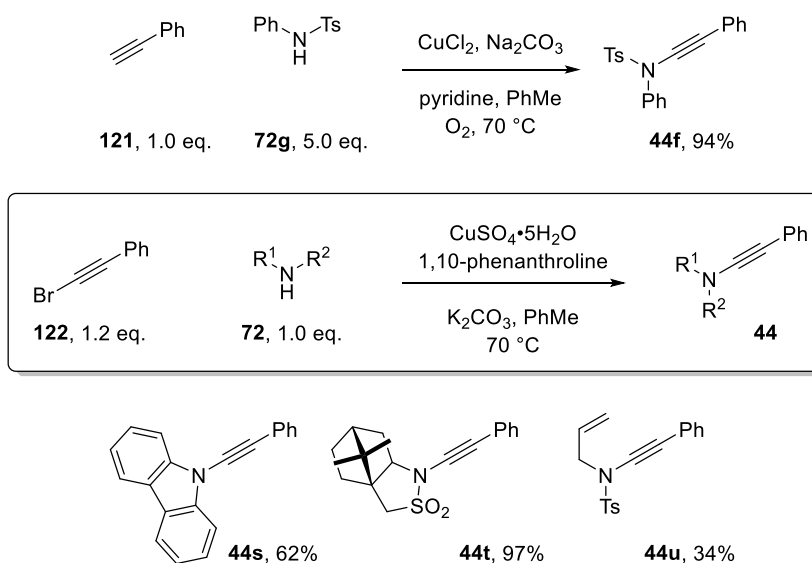
**Scheme 94:** Attempted syntheses of oxazole annulated imidazolium **353•HX** performed by ADG.

In view of these initial results, ylide **356a** was prepared on a multigram scale (Scheme 95). A two-step process afforded formamide **367** through alkylation of **275b** with methyl bromoacetate, followed by formylation through treatment with acetic anhydride and formic acid. **367** was then reacted with *N*-aminopyridinium iodide and K<sub>2</sub>CO<sub>3</sub> in MeOH to access ylide **356a**.



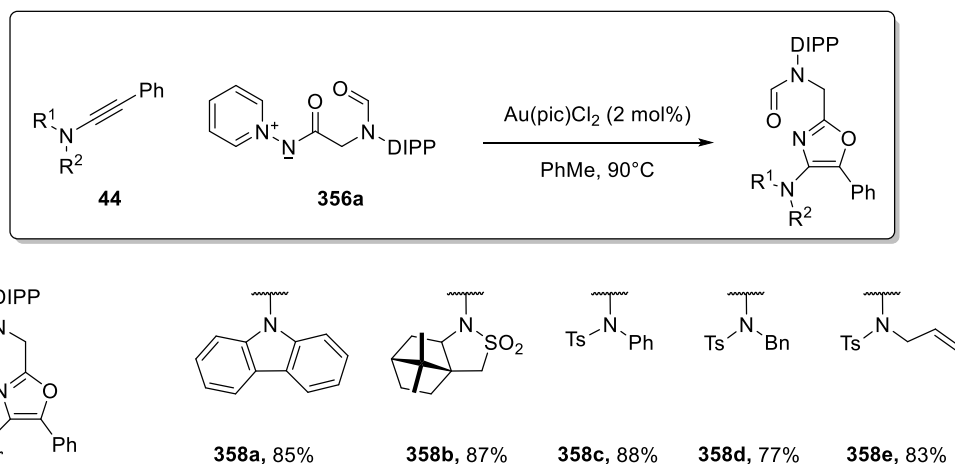
Scheme 95: Multigram synthesis of formamide ylide **356a**.

Ynamides **44** were then prepared according to literature procedures (Scheme 96). **44s** was chosen for both its size and aromaticity, with the  $\pi$ -system of the carbazole offering potential sites for secondary coordination. Camphor sultam **44t** was selected for its significant three-dimensional bulk and chirality, presenting an opportunity for asymmetric catalysis. Allyl containing ynamide **44u** was selected due to the known ability of allyl groups to coordinate to transition metals through  $\pi$ -interactions.



Scheme 96: Ynamide synthesis employing the Stahl<sup>55</sup> and Hsung<sup>54</sup> methodologies.

With the precursors in hand, ylide **356a** was combined with ynamides **44** under the gold-catalysed protocol to access oxazoles **358a-e** (Scheme 97). In all cases the ynamide was consumed within 6 h, resulting in simple purification procedures, albeit with double-banding in the TLC analysis due to the presence of amide rotamers.



**Scheme 97: Gold-catalysed oxazole formation utilising ylide 356a.**

To confirm the presence of amide rotamers, clearly visible in the  $^1\text{H}$ - and  $^{13}\text{C}$ - NMR spectra at r.t., a variable temperature  $^1\text{H}$ -NMR spectroscopic study was performed on **358a** (Figure 39). The results demonstrated that even at 125 °C the formamide shows a remarkable preference for the *Z* conformation, with only a minor shift in the *E*:*Z* ratio.

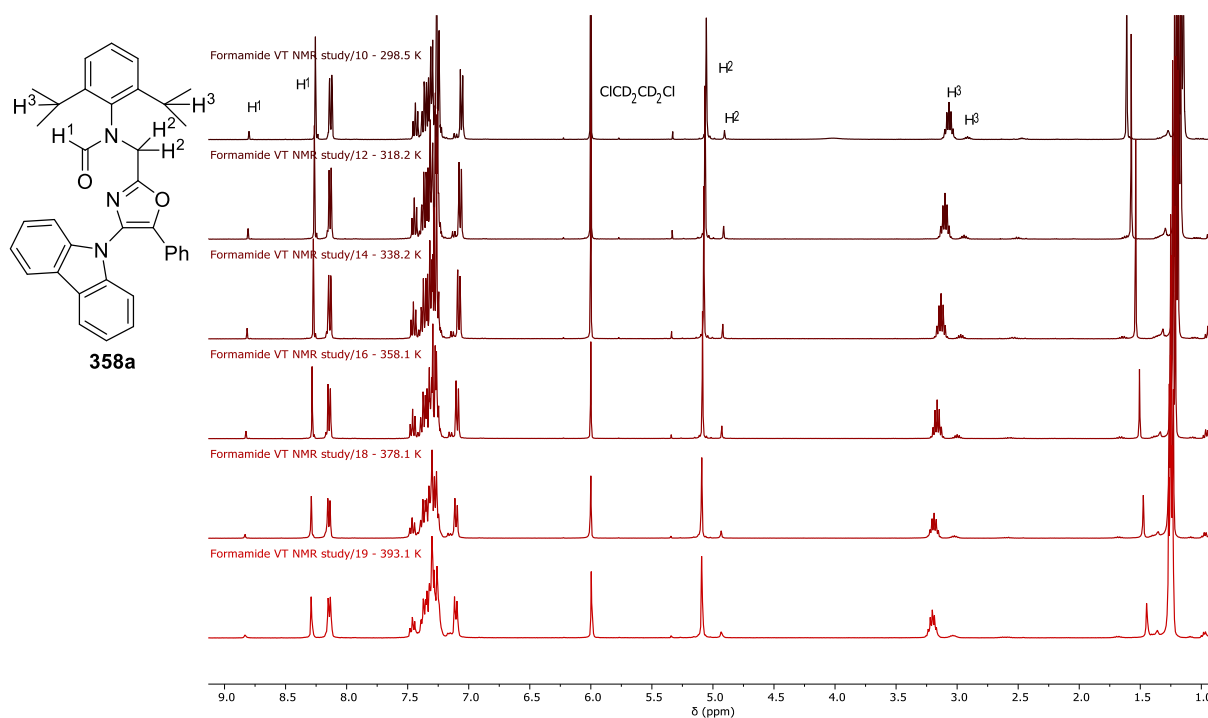


**Figure 39: Variable temperature  $^1\text{H}$ -NMR study of formamide 358a, increasing temperature down the series. Amide rotamers present in a 10.5:1.0 ratio at 298.5 K, shifting to 7.5:1.0 at 393 K.**

Assignment of the major amide conformer was made through single crystal XRD analysis of **358a**, which showed the carbazole unit to be out of plane with the oxazole and the formamide likely preferring the *Z* conformation (Figure 40).<sup>k</sup> Free rotation around the C<sub>2</sub>-C<sub>3</sub> σ-bond would allow the formamide to reposition such that interaction with N<sub>2</sub> would be possible. It was postulated that the harsh reaction temperature required in the subsequent imidazolium formation may be due to the preference for an unreactive amide configuration for cyclisation, with a high energy barrier for rotation requiring significant thermal energy.

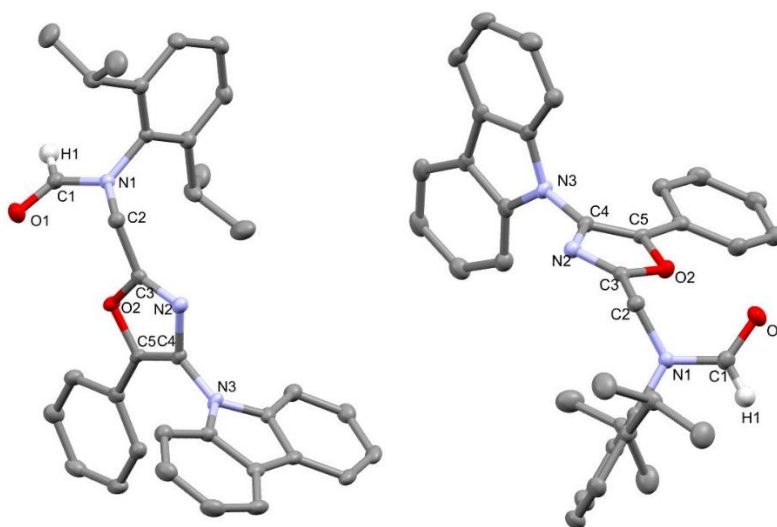
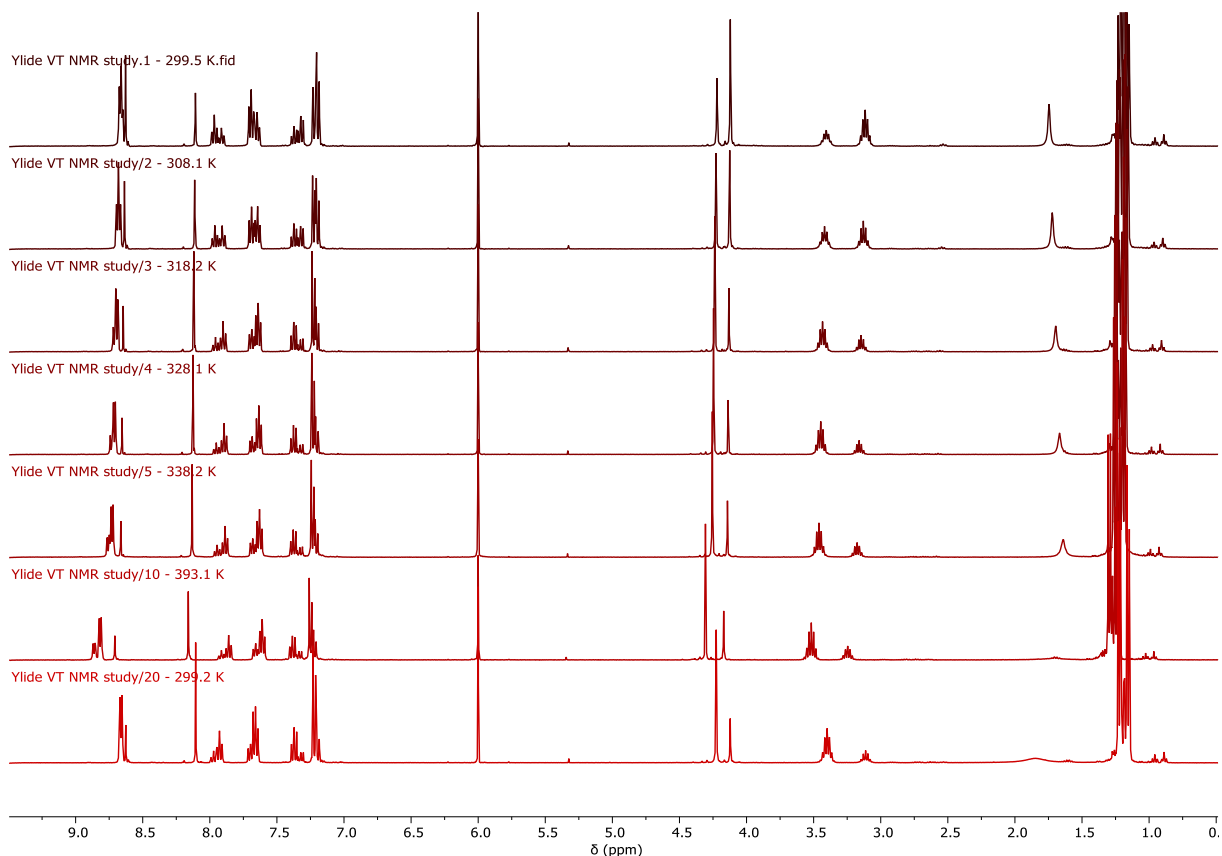


Figure 40: X-ray structure of **358a**. Ellipsoids at 50% probability, hydrogens omitted for clarity except at the formamide. X-ray data obtained and solved with assistance from Dr Louise Male.

When a variable temperature <sup>1</sup>H-NMR spectroscopy study was performed on ylide **356a**, the rotamer resonance ratio inverted between 35 – 45 °C and did not reverse when cooled to room temperature (Figure 41). This indicated that the energy barrier to rotation in **356a** was much lower, allowing for conversion between the *E*- and *Z*- amide isomers at significantly lower temperatures.

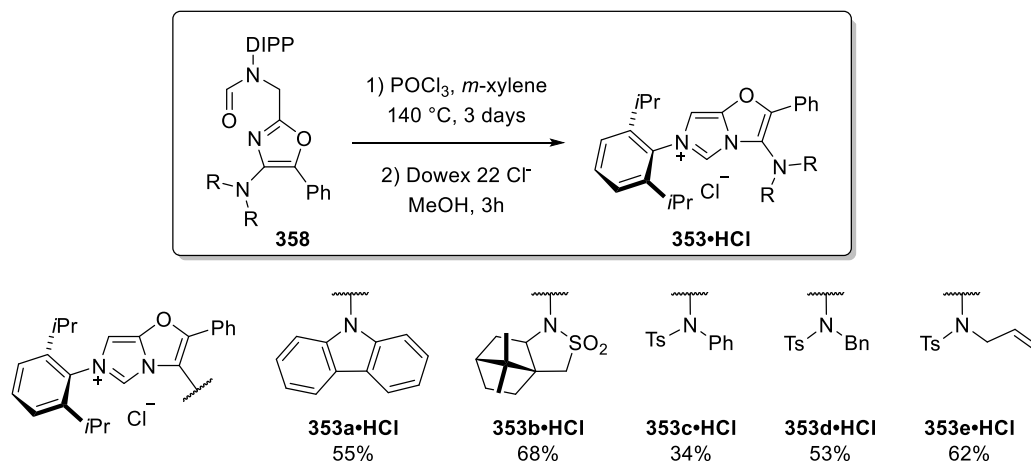
<sup>k</sup> Oxazole **358a** showed a 20:1 mixture of amide rotamers at r.t. in the <sup>1</sup>H-NMR spectra. A single crystal suitable for XRD analysis was grown from this mixture, therefore the *Z* configuration cannot be definitively assigned.





**Figure 41:** Variable temperature  $^1\text{H}$ -NMR study of ylide **356a**. Ratios of amide conformers: 1.0:1.7 at 299.5 K. 2.4:1.0 at 393.1 K. 3.1:1.0 after allowing to cool back to 299.2 K.

Oxazoles **358a-e** were swiftly converted to the corresponding imidazolium salts **353•HCl** by heating with  $\text{POCl}_3$  at 140 °C (Scheme 98). Treatment of the crude reaction mixtures after aqueous work up with Dowex 22  $\text{Cl}^-$  counterion exchange resin, as used by Lassaletta in another  $\text{POCl}_3$  mediated imidazolium formation,<sup>134</sup> followed by flash column chromatography provided the hydrochloride salts with no detectable phosphorus containing impurities within the  $^{31}\text{P}$ -NMR spectra. This negated the need for a counterion exchange with  $\text{KPF}_6$  under aqueous conditions, which had reduced the isolated yields due to poor solubility in water when performed previously in the Davies group (Scheme 93), and provided suitable material for silver transmetalation methods discussed in Chapter 6.1.



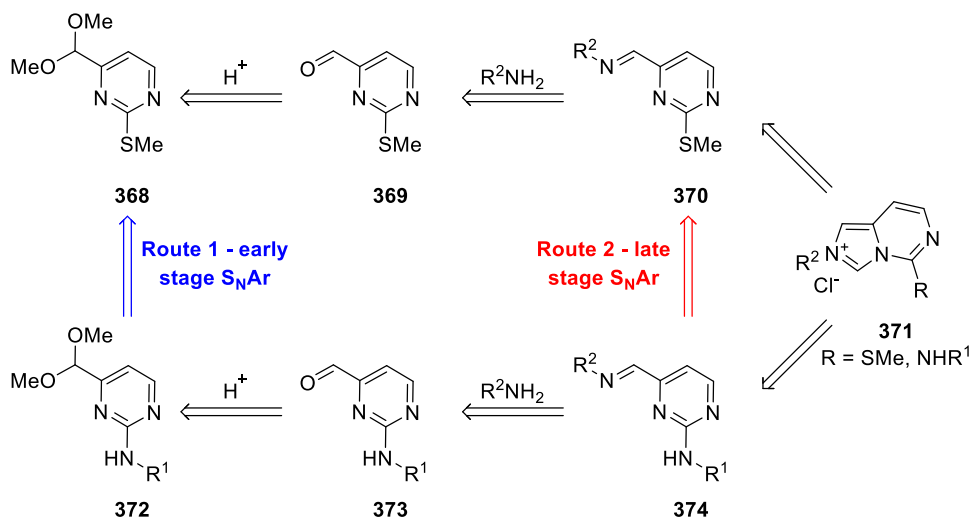
**Scheme 98:** POCl<sub>3</sub> mediated cyclisation to form imidazolium•HCl salts.

With five unique oxazole annulated imidazolium salts in hand, having confirmed the presence of amide rotamers and providing plausible reasoning for the low reactivity of oxazoles **358** towards cyclisation, their complexation to transition metals was studied (*vide infra*, chapter 6.1).

## 5.3 Pyrimidine annulated imidazolium salt synthesis

### 5.3.1 Design of the synthesis route

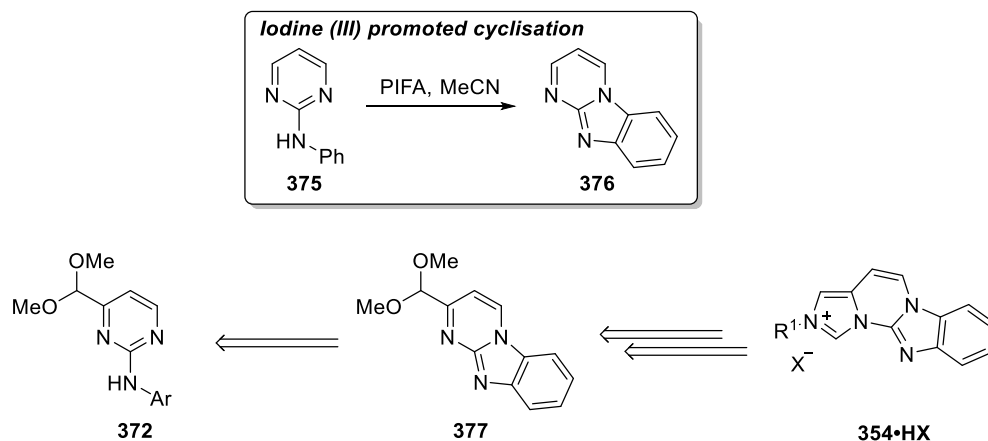
Attention was then turned to developing a robust methodology that provided access to pyrimidine fused imidazolium salts. The planned synthesis route focused on the preparation of dimethylacetal pyrimidine derivative **368** (Scheme 99). The acetal was crucial as a reactive handle to access aldehyde **369** through acetal hydrolysis. Subsequent imine formation and cyclisation would then provide imidazolium salt **371**. A sulfide handle was selected in **368** for S<sub>N</sub>Ar reactivity such that a range of nucleophiles could be installed to modify the ligand properties within TM complexes.



**Scheme 99: Planned synthesis route for pyrimidine annulated imidazolium salts.**

Two approaches were initially considered for the generation of a library of pyrimidine fused NHC precursors. The first approach (route 1) looked to prepare aminopyrimidine **372** with an early stage  $S_NAr$  reaction from **368**, before installation of the imine functionality and cyclisation. The second approach (route 2) looked to install the imine functional group and then attempt  $S_NAr$  reactions upon **370** at a later stage. The latter would provide a modular route and allow late stage introduction of a range of nucleophiles to modify ligand characteristics around the metal centre. However, the sensitivity of imines and amines towards oxidation and nucleophilic addition made the first approach the more attractive option.

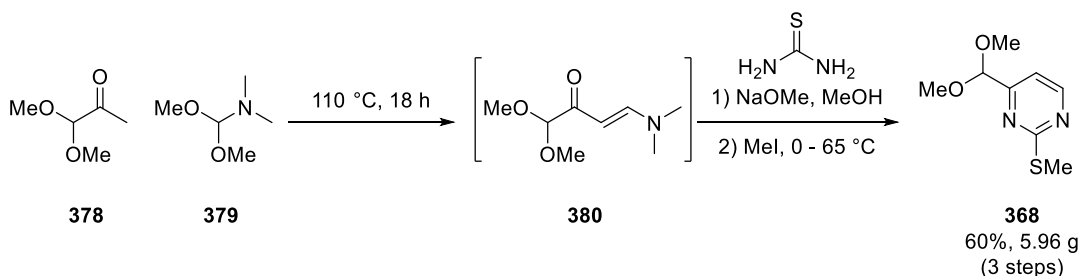
The preparation of imidazopyrimidine **354** was then based on a hypervalent-iodine promoted cycloamination of aminopyrimidine **375** developed in 2014 to deliver **376** (Scheme 100).<sup>212</sup> It was questioned whether the same conditions could be used to access **377** in a regioselective manner in the presence of a dimethyl acetal functional group. If **377** could be accessed under these conditions, the same acetal hydrolysis, imine formation and cyclisation approach could deliver **354·HX**.



Scheme 100: Hypervalent iodine promoted synthesis of imidazo-pyrimidine and retrosynthetic analysis to access 354.

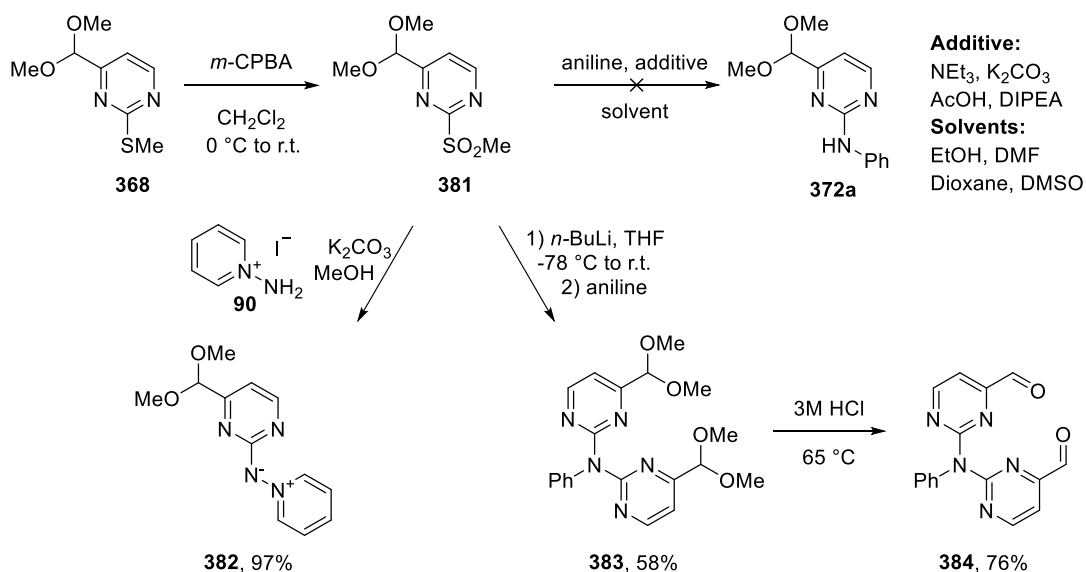
### 5.3.2 Condensation reactions to access functionalised pyrimidines

With a synthetic strategy in hand, sulfide **368** was prepared (Scheme 101). Condensation of **380**, generated *in situ* by heating **378** and **379**, with thiourea and subsequent methylation afforded **368** on a multigram scale. Freshly prepared NaOMe was found to be essential to obtain good yields.



Scheme 101: Condensation reaction utilising thiourea to access 368.

Sulfide **368** showed no reactivity towards  $\text{S}_{\text{N}}\text{Ar}$  reactivity under various conditions. Therefore oxidation of **368** to sulfone **381** was achieved in excellent yield through reaction with *m*-CPBA to increase the electrophilicity of the pyrimidine and provide a superior leaving group (Scheme 102). Subsequently, several  $\text{S}_{\text{N}}\text{Ar}$  conditions were tested to replace the sulfone moiety by a range of amines derivatives.



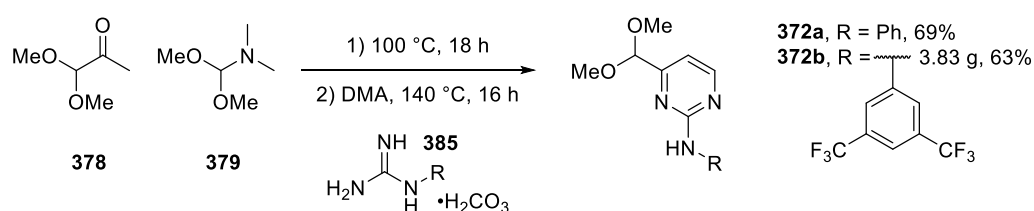
**Scheme 102: Attempted  $\text{S}_{\text{N}}\text{Ar}$  reactions with sulfone **381**.**

Disappointingly anilines proved to be poor nucleophiles with a variety of organic and inorganic bases. When *n*-BuLi was used to access the lithium amide, **383** was recovered as the major product through double alkylation. This stemmed from the higher acidity of **372a** compared to aniline, resulting in the preferential formation of the lithium amide of **372a** in solution. Although an undesired product, conversion of **383** into bis-aldehyde **384** offered potential access into an attractive Schiff base motif through imine formation, with a rigid backbone that would offer an interesting template in metal coordination studies. If mono-substitution could be controlled, that  $\text{S}_{\text{N}}\text{Ar}$  proceeds with alkyl lithium reagents would allow a variety of substituted anilines to be employed. Moreover, **90** proved to be a suitable nucleophile in the presence of  $\text{K}_2\text{CO}_3$  to access ylide **382**; this demonstrated that stronger nucleophiles could be utilised under milder conditions.

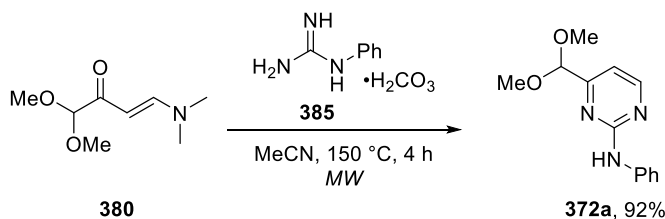
Due to the poor reactivity of sulfone **381** towards substitution, a separate approach was taken to deliver aminopyrimidine **372a**. By replacing thiourea with guanidine derivative **385**, generated by reaction of anilines with cyanamide, condensation with *in-situ* generated **380**

delivered desired aminopyrimidine **372a** (Scheme 103). The use of DMA as the reaction solvent was required for increased reaction temperatures, with a drawback being the removal of residual solvent during the extraction. This was then extended to prepare CF<sub>3</sub>-derivative **372b** on multigram scale. Subsequently this process was found to work under microwave irradiation in excellent yields, while significantly reducing the reaction time and simplifying the work up procedure.

**Hotplate heating:**

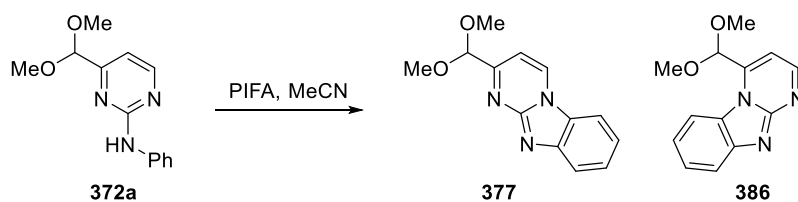


**Microwave irradiation:**



**Scheme 103: Condensation of guanidine derivatives with 380 to form aminopyrimidines.**

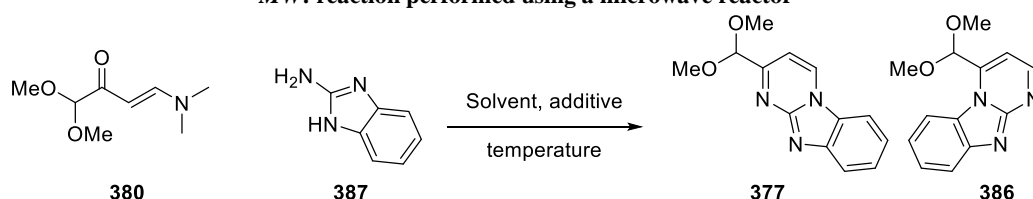
Aminopyrimidine **372a** was then tested under the hypervalent-iodine promoted cycloamination reaction discussed earlier (Scheme 104).<sup>212</sup> Pleasingly the desired cyclisation occurred with PIFA in under 20 minutes, however a 1:1 mixture of separable regioisomers **377** and **386** was isolated.



**Scheme 104: Hypervalent iodine promoted imidazo-pyrimidine synthesis**

Without a handle to modify the regiocontrol, a different method that looked to employ 2-aminobenzimidazole **387** in the condensation reaction was explored to improve the atom economy of the process. A solvent screen was undertaken utilising hotplate and microwave heating to optimise the isolation of **377** (Table 4).

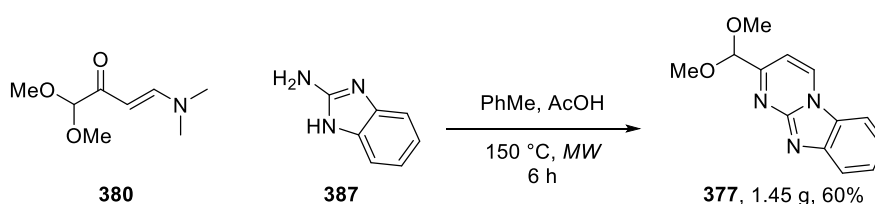
**Table 4: Optimisation for condensation of 380 with 2-aminobenzimidazole 387.** <sup>a</sup> Ratios determined by <sup>1</sup>H-NMR analysis on 1.0 mmol scale reaction. <sup>b</sup> Isolated yield. NR- not recovered. HP: reaction performed using a hotplate. MW: reaction performed using a microwave reactor



Entry	Solvent	T (°C)	Time (h)	Δ	377 <sup>a</sup>	386 <sup>a</sup>	380 <sup>a</sup>
1	DMA	140	18	HP	1.00	3.00	1.20
2	MeCN	88	16	HP	1.00	1.09	1.50
3	MeOH	65	18	HP	0.00	0.00	1.00
4	PhMe	110	18	HP	1.00	2.38	1.79
5	Pyridine	115	18	HP	1.00	2.86	2.17
6	MeCN	150	2	MW	1.00	1.43	4.29
7	MeCN	150	4	MW	1.00	1.75	1.21
8	THF	150	4	MW	1.00	1.92	1.00
9	MeOH	150	4	MW	1.00	2.94	1.47
10	PhMe	150	4	MW	1.00	1.27	0.13
11	PhMe	150	5	MW	30% <sup>b</sup>	35% <sup>b</sup>	20% <sup>b</sup>
12	PhMe	150	6	MW	48% <sup>b</sup>	NR	NR
13	PhMe + AcOH	150	6	MW	1.00	0.27	0.16

Initial attempts heating **380** with **387** in DMA and MeCN at reflux showed moderate conversion to **377** and **386**, with a significant amount of **365** remaining (Table 4, entries 1-2). A solvent screen was then performed to survey the effect of solvent polarities on the selectivity of the condensation (Table 4, entries 1-5). Under hotplate heating, a clear preference for undesired regioisomer **386** was evident in all cases, with MeCN providing the best ratio. No clear trend was observed with regards to solvent polarity; however, it became clear that the condensation required high temperatures for optimum conversion.

To accommodate increased reaction temperatures, the reaction was tested under microwave irradiation at 150 °C in MeCN to assess the effect on rates of reaction and regioselectivity relative to thermal heating (Table 4, entries 6-7). A minimum reaction time of 4 h was necessary for comparable consumption of **380**, however the amount of undesired regioisomer **386** increased. THF, MeOH and PhMe were then tested under microwave heating (Table 4, entries 8-10). PhMe provided the best reaction outcome, with an extended reaction time of 6 h affording 48% of desired compound **377** (Table 4, entry 12). Having observed that pyridine favoured **386**, an acidic additive was tested (Table 4, entries 5 and 13). Addition of 1.0 equivalent of AcOH was advantageous to the selectivity, favouring the formation of **377**. This reaction was then repeated at a larger scale to deliver 1.45 g of **377** (Scheme 105).



**Scheme 105: Gram scale synthesis of imidazopyrimidine **377**.**

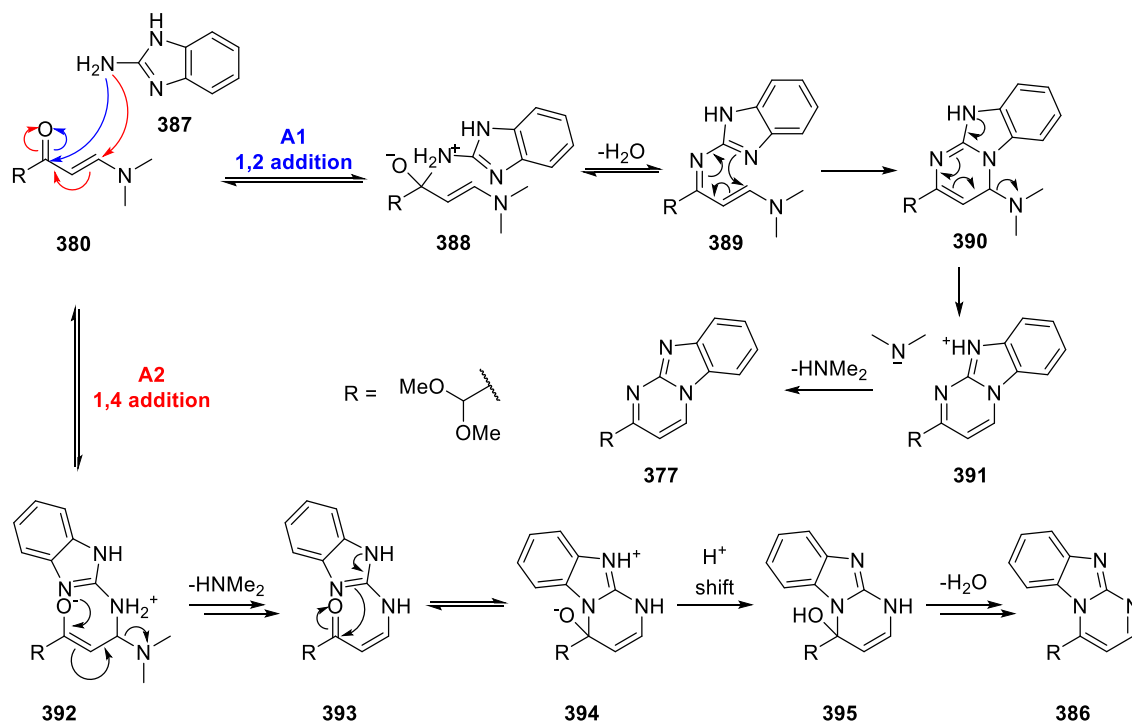
The effect of an acidic additive on the regioselectivity was apparent, however the role of AcOH in favouring desired regioisomer **377** was unclear due to the various mechanisms possible in the condensation reaction. With a primary amine and an activated imidazole, **387** contains two nucleophilic sites that could attack enone **380** in a 1,2- or 1,4- fashion.

If the primary amine acted as the nucleophile, 1,2-addition would deliver imine **389** via dehydration of **388** (Scheme 106, A1). Subsequent electrocyclisation provides **390**, from which HNMe<sub>2</sub> is eliminated to give desired regioisomer **377**. In contrast, a 1,4-addition elimination process would deliver **393** (Scheme 106, A2). Nucleophilic attack of the imidazole into the



ketone to give **395** would then be followed by a proton shift and subsequent loss of water to deliver unwanted regioisomer **386**.

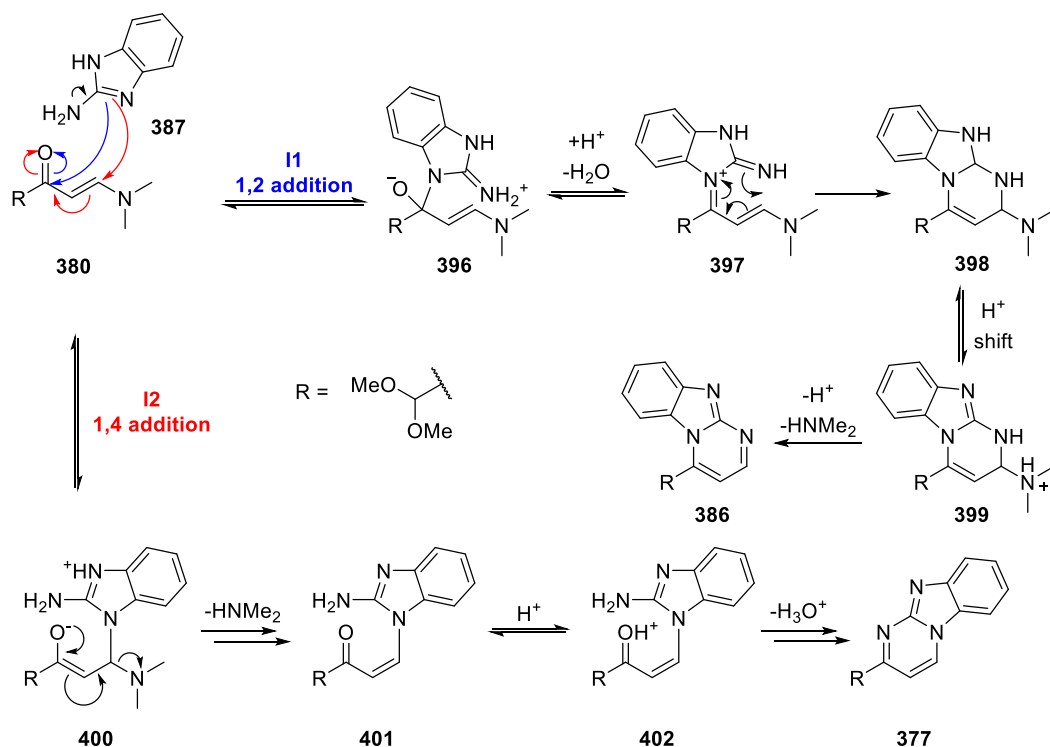
*Nucleophilic attack from the primary amine*



**Scheme 106:** Condensation mechanism with the primary amine as the nucleophile.

The other possibility involves the imidazole nitrogen performing the initial nucleophilic attack. 1,2-Addition would give **397** via iminium formation (Scheme 107, I1). This is then poised to undergo an electrocyclic ring closure to **398**, which undergoes a proton shift, elimination and deprotonation cascade to provide undesired **386**. Finally, if the condensation proceeds by a 1,4-addition elimination process, **401** would be generated and subsequently undergo an imine formation to deliver desired **377** (Scheme 107, I2).

**Nucleophilic attack from the imidazole**



**Scheme 107: Condensation mechanism with the imidazole nitrogen as the nucleophile.**

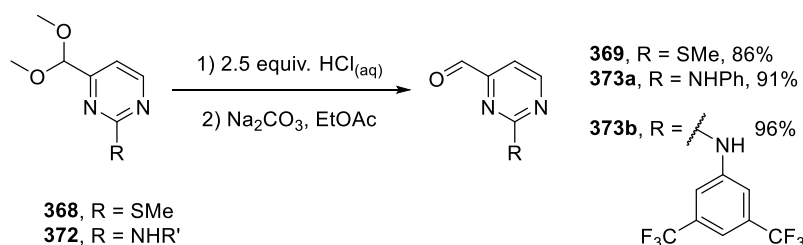
AcOH would promote both 1,2- and 1,4- addition pathways by activation of enone **380**, whilst protonation of the amine or imidazole functional groups in **387** would reduce their nucleophilicity. An acid additive may also increase the rate of reaction by accommodating proton transfer processes.

### 5.3.3 Synthesis of imidazolium salts

#### 5.3.3.1 Initial synthesis of sulfide and aniline functionalised imidazolium salts

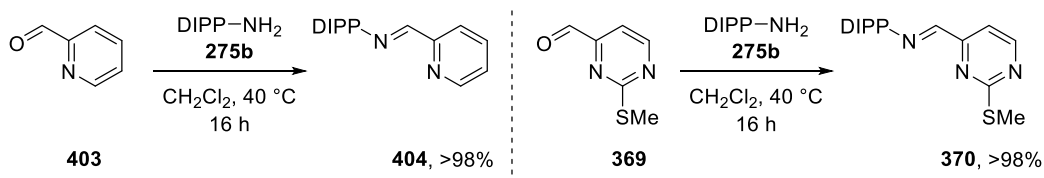
With pyrimidines in hand, conversion into the corresponding imidazolium salts was initially explored with sulfide pyrimidine **368**. Acetal deprotection to aldehyde **369** was achieved under acidic conditions (Scheme 108). Purification by the formation of a bisulfite adduct was attempted to negate flash column chromatography, however the subsequent reversal back to the aldehyde yielded negligible amounts of aldehyde **369** due to its solubility in water.<sup>213</sup> Due to

the solubility of **369** in aqueous media, solid Na<sub>2</sub>CO<sub>3</sub> was used to neutralise the reaction mixture and minimal water was added before extraction and subsequent purification. Aniline derivatives **372** were also hydrolysed to aldehydes **373** following analogous procedures in excellent yields.



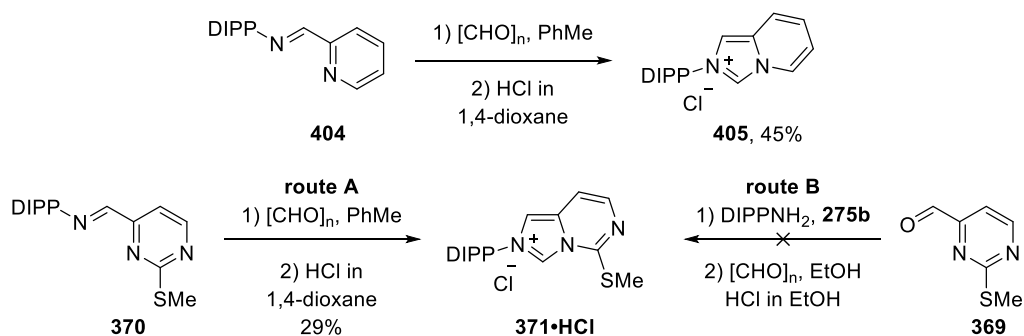
**Scheme 108: Synthesis of aldehyde derivatives through acetal hydrolysis.**

Unlike pyrimidine fused NHC complexes, there are many pyridine-fused backbones described in the literature, from which a suitable pyridine derivative was selected for comparison of the synthesis. Following a literature procedure,<sup>214</sup> condensation of aniline **275b** with picolinaldehyde gave imine **404** in quantitative yields (Scheme 109). Sulfide pyrimidine **369** was subjected to identical conditions and gave access to **370** in excellent yield.



**Scheme 109: Condensation reactions to access imines.**

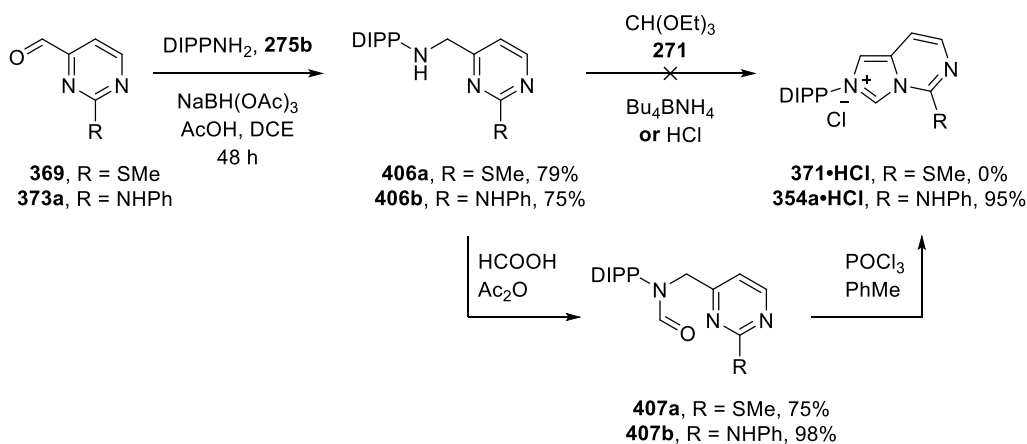
Subsequent treatment of imines **404** and **370** with HCl in 1,4-dioxane and paraformaldehyde in PhMe gave moderate conversion to imidazolium salts **405** and **371•HCl** (Scheme 110, route A). The addition of HCl in 1,4-dioxane to the reaction mixture resulted in immediate precipitation, resulting in ineffective stirring.



**Scheme 110: Imidazolium salt synthesis using paraformaldehyde.**

Attempts at repeating and increasing the scale to access **371•HCl** under the same reaction conditions proved challenging, as poor conversion to the imidazolium was accompanied with various impurities. Another literature procedure was tested using HCl in EtOH that provides a one pot procedure from aldehyde **369** through *in situ* generation of imine **370** (Scheme 110, route B).<sup>215</sup> Whilst using ethanol resulted in a homogenous reaction mixture, TLC analysis showed a complex reaction mixture and no desired product was obtained.

Although the nucleophilicity of the pyrimidine is lower than that of a pyridine, the poor reactivity towards cyclisation was surprising, and so the more nucleophilic aminopyrimidine derivative **373a** was studied alongside sulfide **369** to observe any difference in reactivity towards cyclisation. With various conditions described in the literature for cyclisation of bis-amines, aminopyrimidines **406** were prepared *via* a reductive amination procedure (Scheme 111).



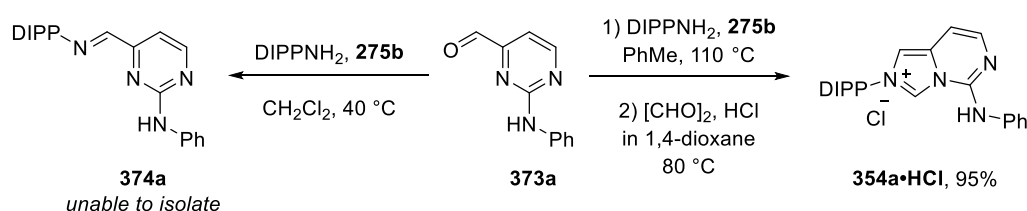
Scheme 111: Synthesis of sulfide and aniline functionalised imidazolium salts.

Amines **406** were then treated with triethyl orthoformate under a variety of acidic media in an attempt to install the precarbenic carbon. In all cases, insignificant amounts of imidazolium salts were observed, with formamides **407** being the major products observed under the reaction conditions. Deliberate formylation through treatment with a mixed anhydride, prepared *in situ*, delivered **407a-b** in excellent yields. On treatment with  $\text{POCl}_3$ , sulfide derivative **407a** once again delivered a disappointing result with no product observed. However aniline derivative **354a•HCl** was isolated in an excellent yield, with the NH moiety intact under the reaction conditions.

### 5.3.3.2 Improved synthesis route to access aniline derivatives

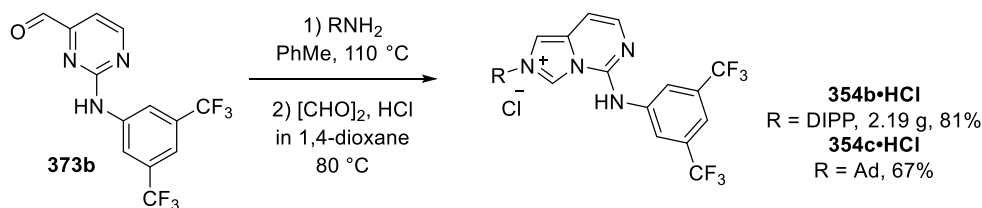
Having recognised that aniline-substituted pyrimidines were significantly reactive towards cyclisation, a more efficient synthesis route was desired. To this end, aldehyde **373a** was combined with **275b** and heated in  $\text{CH}_2\text{Cl}_2$  in an attempt to isolate imine **374a** (Scheme 112). Due to the similar polarity of the two starting materials and the resulting imine, separation by flash column chromatography proved challenging. Nevertheless, it was clear that imine **374a** was forming at only  $40^\circ\text{C}$  and without an acid catalyst. With this observation in hand, a one pot process was envisaged. Aldehyde **373a** was heated at reflux with **275b** in PhMe until

complete consumption of the aldehyde was observed, followed by addition of paraformaldehyde and HCl in 1,4-dioxane at 80 °C (Scheme 112). Almost immediately the reaction mixture turned from yellow to light brown, with a cream solid precipitating. By simply filtering and washing the precipitate, imidazolium salt **354a•HCl** was isolated in excellent yield. The only impurity was PhMe, which was assumed to be trapped in the crystal lattice from precipitation. The remaining PhMe was easily removed by re-dissolving the solid in CHCl<sub>3</sub>, concentration under reduced pressure and drying under high vacuum.



**Scheme 112: Attempted synthesis of imine **374a** and subsequent one pot process to **354a•HCl**.**

The synthetic route was then examined for its ability to modify key parts of the NHC precursors in a modular fashion for tuning of the ligand properties. Trifluoromethyl functionalised pyrimidine **373b**, prepared in Scheme 103, was selected as an electron deficient aniline alternative to **373a** that would increase the acidity of the N-H and provide a hydrogen bonding template. Aldehyde **373b** was combined in the one-pot protocol with **275b** to prepare **354b•HCl** in an excellent yield on a multigram scale (Scheme 113). Modification of the imidazole side chain was then achieved with an alkyl amine to deliver **354c•HCl**. Adamantylamine•HCl was present in the crude material isolated from filtration and purification by flash column chromatography was required. Although not tested, the addition of a sub-stoichiometric amount of an acid catalyst could catalyse imine formation, improving the yield for challenging amines that do not deliver complete consumption of the aldehyde.

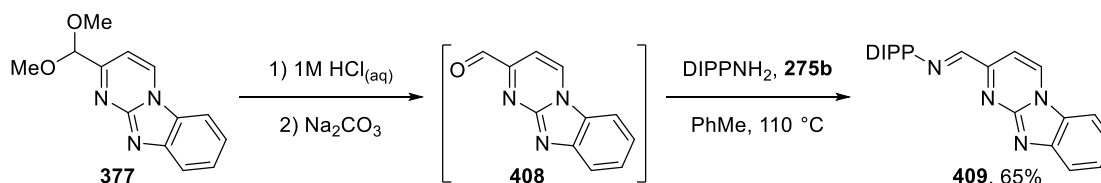


**Scheme 113: Synthesis of fluoro-aniline imidazolium salt derivatives.**

Boosted by evidence that nitrogen substituted pyrimidines appeared more reactive than their sulfide counterparts, a synthesis route to deliver an imidazolium containing a guanidine residue was then explored.

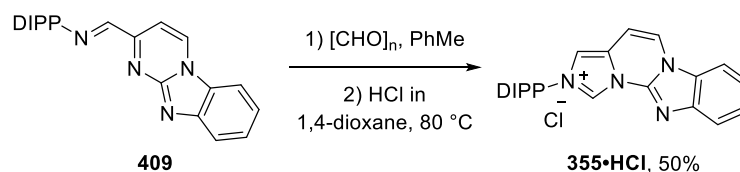
### 5.3.3.3 Synthesis of imidazolium salt containing a guanidine residue

With acetal **377** in hand, hydrolysis under acidic conditions was attempted, however aldehyde **408** proved very polar and was insoluble in  $\text{CDCl}_3$ . When MeOD was used as the NMR solvent the hemiacetal was observed. As the  $^1\text{H}$ -NMR spectra showed that acetal **377** had been consumed, crude aldehyde **408** was then treated with **275b** at reflux, affording iminopyrimidine diisopropylaniline **409** *via* a two-step process (Scheme 114).



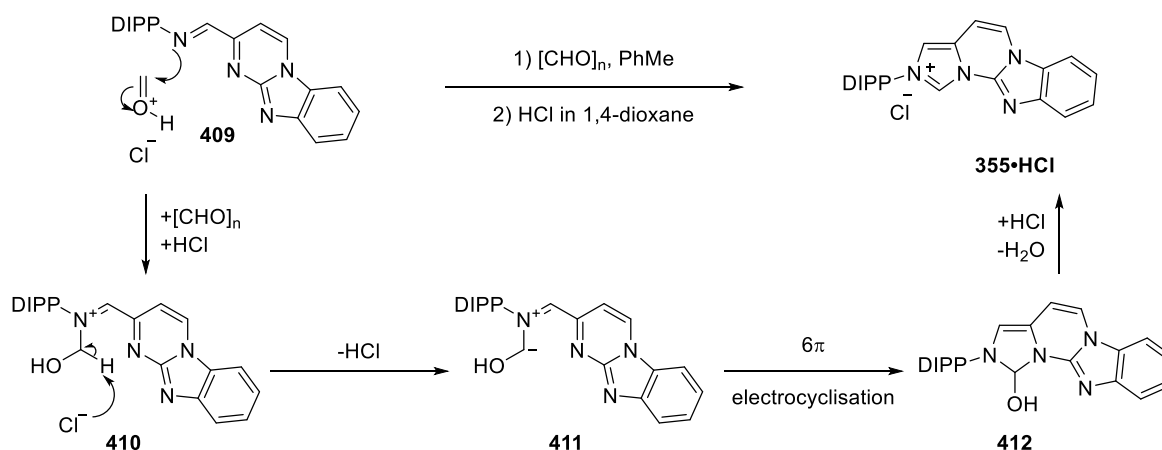
**Scheme 114: Two-step synthesis of iminopyrimidine 409.**

Imine **409** was then treated with paraformaldehyde and HCl in 1,4-dioxane, generating desired imidazolium **355•HCl** in moderate yield (Scheme 115). Due to the basic nature of the guanidine core, 3.0 eq. of acid were used to account for a sacrificial equivalent of acid.



**Scheme 115: Synthesis of imidazolium salt 355•HCl using paraformaldehyde.**

When this reaction was repeated the reproducibility proved low. During several repeat attempts the aldehyde was often recovered alongside the unreacted imine **409**. Examination of the reaction mechanism revealed potential causes of this inconsistency through deactivation of the pyrimidine towards cyclisation through protonation of the imidazole residue (Scheme 116). Attack of imine **409** onto paraformaldehyde generates **410**, which is deprotonated to form 1,5-dipole **411**. This undergoes a  $6\pi$  electrocyclization to produce **412**, which undergoes protonation and dehydration to deliver imidazolium **355•HCl**.

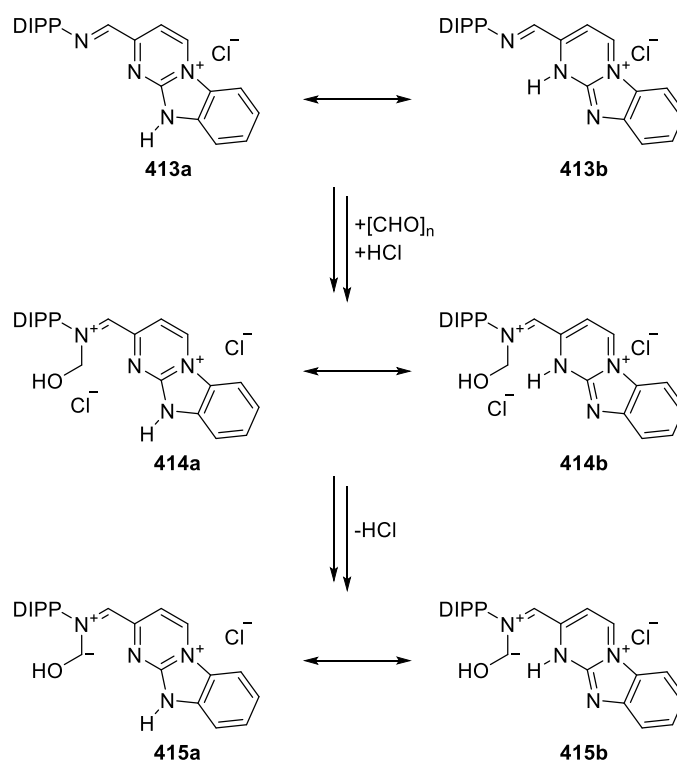


**Scheme 116: Mechanistic considerations for synthesis of 355•HCl.**

HCl is crucial throughout the process: acidic activation of paraformaldehyde; formation of 1,5-dipole **411** through deprotonation from the chloride counterion; and facilitating the final protonation and dehydration steps. However, imine **409** contains a guanidine motif that is more basic than paraformaldehyde. Protonation of either the imidazole or pyrimidine ring generates **413a-b**, which would lead to doubly charged intermediates **414a-b** on attack of



paraformaldehyde (Scheme 117). If 1,5-dipole **415a-b** is generated under the reaction conditions, it contains significantly different electronic properties compared to **411** and may not undergo the  $6\pi$  electrocyclization process.



Scheme 117: Unproductive reaction pathways preventing imidazolium formation.

Due to time constraints, this challenge is yet to be resolved, however the relatively straightforward synthesis of imine precursor **409** and the isolation of **355•HCl** show that with refinement this could be an excellent synthesis route. Single crystal XRD analysis of **355•HCl** demonstrated the potential of the guanidine motif to perform substrate interaction, in this case through hydrogen bonding with water, for the activation of nucleophiles (Figure 42).

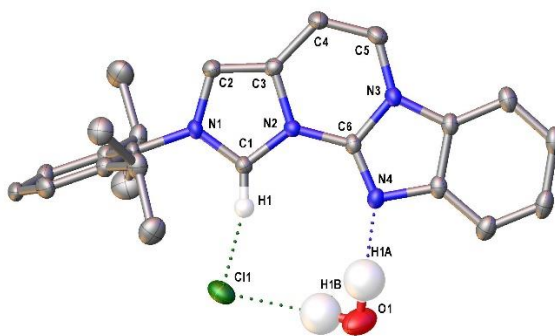


**Figure 42: X-ray structure of 355•HCl revealing hydrogen bond acceptor ability of guanidine residue from crystallisation with a molecule of water. Ellipsoids at 50% probability, majority of hydrogens and CH<sub>2</sub>Cl<sub>2</sub> solvent molecule omitted for clarity. X-ray data was obtained and solved with assistance from Dr Louise Male.**

## 5.4 Conclusion

Five oxazole annulated imidazolium salts have been prepared with varying functionality at the ynamide nitrogen, designed to encumber the coordination sphere of transition metal complexes. These were designed from previous work within the Davies lab and provided a series of tosyl protected sulfonamides with aryl, benzyl and alkyl substituents, alongside an aromatic carbazole unit and a chiral camphor sultam. Improvements to the preparation included the use of a counterion exchange resin, which proved capable of removing phosphorus impurities from the POCl<sub>3</sub> mediated cyclisation, delivering the desirable chloride counterion for transition metal complexation.

Variable temperature <sup>1</sup>H-NMR studies revealed the high energy barrier between *s*-cis and *s*-trans amide conformations in the formyl oxazoles, indicating the forcing reaction temperatures required for imidazolium formation may result from the need to access the minor conformer.

Pyrimidine annulated imidazolium salts were designed and realised comprising of a novel ligand backbone with amine and guanidine residues. Synthesis routes were developed that delivered the desired salts and subsequently improved for the aniline derivatives. This

improvement led to a linear sequence of just four steps to access scaffold **354** (Figure 43). Additionally, there was a reduction in the number of column chromatography purifications required and the synthetic route was validated by successful preparation of **354b•HCl** on a multigram scale. The modular nature of the improved method was demonstrated by functionalisation of the aniline motif and the incorporation of alkyl and sterically demanding aryl groups at the imidazole. Further exhibition of the modular nature of the synthesis route was achieved by an MSci student who utilised this methodology to access derivatives **354d-f•HCl**.

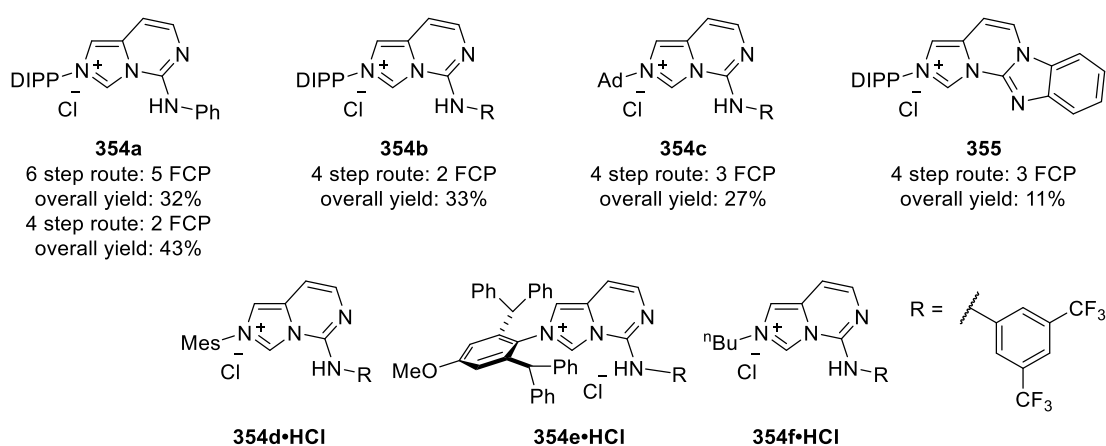


**Figure 43: Overview for ligand syntheses. FCP: Flash column chromatography purifications.**

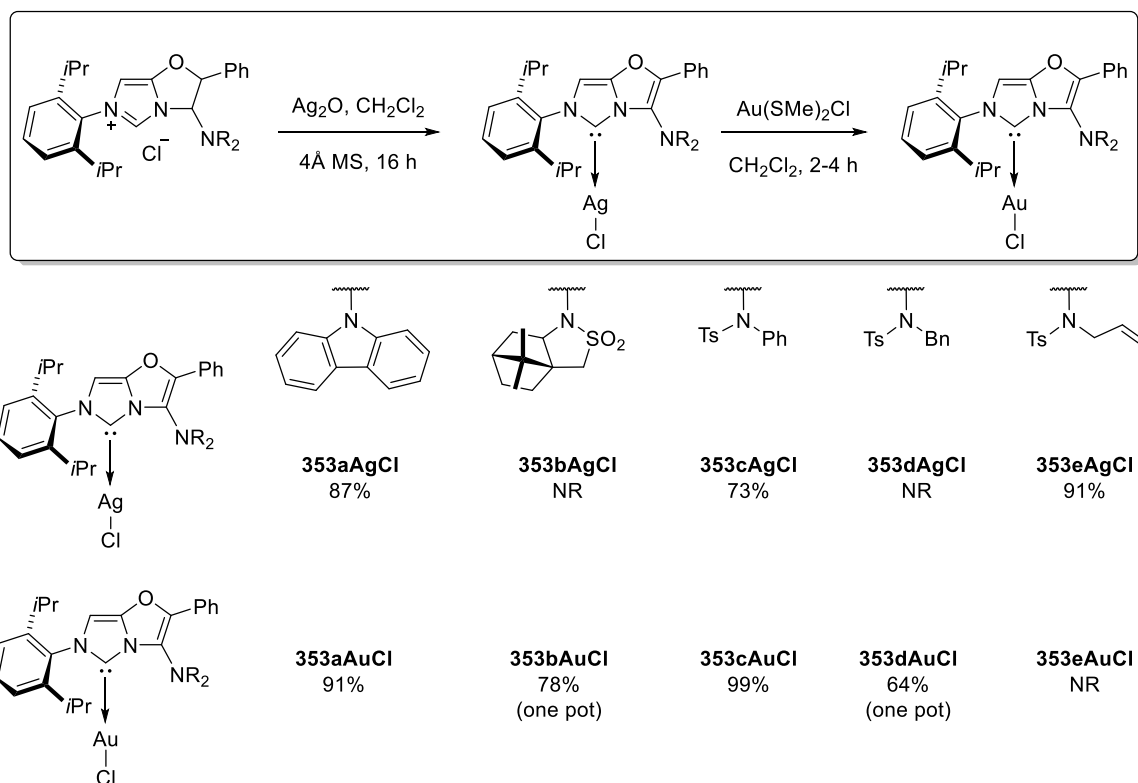
Single crystal analysis of a guanidine containing imidazolium salt highlighted the potential of these systems to undergo substrate interaction through secondary sites on the ligand backbone.

## Chapter 6: NHC transition metal complexes

Following on from the discussion in chapter five, and with a range of NHC precursors in hand, their coordination to transition metals was studied. Complexation with silver, gold, palladium and nickel was targeted due to their widespread use in transition metal catalysed reactions.<sup>195,216,217</sup>

### 6.1 Synthesis of transition metal complexes

Initial focus was placed on the oxazole annulated derivatives **353•HCl**. Complexation with silver followed by transmetalation with Au(SMe<sub>2</sub>)Cl afforded **353AgCl** and **353AuCl** respectively (Scheme 118). In all cases, complete consumption of imidazolium salts **353•HCl** was observed upon treatment with Ag<sub>2</sub>O. **353aAuCl** and **353cAuCl** were prepared from silver complexes **353aAgCl** and **353cAgCl** after filtration through celite, whilst a one-pot process where Au(SMe)<sub>2</sub>Cl was added after 16 h provided direct access to **353bAuCl** and **353dAuCl**. Unfortunately, silver complex **353eAgCl** proved susceptible to rapid degradation in the presence of light.



**Scheme 118: Synthesis of NHCuAuCl complexes from oxazole annulated imidazoliums via transmetalation. NR: not recovered.**

Desymmetrisation of the diisopropyl phenyl group was evident in the <sup>1</sup>H- and <sup>13</sup>C- NMR spectra of gold complexes **353b-dAuCl**, through the separation of all four methyl signals and the attached CH heptets. This stemmed from hindered rotation around the sulfonamide C-N bond upon coordination to transition metals (Figure 42), resulting in atropisomerism. In contrast, the symmetry of carbazole-containing gold-complex **353aAuCl**, precluded this complex from demonstrating atropisomerism. Whilst **353bc-dAuCl**, were prepared as a racemic mixture of enantiomeric atropisomers, the use of enantiopure (1*S*,2*R*)-(-)-10,2-camphorsultam as the sulfonamide introduced diastereotopicity in **353bAuCl**. One diastereomer was observed after purification, with the diastereotopic CH<sub>2</sub> alpha to the sulfonamide providing a single set of *J*<sub>AB</sub> doublets. Single crystals suitable for X-ray diffraction were collected and analysed for comparison of steric properties across the series of ligands (*vide infra*).

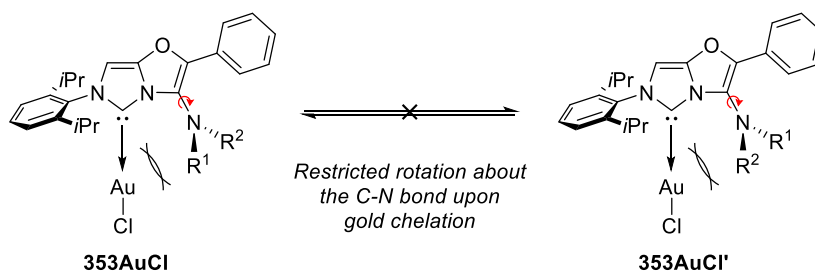
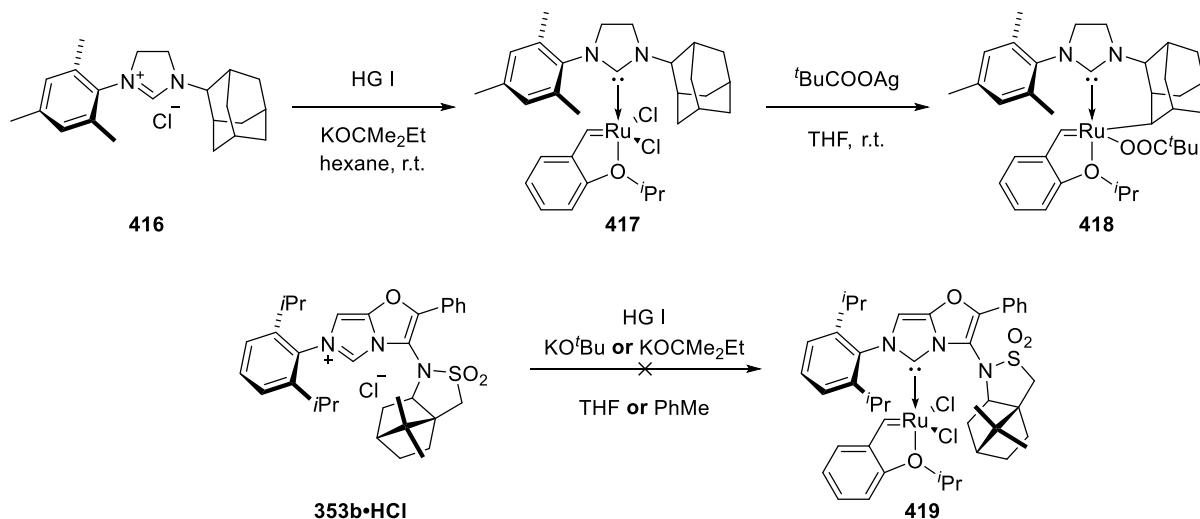


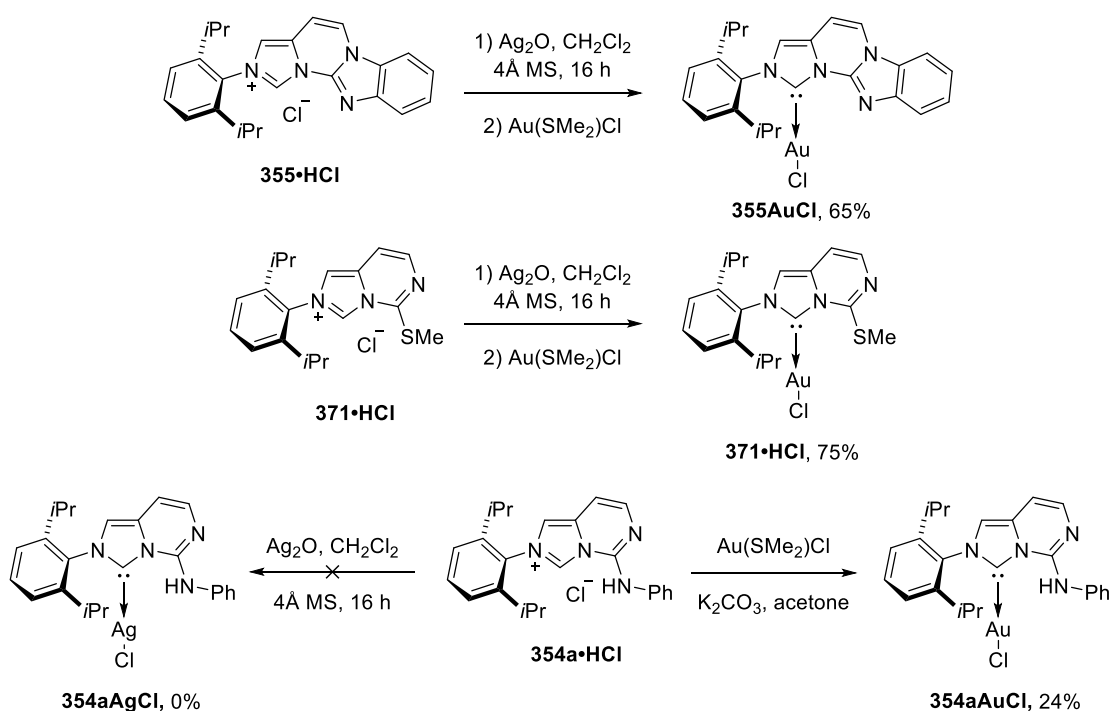
**Figure 44:** Restricted rotation leading to atropisomers in oxazole annulated NHCAuCl complexes.

With carbene transfer onto gold successful, direct coordination to a ruthenium complex was investigated. Recent developments in chelated ruthenium catalysts through intramolecular C-H bond activation has enabled Z-selective cross metathesis and asymmetric ring opening cross metathesis processes.<sup>218,219</sup> C-H activation from the pendant adamantyl group in **417** was observed when performing halide extraction to give cyclo-metalated complex **418** (Scheme 119). With the notion that the camphor sultam unit may undergo a similar C-H insertion process upon halide extraction, the synthesis of **419** was attempted. Unfortunately, no isolable product was obtained, regardless of the base or solvent used.



**Scheme 119:** Top: Cyclometalated ruthenium complex accessed via C-H activation. Bottom: Attempted synthesis of a chiral ruthenium complex.

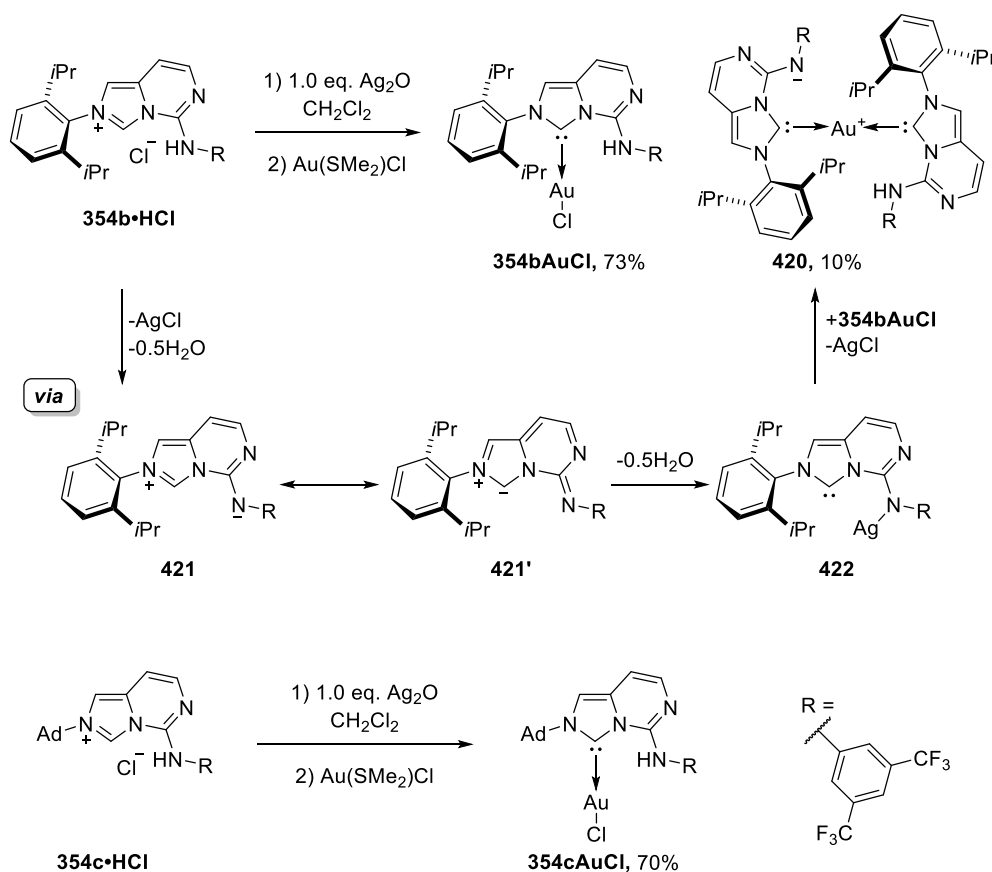
Focus was then turned to the pyrimidine annulated NHC precursors. Treatment of guanidine and sulfide imidazolium salts **355•HCl** and **371•HCl** with the aforementioned one-pot procedure offered access to gold complexes **355AuCl** and **371AuCl** (Scheme 120). In contrast, when aniline derivative **354a•HCl** was treated with Ag<sub>2</sub>O, no starting material consumption was observed by TLC. Instead the reaction turned to a dark colour with visible black precipitation. Direct coordination was achieved through treating **354a•HCl** with Au(SMe<sub>2</sub>)Cl in the presence of K<sub>2</sub>CO<sub>3</sub>, delivering **354aAuCl** in a low yield of 24%.<sup>143</sup> The N-H resonance of **354aAuCl** remained visible in the <sup>1</sup>H-NMR spectrum as a sharp peak at 10.24 ppm, compared to a broad singlet around 11.70 ppm in imidazolium **354a•HCl**.



Scheme 120: Synthesis of pyrimidine annulated NHCAuCl complexes.

Intrigued by the poor reactivity of **354a•HCl** towards coordination, a study was performed with trifluoroaniline imidazolium **354b•HCl**. Noting that the black deposits observed previously resembled AgCl precipitation, and taking into account the presence of an acidic proton in

**354b•HCl**, a second equivalent of  $\text{Ag}_2\text{O}$  was added in the silver coordination step (Scheme 121). This led to consumption of **354b•HCl** by TLC analysis, therefore  $\text{Au}(\text{SMe}_2)\text{Cl}$  was then added. NHC-AuCl complexes are typically white solids, however after filtration through a pad of celite the crude material was a deep green colour. Gratifyingly **354bAuCl** was isolated in 74% yield as an off-white solid, alongside bis-NHC complex **420** as a yellow solid. **420** proved unstable in solution, rapidly turning from yellow to a dark green. Nonetheless, elemental analysis and single crystal XRD analysis confirmed the formation of charged bis-NHC complex **420**.



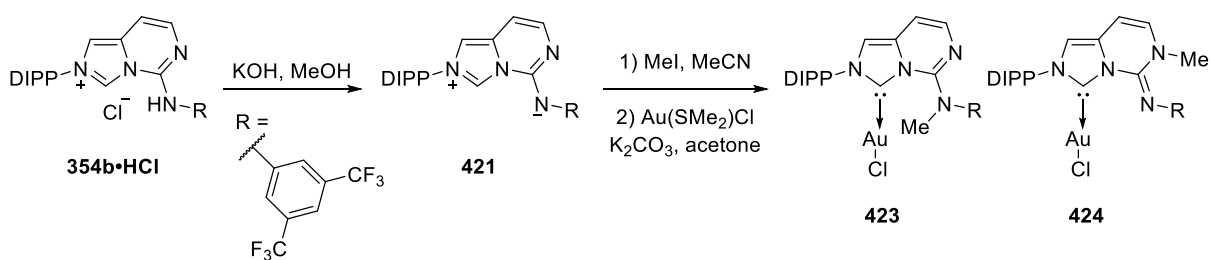
Scheme 121: Formation of mono- and bis- NHC gold complexes.

It was postulated this occurs through the generation of zwitterion **421** upon treatment with the 0.5 equivalents of  $\text{Ag}_2\text{O}$ , with the negative charge delocalised around the aromatic system. The



second 0.5 equivalents of Ag<sub>2</sub>O is then required for deprotonation to generate carbene **422**, with the negative charge stabilised by coordination to Ag(I). Chloride extraction from **354bAuCl** would then deliver cationic bis-NHC complex **420**. Transmetalation *via* the silver complex also provided adamantyl derivative **354cAuCl** in a one pot procedure, from which the same formation of a cationic gold species was observed.

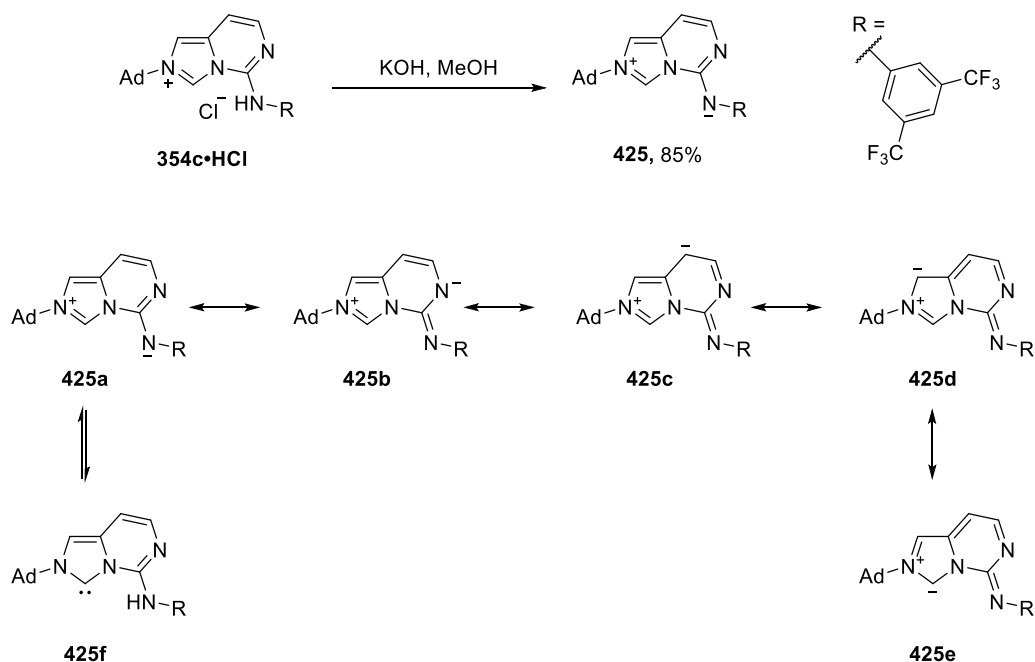
To study the potential reactivity of zwitterion **421**, **354b•HCl** was treated with KOH and the reaction mixture immediately turned bright yellow (Scheme 122). The reaction mixture was filtered, concentrated under reduced pressured and analysed by <sup>1</sup>H-NMR. A clear shift in the <sup>1</sup>H-NMR spectra was observed alongside the disappearance of the N-H resonance. Due to the unknown stability of zwitterion **421**, methylation with MeI was attempted, followed by coordination to gold using analogous reaction conditions as described previously. Purification of the crude reaction mixture delivered a mixture of *N*-methylated products **423** and **424**, although separation of the regioisomers was not successful. A separate attempt at methylation of imidazolium **354b•HCl** in the absence of base yielded no reaction, further evidencing the formation of zwitterion **421**.



Scheme 122: Deprotonation of **354b•HCl** to form a zwitterion and subsequent coordination to gold.

Adamantyl derivative **354c•HCl** was then tested under the same deprotonation conditions, providing isolable zwitterion **425** as a yellow crystalline solid (Scheme 123). The negative charge is delocalised through the  $\pi$ -system of the ligand backbone, highlighted through

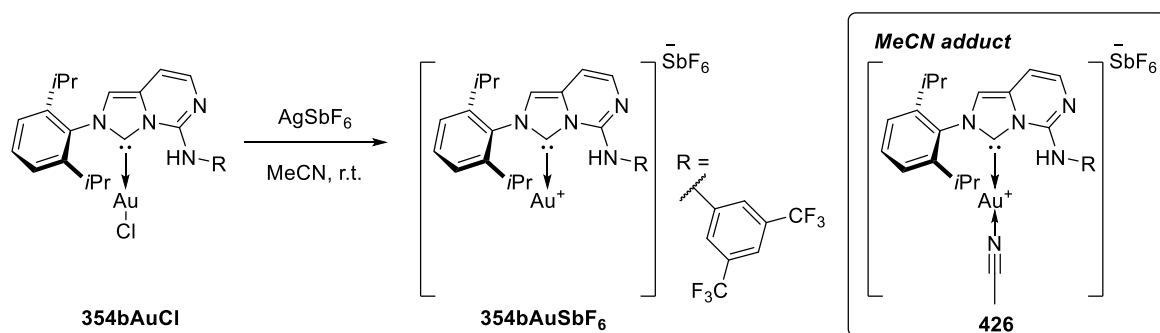
resonance forms **425a-f**, highlighting the unique electronic nature observed with aminopyrimidine motifs. It was hypothesized that this delocalisation reduces the carbene character of **425**, visualised as **425f**, preventing coordination to gold without a second equivalent of Ag<sub>2</sub>O.



**Scheme 123: Formation of a bench stable zwitterion and delocalisation around ligand backbone.**

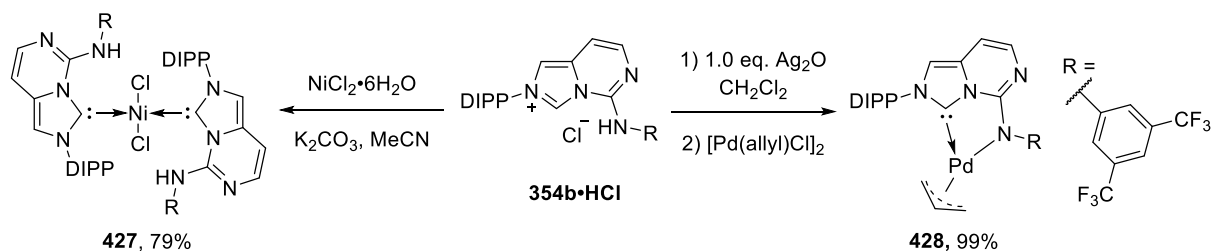
The dissociation energy of chloride counterions in NHCAuCl complexes results in low catalyst activities in most cases as the gold centre remains saturated. This is usually overcome by chloride extraction with a suitable silver salt containing highly delocalised counterions with lower dissociation energies such as AgSbF<sub>6</sub>, AgPF<sub>4</sub> or AgOTf. The comparatively low binding affinity of these counterions result in vacant coordination sites at the gold centre that allow interaction with substrates for catalytic reaction pathways.<sup>220</sup> These reactions are usually performed in coordinating solvents, such as MeCN, that provide additional stability for storage as the solvated gold complex, although they can also be generated *in-situ*. Gold complex **354bAuCl** was then treated with AgSbF<sub>6</sub> in MeCN to determine the stability of a cationic gold

complex containing a secondary amine in close vicinity to the metal centre (Scheme 124). Cationic species **354bAuSbF<sub>6</sub>** proved unstable in solution, rapidly turning dark green and providing a gold mirror during NMR analysis. Full characterisation was obtained by preparing a fresh NMR sample under argon and immediately running <sup>1</sup>H-, <sup>13</sup>C- and <sup>19</sup>F-NMR analysis on a 500 MHz spectrometer to shorten the acquisition times. The N-H was not visible in the <sup>1</sup>H NMR spectra, however whether this was due to deprotonation or rapid exchange in acetone-*d*<sub>6</sub> is not yet known. Confirmation that **354bAuSbF<sub>6</sub>** was isolated rather than solvated complex **426** was achieved through NMR and elemental analysis.



Scheme 124: Halide extraction with AgSbF<sub>6</sub>.

The ability to form bidentate NHC-TM complexes was then explored through coordination to nickel and palladium. Following a literature procedure,<sup>144</sup> direct coordination was achieved to deliver nickel complex **427**, with the aniline moiety protonated without displacing the chlorides (Scheme 125). This assignment was made as the N-H resonances were visible in the <sup>1</sup>H-NMR spectrum and later confirmed by elemental analysis. Palladium compound **428** was obtained *via* transmetalation of the silver complex and determined to be bidentate with the deprotonated aniline displacing the chloride ligand.



Scheme 125: Formation of palladium- and nickel- NHC TM complexes.

## 6.2 Analysis of NHC ligands

With a series of  $\text{NHCAuCl}$  complexes in hand, an investigation into the steric properties and potential secondary coordination abilities of the ligands was performed. The structures of silver and gold complexes **353AgCl** and **353AuCl** were obtained by single crystal XRD analysis (Figure 45-46). Gold complexes **353AuCl** were analysed using SambVca 2.0 to calculate %  $V_{\text{bur}}$  and generate topological steric maps to evaluate the ligands impact on the coordination sphere.<sup>170</sup> Comparison of the bond angles and lengths against literature compounds is summarised below in Table 5.

Examination of the crystal structures of **353aAgCl** and **353cAgCl** revealed potential interactions between the  $\pi$ -system of the carbazole and tosyl functional groups and the metal centre (Figure 45). The carbazole nitrogen adopted a change in geometry from trigonal planar to trigonal pyramidal ( $\text{C}_5\text{N}_3\text{C}_{7/13}$   $152.8(2)^\circ/153.6(2)^\circ$ ), with distances between 3.396(3)-3.658(4) Å separating the carbazole core and silver centre. This resulted in positioning of the silver centrally to the  $\pi$ -system of the interior ring. Whilst  $\text{N}_3$  remains trigonal planar in **353cAgCl**, the aromatic tosyl group again appeared to shield the metal centre through  $\pi$  interactions, with distances between 3.806(3)-3.710(2) Å.

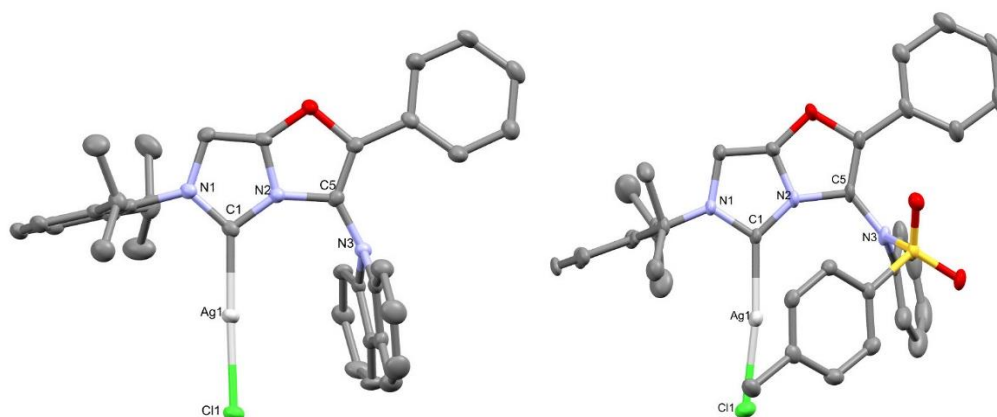


**Figure 45: X-ray structures of 353aAgCl and 353cAgCl.** Ellipsoids drawn at 50% probability, hydrogens omitted for clarity. X-ray data obtained and solved with assistance from Dr Louise Male. **353aAgCl**:  $\text{N}_2\text{C}_1\text{Au}$   $126.0(2)^\circ$  and  $\text{C}_1\text{AuCl}$   $177.4(1)^\circ$ . **353cAgCl**:  $\text{N}_2\text{C}_1\text{Au}$   $134.4(2)^\circ$  and  $\text{C}_1\text{AuCl}$   $172.8(8)^\circ$ .

Gold derivative **353aAuCl** exhibited a similar effect, with an increased distortion angle ( $\text{C}_5\text{N}_3\text{C}_{11/12}$   $153.1(3)^\circ/153.8(3)^\circ$ ) and decreased distances between the gold and interior carbazole atoms ( $3.439(4)$ - $3.740(4)$  Å) (Figure 46, 1). Tosyl containing complexes **353cAuCl** and **353dAuCl** demonstrated similar  $\pi$ -interactions between the tosyl group and metal centre to those observed for **353cAgCl**, maintaining a trigonal planar geometry at  $\text{N}_3$  (Figure 46, 2 and 3). The range of distances between the gold centre and tosyl aromatic group increased in **353cAuCl** ( $3.736(5)$ - $3.914(6)$  Å) in comparison to **353cAgCl**, with **353dAuCl** containing a significantly smaller range ( $3.723(3)$ - $3.758(3)$  Å) and a shorter average distance.

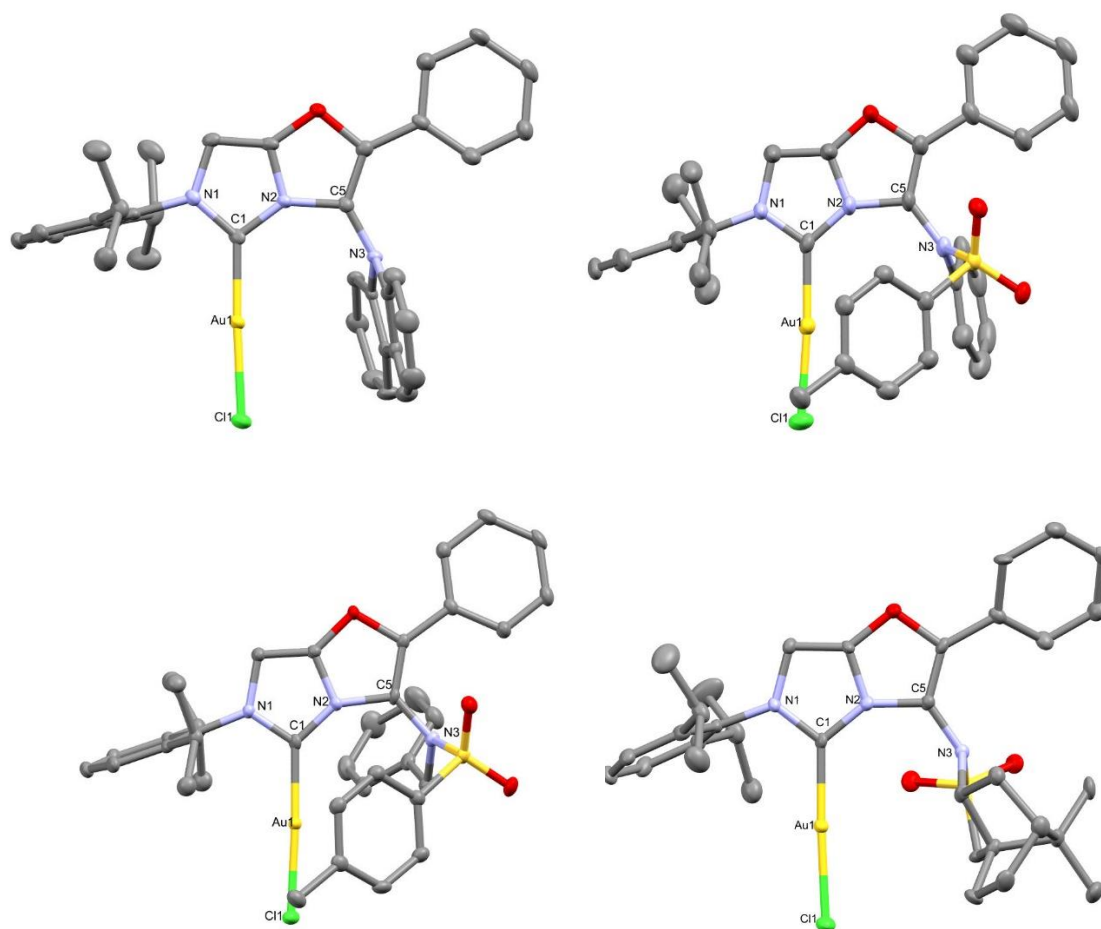


**Figure 46:** X-ray structures of: 1. **353aAuCl**; 2. **353bAuCl**; 3. **353cAuCl**; 4. **353dAuCl** ( $\text{CH}_2\text{Cl}_2$  removed). Ellipsoids drawn at 50% probability, hydrogens and solvent omitted for clarity. X-ray data obtained and solved with assistance from Dr Louise Male. All structures centred on the  $\text{C}_1\text{Au}$  bond.

Distortion of the carbene-Au and AuCl bonds was observed due to the unsymmetrical nature of the ligands (values in Table 5). Carbazole complex **353aAuCl** displayed bending towards the aromatic functionality, whereas sulfonamide derivatives **353b-dAuCl** showed distortion in the opposite direction. The degree of  $\text{N}_2\text{C}_1\text{Au}$  bond angle distortion followed  $\%V_{\text{bur}}$  values, with complementary  $\text{C}_1\text{AuCl}$  bond bending in the opposing fashion.

The X-ray structure of aniline derivative **354aAuCl** revealed even greater bending of the gold carbene bond due to the impact of secondary amine (Figure 47).  $\text{N}_4$  remained trigonal planar with the aryl group positioned away from the metal centre. No bonding interactions were

observed in the crystal structures of **354aAuCl** or **355AuCl**, however both hydrogen bond donor and acceptor sites were accommodated within the coordination sphere.

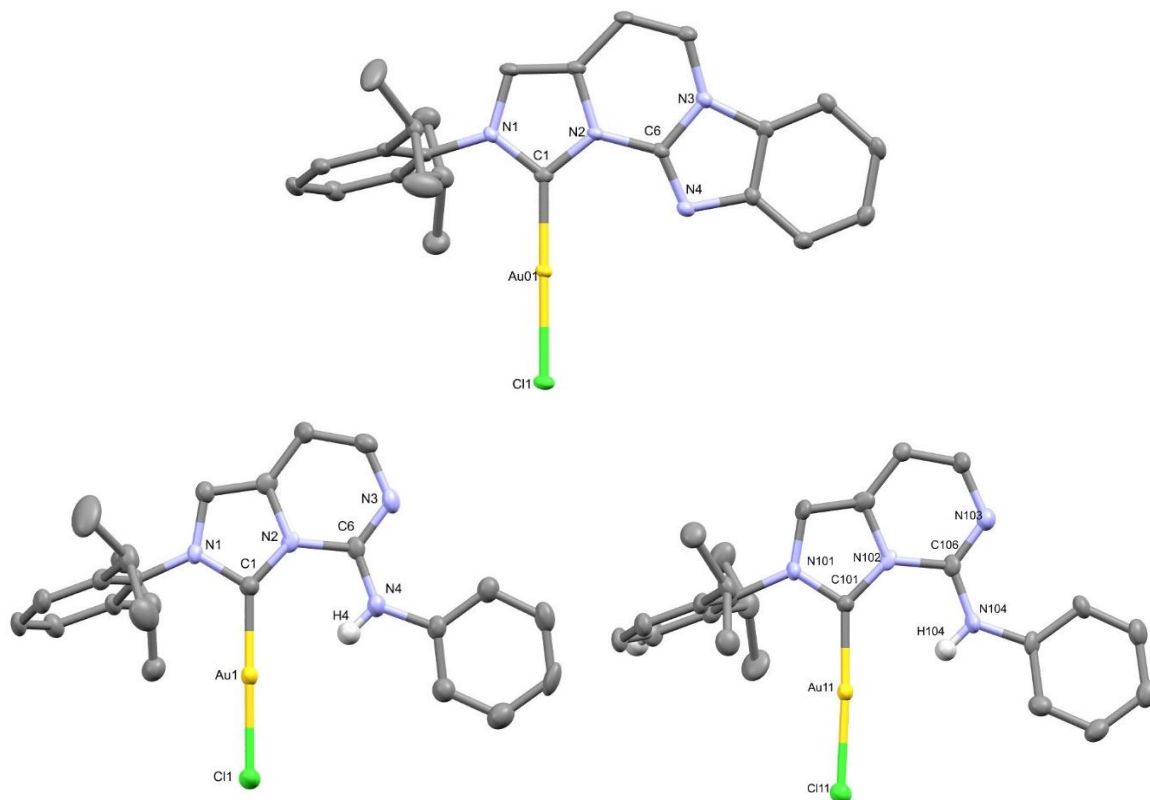
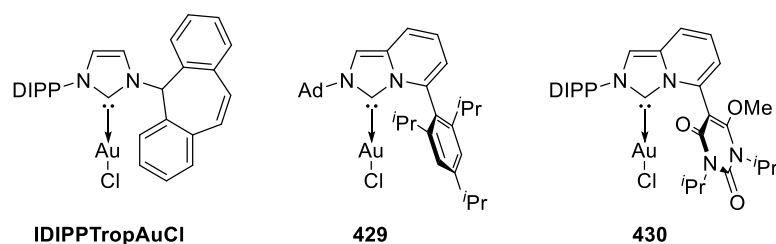


**Figure 47:** X-ray structures of: 1. **355AuCl**; 2 and 3. **354aAuCl** (unique structures within unit cell). Ellipsoids drawn at 50% probability, hydrogens omitted for clarity except for N-Hs. X-ray data obtained and solved with assistance from Dr Louise Male.

The results displayed in Table 5 present comparison against a range of literature **NHCAuCl** complexes. **353dAuCl** was confirmed as the most sterically demanding ligand, providing a % $V_{bur}$  of 56.4, reflecting its ability to wrap around the metal within the coordination sphere. Replacing the flexible benzyl functionality with a more rigid phenyl group in **353cAuCl** reduced the % $V_{bur}$  by 5.4. Camphor derivative **353bAuCl** proved more sterically demanding than **IPrAuCl**, however provided less impact than **IPr\*AuCl** and other heterocyclic ligands. Pyrimidine annulated **354aAuCl** and **355AuCl** had considerably less impact on the % $V_{bur}$ , reflecting the positioning of the aryl groups away from the gold carbene. No significant

deviation from typical C<sub>1</sub>Au or AuCl bond lengths were observed across the oxazole- or pyrimidine- annulated NHCs.

**Table 5: comparison of %V<sub>bur</sub>, bond lengths and angles between literature complexes and synthesised library.**  
<sup>a</sup>Calculated using SambVca 2.0 software.<sup>170</sup> <sup>b</sup>Angle measured clockwise from C<sub>1</sub>. <sup>c</sup>Two unique complexes in unit cell.  
 Literature compound cif files downloaded from CCDC and data produced from X-ray structures.



Entry	Complex	%V <sub>bur</sub> <sup>a</sup>	Au-C <sub>1</sub> (Å)	Au-Cl (Å)	N <sub>2</sub> C <sub>1</sub> Au (°)	N <sub>1</sub> C <sub>1</sub> N <sub>2</sub> (°)	ClAuC <sub>1</sub> (°) <sup>b</sup>
1	<b>353aAuCl</b>	44.1	1.973(4)	2.279(3)	126.6(3)	101.9(3)	177.4(1)
2	<b>353bAuCl</b>	48.5	1.975(7)	2.283(2)	129.4(6)	102.6(9)	177.4(2)
3	<b>353cAuCl</b>	51.0	1.983(5)	2.281(1)	131.8(4)	103.5(5)	183.8(8)
4	<b>353dAuCl</b>	56.4	1.976(3)	2.280(7)	133.5(2)	102.9(2)	183.1(0)
5	<b>355AuCl</b>	36.2	1.972(3)	2.287(0)	128.7(2)	103.2(3)	178.7(4)
6	<b>354aAuCl</b>	40.6	1.972(7) 1.959(7)	2.274(2) 2.270(2)	137.0(5) 135.6(5)	101.7(6) 101.6(6)	184.2(8)/ 182.7(8)
7	<b>IPrAuCl</b> . <sup>221</sup>	45.6	1.941(3)	2.270(1)	125.8(8)	102.3(9)	-
8	<b>IPr*AuCl</b> . <sup>175</sup>	50.4	1.987(8)	2.273(2)	126.1(6)	106.3(6)	-
9	<b>IDIPP-TropAuCl</b> . <sup>169</sup>	51.1	1.972(2)	2.273(3)	124.1(2)	104.5(2)	182.0(0)
10	<b>429</b> . <sup>134</sup>	51.6	1.976(6)	2.271(2)	126.1(4)	103.6(4)	182.9(8)
11	<b>430</b> . <sup>222</sup>	53.4	1.992(4)	2.279(1)	127.1(3)	104.2(3)	175.7(1)

With the above analyses in hand, an understanding of the three-dimensional environment within the coordination sphere beyond a numerical descriptor was desired. Due to the linear nature of NHC<sub>2</sub>AuCl complexes, the vacant coordination site upon halide extraction is *trans* to the NHC ligand. Many sterically demanding ligands, such as **IPr** and **IPr\***, deliver significant stabilisation at the organometallic centre without interacting with substrates at the coordination site. The topographic steric maps of **353AuCl** confirmed that in all cases the immediate vicinity of the metal centre was significantly shielded (Figure 48). Additionally, the carbazole (Figure



48, 1) and sulfonamide motifs (Figure 48, 2-4) were positioned such that they display significant encumbrance in the coordination site of  $[\text{NHCAu}]^+$  complexes (visualised as the orange and red zones). This places them in position for possible substrate interaction as well as significant stabilisation of reactive organometallic intermediates. Replacing the phenyl in **353cAuCl** for flexible benzyl derivative **353dAuCl** provided increased shielding around the gold centre in the southeast sector. These results demonstrated the promising steric characteristics of the oxazole annulated NHC ligands, with the ability to modify the environment within the coordination sphere through selection of an appropriate ynamide in the oxazole formation.

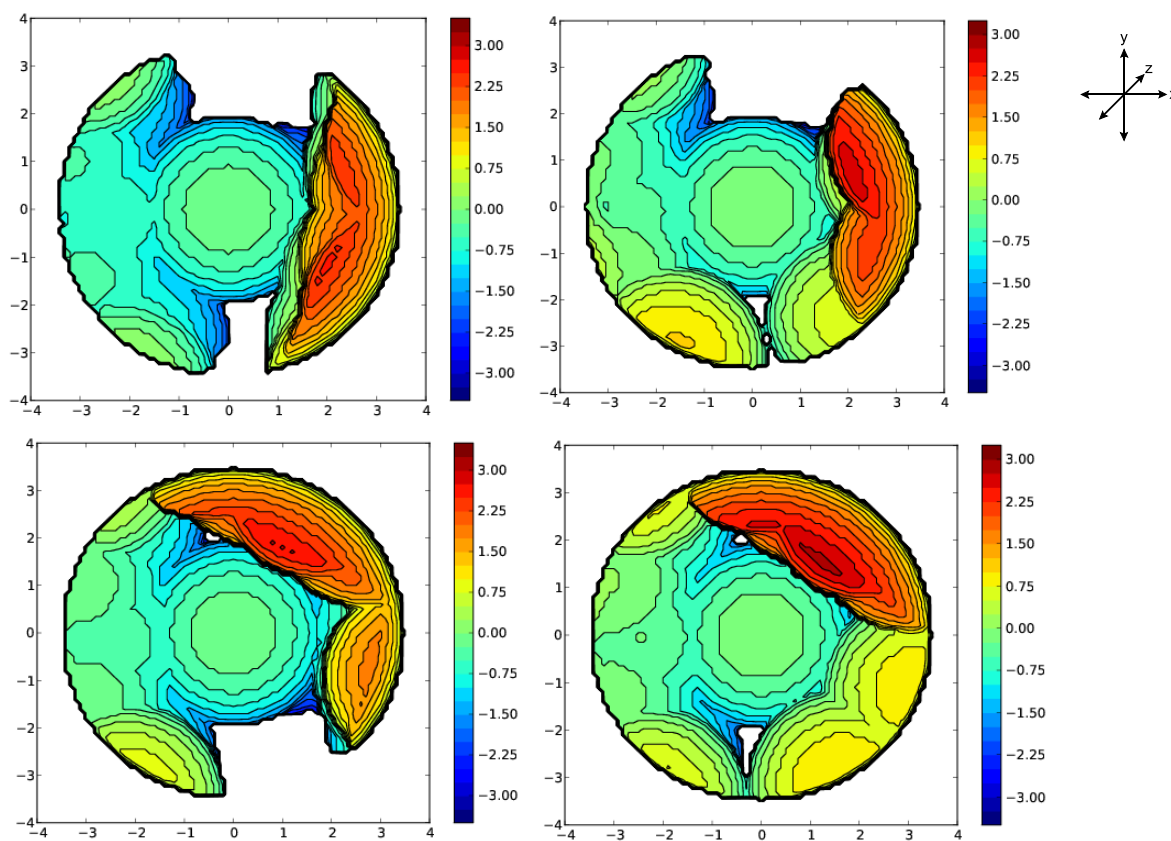
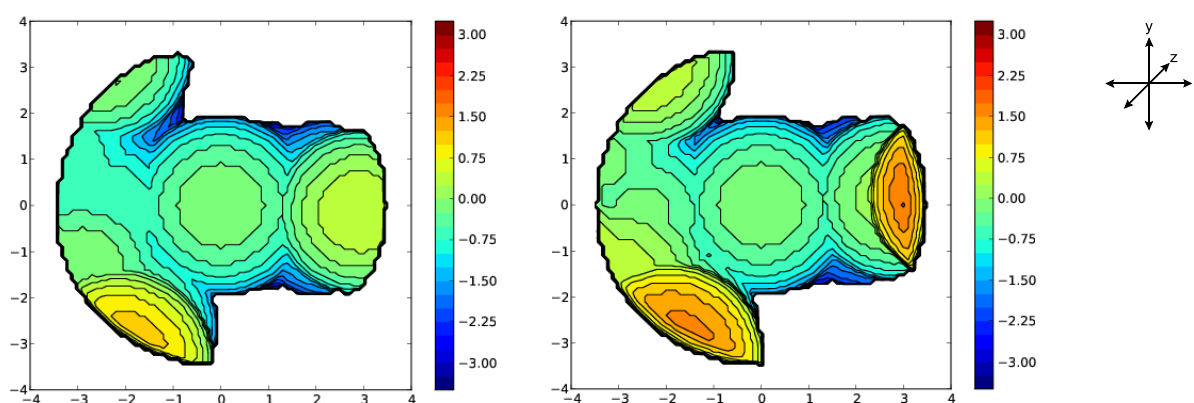


Figure 48: Topographic steric maps: 1. **353aAuCl**; 2. **353bAuCl**; 3. **353cAuCl**; 4. **353dAuCl**. Au-carbene bond selected as Z axis, nitrogens flanking carbene define XZ plane. Bondi radii scaled by 1.17, sphere radius 3.5 Å, mesh spacing 0.10, H atoms removed for calculations. Colour coding represents positioning of steric bulk relative to the centre of the sphere, scale in Å.

The topographic steric maps of pyrimidine complexes **354aAuCl** and **355AuCl** reflected the comparatively limited steric impact on the coordination sphere, with the north-east and south-east regions remaining unshielded (Figure 49). This was attributed to the linear nature of the pyrimidine fragment of the NHC ligands. Nevertheless, in both cases the pendant nitrogen was positioned close to the metal centre, offering opportunities for secondary coordination and substrate interaction in non-linear TM complexes.



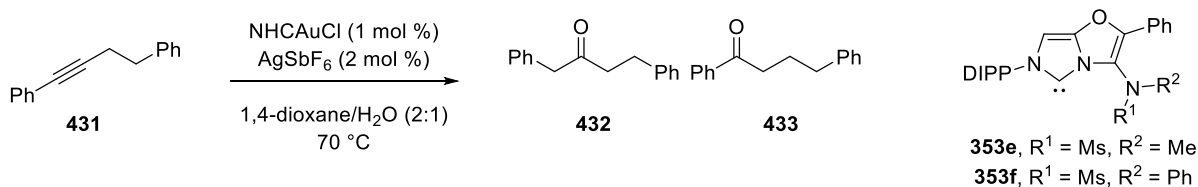
**Figure 49:** Topographic steric maps for **355AuCl** and **354aAuCl**. Au-carbene bond selected as Z axis, nitrogens flanking carbene define XZ plane. Bondi radii scaled by 1.17, sphere radius 3.5 Å, mesh spacing 0.10, H atoms removed for calculations. Colour coding represents positioning of steric bulk relative to the centre of the sphere, scale in Å.

### 6.3 Preliminary catalyst activity study

Having prepared a range of oxazole annulated-gold complexes, a study on the hydration of alkynes was undertaken to assess their activity. Previous work within the Davies group had demonstrated anti-Markovnikov reactivity in the hydration of internal alkyne **431** when adapting conditions developed by Nolan (Table 6).<sup>223</sup> The activity across the series of complexes was good to excellent, with **353b-dAuCl** matching that achieved with **IPrAuCl**. Selectivity for the anti-Markovnikov hydration product was favoured through the oxazole

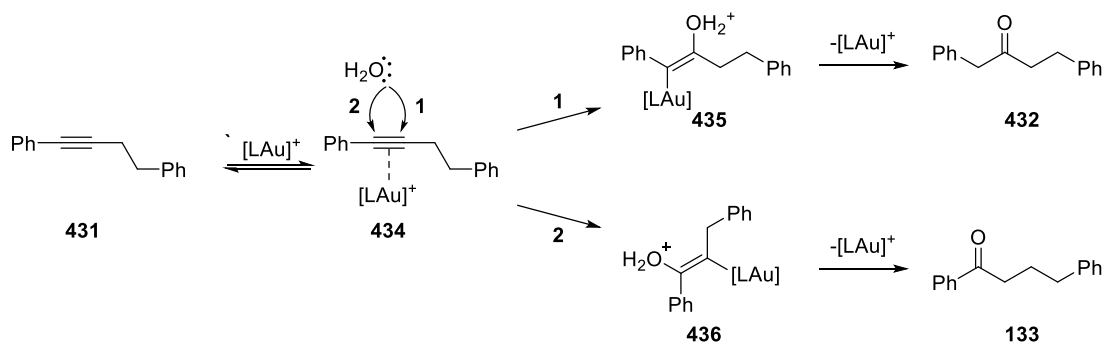
annulated NHC ligands, with camphor complex **353bAuCl** achieving the highest regioselectivity.

**Table 6: Probing the activity and selectivity of oxazole annulated NHCAuCl complexes in the hydration of an internal alkyne.** <sup>a</sup>Calculated by <sup>1</sup>H-NMR ratios of mixture. Performed by ADG.



Entry	NHC	Yield (%)	416:417 <sup>a</sup>
1	<b>IPr</b>	87	1.0:1.0
2 <sup>b</sup>	<b>353e</b>	55	1.8:1.0
3 <sup>b</sup>	<b>353f</b>	76	1.1:1.0
4	<b>353a</b>	78	1.3:1.0
5	<b>353b</b>	89	2.6:1.0
6	<b>353c</b>	94	1.8:1.0
7	<b>353d</b>	90	1.1:1.0
8	No gold	-	-

An increase in selectivity from 1.0:1.0 to 2.6:1.0 represented a significant improvement with respect to that previously reported, yet the observed trend was challenging to elucidate. The rate- and product- determining step has been identified as the attack of H<sub>2</sub>O onto gold activated alkyne **431** through DFT calculations (Scheme 126).<sup>224</sup> Therefore a ligand that affects the vacant coordination site within the [NHCAu]<sup>+</sup> complex has the potential to impact the reaction outcome by differentiation of the energies of **435** and **436**. However, there was no clear correlation between the %V<sub>bur</sub> values or topographic steric maps with the regioselectivity observed.



**Scheme 126: Mechanism of gold-catalysed hydration of internal alkynes.**

Nevertheless, the activity and selectivity achieved across the series demonstrated the potential of the oxazole annulated NHCs to provide unique reaction control.

## 6.4 Conclusion

A library of four oxazole annulated  $NHCAuCl$  complexes has been generated and the corresponding X-ray structures obtained. Secondary  $\pi$ -interactions between aromatic substituents and the metal centre were identified. Analysis of the topographical steric maps revealed the significant steric impact of the ynamide nitrogen substituents on both the metal centre and the potential vacant coordination site. These substituents may allow for substantial shielding of electrophilic metal centres produced during catalytic cycles, whilst their flexibility could also accommodate bulky substrates through rotation or geometry adjustments.

An initial screening of the oxazole derived complexes' reactivity on the hydration of an internal alkyne proved the  $NHCAuCl$  complexes to be active in Au(I) catalysis reactions, providing anti-Markovnikov regioselectivity. Future work on this family of complexes should focus on testing the capabilities of these NHC ligands in various transition metal catalysed reactions to explore the effect of the flexible steric bulk on reaction outcome.

The coordination of pyrimidine annulated imidazoliums to gold, nickel and palladium has been accomplished. Isolation of a bis-NHCAuCl complex revealed the acidic nature of the aniline moiety, through the generation of a zwitterionic imidazolium. Steric characterisation was obtained through X-ray structures, %  $V_{bur}$  and topographic steric maps. The electronic nature of these ligands is yet to be explored. Going forward these ligands should be investigated for their ability to electronically influence reaction outcomes through substrate interaction, switchable response to chemical stimulus or reactive organometallic species stabilisation.

## Chapter 7: Supporting information

### General Experimental

Commercial chemicals were purchased from major suppliers (Sigma-Aldrich, Acros organics, Fisher Scientific or VWR international) and used without prior purification unless otherwise specified. Glassware used for reactions carried out under an argon atmosphere were flame-dried with a Bunsen burner or hot air gun under vacuum at 0.1 mbar and backfilled with argon. The vacuum/argon purge was carried out three times. Reaction set ups were performed with standard air sensitive Schlenk techniques. Solvents were dried under the following conditions: CH<sub>2</sub>Cl<sub>2</sub>, THF and toluene were drawn through a PureSolv EN solvent purification system through alumina packed columns and transferred under argon onto activated 3 Å molecular sieves. DMF, EtOH, 1,2-DCB, 1,2-DCE and 1,4-dioxane were stored over activated 4 Å molecular sieves for 24 h prior to use. All reactions were stirred using Teflon coated magnetic stirrer bars. Reactions which required heating were submerged in preheated paraffin oil baths or aluminium heating mantles and the temperature controlled by an external probe. Reactions which required cooling were submerged in the following baths: 0 °C – ice/water, –40 °C – dry ice/MeCN, –78 °C – dry ice/acetone. All reactions were monitored using thin layer chromatography on Merck silica gel 60 F<sub>254</sub> (aluminium support) plates which were developed using the standard visualising agents: UV fluorescence (254 nm), potassium permanganate/Δ, vanillin/Δ, anisaldehyde/Δ or phosphomolybdic acid/Δ. Flash chromatography was carried out on Sigma Aldrich silica gel (60 Å, 230–400 mesh, 40–63 μm) or Interchim prepacked 4 g spherical silica columns (60 Å, 30 μm) and were run manually or with a CombiFlash® NextGen 300+ using UV detection. Gradient eluent mixtures are described including any isocratic holds: (0→30<sub>hold</sub>→100, hexane/EtOAc). Masses were measured to four significant figures and are

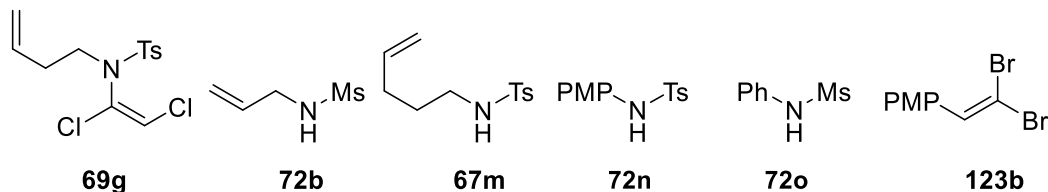
rounded to 3 significant figures, or to the nearest 0.1 mg and 0.01 mmol where appropriate. Reagents measured in mL are recorded to appropriate significant figures to represent the accuracy of measurement. Melting points were measured in open ended capillaries using a Stuart Scientific melting point apparatus and are uncorrected.  $^1\text{H}$  NMR and  $^{13}\text{C}$  NMR experiments were recorded using Bruker AVIII400 ( $^1\text{H}$  = 400 MHz,  $^{13}\text{C}$  = 101 MHz), Bruker AVNEO400 ( $^1\text{H}$  = 400 MHz,  $^{13}\text{C}$  = 101 MHz), AVIII300 ( $^1\text{H}$  = 300 MHz,  $^{13}\text{C}$  = 75 MHz) or Bruker AVNEO500 ( $^1\text{H}$  = 500 MHz,  $^{13}\text{C}$  = 126 MHz) spectrometers at 295–300 K.  $^{13}\text{C}$  NMR spectra were recorded using the UDEFT, JMOD or the PENDANT pulse sequence from the Bruker standard pulse program library. 2D NMR spectra were recorded using the Bruker standard pulse program library. Spectra were processed using MestReNova 12.0.3. Chemical shifts ( $\delta$ ) are given in ppm relative to TMS and are calibrated using residual solvent peaks ( $\text{CDCl}_3$ :  $\delta_{\text{C}} \equiv 77.16$  ppm,  $\text{MeOD}$ :  $\delta_{\text{C}} \equiv 49.00$  ppm,  $\text{DMSO}-d_6$ :  $\delta_{\text{C}} \equiv 39.52$  ppm,  $\text{Acetone}-d_6$ :  $\delta_{\text{C}} \equiv 29.84$  ppm; residual  $\text{CHCl}_3$  in  $\text{CDCl}_3$ :  $\delta_{\text{H}} \equiv 7.26$  ppm, residual  $\text{MeOH}$  in  $\text{MeOD}$ :  $\delta_{\text{H}} \equiv 3.31$  ppm, residual  $\text{DMSO}$  in  $\text{DMSO}-d_6$ :  $\delta_{\text{H}} \equiv 2.50$  ppm, residual acetone in  $\text{Acetone}-d_6$ :  $\delta_{\text{H}} \equiv 2.05$  ppm). Spectral data for  $^1\text{H}$  NMR spectroscopy are reported as follows: chemical shift (multiplicity, number of protons, coupling constant); and for  $^{13}\text{C}$  NMR spectroscopy: chemical shift. The following abbreviations were used for multiplicity: s (singlet), d (doublet), t (triplet), q (quadruplet), quin (quintuplet), hept (heptet), br. (broad), m (multiplet), app. (apparent). Coupling constants ( $J$ ) are quoted in Hz to one decimal place. Where NMR spectra are assigned for a mixture of rotamers the resonances are matched where possible and reported as a pair, with the sum of the integration reported, for example:  $5.07_{\text{maj}}$  and  $4.91_{\text{min}}$  (s, 2H). Where restricted rotation causes broadening of the NMR resonances, the centre of the peak is reported: (br. s). Infrared spectra were recorded neat on a Perkin–Elmer Spectrum 100 FTIR spectrometer. Wavenumbers ( $\nu$ ) are reported in  $\text{cm}^{-1}$ . Mass spectra were obtained using Waters

LCT (ES) or Waters Synapt (ES) spectrometers. High resolution spectra used a lock-mass to adjust the calibrated mass scale.



## Formation of precursors to ynamides

The following compounds were available within the Davies lab.



The following sulfonyl and carbamate protected amines were prepared according to literature procedures, which are referenced alongside the data:

### *N-Allyl-4-methylbenzenesulfonamide 72a*

CC=C[NH]Ts 2.07 g, 98%. Spectroscopic data matched that reported in the literature.<sup>6</sup>

### *4-Methyl-N-methylbenzenesulfonamide 72c*

C[NH]Ts 8.60 g, 93%. Spectroscopic data matched that reported in the literature.<sup>226</sup>

### *Benzyl allylcarbamate 72d*

CC=C[NH]Cbz 9.42 g, 98%. Spectroscopic data matched that reported in the literature.<sup>227</sup>

### *N-Benzylmethanesulfonamide 72e*

Bn[NH]Ms 3.05 g, 82%. Spectroscopic data matched that reported in the literature.<sup>228</sup>

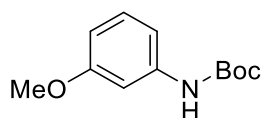
### *4-Methyl-N-phenylbenzenesulfonamide 72g*

c1ccccc1[NH]Ts 4.57 g, 92%. Spectroscopic data matched that reported in the literature.<sup>229</sup>

### *N-Methyl-4-nitrobenzenesulfonamide 72h*

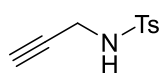
C[NH]Ns 2.04 g, 94%. Spectroscopic data matched that reported in the literature.<sup>230</sup>

***tert-Butyl (3-methoxyphenyl)carbamate 72i***



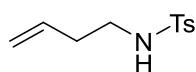
4.13 g, 92%. Spectroscopic data matched that reported in the literature.<sup>231</sup>

***N-Propargyl-4-methylbenzenesulfonamide 72j***



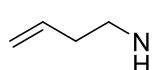
467 mg, 74%. Spectroscopic data matched that reported in the literature.<sup>232</sup>

***N-(But-3-en-1-yl)-4-methylbenzenesulfonamide 72k***



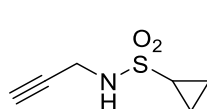
1.03 g, 99%. Spectroscopic data matched that reported in the literature.<sup>233</sup>

***Benzyl but-3-en-1-ylcarbamate 72l***



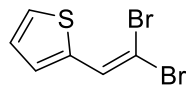
1.58 g, 96%. Spectroscopic data matched that reported in the literature.<sup>234</sup>

***N-(Prop-2-yn-1-yl)cyclopropanesulfonamide 72f***



Propargylamine (771 mg, 14.0 mmol) and  $\text{NEt}_3$  (3.0 mL, 21.0 mmol) were stirred in  $\text{CH}_2\text{Cl}_2$  (28 mL) at 0 °C. Cyclopropanesulfonyl chloride (1.7 mL, 16.8 mmol) was added dropwise over 5 min before the reaction mixture was allowed to warm to r.t. and stirred for 1 h. The reaction mixture was quenched with 2 M  $\text{HCl}_{(\text{aq})}$  (40 mL) and extracted with  $\text{CH}_2\text{Cl}_2$  (2×30 mL). The combined organics were washed with brine (3×50 mL), dried over  $\text{Na}_2\text{SO}_4$ , concentrated under reduced pressure and purified by flash column chromatography (6:4 hexane/EtOAc) to give sulfonamide **72f** as a yellow oil (2.13 g, 96%): IR (neat):  $\nu = 3275, 2118, 1425, 1301, 1139, 1067, 889 \text{ cm}^{-1}$ ;  $^1\text{H}$  NMR (400 MHz,  $\text{CDCl}_3$ ):  $\delta = 4.82$  (br. s, 1H), 3.96 – 3.93 (m, 2H), 2.58 – 2.51 (m, 1H), 2.34 (t,  $J = 2.5 \text{ Hz}$ , 1H), 1.23 – 1.17 (m, 2H), 1.06 – 1.00 (m, 2H) ppm;  $^{13}\text{C}$  NMR (101 MHz,  $\text{CDCl}_3$ ):  $\delta = 79.5$  (C), 73.0 (CH), 32.9 (CH<sub>2</sub>), 30.8 (CH), 6.0 (2CH<sub>2</sub>) ppm; HRMS (ES-TOF):  $m/z$ : calcd for  $\text{C}_6\text{H}_9\text{NO}_2\text{SNa}$ : 182.0246, found 182.0247  $[\text{M}+\text{Na}]^+$ .

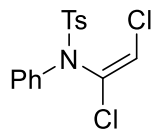
### ***1,1-Dibromo-2-(2-thienyl)ethene 123a***

 PPh<sub>3</sub> (6.55 g, 25.0 mmol) was added to a solution of CBr<sub>4</sub> (4.15 g, 12.5 mmol) in CH<sub>2</sub>Cl<sub>2</sub> (25 mL) at 0 °C and stirred for 10 min. Thiophenecarboxaldehyde (1.12 g, 10.0 mmol) was added dropwise over 5 min and stirred for 10 min at 0 °C. After removing the ice bath, the reaction mixture was stirred for a further 1 h at r.t. The reaction mixture was diluted with H<sub>2</sub>O (50 mL) and extracted with CH<sub>2</sub>Cl<sub>2</sub> (25 mL). The organic phase was dried over Na<sub>2</sub>SO<sub>4</sub>, filtered and concentrated under reduced pressure. Purification by flash column chromatography (hexane) gave **123a** as a light brown solid (2.15 g, 80%); mp: 57–58 °C; IR (neat):  $\nu$  = 2230, 1421, 1355, 1210, 1100, 857 cm<sup>-1</sup>; <sup>1</sup>H NMR (400 MHz, CDCl<sub>3</sub>):  $\delta$  = 7.65 (s, 1H), 7.39 (d,  $J$  = 4.9 Hz, 1H), 7.25 (d,  $J$  = 3.7 Hz, 1H), 7.04 (dd,  $J$  = 4.9, 3.7 Hz, 1H) ppm; <sup>13</sup>C NMR (101 MHz, CDCl<sub>3</sub>):  $\delta$  = 138.2 (C), 131.0 (CH), 130.2 (CH), 127.3 (CH), 126.7 (CH), 87.1 (C) ppm. Spectroscopic data matched that reported in the literature.<sup>235</sup>

### **General procedure 1: dichloroenamides (GP1)**

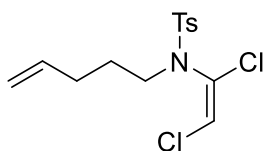
Following the method of Anderson,<sup>56</sup> the relevant sulfonamide (1.0 eq.) and Cs<sub>2</sub>CO<sub>3</sub> (1.5 eq.) were dissolved in DMF (1.33 M sulfonamide) and heated to 50 °C. Trichloroethylene (1.1 eq.) was added via syringe pump over 10 min and the reaction mixture stirred for 2 h at 50 °C. After allowing to cool to r.t., the reaction mixture was diluted with EtOAc and washed with H<sub>2</sub>O (3×) and brine (3×), dried over Na<sub>2</sub>SO<sub>4</sub> and concentrated under reduced pressure.

### ***(E)-N-(1,2-Dichlorovinyl)-4-methyl-N-phenylbenzenesulfonamide 69a***

 Following **GP1** using sulfonamide **72g** (2.85 g, 11.5 mmol). Hot recrystallisation (EtOH) gave **69a** as a colourless crystalline solid (3.43 g, 87%); mp: 120–121 °C (lit. 115°C); IR (neat):  $\nu$  = 3077, 1593, 1488, 1362, 1164, 1087 cm<sup>-1</sup>; <sup>1</sup>H NMR (400 MHz, CDCl<sub>3</sub>):  $\delta$  = 7.65 (d<sub>AA'XX'</sub>,  $J$  = 8.4 Hz, 2H), 7.39 – 7.30 (m, 5H), 7.25 (d<sub>AA'XX'</sub>,  $J$  = 8.0 Hz, 2H),

6.45 (s, 1H), 2.43 (s, 3H) ppm;  $^{13}\text{C}$  NMR (101 MHz,  $\text{CDCl}_3$ ):  $\delta$  = 144.7 (C), 137.8 (C), 135.7 (C), 130.8 (C), 129.5 (2CH), 129.5 (2CH), 129.2 (CH), 128.9 (2CH), 128.8 (2CH), 120.7 (CH), 21.8 ( $\text{CH}_3$ ) ppm. Spectroscopic data matched that reported in the literature.<sup>56</sup>

**(E)-N-(1,2-dichlorovinyl)-4-methyl-N-(pent-4-en-1-yl)benzenesulfonamide 69e**



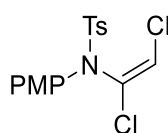
Following **GP1** using sulfonamide **72m** (1.24 g, 5.18 mmol).

Purification by flash column chromatography (9:1 hexane/EtOAc) gave

**69e** as a colourless oil (1.65 g, 95%); mp: 35–36 °C; IR (neat):  $\nu$  = 3085,

2926, 2871, 1597, 1359, 1165  $\text{cm}^{-1}$ ;  $^1\text{H}$  NMR (400 MHz,  $\text{CDCl}_3$ ):  $\delta$  = 7.80 ( $d_{\text{AA'XX'}}$ ,  $J$  = 8.2 Hz, 2H), 7.32 ( $d_{\text{AA'XX'}}$ ,  $J$  = 8.2 Hz, 2H), 6.50 (s, 1H), 5.75 (ddt,  $J$  = 16.9, 10.2, 6.6 Hz, 1H), 5.06 – 4.94 (m, 2H), 3.24 (br. s, 2H), 2.44 (s, 3H), 2.12 (qpp. q,  $J$  = 7.2 Hz, 2H), 1.63 (p,  $J$  = 7.2 Hz, 2H) ppm;  $^{13}\text{C}$  NMR (101 MHz,  $\text{CDCl}_3$ ):  $\delta$  = 144.7 (C), 137.2 (CH), 135.2 (C), 129.9 (C), 129.8 (2CH), 128.5 (2CH), 121.5 (CH), 47.4 ( $\text{CH}_2$ ), 30.7 ( $\text{CH}_2$ ), 26.8 ( $\text{CH}_2$ ), 21.7 ( $\text{CH}_3$ ) ppm; MS (ES–TOF):  $m/z$ : 100% 334.0  $[\text{M}+\text{H}]^+$ , 62% 300.0  $[\text{M}+\text{Cl}]^+$ , 10 % 338.0  $[\text{M}+\text{H}]^+$ ; HRMS (ES–TOF):  $m/z$ : calcd for  $\text{C}_{14}\text{H}_{18}\text{NO}_2\text{S}^{35}\text{Cl}_2$ : 334.0430, found 334.0436  $[\text{M}+\text{H}]^+$ .

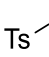
**(E)-N-(1,2-Dichlorovinyl)-N-(4-methoxyphenyl)-4-methylbenzenesulfonamide 69f**



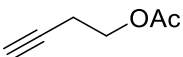
Following **GP1** using sulfonamide **72n** (3.47 g, 12.5 mmol). Hot recrystallisation (EtOH) gave **69f** as a white solid (3.65 g, 79%); mp: 135–

138 °C (lit. 134 °C); IR (neat):  $\nu$  = 1599, 1505, 1361, 1253, 1166, 1090  $\text{cm}^{-1}$ ;  $^1\text{H}$  NMR (300 MHz,  $\text{CDCl}_3$ ):  $\delta$  = 7.64 ( $d_{\text{AA'XX'}}$ ,  $J$  = 8.3 Hz, 2H), 7.28 – 7.21 (m, 4H), 6.82 ( $d_{\text{AA'XX'}}$ ,  $J$  = 9.1 Hz, 2H), 6.41 (s, 1H), 3.80 (s, 3H), 2.43 (s, 3H) ppm; MS (ES–TOF):  $m/z$ : 100% 336.1  $[\text{M}-\text{Cl}]^+$ , 30% 338.1  $[\text{M}-\text{Cl}]^+$ ; Spectroscopic data matched that reported in the literature.<sup>56</sup>

### *S-Methyl 4-Methylbenzenesulfonothioate TsSMe*

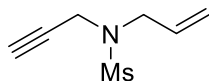
 Sodium *p*-toluenesulfinate (9.98 g, 56.0 mmol) and iodine (10.2 g, 40.2 mmol) were dissolved in CH<sub>2</sub>Cl<sub>2</sub> (60 mL) before dimethyl disulfide (1.78 mL, 19.9 mmol) was added in one portion and stirred for 16 h at r.t. The orange reaction mixture was poured into a separating funnel containing H<sub>2</sub>O (100 mL), Na<sub>2</sub>S<sub>2</sub>O<sub>3</sub> (5.0 g) and NaOH (2.0 g) and shaken vigorously until the solution remained colourless. The phases were separated and the organic layer washed with H<sub>2</sub>O (100 mL), dried over Na<sub>2</sub>SO<sub>4</sub>, filtered and concentrated under reduced pressure to give **TsSMe** as a yellow solid (7.61 g, 94%); mp: 55–57 °C; IR (neat):  $\nu$  = 2194, 1593, 1304, 1296, 1140, 1075 cm<sup>-1</sup>; <sup>1</sup>H NMR (400 MHz, CDCl<sub>3</sub>):  $\delta$  = 7.81 (d<sub>AA'</sub><sub>XX'</sub>,  $J$  = 8.2 Hz, 2H), 7.35 (d<sub>AA'</sub><sub>XX'</sub>,  $J$  = 8.2 Hz, 2H), 2.50 (s, 3H), 2.45 (s, 3H) ppm; <sup>13</sup>C NMR (101 MHz, CDCl<sub>3</sub>):  $\delta$  = 144.9 (C), 141.1 (C), 130.0 (2CH), 127.3 (2CH), 21.8 (CH<sub>3</sub>), 18.1 (CH<sub>3</sub>) ppm. Spectroscopic data matched that reported in the literature.<sup>236</sup>

### *But-3-yn-1-yl acetate 73*

 Homopropargyl alcohol (0.76 mL, 10.0 mmol) and NEt<sub>3</sub> (1.7 mL, 12.2 mmol) were stirred in CH<sub>2</sub>Cl<sub>2</sub> (30 mL) before acetyl chloride (0.85 mL, 12.0 mmol) was added dropwise over 2 min. After stirring at r.t. for 40 min, the reaction mixture was poured into 1 M HCl<sub>(aq)</sub> (50 mL) and the phases separated. The organic layer was washed with H<sub>2</sub>O (50 mL) and brine (50 mL), dried over Na<sub>2</sub>SO<sub>4</sub>, filtered and concentrated under reduced pressure. The crude material was loaded onto a pad of silica (4 cm deep) and eluted with CH<sub>2</sub>Cl<sub>2</sub>. The filtrate was concentrated under reduced pressure (30 min at 250 mbar, 40 °C) to give alkyne **73** as a pale yellow oil (1.08 g, 96%) that was characterised by <sup>1</sup>H NMR and IR only and used immediately in the next reaction; IR (neat):  $\nu$  = 1699, 1668, 1475, 1415, 1366, 1243, 1176 cm<sup>-1</sup>; <sup>1</sup>H NMR (400 MHz, CDCl<sub>3</sub>):  $\delta$  = 4.17 (t,  $J$  = 6.8 Hz, 2H), 2.53 (td,  $J$  = 6.8, 2.7 Hz, 2H), 2.07 (s, 3H),

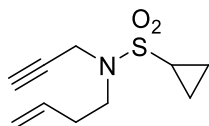
2.00 (t,  $J = 2.7$  Hz, 1H) ppm;  $^{13}\text{C}$  NMR (101 MHz,  $\text{CDCl}_3$ ):  $\delta = 171.0$  (C), 80.2 (CH), 70.0 (C), 62.3 ( $\text{CH}_2$ ), 21.0 ( $\text{CH}_3$ ), 19.1 ( $\text{CH}_2$ ) ppm.

*N-Allyl-N-(prop-2-yn-1-yl)methanesulfonamide 74a*



Sulfonamide **72b** (1.49 g, 11.0 mmol),  $\text{K}_2\text{CO}_3$  (1.82 g, 13.2 mmol) and propargyl bromide (80% in PhMe, 1.46 mL, 13.2 mmol) were dissolved in acetone (55 mL) and heated to 60 °C for 16 h. After allowing to cool to r.t., the reaction mixture was diluted with  $\text{H}_2\text{O}$  (50 mL) and extracted with  $\text{Et}_2\text{O}$  (3×25 mL). The combined organics were washed with  $\text{H}_2\text{O}$  (40 mL) and brine (40 mL), dried over  $\text{Na}_2\text{SO}_4$ , filtered and concentrated under reduced pressure. Purification by flash column chromatography (6:4 hexane/ $\text{Et}_2\text{O}$ ) gave enyne **74a** as a yellow oil (1.49 g, 78%). Spectroscopic data matched that reported in the literature.<sup>237</sup>

*N-(But-3-en-1-yl)-N-(prop-2-yn-1-yl)cyclopropanesulfonamide 76a*



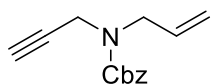
Sulfonamide **72f** (796 mg, 5.00 mmol),  $\text{K}_2\text{CO}_3$  (2.07 g, 15.0 mmol) and 4-bromobutene (761  $\mu\text{L}$ , 7.50 mmol) were dissolved in DMF (10 mL) and heated to 60 °C for 16 h. After allowing to cool to r.t., the reaction mixture was diluted with  $\text{H}_2\text{O}$  (50 mL) and extracted with  $\text{Et}_2\text{O}$  (3×25 mL). The combined organics were washed with  $\text{H}_2\text{O}$  (40 mL) and brine (40 mL), dried over  $\text{Na}_2\text{SO}_4$ , filtered and concentrated under reduced pressure. Purification by flash column chromatography (7:3 hexane/ $\text{EtOAc}$ ) gave enyne **76a** as a pale yellow oil (724 mg, 68%); IR (neat):  $\nu = 3273, 2111, 1329, 1144, 102, 998, 887\text{ cm}^{-1}$ ;  $^1\text{H}$  NMR (400 MHz,  $\text{CDCl}_3$ ):  $\delta = 5.80$  (ddt,  $J = 17.1, 10.2, 6.8$  Hz, 1H), 5.19 – 5.05 (m, 2H), 4.11 (d,  $J = 2.4$  Hz, 2H), 3.42 (t,  $J = 7.4$  Hz, 2H), 2.48 – 2.30 (m, 4H), 1.24 – 1.17 (m, 2H), 1.03 – 0.96 (m, 2H) ppm;  $^{13}\text{C}$  NMR (101 MHz,  $\text{CDCl}_3$ ):  $\delta = 134.6$  (CH), 117.5 ( $\text{CH}_2$ ), 78.0 (C),

73.9 (CH), 46.0 (CH<sub>2</sub>), 36.4 (CH<sub>2</sub>), 32.5 (CH<sub>2</sub>), 28.8 (CH), 5.4 (2CH<sub>2</sub>) ppm; HRMS (ES–TOF): *m/z*: calcd for C<sub>10</sub>H<sub>15</sub>NO<sub>2</sub>SNa: 236.0716, found 236.0720 [M+Na]<sup>+</sup>.

### General procedure 2: NaH alkylations (GP2)

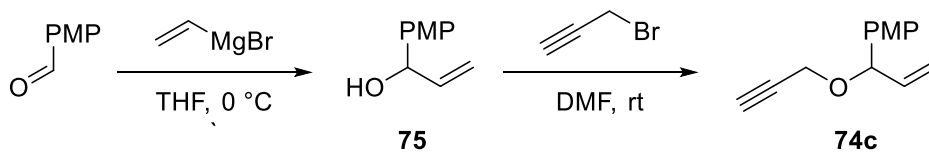
NaH (60% dispersion in mineral oil) (1.2 eq.) was transferred to a flame dried Schlenk tube and DMF (0.5 M wrt amide) was added. After stirring for 5 min, the reaction mixture was cooled to 0 °C and the amide/alcohol (1.0 eq.) added portionwise. The reaction mixture was stirred at 0 °C until the evolution of H<sub>2(g)</sub> ceases, at which point the alkyl bromide (1.2 eq.) was added dropwise over 2–5 min. After 30 min at 0 °C, the ice bath is removed and stirred overnight. The reaction mixture was then poured into H<sub>2</sub>O (3× volume of DMF) and extracted with Et<sub>2</sub>O (3×). The combined organics are washed with H<sub>2</sub>O (2×), brine (2×), dried over Na<sub>2</sub>SO<sub>4</sub>, filtered and concentrated under reduced pressure. Crude reaction mixtures were then purified by flash column chromatography to give the corresponding enynes.

### *Benzyl allyl(prop-2-yn-1-yl)carbamate 74b*



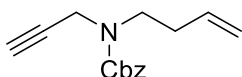
Synthesised following **GP2** from **72d** (1.13 g, 54%). Spectroscopic data matched that reported in the literature.<sup>238</sup>

### *1-Methoxy-4-(1-(prop-2-yn-1-yloxy)allyl)benzene 74c*



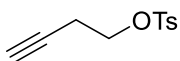
**75** synthesised according to a literature procedure (759 mg, 93%).<sup>39</sup> **74c** synthesis following **GP2** from **75** (498 mg, 91%). Spectroscopic data matched that reported in the literature.<sup>39</sup>

***Benzyl but-3-en-1-yl(prop-2-yn-1-yl)carbamate 76b***



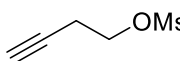
Synthesised following **GP2** from **72g** (1.04 g, 66%). Spectroscopic data matched that reported in the literature.<sup>239</sup>

***But-3-yn-1-yl 4-methylbenzenesulfonate 83a***



3-Butyn-1-ol (0.76 mL, 10.0 mmol) and NEt<sub>3</sub> (1.5 mL, 10.8 mmol) were dissolved in CH<sub>2</sub>Cl<sub>2</sub> (20 mL) and cooled to 0 °C. *p*-Toluenesulfonyl chloride (2.10 g, 11.0 mmol) was added portion wise over 10 min and stirred at 0 °C for 15 min before the ice bath was removed and the reaction mixture stirred for 2 h at r.t. The reaction mixture was poured into a separating funnel and washed with satd NaHCO<sub>3(aq)</sub> (50 mL) and brine (50 mL). The organic layer was dried over Na<sub>2</sub>SO<sub>4</sub>, filtered, concentrated under reduced pressure and purified by flash column chromatography (8:2 hexane/EtOAc) to give protected alcohol **83a** as a colourless oil (2.18 g, 97%); IR (neat):  $\nu$  = 3292, 2962, 1924, 1598, 1356, 1189, 1173, 1096, 975 cm<sup>-1</sup>; <sup>1</sup>H NMR (400 MHz, CDCl<sub>3</sub>):  $\delta$  = 7.80 (d<sub>AA'XX'</sub>, *J* = 8.2 Hz, 2H), 7.35 (d<sub>AA'XX'</sub>, *J* = 8.2 Hz, 1H), 4.10 (t, *J* = 7.1 Hz, 2H), 2.55 (td *J* = 7.1, 2.7 Hz, 2H), 2.45 (s, 3H), 1.97 (t, *J* = 2.7 Hz, 1H) ppm; <sup>13</sup>C NMR (101 MHz, CDCl<sub>3</sub>):  $\delta$  = 145.1 (C), 133.0 (C), 130.0 (2CH), 128.1 (2CH), 78.5 (C), 70.9 (CH), 67.6 (CH<sub>2</sub>), 21.8 (CH<sub>2</sub>), 19.6 (CH<sub>3</sub>) ppm; MS (ES-TOF): *m/z*: 100% 225.1 [M+H]<sup>+</sup>. Spectroscopic data matched that reported in the literature.<sup>240</sup>

***But-3-yn-1-yl methanesulfonate 83b***



3-Butyn-1-ol (2.27 mL, 30.0 mmol) and NEt<sub>3</sub> (4.6 mL, 33.0 mmol) were dissolved in CH<sub>2</sub>Cl<sub>2</sub> (60 mL) and cooled to 0 °C. Methanesulfonyl chloride (2.33 mL, 30.0 mmol) was added dropwise over 10 min and stirred at 0 °C for 15 min before the ice bath was removed and the reaction mixture stirred for 2 h at r.t. The reaction mixture was poured into a separating funnel and washed with 1 M HCl<sub>(aq)</sub> (50 mL), satd NaHCO<sub>3(aq)</sub> (50 mL) and

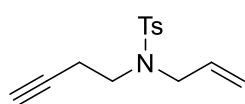


brine (50 mL). The organic layer was dried over Na<sub>2</sub>SO<sub>4</sub>, filtered and concentrated under reduced pressure to give protected alcohol **83b** as a colourless oil characterised by <sup>1</sup>H NMR only and used immediately in the next reaction (4.19 g, 94%); <sup>1</sup>H NMR (300 MHz, CDCl<sub>3</sub>): δ = 4.31 (t, *J* = 6.7 Hz, 2H), 3.06 (s, 3H), 2.66 (td, *J* = 6.7, 2.7 Hz, 2H), 2.07 (t, *J* = 2.7 Hz, 1H) ppm.

### General procedure 3: alkylation of allylamine (GP3)

Protected alkyne **83a** or **83b** (1.0 eq.), allylamine (3.0 eq.) and NaI (0.20 eq.) were combined in DMSO (0.6 M alkyne) and the mixture stirred at 50 °C overnight. The reaction mixture was poured into 2 M NaOH and extracted with Et<sub>2</sub>O (3×), before the combined organics were washed with brine (1×), dried over Na<sub>2</sub>SO<sub>4</sub>, filtered and concentrated under reduced pressure (10 mbar 10 min). The crude amine and NEt<sub>3</sub> (1.5 eq.) were dissolved in CH<sub>2</sub>Cl<sub>2</sub> (0.6 M wrt alkyne) and sulfonyl chloride (1.1 eq.) or Boc<sub>2</sub>O (1.1 eq.) were added and the reaction mixture stirred for 3 h at r.t. The reaction mixture was diluted with CH<sub>2</sub>Cl<sub>2</sub>, washed with 2 M HCl<sub>(aq)</sub>, H<sub>2</sub>O and brine before drying over Na<sub>2</sub>SO<sub>4</sub>, filtration and concentration under reduced pressure.

#### *N*-Allyl-*N*-(but-3-yn-1-yl)-4-methylbenzenesulfonamide **81a**

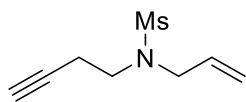


Following **GP3** with alkyne **83a** (2.80 g, 12.5 mmol). Purification by flash column chromatography gave enyne **81a** as a pale yellow oil (2.93 g, 90%); IR (neat): ν = 3288, 2921, 1598, 1451, 1338, 1305, 1153, 1091, 983, 918 cm<sup>-1</sup>; <sup>1</sup>H NMR (300 MHz, CDCl<sub>3</sub>): δ = 7.70 (d<sub>AA'XX'</sub>, *J* = 8.1 Hz, 2H), 7.30 (d<sub>AA'XX'</sub>, *J* = 8.1 Hz, 2H), 5.66 (ddt, *J* = 17.1, 10.0, 6.4 Hz, 1H), 5.25 – 5.14 (m, 2H), 3.84 (dt, *J* = 6.4, 1.3 Hz, 2H), 3.32 – 3.25 (m, 2H), 2.50 – 2.40 (m, 5H), 1.97 (t, *J* = 2.7 Hz, 1H) ppm; <sup>13</sup>C NMR (75 MHz, CDCl<sub>3</sub>): δ = 143.6 (C), 136.9 (C), 133.1 (CH), 129.9 (2CH), 127.3 (2CH), 119.4 (CH<sub>2</sub>), 81.1 (CH), 70.3 (C), 51.5

(CH<sub>2</sub>), 46.1 (CH<sub>2</sub>), 21.7 (CH<sub>3</sub>), 19.5 (CH<sub>2</sub>) ppm; MS (ES–TOF): *m/z*: 100% 264.1 [M+H]<sup>+</sup>.

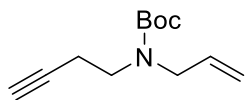
Spectroscopic data matched that reported in the literature.<sup>241</sup>

***N-Allyl-N-(but-3-yn-1-yl)-methanesulfonamide 81b***



Following **GP3** with alkyne **83b** (4.15 g, 28.0 mmol). Aqueous work up provided pure enyne **81b** as a pale yellow oil (3.13 g, 60%); IR (neat):  $\nu$  = 3282, 2934, 2175, 1643, 1321, 1143, 1081, 963 cm<sup>-1</sup>; <sup>1</sup>H NMR (400 MHz, CDCl<sub>3</sub>):  $\delta$  = 5.83 (ddt, *J* = 16.8, 10.1, 6.4 Hz, 1H), 5.34 – 5.24 (m, 2H), 3.92 (dt, *J* = 6.4, 1.4 Hz, 2H), 3.39 (t, *J* = 7.0 Hz, 2H), 2.93 (s, 3H), 2.50 (td, *J* = 7.0, 2.7 Hz, 2H), 2.02 (t, *J* = 2.7 Hz, 1H) ppm; <sup>13</sup>C NMR (101 MHz, CDCl<sub>3</sub>):  $\delta$  = 132.8 (CH), 119.6 (CH<sub>2</sub>), 81.2 (C), 70.6 (CH), 50.7 (CH<sub>2</sub>), 45.8 (CH<sub>2</sub>), 39.8 (CH<sub>3</sub>), 19.3 (CH<sub>2</sub>) ppm; HRMS (ES–TOF): *m/z*: calcd for C<sub>8</sub>H<sub>14</sub>NO<sub>2</sub>S: 188.0740, found 188.0746 [M+H]<sup>+</sup>.

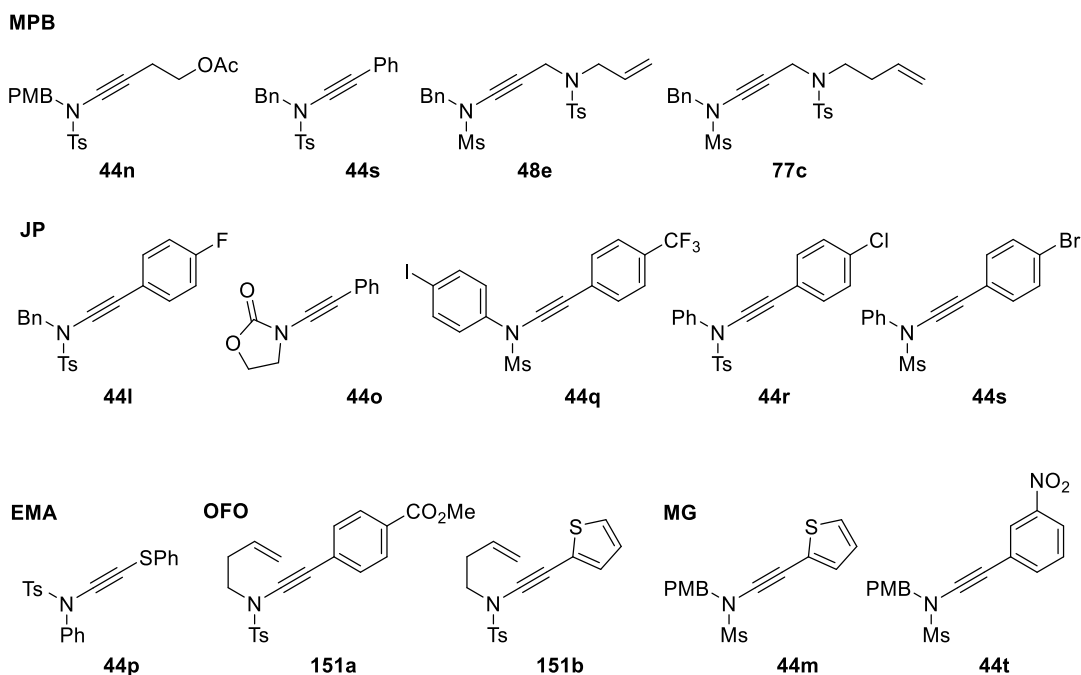
***N-Allyl-N-(but-3-yn-1-yl)-tert-butyl carbamate 81c***



Following **GP3** with alkyne **83a** (1.12 g, 4.99 mmol). Purification by flash column chromatography (8:2 hexane/Et<sub>2</sub>O) gave enyne **81c** as a colourless oil (986 mg, 94%); IR (neat):  $\nu$  = 3309, 2980, 1810, 1691, 1463, 1407, 1366, 1248, 1165, 1117 cm<sup>-1</sup>; *NMR spectra display a mixture of rotamers*: <sup>1</sup>H NMR (400 MHz, CDCl<sub>3</sub>):  $\delta$  = 5.83 – 5.71 (m, 1H), 5.13 (br. d, 2H), 3.88 (br. s, 2H), 3.34 (br. s, 2H), 2.41 (s, 2H), 1.96 (t, *J* = 2.7 Hz, 1H), 1.46 (s, 9H) ppm; <sup>13</sup>C NMR (101 MHz, CDCl<sub>3</sub>):  $\delta$  = 155.4 and 146.9 (C), 134.2 (CH), 116.8 (CH<sub>2</sub>), 85.3 (C), 80.0 (CH), 69.6 (C), 52.4 (CH<sub>2</sub>), 45.9 (CH<sub>2</sub>), 28.5 and 27.6 (3CH<sub>3</sub>), 18.7 (CH<sub>2</sub>) ppm; HRMS (ES–TOF): *m/z*: calcd for C<sub>12</sub>H<sub>19</sub>NO<sub>2</sub>Na: 232.1308, found 232.1312 [M+Na]<sup>+</sup>.

## Formation of ynamides

The following ynamides were prepared by previous Davies' group members Matthew P. Ball-Jones (MPB), Miguel Garzon (MG), Joshua D. Priest (JP), Elsa Martinez-Arce (EMA) and Onyeka F. Obumselu (OFO):



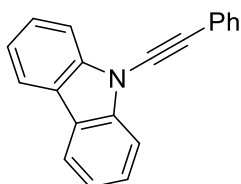
### General procedure 4: Hsung ynamide synthesis (GP4a and GP4b)

**GP4a** – The relevant terminal alkyne (1.0 eq.),  $\text{AgNO}_3$  (0.1 eq.) and NBS (1.1 eq.) were dissolved in acetone (0.2 M wrt alkyne) and stirred at r.t. for 1–4 h in darkness. The solvent was removed under reduced pressure and the crude material loaded onto a pad of silica gel and eluted with hexane/ $\text{Et}_2\text{O}$ .

**GP4b** – Following the method of Hsung,<sup>54</sup> bromoalkyne (1.2 eq.), amide (1.0 eq.)  $\text{K}_2\text{CO}_3$  (2.4 eq.),  $\text{Cu}_2\text{SO}_4 \cdot \text{H}_2\text{O}$  (0.1 eq.), 1,10-phenanthroline (0.2 eq.) and PhMe (0.1–1.0 M wrt amide) were combined in a flame dried Schlenk tube and heated to 70 °C for 16 h. After allowing to

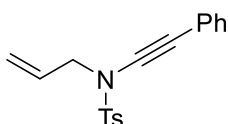
cool to r.t., the reaction mixture was filtered through a 3 cm pad of silica (EtOAc) and the solvent removed under reduced pressure. The crude material was purified through flash column chromatography or recrystallisation to give the corresponding ynamide.

***9-(Phenylethynyl)-9H-carbazole 44s***



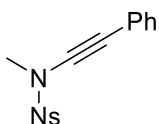
Synthesised following **GP4** (1.10 g, 62%) at 1.0M. Spectroscopic data matched that reported in the literature.<sup>242</sup>

***N-Allyl-4-methyl-N-(phenylethynyl)benzenesulfonamide 44u***



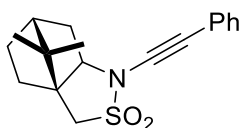
Synthesised following **GP4** (451 mg, 34%) at 1.0M. Spectroscopic data matched that reported in the literature.<sup>54</sup>

***N-Methyl-4-nitro-N-(phenylethynyl)benzenesulfonamide 44h***



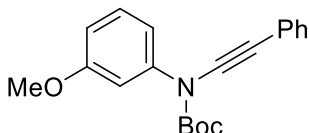
Synthesised following **GP4** (1.93 g, 76%) at 1.0M. Spectroscopic data matched that reported in the literature.<sup>243</sup>

***(3a*S*,6*R*)-8,8-dimethyl-1-(phenylethynyl)hexahydro-3*H*-3*a*,6-methanobenzo[*c*]isothiazole 2,2-dioxide 44t***



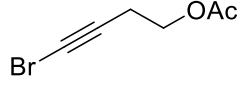
Synthesised following **GP4** (918 mg, 97%) at 1.0M. Spectroscopic data matched that reported in the literature.<sup>244</sup>

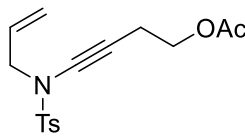
***tert-Butyl (3-methoxyphenyl)(phenylethynyl)carbamate 44g***



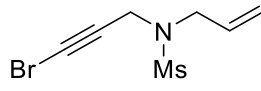
Synthesised following **GP4** (1.60 g, 62%) at 0.5M. Spectroscopic data matched that reported in the literature.<sup>245</sup>

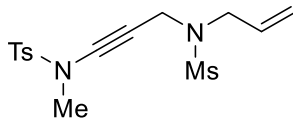
**4-((N-Allyl-4-methylphenyl)sulfonamido)but-3-yn-1-yl acetate 44e**

 Following **GP4a** with alkyne **73** (1.06 g, 9.42 mmol), NBS (1.86 g, 10.5 mmol), AgNO<sub>3</sub> (161 mg, 10 mol%) and acetone (48 mL). Filtration through a 4 cm pad of silica (7:3 hexane/Et<sub>2</sub>O) gave bromoalkyne **73'** as a pale yellow oil (1.43 g, 79%) that was used directly in the next reaction without characterisation.

 Following **GP4b** with bromoalkyne **73'** (1.43 g, 7.49 mmol) and sulfonamide **72a** (1.32 g, 6.25 mmol) at 0.5M. Purification by flash column chromatography (7:3 hexane/EtOAc) gave ynamide **44e** as a yellow oil (1.71 g, 85%); IR (neat):  $\nu = 2963, 2245, 1736, 1597, 1352, 1330, 1232, 1152, 1086 \text{ cm}^{-1}$ ; <sup>1</sup>H NMR (400 MHz, CDCl<sub>3</sub>):  $\delta = 7.77 (\text{d}_{\text{AA'XX'}}, J = 8.2 \text{ Hz}, 2\text{H}), 7.33 (\text{d}_{\text{AA'XX'}}, J = 8.2 \text{ Hz}, 2\text{H}), 5.70 (\text{ddt}, J = 17.1, 10.1, 6.3 \text{ Hz}, 1\text{H}), 5.24 - 5.16 (\text{m}, 2\text{H}), 4.09 (\text{t}, J = 6.9 \text{ Hz}, 2\text{H}), 3.91 (\text{app. dt}, J = 6.3, 1.3 \text{ Hz}, 2\text{H}), 2.59 (\text{t}, J = 6.9, 2\text{H}), 2.44 (\text{s}, 3\text{H}), 2.04 (\text{s}, 3\text{H}) \text{ ppm}$ ; <sup>13</sup>C NMR (101 MHz, CDCl<sub>3</sub>):  $\delta = 170.9 (\text{C}), 144.7 (\text{C}), 134.8 (\text{C}), 131.1 (\text{CH}), 129.8 (2\text{CH}), 127.8 (2\text{CH}), 119.9 (\text{CH}_2), 74.6 (\text{C}), 66.3 (\text{C}), 62.7 (\text{CH}_2), 54.3 (\text{CH}_2), 21.8 (\text{CH}_3), 21.0 (\text{CH}_3), 19.1 (\text{CH}_2) \text{ ppm}$ ; HRMS (ES-TOF):  $m/z$ : calcd for C<sub>16</sub>H<sub>20</sub>NO<sub>4</sub>S: 322.1108, found 322.1115 [M+H]<sup>+</sup>.

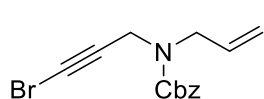
**N-(3-(N-Allylmethylsulfonamido)prop-1-yn-1-yl)-N,4-dimethylbenzenesulfonamide 48a**

 Following **GP4a** with alkyne **74a** (1.49 g, 8.61 mmol), NBS (1.68 g, 6.47 mmol), AgNO<sub>3</sub> (146 mg, 10 mol%) and acetone (43 mL). Filtration through a 4 cm pad of silica (6:4 hexane/Et<sub>2</sub>O) gave bromoalkyne **74a'** as a pale yellow oil (1.82 g, 84%) that was used directly in the next reaction without characterisation.

 Following **GP4b** with bromoalkyne **74a'** (1.82 g, 7.22 mmol) and sulfonamide **72c** (1.11 g, 6.00 mmol) at 0.5M. Purification by flash column chromatography (65:35 hexane/EtOAc) gave enynamide **48a** as a colourless oil that

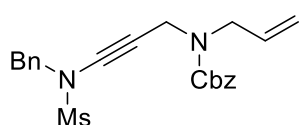
solidified upon standing (1.95 g, 91%); mp: 73–74 °C; IR (neat):  $\nu$  = 2929, 2246, 1598, 1364, 1323, 1168, 1155, 1145, 1105, 1087, 1017  $\text{cm}^{-1}$ ;  $^1\text{H}$  NMR (400 MHz,  $\text{CDCl}_3$ ):  $\delta$  = 7.75 ( $d_{\text{AA'XX'}}$ ,  $J$  = 8.2 Hz, 2H), 7.38 ( $d_{\text{AA'XX'}}$ ,  $J$  = 8.2 Hz, 2H), 5.80 (ddt,  $J$  = 16.6, 10.0, 6.4 Hz, 1H), 5.41 – 5.26 (m, 2H), 4.14 (s, 2H), 3.85 (d,  $J$  = 6.3 Hz, 2H), 3.06 (s, 3H), 2.92 (s, 3H), 2.46 (s, 3H) ppm;  $^{13}\text{C}$  NMR (101 MHz,  $\text{CDCl}_3$ ):  $\delta$  = 145.3 (C), 133.3 (C), 132.2 (CH), 130.1 (2CH), 127.8 (2CH), 120.0 ( $\text{CH}_2$ ), 80.8 (C), 62.8 (C), 49.2 ( $\text{CH}_2$ ), 39.0 ( $\text{CH}_3$ ), 38.4 ( $\text{CH}_3$ ), 36.2 ( $\text{CH}_2$ ), 21.8 ( $\text{CH}_3$ ) ppm; HRMS (ES–TOF):  $m/z$ : calcd for  $\text{C}_{15}\text{H}_{21}\text{N}_2\text{O}_4\text{S}_2$ : 357.0937, found 357.0947  $[\text{M}+\text{H}]^+$ .

***Benzyl allyl(3-(N-benzylmethylsulfonamido)prop-2-yn-1-yl)carbamate 48b***



Following **GP4a** with alkyne **74b** (1.13 g, 4.91 mmol), NBS (961 mg, 3.40 mmol),  $\text{AgNO}_3$  (84 mg, 10 mol%) and acetone (25 mL).

Purification by flash column chromatography (8:2 hexane/ $\text{Et}_2\text{O}$ ) gave bromoalkyne **74b'** as a pale yellow oil (1.17 g, 78%) that was used directly in the next reaction without characterisation.

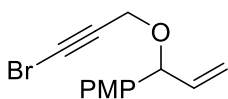


Following **GP4b** with bromoalkyne **74b'** (1.17 g, 3.81 mmol) and sulfonamide **72e** (589 mg, 3.18 mmol) at 0.5M. Purification by flash

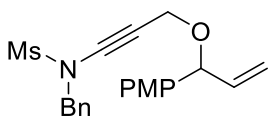
column chromatography (7:3 hexane/ $\text{EtOAc}$ ) gave enynamide **48b** as a yellow oil (1.24 g, 94%); IR (neat):  $\nu$  = 3033, 2933, 2695, 1455, 1416, 1428, 1323, 1152  $\text{cm}^{-1}$ ; *NMR spectra display a mixture of rotamers*:  $^1\text{H}$  NMR (400 MHz,  $\text{CDCl}_3$ ):  $\delta$  = 7.42 – 7.28 (m, 10H), 5.72 (br. s, 1H), 5.16 (s, 2H), 5.12 (br. s, 2H), 4.57 (br. s, 2H), 4.19 (br. d, 2H), 3.93 – 3.87 (m, 2H), 2.83 (br. d, 3H) ppm;  $^{13}\text{C}$  NMR (101 MHz,  $\text{CDCl}_3$ ):  $\delta$  = 155.6 (C), 136.6 (C), 134.6 (C), 133.0 (CH), 129.0 (CH), 128.9 (CH), 128.8 (CH), 128.6 (CH), 128.2 (CH), 128.0 (CH), 118.0 ( $\text{CH}_2$ ) 67.5 ( $\text{CH}_2$ ), 55.6 ( $\text{CH}_2$ ), 48.2 ( $\text{CH}_2$ ) 38.9 ( $\text{CH}_3$ ), 36.1 ( $\text{CH}_2$ ) ppm; *equivalent aromatic CH*

groups cannot be determined due to overlap. Neither quaternary alkyne carbon resonances not observed in  $^{13}\text{C}$  NMR spectra; HRMS (ES–TOF):  $m/z$ : calcd for  $\text{C}_{22}\text{H}_{25}\text{N}_2\text{O}_4\text{S}$ : 413.1530, found 513.1526  $[\text{M}+\text{H}]^+$ .

***N*-Benzyl-*N*-(3-((1-(4-methoxyphenyl)allyl)oxy)prop-1-yn-1-yl)methanesulfonamide **48c****

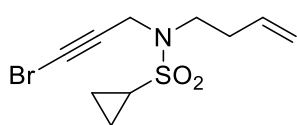


Following **GP4a** with alkyne **74c** (495 mg, 2.45 mmol), NBS (481 mg, 2.80 mmol),  $\text{AgNO}_3$  (41.6 mg, 10 mol%) and acetone (13 mL). Filtration through a pad of 4 cm silica (7:3 pentane/ $\text{Et}_2\text{O}$ ) gave bromoalkyne **74c'** as a pale yellow oil (683 mg, 99%) that was used directly in the next reaction without characterisation.



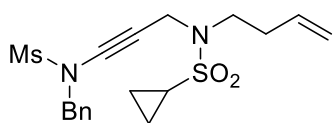
Following **GP4b** with bromoalkyne **74c'** (683 mg, 2.43 mmol) and sulfonamide **72e** (370 mg, 2.00 mmol) at 0.5M. Purification by flash column chromatography (3:1 hexane/ $\text{EtOAc}$ ) gave enynamide **48c** as a yellow oil (725 mg, 94%); IR (neat):  $\nu = 2934, 2839, 2243, 1604, 1511, 1347, 1246, 1155, 1028\text{ cm}^{-1}$ ;  $^1\text{H}$  NMR (400 MHz,  $\text{CDCl}_3$ ):  $\delta = 7.47 - 7.33$  (m, 5H), 7.20 ( $d_{\text{AA'XX'}}$ ,  $J = 8.5\text{ Hz}$ , 2H), 6.87 ( $d_{\text{AA'XX'}}$ ,  $J = 8.5\text{ Hz}$ , 2H), 5.91 (ddd,  $J = 17.0, 10.3, 6.6\text{ Hz}$ , 1H), 5.25 – 5.18 (m, 2H), 4.86 (d,  $J = 6.6\text{ Hz}$ , 1H), 4.63 (s, 2H), 4.27 (d,  $J_{\text{AB}} = 16.3\text{ Hz}$ , 1H), 4.17 (d,  $J_{\text{AB}} = 16.3\text{ Hz}$ , 1H), 3.80 (s, 3H), 2.89 (s, 3H) ppm;  $^{13}\text{C}$  NMR (101 MHz,  $\text{CDCl}_3$ ):  $\delta = 159.4$  (C), 138.3 (CH), 134.7 (C), 132.2 (C), 129.0 (2CH), 128.9 (2CH), 128.8 (2CH), 128.6 (2CH), 116.9 ( $\text{CH}_2$ ), 114.0 (CH), 80.5 (CH), 79.4 (C), 68.7 (C), 55.7 ( $\text{CH}_2$ ), 55.6 ( $\text{CH}_2$ ), 55.4 ( $\text{CH}_3$ ), 39.1 ( $\text{CH}_3$ ) ppm; HRMS (ES–TOF):  $m/z$ : calcd for  $\text{C}_{21}\text{H}_{23}\text{NO}_4\text{SNa}$ : 408.1240, found 408.1248  $[\text{M}+\text{Na}]^+$ .

***N*-(3-(*N*-Benzylmethylsulfonamido)prop-2-yn-1-yl)-*N*-(but-3-en-1-yl)cyclopropanesulfonamide **77a****



Following **GP4a** with alkyne **76a** (1.58 g, 7.40 mmol), NBS (1.45 g, 8.15 mmol), AgNO<sub>3</sub> (126 mg, 10 mol%) and acetone (37 mL).

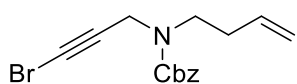
Filtration through a 5 cm pad of silica (6:4 hexane/Et<sub>2</sub>O) gave bromoalkyne **76a'** as a pale yellow oil (2.13 g, 98%) that was used directly in the next reaction without characterisation.



Following **GP4b** with bromoalkyne **76a'** (2.10 g, 7.19 mmol) and sulfonamide **72e** (1.11 g, 5.99 mmol) at 0.5M. Purification by flash

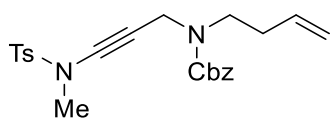
column chromatography (0→100% hexane:Et<sub>2</sub>O) gave enynamide **77a** as a brown oil (1.67 g, 70%); IR (neat):  $\nu$  = 2248, 1455, 1330, 1145, 1043, 888 = cm<sup>-1</sup>; <sup>1</sup>H NMR (400 MHz, CDCl<sub>3</sub>):  $\delta$  = 7.42 – 7.33 (m, 5H), 5.73 (ddt,  $J$  = 17.0, 10.2, 6.7 Hz, 1H), 5.14 – 5.01 (m, 2H), 4.59 (s, 2H), 4.19 (s, 2H), 3.21 (t,  $J$  = 7.1 Hz 2H), 2.96 (s, 3H), 2.29 – 2.22 (m, 2H), 2.18 (tt,  $J$  = 8.1, 4.9 Hz, 1H), 1.10 – 1.01 (m, 2H), 0.87 – 0.77 (m, 2H) ppm; <sup>13</sup>C NMR (101 MHz, CDCl<sub>3</sub>):  $\delta$  = 134.7 (CH), 134.5 (C), 129.0 (2CH), 128.94 (CH), 128.87 (2CH), 117.3 (CH<sub>2</sub>), 78.3 (C), 66.4 (C), 55.4 (CH<sub>2</sub>), 45.8 (CH<sub>2</sub>), 39.1 (CH<sub>3</sub>), 36.8 (CH<sub>2</sub>), 32.4 (CH<sub>2</sub>), 28.5 (CH), 5.1 (2CH<sub>2</sub>) ppm; HRMS (ES-TOF):  $m/z$ : calcd for C<sub>18</sub>H<sub>24</sub>N<sub>2</sub>O<sub>4</sub>S<sub>2</sub>Na: 419.1070, found 419.1072 [M+Na]<sup>+</sup>.

***Benzyl but-3-en-1-yl*(3-((*N*,4-dimethylphenyl)sulfonamido)prop-2-yn-1-yl)carbamate **77b****



Following **GP4a** with alkyne **76b** (1.02 g, 4.19 mmol), NBS (819 mg, 4.62 mmol), AgNO<sub>3</sub> (71 mg, 10 mol%) and acetone (21 mL).

Purification by flash column chromatography (9:1 hexane/Et<sub>2</sub>O) gave bromoalkyne **76b'** as a yellow oil (1.29 g, 96%) that was used directly in the next reaction without characterisation.

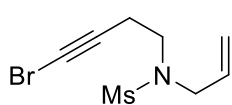


Following **GP4b** with bromoalkyne **76b'** (1.29 g, 4.01 mmol) and sulfonamide **72c** (611 mg, 3.30 mmol) at 0.5M. Purification by

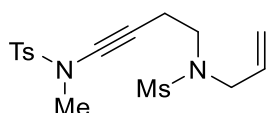


flash column chromatography (3:1 hexane/EtOAc) gave enynamide **77b** as colourless oil (1.26 g, 90%); IR (neat):  $\nu = 2923, 1693, 1597, 1455, 1417, 1354, 1216, 1146, 1148 \text{ cm}^{-1}$ ; *NMR spectra display a mixture of rotamers*:  $^1\text{H}$  NMR (400 MHz,  $\text{CDCl}_3$ ):  $\delta = 7.74$  (br. s, 2H), 7.43 – 7.27 (m, 7H), 5.84 – 5.64 (m, 1H), 5.14 (s, 2H), 5.11 – 4.97 (m, 2H), 4.28 – 4.14 (m, 2H), 3.39 (t,  $J = 7.3 \text{ Hz}$ , 2H), 3.06 – 2.98 (m, 3H), 2.43 (s, 3H), 2.35 – 2.25 (m, 2H) ppm;  $^{13}\text{C}$  NMR (101 MHz,  $\text{CDCl}_3$ ):  $\delta = 144.9$  (C), 136.7 (C), 135.2 (CH), 133.3 (C), 129.9 (2CH), 128.6 (CH), 128.1 (CH), 127.9 (CH), 127.8 (CH), 117.0 ( $\text{CH}_2$ ), 78.6 (C), 67.4 ( $\text{CH}_2$ ), 64.7 (C), 46.5 ( $\text{CH}_2$ ) and 45.5, 39.2 ( $\text{CH}_3$ ), 36.8 ( $\text{CH}_2$ ), 32.8 and 32.4 ( $\text{CH}_2$ ), 21.8 ( $\text{CH}_3$ ) ppm; *equivalent aromatic CH groups cannot be determined due to overlap in  $^{13}\text{C}$  NMR spectra*; HRMS (ES–TOF):  $m/z$ : calcd for  $\text{C}_{23}\text{H}_{29}\text{N}_2\text{O}_5\text{S}$ : 445.1792, found 445.1798  $[\text{M}+\text{H}_3\text{O}]^+$ .

***N*-(4-(*N*-Allylmethylsulfonamido)but-1-yn-1-yl)-*N*,4-dimethylbenzenesulfonamide 85a**



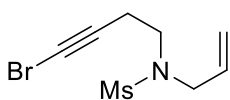
Following **GP4a** with alkyne **81b** (3.09 g, 16.5 mmol), NBS (3.22 g, 18.2 mmol),  $\text{AgNO}_3$  (280 mg, 10 mol%) and acetone (85 mL). Filtration through a 6 cm pad of silica (1:1 hexane/ $\text{Et}_2\text{O}$ ) gave bromoalkyne **81b'** as a yellow oil (3.87 g, 88%) that was used directly in the next reaction without characterisation.



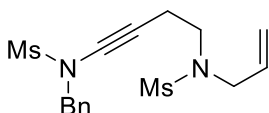
Following **GP4b** with bromoalkyne **81b'** (3.87 g, 14.5 mmol) and sulfonamide **72c** (2.24 g, 12.1 mmol) at 0.4M. Purification by flash column chromatography (6:4 hexane/ $\text{EtOAc}$ ) gave enynamide **85a** as a pale yellow oil (4.04 g, 75%); IR (neat):  $\nu = 2930, 2255, 2059, 1676, 1323, 1160, 1147, 1089, 1040 \text{ cm}^{-1}$ ;  $^1\text{H}$  NMR (300 MHz,  $\text{CDCl}_3$ ):  $\delta = 7.76$  ( $d_{\text{AA}'\text{XX}'}$ ,  $J = 8.1 \text{ Hz}$ , 2H), 7.36 ( $d_{\text{AA}'\text{XX}'}$ ,  $J = 8.1 \text{ Hz}$ , 2H), 5.81 (ddt,  $J = 17.1, 10.1, 6.3 \text{ Hz}$ , 1H), 5.33 – 5.23 (m, 2H), 3.89 (dt,  $J = 6.3, 1.4 \text{ Hz}$ , 2H), 3.32 (t,  $J = 7.1 \text{ Hz}$ , 2H), 3.01 (s, 3H), 2.87 (s, 3H), 2.56 (t,  $J = 7.1 \text{ Hz}$ , 2H), 2.45 (s, 3H) ppm;  $^{13}\text{C}$  NMR (101 MHz,  $\text{CDCl}_3$ ):  $\delta = 144.9$  (C), 133.3 (C), 132.9 (CH), 129.9 (2CH), 127.8 (2CH), 119.5 ( $\text{CH}_2$ ),

76.7 (C), 65.4 (C), 50.7 (CH<sub>2</sub>), 46.2 (CH<sub>2</sub>), 39.7 (CH<sub>3</sub>), 39.3 (CH<sub>3</sub>), 21.8 (CH<sub>3</sub>), 19.3 (CH<sub>2</sub>) ppm; HRMS (ES–TOF): *m/z*: calcd for C<sub>16</sub>H<sub>23</sub>N<sub>2</sub>O<sub>4</sub>S<sub>2</sub>: 371.1094, found 371.1101 [M+H]<sup>+</sup>.

***N*-Allyl-*N*-(4-(*N*-benzylmethylsulfonamido)but-3-yn-1-yl)methanesulfonamide **85b****

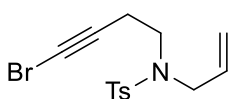


Following **GP4a** with alkyne **81b** (514 mg, 2.75 mmol), NBS (538 mg, 3.03 mmol), AgNO<sub>3</sub> (46.8 mg, 10 mol%) and acetone (14 mL). Filtration through a 6 cm pad of silica (1:1 hexane/Et<sub>2</sub>O) gave bromoalkyne **81b'** as a yellow oil (732 mg, quant.) that was used directly in the next reaction without characterisation.

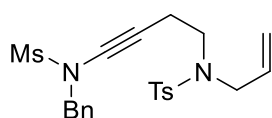


Following **GP4b** with bromoalkyne **81b'** (732 mg, 2.75 mmol) and sulfonamide **72e** (426 mg, 2.30 mmol) at 0.5 M. Purification by flash column chromatography (6:4 hexane/EtOAc) gave enynamide **85b** as a pale yellow oil (596 mg, 70%); IR (neat):  $\nu$  = 2933, 2254, 1662, 1584, 1316, 1148, 962 cm<sup>-1</sup>; <sup>1</sup>H NMR (400 MHz, CDCl<sub>3</sub>):  $\delta$  = 7.44 – 7.34 (m, 5H), 5.77 (ddt, *J* = 17.2, 10.1, 6.3 Hz, 1H), 5.29 – 5.21 (m, 2H), 4.57 (s, 2H), 3.82 (dt, *J* = 6.3, 1.3 Hz, 2H), 3.30 (t, *J* = 6.9 Hz, 2H), 2.90 (s, 3H), 2.82 (s, 3H), 2.57 (t, *J* = 6.9 Hz, 2H) ppm; <sup>13</sup>C NMR (101 MHz, CDCl<sub>3</sub>):  $\delta$  = 134.8 (C), 132.8 (CH), 128.93 (2CH), 128.90 (2CH), 128.8 (CH), 119.5 (CH<sub>2</sub>), 75.0 (C), 67.9 (C), 55.6 (CH<sub>2</sub>), 50.5 (CH<sub>2</sub>), 46.0 (CH<sub>2</sub>), 39.6 (CH<sub>3</sub>), 38.7 (CH<sub>3</sub>), 19.3 (CH<sub>2</sub>) ppm; HRMS (ES–TOF): *m/z*: calcd for C<sub>16</sub>H<sub>23</sub>N<sub>2</sub>O<sub>4</sub>S<sub>2</sub>: 371.1094, found 371.1010 [M+H]<sup>+</sup>.

***N*-Allyl-*N*-(4-(*N*-benzylmethylsulfonamido)but-3-yn-1-yl)-4-methylbenzenesulfonamide **85c****



Following **GP4a** with alkyne **81a** (1.87 g, 7.16 mmol), NBS (1.40 g, 7.87 mmol), AgNO<sub>3</sub> (121 mg, 10 mol%) and acetone (35 mL). Filtration through a pad of silica (7:3 hexane/Et<sub>2</sub>O) gave bromoalkyne **81a'** as a yellow oil (2.05 g, 83%) that was used directly in the next reaction without characterisation.

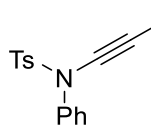


Following **GP4b** with bromoalkyne **81a'** (1.64 g, 4.80 mmol) and sulfonamide **72e** (470 mg, 3.99 mmol) at 0.5M. Purification by flash column chromatography (0→100% hexane:Et<sub>2</sub>O) gave enynamide **85c** as a pale yellow oil (1.71 g, 96%); IR (neat):  $\nu$  = 2925, 2255, 1686, 1344, 1153, 1091 cm<sup>-1</sup>; <sup>1</sup>H NMR (400 MHz, CDCl<sub>3</sub>):  $\delta$  = 7.68 (d<sub>AA'</sub><sub>XX'</sub>,  $J$  = 8.1 Hz, 2H), 7.45 – 7.35 (m, 5H), 7.30 (d<sub>AA'</sub><sub>XX'</sub>,  $J$  = 8.1 Hz, 2H), 5.57 (ddt,  $J$  = 17.1, 10.0, 6.4 Hz, 1H), 5.17 – 5.10 (m, 2H), 4.57 (s, 2H), 3.77 (dt,  $J$  = 6.4, 1.4 Hz, 2H), 3.22 (t,  $J$  = 7.2 Hz, 2H), 2.89 (s, 3H), 2.54 (t,  $J$  = 7.2 Hz, 2H), 2.43 (s, 3H) ppm; <sup>13</sup>C NMR (101 MHz, CDCl<sub>3</sub>):  $\delta$  = 143.6 (C), 137.0 (C), 134.8 (C), 133.0 (CH), 129.9 (2CH), 129.0 (2CH), 128.9 (2CH), 128.7 (CH), 127.2 (2CH), 119.3 (CH<sub>2</sub>), 74.9 (C), 67.9 (C), 55.7 (CH<sub>2</sub>), 51.3 (CH<sub>2</sub>), 46.5 (CH<sub>2</sub>), 38.7 (CH<sub>3</sub>), 21.7 (CH<sub>3</sub>), 19.5 (CH<sub>2</sub>) ppm; HRMS (ES–TOF):  $m/z$ : calcd for C<sub>22</sub>H<sub>27</sub>N<sub>2</sub>O<sub>4</sub>S<sub>2</sub>: 447.1407, found 447.1409 [M+H]<sup>+</sup>.

### General procedure 5: Anderson ynamide synthesis (GP5)

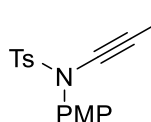
Following the method of Anderson,<sup>56</sup> the relevant dichloroenamide (1.0 eq.) was dissolved in THF (0.25 M wrt dichloroenamide) and cooled to –78 °C. A solution of *n*-BuLi in hexanes (1.6 M, 1.2 eq.) was added via syringe pump over 10 min and the reaction stirred for 5 min at –78 °C before warming to –40 °C and stirring for 30 min. After cooling the reaction mixture back to –78 °C, *n*-BuLi in hexanes (1.6 M, 1.0 eq.) was added via syringe pump over 10 min and the mixture stirred for an additional 10 min before the relevant electrophile (1.2 eq.) was added portion wise. After 10 min at –78 °C, the cooling bath was removed and the reaction stirred at r.t. for 2 h before quenching the reaction with H<sub>2</sub>O. The organics were extracted with Et<sub>2</sub>O (3×) and the combined organics were washed with H<sub>2</sub>O (1×) and brine (1×), dried over Na<sub>2</sub>SO<sub>4</sub>, filtered and concentrated under reduced pressure. The crude material was purified by flash column chromatography or recrystallisation to give the corresponding ynamide.

#### **4-Methyl-N-phenyl-N-((methylthio)ethynyl)benzenesulfonamide 44a**



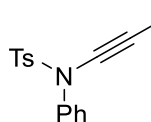
Following **GP5** with dichloroenamide **69a** (1.71 g, 5.00 mmol) and **TsSMe** (1.31 g, 6.50 mmol). Purification by flash column chromatography (9:1 heptane:EtOAc) gave ynamide **44a** as a yellow solid (1.58 g, 99%); mp: 122–124 °C; IR (neat):  $\nu = 2934, 2168, 1594, 1487, 1537, 1172, 1453, 1089 \text{ cm}^{-1}$ ;  $^1\text{H}$  NMR (400 MHz,  $\text{CDCl}_3$ ):  $\delta = 7.60 (\text{d}_{\text{AA'XX}}, J = 8.3 \text{ Hz}, 2\text{H}), 7.34 - 7.27 (\text{m}, 5\text{H}), 7.24 - 7.20 (\text{m}, 2\text{H}), 2.44 (\text{s}, 3\text{H}), 2.34 (\text{s}, 3\text{H})$  ppm;  $^{13}\text{C}$  NMR (101 MHz,  $\text{CDCl}_3$ ):  $\delta = 145.1 (\text{C}), 139.2 (\text{C}), 133.43 (\text{C}), 129.6 (2\text{CH}), 129.2 (2\text{CH}), 128.4 (3\text{CH}), 126.4 (2\text{CH}), 86.7 (\text{C}), 66.7 (\text{C}), 21.8 (\text{CH}_3), 20.6 (\text{CH}_3)$  ppm; HRMS (ES-TOF):  $m/z$ : calcd for  $\text{C}_{16}\text{H}_{15}\text{NO}_2\text{S}_2\text{Na}$ : 340.0436, found 340.0445  $[\text{M}+\text{Na}]^+$ .

#### **4-Methyl-N-(4-methoxybenzyl)-N-((methylthio)ethynyl)benzenesulfonamide 44b**



Following **GP5** with dichloroenamide **69f** (1.49 g, 4.00 mmol) and **TsSMe** (890 mg, 4.40 mmol). Purification by flash column chromatography (7:3 hexane/EtOAc) gave ynamide **44b** as a yellow solid (1.05 g, 75%); mp: 129–131 °C; IR (neat):  $\nu = 2169, 2027, 1593, 1505, 1357, 1252, 1163, 1087, 1038 \text{ cm}^{-1}$ ;  $^1\text{H}$  NMR (400 MHz,  $\text{CDCl}_3$ ):  $\delta = 7.60 (\text{d}_{\text{AA'XX}}, J = 8.1 \text{ Hz}, 2\text{H}), 7.29 (\text{d}_{\text{AA'XX}}, J = 8.1 \text{ Hz}, 2\text{H}), 7.08 (\text{d}_{\text{AA'XX}}, J = 9.0 \text{ Hz}, 2\text{H}), 6.81 (\text{d}_{\text{AA'XX}}, J = 9.0 \text{ Hz}, 2\text{H}), 3.79 (\text{s}, 3\text{H}), 2.44 (\text{s}, 3\text{H}), 2.32 (\text{s}, 3\text{H})$  ppm;  $^{13}\text{C}$  NMR (101 MHz,  $\text{CDCl}_3$ ):  $\delta = 159.6 (\text{C}), 145.0 (\text{C}), 133.3 (\text{C}), 131.8 (\text{C}), 129.6 (2\text{CH}), 128.4 (2\text{CH}), 128.0 (2\text{CH}), 114.4 (2\text{CH}), 87.1 (\text{C}), 65.9 (\text{C}), 55.6 (\text{CH}_3), 21.8 (\text{CH}_3), 20.6 (\text{CH}_3)$  ppm; HRMS (ES-TOF):  $m/z$ : calcd for  $\text{C}_{17}\text{H}_{17}\text{NO}_3\text{S}_2\text{Na}$ : 370.0542, found 370.0549  $[\text{M}+\text{Na}]^+$ .

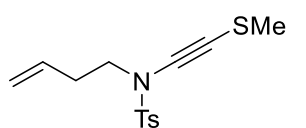
#### **Methyl 3-((N-phenyl-4-methylphenyl)sulfonamido)propiolate 44k**



Following **GP5** with dichloroenamide **69a** (342 mg, 1.00 mmol) and methyl chloroformate (93  $\mu\text{L}$ , 1.20 mmol). Purification by flash column chromatography (7:3 hexane/EtOAc) gave ynamide **44k** as a white solid (210 mg, 60%); mp:

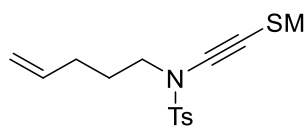
134–135 °C; IR (neat):  $\nu$  = 2221, 1710, 1594, 1491, 1381, 1355, 1208, 1190, 1175, 1125  $\text{cm}^{-1}$ ;  $^1\text{H}$  NMR (400 MHz,  $\text{CDCl}_3$ ):  $\delta$  = 7.63 ( $d_{\text{AA'XX'}}$ ,  $J$  = 8.4 Hz, 2H), 7.38 – 7.30 (m, 5H), 7.22 – 7.18 (m, 2H), 3.77 (s, 3H), 2.45 (s, 3H) ppm;  $^{13}\text{C}$  NMR (101 MHz,  $\text{CDCl}_3$ ):  $\delta$  = 154.6 (C), 146.0 (C), 137.2 (C), 133.0 (C), 130.0 (2CH), 129.6 (2CH), 129.3 (CH), 128.5 (2CH), 126.7 (2CH), 82.8 (C), 66.4 (C), 52.6 ( $\text{CH}_3$ ), 21.9 ( $\text{CH}_3$ ) ppm; HRMS (ES–TOF):  $m/z$ : calcd for  $\text{C}_{17}\text{H}_{16}\text{NO}_4\text{S}$ : 330.0795, found 330.0801  $[\text{M}+\text{H}]^+$ .

**4-Methyl-N-(but-3-en-1-yl)-N-((methylthio)ethynyl)benzenesulfonamide 151c**



Following **GP5** with dichloroenamide **69g** (320 mg, 1.00 mmol) and **TsSMe** (243 mg, 1.20 mmol). Purification by flash column chromatography (9:1 hexane/EtOAc) gave **151c** as a pale yellow oil (261 mg, 88%); IR (neat):  $\nu$  = 2926, 2151, 1597, 1361, 1167  $\text{cm}^{-1}$ ;  $^1\text{H}$  NMR (400 MHz,  $\text{CDCl}_3$ ):  $\delta$  = 7.79 ( $d_{\text{AA'XX'}}$ ,  $J$  = 8.4 Hz, 2H), 7.34 ( $d_{\text{AA'XX'}}$ ,  $J$  = 8.4 Hz, 2H), 5.68 (ddt,  $J$  = 17.0, 10.2, 6.8 Hz, 1H), 5.11 – 5.00 (m, 2H), 3.41 (t,  $J$  = 7.4 Hz, 2H), 2.45 (s, 3H), 2.41 – 2.33 (m, 2H), 2.31 (s, 3H) ppm;  $^{13}\text{C}$  NMR (101 MHz,  $\text{CDCl}_3$ ):  $\delta$  = 144.8 (C), 134.9 (C), 133.8 (CH), 129.8 (2CH), 127.8 (2CH), 117.9 ( $\text{CH}_2$ ), 86.2 (C), 67.1 (C), 51.1 ( $\text{CH}_2$ ), 32.4 ( $\text{CH}_2$ ), 21.8 ( $\text{CH}_3$ ), 20.8 ( $\text{CH}_3$ ) ppm; HRMS (ES–TOF):  $m/z$ : calcd for  $\text{C}_{14}\text{H}_{17}\text{NO}_2\text{S}_2$ : 295.0695, found 295.0699  $[\text{M}]^+$ .

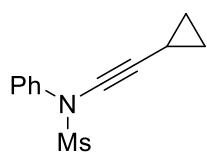
**4-Methyl-N-(pent-4-en-1-yl)-N-((methylthio)ethynyl)benzenesulfonamide 151d**



Following **GP5** with dichloroenamide **69e** (320 mg, 0.957 mmol) and **TsSMe** (243 mg, 1.20 mmol). Purification by flash column chromatography (9:1 hexane/EtOAc) gave **151d** as a pale yellow oil (290 mg, 98%); IR (neat):  $\nu$  = 2927, 2156, 1642, 1597, 1362, 1167, 1090, 912, 813, 731, 660  $\text{cm}^{-1}$ ;  $^1\text{H}$  NMR (400 MHz,  $\text{CDCl}_3$ ):  $\delta$  = 7.78 ( $d_{\text{AA'XX'}}$ ,  $J$  = 8.0 Hz, 2H), 7.34 ( $d_{\text{AA'XX'}}$ ,  $J$  = 8.0 Hz, 2H), 5.75 (ddt,  $J$  = 16.9, 10.2, 6.6 Hz, 1H), 5.05 – 4.96 (m, 2H), 3.35 (t,  $J$  = 7.2 Hz, 2H), 2.45 (s, 3H), 2.31 (s, 3H), 2.10

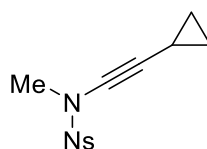
– 2.02 (m, 2H), 1.73 (p,  $J = 7.2$  Hz, 2H) ppm;  $^{13}\text{C}$  NMR (101 MHz,  $\text{CDCl}_3$ ):  $\delta = 144.7$  (C), 137.2 (CH), 134.9 (C), 129.9 (2CH), 127.8 (2CH), 115.7 ( $\text{CH}_2$ ), 86.4 (C), 66.7 (C), 51.3 ( $\text{CH}_2$ ), 30.4 ( $\text{CH}_2$ ), 27.3 ( $\text{CH}_2$ ), 21.8 ( $\text{CH}_3$ ), 20.8 ( $\text{CH}_3$ ) ppm; HRMS (ES–TOF):  $m/z$ : calcd for  $\text{C}_{15}\text{H}_{20}\text{NO}_2\text{S}_2$ : 310.0930, found 310.0937  $[\text{M}+\text{H}]^+$ .

***N*–(Cyclopropylethynyl)–*N*–phenylmethanesulfonamide **44c****



Sulfonamide **72o** (1.71 g, 10.0 mmol),  $\text{CuCl}_2$  (26.9 mg, 0.20 mmol) and  $\text{Na}_2\text{CO}_3$  (420 mg, 4.00 mmol) were combined in a flame dried Schlenk tube and purged with  $\text{O}_{2(\text{g})}$  for 10 min. A 0.4 M solution of pyridine (0.32 mL, 4.00 mmol) in PhMe (10 mL) was added and a balloon of  $\text{O}_{2(\text{g})}$  attached before heating to 70 °C. After 15 min, a 0.2 M solution of ethynylcyclopropane (170  $\mu\text{L}$ , 2.01 mmol) in PhMe (10 mL) was added over 4 h using a syringe pump and the reaction then left to stir at 70 °C for 4 h. After allowing to cool to r.t., the reaction mixture was filtered through a 3 cm pad of silica (EtOAc) and concentrated under reduced pressure. Purification by flash column chromatography (85:15 hexane/EtOAc) gave ynamide **44c** as a colourless solid (466 mg, 99%); mp: 73–75 °C; IR (neat):  $\nu = 3010, 2160, 1487, 1359, 1327, 1270, 1159, 1080\text{ cm}^{-1}$ ;  $^1\text{H}$  NMR (400 MHz,  $\text{CDCl}_3$ ):  $\delta = 7.50 - 7.46$  (m, 2H), 7.43 – 7.38 (m, 2H), 7.35 – 7.30 (m, 1H), 3.06 (s, 3H), 1.38 (tt,  $J = 8.1, 4.9$  Hz, 1H), 0.86 – 0.80 (m, 2H), 0.77 – 0.71 (m, 2H) ppm;  $^{13}\text{C}$  NMR (101 MHz,  $\text{CDCl}_3$ ):  $\delta = 139.2$  (C), 129.4 (2CH), 128.1 (CH), 125.6 (2CH), 75.3 (C), 68.7 (C), 36.4 ( $\text{CH}_3$ ), 9.0 ( $2\text{CH}_2$ ), –0.6 (CH) ppm; HRMS (ES–TOF):  $m/z$ : calcd for  $\text{C}_{12}\text{H}_{14}\text{NO}_2\text{S}$ : 236.0740, found 236.0742  $[\text{M}+\text{H}]^+$ .

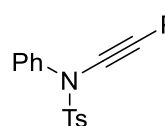
***N*–(Cyclopropylethynyl)–*N*–methyl–4–nitrobenzenesulfonamide **44d****



Sulfonamide **72h** (2.16 g, 10.0 mmol),  $\text{CuCl}_2$  (26.9 mg, 0.20 mmol) and  $\text{Na}_2\text{CO}_3$  (420 mg, 4.00 mmol) were combined in a flame dried Schlenk tube

and purged with O<sub>2(g)</sub> for 10 min. A 0.4 M solution of pyridine (0.32 mL, 4.00 mmol) in PhMe (10 mL) was added and a balloon of O<sub>2(g)</sub> attached before heating to 70 °C. After 15 min, a 0.2 M solution of ethynylcyclopropane (170 µL, 2.01 mmol) in PhMe (10 mL) was added via syringe pump over 4 h and the reaction left to stir at 70 °C for an additional 4 h. After allowing to cool to r.t., the reaction mixture was filtered through a 3 cm pad of silica (EtOAc) and concentrated under reduced pressure. Purification by flash column chromatography (85:15 hexane/EtOAc) gave ynamide **44d** as a yellow solid (548 mg, 98%); mp: 86–90 °C; IR (neat):  $\nu = 3112, 2210, 1530, 1370, 1349, 1313, 1171 \text{ cm}^{-1}$ ; <sup>1</sup>H NMR (300 MHz, CDCl<sub>3</sub>):  $\delta = 8.42$  (d<sub>AA'XX'</sub>,  $J = 8.9 \text{ Hz}$ , 2H), 8.08 (d<sub>AA'XX'</sub>,  $J = 8.9 \text{ Hz}$ , 2H), 3.07 (s, 3H), 1.28 (tt,  $J = 8.1, 4.9$ , 1H), 0.85 – 0.77 (m, 2H), 0.67 – 0.60 (m, 2H) ppm; <sup>13</sup>C NMR (101 MHz, CDCl<sub>3</sub>):  $\delta = 150.7$  (C), 141.8 (C), 129.1 (2CH), 124.4 (2CH), 74.2 (C), 69.4 (C), 39.8 (CH<sub>3</sub>), 9.0 (2CH<sub>2</sub>), –0.9 (CH) ppm; HRMS (ES–TOF):  $m/z$ : calcd for C<sub>12</sub>H<sub>13</sub>N<sub>2</sub>O<sub>4</sub>S: 281.0591, found 281.0604 [M+H]<sup>+</sup>.

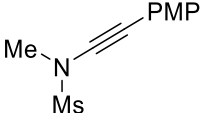
**4-Methyl-N-phenyl-N-(phenylethynyl)benzenesulfonamide 44f**



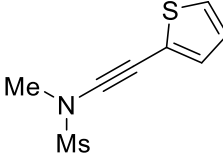
Sulfonamide **72g** (4.94 g, 20.0 mmol), CuCl<sub>2</sub> (107 mg, 0.80 mmol) and Na<sub>2</sub>CO<sub>3</sub> (845 mg, 8.00 mmol) were combined in a flame dried Schlenk tube and purged with O<sub>2(g)</sub> for 10 min. A 0.4 M solution of pyridine (0.94 mL, 8.00 mmol) in PhMe (20 mL) was added and a balloon of O<sub>2(g)</sub> attached before heating to 70 °C. After 15 min, a 0.2 M solution of phenyl acetylene (0.45 mL, 4.00 mmol) in PhMe (20 mL) was added via syringe pump over 4 h and the reaction left to stir at 70 °C for an additional 4 h. After allowing to cool to r.t., the reaction mixture was filtered through a 3 cm pad of silica (EtOAc) and concentrated under reduced pressure. Purification by flash column chromatography (95:5 hexane/EtOAc) gave ynamide **44f** as a white solid (1.30 g, 94%); mp (EtOH): 107–109 °C (lit. 103–105 °C); IR (neat):  $\nu = 2245, 1592, 1491, 1366, 1172 \text{ cm}^{-1}$ ; <sup>1</sup>H NMR (300 MHz, CDCl<sub>3</sub>):  $\delta = 7.62$

( $d_{AA'XX'}$ ,  $J = 8.4$  Hz, 2H), 7.41 – 7.27 (m, 12H), 2.44 (s, 3H) ppm. Spectroscopic data matched that reported in the literature.<sup>246</sup>

***N-Methyl-N-((4-methoxyphenyl)ethynyl)methanesulfonamide 44i***

 1-(2,2-Dibromovinyl)-4-methoxybenzene **123b** (1.49 g, 5.10 mmol), sulfonamide **72g** (434 mg, 4.00 mmol), CuI (91.4 mg, 0.48 mmol), DMEDA (82  $\mu$ L, 0.76 mmol), Cs<sub>2</sub>CO<sub>3</sub> (5.20 g, 16.0 mmol) and degassed 1,4-dioxane (8.0 mL) were combined in a Schlenk tube and heated to 70 °C for 16 h. After allowing to cool to r.t., the reaction mixture was filtered through a 3 cm pad of silica (EtOAc) and concentrated under reduced pressure. Purification by flash column chromatography (7:3 hexane/EtOAc) gave ynamide **44i** as a white solid (701 mg, 73%); mp: 81–83 °C (lit. oil); <sup>1</sup>H NMR (300 MHz, CDCl<sub>3</sub>):  $\delta$  = 7.36 ( $d_{AA'XX'}$ ,  $J = 8.9$  Hz, 2H), 6.83 ( $d_{AA'XX'}$ ,  $J = 8.9$  Hz, 2H), 3.81 (s, 3H), 3.28 (s, 3H), 3.12 (s, 3H) ppm; <sup>13</sup>C NMR (101 MHz, CDCl<sub>3</sub>):  $\delta$  = 159.9 (C), 133.8 (2CH), 114.5 (C), 114.2 (2CH), 81.8 (C), 69.4 (C), 55.5 (CH<sub>3</sub>), 39.5 (CH<sub>3</sub>), 36.8 (CH<sub>3</sub>) ppm; MS (ES–TOF):  $m/z$ : 100% 262.1 [M+Na]<sup>+</sup>. Spectroscopic data matched that reported in the literature.<sup>247</sup>

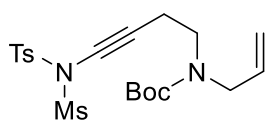
***N-Methyl-N-(thiophen-2-ylethynyl)methanesulfonamide 44j***

 Dibromoolefin **123a** (971 mg, 3.60 mmol), sulfonamide **72g** (327 mg, 3.00 mmol), CuI (69.0 mg, 0.36 mmol), DMEDA (58  $\mu$ L, 0.54 mmol), Cs<sub>2</sub>CO<sub>3</sub> (3.91 g, 12.0 mmol) and degassed 1,4-dioxane (6.0 mL) were combined in a Schlenk tube and heated to 70 °C for 16 h. After allowing to cool to r.t., the reaction mixture was filtered through a 3 cm pad of silica (EtOAc) and concentrated under reduced pressure. Purification by flash column chromatography (3:1 hexane/EtOAc) gave ynamide **44j** as an orange oil that solidified upon standing (605 mg, 94%); mp: 81–83 °C (lit. oil); IR (neat):  $\nu$  = 2230, 1421, 1355, 1301, 1100, 1158, 937 cm<sup>-1</sup>; <sup>1</sup>H NMR (300 MHz, CDCl<sub>3</sub>):  $\delta$  = 7.29 (dd,  $J = 5.2, 1.1$  Hz, 1H),



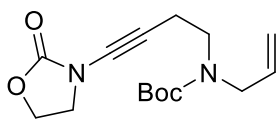
7.22 (dd,  $J = 3.6, 1.1$  Hz, 1H), 6.98 (dd,  $J = 5.2, 3.6$  Hz, 1H), 3.30 (s, 3H), 3.13 (s, 3H) ppm;  $^{13}\text{C}$  NMR (101 MHz,  $\text{CDCl}_3$ ):  $\delta = 133.5$  (CH), 128.2 (CH), 127.2 (CH), 122.5 (C), 86.5 (C), 63.0 (C), 39.4 ( $\text{CH}_3$ ), 37.3 ( $\text{CH}_3$ ) ppm. Spectroscopic data matched that reported in the literature.<sup>247</sup>

***Tert-butyl but-3-en-1-yl(3-((*N*,4-dimethylphenyl)sulfonamido)prop-2-yn-1-yl)carbamate 85d***



Sulfonamide **72c** (3.24 g, 17.5 mmol),  $\text{CuCl}_2$  (47.1 mg, 0.35 mmol) and  $\text{Na}_2\text{CO}_3$  (735 mg, 7.00 mmol) were combined in a flame dried Schlenk tube and purged with  $\text{O}_{2(g)}$  for 10 min. A 0.4 M solution of pyridine (0.56 mL, 6.95 mmol) in PhMe (17.5 mL) was added and a balloon of  $\text{O}_{2(g)}$  attached before heating to 70 °C. After 15 min, a 0.2 M solution of alkyne **81c** (732 mg, 3.50 mmol) in PhMe (10 mL) was added over 4 h using a syringe pump and the reaction then left to stir at 70 °C for 16 h. After allowing to cool to r.t., the reaction mixture was filtered through a 3 cm pad of silica (EtOAc) and concentrated under reduced pressure. Purification by flash column chromatography (8:2 hexane/EtOAc) gave enynamide **85d** as a pale yellow oil (980 mg, 71%); IR (neat):  $\nu = 2979, 2929, 2256, 1689, 1461, 1406, 1363, 1247, 1163, 1140$   $\text{cm}^{-1}$ ; *NMR spectra display a mixture of rotamers*:  $^1\text{H}$  NMR (400 MHz,  $\text{CDCl}_3$ ):  $\delta = 7.76$  ( $d_{\text{AA'XX'}}$ ,  $J = 8.1$  Hz, 2H), 7.35 ( $d_{\text{AA'XX'}}$ ,  $J = 8.1$  Hz, 2H), 5.81 – 5.69 (m, 1H), 5.15 – 5.06 (m, 2H), 3.83 (br. s, 2H), 3.35 – 3.21 (m, 2H), 3.01 (s, 3H), 2.49 – 2.43 (m, 5H), 1.44 (s, 9H) ppm;  $^{13}\text{C}$  NMR (101 MHz,  $\text{CDCl}_3$ ):  $\delta = 155.4$  (C), 144.7 (C), 134.3 (CH), 133.4 (C), 129.9 (2CH), 127.9 (2CH), 116.7 and 116.1 ( $\text{CH}_2$ ), 82.4 (C), 79.9 (C), 76.0 (C), 50.6 and 50.0 ( $\text{CH}_2$ ), 46.3 and 46.2 ( $\text{CH}_2$ ), 39.4 ( $\text{CH}_3$ ), 28.5 (3 $\text{CH}_3$ ), 21.8 ( $\text{CH}_3$ ), 18.7 and 18.5 ( $\text{CH}_2$ ) ppm; HRMS (ES–TOF):  $m/z$ : calcd for  $\text{C}_{20}\text{H}_{28}\text{N}_2\text{O}_4\text{SNa}$ : 415.1662, found 415.1673  $[\text{M}+\text{Na}]^+$ .

***Tert-butyl allyl(4-(2-oxooxazolidin-3-yl)but-3-yn-1-yl)carbamate 85e***



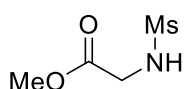
Oxazolidinone (870 mg, 10.0 mmol), CuCl<sub>2</sub> (26.9 mg, 0.20 mmol) and Na<sub>2</sub>CO<sub>3</sub> (420 mg, 4.00 mmol) were combined in a flame dried Schlenk

tube and purged with O<sub>2(g)</sub> for 10 min. A 0.4 M solution of pyridine (0.32 mL, 4.00 mmol) in PhMe (10 mL) was added and a balloon of O<sub>2(g)</sub> attached before heating to 70 °C. After 15 min, a 0.2 M solution of alkyne **81c** (418 mg, 2.00 mmol) in PhMe (10 mL) was added over 4 h using a syringe pump and the reaction then left to stir at 70 °C for 16 h. After allowing to cool to r.t., the reaction mixture was filtered through a 3 cm pad of silica (EtOAc) and concentrated under reduced pressure. Purification by flash column chromatography (1:1 hexane/EtOAc) gave enynamide **85e** as a colourless oil (389 mg, 66%); IR (neat):  $\nu$  = 2979, 1919, 2265, 1176, 1686, 1479, 1407, 1366, 1163, 1111, 1034 cm<sup>-1</sup>; *NMR spectra display a mixture of rotamers*: <sup>1</sup>H NMR (400 MHz, CDCl<sub>3</sub>):  $\delta$  = 5.83 – 5.68 (m, 1H), 5.11 (br. d,  $J$  = 12.4 Hz, 2H), 4.43 – 4.37 (m, 2H), 3.90 – 3.80 (m, 4H), 3.33 (br. s, 2H), 2.52 (br. t,  $J$  = 7.2 Hz, 2H), 1.44 (s, 9H) ppm; <sup>13</sup>C NMR (101 MHz, CDCl<sub>3</sub>):  $\delta$  = 156.6 (C), 155.4 (C), 134.2 and 134.1 (CH), 116.8 and 116.2 (CH<sub>2</sub>), 84.0 (C), 80.0 and 79.9 (C), 71.2 (C), 63.0 (CH<sub>2</sub>), 50.7 and 50.0 (CH<sub>2</sub>) 47.0 (CH<sub>2</sub>) 46.1 and 46.0 (CH<sub>2</sub>), 28.5 and 28.1 (3CH<sub>3</sub>), 18.6 and 18.4 (CH<sub>2</sub>) ppm; HRMS (ES–TOF):  $m/z$ : calcd for C<sub>15</sub>H<sub>22</sub>N<sub>2</sub>O<sub>4</sub>Na: 317.1472, found 317.1481 [M+Na]<sup>+</sup>.

**Formation of *N*-acyl pyridinium ylide and *N*-(pivaloyloxy)amide precursors**

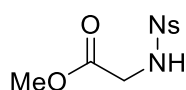
The following compounds were synthesised according to literature procedures which are referenced alongside spectroscopic data:

***Methyl (methylsulfonyl)glycinate 78e***



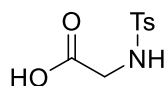
1.85 g, 96%. Spectroscopic data matched that reported in the literature.<sup>248</sup>

**Methyl ((4-nitrophenyl)sulfonyl)glycinate 88f**



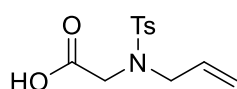
4.00 g, 73%. Spectroscopic data matched that reported in the literature.<sup>249</sup>

**Tosylglycine 116**



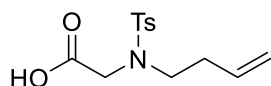
14.0 g, 61%. Spectroscopic data matched that reported in the literature.<sup>250</sup>

**N-Allyl-N-tosylglycine 117a**



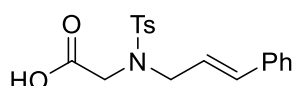
From **116**: 3.56 g, 80%. Spectroscopic data matched that reported in the literature.<sup>251</sup>

**N-(But-3-en-1-yl)-N-tosylglycine 125a**



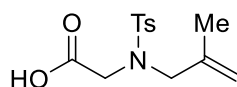
From **116**: 939 mg, 83%. Spectroscopic data matched that reported in the literature.<sup>252</sup>

**N-Cinnamyl-N-tosylglycine 125b**



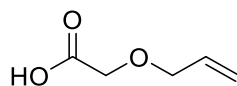
655 mg, 95% over 2 steps. Spectroscopic data matched that reported in the literature.<sup>253</sup>

**N-(2-Methylallyl)-N-tosylglycine 125c**



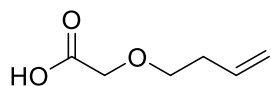
673 mg, 95%. Spectroscopic data matched that reported in the literature.<sup>251</sup>

**2-(Allyloxy)acetic acid 125d**



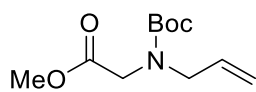
1.23 g, 53%. Spectroscopic data matched that reported in the literature.<sup>252</sup>

**2-(But-3-en-1-yloxy)acetic acid 96**



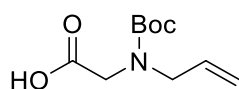
625 mg, 48%. Spectroscopic data matched that reported in the literature.<sup>254</sup>

***Methyl N-allyl-N-(tert-butoxycarbonyl)glycinate 89c***



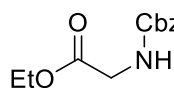
592 mg, 52%. Spectroscopic data matched that reported in the literature.<sup>255</sup>

***Methyl N-allyl-N-(tert-butoxycarbonyl)glycine 125e***



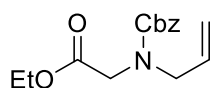
543 mg, quant. Spectroscopic data matched that reported in the literature.<sup>256</sup>

***Ethyl ((benzyloxy)carbonyl)glycinate 88d***



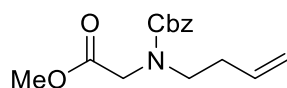
2.81 g, 99%. Spectroscopic data matched that reported in the literature.<sup>257</sup>

***Ethyl N-allyl-N-((benzyloxy)carbonyl)glycinate 89d***



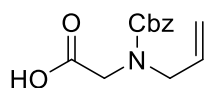
From **78d**: 245 mg, 29%. Spectroscopic data matched that reported in the literature.<sup>257</sup>

***Methyl N-((benzyloxy)carbonyl)-N-(but-3-en-1-yl)glycinate 89e***



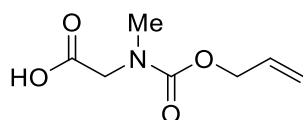
224 mg, 25%. Spectroscopic data matched that reported in the literature.<sup>258</sup>

***N-allyl-N-((benzyloxy)carbonyl)glycine 134***



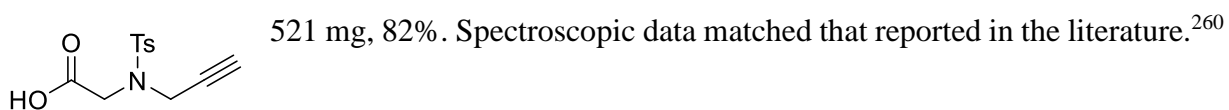
From **79d**: 203 mg, 91%. Spectroscopic data matched that reported in the literature.<sup>257</sup>

***N-((Allyloxy)carbonyl)-N-methylglycine 125f***

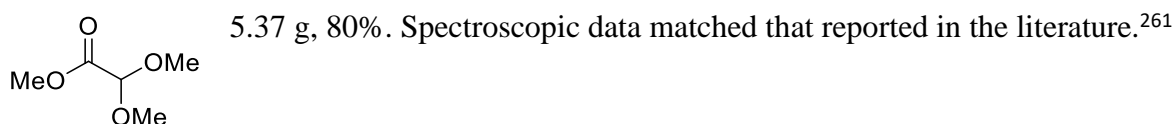


3.40 g, 98%. Spectroscopic data matched that reported in the literature.<sup>259</sup>

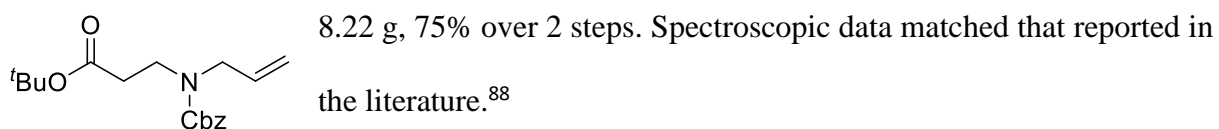
***N-(prop-2-yn-1-yl)-N-tosylglycine 125g***



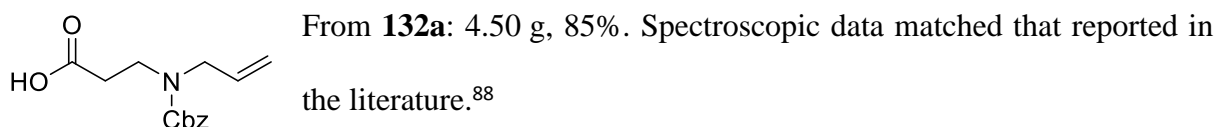
***Methyl 2,2-dimethoxyacetate 126a***



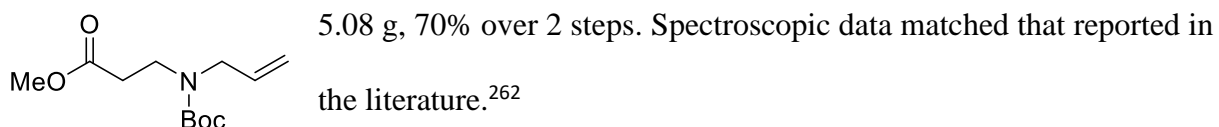
***tert-Butyl 3-(allyl((benzyloxy)carbonyl)amino)propanoate 147a***



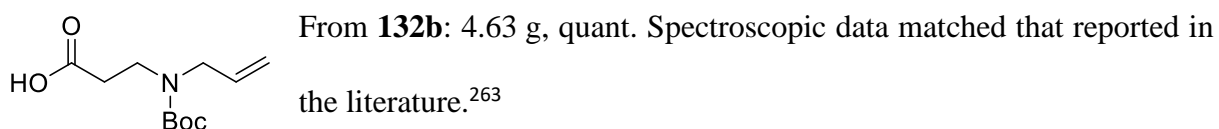
***3-(Allyl((benzyloxy)carbonyl)amino)propanoic acid 148a***



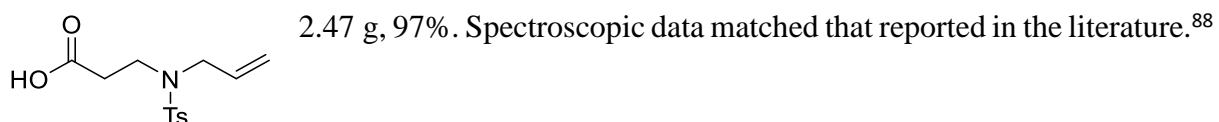
***Methyl 3-(allyl(tert-butoxycarbonyl)amino)propanoate 147b***



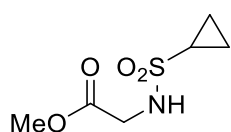
***3-(Allyl(tert-butoxycarbonyl)amino)propanoic acid 148b***



***3-((N-Allyl-4-methylphenyl)sulfonamido)propanoic acid 148c***

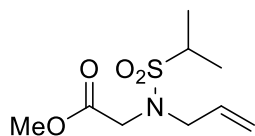


### ***Methyl (cyclopropylsulfonyl)glycinate 88g***



Cyclopropanesulfonyl chloride (2.0 mL, 20.0 mmol) was added dropwise over 10 min to a solution of glycine methyl ester hydrochloride (2.45 g, 20.0 mmol) and NEt<sub>3</sub> (5.6 mL, 40.2 mmol) in CH<sub>2</sub>Cl<sub>2</sub> (100 mL) and the reaction mixture was stirred at r.t. for 18 h. The reaction mixture was transferred into a separating funnel, washed with 2 M HCl<sub>(aq)</sub> (100 mL) and brine (100 mL), dried over Na<sub>2</sub>SO<sub>4</sub>, filtered, and concentrated under reduced pressure. The crude material was flushed through a 6 cm pad of silica (Et<sub>2</sub>O) to give methyl ester **88g** as a colourless oil (3.57 g, 92%); IR (neat):  $\nu$  = 3290, 1741, 1436, 1327, 1214, 1142 cm<sup>-1</sup>; <sup>1</sup>H NMR (400 MHz, CDCl<sub>3</sub>):  $\delta$  = 5.08 (br. s, 1H), 3.93 (d,  $J$  = 5.5 Hz, 2H), 3.77 (s, 3H), 2.47 (tt,  $J$  = 8.0, 4.9 Hz, 1H), 1.18 – 1.11 (m, 2H), 1.01 – 0.95 (m, 2H) ppm; <sup>13</sup>C NMR (101 MHz, CDCl<sub>3</sub>):  $\delta$  = 170.4 (C), 52.8 (CH<sub>3</sub>), 44.5 (CH<sub>2</sub>), 30.5 (CH), 5.5 (2CH<sub>2</sub>) ppm; HRMS (ES–TOF):  $m/z$ : calcd for C<sub>6</sub>H<sub>12</sub>NO<sub>4</sub>S: 194.0482, found 194.0483 [M+H]<sup>+</sup>.

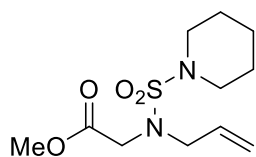
### ***Methyl N-allyl-N-(isopropylsulfonyl)glycinate 89a***



2-Propanesulfonyl chloride (2.25 mL, 20.0 mmol) was added dropwise over 10 min to a solution of glycine methyl ester hydrochloride (2.57 g, 21.0 mmol) and NEt<sub>3</sub> (5.6 mL, 40.2 mmol) in CH<sub>2</sub>Cl<sub>2</sub> (100 mL) and the reaction mixture was stirred at r.t. for 18 h. The reaction mixture was transferred into a separating funnel, washed with 2 M HCl<sub>(aq)</sub> (100 mL) and brine (100 mL), dried over Na<sub>2</sub>SO<sub>4</sub>, filtered, and concentrated under reduced pressure to give the protected amine as a pale yellow oil (1.24 g, 32%). The crude material (1.24 g, 6.34 mmol) was combined with K<sub>2</sub>CO<sub>3</sub> (1.75 g, 12.7 mmol) and allyl bromide (827  $\mu$ L, 9.50 mmol) in MeCN (32 mL) and heated to reflux for 16 h. After cooling to r.t., the solvent was removed under reduced pressure and taken up in EtOAc/H<sub>2</sub>O (1:1, 100 mL). The phases were separated and the organic layer washed with

H<sub>2</sub>O (40 mL) and brine (50 mL), dried over Na<sub>2</sub>SO<sub>4</sub>, filtered and concentrated under reduced pressure to give **89a** as a yellow oil (1.42 g, 30% over 2 steps); IR (neat):  $\nu$  = 2982, 1750, 1326, 1214, 1174, 1136 cm<sup>-1</sup>; <sup>1</sup>H NMR (400 MHz, CDCl<sub>3</sub>):  $\delta$  = 5.78 (ddt,  $J$  = 16.7, 10.2, 6.5 Hz, 1H), 5.28 – 5.21 (m, 2H), 4.05 (s, 2H), 3.96 (dt,  $J$  = 6.5, 1.3 Hz, 2H), 3.75 (s, 3H), 3.26 (hept,  $J$  = 6.8 Hz, 1H), 1.40 (d,  $J$  = 6.8 Hz, 6H) ppm; <sup>13</sup>C NMR (101 MHz, CDCl<sub>3</sub>):  $\delta$  = 170.4 (C), 133.0 (CH), 119.9 (CH<sub>2</sub>), 55.3 (CH<sub>3</sub>), 52.3 (CH), 51.8 (CH<sub>2</sub>), 47.1 (CH<sub>2</sub>), 16.8 (2CH<sub>3</sub>) ppm; HRMS (ES–TOF):  $m/z$ : calcd for C<sub>9</sub>H<sub>17</sub>NO<sub>4</sub>SNa: 258.0770, found 258.0778 [M+Na]<sup>+</sup>.

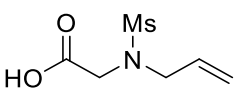
***Methyl N-allyl-N-(piperidin-1-ylsulfonyl)glycinate 89b***



Piperidine-1-sulfonyl chloride (2.81 mL, 20.0 mmol) was added dropwise over 10 min to a solution of glycine methyl ester hydrochloride (2.57 g, 21.0 mmol) and NEt<sub>3</sub> (5.6 mL, 40.2 mmol) in CH<sub>2</sub>Cl<sub>2</sub> (100 mL) and the reaction mixture was stirred at r.t. for 18 h. The reaction mixture was transferred into a separating funnel, washed with 2 M HCl<sub>(aq)</sub> (100 mL) and brine (100 mL), dried over Na<sub>2</sub>SO<sub>4</sub>, filtered, and concentrated under reduced pressure to give the protected amine as a yellow oil (2.37 g, 50%). The crude material (2.36 g, 10.0 mmol) was combined with K<sub>2</sub>CO<sub>3</sub> (2.76 g, 20.0 mmol) and allyl bromide (1.31 mL, 15.0 mmol) in MeCN (50 mL) and heated to reflux for 16 h. After cooling to r.t., the solvent was removed under reduced pressure and taken up in EtOAc/H<sub>2</sub>O (1:1, 100 mL). The phases were separated and the organic layer washed with H<sub>2</sub>O (40 mL) and brine (50 mL), dried over Na<sub>2</sub>SO<sub>4</sub>, filtered and concentrated under reduced pressure to give **89b** a pale yellow oil (2.62 g, 48% over 2 steps); IR (neat):  $\nu$  = 2940, 2855, 1752, 1334, 1212, 1144, 1054 cm<sup>-1</sup>; <sup>1</sup>H NMR (400 MHz, CDCl<sub>3</sub>):  $\delta$  = 5.80 (ddt,  $J$  = 17.5, 9.7, 6.5 Hz, 1H), 5.27 – 5.20 (m, 2H), 3.94 (s, 2H), 3.91 (dt,  $J$  = 6.5, 1.3 Hz, 2H), 3.74 (s, 3H), 3.23 – 3.19 (m, 4H), 1.65 – 1.57 (m, 4H), 1.57 – 1.49 (m, 2H) ppm; <sup>13</sup>C NMR (101 MHz, CDCl<sub>3</sub>):

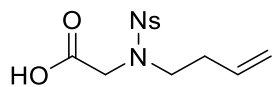
$\delta$  = 170.2 (C), 132.9 (CH), 119.7 (CH<sub>2</sub>), 52.3 (CH<sub>3</sub>), 51.8 (CH<sub>2</sub>), 47.6 (CH<sub>2</sub>), 47.0 (2CH<sub>2</sub>), 25.5 (2CH<sub>2</sub>), 23.9 (CH<sub>2</sub>) ppm; HRMS (ES–TOF):  $m/z$ : calcd for C<sub>11</sub>H<sub>20</sub>N<sub>2</sub>O<sub>4</sub>SNa: 299.1036, found 299.1043 [M+Na]<sup>+</sup>.

***N*-Allyl-*N*-(methylsulfonyl)glycine **125g****

 **88e** (1.67 g, 10.0 mmol), K<sub>2</sub>CO<sub>3</sub> (3.31 g, 24.0 mmol) and allyl bromide (1.30 mL, 15.0 mmol) were dissolved in MeCN (50 mL) and the mixture was heated to reflux for 16 h. After cooling to r.t., the solvent was removed under reduced pressure and the residue taken up in EtOAc/H<sub>2</sub>O (1:1, 100 mL). The phases were separated and the organic layer washed with H<sub>2</sub>O (40 mL) and brine (50 mL), dried over Na<sub>2</sub>SO<sub>4</sub>, filtered and concentrated under reduced pressure. The crude methyl ester was dissolved in MeOH (10 mL) and cooled to 0 °C. A solution of 4 M NaOH<sub>(aq)</sub> (6.25 mL, 25 mmol) was added dropwise over 2 min and the cooling bath was removed. After stirring for 2 h at r.t., the reaction mixture was diluted with H<sub>2</sub>O (40 mL) and the organics were extracted with Et<sub>2</sub>O (2×50 mL) before the aqueous phase was acidified to pH 2 with 2 M HCl<sub>(aq)</sub>. After leaving for 2 h at 0 °C, the precipitate was collected and dried under high vacuum (0.02 mbar) to yield **125g** as a white solid (1.77 g, 92% over 2 steps); mp: 110–112 °C; IR (neat):  $\nu$  = 3320 (br.), 1744, 1324, 1144, 1215, 1177, 923, 794 cm<sup>-1</sup>; <sup>1</sup>H NMR (400 MHz, CDCl<sub>3</sub>):  $\delta$  = 5.81 (ddt,  $J$  = 17.3, 9.8, 6.4 Hz, 1H), 5.34 – 5.28 (m, 2H), 4.14 (s, 2H), 3.92 (dt,  $J$  = 6.4, 1.3 Hz, 2H), 3.03 (s, 3H) ppm; <sup>13</sup>C NMR (101 MHz, CDCl<sub>3</sub>):  $\delta$  = 174.7 (C), 132.2 (CH), 120.3 (CH<sub>2</sub>), 50.7 (CH<sub>2</sub>), 47.0 (CH<sub>2</sub>), 40.5 (CH<sub>3</sub>) ppm; HRMS (ES–TOF):  $m/z$ : calcd for C<sub>6</sub>H<sub>11</sub>NO<sub>4</sub>SNa: 216.0301, found 216.0306 [M+H]<sup>+</sup>.

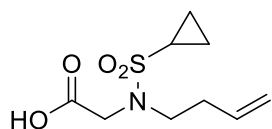


***N*-(But-3-en-1-yl)-*N*-((4-nitrophenyl)sulfonyl)glycine 125h**



**88f** (1.65 g, 6.00 mmol), K<sub>2</sub>CO<sub>3</sub> (1.66 g, 12.0 mmol) and 4-bromo-1-butene (910  $\mu$ L, 8.97 mmol) were dissolved in MeCN (30 mL) and the mixture heated to reflux for 16 h. After cooling to r.t., the solvent was removed under reduced pressure and the residue taken up in EtOAc/H<sub>2</sub>O (1:1, 100 mL). The phases were separated and the organic layer washed with H<sub>2</sub>O (40 mL) and brine (50 mL), dried over Na<sub>2</sub>SO<sub>4</sub>, filtered and concentrated under reduced pressure. The crude ester was dissolved in MeOH (12 mL) and cooled to 0 °C. A solution of 4 M NaOH<sub>(aq)</sub> (3.75 mL, 15 mmol) was added dropwise over 2 min and the cooling bath was removed. After stirring for 2 h at r.t., the reaction mixture was diluted with H<sub>2</sub>O (40 mL) and the organics were extracted with Et<sub>2</sub>O (2×50 mL) before the aqueous phase was acidified to pH 2 with 2 M HCl<sub>(aq)</sub>. After leaving for 2 h at 0 °C, the precipitate was collected and dried under high vacuum (0.02 mbar) to yield **125h** as a pale yellow solid (1.31 g, 70% over 2 steps); mp: 174–176 °C; IR (neat):  $\nu$  = 3102 (br.), 1716, 1525, 1403, 1345, 1313, 1229, 1157, 1098 cm<sup>-1</sup>; <sup>1</sup>H NMR (400 MHz, DMSO-*d*<sub>6</sub>):  $\delta$  = 12.85 (s, 1H), 8.38 (d<sub>AA'</sub>XX', *J* = 8.9 Hz, 2H), 8.09 (d<sub>AA'</sub>XX', *J* = 8.9 Hz, 2H), 5.70 (ddt, *J* = 17.0, 10.2, 6.7 Hz, 1H), 5.04 (app. dq, *J* = 17.0, 1.6 Hz, 1H), 4.98 (ddt, *J* = 10.2, 2.2, 1.2 Hz, 1H), 4.07 (s, 2H), 3.30 (t, *J* = 7.2 Hz, 2H), 2.27 (app. q, *J* = 7.2 Hz, 2H) ppm; <sup>13</sup>C NMR (101 MHz, DMSO-*d*<sub>6</sub>):  $\delta$  = 170.0 (C), 149.7 (C), 145.2 (C), 135.0 (CH), 128.6 (2CH), 124.5 (2CH), 117.1 (CH<sub>2</sub>), 48.0 (CH<sub>2</sub>), 47.7 (CH<sub>2</sub>), 32.1 ppm (CH<sub>2</sub>) ppm; HRMS (ES-TOF): *m/z*: calcd for C<sub>12</sub>H<sub>14</sub>N<sub>2</sub>O<sub>6</sub>Na: 337.0465, found 337.0471 [M+Na]<sup>+</sup>.

***N*-(But-3-en-1-yl)-*N*-(cyclopropylsulfonyl)glycine 135**



**88g** (1.93 g, 10.0 mmol), K<sub>2</sub>CO<sub>3</sub> (3.31 g, 24.0 mmol) and 4-bromo-1-butene (1.52 mL, 15.0 mmol) were dissolved in MeCN (50 mL) and the

mixture was heated to reflux for 16 h. After cooling to r.t., the solvent was removed under reduced pressure and the residue taken up in EtOAc/H<sub>2</sub>O (1:1, 100 mL). The phases were separated and the organic layer washed with H<sub>2</sub>O (40 mL) and brine (50 mL), dried over Na<sub>2</sub>SO<sub>4</sub>, filtered and concentrated under reduced pressure. The crude methyl ester was dissolved in MeOH (10 mL) and cooled to 0 °C. A solution of 4 M NaOH<sub>(aq)</sub> (6.25 mL, 25 mmol) was added dropwise over 2 min and the cooling bath was removed. After stirring for 2 h at r.t., the reaction mixture was diluted with H<sub>2</sub>O (40 mL) and the organics were extracted with Et<sub>2</sub>O (2×50 mL) before the aqueous phase was acidified to pH 2 with 2 M HCl<sub>(aq)</sub>. After leaving for 2 h at 0 °C, the precipitate was collected and dried under high vacuum (0.02 mbar) to yield **135** as a white solid (1.14 g, 49% over 2 steps); mp: 65–66 °C; IR (neat):  $\nu$  = 3194 (br.), 2942, 1738, 1329, 1140, 1066 cm<sup>-1</sup>; <sup>1</sup>H NMR (400 MHz, CDCl<sub>3</sub>):  $\delta$  = 5.77 (ddt,  $J$  = 17.1, 10.3, 6.8 Hz, 1H), 5.17 – 5.06 (m, 2H), 4.16 (s, 2H), 3.44 – 3.39 (m, 2H), 2.53 (tt,  $J$  = 8.1, 4.9, 1H), 2.40 – 2.33 (m, 2H), 1.21 – 1.15 (m, 2H), 1.03 – 0.97 (m, 2H) ppm; <sup>13</sup>C NMR (101 MHz, CDCl<sub>3</sub>):  $\delta$  = 175.0 (C), 134.4 (CH), 117.8 (CH<sub>2</sub>), 48.3 (CH<sub>2</sub>), 47.9 (CH<sub>2</sub>), 33.0 (CH<sub>2</sub>), 30.2 (CH), 5.6 (2CH<sub>2</sub>) ppm; HRMS (ES–TOF):  $m/z$ : calcd for C<sub>9</sub>H<sub>15</sub>NO<sub>4</sub>SNa: 256.0614, found 256.0623 [M+Na]<sup>+</sup>.

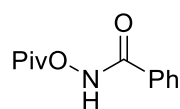
## Formation of *N*–(pivaloyloxy)amides

### *O*–Pivaloylhydroxyamine triflic acid

PivONH<sub>2</sub>•HOTf Hydroxylamine hydrochloride (5.56 g, 80.0 mmol) and Boc<sub>2</sub>O (17.5 g, 80.0 mmol) were dissolved in a rigorously stirred biphasic mixture of THF (80 mL) and H<sub>2</sub>O (80 mL) and cooled to 0 °C. NaHCO<sub>3</sub> (13.4 g, 160 mmol) was added at a rate of 1 g/min and the reaction mixture was allowed to warm to r.t. and stirred for 3 h. After transferring to a separating funnel, the aqueous phase was extracted with EtOAc (3×60 mL) and the combined

organic layers washed with satd  $\text{NaHCO}_{3(\text{aq})}$  (50 mL),  $\text{H}_2\text{O}$  (50 mL) and brine (50 mL), then dried over  $\text{Na}_2\text{SO}_4$ , filtered and concentrated under reduced pressure to leave a colourless oil (7.96 g, 59.0 mmol). The crude oil was combined with pivalic anhydride (14.3 mL, 70.0 mmol) and  $\text{CHCl}_3$  (150 mL) under an argon atmosphere and heated at reflux for 16 h. After allowing to cool to r.t., satd  $\text{NaHCO}_{3(\text{aq})}$  (80 mL) was added and the layers were separated. The organic layer was washed with satd  $\text{NaHCO}_{3(\text{aq})}$  (2×50 mL), dried over  $\text{Na}_2\text{SO}_4$ , filtered and concentrated under reduced pressure. The residue was dissolved in  $\text{Et}_2\text{O}$  (150 mL) and cooled to 0 °C before  $\text{TfOH}$  (5.20 mL, 59.0 mmol) was added dropwise over 10 min and stirred at 0 °C for 10 min. Pentane (100 mL) was added in one portion and the ice bath was removed with continued stirring for 2 h before the solid was collected by vacuum filtration and dried in a vacuum desiccator ( $\text{P}_2\text{O}_5$  desiccant) overnight to give *O*-Pivaloylhydroxyamine triflic acid as a white solid (10.8 g, 51%).

***N*-(Pivaloyloxy)benzamide **111a****



*O*-Pivaloylhydroxyamine triflic acid (800 mg, 3.00 mmol) was added to a biphasic mixture of  $\text{Na}_2\text{CO}_3$  (630 mg, 6.00 mmol) in  $\text{EtOAc}$  (20 mL) and  $\text{H}_2\text{O}$  (10 mL) and the reaction mixture was cooled to 0 °C. Benzoyl chloride (350  $\mu\text{L}$ , 3.00 mmol) was added dropwise over 2 min and the reaction mixture was allowed to warm to rt. After stirring for 24 h, the reaction mixture was diluted with  $\text{EtOAc}$  (10 mL) and the phases separated. The organic phase was washed with satd  $\text{NaHCO}_{3(\text{aq})}$  (2×10 mL) and brine (10 mL), dried over  $\text{Na}_2\text{SO}_4$ , filtered and concentrated under reduced pressure. Purification by flash column chromatography (85:15 hexane/ $\text{EtOAc}$ ) gave **111a** as a white solid (468 mg, 71%); mp: 106–109 °C (lit. 111 °C);  $^1\text{H}$  NMR (400 MHz,  $\text{CDCl}_3$ ):  $\delta$  = 9.33 (br. s, 1H), 7.82 (dt,  $J$  = 7.1, 1.7 Hz, 2H), 7.57 (tt,  $J$  = 7.4, 1.5 Hz, 1H), 7.46 (tt,  $J$  = 7.6, 1.4 Hz, 2H), 1.37 (s, 9H) ppm;  $^{13}\text{C}$  NMR

(101 MHz, CDCl<sub>3</sub>):  $\delta$  = 177.2 (C), 168.0 (C), 132.9 (CH), 131.1 (C), 129.0 (2CH), 127.6 (2CH), 38.6 (C), 27.2 (3CH<sub>3</sub>) ppm; MS (ES–TOF):  $m/z$ : 100% 244.1 [M+Na]<sup>+</sup>. Spectroscopic data matched that reported in the literature.<sup>81</sup>

#### **General Procedure 6a: *N*–(pivaloyloxy)amide synthesis (GP6a)**

Following the general procedure of Fagnou:<sup>80</sup> The relevant acid derivative (1.0 eq.) and DMF (2 drops) were dissolved in CH<sub>2</sub>Cl<sub>2</sub> (0.3 M wrt acid) and cooled to 0 °C. Oxalyl chloride (1.2 eq.) was added dropwise over 10 min before the reaction mixture was allowed to warm to r.t. and stirred for 3 h. The solvent was removed under reduced pressure (bath at 23 °C) to give the crude acid chloride. *O*–Pivaloylhydroxyamine triflic acid (1.0 eq.) was added to a biphasic mixture of Na<sub>2</sub>CO<sub>3</sub> (2.0 eq.) in EtOAc/H<sub>2</sub>O (2:1, 0.1 M wrt acid) and the reaction mixture was cooled to 0 °C. The crude acid chloride was dissolved in a minimal amount of EtOAc and added dropwise over 5 min. Upon complete addition, the reaction mixture was allowed to warm to r.t. and stirred for 16–18 h, diluted with H<sub>2</sub>O and the phases separated. The aqueous layer was washed with EtOAc and the combined organics washed with brine. If required, the crude product was purified by flash column chromatography.

#### **General Procedure 6b: *N*–(pivaloyloxy)amide synthesis (GP6b)**

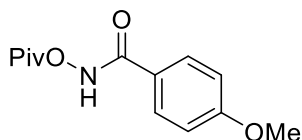
Adapted from procedure of Zhu,<sup>74</sup> the relevant acid derivative (1.0 eq.) and DMF (2 drops) were dissolved in CH<sub>2</sub>Cl<sub>2</sub> (0.3 M wrt acid) and cooled to 0 °C. Oxalyl chloride (1.2 eq.) was added dropwise over 10 min before the reaction mixture was allowed to warm to r.t. and stirred for 3 h. The solvent was removed under reduced pressure (bath at 23 °C) to give the crude acid chloride. Hydroxylamine hydrochloride (1.2 eq.) was added to a biphasic mixture of K<sub>2</sub>CO<sub>3</sub> (2.0 eq.) in EtOAc/H<sub>2</sub>O (2:1, 0.2 M wrt acid) and the reaction mixture was cooled to 0 °C. The

crude acid chloride was dissolved in a minimal amount of EtOAc and added dropwise over 5 min. Upon complete addition, the reaction mixture was allowed to warm to r.t. and stirred for 2–3 h, diluted with H<sub>2</sub>O and the phases separated. The aqueous layer was washed with EtOAc and the combined organics washed with brine. The residue was dissolved in CH<sub>2</sub>Cl<sub>2</sub> (1.0 M), NEt<sub>3</sub> (1.2 eq.) was added and the reaction mixture cooled to 0 °C. Pivaloyl chloride (1.0 eq.) was added dropwise over 2 min and the reaction allowed to warm to r.t. and stir for 2 h. After concentrating under reduced pressure, H<sub>2</sub>O was added and the organics extracted with EtOAc (3 washes). The combined organic phases were dried over Na<sub>2</sub>SO<sub>4</sub>, filtered and concentrated under reduced pressure. The crude product was purified by flash column chromatography.

#### General Procedure 6c: *N*–(pivaloyloxy)amide synthesis (GP6c)

The relevant acid derivative (1.0 eq.) and *N*–methylmorpholine (3.0 eq.) were dissolved in dry THF (0.33 M wrt acid) in flame dried glassware under argon and cooled to 0 °C. Isobutyl chloroformate (1.1 eq.) was added dropwise over 5 min and the reaction stirred at 0 °C for 15 min. *o*–Pivaloylhydroxyamine triflic acid (1.1 eq.) was added in 3 portions over 5 min, the ice bath was removed, and the reaction mixture stirred at r.t. overnight. The solvent was removed under reduced pressure and the crude products purified by flash column chromatography.

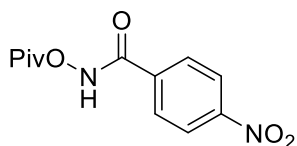
#### 4–Methoxy–*N*–(pivaloyloxy)benzamide **111b**



Following **GP6a** using *p*–anisic acid (457 mg, 3.00 mmol), oxalyl chloride (310 μL, 3.60 mmol), *o*–pivaloylhydroxyamine triflic acid (801 mg, 3.00 mmol) and Na<sub>2</sub>CO<sub>3</sub> (630 mg, 6.00 mmol). Purification by flash column chromatography (6:4 hexane/EtOAc) gave **111b** as an off white solid (574 mg, 76%); mp: 138–140 °C (lit. not given); IR (neat):  $\nu$  = 3230, 2975, 2940, 1772, 1646, 1604, 1530, 1483, 1319, 1258, 1069, 1028 cm<sup>–1</sup>; <sup>1</sup>H NMR (400 MHz, CDCl<sub>3</sub>):  $\delta$  = 9.32 (br. s, 1H), 7.78 (d<sub>AA'XX'</sub>, *J* =

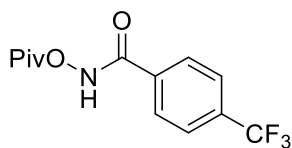
8.9 Hz, 2H), 6.93 (d<sub>AA'XX'</sub>, *J* = 8.9 Hz, 2H), 3.85 (s, 3H), 1.35 (s, 9H) ppm; <sup>13</sup>C NMR (101 MHz, CDCl<sub>3</sub>): δ = 177.4 (C), 166.9 (C), 163.3 (C), 129.6 (2CH), 123.2 (C), 114.2 (2CH), 55.6 (CH<sub>3</sub>), 38.6 (C), 27.2 (3CH<sub>3</sub>) ppm; MS (ES–TOF): *m/z*: 100% 274.1 [M+Na]<sup>+</sup>. Spectroscopic data matched that reported in the literature.<sup>81</sup>

**4–Nitro–*N*–(pivaloyloxy)benzamide **111c****



Following **GP6a** using 4–nitrobenzoic acid (501 mg, 3.00 mmol), oxalyl chloride (310 μL, 3.60 mmol), *o*–pivaloylhydroxyamine triflic acid (801 mg, 3.00 mmol) and Na<sub>2</sub>CO<sub>3</sub> (630 mg, 6.00 mmol). Purification by flash column chromatography (8:2 hexane/EtOAc) gave **111c** as a pale yellow solid (574 mg, 76%); IR (neat): ν = 3346, 2983, 2934, 1783, 1692, 1605, 1522, 1462, 1345, 1069 cm<sup>–1</sup>; <sup>1</sup>H NMR (400 MHz, CDCl<sub>3</sub>): δ 9.37 (br. s, 1H), 8.33 (d<sub>AA'XX'</sub>, *J* = 8.9 Hz, 2H), 7.99 (d<sub>AA'XX'</sub>, *J* = 8.9 Hz, 2H), 1.37 (s, 9H) ppm; <sup>13</sup>C NMR (101 MHz, CDCl<sub>3</sub>): δ = 177.0 (C), 160.2 (C), 150.5 (C), 136.6 (C), 128.9 (2CH), 124.2 (2CH), 38.7 (C), 27.1 (3CH<sub>3</sub>) ppm; MS (ES–TOF): *m/z*: 100% 298.1 [M+Na]<sup>+</sup>. Spectroscopic data matched that reported in the literature.<sup>75</sup>

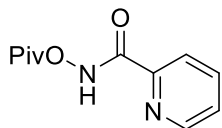
***N*–(Pivaloyloxy)–4–(trifluoromethyl)benzamide **111d****



Following **GP6a** using 4–(trifluoromethyl)benzoic acid (570 mg, 3.00 mmol), oxalyl chloride (310 μL, 3.60 mmol), *o*–pivaloylhydroxyamine triflic acid (801 mg, 3.00 mmol) and Na<sub>2</sub>CO<sub>3</sub> (630 mg, 6.00 mmol). Purification by flash column chromatography (85:15 hexane/EtOAc) gave **111d** as an off white solid (756 mg, 87%); mp: 103–105 °C (lit. not given); IR (neat): ν = 3194, 2976, 1782, 1669, 1523, 1325, 1169, 1118, 1066 cm<sup>–1</sup>; <sup>1</sup>H NMR (400 MHz, CDCl<sub>3</sub>): δ = 9.40 (s, 1H), 7.92 (d<sub>AA'XX'</sub>, *J* = 8.1 Hz, 2H), 7.73 (d<sub>AA'XX'</sub>, *J* = 8.1 Hz, 2H), 1.36 (s, 9H) ppm; <sup>13</sup>C NMR (101 MHz, CDCl<sub>3</sub>): δ = 177.1 (C), 165.5 (C), 134.5 (q, *J* = 32.0 Hz, C), 134.4 (C), 128.1 (2CH),

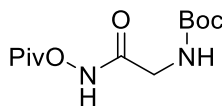
126.1 (q,  $J = 3.5$  Hz, 2CH), 123.6 (q,  $J = 272.7$  Hz  $\text{CF}_3$ ), 38.7 (C), 27.1 (3 $\text{CH}_3$ ) ppm; MS (ES-TOF):  $m/z$ : 100% 312.1  $[\text{M}+\text{Na}]^+$ . Spectroscopic data matched that reported in the literature.<sup>75</sup>

***N*-(Pivaloyloxy)picolinamide 111e**



Following **GP6a** using picolinic acid (369 mg, 3.00 mmol), oxalyl chloride (310  $\mu\text{L}$ , 3.60 mmol), *o*-pivaloylhydroxyamine triflic acid (801 mg, 3.00 mmol) and  $\text{Na}_2\text{CO}_3$  (630 mg, 6.00 mmol) gave **111e** as an off white solid (408 mg, 61%); mp: 58–60 °C; IR (neat):  $\nu = 3085, 3976, 2906, 1773, 1689, 1591, 1504, 1469, 1287, 1080\text{ cm}^{-1}$ ;  $^1\text{H}$  NMR (400 MHz,  $\text{CDCl}_3$ ):  $\delta = 10.78$  (br. s, 1H), 8.57 (ddd,  $J = 4.8, 1.7, 0.9$  Hz, 1H), 8.14 (dt,  $J = 7.9, 1.1$  Hz, 1H), 7.87 (td,  $J = 7.9, 1.7$  Hz, 1H), 7.48 (ddd,  $J = 7.7, 4.8, 1.1$  Hz, 1H), 1.38 (s, 9H) ppm;  $^{13}\text{C}$  NMR (101 MHz,  $\text{CDCl}_3$ ):  $\delta = 176.4$  (C), 162.0 (C), 148.6 (CH), 137.6 (CH), 127.2 (CH), 122.8 (CH), 38.6 (C), 27.2 (3 $\text{CH}_3$ ) ppm; *one quaternary carbon resonance not observed in  $^{13}\text{C}$  NMR spectra*; MS (SQD-ES):  $m/z$ : 100% 245.0  $[\text{N}+\text{Na}]^+$ .

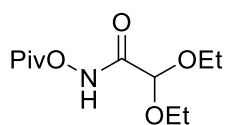
***tert*-Butyl (2-oxo-2-((pivaloyloxy)amino)ethyl)carbamate 111f**



A solution of KOH (85%, 1.32 g, 20.0 mmol) in MeOH (5.0 mL) was added to a solution of hydroxylamine hydrochloride (695 mg, 10.0 mmol) in MeOH (5.0 mL) and the mixture was cooled to 0 °C (KCl precipitates) and stirred for 30 min. The reaction mixture was filtered through a pad of cotton wool into a flask containing methyl (*tert*-butoxycarbonyl)glycinate (950 mg, 5.03 mmol) and the reaction mixture stirred at r.t. overnight. After removing the solvent under reduced pressure, the reaction mixture was diluted with  $\text{H}_2\text{O}$  (15 mL) and acidified with 2 M  $\text{HCl}_{(\text{aq})}$  until it reached pH 2. The organic layer were extracted with EtOAc (3 $\times$ 20 mL) and combined before being washed with brine (2 $\times$ 30mL), drying over  $\text{Na}_2\text{SO}_4$ , filtering and concentrated under reduced pressure to give crude the hydroxamic acid (474 mg, 50%). The crude hydroxamic acid (474 mg, 2.50 mmol) and  $\text{NEt}_3$

(0.42 mL, 3.00 mmol) were dissolved in dry THF (12.5 mL) and cooled to 0 °C. Pivaloyl chloride (332  $\mu$ L, 2.49 mmol) was added dropwise over 5 min, the ice bath was removed and the reaction stirred at r.t. for 2 h. The reaction mixture was diluted with EtOAc (40 mL) and H<sub>2</sub>O (30 mL) and the phases separated. The organic phase was washed with 1 M HCl<sub>(aq)</sub> (30 mL), brine (40 mL), dried over Na<sub>2</sub>SO<sub>4</sub>, filtered and concentrated under reduced pressure. Purification by flash column chromatography (7:3 hexane/EtOAc) gave **111f** as a white solid (550 mg, 40% over 2 steps); mp: 104–107 °C; IR (neat):  $\nu$  = 3230 (br.), 3123 (br.) 2974, 2941, 1780, 1697, 1670, 1442, 1398, 1366, 1149, 1084 cm<sup>-1</sup>; *NMR spectra display a mixture of rotamers*: <sup>1</sup>H NMR (400 MHz, CDCl<sub>3</sub>):  $\delta$  = 9.83 (br. s, 1H), 5.26 (br. s, 1H), 3.89 (br. s, 2H), 1.45 (s, 9H), 1.30 (s, 9H) ppm; <sup>13</sup>C NMR (101 MHz, CDCl<sub>3</sub>):  $\delta$  = 42.5 and 42.5 (CH<sub>2</sub>), 38.4 (C), 28.3 (3CH<sub>3</sub>), 27.0 (3CH<sub>3</sub>), *three quaternary carbon resonances not observed in <sup>13</sup>C NMR spectra*; HRMS (ES–TOF): *m/z*: calcd for C<sub>12</sub>H<sub>22</sub>N<sub>2</sub>O<sub>5</sub>Na: 297.1421, found 297.1425 [M+Na]<sup>+</sup>.

### 2,2-Diethoxy-N-(pivaloyloxy)acetamide **111g**

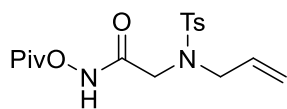


A solution of KOH (85%, 1.22 g, 18.6 mmol) in MeOH (5.0 mL) was added to a solution of hydroxylamine hydrochloride (646 mg, 9.30 mmol) in MeOH (5.0 mL) and the mixture was cooled to 0 °C (KCl precipitates) and stirred for 30 min. The reaction mixture was filtered through a pad of cotton wool into a flask containing ethyl 2,2-diethoxyacetate (820 mg, 4.65 mmol) and the reaction mixture stirred at r.t. overnight. After removing the solvent under reduced pressure, the reaction mixture was diluted with H<sub>2</sub>O (15 mL) and acidified with 2 M HCl<sub>(aq)</sub> until it reached pH 2. The organic layers were extracted with EtOAc (3×20 mL) and combined before being washed with brine (2×30mL), drying over Na<sub>2</sub>SO<sub>4</sub>, filtering and concentrated under reduced pressure to give crude the hydroxamic acid (578 mg, 76%). The crude hydroxamic acid (578 mg, 3.54 mmol) and NEt<sub>3</sub> (0.59 mL, 4.25



mmol) were dissolved in dry THF (18 mL) and cooled to 0 °C. Pivaloyl chloride (471  $\mu$ L, 3.54 mmol) was added dropwise over 5 min, the ice bath was removed and the reaction stirred at r.t. for 2 h. The reaction mixture was diluted with EtOAc (40 mL) and H<sub>2</sub>O (30 mL) and the phases separated. The organic phase was washed with 2 M HCl<sub>(aq)</sub> (30 mL), brine (40 mL), dried over Na<sub>2</sub>SO<sub>4</sub>, filtered and concentrated under reduced pressure. Purification by flash column chromatography (8:2 hexane/EtOAc) gave **111g** as a white solid (825 mg, 71% over 2 steps); mp: 28–30 °C; IR (neat):  $\nu$  = 3234 (br.), 2977, 1782, 1698, 1481, 1369, 1072 cm<sup>-1</sup>; <sup>1</sup>H NMR (400 MHz, CDCl<sub>3</sub>):  $\delta$  = 9.54 (br. s, 1H), 4.99 (s, 1H), 3.78 – 3.60 (m, 4H), 1.32 (s, 9H), 1.26 (t,  $J$  = 7.1 Hz, 6H) ppm; <sup>13</sup>C NMR (101 MHz, CDCl<sub>3</sub>):  $\delta$  = 176.2 (C), 164.7 (C), 98.2 (CH), 62.6 (2CH<sub>2</sub>), 38.5 (C), 27.1 (3CH<sub>3</sub>), 15.2 (2CH<sub>3</sub>) ppm; HRMS (ES–TOF):  $m/z$ : calcd for C<sub>11</sub>H<sub>21</sub>NO<sub>5</sub>Na: 270.1312, found 270.1318 [M+Na]<sup>+</sup>.

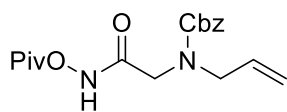
**2-((*N*-Allyl-4-methylphenyl)sulfonamido)-*N*-(pivaloyloxy)acetamide 118a**



Following **GP6a** using **117** (539 mg, 2.00 mmol), oxalyl chloride (0.21 mL, 2.40 mmol), *o*-pivaloylhydroxyamine triflic acid (534 mg, 2.00

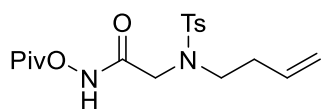
mmol) and Na<sub>2</sub>CO<sub>3</sub> (420 mg, 4.00 mmol). Purification by flash column chromatography (7:3 hexane/EtOAc) gave **118a** as a white solid (580 mg, 79%); mp: 93–95 °C; IR (neat):  $\nu$  = 3260, 2975, 1699, 1633, 1598, 1328, 1304, 1155 cm<sup>-1</sup>; <sup>1</sup>H NMR (300 MHz, CDCl<sub>3</sub>):  $\delta$  = 9.59 (br. s, 1H), 7.72 (d<sub>AA'XX'</sub>,  $J$  = 8.1 Hz, 2H), 7.35 (d<sub>AA'XX'</sub>,  $J$  = 8.1 Hz, 2H), 5.67 (ddt,  $J$  = 17.6, 9.1, 6.7 Hz, 1H), 5.27 – 5.18 (m, 2H), 3.90 (dt,  $J$  = 6.8, 1.2 Hz, 2H), 3.80 (s, 2H), 2.45 (s, 3H), 1.32 (s, 9H) ppm; <sup>13</sup>C NMR (101 MHz, CDCl<sub>3</sub>):  $\delta$  = 176.1 (C), 166.0 (C), 144.5 (C), 135.1 (C), 131.2 (CH), 130.2 (2CH), 127.7 (2CH), 121.5 (CH<sub>2</sub>), 52.6 (CH<sub>2</sub>), 49.0 (CH<sub>2</sub>), 38.5 (C), 27.1 (3CH<sub>3</sub>), 21.7 (CH<sub>3</sub>) ppm; HRMS (ES–TOF):  $m/z$ : calcd for C<sub>17</sub>H<sub>24</sub>N<sub>2</sub>O<sub>5</sub>SSNa: 3913.1298, found 391.1309 [M+Na]<sup>+</sup>.

***Benzyl allyl(2-oxo-2-((pivaloyloxy)amino)ethyl)carbamate 118b***



Following **GP6c** with acid **134** (966 mg, 4.00 mmol), *N*-methylmorpholine (1.32 mL, 12.0 mmol), isobutyl chloroformate (0.57 mL, 4.40 mmol) and *o*-Pivaloylhydroxyamine triflic acid (1.17 g, 4.40 mmol). Purification by flash column chromatography (3:1 hexane/EtOAc) gave **118b** as a colourless oil (926 mg, 66%); IR (neat):  $\nu = 3219$  (br.), 2976, 1780, 1678, 1462, 1416, 1243, 1082  $\text{cm}^{-1}$ ; *NMR spectra display a mixture of rotamers*:  $^1\text{H}$  NMR (400 MHz,  $\text{CDCl}_3$ ):  $\delta = 9.64$  and 8.98 (br. s, 1H), 7.43 – 7.32 (m, 5H), 5.89 – 5.75 (m, 1H), 5.27 – 5.17 (m, 4H), 4.08 – 4.02 (m, 2H), 3.98 (br. s, 2H), 1.33 (s, 9H) ppm;  $^{13}\text{C}$  NMR (101 MHz,  $\text{CDCl}_3$ ):  $\delta = 132.4$  (CH), 128.7 (2CH), 128.4 (2CH), 128.0 (CH), 118.3 ( $\text{CH}_2$ ), 68.2 ( $\text{CH}_2$ ), 60.6 ( $\text{CH}_2$ ), 51.1 ( $\text{CH}_2$ ), 38.5 (C), 27.1 (3 $\text{CH}_3$ ) ppm; *three quaternary carbon resonances not observed in  $^{13}\text{C}$  NMR spectra*; HRMS (ES-TOF):  $m/z$ : calcd for  $\text{C}_{18}\text{H}_{24}\text{N}_2\text{O}_5\text{Na}$ : 371.5177, found 371.1584  $[\text{M}+\text{Na}]^+$ .

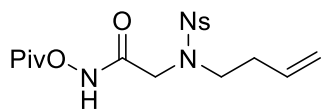
***2-((N-(But-3-en-1-yl)-4-methylphenyl)sulfonamido)-N-(pivaloyloxy)acetamide 128a***



Following **GP6b** using **125a** (566 mg, 2.00 mmol), oxalyl chloride (0.21 mL, 2.45 mmol), hydroxylamine hydrochloride (167 mg, 2.40 mmol) and  $\text{K}_2\text{CO}_3$  (552 mg, 4.00 mmol). Purification by flash column chromatography (75:25 hexane/EtOAc) gave **128a** as a white solid (306 mg, 40%); mp: 74–75  $^\circ\text{C}$ ; IR (neat):  $\nu = 3247$  (br.), 2978, 2932, 1782, 1671, 1481, 1338, 1161  $\text{cm}^{-1}$ ;  $^1\text{H}$  NMR (300 MHz,  $\text{CDCl}_3$ ):  $\delta = 9.68$  (br. s, 1H), 7.71 ( $d_{\text{AA}'\text{XX}'}$ ,  $J = 8.1$ , Hz, 2H), 7.35 ( $d_{\text{AA}'\text{XX}'}$ ,  $J = 8.1$  Hz, 2H), 5.72 (ddt,  $J = 17.0$ , 10.3, 6.7 Hz, 1H), 5.17 – 5.01 (m, 2H), 3.79 (br. s, 2H), 3.35 – 3.27 (m, 2H), 2.44 (s, 3H), 2.40 – 2.31 (m, 2H), 1.33 (s, 9H) ppm;  $^{13}\text{C}$  NMR (101 MHz,  $\text{CDCl}_3$ ):  $\delta = 175.9$  (C), 163.0 (C), 144.6 (C), 139.9 (C), 134.3 (CH), 130.2 (2CH), 127.6 (2CH), 118.0 ( $\text{CH}_2$ ), 51.0 ( $\text{CH}_2$ ), 50.2 ( $\text{CH}_2$ ),

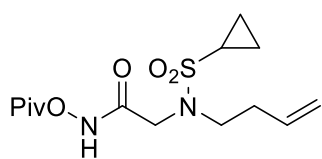
38.5 (C), 32.6 (CH<sub>2</sub>), 27.2 (3CH<sub>3</sub>), 21.7 (CH<sub>3</sub>) ppm; HRMS (ES–TOF): *m/z*: calcd for C<sub>18</sub>H<sub>26</sub>N<sub>2</sub>O<sub>5</sub>SNa: 405.1455, found 405.1461 [M+Na]<sup>+</sup>.

**2-((*N*-(*But-3-en-1-yl*)-4-nitrophenyl)sulfonamido)-*N*-(pivaloyloxy)acetamide 128b**



Following **GP6a** using **125h** (1.26 g, 4.01 mmol), oxalyl chloride (0.41 mL, 4.78 mmol), *O*-pivaloylhydroxyamine triflic acid (1.07 g, 4.01 mmol) and Na<sub>2</sub>CO<sub>3</sub> (840 mg, 8.00 mmol). Purification by flash column chromatography (4:6 hexane/Et<sub>2</sub>O) gave **128b** as a pale yellow solid (1.47 g, 89%); mp: 89–90 °C; IR (neat):  $\nu$  = 3215 (br.), 2980, 1779, 1682, 1528, 1374, 1311, 1161, 1080 cm<sup>-1</sup>; <sup>1</sup>H NMR (400 MHz, CDCl<sub>3</sub>):  $\delta$  = 9.36 (br. s, 1H), 8.37 (d<sub>AA'</sub>XX', *J* = 8.9 Hz, 2H), 8.04 (d<sub>AA'</sub>XX', *J* = 8.9 Hz, 2H), 5.71 (ddt, *J* = 17.1, 10.3, 6.7 Hz, 1H), 5.15 – 5.06 (m, 2H), 3.98 (br. s, 2H), 3.38 (t, *J* = 7.9 Hz, 2H), 2.38 (dt, *J* = 7.9, 6.7 Hz, 2H), 1.31 (s, 9H) ppm; <sup>13</sup>C NMR (101 MHz, CDCl<sub>3</sub>):  $\delta$  = 176.1 (C), 165.6 (C), 150.2 (C), 144.2 (C), 133.9 (CH), 128.8 (2CH), 124.4 (2CH), 117.9 (CH<sub>2</sub>), 49.0 (CH<sub>2</sub>), 48.5 (CH<sub>2</sub>), 38.3 (C), 32.3 (CH<sub>2</sub>), 26.9 (3CH<sub>3</sub>) ppm; HRMS (ES–TOF): *m/z*: calcd for C<sub>17</sub>H<sub>23</sub>N<sub>3</sub>O<sub>7</sub>SNa: 436.1149, found 436.1153 [M+Na]<sup>+</sup>.

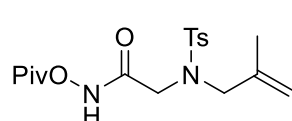
**2-((*N*-(*But-3-en-1-yl*)cyclopropanesulfonamido)-*N*-(pivaloyloxy)acetamide 128c**



Acid **135** (933 mg, 4.00 mmol) and NMM (1.1 mL, 9.64 mmol) were combined in dry CH<sub>2</sub>Cl<sub>2</sub> (12 mL) and cooled to 0 °C. 1-Propylphosphonic acid cyclic anhydride (50% w/w soln in CH<sub>2</sub>Cl<sub>2</sub>) (2.80 g, 4.4 mmol) was added dropwise over 5 min and the reaction stirred for 10 min at 0 °C. *o*-pivaloylhydroxyamine triflic acid (1.18 g, 4.42 mmol) was added and the ice bath removed. After stirring at r.t. for 16 h and removing the solvent under reduced pressure, the reaction mixture was diluted with EtOAc (50 mL) and washed with H<sub>2</sub>O (3×30 mL), brine (50 mL), dried over Na<sub>2</sub>SO<sub>4</sub>, filtered, and concentrated under reduced pressure. Purification by

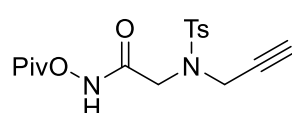
flash column chromatography (6:4 hexane/EtOAc) gave **128c** as a white solid (2.05 g, 65%); mp: 133–136 °C; IR (neat):  $\nu = 3121$  (br.), 2979, 1785, 1671, 1325, 1143, 1094  $\text{cm}^{-1}$ ;  $^1\text{H}$  NMR (400 MHz,  $\text{CDCl}_3$ ):  $\delta = 9.48$  (br. s, 1H), 5.77 (ddt,  $J = 17.1, 10.3, 6.8$  Hz, 1H), 5.18 – 5.07 (m, 2H), 4.03 (s, 2H), 3.48 – 3.42 (m, 2H), 2.54 – 2.45 (m, 1H), 2.45 – 2.37 (m, 2H), 1.31 (s, 9H), 1.24 – 1.19 (m, 2H), 1.07 – 1.01 (m, 2H) ppm;  $^{13}\text{C}$  NMR (101 MHz,  $\text{CDCl}_3$ ):  $\delta = 176.1$  (C), 134.4 (CH), 117.9 ( $\text{CH}_2$ ), 49.7 ( $\text{CH}_2$ ), 49.0 ( $\text{CH}_2$ ), 38.5 (C), 32.9 ( $\text{CH}_2$ ), 29.3 (CH), 27.1 (3 $\text{CH}_3$ ), 5.5 (2 $\text{CH}_2$ ) ppm; *one quaternary carbon resonance not observed in  $^{13}\text{C}$  NMR spectra*; HRMS (ES–TOF):  $m/z$ : calcd for  $\text{C}_{14}\text{H}_{24}\text{N}_2\text{O}_5\text{SNa}$ : 355.1298, found 355.1303  $[\text{M}+\text{Na}]^+$ .

**2-((4-Methyl-N-(2-methylallyl)phenyl)sulfonamido)-N-(pivaloyloxy)acetamide 129**



Following **GP6a** using **125c** (425 mg, 1.50 mmol), oxalyl chloride (0.15 mL, 1.75 mmol), *o*-pivaloylhydroxyamine triflic acid (400 mg, 1.50 mmol) and  $\text{Na}_2\text{CO}_3$  (315 mg, 3.00 mmol). Purification by flash column chromatography (7:3 hexane/EtOAc) gave **129** as a colourless oil (206 mg, 36%); IR (neat):  $\nu = 3253$  (br.), 2976, 2921, 1781, 1718, 1339, 1159, 1093  $\text{cm}^{-1}$ ;  $^1\text{H}$  NMR (400 MHz,  $\text{CDCl}_3$ ):  $\delta = 9.68$  (br. s, 1H), 7.76 (d,  $J = 8.1$  Hz, 2H), 7.35 (d,  $J = 8.1$  Hz, 2H), 4.98 (t,  $J = 1.5$  Hz, 1H), 4.88 (t,  $J = 1.5$  Hz, 1H), 3.85 – 3.81 (m, 4H), 2.46 (s, 3H), 1.73 (s, 3H), 1.34 (s, 9H) ppm;  $^{13}\text{C}$  NMR (101 MHz,  $\text{CDCl}_3$ ):  $\delta = 176.0$  (C), 166.3 (C), 144.4 (C), 134.9 (C), 139.0 (C), 130.1 (2CH), 127.8 (2CH), 116.8 ( $\text{CH}_2$ ), 55.9 ( $\text{CH}_2$ ), 48.8 ( $\text{CH}_2$ ), 38.5 (C), 27.1 (3 $\text{CH}_3$ ), 21.7 ( $\text{CH}_3$ ), 20.0 ( $\text{CH}_3$ ) ppm; HRMS (ES–TOF):  $m/z$ : calcd for  $\text{C}_{18}\text{H}_{26}\text{N}_2\text{O}_5\text{SNa}$ : 405.1460, found 405.1464  $[\text{M}+\text{Na}]^+$ .

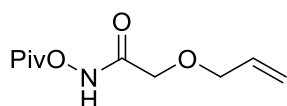
**2-((4-Methyl-N-(prop-2-yn-1-yl)phenyl)sulfonamido)-N-(pivaloyloxy)acetamide 130**



Following **GP6a** using **125g** (267 mg, 1.00 mmol), oxalyl chloride (0.10 mL, 1.19 mmol), *o*-pivaloylhydroxyamine triflic acid (267 mg, 1.00 mmol) and  $\text{Na}_2\text{CO}_3$  (210 mg, 2.00 mmol). Purification by flash column chromatography

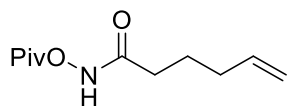
(7:3 hexane/EtOAc) gave **130** as a white solid (242 mg, 66%); mp: 96–98 °C; IR (neat):  $\nu$  = 3267, 3269 (br.), 2980, 2120, 7185, 1684, 1500, 1348, 1163, 1085  $\text{cm}^{-1}$ ;  $^1\text{H}$  NMR (400 MHz,  $\text{CDCl}_3$ ):  $\delta$  = 9.51 (br. s, 1H), 7.75 ( $d_{\text{AA'XX'}}$ ,  $J$  = 8.1 Hz, 2H), 7.33 ( $d_{\text{AA'XX'}}$ ,  $J$  = 8.1 Hz, 2H), 4.27 (d,  $J$  = 2.5 Hz, 2H), 3.96 (s, 2H), 2.44 (s, 3H), 2.12 (t,  $J$  = 2.5 Hz, 1H), 1.33 (s, 9H) ppm;  $^{13}\text{C}$  NMR (101 MHz,  $\text{CDCl}_3$ ):  $\delta$  = 147.7 (C), 144.8 (C), 130.0 (2CH), 128.1 (2CH), 75.4 (C), 68.0 (CH), 52.4 ( $\text{CH}_2$ ), 48.9 ( $\text{CH}_2$ ), 38.7 (C), 27.1 (3 $\text{CH}_3$ ), 21.8 ( $\text{CH}_3$ ) ppm; *two quaternary carbon resonances not observed in  $^{13}\text{C}$  NMR spectra*; HRMS (ES–TOF):  $m/z$ : calcd for  $\text{C}_{17}\text{H}_{22}\text{N}_2\text{O}_5\text{SNa}$ : 389.1142, found 389.1148  $[\text{M}+\text{Na}]^+$ .

### 2-(Allyloxy)-N-(pivaloyloxy)acetamide **131a**



Following **GP6a** using **125d** (348 mg, 3.00 mmol), oxalyl chloride (0.31 mL, 3.60 mmol), *o*-pivaloylhydroxyamine triflic acid (801 mg, 3.00 mmol) and  $\text{Na}_2\text{CO}_3$  (630 mg, 6.00 mmol). Purification by flash column chromatography (7:3 hexane/EtOAc) gave **131a** as a colourless oil (422 mg, 65%); IR (neat):  $\nu$  = 3202 (br.), 2976, 1779, 1688, 1481, 1082  $\text{cm}^{-1}$ ; *NMR spectra display a mixture of rotamers*:  $^1\text{H}$  NMR (400 MHz,  $\text{CDCl}_3$ ):  $\delta$  = 9.49 (br. s, 1H), 5.94 – 5.83 (m, 1H), 5.36 – 5.22 (m, 2H), 4.13 – 4.11 (m, 2H), 4.10 – 4.07 (m, 2H), 1.32 (m, 9H) ppm;  $^{13}\text{C}$  NMR (101 MHz,  $\text{CDCl}_3$ ):  $\delta$  = 176.3 (C), 166.9 (C), 133.2 (CH), 118.8 ( $\text{CH}_2$ ), 72.8 ( $\text{CH}_2$ ), 69.1 ( $\text{CH}_2$ ), 38.5 (C), 27.1 (3 $\text{CH}_3$ ) ppm; HRMS (ES–TOF):  $m/z$ : calcd for  $\text{C}_{10}\text{H}_{17}\text{NO}_4\text{Na}$ : 238.1050, found 238.1057  $[\text{M}+\text{Na}]^+$ .

### N-(Pivaloyloxy)hex-5-enamide **131b**



Following **GP6a** using 5-hexenoic acid (360  $\mu\text{L}$ , 3.00 mmol), oxalyl chloride (0.31 mL, 3.60 mmol), *o*-pivaloylhydroxyamine triflic acid (801 mg, 3.00 mmol) and  $\text{Na}_2\text{CO}_3$  (630 mg, 6.00 mmol). Purification by flash column chromatography (8:2 hexane/EtOAc) gave **131b** as a colourless oil (501 mg, 78%); IR (neat):

$\nu = 3177$  (br.), 2977, 1780, 1668, 1481, 1080  $\text{cm}^{-1}$ ;  $^1\text{H}$  NMR (400 MHz,  $\text{CDCl}_3$ ):  $\delta = 8.73$  (br. s, 1H), 5.83 – 5.70 (m, 1H), 5.11 – 4.93 (m, 2H), 2.25 (t,  $J = 7.4$ , 2H), 2.17 – 2.09 (m, 2H), 1.83 – 1.74 (m, 2H), 1.32 – 1.30 (m, 9H) ppm;  $^{13}\text{C}$  NMR (101 MHz,  $\text{CDCl}_3$ ):  $\delta = 176.9$  (C), 137.6 (CH), 115.8 ( $\text{CH}_2$ ), 38.5 (C), 33.0 ( $\text{CH}_2$ ), 32.1 ( $\text{CH}_2$ ), 27.1 (3 $\text{CH}_3$ ), 24.0 ( $\text{CH}_2$ ) ppm; *one quaternary carbon resonance not observed in  $^{13}\text{C}$  NMR spectra*; HRMS (ES–TOF):  $m/z$ : calcd for  $\text{C}_{11}\text{H}_{19}\text{NO}_3\text{Na}$ : 236.1257, found 236.1265  $[\text{M}+\text{Na}]^+$ .

### 2-((*N*-Cinnamyl-4-methylphenyl)sulfonamido)-*N*-(pivaloyloxy)acetamide **132**

Following **GP6c** with acid **125b** (517 mg, 1.50 mmol), *N*-methylmorpholine (0.50 mL, 4.50 mmol), isobutyl chloroformate (0.22 mL, 1.69 mmol) and *o*-Pivaloylhydroxyamine triflic acid (444 mg, 1.65 mmol). Purification by flash column chromatography (8:2 hexane/EtOAc) gave **132** as a white solid (260 mg, 39%); mp: 80–81 °C; IR (neat):  $\nu = 3223$  (br.) 2976, 2935, 1784, 1682, 1479, 1340, 1159, 1089  $\text{cm}^{-1}$ ;  $^1\text{H}$  NMR (400 MHz,  $\text{CDCl}_3$ ):  $\delta = 9.60$  (br. s, 1H), 7.76 ( $d_{\text{AA'XX'}}$ ,  $J = 8.1$  Hz, 2H), 7.35 ( $d_{\text{AA'XX'}}$ ,  $J = 8.1$ , 2H), 7.32 – 7.22 (m, 5H), 6.48 (dt,  $J = 15.7$ , 1.3 Hz, 1H), 5.98 (dt,  $J = 15.7$ , 7.0 Hz, 1H), 4.07 (dd,  $J = 7.0$ , 1.3 Hz, 2H), 3.87 (s, 2H), 2.45 (s, 3H), 1.30 (s, 9H) ppm;  $^{13}\text{C}$  NMR (101 MHz,  $\text{CDCl}_3$ ):  $\delta = 144.6$  (C), 136.3 (CH), 135.9 (C), 130.2 (2CH), 129.9 (C), 128.7 (2CH), 128.4 (CH), 127.7 (2CH), 126.8 (2CH), 121.9 (CH), 52.1 ( $\text{CH}_2$ ), 49.2 ( $\text{CH}_2$ ), 38.5 (C), 27.1 (3 $\text{CH}_3$ ), 21.7 ( $\text{CH}_3$ ) ppm; *two quaternary carbon resonances not observed in  $^{13}\text{C}$  NMR spectra*; HRMS (ES–TOF):  $m/z$ : calcd for  $\text{C}_{23}\text{H}_{29}\text{N}_2\text{O}_5\text{S}$ : 445.1792, found 445.1794  $[\text{M}+\text{H}]^+$ .

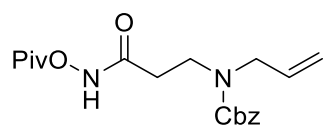
### Allyl methyl(2-oxo-2-((pivaloyloxy)amino)ethyl)carbamate **133**

Following **GP6a** using acid **125f** (520 mg, 3.00 mmol), oxalyl chloride (0.31 mL, 3.60 mmol), *o*-pivaloylhydroxyamine triflic

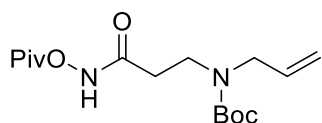
acid (801 mg, 3.00 mmol) and Na<sub>2</sub>CO<sub>3</sub> (630 mg, 6.00 mmol). Purification by flash column chromatography (6:4 hexane/EtOAc) gave **133** as a colourless oil (322 mg, 40%); IR (neat):  $\nu$  = 3210 (br.) 2975, 1780, 1677, 1481, 1401, 1219, 1152, 1082 cm<sup>-1</sup>; *NMR spectra display a mixture of rotamers*: <sup>1</sup>H NMR (400 MHz, CDCl<sub>3</sub>):  $\delta$  = 9.70 – 9.06 (br. s, 1H), 6.01 – 5.87 (m, 1H), 5.36 – 5.27 (m, 1H), 5.26 – 5.19 (m, 1H), 4.67 – 4.58 (m, 2H), 4.10 – 3.92 (m, 2H), 3.06 (s, 3H), 1.31 (br. s, 9H) ppm; <sup>13</sup>C NMR (101 MHz, CDCl<sub>3</sub>):  $\delta$  = 176.2 (C), 132.5 (CH), 118.1 (CH<sub>2</sub>), 67.0 (CH<sub>2</sub>), 51.6 and 51.0 (CH<sub>2</sub>), 38.5 (C), 35.9 (CH<sub>3</sub>), 27.1 (3CH<sub>3</sub>) ppm; *two quaternary carbon resonances not observed in <sup>13</sup>C NMR spectra*; HRMS (ES–TOF): *m/z*: calcd for C<sub>12</sub>H<sub>20</sub>N<sub>2</sub>O<sub>5</sub>Na: 295.1264, found 295.1272 [M+Na]<sup>+</sup>.

***Benzyl allyl(3-oxo-3-((pivaloyloxy)amino)propyl)carbamate 149a***

Following **GP6c** with acid **148a** (3.95 g, 15.0 mmol), *N*-methylmorpholine (5.0 mL, 45.5 mmol), isobutyl chloroformate (2.1 mL, 16.2 mmol) and *o*-pivaloylhydroxyamine triflic acid (4.00 g, 15.0 mmol). Purification by flash column chromatography (8:2→7:3 hexane/EtOAc) gave **149a** as a colourless oil (2.52 g, 46%); IR (neat):  $\nu$  = 3215 (br.), 2975, 1778, 1670, 1477, 1415, 1245, 1083 cm<sup>-1</sup>; *NMR spectra display a mixture of rotamers*: <sup>1</sup>H NMR (400 MHz, CDCl<sub>3</sub>):  $\delta$  = 9.83 and 8.97 (br. s, 1H), 7.38 – 7.28 (m, 5H), 5.83 – 5.67 (m, 1H), 5.19 – 5.08 (m, 4H), 3.92 (d t, *J* = 5.9, 1.5 Hz, 2H), 3.58 (t, *J* = 6.8 Hz, 2H), 2.65 – 2.40 (m, 2H), 1.30 (s, 9H) ppm; <sup>13</sup>C NMR (101 MHz, CDCl<sub>3</sub>):  $\delta$  = 176.5 (C), 169.2 (C), 156.8 (C), 136.5 (C), 133.4 (CH), 128.6 (2CH), 128.2 (2CH), 127.9 (CH), 117.3 and 117.2 (CH<sub>2</sub>), 67.6 (CH<sub>2</sub>), 50.6 (CH<sub>2</sub>), 43.4 (CH<sub>2</sub>), 38.4 (C), 32.7 (CH<sub>2</sub>), 27.1 (3CH<sub>3</sub>) ppm; HRMS (ES–TOF): *m/z*: calcd for C<sub>19</sub>H<sub>26</sub>N<sub>2</sub>NaO<sub>5</sub>: 385.1734, found 385.1744 [M+Na]<sup>+</sup>.

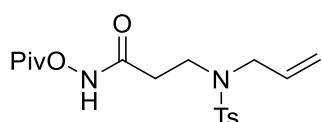


***tert-Butyl allyl(3-oxo-3-((pivaloyloxy)amino)propyl)carbamate 149b***



Following **GP6c** with acid **148b** (3.44 g, 15.0 mmol), *N*-methylmorpholine (5.0 mL, 45.5 mmol), isobutyl chloroformate (2.1 mL, 16.2 mmol) and *o*-pivaloylhydroxyamine triflic acid (4.00 g, 15.0 mmol). After 18 h at r.t., the mixture was heated to 45 °C for 3 h before the aqueous work up. Purification by flash column chromatography (9:1→7:3 hexane/EtOAc) gave **149b** as a colourless oil (3.44 g, 70%); IR (neat):  $\nu = 3214$  (br.), 2975, 1780, 1665, 1479, 1410, 1367, 1164, 1086  $\text{cm}^{-1}$ ; *NMR spectra display a mixture of rotamers*:  $^1\text{H}$  NMR (400 MHz,  $\text{CDCl}_3$ ):  $\delta = 10.13$  and  $9.13$  (br. s, 1H), 5.75 (ddt,  $J = 17.6, 9.8, 5.6$  Hz, 1H), 5.16 – 5.08 (m, 2H), 3.86 – 3.79 (m, 2H), 3.52 (t,  $J = 6.7$  Hz, 2H), 2.55 (br. s, 2H), 1.44 (s, 9H), 1.29 (s, 9H) ppm;  $^{13}\text{C}$  NMR (101 MHz,  $\text{CDCl}_3$ ):  $\delta = 176.9$  (C), 169.2 (C), 133.7 (CH), 116.8 ( $\text{CH}_2$ ), 80.7 (C), 50.4 ( $\text{CH}_2$ ), 42.7 ( $\text{CH}_2$ ), 38.4 (C), 33.2 and 33.0 ( $\text{CH}_2$ ), 28.5 ( $3\text{CH}_3$ ), 27.3 and 27.1 ( $3\text{CH}_3$ ) ppm; *one quaternary carbon resonance not observed in  $^{13}\text{C}$  NMR spectra*; HRMS (ES-TOF):  $m/z$ : calcd for  $\text{C}_{16}\text{H}_{28}\text{N}_2\text{O}_5\text{Na}$ : 351.1890, found 351.1892  $[\text{M}+\text{Na}]^+$ .

***3-((N-Allyl-4-methylphenyl)sulfonamido)-N-(pivaloyloxy)propenamide 149c***



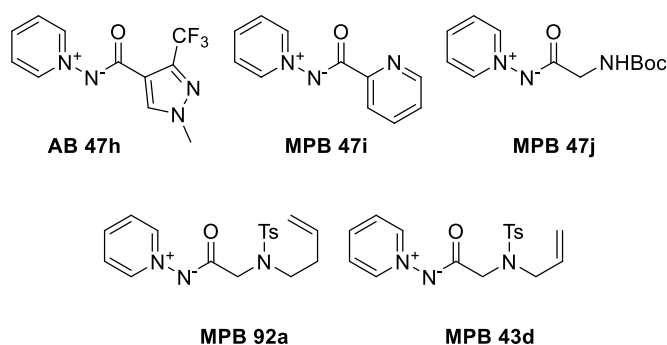
Following **GP6b** using acid **148c** (1.70 g, 6.00 mmol), oxalyl chloride (0.62 mL, 7.19 mmol), hydroxylamine hydrochloride (500 mg, 7.20 mmol) and  $\text{K}_2\text{CO}_3$  (1.66 g, 12.0 mmol). Purification by flash column chromatography (7:3 hexane/EtOAc) gave **149c** as a colourless oil (1.85 g, 81%); IR (neat):  $\nu = 3230$  (br.), 2976, 1778, 1674, 1332, 1154, 1085  $\text{cm}^{-1}$ ;  $^1\text{H}$  NMR (400 MHz,  $\text{CDCl}_3$ ):  $\delta = 8.90$  (br. s, 1H), 7.70 ( $d_{\text{AA}'\text{XX}'}$ ,  $J = 8.0$  Hz, 2H), 7.31 ( $d_{\text{AA}'\text{XX}'}$ ,  $J = 8.0$  Hz, 2H), 5.62 (ddt,  $J = 16.6, 10.1, 6.4$  Hz, 1H), 5.22 – 5.13 (m, 2H), 3.81 (dt,  $J = 6.4, 1.3$  Hz, 2H), 3.39 (t,  $J = 7.2$  Hz, 2H), 2.63 (t,  $J = 7.2$  Hz, 2H), 2.43 (s, 3H), 1.31 (s, 9H) ppm;  $^{13}\text{C}$  NMR (101 MHz,  $\text{CDCl}_3$ ):  $\delta = 143.9$



(C), 136.0 (C), 132.8 (CH), 130.0 (2CH), 127.4 (2CH), 119.8 (CH<sub>2</sub>), 52.3 (CH<sub>2</sub>), 43.5 (CH<sub>2</sub>), 38.5 (C), 33.7 (CH<sub>2</sub>), 27.1 (3CH<sub>3</sub>), 21.7 (CH<sub>3</sub>) ppm; *two quaternary carbon resonances not observed in <sup>13</sup>C NMR spectra*; HRMS (ES–TOF): *m/z*: calcd for C<sub>18</sub>H<sub>26</sub>N<sub>2</sub>O<sub>5</sub>SNa: 405.1455, found 405.1459 [M+Na]<sup>+</sup>.

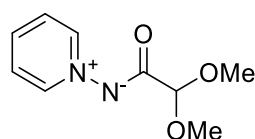
## Formation of *N*-acyl pyridinium ylides

The following ynamides were prepared by current and previous Davies group members Alessandro Ballela (AB) and Matthew P. Ball–Jones (MPB):



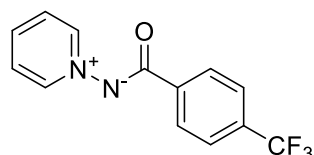
The following compounds were synthesised according to literature procedures, which are referenced alongside the data:

### *(2,2-Dimethoxyacetyl)(pyridin-1-ium-1-yl)amide 47a*



3.52 g, 90%. Spectroscopic data matched that reported in the literature.<sup>49</sup>

### *Pyridin-1-ium-1-yl(4-(trifluoromethyl)benzoyl)amide 47f*

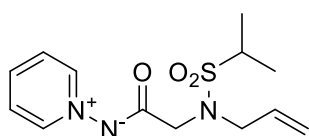


750 mg, 94%. Spectroscopic data matched that reported in the literature.<sup>264</sup>

### General Procedure 7: *N*-acyl pyridinium ylide synthesis (GP7)

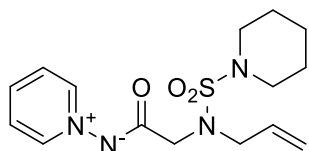
The relevant ester (1.2 eq.), 1-aminopyridinium iodide (1.0 eq.) and K<sub>2</sub>CO<sub>3</sub> (2.4 eq.) were dissolved in MeOH (0.12 M) and stirred at r.t. for 3 days. The solvent was removed under reduced pressure and the resulting solution passed through a 3 cm alumina pad with CH<sub>2</sub>Cl<sub>2</sub>/MeOH (9:1). The crude material was then purified by flash column chromatography to yield the corresponding ylide.

#### *(N-Allyl-N-(isopropylsulfonyl)glycyl)(pyridin-1-ium-1-yl)amide 43a*



Following **GP7** using ester **89a** (1.41 g, 5.99 mmol) and 1-aminopyridinium iodide (1.11 g, 5.00 mmol). Purification by flash column chromatography (9:1 CH<sub>2</sub>Cl<sub>2</sub>/MeOH) gave ylide **43a** as a brown oil (1.05 g, 71%); IR (neat):  $\nu$  = 2934, 1583, 1470, 1314, 1269, 1130, 1054 cm<sup>-1</sup>; <sup>1</sup>H NMR (400 MHz, CDCl<sub>3</sub>):  $\delta$  = 8.65 – 8.62 (m, 2H), 7.93 (tt,  $J$  = 7.7, 1.3 Hz, 1H), 7.69 – 7.64 (m, 2H), 5.84 (ddt,  $J$  = 17.1, 10.2, 6.3 Hz, 1H), 5.30 – 5.19 (m, 2H), 4.07 – 4.03 (m, 4H), 3.47 (hept,  $J$  = 6.8 Hz, 1H), 1.39 (d,  $J$  = 6.9 Hz, 6H) ppm; <sup>13</sup>C NMR (101 MHz, CDCl<sub>3</sub>):  $\delta$  = 172.6 (C), 143.0 (2CH), 137.5 (CH), 133.9 (CH), 126.3 (2CH), 118.6 (CH<sub>2</sub>), 55.0 (CH), 51.5 (CH<sub>2</sub>), 49.3 (CH<sub>2</sub>), 16.9 (2CH<sub>3</sub>) ppm; HRMS (ES-TOF):  $m/z$ : calcd for C<sub>13</sub>H<sub>20</sub>N<sub>3</sub>O<sub>3</sub>S: 298.1220, found 298.1223 [M+H]<sup>+</sup>.

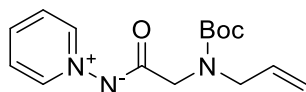
#### *(N-Allyl-N-(piperidin-1-ylsulfonyl)glycyl)(pyridin-1-ium-1-yl)amide 43b*



Following **GP7** using ester **89b** (2.60 g, 9.62 mmol) and 1-aminopyridinium iodide (1.78 g, 8.01 mmol). Purification by flash column chromatography (9:1 CH<sub>2</sub>Cl<sub>2</sub>/MeOH) gave ylide **43b** as a brown oil (1.92 g, 71%); IR (neat):  $\nu$  = 2936, 2853, 1583, 1470, 1324, 1138, 1052 cm<sup>-1</sup>; <sup>1</sup>H NMR (400 MHz, CDCl<sub>3</sub>):  $\delta$  = 8.67 – 8.63 (m, 2H), 7.91 (tt,  $J$  = 7.7, 1.3 Hz 1H), 7.68 – 7.62 (m, 2H), 5.89 (ddt,  $J$  = 17.2, 10.1, 6.4 Hz, 1H), 5.25 (app. dq, 17.2, 1.4 Hz, 1H), 5.19 (app. dq,  $J$  = 10.1, 1.4 Hz, 1H), 4.01 (dt,  $J$

= 6.5, 1.4 Hz, 2H), 3.94 (s, 2H), 3.28 – 3.24 (m, 4H), 1.63 – 1.55 (m, 4H), 1.52 – 1.45 (m, 2H) ppm;  $^{13}\text{C}$  NMR (101 MHz,  $\text{CDCl}_3$ ):  $\delta$  = 172.6 (C), 143.0 (2CH), 137.3 (CH), 133.8 (CH), 126.2 (2CH), 118.5 ( $\text{CH}_2$ ), 51.6 ( $\text{CH}_2$ ), 50.0 ( $\text{CH}_2$ ), 46.9 (2 $\text{CH}_2$ ), 25.5 (2 $\text{CH}_2$ ), 23.9 ( $\text{CH}_2$ ) ppm; HRMS (ES–TOF):  $m/z$ : calcd for  $\text{C}_{15}\text{H}_{23}\text{N}_4\text{O}_3\text{S}$ : 339.1485, found 339.1489  $[\text{M}+\text{H}]^+$ .

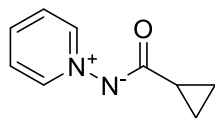
**(*N*-Allyl-*N*-(*tert*-butoxycarbonyl)glycyl)(pyridin-1-ium-1-yl)amide **43c****



Following **GP7** using ester **89c** (687 mg, 3.00 mmol) and 1-aminopyridinium iodide (555 mg, 2.50 mmol). Purification by flash

column chromatography (9:1  $\text{CH}_2\text{Cl}_2/\text{MeOH}$ ) gave ylide **43c** as a brown oil (301 mg, 41%); IR (neat):  $\nu$  = 3110, 2985, 2968, 1679, 1583, 1565, 1469, 1251, 1166, 1122  $\text{cm}^{-1}$ ; *NMR spectra display a mixture of rotamers*:  $^1\text{H}$  NMR (300 MHz,  $\text{CDCl}_3$ ):  $\delta$  = 8.72 – 8.62 (m, 2H), 7.93 – 7.84 (s, 1H), 7.68 – 7.57 (m, 2H), 5.93 – 5.77 (m, 1H), 5.23 – 5.03 (m, 2H), 4.09 – 3.90 (m, 4H), 1.47 (s, 9H) ppm;  $^{13}\text{C}$  NMR (101 MHz,  $\text{CDCl}_3$ ):  $\delta$  = 172.8 (C), 155.8 (C), 142.9 and 142.7 (2CH), 137.6 and 137.4 (CH), 134.1 and 134.0 (CH), 126.2 and 126.1 (2CH), 116.3 and 115.7 ( $\text{CH}_2$ ), 79.3 and 79.2 (C), 50.4 and 49.9 ( $\text{CH}_2$ ), 49.5 and 49.3 ( $\text{CH}_2$ ), 28.2 and 28.2 (3 $\text{CH}_3$ ) ppm; HRMS (ES–TOF):  $m/z$ : calcd for  $\text{C}_{15}\text{H}_{22}\text{N}_3\text{O}_3$ : 292.1656, found 292.1664  $[\text{M}+\text{H}]^+$ .

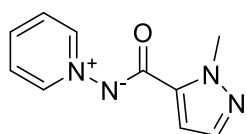
**Cyclopropanecarbonyl(pyridin-1-ium-1-yl)amide **47d****



1-Aminopyridinium iodide (4.44 g, 20.0 mmol) dissolved in 2.5 M NaOH (200 mL) with vigorous stirring and cooled to 0 °C. After 10 min stirring at 0 °C, cyclopropanecarbonyl chloride (3.63 mL, 40.0 mmol) was added via syringe pump over 20 min, the ice bath was removed, and the reaction mixture stirred at r.t. for 16 h. The organics were extracted with  $\text{CH}_2\text{Cl}_2$  (3×100 mL), combined and washed with brine (200 mL), dried over  $\text{Na}_2\text{SO}_4$ , filtered and concentrated under reduced pressure. Purification by flash column chromatography (9:1  $\text{CH}_2\text{Cl}_2/\text{MeOH}$ ) gave **47d** as pale yellow crystals (2.01 g, 62%); mp: 158–

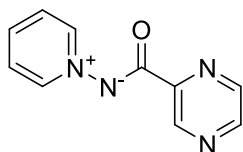
160 °C; IR (neat):  $\nu$  = 3104, 3034, 1562, 1478, 1436, 1393, 1246  $\text{cm}^{-1}$ ;  $^1\text{H}$  NMR (300 MHz,  $\text{CDCl}_3$ ):  $\delta$  = 8.73 – 8.68 (m, 2H), 7.87 (tt,  $J$  = 7.7, 1.4 Hz, 1H), 7.65 – 7.58 (m, 2H), 1.68 (tt,  $J$  = 8.0, 4.8 Hz, 1H), 0.97 – 0.90 (m, 2H), 0.75 – 0.68 (m, 2H) ppm;  $^{13}\text{C}$  NMR (101 MHz,  $\text{CDCl}_3$ ):  $\delta$  = 177.6 (C), 143.2 (2CH), 136.7 (CH), 125.9 (2CH), 14.7 (CH), 6.4 (2CH<sub>2</sub>) ppm; HRMS (ES–TOF):  $m/z$ : calcd for  $\text{C}_9\text{H}_{11}\text{N}_2\text{O}$ : 163.0866, found 163.0863  $[\text{M}+\text{H}]^+$ .

**(1-Methyl-1H-pyrazole-5-carbonyl)(pyridin-1-ium-1-yl)amide 47e**



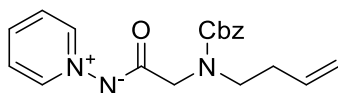
1-Methyl-pyrazole-5-carboxylic acid (348 mg, 3.00 mmol) and  $\text{NEt}_3$  (0.84 mL, 6.10 mmol) were dissolved in dry  $\text{CH}_2\text{Cl}_2$  (15 mL) under argon and cooled to 0 °C. Isobutyl chloroformate (430  $\mu\text{L}$ , 3.32 mmol) was added dropwise over 5 min and the reaction mixture was stirred for 1 h before  $\text{K}_2\text{CO}_3$  (993 mg, 7.20 mmol), 1-aminopyridinium iodide (732 mg, 3.30 mmol) and MeOH (6.0 mL) were added and the ice bath removed. After stirring at r.t. for 16 h, 2 M  $\text{NaOH}_{(\text{aq})}$  (20 mL) was added and the organics extracted with  $\text{CH}_2\text{Cl}_2$  (3 $\times$ 20 mL). The combined organics were washed with brine (40 mL), dried over  $\text{Na}_2\text{SO}_4$ , filtered and concentrated under reduced pressure. Purification by flash column chromatography (9:1  $\text{CH}_2\text{Cl}_2/\text{MeOH}$ ) gave ylide **47e** as a brown solid (422 mg, 70%); mp: 133–134 °C; IR (neat):  $\nu$  = 3104, 3080, 3037, 1582, 1568, 1462 1324, 1265  $\text{cm}^{-1}$ ;  $^1\text{H}$  NMR (300 MHz,  $\text{CDCl}_3$ ):  $\delta$  = 8.79 – 8.74 (m, 2H), 7.97 (tt,  $J$  = 7.7, 1.4 Hz, 1H), 7.75 – 7.67 (m, 2H), 7.44 (d,  $J$  = 2.0 Hz, 1H), 6.76 (d,  $J$  = 2.0 Hz, 1H), 4.24 (s, 3H) ppm;  $^{13}\text{C}$  NMR (101 MHz,  $\text{CDCl}_3$ ):  $\delta$  = 165.2 (C), 143.4 (2CH), 138.7 (C), 137.6 (CH), 137.5 (CH), 126.3 (2CH), 107.8 (CH), 39.5 (CH<sub>3</sub>) ppm; HRMS (ES–TOF):  $m/z$ : calcd for  $\text{C}_{10}\text{H}_{11}\text{N}_4\text{O}$ : 203.0927, found 203.0929  $[\text{M}+\text{H}]^+$ .

**(Pyrazine-2-carbonyl)(pyridin-1-ium-1-yl)amide 47b**



Pyrazine carboxylic acid (372 mg, 3.00 mmol) and conc. H<sub>2</sub>SO<sub>4</sub> (2 drops) were dissolved in MeOH (16 mL) and heated to reflux for 2 h. After allowing to cool to r.t., the solvent was removed under reduced pressure and the residue taken up in EtOAc (40 mL). The organics were washed with satd NaHCO<sub>3(aq)</sub> (25 mL) and brine (40 mL), dried over Na<sub>2</sub>SO<sub>4</sub>, filtered and concentrated under reduced pressure to give crude ester (352 mg, 85%). Following **GP6** using crude ester (352 mg, 2.55 mmol) and 1-aminopyridinium iodide (466 mg, 2.10 mmol). Purification by flash column chromatography (9:1 CH<sub>2</sub>Cl<sub>2</sub>/MeOH) gave ylide **47b** as a brown solid (366 mg, 87%); mp: 245–249 °C; IR (neat):  $\nu$  = 3059, 1591, 1583, 1558, 1470, 1333, 1194, 1154, 1017 cm<sup>-1</sup>; <sup>1</sup>H NMR (300 MHz, CDCl<sub>3</sub>):  $\delta$  = 9.42 (d,  $J$  = 1.2 Hz, 1H), 8.91 – 8.83 (m, 2H), 8.68 – 8.61 (m, 2H), 8.07 – 7.93 (m, 1H), 7.79 – 7.70 (m, 2H) ppm; <sup>13</sup>C NMR (101 MHz, CDCl<sub>3</sub>):  $\delta$  = 168.3 (C), 150.1 (C), 145.7 (CH), 145.5 (CH), 143.6 (CH), 143.4 (2CH), 137.9 (CH), 126.4 (2CH) ppm; HRMS (ES-TOF):  $m/z$ : calcd for C<sub>10</sub>H<sub>9</sub>N<sub>4</sub>O: 201.0771, found 201.0776 [M+H]<sup>+</sup>.

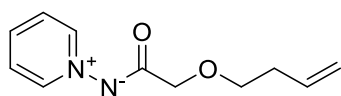
**(N-((Benzyloxy)carbonyl)-N-(but-3-en-1-yl)glycyl)(pyridin-1-ium-1-yl)amide 92b**



Following **GP7** using ester **89e** (308 mg, 0.75 mmol) and 1-aminopyridinium iodide (139 mg, 0.63 mmol). Purification by flash column chromatography (9:1 CH<sub>2</sub>Cl<sub>2</sub>/MeOH) gave ylide **92b** as a brown oil (109 mg, 51%); IR (neat):  $\nu$  = 3068, 2938, 1689, 1579, 1471, 1218, 1141 cm<sup>-1</sup>; NMR spectra display a mixture of rotamers: <sup>1</sup>H NMR (400 MHz, CDCl<sub>3</sub>):  $\delta$  = 8.62 (d,  $J$  = 5.6 Hz, 1H), 8.33 (d,  $J$  = 5.6 Hz, 1H), 7.88 – 7.77 (m, 1H), 7.56 (t,  $J$  = 7.2 Hz, 1H), 7.50 (t,  $J$  = 7.2 Hz, 1H), 7.35 – 7.18 (m, 5H), 5.73 (ddt,  $J$  = 17.1, 10.2, 6.8 Hz, 1H), 5.12 (s, 2H), 5.06 – 4.99 (m, 1H), 4.98 – 4.90 (m, 1H), 4.04 and 3.96 (s, 2H), 3.49 – 3.40 (m, 2H), 2.42 – 2.24 (m, 2H) ppm; <sup>13</sup>C NMR (101

MHz, CDCl<sub>3</sub>):  $\delta$  = 172.9 (C), 156.8 and 156.7 (C), 143.3 and 143.2 (2CH), 137.6 (C), 137.2 and 137.1 (CH), 135.8 and 135.7 (CH), 128.5 and 128.4 (2CH), 128.0 (CH), 127.8 and 127.7 (2CH), 126.1 (2CH), 116.6 and 116.5 (CH<sub>2</sub>), 67.2 and 66.8 (CH<sub>2</sub>), 51.1 and 51.0 (CH<sub>2</sub>), 48.6 and 47.8 (CH<sub>2</sub>), 33.1 and 32.7 (CH<sub>2</sub>) ppm; HRMS (ES–TOF):  $m/z$ : calcd for C<sub>19</sub>H<sub>22</sub>N<sub>3</sub>O<sub>3</sub>: 340.1656, found 340.1664 [M+H]<sup>+</sup>.

**(2-(But-3-en-1-yloxy)acetyl)(pyridin-1-ium-1-yl)amide 92c**



Acid **86** (585 mg, 4.50 mmol) and DMF (1 drop) were dissolved in dry CH<sub>2</sub>Cl<sub>2</sub> (9.0 mL) under argon. Oxalyl chloride (430  $\mu$ L, 5.01 mmol) was added dropwise over 5 min and the reaction mixture stirred at r.t. for 2 h. The reaction mixture was concentrated under reduced pressure (water bath at 23 °C, 10 min at 10 mbar) and then re-dissolved in CH<sub>2</sub>Cl<sub>2</sub> (9.0 mL) with vigorous stirring. Finely ground K<sub>2</sub>CO<sub>3</sub> (1.35 g, 9.87 mmol) and 1-aminopyridinium iodide (910 mg, 4.10 mmol) were added and the reaction stirred at r.t. for 16 h. 1 M NaOH (20 mL) was added and the organics extracted with CH<sub>2</sub>Cl<sub>2</sub> (3 $\times$ 20 mL). The combined organic phases were washed with brine (30 mL), dried over Na<sub>2</sub>SO<sub>4</sub>, filtered and concentrated under reduced pressure. Purification by flash column chromatography gave ylide **92c** as a brown solid (418 mg, 45%); mp: 75–77 °C; IR (neat):  $\nu$  = 3395 (br.), 2922, 2859, 1567, 1471, 1281, 1108 cm<sup>-1</sup>; <sup>1</sup>H NMR (400 MHz, CDCl<sub>3</sub>):  $\delta$  = 8.73 – 8.67 (m, 2H), 7.91 (tt,  $J$  = 7.7, 1.3 Hz, 1H), 7.67 – 7.62 (m, 2H), 5.86 (ddt,  $J$  = 17.1, 10.2, 6.9 Hz, 1H), 5.11 (app. dq,  $J$  = 17.1, 1.7 Hz, 1H), 5.03 (ddt,  $J$  = 10.2, 2.3, 1.3 Hz, 1H), 4.15 (s, 2H), 3.67 (t,  $J$  = 6.9 Hz, 2H), 2.45 (app. qt,  $J$  = 6.9, 1.4 Hz, 2H) ppm; <sup>13</sup>C NMR (101 MHz, CDCl<sub>3</sub>):  $\delta$  = 173.6 (C), 143.3 (2CH), 137.3 (CH), 135.3 (CH), 126.2 (2CH), 116.5 (CH<sub>2</sub>), 71.8 (CH<sub>2</sub>), 70.9 (CH<sub>2</sub>), 34.3 (CH<sub>2</sub>) ppm; HRMS (ES–TOF):  $m/z$ : calcd for C<sub>11</sub>H<sub>15</sub>N<sub>2</sub>O<sub>2</sub>: 207.1128, found 207.1133 [M+H]<sup>+</sup>.

## Polycyclisation catalysis products

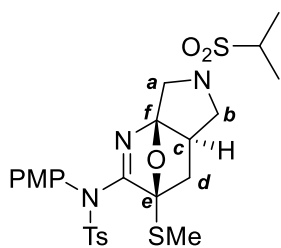
### Gold-catalysed polycyclisation products

#### General Procedure 8: gold-catalysed cascade (GP8)

Adapted from the method developed within our group.<sup>48,49</sup> The relevant ynamide (1.0 eq.), ylide (1.1–1.5 eq.), AuPicCl<sub>2</sub> (2–5 mol%) and PhMe (0.1 M wrt ynamide) were combined in a flame dried Schlenk tube and the mixture heated to 90 °C. The reaction was monitored for consumption of the ynamide (typically 1–4 h) and then stirred at the stated temperature for the stated time (typically 24 h). After allowing to cool to r.t., the reaction mixture was passed through a 3 cm pad of silica (EtOAc) and concentrated under reduced pressure. Purification by flash column chromatography or recrystallisation gave the corresponding Diels–Alder product.

#### Products derived from alkene tethered *N*-acyl pyridinium ylides (Chapter 2.1.3)

*N*-((3*S*,4*aR*,7*aR*)-6-(Isopropylsulfonyl)-3-(methylthio)-3,4,4*a*,5,6,7-hexahydro-3,7*a*-epoxypyrrolo[3,4-*b*]pyridin-2-yl)-*N*-(4-methoxyphenyl)-4-methylbenzenesulfonamide **91a**

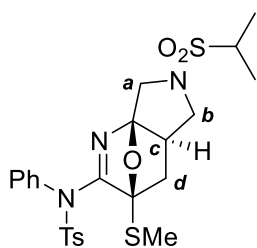


Following **GP8** with ynamide **44b** (104 mg, 0.30 mmol), ylide **43a** (107 mg, 0.36 mmol), AuPicCl<sub>2</sub> (5.6 mg, 5 mol%) and PhMe (4.0 mL) for 20 h at 90 °C. Purification by flash column chromatography (6:4 hexane/EtOAc) gave **91a** as a white powder (165 mg, 97%); mp: 135–

136 °C; IR (neat):  $\nu$  = 2990, 2935, 1597, 1507, 1327, 1168, 1143 cm<sup>-1</sup>; <sup>1</sup>H NMR (400 MHz, CDCl<sub>3</sub>):  $\delta$  = 7.71 (d<sub>AA'XX'</sub>, *J* = 8.3 Hz, 2H), 7.25 (d<sub>AA'XX'</sub>, *J* = 8.3 Hz, 2H), 7.13 (d<sub>AA'XX'</sub>, *J* = 8.9 Hz, 2H), 6.85 (d<sub>AA'XX'</sub>, *J* = 8.9, 2H), 4.22 (d, *J*<sub>AB</sub> = 11.6 Hz, 1H<sub>a</sub>), 3.97 (dd, *J* = 9.5, 8.4 Hz, 1H<sub>b</sub>), 3.86 (d, *J*<sub>AB</sub> = 11.6 Hz, 1H<sub>a</sub>), 3.83 (s, 3H), 3.26 (p, *J* = 6.8 Hz, 1H), 3.02 (app. t, *J* = 9.9 Hz, 1H<sub>b</sub>), 2.58 – 2.47 (m, 1H<sub>c</sub>), 2.43 (s, 3H), 1.83 (s, 3H), 1.76 – 1.71 (m, 2H<sub>d</sub>),

1.38 (d,  $J = 6.8$  Hz, 3H), 1.38 (d,  $J = 6.8$  Hz, 3H) ppm;  $^{13}\text{C}$  NMR (101 MHz,  $\text{CDCl}_3$ ):  $\delta = 166.3$  (C), 160.8 (C), 144.8 (C), 134.5 (C), 131.9 (2CH), 129.9 (2CH), 129.2 (2CH), 127.9 (C), 114.2 (2CH), 107.5 (C), 96.5 (C), 55.7 ( $\text{CH}_3$ ), 53.8 (CH), 53.1 ( $\text{C}_b\text{H}_2$ ), 50.0 ( $\text{C}_a\text{H}_2$ ), 46.5 ( $\text{C}_c\text{H}$ ), 33.8 ( $\text{C}_d\text{H}_2$ ), 21.9 ( $\text{CH}_3$ ), 16.83 ( $\text{CH}_3$ ), 16.80 ( $\text{CH}_3$ ), 12.6 ( $\text{SCH}_3$ ) ppm; HRMS (ES–TOF):  $m/z$ : calcd for  $\text{C}_{25}\text{H}_{32}\text{N}_3\text{O}_6\text{S}_3$ : 566.1448, found 566.1449  $[\text{M}+\text{H}]^+$ .

***N*–((3*S*,4*aR*,7*aR*)–6–(Isopropylsulfonyl)–3–(methylthio)–3,4,4*a*,5,6,7–hexahydro–3,7*a*–epoxypyrrolo[3,4–*b*]pyridin–2–yl)–4–methyl–*N*–phenylbenzenesulfonamide **91b****

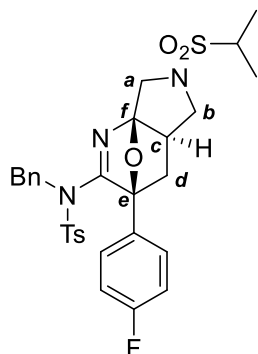


Following **GP8** with ynamide **44a** (397 mg, 1.25 mmol), ylide **43a** (446 mg, 1.50 mmol), AuPicCl<sub>2</sub> (9.7 mg, 2mol%) and PhMe (12.5 mL) for 14 h at 90 °C. Purification by flash column chromatography (linear 0→100 hexane/EtOAc) gave **91b** as a yellow foam (636 mg, 95%); IR

(neat):  $\nu = 2932, 1283, 1361, 1236, 1166, 1141, 1088, 1054\text{ cm}^{-1}$ ;  $^1\text{H}$  NMR (400 MHz,  $\text{CDCl}_3$ ):  $\delta = 7.70$  ( $d_{\text{AA}'\text{XX}'}$ ,  $J = 8.4$ , 2H), 7.46 – 7.41 (m, 1H), 7.39 – 7.34 (m, 2H), 7.28 – 7.20 (m, 4H), 4.24 (d,  $J_{\text{AB}} = 11.6$  Hz, 1H<sub>a</sub>), 3.98 (dd,  $J = 9.5, 8.3$  Hz, 1H<sub>b</sub>), 3.87 (d,  $J_{\text{AB}} = 11.6$  Hz, 1H<sub>a</sub>), 3.26 (p,  $J = 6.8$  Hz, 1H), 3.03 (app. t,  $J = 9.9$  Hz, 1H<sub>b</sub>), 2.55 (dddd,  $J = 10.2, 8.3, 7.1, 3.4$  Hz, 1H<sub>c</sub>), 2.43 (s, 3H), 1.79 (dd,  $J = 12.4, 7.1$  Hz, 1H<sub>d</sub>), 1.78 (s, 3H), 1.73 (dd,  $J = 12.4, 3.4$  Hz, 1H<sub>d</sub>), 1.38 (d,  $J = 6.8$  Hz, 3H), 1.38 (d,  $J = 6.8$  Hz, 3H) ppm;  $^{13}\text{C}$  NMR (101 MHz,  $\text{CDCl}_3$ ):  $\delta = 166.3$  (C), 144.7 (C), 135.5 (C), 134.3 (C), 130.4 (2CH), 129.8 (CH), 129.7 (2CH), 129.1 (2CH), 128.9 (2CH), 107.4 (C), 96.4 (C), 53.7 (CH), 53.0 ( $\text{C}_b\text{H}_2$ ), 49.9 ( $\text{C}_a\text{H}_2$ ), 46.3 ( $\text{C}_c\text{H}$ ), 33.7 ( $\text{C}_d\text{H}_2$ ), 21.7 ( $\text{CH}_3$ ), 16.69 ( $\text{CH}_3$ ), 16.67 ( $\text{CH}_3$ ), 12.4 ( $\text{CSH}_3$ ) ppm; HRMS (ES–TOF):  $m/z$ : calcd for  $\text{C}_{24}\text{H}_{30}\text{N}_3\text{O}_5\text{S}_3$ : 536.1342, found 536.1351  $[\text{M}+\text{H}]^+$ .



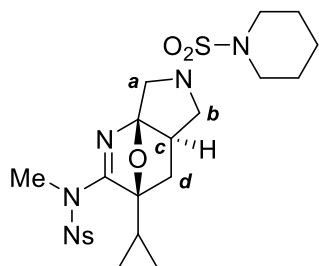
***N*-Benzyl-*N*-((3*S*,4*aR*,7*aR*)-3-(4-fluorophenyl)-6-(isopropylsulfonyl)-3,4,4*a*,5,6,7-hexahydro-3,7*a*-epoxypyrrolo[3,4-*b*]pyridin-2-yl)-4-methylbenzenesulfonamide **91d****



Following **GP8** with ynamide **44i** (152 mg, 0.40 mmol), ylide **43a** (143 mg, 0.48 mmol), AuPicCl<sub>2</sub> (7.8 mg, 5 mol%) and PhMe (4.0 mL) for 20 h at 90 °C. Purification by flash column chromatography (7:3→6:4 hexane/EtOAc) gave **91d** as a white powder (153 mg, 64%); mp: 153–155 °C; IR (neat):  $\nu$  = 2944, 1582, 1514, 1353, 1326, 1228,

1164, 1107, 1090 cm<sup>-1</sup>; <sup>1</sup>H NMR (400 MHz, CDCl<sub>3</sub>):  $\delta$  = 7.46 (d<sub>AA'XX'</sub>,  $J$  = 8.4 Hz, 2H), 7.24 – 7.13 (m, 7H), 6.99 (app. t,  $J$  = 8.7 Hz, 2H), 6.91 (d<sub>AA'XX'</sub>,  $J$  = 7.9 Hz, 2H), 4.56 (d,  $J_{AB}$  = 15.3 Hz, 1H), 4.31 (d,  $J_{AB}$  = 15.3 Hz, 1H), 4.24 (d,  $J_{AB}$  = 11.6 Hz, 1H<sub>a</sub>), 3.99 (dd,  $J$  = 9.5, 8.4 Hz, 1H<sub>b</sub>), 3.83 (d,  $J$  = 11.6 Hz, 1H<sub>a</sub>), 3.22 (p,  $J$  = 6.8 Hz, 1H), 3.01 (app. t,  $J$  = 9.8 Hz, 1H<sub>b</sub>), 2.49 – 2.40 (m, 1H<sub>c</sub>), 2.42 (s, 3H), 2.20 (dd,  $J$  = 12.1, 7.5 Hz, 1H<sub>d</sub>), 1.84 (dd,  $J$  = 12.1, 3.3 Hz, 1H<sub>d</sub>), 1.34 (d,  $J$  = 6.8 Hz, 6H) ppm; <sup>13</sup>C NMR (101 MHz, CDCl<sub>3</sub>):  $\delta$  = 170.2 (C), 163.1 (d,  $J$  = 248.6 Hz, CF), 144.8 (C), 135.3 (C), 135.2 (C), 130.8 (d,  $J$  = 3.2 Hz, C), 129.7 (CH), 129.6 (2CH), 128.43 (2CH), 128.41 (2CH), 128.3 (2CH), 128.0 (2CH), 115.4 (d,  $J$  = 21.6 Hz, 2CH), 107.9 (C<sub>f</sub>), 94.0 (C<sub>e</sub>), 53.7 (CH), 53.6 (C<sub>b</sub>H<sub>2</sub>), 51.9 (CH<sub>2</sub>), 50.1 (C<sub>a</sub>H<sub>2</sub>), 45.7 (C<sub>c</sub>H), 33.1 (C<sub>d</sub>H<sub>2</sub>), 21.8 (CH<sub>3</sub>), 16.8 (CH<sub>3</sub>), 16.7 (CH<sub>3</sub>) ppm; HRMS (ES–TOF):  $m/z$ : calcd for C<sub>30</sub>H<sub>33</sub>N<sub>3</sub>O<sub>5</sub>FS<sub>2</sub>: 598.1840, found 598.1848 [M+H]<sup>+</sup>.

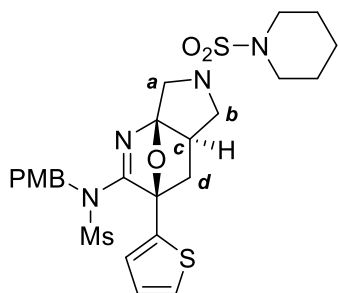
***N*-((3*S*,4*aR*,7*aR*)-3-Cyclopropyl-6-(piperidin-1-ylsulfonyl)-3,4,4*a*,5,6,7-hexahydro-3,7*a*-epoxypyrrolo[3,4-*b*]pyridin-2-yl)-*N*-methyl-4-nitrobenzenesulfonamide **91c****



Following **GP8** with ynamide **44d** (112 mg, 0.40 mmol), ylide **43b** (162 mg, 0.48 mmol), AuPicCl<sub>2</sub> (7.8 mg, 5 mol%) and PhMe (4.0 mL) for 24 h at 90 °C. Purification by flash column chromatography (65:35 hexane/EtOAc) gave **91c** as a yellow

powder (210 mg, 97%); IR (neat):  $\nu$  = 2943, 2855, 1589, 1531, 1349, 1162, 1084, 1053  $\text{cm}^{-1}$ ;  $^1\text{H}$  NMR (400 MHz,  $\text{CDCl}_3$ ):  $\delta$  = 8.39 (d<sub>AA'XX'</sub>,  $J$  = 9.1 Hz, 2H), 8.21 (d<sub>AA'XX'</sub>,  $J$  = 9.1 Hz, 2H), 3.94 (d,  $J_{AB}$  = 11.7 Hz, 1H<sub>a</sub>), 3.80 (dd,  $J$  = 9.4, 8.2 Hz, 1H<sub>b</sub>), 3.69 (d,  $J_{AB}$  = 11.7 Hz, 1H<sub>a</sub>), 3.36 (s, 3H), 3.23 – 3.19 (m, 4H), 2.93 (dd,  $J$  = 10.2, 9.5 Hz, 1H<sub>b</sub>), 2.44 – 2.35 (m, 1H<sub>c</sub>), 1.76 (dd,  $J$  = 12.3, 7.6 Hz, 1H<sub>d</sub>), 1.66 – 1.59 (m, 4H), 1.58 – 1.47 (m, 4H), 0.79 – 0.71 (m, 1H), 0.66 – 0.60 (m, 3H) ppm;  $^{13}\text{C}$  NMR (101 MHz,  $\text{CDCl}_3$ ):  $\delta$  = 169.9 (C), 150.7 (C), 143.6 (C), 130.1 (2CH), 124.3 (2CH), 106.9 (C), 93.6 (C), 53.4 (C<sub>b</sub>H<sub>2</sub>), 50.0 (C<sub>a</sub>H<sub>2</sub>), 47.1 (2CH<sub>2</sub>), 45.1 (C<sub>c</sub>H), 35.7 (CH<sub>3</sub>), 32.1 (C<sub>d</sub>H<sub>2</sub>), 25.6 (2CH<sub>2</sub>), 23.9 (CH<sub>2</sub>), 11.1 (CH), 3.58 (CH<sub>2</sub>), 3.56 (CH<sub>2</sub>) ppm; HRMS (ES–TOF):  $m/z$ : calcd for C<sub>22</sub>H<sub>30</sub>N<sub>5</sub>O<sub>7</sub>S<sub>2</sub>: 540.1581, found 540.1589 [M+H]<sup>+</sup>.

***N*–(4–Methoxybenzyl)–N–((3*R*,4*aR*,7*aR*)–6–(piperidin–1–ylsulfonyl)–3–(thiophen–2–yl)–3,4,4*a*,5,6,7–hexahydro–3,7*a*–epoxypyrrolo[3,4–*b*]pyridin–2–yl)methanesulfonamide **91e****

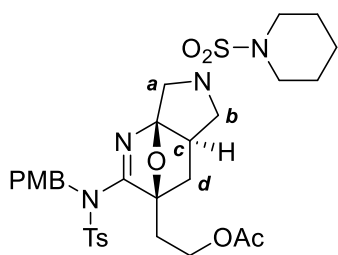


Following **GP8** with ynamide **44m** (129 mg, 0.40 mmol), ylide **43b** (162 mg, 0.48 mmol), AuPicCl<sub>2</sub> (7.8 mg, 5 mol%) and PhMe (4.0 mL) for 24 h at 90 °C. Purification by flash column chromatography (65:35 hexane/EtOAc) gave **91e** as a pale yellow foam (138 mg, 60%); IR (neat):  $\nu$  = 2941, 2854, 1607, 1580, 1513,

1443, 1346, 1246, 1157, 1148, 1052, 1030  $\text{cm}^{-1}$ ;  $^1\text{H}$  NMR (400 MHz,  $\text{CDCl}_3$ ):  $\delta$  = 7.38 (dd,  $J$  = 5.1, 1.2 Hz, 1H), 7.21 (dd,  $J$  = 3.6, 1.2 Hz, 1H), 7.16 (d<sub>AA'XX'</sub>,  $J$  = 8.7 Hz, 2H), 7.06 (dd,  $J$  = 5.1, 3.6 Hz, 1H), 6.86 (d<sub>AA'XX'</sub>,  $J$  = 8.7 Hz, 2H), 4.69 (d,  $J_{AB}$  = 15.4 Hz, 1H), 4.10 (d,  $J_{AB}$  = 15.4 Hz, 1H), 4.09 (d,  $J_{AB}$  = 11.7 Hz, 1H<sub>a</sub>), 3.94 (d,  $J_{AB}$  = 11.7 Hz, 1H<sub>a</sub>), 3.86 (dd,  $J$  = 9.5, 8.3 Hz, 1H<sub>b</sub>), 3.79 (s, 3H), 3.24 – 3.20 (m, 4H), 3.07 (app. t,  $J$  = 9.9, 1H<sub>b</sub>), 2.66 – 2.57 (m, 1H<sub>c</sub>), 2.48 (s, 3H), 2.38 (dd,  $J$  = 12.0, 7.6 Hz, 1H<sub>d</sub>), 1.97 (dd,  $J$  = 12.0, 3.2 Hz, 1H<sub>d</sub>), 1.68 – 1.58 (m, 4H), 1.57 – 1.50 (m, 2H) ppm;  $^{13}\text{C}$  NMR (101 MHz,  $\text{CDCl}_3$ ):  $\delta$  = 169.3 (C), 159.7 (C), 137.3 (C), 130.1 (2CH), 127.9 (CH), 127.6 (CH), 127.5 (CH), 127.1 (C), 114.3 (2CH), 108.2 (C), 91.1

(C), 55.4 (CH<sub>3</sub>), 53.3 (C<sub>b</sub>H<sub>2</sub>), 51.2 (C<sub>a</sub>H<sub>2</sub>), 50.0 (C<sub>a</sub>H<sub>2</sub>), 47.2 (2CH<sub>2</sub>), 46.0 (C<sub>c</sub>H), 42.7 (CH<sub>3</sub>), 34.6 (C<sub>d</sub>H<sub>2</sub>), 25.6 (2CH<sub>2</sub>), 23.9 (CH<sub>2</sub>) ppm; HRMS (ES–TOF): m/z: calcd for C<sub>25</sub>H<sub>32</sub>N<sub>4</sub>O<sub>6</sub>S<sub>3</sub>Na: 603.1376, found 603.1381 [M+Na]<sup>+</sup>.

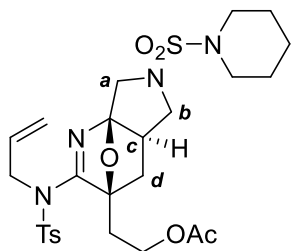
**2-((3*S*,4*aR*,7*aR*)-2-((*N*-(4-Methoxybenzyl)-4-methylphenyl)sulfonamido)-6-(piperidin-1-ylsulfonyl)-4*a*,5,6,7-tetrahydro-3,7*a*-epoxypyrrolo[3,4-*b*]pyridin-3(4*H*)-yl)ethyl acetate **9If****



Following **GP8** with ynamide **44n** (120 mg, 0.30 mmol), ylide **43b** (122 mg, 0.36 mmol), AuPicCl<sub>2</sub> (5.8 mg, 5 mol%) and PhMe (3.0 mL) for 24 h at 90 °C. Purification by flash column chromatography gave **9If** as a white foam (114 mg, 57%); IR

(neat):  $\nu$  = 2940, 2362, 2335, 1739, 1583, 1514, 1360, 1245, 1165, 1044 cm<sup>-1</sup>; <sup>1</sup>H NMR (400 MHz, CDCl<sub>3</sub>):  $\delta$  = 7.63 (d<sub>AA'XX'</sub>,  $J$  = 8.4 Hz, 2H), 7.36 (d<sub>AA'XX'</sub>,  $J$  = 8.4 Hz, 2H), 7.17 (d<sub>AA'XX'</sub>,  $J$  = 8.7 Hz, 2H), 6.80 (d<sub>AA'XX'</sub>,  $J$  = 8.7 Hz, 2H), 4.43 (d,  $J_{AB}$  = 13.4 Hz, 1H), 4.35 (d,  $J_{AB}$  = 13.4 Hz, 1H), 4.15 – 4.05 (m, 2H), 3.98 (d,  $J_{AB}$  = 11.6 Hz, 1H<sub>a</sub>), 3.80 (dd,  $J$  = 9.5, 8.3 Hz, 1H<sub>b</sub>), 3.78 (s, 3H), 3.65 (d,  $J_{AB}$  = 11.6 Hz, 1H<sub>a</sub>), 3.22 – 3.15 (m, 4H), 2.90 (app. t,  $J$  = 9.9 Hz, 1H<sub>b</sub>), 2.53 – 2.47 (m, 2H), 2.46 (s, 3H), 2.23 – 2.13 (m, 1H<sub>c</sub>), 2.01 (s, 3H), 1.69 – 1.51 (m, 6H+2H<sub>d</sub>) ppm; <sup>13</sup>C NMR (101 MHz, CDCl<sub>3</sub>):  $\delta$  = 172.3 (C), 170.9 (C), 159.7 (C), 145.1 (C), 134.4 (C), 130.7 (2CH), 130.2 (2CH), 128.0 (2CH), 126.8 (C), 114.0 (2CH), 107.4 (C), 92.6 (C), 60.2 (CH<sub>2</sub>), 55.4 (CH<sub>3</sub>), 53.8 (C<sub>b</sub>H<sub>2</sub>), 52.9 (CH<sub>2</sub>), 50.3 (C<sub>a</sub>H<sub>2</sub>), 47.2 (2CH<sub>2</sub>), 44.7 (C<sub>c</sub>H), 32.4 (C<sub>d</sub>H<sub>2</sub>), 29.0 (CH<sub>2</sub>), 25.6 (2CH<sub>2</sub>), 23.9 (CH<sub>2</sub>), 21.8 (CH<sub>3</sub>), 21.1 (CH<sub>3</sub>) ppm; HRMS (ES–TOF): m/z: calcd for C<sub>31</sub>H<sub>40</sub>N<sub>4</sub>O<sub>8</sub>S<sub>2</sub>Na: 683.2180, found 683.2191 [M+Na]<sup>+</sup>.

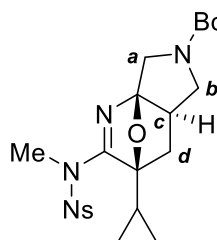
**2-((3*S*,4*aR*,7*aR*)-2-((*N*-Allyl-4-methylphenyl)sulfonamido)-6-(piperidin-1-ylsulfonyl)-4*a*,5,6,7-tetrahydro-3,7*a*-epoxypyrrolo[3,4-*b*]pyridin-3(4*H*)-yl)ethyl acetate **91g****



Following **GP8** with ynamide **44e** (129 mg, 0.40 mmol), ylide **43b** (162 mg, 0.48 mmol), AuPicCl<sub>2</sub> (3.11 mg, 2 mol%) and PhMe (4.0 mL) for 24 h at 90 °C. Purification by flash column chromatography (7:3→6:4 hexane/EtOAc) gave **91g** as a white foam

(162 mg, 70%); IR (neat):  $\nu$  = 2942, 2360, 2335, 1739, 1645, 1580, 1361, 1250, 1168 cm<sup>-1</sup>; <sup>1</sup>H NMR (400 MHz, CDCl<sub>3</sub>):  $\delta$  = 7.54 (d<sub>AA'XX'</sub>,  $J$  = 8.4 Hz, 2H), 7.27 (d<sub>AA'XX'</sub>,  $J$  = 8.4 Hz, 2H), 5.65 (dddd,  $J$  = 17.5, 9.8, 6.6, 5.9 Hz, 1H), 5.12 – 5.05 (m, 2H), 4.25 – 4.15 (m, 2H), 4.00 – 3.85 (m, 2H), 3.90 (d,  $J_{AB}$  = 11.7 Hz, 1H<sub>a</sub>), 3.79 (dd,  $J$  = 9.6, 8.3 Hz, 1H<sub>b</sub>), 3.63 (d,  $J_{AB}$  = 11.7 Hz, 1H<sub>a</sub>), 3.17 – 3.08 (m, 4H), 2.92 (app. t,  $J$  = 9.8 Hz, 1H<sub>b</sub>), 2.61 (ddd,  $J$  = 14.8, 7.5, 6.6 Hz, 1H), 2.49 (ddd,  $J$  = 14.8, 7.5, 6.6 Hz, 1H), 2.38 (s, 3H), 2.33 – 2.25 (m, 1H<sub>c</sub>), 2.05 (dd,  $J$  = 12.6, 7.6, 1H<sub>d</sub>), 1.99 (s, 3H), 1.66 (dd,  $J$  = 12.6, 3.5, 1H<sub>d</sub>), 1.60 – 1.52 (m, 4H), 1.52 – 1.42 (m, 2H) ppm; <sup>13</sup>C NMR (101 MHz, CDCl<sub>3</sub>):  $\delta$  = 171.8 (C), 170.9 (C), 145.1 (C), 134.4 (C), 131.3 (CH), 130.1 (2CH), 127.8 (2CH), 120.1 (CH<sub>2</sub>), 107.3 (C), 92.6 (C), 60.2 (CH<sub>2</sub>), 53.8 (C<sub>b</sub>H<sub>2</sub>), 51.9 (CH<sub>2</sub>), 50.2 (C<sub>a</sub>H<sub>2</sub>), 47.1 (2CH<sub>2</sub>), 44.7 (C<sub>c</sub>H), 32.8 (C<sub>d</sub>H<sub>2</sub>), 29.2 (CH<sub>2</sub>), 25.5 (2CH<sub>2</sub>), 23.8 (CH<sub>2</sub>), 21.7 (CH<sub>3</sub>), 21.1 (CH<sub>3</sub>) ppm; HRMS (ES-TOF):  $m/z$ : calcd for C<sub>26</sub>H<sub>36</sub>N<sub>4</sub>O<sub>7</sub>S<sub>2</sub>Na: 603.1923, found 603.1931 [M+Na]<sup>+</sup>.

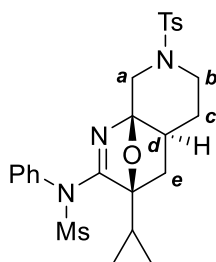
***tert*-Butyl (3*S*,4*aR*,7*aR*)-3-cyclopropyl-2-((*N*-methyl-4-nitrophenyl)sulfonamido)-3,4,4*a*,5-tetrahydro-3,7*a*-epoxypyrrolo[3,4-*b*]pyridine-6(7*H*)-carboxylate **91h****



Following **GP8** with ynamide **44d** (196 mg, 0.70 mmol), ylide **43c** (245 mg, 0.84 mmol), AuPicCl<sub>2</sub> (13.6 mg, 5 mol%) and PhMe (7.0 mL) for 24 h at 90 °C. Purification by flash column chromatography (0→100 hexane/EtOAc) gave **91h** as a pale yellow foam (286 mg, 83%); IR (neat):

$\nu = 2954, 1701, 1592, 1528, 1398, 1364, 1179, 1166, 1101 \text{ cm}^{-1}$ ; NMR spectra display a mixture of rotamers;  $^1\text{H}$  NMR (400 MHz,  $\text{CDCl}_3$ ):  $\delta = 8.38$  ( $d_{\text{AA'XX'}}$ ,  $J = 8.9 \text{ Hz}$ , 2H),  $8.21$  ( $d_{\text{AA'XX'}}$ ,  $J = 8.9 \text{ Hz}$ , 2H),  $3.96$  and  $3.91$  ( $d$ ,  $J_{\text{AB}} = 12.7 \text{ Hz}$ ,  $1\text{H}_a$ ),  $3.94$  and  $3.95$  ( $dd$ ,  $J = 10.4, 8.9 \text{ Hz}$ ,  $1\text{H}_b$ ),  $3.75$  and  $3.72$  ( $d$ ,  $J_{\text{AB}} = 12.7 \text{ Hz}$ ,  $1\text{H}_a$ ),  $3.38$  and  $3.37$  ( $s$ , 3H),  $2.90$  (app. t,  $J = 10.3 \text{ Hz}$ ,  $1\text{H}_b$ ),  $2.38 - 2.26$  (m,  $1\text{H}_c$ ),  $1.71$  ( $dd$ ,  $J = 12.3, 7.6 \text{ Hz}$ ,  $1\text{H}_d$ ),  $1.46$  (m,  $10\text{H}+1\text{H}_d$ ),  $0.78 - 0.70$  (m,  $1\text{H}$ ),  $0.67 - 0.58$  (m, 3H) ppm; only the major peaks are reported:  $^{13}\text{C}$  NMR (101 MHz,  $\text{CDCl}_3$ ):  $\delta = 169.6$  (C),  $154.2$  (C),  $150.6$  (C),  $143.8$  (C),  $130.1$  (2CH),  $124.2$  (2CH),  $107.0$  (C),  $93.5$  (C),  $79.9$  (C),  $50.6$  ( $\text{C}_b\text{H}_2$ ),  $48.3$  ( $\text{CH}_2$ ),  $43.8$  ( $\text{C}_c\text{H}$ ),  $35.7$  ( $\text{CH}_3$ ),  $32.0$  ( $\text{C}_d\text{H}_2$ ),  $28.6$  ( $3\text{CH}_3$ ),  $11.2$  (CH),  $3.5$  ( $2\text{CH}_2$ ) ppm; HRMS (ES-TOF):  $m/z$ : calcd for  $\text{C}_{22}\text{H}_{29}\text{N}_4\text{O}_7\text{S}$ : 493.1751, found 493.1765  $[\text{M}+\text{H}]^+$ .

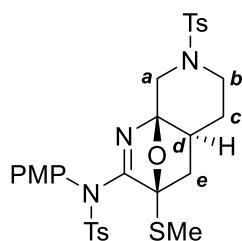
***N-((3S,4aS,8aR)-3-Cyclopropyl-7-tosyl-4,4a,5,6,7,8-hexahydro-3H-3,8a-epoxy-1,7-naphthyridin-2-yl)-N-phenylmethanesulfonamide 93a***



Following **GP8** with ynamide **44c** (177 mg, 0.75 mmol), ylide **92a** (324 mg, 0.90 mmol),  $\text{AuPicCl}_2$  (14.6 mg, 5 mol%) and PhMe (7.5 mL) for 24 h at  $90^\circ\text{C}$ . Purification by flash column chromatography ( $0 \rightarrow 30_{\text{hold}} \rightarrow 100$  hexane/EtOAc) gave **93a** as a fluffy white powder (348 mg, 90%); mp:  $202 - 203^\circ\text{C}$ ; IR (neat):  $\nu = 2948, 1589, 1357, 1161, 1124, 1103 \text{ cm}^{-1}$ ;  $^1\text{H}$  NMR (400 MHz,  $\text{CDCl}_3$ ):  $\delta = 7.69$  ( $d_{\text{AA'XX'}}$ ,  $J = 8.3 \text{ Hz}$ , 2H),  $7.46 - 7.34$  (m, 5H),  $7.33$  ( $d_{\text{AA'XX'}}$ ,  $J = 8.3 \text{ Hz}$ , 2H),  $4.36$  ( $dd$ ,  $J = 13.2, 1.7 \text{ Hz}$ ,  $1\text{H}_a$ ),  $3.83 - 3.77$  (m,  $1\text{H}_b$ ),  $3.28$  (s, 3H),  $3.24$  ( $d$ ,  $J_{\text{AB}} = 13.2 \text{ Hz}$ ,  $1\text{H}_a$ ),  $2.45$  (s, 3H),  $2.39$  (app. td,  $J = 12.5, 2.1 \text{ Hz}$ ,  $1\text{H}_b$ ),  $1.95 - 1.87$  (m,  $1\text{H}$ ),  $1.83 - 1.74$  (m,  $1\text{H}$ ),  $1.66$  ( $dd$ ,  $J = 11.9, 7.6 \text{ Hz}$ ,  $1\text{H}_c$ ),  $1.43$  (app. qd,  $J = 12.9, 3.8 \text{ Hz}$ ,  $1\text{H}$ ),  $0.98$  ( $dd$ ,  $J = 11.9, 2.7 \text{ Hz}$ ,  $1\text{H}_c$ ),  $0.38$  (tt,  $J = 8.3, 5.3 \text{ Hz}$ ,  $1\text{H}$ ),  $0.32 - 0.21$  (m,  $1\text{H}$ ),  $0.21 - 0.15$  (m,  $1\text{H}$ ),  $0.14 - 0.07$  (m,  $1\text{H}$ ),  $-0.10 - -0.19$  (m,  $1\text{H}$ ) ppm;  $^{13}\text{C}$  NMR (101 MHz,  $\text{CDCl}_3$ ):  $\delta = 169.3$  (C),  $143.8$  (C),  $136.4$  (C),  $133.6$  (C),  $129.8$  (2CH),  $129.6$  (CH),  $129.5$  (2CH),  $129.3$  (2CH),  $127.9$  (2CH),

97.4 (C), 91.8 (C), 48.4 (C<sub>a</sub>H<sub>2</sub>), 45.5 (C<sub>b</sub>H<sub>2</sub>), 39.8 (CH<sub>3</sub>), 37.8 (C<sub>d</sub>H), 33.8 (C<sub>e</sub>H<sub>2</sub>), 30.3 (C<sub>c</sub>H<sub>2</sub>), 21.7 (CH<sub>3</sub>), 10.8 (CH), 3.2 (CH<sub>2</sub>), 3.0 (CH<sub>2</sub>) ppm; HRMS (ES-TOF): m/z: calcd for C<sub>25</sub>H<sub>29</sub>N<sub>3</sub>O<sub>5</sub>S<sub>2</sub>Na: 538.1441, found 538.1450 [M+Na]<sup>+</sup>.

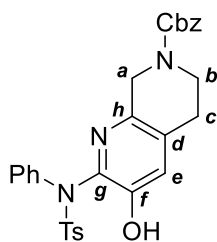
***N*-(4-Methoxyphenyl)-4-methyl-N-((3*S*,4*aS*,8*aR*)-3-(methylthio)-7-tosyl-4,4*a*,5,6,7,8-hexahydro-3*H*-3,8*a*-epoxy-1,7-naphthyridin-2-yl)benzenesulfonamide **93b****



Following **GP8** with ynamide **44b** (86.8 mg, 0.25 mmol), ylide **92a** (108 mg, 0.30 mmol), AuPicCl<sub>2</sub> (4.86 mg, 5 mol%) and PhMe (2.5 mL) for 20 h at 90 °C. Purification by flash column chromatography (6:4 hexane/EtOAc) gave **93b** as a yellow foam (128 mg, 81%); IR (neat): ν =

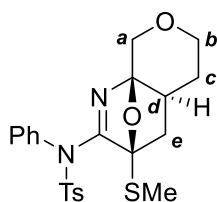
2916, 2849, 1450, 1328, 1174 cm<sup>-1</sup>; <sup>1</sup>H NMR (400 MHz, CDCl<sub>3</sub>): δ = 7.70 (d<sub>AA'XX'</sub>, *J* = 8.3 Hz, 2H), 7.67 (d<sub>AA'XX'</sub>, *J* = 8.4 Hz, 2H), 7.34 (d<sub>AA'XX'</sub>, *J* = 8.3 Hz, 2H), 7.22 (d<sub>AA'XX'</sub>, *J* = 8.4 Hz, 2H), 7.09 (d<sub>AA'XX'</sub>, *J* = 8.9 Hz, 2H), 6.81 (d<sub>AA'XX'</sub>, *J* = 8.9 Hz, 2H), 4.36 (dd, *J* = 13.3, 1.7 Hz, 1H<sub>a</sub>), 3.84 – 3.78 (m, 1H<sub>b</sub>), 3.81 (s, 3H), 3.24 (d, *J*<sub>AB</sub> = 13.3 Hz, 1H<sub>a</sub>), 2.48 – 2.41 (m, 1H<sub>b</sub>) 2.45 (s, 3H), 2.41 (s, 3H), 1.99 – 1.92 (m, 1H), 1.90 – 1.81 (m, 1H<sub>d</sub>+1H), 1.70 (s, 3H), 1.56 – 1.45 (m, 1H) 1.46 – 1.38 (m, 1H) ppm; <sup>13</sup>C NMR (101 MHz, CDCl<sub>3</sub>): δ = 166.2 (C), 160.6 (C), 144.6 (C), 143.7 (C), 134.4 (C), 133.8 (C), 131.9 (2CH), 129.8 (2CH), 129.7 (2CH), 129.1 (2CH), 127.9 (2CH), 127.8 (C), 114.0 (2CH), 97.3 (C), 94.6 (C), 55.6 (CH<sub>3</sub>), 48.2 (C<sub>a</sub>H<sub>2</sub>), 45.2 (C<sub>b</sub>H<sub>2</sub>), 38.9 (C<sub>d</sub>H), 36.3 (C<sub>e</sub>H<sub>2</sub>), 30.2 (C<sub>c</sub>H<sub>2</sub>), 21.8 (CH<sub>3</sub>), 21.7 (CH<sub>3</sub>), 12.4 (SCH<sub>3</sub>) ppm; HRMS (ES-TOF): m/z: calcd for C<sub>30</sub>H<sub>34</sub>N<sub>3</sub>O<sub>6</sub>S<sub>3</sub>: 628.1604, found 628.1624 [M+H]<sup>+</sup>.

***Benzyl 3-hydroxy-2-((4-methyl-N-phenylphenyl)sulfonamido)-5,8-dihydro-1,7-naphthyridine-7(6H)-carboxylate 94***



Following **GP8** with ynamide **44a** (76.2 mg, 0.24 mmol), ylide **92b** (89.6 mg, 0.26 mmol), AuPicCl<sub>2</sub> (4.7 mg, 5 mol%) and PhMe (2.4 mL) for 24 h at 90 °C and 24 h at 110 °C. Purification by flash column chromatography (7:3 hexane/EtOAc) and hot recrystallisation (EtOH) gave hydroxypyridine **94** as a white powder (100 mg, 79%); mp: 154–155 °C; IR (neat):  $\nu$  = 3406 (br.), 2930, 1687, 1620, 1604, 1521, 1458, 1429, 1351, 1227, 1217, 1068 cm<sup>-1</sup>; *NMR spectra display a mixture of rotamers*: <sup>1</sup>H NMR (400 MHz, CDCl<sub>3</sub>):  $\delta$  = 7.75 (d,  $J$  = 7.9 Hz, 2H), 7.45 – 7.18 (m, 12H), 6.95 (tt,  $J$  = 7.4, 1.3 Hz, 1H), 6.37 and 6.29 (br. s, OH), 5.19 (s, 2H), 4.59 (br. app. s, 2H<sub>a</sub>), 3.73 (t,  $J$  = 5.8 Hz, 2H<sub>b</sub>), 2.73 (t,  $J$  = 5.8 Hz, 2H<sub>c</sub>), 2.33 (s, 3H) ppm; <sup>13</sup>C NMR (101 MHz, CDCl<sub>3</sub>):  $\delta$  = 155.5 and 155.4 (C), 149.0 (C<sub>h</sub>), 146.6 (C), 139.6 (C), 136.7 (C), 132.3 (C), 131.3 (C), 131.0 (C<sub>e</sub>H), 130.3 (4CH), 128.8 (2CH), 128.7 (CH), 128.3 (4CH), 122.2 (CH), 120.6 and 120.4 (C<sub>d</sub>), 118.5 (2CH), 67.5 (CH<sub>2</sub>), 48.3 (C<sub>a</sub>H<sub>2</sub>), 41.1 and 41.0 (C<sub>b</sub>H<sub>2</sub>), 27.4 and 27.2 (C<sub>c</sub>H<sub>2</sub>), 21.8 (CH<sub>3</sub>) ppm; *one quaternary carbon not observed in <sup>13</sup>C NMR spectra*; HRMS (ES–TOF):  $m/z$ : calcd for C<sub>29</sub>H<sub>28</sub>N<sub>3</sub>O<sub>5</sub>S: 530.1744, found 530.1750 [M+H]<sup>+</sup>.

***4-Methyl-N-((3S,4aS,8aR)-3-(methylthio)-4,4a,5,6-tetrahydro-3H,8H-3,8a-epoxypyran[3,4-b]pyridin-2-yl)-N-phenylbenzenesulfonamide 97***

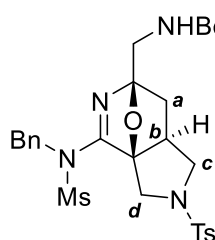


Following **GP8** with ynamide **44a** (159 mg, 0.50 mmol), ylide **92c** (124 mg, 0.60 mmol), AuPicCl<sub>2</sub> (3.9 mg, 2 mol%) and PhMe (5.0 mL) for 24 h at 90 °C and 24 h at 110 °C. Purification by flash column chromatography (0→100 hexane/EtOAc) gave **97** as a white powder (198 mg, 89%); mp: 181–183 °C; IR (neat):  $\nu$  = 2952, 2849, 1594, 1589, 1362, 1168, 1091, 885 cm<sup>-1</sup>; <sup>1</sup>H NMR (400 MHz, CDCl<sub>3</sub>):  $\delta$  = 7.70 (d<sub>AA'XX'</sub>,  $J$  = 8.3 Hz, 2H), 7.44 – 7.38 (m, 1H), 7.36 – 7.31 (m, 2H), 7.25 – 7.21 (m, 4H),

4.38 (d,  $J_{AB} = 13.1$  Hz, 1H<sub>a</sub>), 4.18 (d,  $J_{AB} = 13.1$  Hz, 1H<sub>a</sub>), 3.97 (ddd,  $J = 11.8, 4.3, 1.8$  Hz, 1H<sub>b</sub>), 3.49 (ddd,  $J = 13.4, 11.8, 1.8$  Hz, 1H<sub>b</sub>), 2.42 (s, 3H), 2.16 – 2.07 (m, 1H<sub>d</sub>), 1.95 (dd,  $J = 12.0, 7.5$  Hz, 1H<sub>e</sub>), 1.96 – 1.87 (m, 1H<sub>c</sub>), 1.72 (s, 3H), 1.68 – 1.57 (m, 1H<sub>c</sub>), 1.51 (dd,  $J = 12.0, 2.9, 1H_e$ ) ppm;  $^{13}\text{C}$  NMR (101 MHz, CDCl<sub>3</sub>):  $\delta = 166.2$  (C), 144.6 (C), 135.9 (C), 134.7 (C), 130.7 (2CH), 129.9 (2CH), 129.7 (CH), 129.1 (2CH), 128.9 (2CH), 97.2 (C), 94.7 (C), 68.6 (C<sub>a</sub>H<sub>2</sub>), 67.0 (C<sub>b</sub>H<sub>2</sub>), 38.5 (C<sub>d</sub>H), 36.5 (C<sub>e</sub>H<sub>2</sub>), 31.6 (C<sub>c</sub>H<sub>2</sub>), 21.8 (CH<sub>3</sub>), 12.4 (SCH<sub>3</sub>) ppm; HRMS (ES-TOF):  $m/z$ : calcd for C<sub>22</sub>H<sub>25</sub>N<sub>2</sub>O<sub>4</sub>S<sub>2</sub>: 445.1250, found 445.1258 [M+H]<sup>+</sup>.

### Products derived from enynamides (Chapter 2.1.4)

***tert*-Butyl (((3*a*S,6*R*,7*a*S)-4-(*N*-benzylmethylsulfonamido)-2-tosyl-2,3,7,7*a*-tetrahydro-3*a*,6-epoxypyrrolo[3,4-*c*]pyridin-6(1*H*)-yl)methyl)carbamate 50*a***

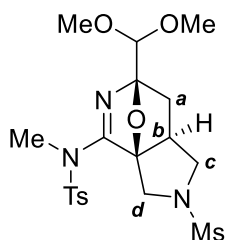


Following **GP8** with ynamide **48d** (173 mg, 0.40 mmol), ylide **47j** (131 mg, 0.52 mmol), AuPicCl<sub>2</sub> (7.8 mg, 5 mol%) and PhMe (4.0 mL) for 24 h at 90 °C. Purification by flash column chromatography (1:1 hexane/EtOAc) gave **50a** as a white foam (195 mg, 81%); IR (neat):  $\nu = 2984, 2934, 1712, 1595, 1511, 1349, 1161$  cm<sup>-1</sup>; NMR spectra display a mixture of rotamers:  $^1\text{H}$  NMR (400 MHz, CDCl<sub>3</sub>):  $\delta = 7.77$  and  $7.68$  (d<sub>AA'XX'</sub>,  $J = 8.3$  Hz, 2H),  $7.35$  (d<sub>AA'XX'</sub>,  $J = 8.3$  Hz, 2H),  $7.32 - 7.27$  (m, 3H),  $7.23 - 7.16$  (m, 2H),  $5.07$  and  $4.79$  (d,  $J_{AB} = 13.4$  Hz, 1H),  $4.86$  and  $4.58$  (d,  $J_{AB} = 13.4$  Hz, 1H),  $4.55$  (br. t,  $J = 5.8$  Hz, NH),  $4.04$  (d,  $J_{AB} = 13.3$  Hz, 1H<sub>d</sub>),  $3.73 - 3.57$  (m, 2H+1H<sub>b</sub>+1H<sub>c</sub>+1H<sub>d</sub>),  $2.99$  and  $2.97$  (s, 3H),  $2.65$  (app. t,  $J = 9.8$  Hz, 1H<sub>c</sub>),  $2.46$  and  $2.44$  (s, 3H),  $1.44$  (s, 9H),  $1.37$  (dd,  $J = 11.9, 2.7$  Hz, 1H<sub>a</sub>),  $1.01$  (dd,  $J = 11.9, 7.5$  Hz, 1H<sub>a</sub>) ppm;  $^{13}\text{C}$  NMR (101 MHz, CDCl<sub>3</sub>):  $\delta = 167.3$  (C), 143.8 (C), 134.6 (C), 134.0 (C), 129.9 (2CH), 129.5 (2CH), 128.9 (CH), 128.8 (2CH), 127.7 (2CH), 103.9 (C), 96.6 (C), 80.0 (C), 53.1 (CH<sub>2</sub>), 52.2 (CH<sub>2</sub>), 47.9 (CH<sub>2</sub>), 42.1 (CH<sub>2</sub>), 41.9 (CH), 39.2 (CH<sub>3</sub>), 33.9 (C<sub>a</sub>H<sub>2</sub>), 28.5 (3CH<sub>3</sub>), 21.7



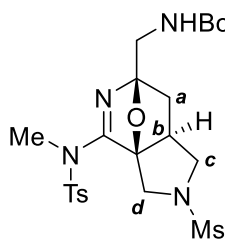
(CH<sub>3</sub>) ppm; one quaternary carbon resonance not observed in <sup>13</sup>C NMR spectra; HRMS (ES-TOF): m/z: calcd for C<sub>28</sub>H<sub>36</sub>N<sub>4</sub>O<sub>7</sub>S<sub>2</sub>Na: 627.1918, found 627.1928 [M+Na]<sup>+</sup>.

***N-((3a*S*,6*R*,7a*S*)-6-(Dimethoxymethyl)-2-(methylsulfonyl)-1,2,3,6,7,7a-hexahydro-3a,6-epoxypyrrolo[3,4-*c*]pyridin-4-yl)-N,4-dimethylbenzenesulfonamide 50b***



Following **GP8** with ynamide **48a** (537 mg, 1.51 mmol), ylide **47a** (353 mg, 1.80 mmol), AuPicCl<sub>2</sub> (29.2 mg, 5 mol%) and PhMe (15.0 mL) for 24 h at 90 °C. Purification by flash column chromatography (0→100 hexane/EtOAc) gave **50b** as a white foam (473 mg, 66%); IR (neat): ν = 2944, 1585, 1331, 1154, 1083, 953, 809, 729, 666 cm<sup>-1</sup>; <sup>1</sup>H NMR (400 MHz, CDCl<sub>3</sub>): δ = 7.64 (d<sub>AA'</sub>XX', *J* = 8.3 Hz, 2H), 7.33 (d<sub>AA'</sub>XX', *J* = 8.3 Hz, 2H), 4.68 (s, 1H), 4.42 (d, *J*<sub>AB</sub> = 13.2 Hz, 1H<sub>d</sub>), 3.91 (dd, *J* = 10.1, 7.9 Hz, 1H<sub>c</sub>), 3.87 (d, *J*<sub>AB</sub> = 13.2 Hz, 1H<sub>d</sub>), 3.54 (s, 3H), 3.52 (s, 3H), 3.03 (dd, *J* = 10.1, 9.4 Hz, 1H<sub>c</sub>), 2.95 (s, 3H), 2.86 (s, 3H), 2.53 – 2.42 (m, 1H<sub>b</sub>), 2.44 (s, 3H), 1.95 (dd, *J* = 12.1, 2.8 Hz, 1H<sub>a</sub>), 1.68 (dd, *J* = 12.1, 7.7 Hz, 1H<sub>a</sub>) ppm; <sup>13</sup>C NMR (101 MHz, CDCl<sub>3</sub>): δ = 168.7 (C), 145.3 (C), 132.8 (C), 130.1 (2CH), 128.2 (2CH), 104.4 (C), 103.0 (CH), 97.0 (C), 57.2 (CH<sub>3</sub>), 56.1 (CH<sub>3</sub>), 52.6 (C<sub>c</sub>H<sub>2</sub>), 48.6 (C<sub>d</sub>H<sub>2</sub>), 42.6 (C<sub>b</sub>H), 37.4 (CH<sub>3</sub>), 35.3 (CH<sub>3</sub>), 33.3 (C<sub>a</sub>H<sub>2</sub>), 21.8 (CH<sub>3</sub>) ppm; HRMS (ES-TOF): m/z: calcd for C<sub>19</sub>H<sub>28</sub>N<sub>3</sub>O<sub>7</sub>S<sub>2</sub>: 474.1363, found 474.1366 [M+H]<sup>+</sup>.

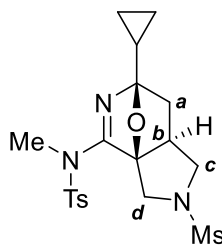
***tert-Butyl (((3a*S*,6*R*,7a*S*)-4-((*N*,4-dimethylphenyl)sulfonamido)-2-(methylsulfonyl)-2,3,7,7a-tetrahydro-3a,6-epoxypyrrolo[3,4-*c*]pyridin-6(1*H*)-yl)methyl)carbamate 50c***



Following **GP8** with ynamide **48a** (537 mg, 1.51 mmol), ylide **47j** (452 mg, 1.80 mmol), AuPicCl<sub>2</sub> (29.2 mg, 5 mol%) and PhMe (15.0 mL) for 24 h at 90 °C. Purification by flash column chromatography (0→100 hexane/EtOAc) gave **50c** as a bright yellow foam (486 mg, 61%); IR (neat): ν = 2933, 1709, 1583, 1333, 1155, 1088, 959, 806, 667 cm<sup>-1</sup>; NMR spectra display a

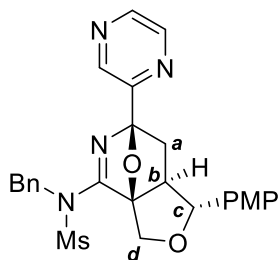
mixture of rotamers:  $^1\text{H}$  NMR (400 MHz,  $\text{CDCl}_3$ ):  $\delta$  = 7.63 ( $d_{\text{AA'XX'}}$ ,  $J$  = 8.4 Hz, 2H), 7.37 ( $d_{\text{AA'XX'}}$ ,  $J$  = 8.4 Hz, 2H), 4.77 (br. t,  $J$  = 5.6 Hz, NH), 4.39 (dd,  $J$  = 13.3, 1.1 Hz,  $1\text{H}_d$ ), 3.90 (dd,  $J$  = 9.9, 8.6 Hz,  $1\text{H}_c$ ), 3.86 (d,  $J_{AB}$  = 13.3 Hz,  $1\text{H}_d$ ), 3.80 – 3.71 (m, 2H), 3.01 (app. t,  $J$  = 9.7,  $1\text{H}_c$ ), 2.90 (s, 3H), 2.87 (s, 3H), 2.52 – 2.43 (m,  $1\text{H}_b$ ), 2.45 (s, 3H), 1.78 (dd,  $J$  = 12.2, 2.9 Hz,  $1\text{H}_a$ ), 1.66 (dd,  $J$  = 12.2, 7.5 Hz,  $1\text{H}_a$ ), 1.46 (s, 9H) ppm; only the majors peak are reported:  $^{13}\text{C}$  NMR (101 MHz,  $\text{CDCl}_3$ ):  $\delta$  = 169.5 (C), 156.0 (C), 145.5 (C), 132.4 (C), 130.1 (2CH), 128.3 (2CH), 103.6 (C), 96.9 (C), 80.0 (C), 52.6 ( $\text{C}_c\text{H}_2$ ), 48.6 ( $\text{C}_d\text{H}_2$ ), 43.5 ( $\text{C}_b\text{H}$ ), 42.5 ( $\text{CH}_2$ ), 37.4 ( $\text{CH}_3$ ), 35.4 ( $\text{CH}_3$ ), 35.0 ( $\text{C}_a\text{H}_2$ ), 28.5 (3 $\text{CH}_3$ ), 21.8 ( $\text{CH}_3$ ) ppm; HRMS (ES–TOF):  $m/z$ : calcd for  $\text{C}_{22}\text{H}_{33}\text{N}_4\text{O}_7\text{S}_2$ : 529.1785, found 529.1794  $[\text{M}+\text{H}]^+$ .

***N*–((3*aS*,6*R*,7*aS*)–6–Cyclopropyl–2–(methylsulfonyl)–1,2,3,6,7,7*a*–hexahydro–3*a*,6–epoxypyrrolo[3,4–*c*]pyridin–4–yl)–*N*,4–dimethylbenzenesulfonamide 50d**



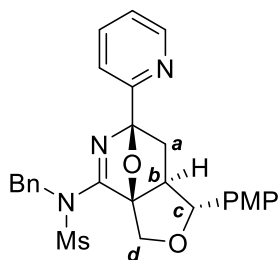
Following **GP8** with ynamide **48a** (537 mg, 1.51 mmol), ylide **47d** (292 mg, 1.80 mmol),  $\text{AuPicCl}_2$  (29.2 mg, 5 mol%) and PhMe (15.0 mL) for 24 h at 90 °C. Purification by flash column chromatography (0→40<sub>hold</sub>→100 hexane/EtOAc) gave **50d** as an off white foam (474 mg, 72%); IR (neat):  $\nu$  = 2956, 1587, 349, 1328, 1149, 1084, 946, 927, 758, 804, 666  $\text{cm}^{-1}$ ;  $^1\text{H}$  NMR (400 MHz,  $\text{CDCl}_3$ ):  $\delta$  = 7.62 ( $d_{\text{AA'XX'}}$ ,  $J$  = 8.4 Hz, 2H), 7.34 ( $d_{\text{AA'XX'}}$ ,  $J$  = 8.4 Hz, 2H), 4.37 (d,  $J_{AB}$  = 13.3 Hz,  $1\text{H}_d$ ), 3.89 (dd,  $J$  = 10.4, 8.5 Hz,  $1\text{H}_c$ ), 3.85 (d,  $J_{AB}$  = 13.3 Hz,  $1\text{H}_d$ ), 3.00 (app. t,  $J$  = 9.7 Hz,  $1\text{H}_c$ ), 2.88 (s, 3H), 2.86 (s, 3H), 2.45 (s, 3H), 2.45 – 2.38 (m,  $1\text{H}_b$ ), 1.73 – 1.62 (m,  $2\text{H}_a$ ), 1.44 – 1.36 (m, 1H), 0.69 – 0.61 (m, 3H), 0.51 – 0.42 (m, 1H) ppm;  $^{13}\text{C}$  NMR (101 MHz,  $\text{CDCl}_3$ ):  $\delta$  = 168.6 (C), 145.3 (C), 132.4 (C), 129.9 (2CH), 128.4 (2CH), 105.4 (C), 96.1 (C), 52.8 ( $\text{C}_c\text{H}_2$ ), 48.6 ( $\text{C}_d\text{H}_2$ ), 43.7 ( $\text{C}_b\text{H}$ ), 37.4 ( $\text{CH}_3$ ), 36.8 ( $\text{C}_c\text{H}_2$ ), 35.1 ( $\text{CH}_3$ ), 21.8 ( $\text{CH}_3$ ), 13.0 (CH), 2.2 ( $\text{CH}_2$ ), 2.1 ( $\text{CH}_2$ ) ppm; HRMS (ES–TOF):  $m/z$ : calcd for  $\text{C}_{19}\text{H}_{26}\text{N}_3\text{O}_5\text{S}_2$ : 440.1308, found 440.1312  $[\text{M}+\text{H}]^+$ .

***N*-Benzyl-*N*-((1*R*,3*aR*,6*R*,7*aS*)-1-(4-methoxyphenyl)-6-(pyrazin-2-yl)-1,6,7,7*a*-tetrahydro-3*H*-3*a*,6-epoxyfuro[3,4-*c*]pyridin-4-yl)methanesulfonamide 50e**



Following **GP8** with ynamide **48c** (116 mg, 0.30 mmol), ylide **47b** (90.1 mg, 0.45 mmol), AuPicCl<sub>2</sub> (3.5 mg, 3 mol%) and 1,2-DCB (3.0 mL) for 24 h at 90 °C. Purification by hot recrystallisation (EtOH) gave **50e** as a pale yellow powder (108 mg, 71%); mp: 163–166 °C; IR (neat):  $\nu$  = 2996, 2915, 2872, 1612, 1590, 1517, 1339, 1256, 1153, 1023 cm<sup>-1</sup>; <sup>1</sup>H NMR (400 MHz, CDCl<sub>3</sub>):  $\delta$  = 9.02 (d,  $J$  = 1.5 Hz, 1H), 8.69 (dd,  $J$  = 2.5, 1.5 Hz, 1H), 8.66 (d,  $J$  = 2.5 Hz, 1H), 7.41 – 7.38 (m, 2H), 7.33 (tt,  $J$  = 6.3, 1.1 Hz, 2H), 7.30 – 7.27 (m, 1H), 7.11 (d<sub>AA'XX'</sub>,  $J$  = 8.7 Hz, 2H), 6.84 (d<sub>AA'XX'</sub>,  $J$  = 8.7, 2H), 4.98 (d,  $J_{AB}$  = 13.7 Hz, 1H), 4.81 (d,  $J_{AB}$  = 13.7 Hz, 1H), 4.78 (d,  $J$  = 11.9 Hz, 1H<sub>d</sub>), 4.59 (d,  $J_{AB}$  = 9.1 Hz, 1H<sub>c</sub>), 4.31 (d,  $J_{AB}$  = 11.9 Hz, 1H<sub>d</sub>), 3.80 (s, 3H), 3.08 (s, 3H), 2.23 – 2.05 (m, 1H<sub>a</sub>), 1.63 – 1.54 (m, 1H<sub>a</sub>+1H<sub>b</sub>) ppm; <sup>13</sup>C NMR (101 MHz, CDCl<sub>3</sub>):  $\delta$  = 168.4 (C), 159.7 (C), 151.0 (C), 145.3 (CH), 144.2 (CH), 144.0 (CH), 135.0 (C), 131.2 (C), 129.4 (2CH), 128.94 (2CH), 128.90 (CH), 127.9 (2CH), 114.0 (2CH), 103.8 (C), 101.5 (C), 85.3 (C<sub>c</sub>H), 66.5 (C<sub>d</sub>H<sub>2</sub>), 55.5 (CH<sub>3</sub>), 53.2 (CH<sub>2</sub>), 51.7 (C<sub>b</sub>H), 39.6 (CH<sub>3</sub>), 35.4 (C<sub>a</sub>H<sub>2</sub>) ppm; HRMS (ES–TOF):  $m/z$ : calcd for C<sub>26</sub>H<sub>27</sub>N<sub>4</sub>O<sub>5</sub>S: 507.1697, found 507.1702 [M+H]<sup>+</sup>.

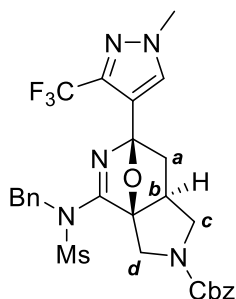
***N*-Benzyl-*N*-((1*R*,3*aR*,6*R*,7*aS*)-1-(4-methoxyphenyl)-6-(pyridin-2-yl)-1,6,7,7*a*-tetrahydro-3*H*-3*a*,6-epoxyfuro[3,4-*c*]pyridin-4-yl)methanesulfonamide 50f**



Following **GP8** with ynamide **48c** (116 mg, 0.30 mmol), ylide **47i** (120 mg, 0.60 mmol), AuPicCl<sub>2</sub> (5.8 mg, 5 mol%) and PhMe (3.0 mL) for 24 h at 90 °C. Purification by hot recrystallisation (EtOH, 62.0 mg) and flash column chromatography of the filtrate (0→50<sub>hold</sub>→100 hexane/EtOAc, 33.6 mg) gave **50f** as a brown powder (95.6 mg, 63%); mp: 159–161 °C; IR (neat):  $\nu$  = 2935, 1580, 1338, 1246, 1163, 1028, 1016, 937 cm<sup>-1</sup>; <sup>1</sup>H NMR (400 MHz, CDCl<sub>3</sub>):

$\delta$  = 8.73 (ddd,  $J$  = 4.9, 1.8, 1.0 Hz, 1H), 7.79 (app. td,  $J$  = 7.6, 1.7 Hz, 1H), 7.74 (app. dt,  $J$  = 7.9, 1.3 Hz, 1H), 7.42 – 7.38 (m, 2H), 7.36 – 7.29 (m, 3H), 7.28 – 7.23 (m, 1H), 7.09 (d<sub>AA'XX'</sub>,  $J$  = 8.7 Hz, 2H), 6.83 (d<sub>AA'XX'</sub>,  $J$  = 8.7 Hz, 2H), 4.94 (d,  $J_{AB}$  = 13.6 Hz, 1H), 4.81 (d,  $J_{AB}$  = 13.6 Hz, 1H), 4.76 (d,  $J_{AB}$  = 11.9 Hz, 1H<sub>d</sub>), 4.59 (d,  $J_{AB}$  = 9.4 Hz, 1H<sub>c</sub>), 4.31 (d,  $J_{AB}$  = 11.9 Hz, 1H<sub>d</sub>), 3.79 (s, 3H), 3.05 (s, 3H), 2.10 (dd,  $J$  = 11.9, 3.0 Hz, 1H<sub>a</sub>), 1.61 (dd,  $J$  = 11.9, 7.7 Hz, 1H<sub>a</sub>), 1.47 (ddd,  $J$  = 9.4, 7.7, 3.0 Hz, 1H<sub>b</sub>) ppm; <sup>13</sup>C NMR (101 MHz, CDCl<sub>3</sub>):  $\delta$  = 168.1 (C), 159.6 (C), 155.5 (C), 149.7 (CH), 136.9 (CH), 135.2 (C), 131.4 (C), 129.4 (2CH), 128.8 (2CH), 128.7 (CH), 127.8 (2CH), 124.0 (CH), 121.9 (CH), 113.9 (2CH), 105.2 (C), 101.0 (C), 85.2 (C<sub>c</sub>H), 66.5 (C<sub>d</sub>H<sub>2</sub>), 55.4 (CH<sub>3</sub>), 53.1 (CH<sub>2</sub>), 51.8 (C<sub>b</sub>H), 39.3 (CH<sub>3</sub>), 35.4 (C<sub>a</sub>H<sub>2</sub>) ppm; HRMS (ES–TOF):  $m/z$ : calcd for C<sub>27</sub>H<sub>28</sub>N<sub>3</sub>O<sub>5</sub>S: 506.1744, found 506.1751 [M+H]<sup>+</sup>.

***Benzyl (3aS,6R,7aS)–4–(N–benzylmethylsulfonamido)–6–(1–methyl–3–(trifluoromethyl)–1H–pyrazol–4–yl)–1,6,7,7a–tetrahydro–3a,6–epoxypyrrolo[3,4–c]pyridine–2(3H)–carboxylate 50g***

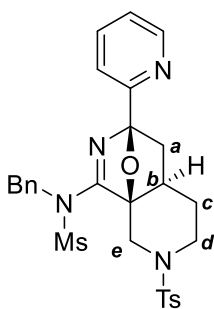


Following **GP8** with ynamide **48b** (412 mg, 1.00 mmol), ylide **47h** (408 mg, 1.50 mmol), AuPicCl<sub>2</sub> (19.5 mg, 5 mol%) and PhMe (10.0 mL) for 24 h at 90 °C. Purification by flash column chromatography (0→40<sub>hold</sub>→100 hexane/EtOAc) gave **50g** as a white foam (337 mg, 56%); IR (neat):  $\nu$  = 2953, 1699, 1587, 1498, 1417, 1350, 1158, 1122, 961 cm<sup>–1</sup>;

<sup>1</sup>H NMR (400 MHz, CDCl<sub>3</sub>):  $\delta$  = 7.64 – 7.60 (m, 1H), 7.41 – 7.28 (m, 10H), 5.18 – 5.09 (m, 2H), 4.86 (dd,  $J$  = 18.1, 13.4 Hz, 1H), 4.66 (d,  $J_{AB}$  = 13.3 Hz, 1H), 4.10 (dd,  $J$  = 24.0, 13.8 Hz, 1H), 4.00 – 3.85 (m, 4H), 3.80 (ddd,  $J$  = 10.6, 8.7, 3.2 Hz, 1H), 3.02 – 2.94 (m, 4H), 1.82 – 1.74 (m, 1H), 1.56 (dd,  $J$  = 11.8, 7.6 Hz, 1H), 1.47 – 1.38 (m, 1H) ppm; <sup>13</sup>C NMR (101 MHz, CDCl<sub>3</sub>):  $\delta$  = 207.0 (C), 166.5 and 166.4 (C), 154.29 and 154.27 (C), 136.61 and 136.58 (C), 134.5 and 134.4 (C), 131.6 and 131.5 (CH), 129.7 and 129.6 (2CH), 128.8 (CH), 128.69 and 128.66

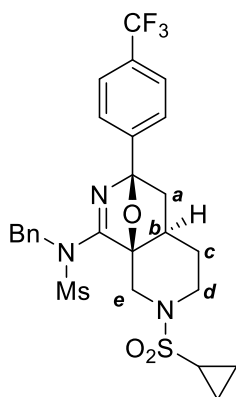
(2CH), 128.5 (2CH), 128.2 (CH), 128.11 and 128.06 (2CH), 121.1 (q,  $J = 269.0$  Hz, CF<sub>3</sub>), 99.2 (C), 96.7 (C), 95.7 (C), 67.01 and 66.99 (CH<sub>2</sub>), 53.1 and 52.9 (CH<sub>2</sub>), 50.5 and 50.3 (CH<sub>2</sub>), 46.6 and 46.2 (CH<sub>2</sub>), 42.0 (CH), 39.61 and 39.57 (CH<sub>3</sub>), 39.1 (CH<sub>2</sub>), 38.6 (CH<sub>3</sub>) ppm; <sup>19</sup>F NMR (377 MHz, CDCl<sub>3</sub>):  $\delta = -59.49$  ppm; HRMS (ES–TOF):  $m/z$ : calcd for C<sub>28</sub>H<sub>29</sub>N<sub>5</sub>O<sub>5</sub>SF<sub>3</sub>: 604.1836, found 604.1853 [M+H]<sup>+</sup>.

***N*–Benzyl–N–((3*R*,4*aR*,8*aS*)–3–(pyridin–2–yl)–7–tosyl–4,4*a*,5,6,7,8–hexahydro–3*H*–3,8*a*–epoxy–2,7–naphthyridin–1–yl)methanesulfonamide 106a**



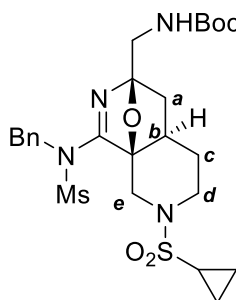
Following **GP8** with ynamide **77c** (112 mg, 0.25 mmol), ylide **47i** (99.6 mg, 0.50 mmol), AuPicCl<sub>2</sub> (4.9 mg, 5 mol%) and PhMe (2.5 mL) for 20 h at 90 °C. Purification by flash column chromatography (4:6 hexane/EtOAc) gave **106a** as a white powder (62.3 mg, 44%); mp: 155–156 °C; IR (neat):  $\nu = 3663, 2989, 2905, 1590, 1328, 1159, 1087, 1051, 960$  cm<sup>–1</sup>; <sup>1</sup>H NMR (400 MHz, CDCl<sub>3</sub>):  $\delta = 8.69$  (ddd,  $J = 4.9, 1.8, 1.0$  Hz, 1H), 7.75 (app. td,  $J = 7.7, 1.8$  Hz, 1H), 7.64 (d<sub>AA'XX'</sub>,  $J = 8.3$  Hz, 2H), 7.59 (app. dt,  $J = 12.8, 3.8$  Hz, 1H), 7.38 – 7.25 (m, 8H), 4.78 (d,  $J_{AB} = 13.9$  Hz, 1H), 4.60 (d,  $J_{AB} = 13.9$  Hz, 1H), 4.24 (dd,  $J = 13.5, 1.8$  Hz, 1H<sub>e</sub>), 3.72 (dtd,  $J = 12.4, 3.6, 1.8$  Hz, 1H<sub>d</sub>), 3.11 (d,  $J_{AB} = 13.5$  Hz, 1H<sub>e</sub>), 2.94 (s, 3H), 2.45 (s, 3H), 2.20 (app. td,  $J = 12.5, 2.1$  Hz, 1H<sub>d</sub>), 1.97 (dd,  $J = 11.9, 7.6$  Hz, 1H<sub>a</sub>), 1.83 (ddt,  $J = 13.5, 5.5, 2.5$ , 1H<sub>c</sub>), 1.73 (dd,  $J = 7.6, 1.8$  Hz, 1H<sub>a</sub>), 1.56 (app. qd,  $J = 12.8, 3.8$ , 1H<sub>c</sub>), 1.31 – 1.20 (m, 1H<sub>b</sub>) ppm; <sup>13</sup>C NMR (101 MHz, CDCl<sub>3</sub>):  $\delta = 169.4$  (C), 155.6 (C), 149.5 (CH), 143.8 (C), 136.8 (CH), 134.7 (C), 133.5 (C), 129.8 (2CH), 129.3 (2CH), 128.9 (2CH), 128.8 (CH), 127.8 (2CH), 123.9 (CH), 121.7 (CH), 103.9 (C), 86.7 (C), 53.8 (CH<sub>2</sub>), 45.3 (C<sub>e</sub>H<sub>2</sub>), 44.9 (C<sub>d</sub>H<sub>2</sub>), 39.5 (CH<sub>3</sub>), 39.4 (C<sub>a</sub>H<sub>2</sub>), 32.8 (C<sub>b</sub>H), 29.4 (C<sub>c</sub>H<sub>2</sub>), 21.7 (CH<sub>3</sub>) ppm; HRMS (ES–TOF):  $m/z$ : calcd for C<sub>28</sub>H<sub>31</sub>N<sub>4</sub>O<sub>5</sub>S<sub>2</sub>: 567.1730, found 567.1735 [M+H]<sup>+</sup>.

***N*-Benzyl-*N*-((3*R*,4*aR*,8*aS*)-7-(cyclopropylsulfonyl)-3-(4-(trifluoromethyl)phenyl)-4,4*a*,5,6,7,8-hexahydro-3*H*-3,8*a*-epoxy-2,7-naphthyridin-1-yl)methanesulfonamide **106b****



Following **GP8** with ynamide **77a** (119 mg, 0.30 mmol), ylide **47f** (120 mg, 0.45 mmol), AuPicCl<sub>2</sub> (5.8 mg, 5 mol%) and PhMe (3.0 mL) for 36 h at 90 °C. Purification by flash column chromatography (0→50<sub>hold</sub>→100 hexane/EtOAc) gave **106b** as a white solid (135 mg, 69%); IR (neat):  $\nu$  = 2935, 1602, 1324, 1154, 1125, 1068, 958 cm<sup>-1</sup>; <sup>1</sup>H NMR (400 MHz, CDCl<sub>3</sub>):  $\delta$  = 7.74 – 7.67 (m, 4H), 7.37 – 7.33 (m, 5H), 4.85 (d,  $J_{AB}$  = 14.2 Hz, 1H), 4.66 (d,  $J_{AB}$  = 14.2 Hz, 1H), 4.30 (dd,  $J$  = 14.2, 1.7 Hz, 1H<sub>e</sub>), 3.80 (app. dq,  $J$  = 12.7, 2.1, 1H<sub>d</sub>), 3.67 (d,  $J_{AB}$  = 14.2 Hz, 1H<sub>e</sub>), 2.99 (s, 3H), 2.80 (app. td,  $J$  = 12.7, 2.1 Hz, 1H<sub>d</sub>), 2.32 (tt,  $J$  = 8.0, 4.9 Hz, 1H), 1.99 (dd,  $J$  = 11.6, 7.1 Hz, 1H<sub>a</sub>), 1.98 – 1.90 (m, 1H<sub>c</sub>), 1.69 – 1.58 (m, 1H<sub>b</sub>+1H<sub>c</sub>), 1.55 (dd,  $J$  = 11.6, 2.1 Hz, 1H<sub>a</sub>), 1.20 – 1.12 (m, 2H), 1.02 – 0.93 (m, 2H) ppm; <sup>19</sup>F NMR (377 MHz, CDCl<sub>3</sub>):  $\delta$  = –62.66 ppm; <sup>13</sup>C NMR (101 MHz, CDCl<sub>3</sub>):  $\delta$  = 168.5 (C), 140.9 (C), 134.6 (C), 132.3 (q,  $J$  = 262 Hz, CF<sub>3</sub>), 129.3 (2CH), 129.1 (2CH), 129.0 (CH), 126.6 (2CH), 125.6 (q,  $J$  = 4.0 Hz, 2CH), 103.3 (C), 86.5 (C), 53.7 (CH<sub>2</sub>), 45.4 (C<sub>e</sub>H<sub>2</sub>), 44.9 (C<sub>d</sub>H<sub>2</sub>), 42.4 (C<sub>a</sub>H<sub>2</sub>), 40.3 (CH<sub>3</sub>), 33.6 (C<sub>b</sub>H), 30.1 (C<sub>c</sub>H<sub>2</sub>), 27.7 (CH), 5.1 (CH<sub>2</sub>), 5.0 (CH<sub>2</sub>) ppm; one quaternary carbon resonance not observed in <sup>13</sup>C NMR spectra; HRMS (ES–TOF):  $m/z$ : calcd for C<sub>26</sub>H<sub>28</sub>N<sub>3</sub>O<sub>5</sub>S<sub>2</sub>F<sub>3</sub>Na: 606.1315, found 606.1319 [M+Na]<sup>+</sup>.

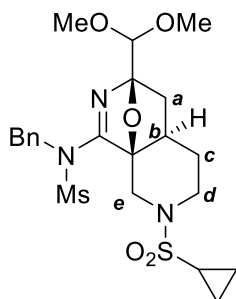
***tert*-Butyl (((3*R*,4*aR*,8*aS*)-1-(*N*-benzylmethylsulfonamido)-7-(cyclopropylsulfonyl)-4,4*a*,5,6,7,8-hexahydro-3*H*-3,8*a*-epoxy-2,7-naphthyridin-3-yl)methyl)carbamate **106c****



Following **GP8** with ynamide **77a** (198 mg, 0.50 mmol), ylide **47j** (151 mg, 0.60 mmol), AuPicCl<sub>2</sub> (9.7 mg, 5 mol%) and PhMe (5.0 mL) for 36 h at 90 °C. Purification by flash column chromatography (4:6 hexane/EtOAc) gave **106c** as a yellow foam (225 mg, 79%); IR (neat):  $\nu$

= 2982, 1707, 1600, 1511, 1336, 1151, 910  $\text{cm}^{-1}$ ; NMR spectra display a mixture of rotamers:  $^1\text{H}$  NMR (400 MHz,  $\text{CDCl}_3$ ):  $\delta$  = 7.41 – 7.28 (m, 5H), 4.78 (d,  $J_{AB}$  = 14.0 Hz, 1H), 4.77 (br. t,  $J$  = 6.1 Hz, NH) 4.60 (d,  $J_{AB}$  = 14.0 Hz, 1H), 4.11 (dd,  $J$  = 14.1, 1.6 Hz,  $1\text{H}_e$ ), 3.84 (dd,  $J$  = 14.4, 6.1 Hz, 1H), 3.77 – 3.69 (m,  $1\text{H}_d$ ), 3.69 (dd,  $J$  = 14.4, 6.1 Hz, 1H), 3.58 (d,  $J_{AB}$  = 14.1 Hz,  $1\text{H}_e$ ), 2.96 (s, 3H), 2.73 (app. td,  $J$  = 12.6, 2.1 Hz,  $1\text{H}_d$ ), 2.30 (tt,  $J$  = 8.3, 4.9 Hz, 1H), 1.93 – 1.82 (m,  $1\text{H}_c$ ), 1.60 – 1.50 (m,  $1\text{H}_a+1\text{H}_b+1\text{H}_c$ ), 1.46 (s, 9H), 1.34 (dd,  $J$  = 11.4, 1.7 Hz,  $1\text{H}_a$ ), 1.17 – 1.10 (m, 2H), 0.99 – 0.95 (m, 2H) ppm; only the major peaks are reported:  $^{13}\text{C}$  NMR (101 MHz,  $\text{CDCl}_3$ ):  $\delta$  = 169.6 (C), 156.1 (C), 134.6 (C), 129.3 (2CH), 129.02 (2CH), 128.95 (CH), 103.1 (C), 86.0 (C), 79.8 (C), 53.6 ( $\text{CH}_2$ ), 45.2 ( $\text{C}_e\text{H}_2$ ), 44.9 ( $\text{C}_d\text{H}_2$ ), 42.5 ( $\text{CH}_2$ ), 39.7 ( $\text{CH}_3$ ), 36.9 ( $\text{C}_a\text{H}_2$ ), 32.9 ( $\text{C}_b\text{H}$ ), 29.9 ( $\text{C}_e\text{H}_2$ ), 28.5 (3 $\text{CH}_3$ ), 27.5 (CH), 5.03 ( $\text{CH}_2$ ), 4.97 ( $\text{CH}_2$ ) ppm; HRMS (ES–TOF):  $m/z$ : calcd for  $\text{C}_{25}\text{H}_{36}\text{N}_4\text{O}_7\text{S}_2\text{Na}$ : 591.1918, found 591.1926  $[\text{M}+\text{Na}]^+$ .

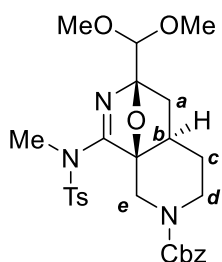
***N*-Benzyl-*N*-((3*R*,4*aR*,8*aS*)-7-(cyclopropylsulfonyl)-3-(dimethoxymethyl)-4,4*a*,5,6,7,8-hexahydro-3*H*-3,8*a*-epoxy-2,7-naphthyridin-1-yl)methanesulfonamide 106d**



Following **GP8** with ynamide **77a** (198 mg, 0.50 mmol), ylide **47a** (118 mg, 0.60 mmol), AuPicCl<sub>2</sub> (9.7 mg, 5 mol%) and PhMe (5.0 mL) for 36 h at 90 °C. Purification by flash column chromatography (4:6 hexane/EtOAc) gave **106d** as a white foam (171 mg, 66%); IR (neat):  $\nu$  = 2932, 1599, 1455, 1337, 1150, 1082, 953, 914  $\text{cm}^{-1}$ ;  $^1\text{H}$  NMR (400 MHz,  $\text{CDCl}_3$ ):  $\delta$  = 7.41 – 7.30 (m, 5H), 4.81 (d,  $J_{AB}$  = 13.9 Hz, 1H), 4.65 (s, 1H), 4.64 (d,  $J_{AB}$  = 13.9 Hz, 1H), 4.12 (dd,  $J$  = 14.2, 1.7 Hz,  $1\text{H}_e$ ), 3.71 (app. d,  $J$  = 12.8 Hz,  $1\text{H}_d$ ), 3.59 (d,  $J_{AB}$  = 14.2 Hz, 1H), 3.52 (s, 3H), 3.51 (s, 3H), 2.98 (s, 3H), 2.71 (app. td,  $J$  = 12.8, 2.1 Hz,  $1\text{H}_d$ ), 2.31 (tt,  $J$  = 8.0, 4.9 Hz, 1H), 1.89 – 1.81 (m,  $1\text{H}_c$ ), 1.57 (dd,  $J$  = 11.7, 7.4 Hz,  $1\text{H}_a$ ), 1.57 – 1.49 (m,  $1\text{H}_c$ ), 1.49 (dd,  $J$  = 11.7, 2.6 Hz,  $1\text{H}_a$ ), 1.46 – 1.35 (m,  $1\text{H}_b$ ), 1.14 – 1.10 (m, 2H), 0.97 – 0.89 (m, 2H) ppm;  $^{13}\text{C}$  NMR (101 MHz,  $\text{CDCl}_3$ ):  $\delta$  = 169.5 (C), 134.9 (C), 129.3 (2CH), 128.9 (2CH), 128.8

(CH), 104.0 (C), 103.1 (C), 85.9 (CH), 56.7 (CH<sub>3</sub>), 56.3 (CH<sub>3</sub>), 53.7 (CH<sub>2</sub>), 45.1 (C<sub>e</sub>H<sub>2</sub>), 44.8 (C<sub>d</sub>H<sub>2</sub>), 39.6 (CH<sub>3</sub>), 35.3 (C<sub>a</sub>H<sub>2</sub>), 32.0 (C<sub>b</sub>H), 29.7 (C<sub>c</sub>H<sub>2</sub>), 27.5 (CH), 5.05 (CH<sub>2</sub>), 4.99 (CH<sub>2</sub>) ppm; HRMS (ES–TOF): m/z: calcd for C<sub>22</sub>H<sub>31</sub>N<sub>3</sub>O<sub>7</sub>S<sub>2</sub>Na: 536.1496, found 536.1506 [M+Na]<sup>+</sup>.

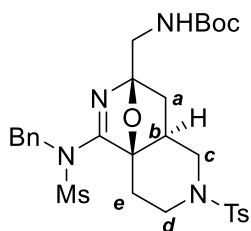
***Benzyl (3R,4aR,8aS)–3–(dimethoxymethyl)–1–((N,4–dimethylphenyl)sulfonamido)–4,4a,5,6–tetrahydro–3H–3,8a–epoxy–2,7–naphthyridine–7(8H)–carboxylate 106e***



Following **GP8** with ynamide **77C** (640 mg, 1.50 mmol), ylide **47a** (353 mg, 1.80 mmol), AuPicCl<sub>2</sub> (29.2 mg, 5 mol%) and PhMe (15.0 mL) for 1 h at 90 °C and 24 h at 110 °C. Purification by flash column chromatography (0→50<sub>hold</sub>→100 hexane/EtOAc) gave **106e** as a yellow foam (534 mg, 66%); IR (neat): ν = 2944, 1698, 1596, 1432, 1355, 1275, 1162, 1109, 1083 cm<sup>-1</sup>; *NMR spectra display a mixture of rotamers*: <sup>1</sup>H NMR (400 MHz, CDCl<sub>3</sub>): δ = 7.70 – 7.58 (m, 2H), 7.41 – 7.28 (m, 7H), 5.21 – 5.05 (m, 2H), 4.63 (s, 1H), 4.71 – 4.57 (m, 1H<sub>e</sub>), 4.28 – 4.17 (m, 1H<sub>d</sub>), 4.17 – 4.02 (m, 1H<sub>e</sub>), 3.51 (m, 3H), 3.50 (s, 3H), 2.96 – 2.88 (m, 1H<sub>d</sub>+3H), 2.43 (s, 3H), 2.37 – 2.26 (m, 1H<sub>b</sub>), 2.02 – 1.90 (m, 1H<sub>c</sub>), 1.75 (dd, *J* = 11.8, 7.7 Hz, 1H<sub>a</sub>), 1.63 (dd, *J* = 11.8, 2.8 Hz, 1H<sub>a</sub>), 1.61 – 1.45 (m, 1H<sub>c</sub>) ppm; <sup>13</sup>C NMR resonances assigned with assistance from HSQC and HMBC spectra due to the broadening of the resonances owing to the rotamer effect: <sup>13</sup>C NMR (101 MHz, CDCl<sub>3</sub>): δ = 171.3 (C), 155.7 (C), 145.1 (C), 137.0 (C), 130.0 (2CH), 128.6 (CH), 128.3 (4CH), 128.0 (2CH), 120.1 (C), 103.4 and 103.3 (CH), 103.0 (C), 87.2 (C), 67.3 (CH<sub>2</sub>), 56.98 and 56.95(CH<sub>3</sub>), 55.9 (CH<sub>3</sub>), 43.54 and 43.48 (C<sub>e</sub>H<sub>2</sub>), 42.84 and 42.80 (C<sub>d</sub>H<sub>2</sub>), 37.4 (CH<sub>3</sub>), 35.44 and 35.41 (C<sub>a</sub>H<sub>2</sub>), 33.20 and 33.18 (C<sub>b</sub>H), 30.0 and 29.9 (C<sub>c</sub>H<sub>2</sub>), 21.8 (CH<sub>3</sub>) ppm; HRMS (ES–TOF): m/z: calcd for C<sub>27</sub>H<sub>34</sub>N<sub>3</sub>O<sub>7</sub>S: 544.2112, found 544.2120 [M+H]<sup>+</sup>.

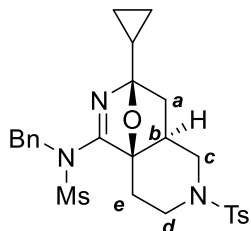


***tert*-Butyl (((3*R*,4*aS*,8*aR*)-1-(*N*-benzylmethylsulfonamido)-6-tosyl-4,4*a*,5,6,7,8-hexahydro-3*H*-3,8*a*-epoxy-2,6-naphthyridin-3-yl)methyl)carbamate 107*a***



Following **GP8** with ynamide **85c** (446 mg, 1.00 mmol), ylide **47j** (302 mg, 1.20), AuPicCl<sub>2</sub> (19.5 mg, 5 mol%) and PhMe (10.0 mL) for 1 h at 90 °C and 24 h at 110 °C. Purification by flash column chromatography (0→50<sub>hold</sub>→100 hexane/EtOAc) gave **107a** as a yellow foam (503 mg, 81%); IR (neat):  $\nu$  = 2922, 1709, 1599, 1510, 1346, 1157 cm<sup>-1</sup>; <sup>1</sup>H NMR (400 MHz, CDCl<sub>3</sub>):  $\delta$  = 7.62 (d<sub>AA'XX'</sub>,  $J$  = 8.3 Hz, 2H), 7.39 – 7.31 (m, 5H), 7.27 (dd,  $J$  = 7.8, 2.2 Hz, 2H), 4.82 (d,  $J_{AB}$  = 14.4 Hz, 1H), 4.71 (br. t,  $J$  = 5.7 Hz, NH), 4.59 (d,  $J_{AB}$  = 14.4 Hz, 1H), 3.85 (dd,  $J$  = 11.5, 6.7 Hz, 1H<sub>c</sub>), 3.83 – 3.72 (m, 1H<sub>d</sub>), 3.77 (dd,  $J$  = 14.4, 5.7 Hz, 1H), 3.59 (dd,  $J$  = 14.4, 5.7 Hz, 1H), 2.90 (s, 3H), 2.50 – 2.38 (m, 1H<sub>e</sub>), 2.44 (s, 3H), 2.33 (ddd,  $J$  = 12.8, 11.4, 2.4 Hz, 1H<sub>d</sub>), 2.12 (app. dt,  $J$  = 13.8, 2.2 Hz, 1H<sub>e</sub>), 1.97 (app. t,  $J$  = 11.6, 1H<sub>c</sub>), 1.78 – 1.67 (m, 1H<sub>b</sub>), 1.50 – 1.41 (m, 1H<sub>a</sub>), 1.43 (s, 9H), 1.12 (dd,  $J$  = 12.0, 2.6 Hz, 1H<sub>a</sub>) ppm; <sup>13</sup>C NMR (101 MHz, CDCl<sub>3</sub>):  $\delta$  = 169.8 (C), 156.0 (C), 144.0 (C), 134.6 (C), 133.6 (C), 130.0 (2CH), 129.3 (2CH), 129.0 (2CH), 128.9 (CH), 127.7 (2CH), 102.6 (C), 86.6 (C), 79.8 (C), 53.1 (CH<sub>2</sub>), 49.8 (C<sub>c</sub>H<sub>2</sub>), 42.9 (C<sub>d</sub>H<sub>2</sub>), 42.5 (CH<sub>2</sub>), 40.7 (CH<sub>3</sub>), 34.5 (C<sub>a</sub>H<sub>2</sub>), 33.9 (C<sub>b</sub>H), 28.5 (3CH<sub>3</sub>), 25.9 (C<sub>e</sub>H<sub>2</sub>), 21.7 (CH<sub>3</sub>) ppm; HRMS (ES-TOF):  $m/z$ : calcd for C<sub>29</sub>H<sub>39</sub>N<sub>4</sub>O<sub>7</sub>S<sub>2</sub>: 619.2255, found 619.2272 [M+H]<sup>+</sup>.

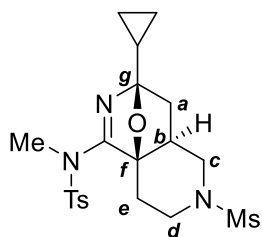
***N*-Benzyl-*N*-((3*R*,4*aS*,8*aR*)-3-cyclopropyl-6-tosyl-4,4*a*,5,6,7,8-hexahydro-3*H*-3,8*a*-epoxy-2,6-naphthyridin-1-yl)methanesulfonamide 107*b***



Following **GP8** with ynamide **85c** (335 mg, 0.75 mmol), ylide **47d** (146 mg, 0.90 mmol), AuPicCl<sub>2</sub> (14.6 mg, 5 mol%) and PhMe (7.5 mL) for 2 h at 90 °C and 22 h at 110 °C. Purification by flash column chromatography (0→30<sub>hold</sub>→100 hexane/EtOAc hexane/EtOAc, EtOAc

gradient at 0–30–100%) gave **107b** as a pale yellow foam (308 mg, 78%); IR (neat):  $\nu = 3034$ , 1566, 1395, 1344, 1249, 1155, 979, 761  $\text{cm}^{-1}$ ;  $^1\text{H}$  NMR (400 MHz,  $\text{CDCl}_3$ ):  $\delta = 7.63$  ( $d_{\text{AA'XX'}}$ ,  $J = 8.3$  Hz, 2H), 7.38 – 7.30 (m, 5H), 7.29 – 7.24 (m, 2H), 4.79 (d,  $J_{\text{AB}} = 14.5$  Hz, 1H), 4.56 (d,  $J_{\text{AB}} = 14.5$  Hz, 1H), 3.88 (ddd,  $J = 11.9, 6.5, 2.1$  Hz, 1H<sub>c</sub>), 3.78 (app. dt,  $J = 6.2, 2.1$  Hz, 1H), 2.84 (s, 3H), 2.44 (s, 3H), 2.43 – 2.33 (m, 1H<sub>d</sub>+1H<sub>e</sub>), 2.17 – 2.10 (m, 1H<sub>e</sub>), 2.05 (app. t,  $J = 11.6$  Hz, 1H<sub>c</sub>), 1.76 – 1.69 (m, 1H), 1.45 (dd,  $J = 11.9, 7.6$  Hz, 1H<sub>a</sub>), 1.32 – 1.23 (m, 1H), 1.08 (dd,  $J = 11.9, 2.7$  Hz, 1H<sub>a</sub>), 0.68 – 0.57 (m, 3H), 0.52 – 0.42 (m, 1H) ppm;  $^{13}\text{C}$  NMR (101 MHz,  $\text{CDCl}_3$ ):  $\delta = 168.8$  (C), 143.9 (C), 134.6 (C), 133.9 (C), 130.0 (2CH), 129.3 (2CH), 129.0 (2CH), 128.8 (CH), 127.7 (2CH), 104.4 (C), 86.0 (C), 53.0 ( $\text{CH}_2$ ), 49.9 ( $\text{C}_6\text{H}_2$ ), 42.9 ( $\text{C}_d\text{H}_2$ ), 40.9 ( $\text{CH}_3$ ), 36.2 ( $\text{C}_a\text{H}_2$ ), 34.1 ( $\text{C}_b\text{H}$ ), 26.0 ( $\text{C}_e\text{H}_2$ ), 21.7 ( $\text{CH}_3$ ), 12.7 (CH), 2.3 ( $\text{CH}_2$ ), 1.9 ( $\text{CH}_2$ ) ppm; HRMS (ES–TOF):  $m/z$ : calcd for  $\text{C}_{26}\text{H}_{32}\text{N}_3\text{O}_5\text{S}_2$ : 530.1778, found 530.1788  $[\text{M}+\text{H}]^+$ .

***N*–((3*R*,4*aS*,8*aR*)–3–Cyclopropyl–6–(methylsulfonyl)–4,4*a*,5,6,7,8–hexahydro–3*H*–3,8*a*–epoxy–2,6–naphthyridin–1–yl)–*N*,4–dimethylbenzenesulfonamide **107c****

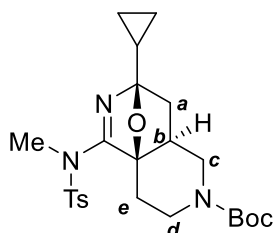


Following **GP8** with ynamide **85a** (926 mg, 2.50 mmol), ylide **47d** (487 mg, 3.00 mmol), AuPicCl<sub>2</sub> (48.6 mg, 5 mol%) and PhMe (25.0 mL) for 1.5 h at 90 °C and 20 h at 110 °C. Purification by hot recrystallisation (EtOH) gave **107c** as a white powder (782 mg, 69%); mp: 214–216 °C;

IR (neat):  $\nu = 3009$ , 1607, 1347, 1328, 1312, 1158, 1150, 978  $\text{cm}^{-1}$ ;  $^1\text{H}$  NMR (400 MHz,  $\text{CDCl}_3$ ):  $\delta = 7.66$  ( $d_{\text{AA'XX'}}$ ,  $J = 8.3$  Hz, 2H), 7.32 ( $d_{\text{AA'XX'}}$ ,  $J = 8.3$  Hz, 2H), 4.01 (ddd,  $J = 12.4, 6.5, 2.1$  Hz, 1H<sub>c</sub>), 3.92 – 3.83 (m, 1H<sub>d</sub>), 2.93 – 2.83 (m, 1H<sub>d</sub>), 2.90 (s, 3H), 2.85 (s, 3H), 2.80 (app. td,  $J = 13.0, 5.6$  Hz, 1H<sub>e</sub>), 2.57 (dd,  $J = 12.4, 11.2$  Hz, 1H<sub>c</sub>), 2.44 (s, 3H), 2.35 – 2.23 (m, 1H<sub>e</sub>+1H<sub>b</sub>), 1.62 (dd,  $J = 12.1, 7.6$  Hz, 1H<sub>a</sub>), 1.40 – 1.30 (m, 1H), 1.25 (dd,  $J = 12.1, 2.6$ , 1H<sub>a</sub>), 0.68 – 0.59 (m, 3H), 0.55 – 0.47 (m, 1H) ppm;  $^{13}\text{C}$  NMR (101 MHz,  $\text{CDCl}_3$ ):  $\delta = 170.7$  (C), 144.9 (C), 133.2 (C), 129.8 (2CH), 128.5 (2CH), 103.8 ( $\text{C}_g$ ), 86.6 ( $\text{C}_f$ ), 49.7 ( $\text{C}_c\text{H}_2$ ), 42.8 ( $\text{C}_d\text{H}_2$ ),

37.3 (CH<sub>3</sub>), 36.8 (CH<sub>3</sub>), 36.1 (C<sub>a</sub>H<sub>2</sub>), 34.7 (C<sub>b</sub>H), 25.8 (C<sub>e</sub>H<sub>2</sub>), 21.8 (CH<sub>3</sub>), 13.0 (CH), 2.1 (CH<sub>2</sub>), 1.9 (CH<sub>2</sub>) ppm; HRMS (ES–TOF): m/z: calcd for C<sub>20</sub>H<sub>28</sub>N<sub>3</sub>O<sub>5</sub>S<sub>2</sub>: 454.1465, found 454.1465 [M+H]<sup>+</sup>.

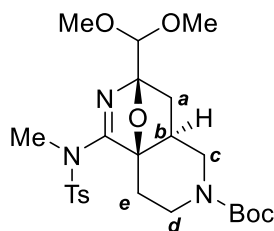
***tert*-Butyl (3*R*,4*aS*,8*aR*)–3–cyclopropyl–1–((*N*,4–dimethylphenyl)sulfonamido)–3,4,4*a*,5,7,8–hexahydro–6*H*–3,8*a*–epoxy–2,6–naphthyridine–6–carboxylate **107d****



Following **GP8** with ynamide **85d** (530 mg, 1.35 mmol), ylide **47d** (318 mg, 1.62 mmol), AuPicCl<sub>2</sub> (26.3 mg, 5 mol%) and PhMe (13.5 mL) for 2 h at 90 °C and 18.5 at 110 °C. Purification by flash column chromatography (0→40<sub>hold</sub>→100 hexane/EtOAc) gave **107d** as a white

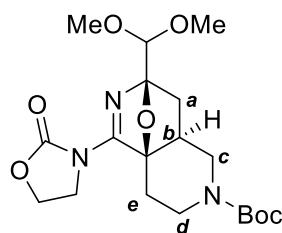
foam (465 mg, 68%); mp: 159–161 °C; IR (neat):  $\nu$  = 2971, 2929, 1690, 1592, 1427, 1355, 1160 cm<sup>-1</sup>; <sup>1</sup>H NMR (400 MHz, CDCl<sub>3</sub>):  $\delta$  = 7.79 – 7.59 (m, 2H), 7.31 (d<sub>AA'XX'</sub>, *J* = 8.3 Hz, 2H), 4.42 – 4.03 (m, 2H), 2.98 – 2.80 (m, 4H), 2.66 – 2.46 (m, 2H), 2.43 (s, 3H), 2.17 – 2.04 (m, 2H), 1.61 – 1.50 (m, 1H), 1.48 (s, 9H), 1.40 – 1.30 (m, 1H), 1.24 – 1.18 (m, 1H), 0.68 – 0.58 (m, 3H), 0.54 – 0.46 (m, 1H) ppm; <sup>13</sup>C NMR resonances assigned with assistance from HSQC and HMBC spectra due to the broadening of the resonances owing to the rotamer effect: <sup>13</sup>C NMR (101 MHz, CDCl<sub>3</sub>):  $\delta$  = 154.5 (C), 144.7 (C), 129.7 (2CH), 128.7 (2CH), 103.9 (C), 87.5 (C), 80.0 (C), 47.7 (CH<sub>2</sub>), 41.3 (CH<sub>2</sub>), 37.6 (CH<sub>3</sub>), 35.8 (CH<sub>2</sub>), 34.3 (CH), 28.6 (3CH<sub>3</sub>), 25.8 (CH<sub>2</sub>), 21.8 (CH<sub>3</sub>), 13.0 (CH), 2.1 (CH<sub>2</sub>), 1.9 (CH<sub>2</sub>) ppm; two quaternary carbon not visible in <sup>13</sup>C NMR spectra; HRMS (ES–TOF): m/z: calcd for C<sub>24</sub>H<sub>34</sub>N<sub>3</sub>O<sub>5</sub>S: 476.2214, found 476.2218 [M+H]<sup>+</sup>.

***tert*-Butyl (3*R*,4*aS*,8*aR*)-3-(dimethoxymethyl)-1-((*N*,4-dimethylphenyl)sulfonamido)-3,4,4*a*,5,7,8-hexahydro-6*H*-3,8*a*-epoxy-2,6-naphthyridine-6-carboxylate **107e****



Following **GP8** with ynamide **85d** (942 mg, 2.40 mmol), ylide **47a** (467 mg, 2.88 mmol), AuPicCl<sub>2</sub> (46.7 mg, 5 mol%) and PhMe (24.0 mL) for 1 h at 90 °C and 24 h at 110 °C. Purification by flash column chromatography (0→25<sub>hold</sub>→100 hexane/EtOAc) followed by hot recrystallisation (EtOH) gave **107e** as a white solid (571 mg, 50%); IR (neat):  $\nu$  = 2932, 1691, 1596, 1421, 1358, 1161, 1119, 1085 cm<sup>-1</sup>; *NMR spectra display a mixture of rotamers*: <sup>1</sup>H NMR (400 MHz, CDCl<sub>3</sub>):  $\delta$  = 7.71 – 7.56 (m, 2H), 7.26 (d<sub>AA'XX'</sub>, *J* = 8.3 Hz, 2H), 4.65 (s, 1H), 4.37 – 3.98 (m, 2H), 3.50 (s, 3H), 3.47 (s, 3H), 2.97 – 2.83 (m, 3H), 2.77 – 2.46 (m, 3H), 2.38 (s, 3H), 2.24 – 2.04 (m, 2H), 1.65 – 1.51 (m, 1H), 1.49 – 1.38 (m, 1H), 1.44 (s, 9H) ppm; <sup>13</sup>C NMR (101 MHz, CDCl<sub>3</sub>):  $\delta$  = 171.5 and 170.4 (C), 154.4 (C), 144.7 (C), 133.7 and 132.9 (C), 129.7 (2CH), 128.4 (2CH), 102.90 (CH), 102.86 (C), 88.3 (C), 79.9 (C), 56.7 (CH<sub>3</sub>), 55.6 (CH<sub>3</sub>), 48.1 and 47.4 (CH<sub>2</sub>), 41.2 and 40.1 (CH<sub>2</sub>), 37.3 and 36.7 (CH<sub>3</sub>), 33.1 (CH), 32.6 (CH<sub>2</sub>), 28.4 (3CH<sub>3</sub>), 25.3 (CH<sub>2</sub>), 21.6 (CH<sub>3</sub>) ppm; HRMS (ES-TOF): *m/z*: calcd for C<sub>24</sub>H<sub>36</sub>N<sub>3</sub>O<sub>7</sub>S: 510.2268, found 510.2280 [M+H]<sup>+</sup>.

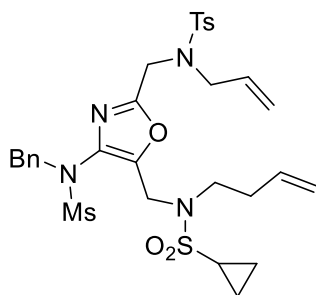
***tert*-Butyl (3*R*,4*aS*,8*aR*)-3-(dimethoxymethyl)-1-(2-oxooxazolidin-3-yl)-3,4,4*a*,5,7,8-hexahydro-6*H*-3,8*a*-epoxy-2,6-naphthyridine-6-carboxylate **107f****



Following **GP8** with ynamide **85e** (235 mg, 0.80 mmol), ylide **47a** (188 mg, 0.96 mmol), AuPicCl<sub>2</sub> (15.6 mg, 5 mol%) and PhMe (8.0 mL) for 22 h at 90 °C. Purification by flash column chromatography (0→100 hexane/EtOAc) gave **107f** as a colourless oil that solidified upon standing (200 mg, 61%); mp: 178–191 °C; IR (neat):  $\nu$  = 2989, 2935, 1774, 1694, 1599, 1471, 1425, 1400, 1171, 1121, 1086, 752 cm<sup>-1</sup>; *NMR spectra display a mixture of rotamers*: <sup>1</sup>H

NMR (400 MHz, CDCl<sub>3</sub>):  $\delta$  = 4.70 (s, 1H), 4.49 – 4.39 (m, 2H), 4.36 – 3.93 (m, 3H), 3.92 – 3.80 (m, 1H), 3.57 (s, 3H), 3.56 (s, 3H), 3.11 – 2.80 (m, 2H), 2.67 – 2.50 (m, 1H), 2.23 – 2.14 (m, 1H), 2.04 (app. dt,  $J$  = 14.1, 2.4 Hz, 1H), 1.63 (dd,  $J$  = 12.0, 7.5 Hz, 1H), 1.49 – 1.42 (m, 1H), 1.46 (s, 9H) ppm; <sup>13</sup>C NMR resonances assigned with assistance from HSQC and HMBC spectra due to the broadening of the resonances owing to the rotamer effect: <sup>13</sup>C NMR (101 MHz, CDCl<sub>3</sub>):  $\delta$  = 167.0 (C), 154.6 (C), 154.0 (C), 103.4 (CH), 102.6 (C), 88.2 (C), 79.9 (C), 63.5 (CH<sub>2</sub>), 57.0 (CH<sub>3</sub>), 56.1 (CH<sub>3</sub>), 47.5 (CH<sub>2</sub>), 45.6 (CH<sub>2</sub>), 41.4 (CH<sub>2</sub>), 33.4 (CH<sub>2</sub>), 32.7 (CH), 28.5 (3CH<sub>3</sub>), 25.1 (CH<sub>2</sub>) ppm; HRMS (ES–TOF):  $m/z$ : calcd for C<sub>19</sub>H<sub>30</sub>N<sub>3</sub>O<sub>7</sub>: 412.2078, found 412.2079 [M+H]<sup>+</sup>.

*N*-Allyl-*N*-((4-(*N*-benzylmethylsulfonamido)-5-((*N*-(but-3-en-1-yl)cyclopropanesulfonamido)methyl)oxazol-2-yl)methyl)-4-methylbenzenesulfonamide **108**

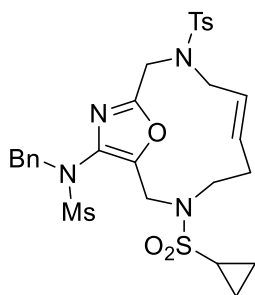


Following **GP8** with ynamide **77a** (277 mg, 0.70 mmol), ylide **43d** (290 mg, 0.84 mmol), AuPicCl<sub>2</sub> (8.17 mg, 3 mol%) and PhMe (7.0 mL) for 1 h at 80 °C and 30 min at 90 °C. Purification by flash column chromatography (6:4 hexane/EtOAc) gave **108** as a colourless oil (354 mg, 76%); IR (neat):  $\nu$  = 2930, 1597, 1456, 1333,

1152, 1091, 960 cm<sup>-1</sup>; <sup>1</sup>H NMR (400 MHz, CDCl<sub>3</sub>):  $\delta$  = 7.64 (d<sub>AA'XX'</sub>,  $J$  = 8.3 Hz, 2H), 7.30 – 7.19 (m, 7H), 5.65 – 5.48 (m, 2H), 5.16 – 5.07 (m, 2H), 5.03 – 4.96 (m, 2H), 4.63 (s, 2H), 4.37 (s, 2H), 4.02 (s, 2H), 3.79 (dt,  $J$  = 6.5, 1.3 Hz, 2H), 2.97 (s, 3H), 2.91 – 2.85 (m, 2H), 2.39 (s, 3H), 2.41 – 2.30 (m, 1H), 2.03 (app. qt,  $J$  = 7.3, 1.3 Hz, 2H), 1.06 – 1.00 (m, 2H), 0.96 – 0.89 (m, 2H) ppm; <sup>13</sup>C NMR (101 MHz, CDCl<sub>3</sub>):  $\delta$  = 158.3 (C), 146.0 (C), 144.1 (C), 136.1 (C), 135.1 (C), 134.7 (CH), 134.3 (C), 131.8 (CH), 130.0 (2CH), 129.4 (2CH), 128.9 (2CH), 128.6 (CH), 127.3 (2CH), 120.4 (CH<sub>2</sub>), 117.2 (CH<sub>2</sub>), 53.9 (CH<sub>2</sub>), 51.1 (CH<sub>2</sub>), 46.3 (CH<sub>2</sub>), 43.6 (CH<sub>2</sub>),

39.9 (CH<sub>2</sub>), 37.9 (CH<sub>3</sub>), 32.9 (CH<sub>2</sub>), 29.9 (CH), 21.6 (CH<sub>3</sub>), 5.3 (2CH<sub>2</sub>) ppm; HRMS (ES-TOF): m/z: calcd for C<sub>30</sub>H<sub>39</sub>N<sub>4</sub>O<sub>7</sub>S<sub>3</sub>: 633.1975, found 663.1991 [M+H]<sup>+</sup>.

**(E)-N-Benzyl-N-(3-(cyclopropylsulfonyl)-9-tosyl-3,9-diaza-1(2,5)-oxazolacyclodecaphan-6-en-14-yl)methanesulfonamide 109**



Diene **108** (140 mg, 0.211 mmol) and Grubbs II catalyst (5.4 mg, 3 mol%) were dissolved in CH<sub>2</sub>Cl<sub>2</sub> (10.5 mL) and heated to reflux for 2 h. After allowing to cool to r.t., the reaction mixture was concentrated under reduced pressure and passed through a 4 cm pad of silica (EtOAc).

The solvent was removed under reduced pressure and crude reaction mixture purified by hot recrystallisation (EtOH) to give trans alkene **109** as a white powder (104 mg, 78%); mp: 149–150 °C; IR (neat): ν = 2925, 2852, 1498, 1330, 1150, 1091 cm<sup>-1</sup>; <sup>1</sup>H NMR (400 MHz, CDCl<sub>3</sub>): δ = 7.73 (d<sub>AA'XX'</sub>, J = 8.3 Hz, 2H), 7.38 – 7.27 (m, 7H), 5.15 (dt, J = 14.3, 6.6 Hz, 1H), 4.71 (s, 2H), 4.48 – 4.38 (m, 1H), 4.41 (s, 2H), 4.00 (s, 2H), 3.49 (app. d, J = 6.6 Hz, 2H), 3.02 (s, 3H), 2.63 (br. s, 2H), 2.44 (s, 3H), 2.34 (tt, J = 7.9, 4.9 Hz, 1H), 1.82 (br. d, J = 7.4 Hz, 2H), 1.19 – 1.09 (m, 2H), 1.08 – 1.02 (m, 2H) ppm; <sup>13</sup>C NMR (101 MHz, CDCl<sub>3</sub>): δ = 158.1 (C), 145.1 (C), 144.1 (C), 135.9 (C), 135.5 (C), 135.0 (C), 130.7 (CH), 130.2 (2CH), 129.8 (2CH), 129.0 (2CH), 128.8 (CH), 127.6 (CH), 127.3 (2CH), 53.5 (CH<sub>2</sub>), 50.6 (CH<sub>2</sub>), 48.2 (CH<sub>2</sub>), 46.4 (CH<sub>2</sub>), 44.0 (CH<sub>2</sub>), 37.8 (CH<sub>3</sub>), 32.9 (CH<sub>2</sub>), 29.1 (CH), 21.7 (CH<sub>3</sub>), 5.4 (2CH<sub>2</sub>) ppm; HRMS (ES-TOF): m/z: calcd for C<sub>28</sub>H<sub>35</sub>N<sub>4</sub>O<sub>7</sub>S<sub>3</sub>: 635.1662, found 635.1680 [M+H]<sup>+</sup>. Crystals suitable for single crystal X-ray diffraction were grown by slow evaporation of a solution of 109 in CH<sub>2</sub>Cl<sub>2</sub>.

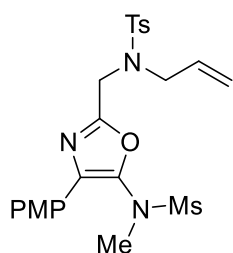
## Cobalt-catalysed polycyclisation products

### General Procedure 9: cobalt catalysis (GP9)

The relevant ynamide (1.0 eq.), *N*-pivaloxy amide (1.0–1.5 eq.), Cp\*CoI<sub>2</sub>(CO) (2.5 mol%) and NaOAc (5 mol%) were dissolved in TFE (0.1 M wrt ynamide) and stirred at the given temperature until TLC indicated consumption of either the ynamide or *N*-pivaloxy amide, at which point the solvent was removed under reduced pressure (10 min at 10 mbar, bath at 40 °C). The residue was dissolved in EtOAc and passed through a 3 cm pad of silica (EtOAc) and concentrated under reduced pressure (10 min at 10 mbar, bath at 40 °C). The residue was then heated at reflux in dioxane (0.1 M wrt ynamide) for the stated time and concentrated under reduced pressure. Purification by flash column chromatography or recrystallisation gave the corresponding Diels–Alder product.

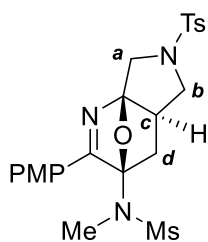
### Products derived from alkene tethered *N*-(pivaloyloxy)amides (Chapter 2.2.4)

#### *N*-Allyl-*N*-((4-(4-methoxyphenyl)-5-(*N*-methylmethylsulfonamido)oxazol-2-yl)methyl)-4-methylbenzenesulfonamide **119**



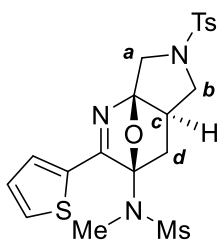
Following **GP9** with amide **118a** (386 mg, 1.05 mmol), ynamide **44i** (233 mg, 1.00 mmol), Cp\*CoI<sub>2</sub>(CO) (11.9 mg, 2.5 mol%) and NaOAc (4.10 mg, 5 mol%) for 2 h at r.t. After filtration through silica, the crude reaction mixture was purified by flash column chromatography (7:3 hexane/EtOAc) to give oxazole **119** as a white foam that was characterised by <sup>1</sup>H NMR only and used in the optimisation study (356 mg, 70%); <sup>1</sup>H NMR (300 MHz, CDCl<sub>3</sub>): δ = 7.77 (d<sub>AA'</sub>XX', *J* = 9.0, 2H), 7.69 (d<sub>AA'</sub>XX', *J* = 8.3 Hz, 2H), 7.27 (d<sub>AA'</sub>XX', *J* = 8.3 Hz, 2H), 6.93 (d<sub>AA'</sub>XX', *J* = 9.0 Hz, 2H), 5.67 (ddt, *J* = 17.5, 9.9, 6.5 Hz, 1H), 5.24 – 5.13 (m, 2H), 4.49 (s, 2H), 3.90 (dt, *J* = 6.5, 1.3 Hz, 2H), 3.83 (s, 3H), 3.25 (s, 3H), 3.07 (s, 3H), 2.35 (s, 3H) ppm.

***N*–((3*R*,4*aR*,7*aR*)–2–(4–Methoxyphenyl)–6–tosyl–4*a*,5,6,7–tetrahydro–3,7*a*–epoxypyrrolo[3,4–*b*]pyridin–3(4*H*)–yl)–*N*–methylethanesulfonamide 120*a***



Following **GP9** with amide **118a** (81.1 mg, 0.22 mmol), ynamide **44i** (46.5 mg, 0.20 mmol), Cp\*CoI<sub>2</sub>(CO) (2.4 mg, 2.5 mol%) and NaOAc (0.84 mg, 5 mol%) for 3 h at r.t. followed by 24 h at 101 °C. Purification by flash column chromatography (6:4 hexane/EtOAc) gave **120a** as a pale beige powder (66.6 mg, 66%); mp: (dec.) 207–209 °C; IR (neat):  $\nu$  = 2926, 1606, 1512, 1345, 1252, 1158 cm<sup>–1</sup>; <sup>1</sup>H NMR (400 MHz, CDCl<sub>3</sub>):  $\delta$  = 7.89 (d<sub>AA'XX'</sub>, *J* = 8.9 Hz, 2H), 7.76 (d<sub>AA'XX'</sub>, *J* = 8.1 Hz, 2H), 7.33 (d<sub>AA'XX'</sub>, *J* = 8.1 Hz, 2H), 6.92 (d<sub>AA'XX'</sub>, *J* = 8.9 Hz, 2H), 4.10 (d, *J*<sub>AB</sub> = 12.0 Hz, 1H<sub>a</sub>), 3.92 – 3.86 (m, 1H<sub>a</sub>+1H<sub>b</sub>), 3.84 (s, 3H), 2.92 – 2.86 (m, 1H<sub>b</sub>+3H), 2.77 (s, 3H), 2.47 (dd, *J* = 13.5, 2.8 Hz, 1H<sub>d</sub>), 2.42 (s, 3H), 2.35 – 2.25 (m, 1H<sub>c</sub>), 1.86 (dd, *J* = 13.5, 7.5 Hz, 1H<sub>d</sub>) ppm; <sup>13</sup>C NMR (101 MHz, CDCl<sub>3</sub>):  $\delta$  = 172.4 (C), 162.8 (C), 143.8 (C), 134.1 (C), 129.9 (2CH), 128.9 (2CH), 127.7 (2CH), 122.1 (C), 114.6 (2CH), 104.5 (C), 102.4 (C), 55.6 (CH<sub>3</sub>), 53.2 (C<sub>b</sub>H<sub>2</sub>), 49.7 (C<sub>a</sub>H<sub>2</sub>), 46.2 (C<sub>c</sub>H), 38.9 (CH<sub>3</sub>), 36.3 (CH<sub>3</sub>), 32.6 (C<sub>d</sub>H<sub>2</sub>), 21.7 (CH<sub>3</sub>) ppm; HRMS (ES–TOF): *m/z*: calcd for C<sub>23</sub>H<sub>28</sub>N<sub>3</sub>O<sub>6</sub>S<sub>2</sub>: 506.1414, found 506.1423 [M+H]<sup>+</sup>. Crystals suitable for single crystal X-ray diffraction were grown by diffusion of hexane into a solution of **120a** in CH<sub>2</sub>Cl<sub>2</sub>.

***N*–Methyl–*N*–((3*R*,4*aR*,7*aR*)–2–(thiophen–2–yl)–6–tosyl–4*a*,5,6,7–tetrahydro–3,7*a*–epoxypyrrolo[3,4–*b*]pyridin–3(4*H*)–yl)methanesulfonamide 120*b***

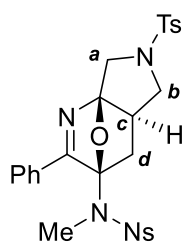


Following **GP9** with amide **118a** (88.4 mg, 0.24 mmol), ynamide **44j** (43.0 mg, 0.20 mmol), Cp\*CoI<sub>2</sub>(CO) (2.4 mg, 2.5 mol%) and NaOAc (0.84 mg, 5 mol%) for 4 h at r.t. followed by 18 h at 101 °C. Purification by flash column chromatography (6:4 hexane/EtOAc) gave **120b** as a white powder (70.1 mg, 73%); mp: (dec.) 230–231 °C; IR (neat):  $\nu$  = 1585, 1343, 1280, 1237, 1159



cm<sup>-1</sup>; <sup>1</sup>H NMR (400 MHz, CDCl<sub>3</sub>): δ = 7.83 (dd, *J* = 3.8, 1.0 Hz, 1H), 7.75 (d<sub>AA'XX'</sub>, *J* = 8.1 Hz, 2H), 7.55 (dd, *J* = 5.0, 1.0 Hz, 1H), 7.33 (d<sub>AA'XX'</sub>, *J* = 8.1 Hz, 2H), 7.11 (dd, *J* = 5.0, 3.8 Hz, 1H), 4.07 (d, *J*<sub>AB</sub> = 12.0 Hz, 1H<sub>a</sub>), 3.90 (d, *J*<sub>AB</sub> = 12.0 Hz, 1H<sub>a</sub>), 3.88 (dd, *J* = 9.8, 8.5 Hz, 1H<sub>b</sub>), 2.99 (s, 3H), 2.90 (app. t, *J* = 9.9 Hz, 1H<sub>b</sub>), 2.82 (s, 3H), 2.43 (s, 3H), 2.38 – 2.27 (m, 1H<sub>c</sub>+1H<sub>d</sub>), 1.84 (dd, *J* = 13.7, 7.8 Hz, 1H<sub>d</sub>) ppm; <sup>13</sup>C NMR (101 MHz, CDCl<sub>3</sub>): δ = 168.1 (C), 143.8 (C), 134.2 (C), 132.4 (C), 132.0 (CH), 131.1 (CH), 129.9 (2CH), 128.7 (CH), 127.7 (2CH), 105.0 (C), 102.3 (C), 53.1 (C<sub>b</sub>H<sub>2</sub>), 49.5 (C<sub>a</sub>H<sub>2</sub>), 46.3 (CH<sub>c</sub>), 39.0 (CH<sub>3</sub>), 36.4 (CH<sub>3</sub>), 32.8 (C<sub>d</sub>H<sub>2</sub>), 21.7 (CH<sub>3</sub>) ppm; HRMS (ES–TOF): *m/z*: calcd for C<sub>20</sub>H<sub>24</sub>N<sub>3</sub>O<sub>5</sub>S<sub>3</sub>: 482.0873, found 482.0883 [M+H]<sup>+</sup>.

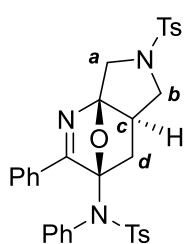
***N*-Methyl-4-nitro-*N*-((3*R*,4*aR*,7*aR*)-2-phenyl-6-tosyl-4*a*,5,6,7-tetrahydro-3,7*a*-epoxypyrrolo[3,4-*b*]pyridin-3(4*H*)-yl)benzenesulfonamide **120c****



Following **GP9** with amide **118a** (133 mg, 0.36 mmol), ynamide **44h** (94.9 mg, 0.30 mmol), Cp\*CoI<sub>2</sub>(CO) (3.6 mg, 2.5 mol%) and NaOAc (1.28 mg, 5 mol%) for 4 h at 50 °C followed by 24 h at 101 °C. Purification by flash column chromatography (7:3 heptane/EtOAc) gave **120c** as a yellow powder (71.2 mg, 41%); mp: 173–176 °C; IR (neat): ν = 2923, 1530, 1348, 1160, 1103, 1058 cm<sup>-1</sup>; <sup>1</sup>H NMR (400 MHz, CDCl<sub>3</sub>): δ = 8.29 (d<sub>AA'XX'</sub>, *J* = 8.9 Hz, 2H), 7.97 (d<sub>AA'XX'</sub>, *J* = 8.9 Hz, 2H), 7.94 – 7.90 (m, 2H), 7.71 (d<sub>AA'XX'</sub>, *J* = 8.1 Hz, 2H), 7.57 – 7.44 (m, 3H), 7.35 (d<sub>AA'XX'</sub>, *J* = 8.1 Hz, 2H), 4.15 (d, *J*<sub>AB</sub> = 11.8 Hz, 1H<sub>a</sub>), 3.85 (dd, *J* = 9.6, 7.8 Hz, 1H<sub>b</sub>), 3.71 (d, *J*<sub>AB</sub> = 11.8 Hz, 1H<sub>a</sub>), 2.96 (s, 3H), 2.61 (app. t, *J* = 9.8 Hz, 1H<sub>b</sub>), 2.47 (s, 3H), 2.35 – 2.25 (m, 1H<sub>c</sub>+H<sub>d</sub>), 2.00 (dd, *J* = 13.6, 8.0 Hz, 1H<sub>d</sub>) ppm; <sup>13</sup>C NMR (101 MHz, CDCl<sub>3</sub>): δ = 173.3 (C), 150.4 (C), 145.2 (C), 144.2 (C), 134.2 (C), 132.2 (CH), 130.0 (2CH), 129.8 (C), 129.3 (2CH), 128.6 (2CH), 127.6 (2CH), 126.8 (2CH), 124.5 (2CH), 105.1 (C), 102.4 (C), 52.8 (C<sub>b</sub>H<sub>2</sub>), 49.5 (C<sub>a</sub>H<sub>2</sub>),

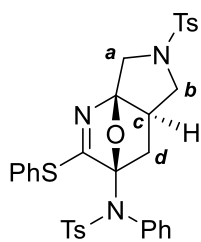
46.0 (C<sub>6</sub>H), 36.2 (CH<sub>3</sub>), 32.4 (C<sub>d</sub>H<sub>2</sub>), 21.6 (CH<sub>3</sub>) ppm; HRMS (ES–TOF): m/z: calcd for C<sub>27</sub>H<sub>26</sub>N<sub>4</sub>O<sub>7</sub>S<sub>2</sub>Na: 605.1135, found 605.1140 [M+Na]<sup>+</sup>.

**4-Methyl-N-phenyl-N-((3R,4aR,7aR)-2-phenyl-6-tosyl-4a,5,6,7-tetrahydro-3,7a-epoxypyrrolo[3,4-b]pyridin-3(4H)-yl)benzenesulfonamide 120d**



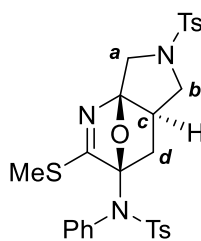
Following **GP9** with amide **118a** (81.1 mg, 0.22 mmol), ynamide **44f** (69.5 mg, 0.20 mmol), Cp\*CoI<sub>2</sub>(CO) (2.4 mg, 2.5 mol%) and NaOAc (0.85 mg, 5 mol%) for 3 h at r.t. followed by 72 h at 101 °C. Purification by flash column chromatography (6:4 hexane/EtOAc) gave **120d** as a white powder (62.4 mg, 51%); mp: (dec.) 200 °C; IR (neat): ν = 1596, 1492, 1450, 1353, 1278, 1162 cm<sup>-1</sup>; *restricted rotation around the NTsPh sulfonamide results in broadening within the NMR*: <sup>1</sup>H NMR (300 MHz, CDCl<sub>3</sub>): δ = 8.03 – 7.92 (m, 2H), 7.73 (d<sub>AA'XX'</sub>, *J* = 8.2 Hz, 2H), 7.53 – 7.43 (m, 3H), 7.38 – 7.18 (m, 8H), 7.12 (d<sub>AA'XX'</sub>, *J* = 8.2 Hz, 2H), 6.61 (br. app. s, 1H), 4.17 (d, *J*<sub>AB</sub> = 11.9 Hz, 1H<sub>a</sub>), 4.07 (d, *J*<sub>AB</sub> = 11.9 Hz, 1H<sub>a</sub>), 3.69 (app. t, *J* = 9.1 Hz, 1H<sub>b</sub>), 2.69 (app. t, *J* = 10.0 Hz, 1H<sub>b</sub>), 2.43 (s, 3H), 2.40 (s, 3H), 2.22 – 2.10 (m, 1H<sub>c</sub>), 1.59 – 1.37 (m, 2H<sub>d</sub>) ppm; <sup>13</sup>C NMR (101 MHz, CDCl<sub>3</sub>): δ = 174.7 (C), 144.2 (C), 143.5 (CH), 137.1 (C), 134.7 (C), 134.2 (C), 132.1 (C), 131.0 (CH), 129.7 (4CH), 129.4 (4CH), 129.3 (C), 128.9 (2CH), 128.7 (2CH), 127.5 (2CH), 126.7 (2CH), 104.4 (C), 101.9 (C), 52.3 (C<sub>b</sub>H<sub>2</sub>), 49.8 (C<sub>a</sub>H<sub>2</sub>), 45.3 (C<sub>c</sub>H), 32.7 (C<sub>d</sub>H<sub>2</sub>), 21.7 (CH<sub>3</sub>), 21.5 (CH<sub>3</sub>) ppm; HRMS (ES–TOF): m/z: calcd for C<sub>33</sub>H<sub>32</sub>N<sub>3</sub>O<sub>5</sub>S<sub>2</sub>: 614.1778, found 614.1788 [M+H]<sup>+</sup>.

**4-Methyl-N-phenyl-N-((3R,4aR,7aR)-2-(phenylthio)-6-tosyl-4a,5,6,7-tetrahydro-3,7a-epoxypyrrolo[3,4-b]pyridin-3(4H)-yl)benzenesulfonamide 120e**



Following **GP9** with amide **118a** (88.4 mg, 0.24 mmol), ynamide **44p** (75.9 mg, 0.20 mmol),  $\text{Cp}^*\text{CoI}_2(\text{CO})$  (2.4 mg, 2.5 mol%) and NaOAc (0.84 mg, 5 mol%) for 2 h at 50 °C followed by 22 h at 101 °C. Purification by flash column chromatography (7:3 hexane/EtOAc) gave **120e** as a white powder (106 mg, 82%); mp: (dec.) 205–207 °C; IR (neat):  $\nu = 2921, 2851, 1597, 1540, 1487, 1347, 1307, 1157 \text{ cm}^{-1}$ ; *restricted rotation around the NTsPh sulfonamide results in broadening within the NMR*:  $^1\text{H}$  NMR (400 MHz,  $\text{CDCl}_3$ ):  $\delta = 7.69 (\text{d}_{\text{AA}'\text{XX}'}, J = 8.2 \text{ Hz}, 2\text{H}), 7.54 - 7.51 (\text{m}, 2\text{H}), 7.49 (\text{d}_{\text{AA}'\text{XX}'}, J = 8.2 \text{ Hz}, 2\text{H}), 7.40 - 7.32 (\text{m}, 4\text{H}), 7.31 - 7.22 (\text{m}, 5\text{H}), 7.17 (\text{d}_{\text{AA}'\text{XX}'}, J = 8.1 \text{ Hz}, 2\text{H}), 7.00 (\text{br. app. s}, 1\text{H}), 3.97 (\text{d}, J_{\text{AB}} = 11.9 \text{ Hz}, 1\text{H}_a), 3.89 (\text{d}, J_{\text{AB}} = 11.9 \text{ Hz}, 1\text{H}_a), 3.62 (\text{dd}, J = 9.5, 8.5 \text{ Hz}, 1\text{H}_b), 2.68 (\text{app. t}, J = 9.9 \text{ Hz}, 1\text{H}_b), 2.44 (\text{s}, 3\text{H}), 2.43 (\text{s}, 3\text{H}), 2.11 - 2.03 (\text{m}, 1\text{H}_c), 1.49 - 1.39 (\text{m}, 2\text{H}_d) \text{ ppm}$ ;  $^{13}\text{C}$  NMR (101 MHz,  $\text{CDCl}_3$ ):  $\delta = 179.0 (\text{C}), 144.4 (\text{C}), 143.6 (\text{C}), 137.2 (\text{C}), 135.3 (\text{C}), 134.6 (\text{C}), 133.9 (2\text{CH}), 131.5 (2\text{CH}), 129.8 (2\text{CH}), 129.53 (\text{CH}), 129.48 (4\text{CH}), 129.4 (2\text{CH}), 129.2 (3\text{CH}), 128.9 (\text{C}), 127.6 (2\text{CH}), 106.4 (\text{C}), 103.1 (\text{C}), 52.1 (\text{C}_b\text{H}_2), 49.7 (\text{C}_a\text{H}_2), 45.9 (\text{C}_c\text{H}), 33.4 (\text{C}_d\text{H}_2), 21.8 (\text{CH}_3), 21.7 (\text{CH}_3) \text{ ppm}$ ; HRMS (ES-TOF):  $m/z$ : calcd for  $\text{C}_{33}\text{H}_{32}\text{N}_3\text{O}_5\text{S}_3$ : 646.1499, found 646.1507  $[\text{M}+\text{H}]^+$ .

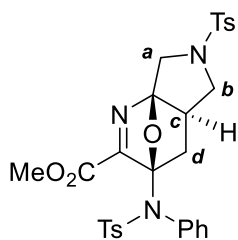
**4-Methyl-N-((3R,4aR,7aR)-2-(methylthio)-6-tosyl-4a,5,6,7-tetrahydro-3,7a-epoxypyrrolo[3,4-b]pyridin-3(4H)-yl)-N-phenylbenzenesulfonamide 120f**



Following **GP9** with amide **118a** (884 mg, 2.40 mmol), ynamide **44a** (635 mg, 2.00 mmol),  $\text{Cp}^*\text{CoI}_2(\text{CO})$  (29.8 mg, 2.5 mol%) and NaOAc (8.2 mg, 5 mol%) for 14 h at 50 °C followed by 20 h at 101 °C. Purification by hot recrystallisation (EtOH, 911 mg) and flash column chromatography of the filtrate (7:3 hexane/EtOAc, 128 mg) gave **120f** as a grey solid (1.04 g, 89%); mp: (dec.)

204–205 °C; IR (neat):  $\nu$  = 2958, 1497, 1535, 1355, 1344, 1174, 1158, 1089, 1051, 1042  $\text{cm}^{-1}$ ; *restricted rotation around the NTsPh sulfonamide results in broadening within the NMR*:  $^1\text{H}$  NMR (400 MHz,  $\text{CDCl}_3$ ):  $\delta$  = 7.73 ( $d_{\text{AA'XX'}}$ ,  $J$  = 8.3 Hz, 2H), 7.47 ( $d_{\text{AA'XX'}}$ ,  $J$  = 8.1 Hz, 2H), 7.34 – 7.29 (m, 3H), 7.22 (t,  $J$  = 7.7, 2H), 7.15 (d,  $J$  = 8.1 Hz, 2H), 6.94 (br. app. s, 2H), 4.05 (d,  $J_{\text{AB}}$  = 11.9 Hz, 1H<sub>a</sub>), 3.94 (d,  $J_{\text{AB}}$  = 11.9 Hz, 1H<sub>a</sub>), 3.67 (dd,  $J$  = 9.7, 8.3 Hz, 1H<sub>b</sub>), 2.70 (app. t,  $J$  = 9.9 Hz, 1H<sub>b</sub>), 2.45 (s, 3H), 2.44 (s, 3H), 2.43 (s, 3H), 2.15 – 2.04 (m, 1H<sub>c</sub>), 1.45 (dd,  $J$  = 12.6, 3.0 Hz, 1H<sub>d</sub>), 1.29 (dd,  $J$  = 12.6, 7.5 Hz, 1H) ppm;  $^{13}\text{C}$  NMR (101 MHz,  $\text{CDCl}_3$ ):  $\delta$  = 180.6 (C), 144.3 (C), 143.6 (C), 137.2 (C), 135.4 (C), 134.5 (C), 131.6 (2CH), 129.8 (2CH), 129.5 (CH), 129.3 (2CH), 129.2 (2CH), 129.1 (2CH), 127.6 (2CH), 106.4 (C), 103.0 (C), 52.4 (C<sub>b</sub>H<sub>2</sub>), 49.7 (C<sub>a</sub>H<sub>2</sub>), 46.2 (C<sub>c</sub>H), 33.7 (C<sub>d</sub>H<sub>2</sub>), 21.8 (CH<sub>3</sub>), 21.7 (CH<sub>3</sub>), 14.5 (SCH<sub>3</sub>) ppm; HRMS (ES–TOF):  $m/z$ : calcd for  $\text{C}_{28}\text{H}_{30}\text{N}_3\text{O}_5\text{S}_3$ : 584.1342, found 584.1350  $[\text{M}+\text{H}]^+$ .

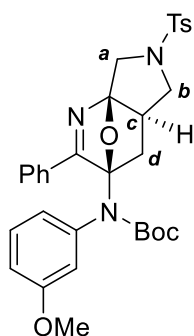
***Methyl (3R,4aR,7aR)–3–((4-methyl-N-phenylphenyl)sulfonamido)–6-tosyl–3,4,4a,5,6,7-hexahydro–3,7a-epoxypyrrolo[3,4-b]pyridine–2-carboxylate 120g***



Following **GP9** with amide **118a** (88.4 mg, 0.24 mmol), ynamide **44k** (68.7 mg, 0.20 mmol),  $\text{Cp}^*\text{CoI}_2(\text{CO})$  (2.4 mg, 2.5 mol%) and NaOAc (0.82 mg, 5 mol%) for 4 h at r.t. followed by 18 h at 101 °C. Purification by flash column chromatography (6:4 hexane/EtOAc) and hot recrystallisation (EtOH) gave **120g** as a white solid (93.0 mg, 78%); mp: 205–206 °C; IR (neat):  $\nu$  = 2951, 1453, 1598, 1344, 1280, 1157, 1142, 1090  $\text{cm}^{-1}$ ; *restricted rotation around the NTsPh sulfonamide results in broadening within the NMR*:  $^1\text{H}$  NMR (400 MHz,  $\text{CDCl}_3$ ):  $\delta$  = 7.67 ( $d_{\text{AA'XX'}}$ ,  $J$  = 8.3 Hz, 2H), 7.50 (br. app. s, 1H), 7.40 ( $d_{\text{AA'XX'}}$ ,  $J$  = 8.2 Hz, 2H), 7.39 – 7.33 (m, 2H), 7.25 ( $d_{\text{AA'XX'}}$ ,  $J$  = 8.3 Hz, 2H), 7.19 ( $d_{\text{AA'XX'}}$ ,  $J$  = 8.2 Hz, 2H), 7.07 (br. app. s, 1H), 6.29 (br. app. s, 1H), 4.15 (d,  $J_{\text{AB}}$  = 12.2 Hz, 1H<sub>a</sub>), 4.01 (d,  $J_{\text{AB}}$  = 12.2 Hz, 1H<sub>a</sub>), 4.00 (s, 3H), 3.67 (dd,  $J$  = 9.9, 8.5 Hz, 1H<sub>b</sub>), 2.57 (app. t,  $J$  = 10.0 Hz, 1H<sub>b</sub>), 2.46 (s, 3H), 2.39 (s, 3H), 2.07 (dddd,

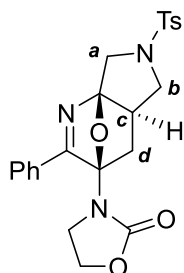
$J = 10.0, 8.5, 7.4, 3.0$  Hz,  $1H_c$ ),  $1.41$  (dd,  $J = 12.8, 7.5$  Hz,  $1H_d$ ),  $1.20$  (dd,  $J = 12.8, 3.0$ ,  $1H_d$ ) ppm;  $^{13}C$  NMR (101 MHz,  $CDCl_3$ ):  $\delta = 169.1$  (C),  $162.1$  (C),  $144.5$  (C),  $143.8$  (C),  $136.4$  (C),  $134.9$  (C),  $134.0$  (C),  $132.5$  (CH),  $129.8$  (2CH),  $129.7$  (2CH),  $129.3$  (2CH),  $129.2$  (2CH),  $128.7$  (2CH),  $127.6$  (2CH),  $105.0$  (C),  $101.4$  (C),  $53.2$  ( $CH_3$ ),  $52.3$  ( $C_{bH_2}$ ),  $49.8$  ( $C_{aH_2}$ ),  $44.1$  ( $C_{cH}$ ),  $32.1$  ( $C_{dH_2}$ ),  $21.8$  ( $CH_3$ ),  $21.6$  ( $CH_3$ ) ppm; HRMS (ES-TOF):  $m/z$ : calcd for  $C_{29}H_{30}N_3O_7S_2$ : 596.1520, found 596.1527  $[M+H]^+$ .

***tert*-Butyl (3-methoxyphenyl)((3*R*,4*aR*,7*aR*)-2-phenyl-6-tosyl-4*a*,5,6,7-tetrahydro-3,7*a*-epoxypyrrolo[3,4-*b*]pyridin-3(4*H*)-yl)carbamate **120h****



Following **GP9** with amide **118a** (166 mg, 0.45 mol), ynamide **44g** (97.0 mg, 0.30 mmol),  $Cp^*CoI_2(CO)$  (3.6 mg, 2.5 mol%) and NaOAc (1.3 mg, 5 mol%) for 4 h at  $50^\circ C$  followed by 20 h at  $101^\circ C$ . Purification by flash column chromatography (7:3 heptane/EtOAc) gave **120h** as a white powder (87.2 mg, 50%); mp:  $176-178^\circ C$ ; IR (neat):  $\nu = 2977, 1714, 1607, 1586, 1485, 1322, 1309, 1159, 1046\text{ cm}^{-1}$ ;  $^1H$  NMR (400 MHz,  $CDCl_3$ ):  $\delta = 7.92$  (d,  $J = 7.1$  Hz, 2H),  $7.75$  ( $d_{AA'XX'}$ ,  $J = 8.0$  Hz, 2H),  $7.51 - 7.24$  (m, 6H),  $7.04 - 6.88$  (m, 2H),  $6.63$  (br. app. s, 1H),  $4.16$  (d,  $J_{AB} = 11.9$  Hz,  $1H_a$ ),  $3.98 - 3.71$  (m, 5H),  $2.73$  (app. t,  $J = 9.9$  Hz, 1H),  $2.44$  (s, 3H),  $2.23 - 2.11$  (m,  $1H_c$ ),  $1.39$  (br. s,  $2H_d$ ),  $1.07$  (s, 9H) ppm;  $^{13}C$  NMR (101 MHz,  $CDCl_3$ ):  $\delta = 174.8$  (C),  $153.6$  (C),  $143.7$  (C),  $140.6$  (C),  $134.3$  (C),  $132.0$  (C),  $131.1$  (CH),  $130.0$  (CH),  $129.9$  (2CH),  $128.8$  (2CH),  $127.7$  (2CH),  $126.2$  (2CH),  $121.4$  (CH),  $116.2$  (C),  $114.5$  (CH),  $113.0$  (CH),  $104.3$  (C),  $100.6$  (C),  $83.1$  (C),  $55.6$  ( $CH_3$ ),  $52.8$  ( $C_{bH_2}$ ),  $49.8$  ( $C_{aH_2}$ ),  $45.4$  ( $C_{cH}$ ),  $32.1$  ( $C_{dH_2}$ ),  $27.7$  ( $3CH_3$ ),  $21.7$  ( $CH_3$ ) ppm; HRMS (ES-TOF):  $m/z$ : calcd for  $C_{32}H_{35}N_3O_6SNa$ : 612.2139, found 612.2143  $[M+Na]^+$ .

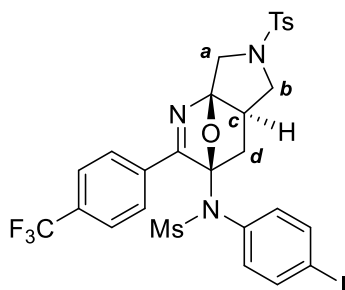
**3-((3*R*,4*aR*,7*aR*)-2-Phenyl-6-tosyl-4*a*,5,6,7-tetrahydro-3,7*a*-epoxypyrrolo[3,4-*b*]pyridin-3(4*H*)-yl)oxazolidin-2-one 120i**



Following **GP9** with amide **118a** (166 mg, 0.45 mmol), ynamide **44o** (56.2 mg, 0.30 mmol), Cp\*CoI<sub>2</sub>(CO) (3.6 mg, 2.5 mol%) and NaOAc (1.25 mg, 5 mol%) for 5 h at r.t. followed by 18 h at 101 °C. Flash column chromatography (4:6 hexane/EtOAc) and hot recrystallisation (EtOH) gave **120i** as a white powder (78.3 mg, 58%); mp: 245–248 °C; IR (neat):  $\nu$  = 3676,

2989, 2902, 1761, 1411, 1342, 1167, 1065 cm<sup>-1</sup>; <sup>1</sup>H NMR (400 MHz, CDCl<sub>3</sub>):  $\delta$  = 7.75 (d<sub>AA'XX'</sub>,  $J$  = 7.9 Hz, 2H), 7.69 (d,  $J$  = 7.5 Hz, 2H), 7.52 (t,  $J$  = 7.5 Hz, 1H), 7.46 (t,  $J$  = 7.5 Hz, 2H), 7.36 (d<sub>AA'XX'</sub>,  $J$  = 7.9 Hz, 2H), 4.31 (app. q,  $J$  = 8.4 Hz, 1H), 4.27 – 4.19 (m, 1H), 4.19 (d,  $J_{AB}$  = 11.7 Hz, 1H<sub>a</sub>), 3.94 (app. t,  $J$  = 8.9 Hz, 1H<sub>b</sub>), 3.78 (d,  $J_{AB}$  = 11.7 Hz, 1H<sub>a</sub>), 3.75 – 3.65 (m, 1H), 3.33 (app. q,  $J$  = 8.4 Hz, 1H), 2.98 (app. t,  $J$  = 9.9 Hz, 1H<sub>b</sub>), 2.73 – 2.67 (m, 1H<sub>d</sub>), 2.44 (s, 3H), 2.42 – 2.30 (m, 1H<sub>c</sub>), 2.08 (dd,  $J$  = 12.9, 7.5 Hz, 1H<sub>d</sub>) ppm; <sup>13</sup>C NMR (101 MHz, CDCl<sub>3</sub>):  $\delta$  = 174.1 (C), 156.1 (C), 143.8 (C), 134.1 (C), 132.1 (CH), 130.1 (C), 130.0 (2CH), 129.4 (2CH), 127.7 (2CH), 126.3 (2CH), 105.4 (C), 99.2 (C), 62.4 (CH<sub>2</sub>), 53.0 (C<sub>b</sub>H<sub>2</sub>), 49.7 (C<sub>a</sub>H<sub>2</sub>), 45.3 (C<sub>c</sub>H), 43.9 (CH<sub>2</sub>), 30.7 (C<sub>d</sub>H<sub>2</sub>), 21.7 (CH<sub>3</sub>) ppm; HRMS (ES–TOF):  $m/z$ : calcd for C<sub>23</sub>H<sub>24</sub>N<sub>3</sub>O<sub>5</sub>S: 451.1431, found 454.1433 [M+H]<sup>+</sup>.

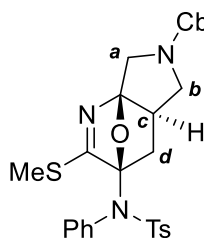
***N*-(4-Iodophenyl)-*N*-((3*R*,4*aR*,7*aR*)-6-tosyl-2-(4-(trifluoromethyl)phenyl)-4*a*,5,6,7-tetrahydro-3,7*a*-epoxypyrrolo[3,4-*b*]pyridin-3(4*H*)-yl)methanesulfonamide 120j**



Following **GP9** with amide **118a** (133 mg, 0.36 mmol), ynamide **44q** (137 mg, 0.30 mmol), Cp\*CoI<sub>2</sub>(CO) (3.6 mg, 2.5 mol%) and NaOAc (1.2 mg, 5 mol%) for 14 h at 50 °C followed by 14 h at 101 °C. Purification by flash column chromatography (7:3 hexane/EtOAc) gave **120j** as a white powder (50.0 mg, 23%); mp:

(dec.) 229–230 °C; IR (neat):  $\nu$  = 2920, 2851, 1480, 1358, 1340, 1320, 1279, 1154, 1127, 1110, 1068, 581, 760, 661  $\text{cm}^{-1}$ ; *restricted rotation around the MsNAr sulfonamide results in broadening within the NMR*:  $^1\text{H}$  NMR (400 MHz,  $\text{CDCl}_3$ ):  $\delta$  = 7.94 ( $d_{\text{AA'XX'}}$ ,  $J$  = 8.1 Hz, 2H), 7.81 ( $d_{\text{AA'XX'}}$ ,  $J$  = 8.0 Hz, 2H), 7.78 (br. app. s, 2H), 7.69 ( $d_{\text{AA'XX'}}$ ,  $J$  = 8.1 Hz, 2H), 7.39 ( $d_{\text{AA'XX'}}$ ,  $J$  = 8.0 Hz, 2H), 6.88 (br. app. s, 2H), 4.16 (d,  $J_{\text{AB}}$  = 12.3 Hz, 1H<sub>a</sub>), 4.08 (d,  $J_{\text{AB}}$  = 12.3 Hz, 1H<sub>a</sub>), 3.83 (dd,  $J$  = 9.9, 8.5, 1H<sub>b</sub>), 2.86 (app. t,  $J$  = 9.9, 1H<sub>b</sub>), 2.78 (s, 3H), 2.43 (s, 3H), 2.31 – 2.22 (m, 1H<sub>c</sub>), 1.73 (br. s, 1H<sub>d</sub>), 1.44 (br. s, 1H<sub>d</sub>) ppm;  $^{13}\text{C}$  NMR (101 MHz,  $\text{CDCl}_3$ ):  $\delta$  = 173.3 (C), 144.0 (C), 139.1 (2CH), 137.0 (C), 135.0 (C), 134.1 (C), 132.9 (C), 129.8 (2CH), 128.0 (2CH), 127.1 (2CH), 125.8 (2CH), 104.9 (C), 96.1 (C), 52.5 (C<sub>b</sub>H<sub>2</sub>), 49.6 (C<sub>a</sub>H<sub>2</sub>), 45.3 (C<sub>c</sub>H), 39.6 (CH<sub>3</sub>), 32.8 (C<sub>d</sub>H<sub>2</sub>), 21.7 (CH<sub>3</sub>) ppm; *one quaternary carbon, CF<sub>3</sub> and 2CH next to CF<sub>3</sub> not observed in  $^{13}\text{C}$  NMR spectra*; HRMS (ES–TOF):  $m/z$ : calcd for  $\text{C}_{28}\text{H}_{25}\text{N}_3\text{O}_5\text{F}_3\text{S}_2\text{INa}$ : 754.0125 found, 754.0139  $[\text{M}+\text{Na}]^+$ .

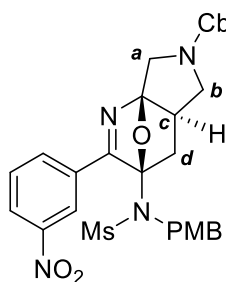
***Benzyl (3R,4aR,7aR)–3–((4-methyl–N-phenylphenyl)sulfonamido)–2–(methylthio)–3,4,4a,5-tetrahydro–3,7a-epoxypyrrolo[3,4-b]pyridine–6(7H)–carboxylate 136a***



Following **GP9** with amide **118b** (125 mg, 0.36 mmol), ynamide **44a** (95.2 mg, 0.30 mmol),  $\text{Cp}^*\text{CoI}_2(\text{CO})$  (3.6 mg, 2.5 mol%) and NaOAc (1.2 mg, 5 mol%) for 12 h at 50 °C followed by 24 h at 101 °C. Purification by hot recrystallisation (EtOH) gave **136a** as a pale brown powder (144 mg, 85%); mp: 198–200 °C; IR (neat):  $\nu$  = 2923, 1710, 1551, 1441, 1409, 1350, 1313, 1165, 1118  $\text{cm}^{-1}$ ; *NMR spectra display a mixture of rotamers in a 1:1 ratio*;  $^1\text{H}$  NMR (400 MHz,  $\text{CDCl}_3$ ):  $\delta$  = 7.55 ( $d_{\text{AA'XX'}}$ ,  $J$  = 8.2 Hz, 2H), 7.43 – 7.32 (m, 6H), 7.26 (s, 2H), 7.18 ( $d_{\text{AA'XX'}}$ ,  $J$  = 8.2 Hz, 2H), 7.08 (br. app. s, 2H), 5.20 and 5.16 (d,  $J_{\text{AB}}$  = 13.5 Hz, 2H), 4.16 (d,  $J_{\text{AB}}$  = 12.6 Hz, 1H), 4.07 and 4.04 (d,  $J_{\text{AB}}$  = 12.7 Hz, 1H<sub>a</sub>), 3.86 and 3.81 (dd,  $J$  = 10.6, 8.6, 1H<sub>b</sub>), 2.86 and 2.86 (app. t,  $J$  = 10.4 Hz, 1H<sub>b</sub>), 2.52 and 2.50 (s, 3H), 2.40 and 2.40 (s, 3H), 2.29 – 2.17 (m, 1H<sub>c</sub>),

1.51 and 1.49 (dd,  $J = 12.6, 3.0$  Hz,  $1H_d$ ), 1.36 (dd,  $J = 12.6, 7.5$  Hz,  $1H_d$ ) ppm;  $^{13}C$  NMR (101 MHz,  $CDCl_3$ ):  $\delta = 180.8$  and  $180.6$  (C),  $154.8$  (C),  $144.3$  and  $144.3$  (C),  $137.3$  and  $137.2$  (C),  $136.8$  (C),  $135.5$  and  $135.5$  (C),  $131.7$  (2CH),  $129.5$  (CH),  $129.4$  (CH),  $129.3$  (2CH),  $129.2$  (2CH),  $128.7$  (2CH),  $128.2$  and  $128.2$  (2CH),  $127.9$  (2CH),  $106.8$  and  $106.1$  (C),  $103.0$  and  $130.0$  (C),  $67.2$  and  $67.1$  ( $CH_2$ ),  $50.9$  and  $50.8$  ( $C_bH_2$ ),  $48.6$  and  $48.4$  ( $C_aH_2$ ),  $46.1$  and  $45.3$  ( $C_cH$ ),  $34.1$  ( $C_dH_2$ ),  $21.8$  ( $CH_3$ ),  $14.5$  and  $14.5$  ( $CH_3$ ) ppm; HRMS (ES-TOF):  $m/z$ : calcd for  $C_{29}H_{30}N_3O_5S_2$ : 564.1621, found 564.1630  $[M+H]^+$ .

***Benzyl (3R,4aR,7aR)-3-(N-(4-methoxybenzyl)methylsulfonamido)-2-(3-nitrophenyl)-3,4,4a,5-tetrahydro-3,7a-epoxypyrrolo[3,4-b]pyridine-6(7H)-carboxylate 136b***

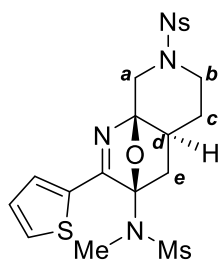


Following **GP9** with amide **118b** (128 mg, 0.37 mmol), ynamide **44t** (108 mg, 0.30 mmol),  $Cp^*CoI_2(CO)$  (3.6 mg, 2.5 mol%) and NaOAc (1.3 mg, 5 mol%) for 4 h at r.t. followed by 72 h at 101 °C. Purification by flash column chromatography (7:3 hexane/EtOAc) gave **136b** as a white powder (83.2 mg, 46%); mp: 158–160 °C; IR (neat):  $\nu = 1701, 1612, 1531, 1501, 1418, 1344, 1234, 1156$   $cm^{-1}$ ;  $^1H$  NMR (400 MHz,  $CDCl_3$ ):  $\delta = 8.51$  (br. s, 1H),  $8.26$  (dd,  $J = 8.1, 1.0$  Hz, 1H),  $8.09$  (tt,  $J = 8.1, 1.3$  Hz, 1H),  $7.56$  (t,  $J = 8.0$  Hz, 1H),  $7.45 - 7.31$  (m, 7H),  $6.82$  (br. s, 2H),  $5.20$  (d,  $J = 8.0$  Hz, 2H),  $4.71$  (br. s, 1H),  $4.52$  (app t,  $J = 14.8$  Hz, 1H),  $4.27$  (dd,  $J = 12.8, 1.8$  Hz, 1H),  $4.16$  (d,  $J_{AB} = 18.3$  Hz, 1H),  $4.15 - 4.03$  (m, 1H),  $3.77$  (s, 3H),  $3.18$  (app. td,  $J = 10.3, 6.5$  Hz, 1H),  $2.94$  (s, 3H),  $2.45 - 2.25$  (m, 2H),  $1.83$  (br. s, 1H) ppm;  $^{13}C$  NMR (101 MHz,  $CDCl_3$ ):  $\delta = 173.1$  and  $173$  (C),  $159.7$  (C),  $154.7$  and  $154.6$  (C),  $148.3$  (C),  $136.64$  and  $136.60$  (C),  $132.59$  and  $132.57$  (CH),  $130.6$  (br. m, C),  $129.8$  (2CH),  $129.7$  (CH),  $128.4$  and  $128.3$  (2CH),  $128.2$  (2CH),  $125.4$  (CH),  $121.8$  (CH),  $114.2$  (br. m, 2CH),  $105.3$  (C),  $104.5$  (C),  $102.10$  and  $102.08$  (C),  $67.4$  and  $67.3$  ( $CH_2$ ),  $55.4$  ( $CH_3$ ),  $51.7$  (br. m,  $CH_2$ ),  $51.5$  and  $51.3$



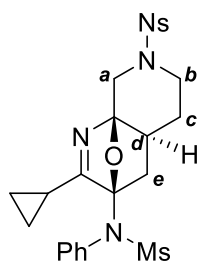
(CH<sub>2</sub>), 48.6 and 48.4 (CH<sub>2</sub>), 45.2 (CH), 44.4 (CH), 42.1 (CH<sub>3</sub>), 34.1 (br, m, CH<sub>2</sub>) ppm; HRMS (ES–TOF): m/z: calcd for C<sub>30</sub>H<sub>30</sub>N<sub>4</sub>O<sub>8</sub>SNa: 629.1677, found 629.1680 [M+Na]<sup>+</sup>.

***N*-Methyl-*N*-((3*R*,4*aS*,8*aR*)-7-((4-nitrophenyl)sulfonyl)-2-(thiophen-2-yl)-4,4*a*,5,6,7,8-hexahydro-3*H*-3,8*a*-epoxy-1,7-naphthyridin-3-yl)methanesulfonamide **137a****



Following **GP9** with amide **128b** (682 mg, 1.65 mmol), ynamide **44j** (323 mg, 1.50 mmol), Cp\*CoI<sub>2</sub>(CO) (17.8 mg, 2.5 mol%) and NaOAc (6.2 mg, 5 mol%) for 12 h at r.t. followed by 24 h at 101 °C. Purification by flash column chromatography (7:3→1:1 hexane/EtOAc) gave **137a** as a beige powder (416 mg, 53%); mp: 158–161 °C; IR (neat): ν = 1590, 1529, 1345, 1320, 1154, 1064, 960 cm<sup>-1</sup>; <sup>1</sup>H NMR (400 MHz, CDCl<sub>3</sub>): δ = 8.41 (d<sub>AA'XX'</sub>, *J* = 8.9 Hz, 2H), 8.00 (d<sub>AA'XX'</sub>, *J* = 8.9 Hz, 2H), 7.87 (dd, *J* = 3.8, 1.1 Hz, 1H), 7.55 (dd, *J* = 5.0, 1.1 Hz, 1H), 7.13 (dd, *J* = 5.1, 3.8 Hz, 1H), 4.50 (dd, *J* = 13.3, 1.8 Hz, 1H<sub>a</sub>), 3.96 – 3.87 (m, 1H<sub>b</sub>), 3.29 (d, *J* = 13.3 Hz, 1H<sub>a</sub>), 3.08 (s, 3H), 3.06 (s, 3H), 2.42 (app. td, *J* = 12.5, 2.1 Hz, 1H<sub>b</sub>), 2.21 – 2.09 (m, 1H<sub>e</sub>+1H<sub>c</sub>), 1.97 (dd, *J* = 13.1, 7.3 Hz, 1H<sub>e</sub>), 1.88 – 1.79 (m, 1H<sub>d</sub>), 1.64 (app. qd, *J* = 12.7, 3.8 Hz, 1H<sub>c</sub>), 1.56 (s, 3H) ppm; <sup>13</sup>C NMR (101 MHz, CDCl<sub>3</sub>): δ = 168.3 (C), 150.4 (C), 142.3 (C), 131.9 (CH), 131.3 (CH), 129.0 (2CH), 128.8 (CH), 124.6 (2CH), 101.6 (C), 95.2 (C), 48.5 (C<sub>a</sub>H<sub>2</sub>), 45.4 (C<sub>b</sub>H<sub>2</sub>), 39.4 (CH<sub>3</sub>), 39.3 (C<sub>d</sub>H), 36.3 (CH<sub>3</sub>), 35.0 (C<sub>e</sub>H<sub>2</sub>), 31.3 (C<sub>c</sub>H<sub>2</sub>) ppm; *one quaternary carbon resonance not observed in <sup>13</sup>C NMR spectra*; HRMS (ES–TOF): m/z: calcd for C<sub>20</sub>H<sub>22</sub>N<sub>4</sub>O<sub>7</sub>S<sub>3</sub>Na: 549.0543, found 549.0546 [M+Na]<sup>+</sup>.

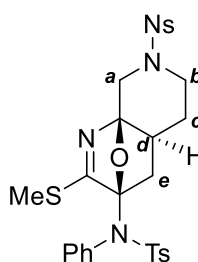
***N*–((3*R*,4*aS*,8*aR*)–2–Cyclopropyl–7–((4–nitrophenyl)sulfonyl)–4,4*a*,5,6,7,8–hexahydro–3*H*–3,8*a*–epoxy–1,7–naphthyridin–3–yl)–*N*–phenylmethanesulfonamide **137b****



Following **GP9** with amide **128b** (114 mg, 0.275 mmol), ynamide **44c** (58.8 mg, 0.25 mmol), Cp\*CoI<sub>2</sub>(CO) (3.0 mg, 2.5 mol%) and NaOAc (1.0 mg, 5 mol%) for 12 h at r.t. followed by 24 h at 101 °C. Purification by flash column chromatography (7:3→1:1 hexane/EtOAc) gave **137b** as a pale

yellow powder (95.6 mg, 70%); mp: (dec.) 202–206 °C; IR (neat):  $\nu$  = 1625, 1349, 1311, 1158, 1095, 936 cm<sup>-1</sup>; <sup>1</sup>H NMR (300 MHz, CDCl<sub>3</sub>):  $\delta$  = 8.39 (d<sub>AA'XX'</sub>,  $J$  = 8.9 Hz, 2H), 7.99 (d<sub>AA'XX'</sub>,  $J$  = 8.9 Hz, 2H), 7.49 – 7.45 (m, 5H), 4.48 (dd,  $J$  = 13.2, 1.8 Hz, 1H<sub>a</sub>), 3.88 (ddd,  $J$  = 10.5, 3.7, 1.8 Hz, 1H<sub>b</sub>), 3.17 (d,  $J_{AB}$  = 13.2 Hz, 1H<sub>a</sub>), 3.09 (s, 3H), 2.36 (app. dt,  $J$  = 12.3, 2.1 Hz, 1H<sub>b</sub>), 2.05 (tt,  $J$  = 8.0, 4.7 Hz, 1H), 1.93 – 1.85 (m, 1H<sub>c</sub>), 1.59 – 1.52 (m, 1H<sub>c</sub>), 1.54 – 1.45 (m, 1H<sub>d</sub>), 1.37 (dd,  $J$  = 12.2, 6.9 Hz, 1H<sub>e</sub>), 1.26 (dd,  $J$  = 12.2, 2.6 Hz, 1H<sub>e</sub>), 1.14 – 0.93 (m, 3H), 0.59 – 0.49 (m, 1H) ppm; <sup>13</sup>C NMR (101 MHz, CDCl<sub>3</sub>):  $\delta$  = 183.7 (C), 150.4 (C), 142.5 (C), 137.8 (C), 129.8 and 129.7 (5CH), 129.0 (2CH), 124.6 (2CH), 101.8 (C), 94.6 (C), 48.6 (C<sub>a</sub>H<sub>2</sub>), 45.4 (C<sub>b</sub>H<sub>2</sub>), 40.2 (CH<sub>3</sub>), 38.3 (C<sub>d</sub>H), 34.7 (C<sub>e</sub>H<sub>2</sub>), 30.4 (C<sub>c</sub>H<sub>2</sub>), 13.9 (CH<sub>2</sub>), 9.6 (CH), 8.2 (CH<sub>2</sub>) ppm; HRMS (ES–TOF):  $m/z$ : calcd for C<sub>24</sub>H<sub>26</sub>N<sub>4</sub>O<sub>7</sub>S<sub>2</sub>Na: 569.1135, found 569.1144 [M+Na]<sup>+</sup>.

***4*–Methyl–*N*–((3*R*,4*aS*,8*aR*)–2–(methylthio)–7–((4–nitrophenyl)sulfonyl)–4,4*a*,5,6,7,8–hexahydro–3*H*–3,8*a*–epoxy–1,7–naphthyridin–3–yl)–*N*–phenylbenzenesulfonamide **137c****

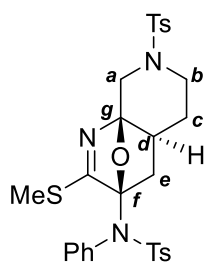


Following **GP9** with amide **128b** (91.8 mg, 0.24 mmol), ynamide **44a** (63.5 mg, 0.20 mmol), Cp\*CoI<sub>2</sub>(CO) (2.4 mg, 2.5 mol%) and NaOAc (0.83 mg, 5 mol%) for 8 h at 50 °C followed by 24 h at 101 °C. Purification by flash column chromatography (65:35 hexane/EtOAc) gave **137c** as a pale

yellow powder (105 mg, 90%); mp: 228–230 °C; IR (neat):  $\nu$  = 1564, 1533, 1358, 1178, 1092 cm<sup>-1</sup>; restricted rotation around the NTsPh sulfonamide results in broadening within the NMR:

$^1\text{H}$  NMR (400 MHz,  $\text{CDCl}_3$ ):  $\delta$  = 8.32 ( $d_{\text{AA'XX'}}$ ,  $J$  = 8.8 Hz, 2H), 8.01 ( $d_{\text{AA'XX'}}$ ,  $J$  = 8.8 Hz, 2H), 7.59 ( $d_{\text{AA'XX'}}$ ,  $J$  = 8.4 Hz, 2H), 7.33 (tt,  $J$  = 7.4, 1.2 Hz, 1H), 7.28 – 7.21 (m, 4H), 7.01 (br. app. s, 2H), 4.63 (dd,  $J$  = 13.6, 1.9 Hz,  $1\text{H}_a$ ), 3.85 – 3.76 (m,  $1\text{H}_b$ ), 3.40 (d,  $J_{AB}$  = 13.6 Hz,  $1\text{H}_a$ ), 2.53 (app. td,  $J$  = 12.8, 2.0 Hz,  $1\text{H}_b$ ), 2.43 (s, 3H), 2.41 (s, 3H), 1.80 – 1.70 (m,  $1\text{H}_c$ ), 1.68 – 1.58 (m,  $1\text{H}_d$ ), 1.43 (dd,  $J$  = 12.4, 7.4 Hz,  $1\text{H}_e$ ), 1.31 – 1.18 (m,  $1\text{H}_c$ ), 1.12 (dd,  $J$  = 12.4, 2.7 Hz,  $1\text{H}_e$ ) ppm;  $^{13}\text{C}$  NMR (101 MHz,  $\text{CDCl}_3$ ):  $\delta$  = 181.0 (C), 150.2 (C), 144.6 (C), 143.7 (C), 137.3 (C), 135.3 (C), 131.4 (2CH), 129.6 (2CH), 129.4 (2CH), 129.3 (2CH), 129.1 (CH), 128.9 (2CH), 124.5 (2CH), 102.1 (C), 96.5 (C), 48.5 ( $\text{C}_a\text{H}_2$ ), 45.0 ( $\text{C}_b\text{H}_2$ ), 39.5 ( $\text{C}_d\text{H}$ ), 36.4 ( $\text{C}_e\text{H}_2$ ), 30.4 ( $\text{C}_c\text{H}_2$ ), 21.8 ( $\text{CH}_3$ ), 14.4 ( $\text{SCH}_3$ ) ppm; HRMS (ES–TOF):  $m/z$ : calcd for  $\text{C}_{28}\text{H}_{29}\text{N}_4\text{O}_7\text{S}_3$ : 629.1193, found 629.1182  $[\text{M}+\text{H}]^+$ .

**4-Methyl-N-((3*R*,4*aS*,8*aR*)-2-(methylthio)-7-tosyl-4,4*a*,5,6,7,8-hexahydro-3*H*-3,8*a*-epoxy-1,7-naphthyridin-3-yl)-N-phenylbenzenesulfonamide **137d****



Following **GP9** with amide **128a** (187 mg, 0.49 mmol), ynamide **44a**

(127 mg, 0.40 mmol),  $\text{Cp}^*\text{CoI}_2(\text{CO})$  (4.8 mg, 2.5 mol%) and NaOAc (1.7

mg, 5 mol%) for 6 h at 50 °C followed by 24 h at 101 °C. Purification hot

recrystallisation (EtOH, 167 mg) and flash column chromatography of the

filtrate (6:4 hexane/EtOAc, 47 mg) gave **137d** as a beige solid (214 mg, 90%); mp: 200–202 °C;

IR (neat):  $\nu$  = 2927, 2842, 1597, 1547, 1363, 1345, 1160, 1145, 1090, 932, 839, 809, 746, 659,

674  $\text{cm}^{-1}$ ; restricted rotation around the  $\text{NTsPh}$  sulfonamide results in broadening within the

NMR:  $^1\text{H}$  NMR (400 MHz,  $\text{CDCl}_3$ ):  $\delta$  = 7.69 ( $d_{\text{AA'XX'}}$ ,  $J$  = 8.1 Hz, 2H), 7.59 ( $d_{\text{AA'XX'}}$ ,  $J$  = 8.2

Hz, 2H), 7.35 – 7.20 (m, 7H), 7.08 (br. app. s, 2H), 4.50 (d,  $J_{AB}$  = 13.2 Hz,  $1\text{H}_a$ ), 3.78 – 3.72

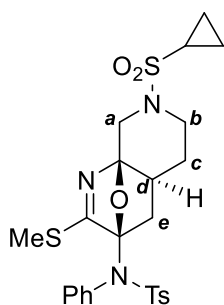
(m,  $1\text{H}_b$ ), 3.17 (d,  $J_{AB}$  = 13.2 Hz,  $1\text{H}_a$ ), 2.44 (s, 3H), 2.41 (s, 3H), 2.41 (s, 3H), 2.29 (app. td,  $J$

= 12.5, 2.1 Hz,  $1\text{H}_b$ ), 1.80 – 1.72 (m,  $1\text{H}_c$ ), 1.62 – 1.54 (m,  $1\text{H}_d$ ), 1.46 – 1.37 (m,  $1\text{H}_c+1\text{H}_e$ ),

1.21 (dd,  $J$  = 12.4, 2.6 Hz,  $1\text{H}_e$ ) ppm;  $^{13}\text{C}$  NMR (101 MHz,  $\text{CDCl}_3$ ):  $\delta$  = 180.7 (C), 144.4 (C),

143.8 (C), 137.5 (C), 135.2 (C), 133.6 (C), 131.6 (2CH), 129.9 (2CH), 129.6 (2CH), 129.3 (4CH), 129.0 (CH), 127.9 (2CH), 102.1 (C<sub>f</sub>), 97.0 (C<sub>g</sub>), 48.7 (C<sub>a</sub>H<sub>2</sub>), 45.2 (C<sub>b</sub>H<sub>2</sub>), 39.6 (C<sub>d</sub>H), 36.3 (C<sub>e</sub>H<sub>2</sub>), 30.6 (C<sub>c</sub>H<sub>2</sub>), 21.8 (CH<sub>3</sub>), 21.7 (CH<sub>3</sub>), 14.4 (SCH<sub>3</sub>) ppm; HRMS (ES–TOF): m/z: calcd for C<sub>29</sub>H<sub>32</sub>N<sub>3</sub>O<sub>5</sub>S<sub>3</sub>: 598.1499, found 598.1510 [M+H]<sup>+</sup>.

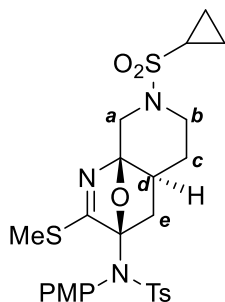
***N*–((3*R*,4*aS*,8*aR*)–7–(Cyclopropylsulfonyl)–2–(methylthio)–4,4*a*,5,6,7,8–hexahydro–3*H*–3,8*a*–epoxy–1,7–naphthyridin–3–yl)–4–methyl–*N*–phenylbenzenesulfonamide **137e****



Following **GP9** with amide **133c** (398 mg, 1.20 mmol), ynamide **44a** (317 mg, 1.00 mmol), Cp\*CoI<sub>2</sub>(CO) (11.9 mg, 2.5 mol%) and NaOAc (4.10 mg, 5 mol%) for 2 h at 50 °C followed by 24 h at 101 °C. Purification by flash column chromatography (4:6 hexane/EtOAc) gave **137e** as a white foam (411 mg, 75%); IR (neat): ν = 2926, 1552, 1491, 1357, 1334, 1310,

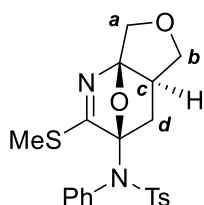
1169, 1153, 1143, 1082 cm<sup>-1</sup>; *restricted rotation around the NTsPh sulfonamide results in broadening within the NMR*: <sup>1</sup>H NMR (400 MHz, CDCl<sub>3</sub>): δ = 7.56 (d<sub>AA'XX'</sub>, *J* = 8.2 Hz, 2H), 7.40 – 7.32 (m, 1H), 7.31 – 7.24 (m, 2H), 7.18 (d<sub>AA'XX'</sub>, *J* = 8.2 Hz, 2H), 7.06 (br. app. s, 2H), 4.54 (dd, *J* = 14.1, 1.8 Hz, 1H<sub>a</sub>), 3.82 – 3.75 (m, 1H<sub>b</sub>), 3.76 (d, *J*<sub>AB</sub> = 14.1 Hz, 1H<sub>a</sub>), 2.87 (app. td, *J* = 13.1, 1.8 Hz, 1H<sub>b</sub>), 2.46 (s, 3H), 2.39 (s, 3H), 2.32 (tt, *J* = 8.0, 4.9 Hz, 1H), 1.86 – 1.72 (m, 1H<sub>c</sub>+1H<sub>d</sub>), 1.50 (dd, *J* = 12.5, 7.6 Hz, 1H<sub>e</sub>), 1.50 – 1.38 (m, 1H<sub>c</sub>) 1.27 – 1.16 (m, 1H<sub>e</sub>+2H), 0.97 – 0.84 (m, 2H) ppm; <sup>13</sup>C NMR (101 MHz, CDCl<sub>3</sub>): δ = 180.7 (C), 144.3 (C), 137.5 (C), 135.4 (C), 131.4 (2CH), 129.6 (2CH), 129.3 (CH), 129.2 (2CH), 129.1 (2CH), 102.2 (C), 96.8 (C), 48.6 (C<sub>a</sub>H<sub>2</sub>), 45.1 (C<sub>b</sub>H<sub>2</sub>), 39.8 (C<sub>d</sub>H), 36.6 (C<sub>e</sub>H<sub>2</sub>), 31.0 (C<sub>c</sub>H<sub>2</sub>), 27.9 (CH), 21.7 (CH<sub>3</sub>), 14.4 (CH<sub>3</sub>), 5.2 (CH<sub>2</sub>), 4.8 (CH<sub>2</sub>) ppm; HRMS (ES–TOF): m/z: calcd for C<sub>25</sub>H<sub>30</sub>N<sub>3</sub>O<sub>5</sub>S<sub>3</sub>: 548.1342, found 548.1350 [M+H]<sup>+</sup>.

***N*–((3*R*,4*aS*,8*aR*)–7–(Cyclopropylsulfonyl)–2–(methylthio)–4*a*,5,6,7,8–hexahydro–3*H*–3,8*a*–epoxy–1,7–naphthyridin–3–yl)–*N*–(4–methoxyphenyl)–4–methylbenzenesulfonamide **137f****



Following **GP9** with amide **128c** (99.6 mg, 0.30 mmol), ynamide **44b** (86.9 mg, 0.25 mmol), Cp\*CoI<sub>2</sub>(CO) (3.6 mg, 2.5 mol%) and NaOAc (1.3 mg, 5 mol%) for 5 h at 50 °C followed by 24 h at 101 °C. Purification by flash column chromatography (3:7 hexane/EtOAc) gave **137f** as a white powder (109 mg, 76%); mp: 185–187 °C; IR (neat):  $\nu$  = 2996, 1603, 1558, 1508, 1340, 1248, 1165, 1087 cm<sup>-1</sup>; <sup>1</sup>H NMR (400 MHz, CDCl<sub>3</sub>):  $\delta$  = 7.54 (d<sub>AA'XX'</sub>,  $J$  = 8.2 Hz, 2H), 7.16 (d<sub>AA'XX'</sub>,  $J$  = 8.2 Hz, 2H), 7.26 – 6.20 (br. m, 2H), 6.73 (br. app s, 2H), 4.48 (dd,  $J$  = 14.1, 1.6 Hz, 1H<sub>a</sub>), 3.78 – 3.70 (m, 3H+1H<sub>a</sub>+1H<sub>b</sub>), 2.85 (app. t,  $J$  = 12.9 Hz, 1H<sub>b</sub>), 2.42 (s, 3H), 2.36 (s, 3H), 2.29 (tt,  $J$  = 7.9, 4.8 Hz, 1H), 1.84 – 1.70 (m, 1H<sub>d</sub>+1H<sub>c</sub>), 1.51 – 1.38 (m, 1H<sub>c</sub>+1H<sub>e</sub>), 1.26 – 1.18 (m, 1H<sub>e</sub>), 1.18 – 1.09 (m, 2H), 0.91 – 0.82 (m, 2H) ppm; <sup>13</sup>C NMR (101 MHz, CDCl<sub>3</sub>):  $\delta$  = 180.6 (C), 159.9 (C), 144.1 (C), 135.4 (C), 132.4 (2CH), 129.8 (C), 129.4 (2CH), 129.1 (2CH), 114.0 (2CH), 102.3 (C), 96.6 (C), 55.5 (CH<sub>3</sub>), 48.5 (C<sub>a</sub>H<sub>2</sub>), 45.0 (C<sub>b</sub>H<sub>2</sub>), 39.6 (C<sub>d</sub>H), 36.5 (C<sub>e</sub>H<sub>2</sub>), 30.9 (C<sub>c</sub>H<sub>2</sub>), 27.8 (CH), 21.6 (CH<sub>3</sub>), 14.3 (SCH<sub>3</sub>), 5.2 (CH<sub>2</sub>), 4.7 (CH<sub>2</sub>) ppm; HRMS (ES–TOF):  $m/z$ : calcd for C<sub>26</sub>H<sub>31</sub>N<sub>3</sub>O<sub>6</sub>S<sub>3</sub>Na: 600.1267, found 600.1277 [M+Na]<sup>+</sup>.

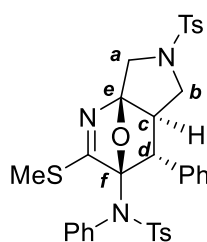
***4*–Methyl–*N*–((3*R*,4*aR*,7*aR*)–2–(methylthio)–4*a*,5–dihydro–7*H*–3,7*a*–epoxyfuro[3,4–*b*]pyridin–3(4*H*)–yl)–*N*–phenylbenzenesulfonamide **138****



Following **GP9** with amide **131a** (77.5 mg, 0.36 mmol), ynamide **44a** (95.3 mg, 0.30 mmol), Cp\*CoI<sub>2</sub>(CO) (3.6 mg, 2.5 mol%) and NaOAc (1.3 mg, 5 mol%) for 4 h at 50 °C followed by 24 h at 101 °C. Purification by flash column chromatography (6:4 hexane/EtOAc) gave **138** as a fluffy white powder (101 mg, 78%); mp: 157–158 °C; IR (neat):  $\nu$  = 2985, 1596, 1541, 1351, 1307, 1168, 1144, 1090, 820, 687, 670 cm<sup>-1</sup>; *restricted rotation around the NTsPh sulfonamide results in*

broadening within the NMR:  $^1\text{H}$  NMR (300 MHz,  $\text{CDCl}_3$ ):  $\delta$  = 7.58 ( $d_{\text{AA'XX'}}$ ,  $J$  = 8.2 Hz, 2H), 7.38 – 7.24 (m, 3H), 7.19 ( $d_{\text{AA'XX'}}$ ,  $J$  = 8.2 Hz, 2H), 7.11 (br. app. s, 2H), 4.43 (d,  $J_{\text{AB}}$  = 10.6 Hz, 1H<sub>a</sub>), 4.23 (d,  $J_{\text{AB}}$  = 10.6 Hz, 1H<sub>a</sub>), 4.05 (app. t,  $J$  = 8.0 Hz, 1H<sub>b</sub>), 3.29 (dd,  $J$  = 10.5, 8.2 Hz, 1H<sub>b</sub>), 2.52 (s, 3H), 2.41 (s, 3H), 2.33 – 2.22 (m, 1H<sub>c</sub>), 1.53 (dd,  $J$  = 12.5, 3.2 Hz, 1H<sub>d</sub>), 1.32 (dd,  $J$  = 12.5, 7.6 Hz, 1H<sub>d</sub>) ppm;  $^{13}\text{C}$  NMR (101 MHz,  $\text{CDCl}_3$ ):  $\delta$  = 180.4 (C), 144.3 (C), 137.4 (C), 135.7 (C), 131.8 (CH), 129.4 (2CH), 129.3 (2CH), 129.2 (2CH), 129.1 (2CH), 109.6 (C), 103.4 (C), 72.3 (C<sub>b</sub>H<sub>2</sub>), 68.0 (C<sub>a</sub>H<sub>2</sub>), 48.6 (C<sub>c</sub>H), 32.4 (C<sub>d</sub>H<sub>2</sub>), 21.8 (CH<sub>3</sub>), 14.5 (SCH<sub>3</sub>) ppm; HRMS (ES–TOF):  $m/z$ : calcd for  $\text{C}_{21}\text{H}_{23}\text{N}_2\text{O}_4\text{S}_2$ : 431.1094, found 431.1100  $[\text{M}+\text{H}]^+$ .

**4-Methyl-N-((3R,4R,4aR,7aR)-2-(methylthio)-4-phenyl-6-tosyl-4a,5,6,7-tetrahydro-3,7a-epoxypyrrolo[3,4-b]pyridin-3(4H)-yl)-N-phenylbenzenesulfonamide 139**



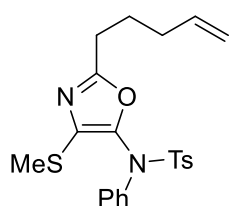
Following **GP9** with amide **132** (80.0 mg, 0.18 mmol), ynamide **44a** (47.6 mg, 0.15 mmol),  $\text{Cp}^*\text{CoI}_2(\text{CO})$  (1.8 mg, 2.5 mol%) and NaOAc (0.62 mg, 5 mol%) for 12 h at 50 °C followed by 72 h at 101 °C. Purification by flash column chromatography (3:1 hexane/EtOAc) gave **139** as a pale

yellow powder (45.1 mg, 45%); mp: 151–154 °C; IR (neat):  $\nu$  = 2923, 1528, 1490, 1457, 1348, 1308, 1156, 1089  $\text{cm}^{-1}$ ;  $^1\text{H}$  NMR (400 MHz,  $\text{CDCl}_3$ ):  $\delta$  = 7.80 ( $d_{\text{AA'XX'}}$ ,  $J$  = 8.0 Hz, 2H), 7.38 (d,  $J$  = 8.0 Hz, 2H), 7.33 (tt,  $J$  = 7.5, 1.2 Hz, 1H), 7.30 ( $d_{\text{AA'XX'}}$ ,  $J$  = 8.2 Hz, 2H), 7.24 – 7.09 (m, 5H), 7.05 ( $d_{\text{AA'XX'}}$ ,  $J$  = 8.2 Hz, 2H), 6.90 (br. d,  $J$  = 8.2 Hz, 1H), 6.86 (br. d,  $J$  = 8.2 Hz, 1H), 6.63 (br. app. d,  $J$  = 7.5 Hz, 2H), 4.15 (d,  $J_{\text{AB}}$  = 11.8 Hz, 1H<sub>a</sub>), 3.92 – 3.82 (m, 1H<sub>d</sub>), 3.90 (d,  $J_{\text{AB}}$  = 11.8 Hz, 1H<sub>a</sub>), 3.86 (dd,  $J$  = 9.5, 8.2 Hz, 1H<sub>b</sub>), 3.10 (app. t,  $J$  = 9.7 Hz, 1H<sub>b</sub>), 2.57 (ddd,  $J$  = 9.9, 8.2, 3.3, 1H<sub>c</sub>), 2.47 (s, 3H), 2.41 (s, 3H), 2.27 (s, 3H) ppm;  $^{13}\text{C}$  NMR (101 MHz,  $\text{CDCl}_3$ ):  $\delta$  = 179.2 (C), 144.3 (C), 143.7 (C), 137.2 (C), 134.6 (C), 134.4 (C), 133.9 (C), 132.5 (CH), 132.2 (CH), 130.0 (2CH), 129.5 (2CH), 128.9 (2CH), 128.9 (2CH), 128.8 (2CH), 128.6 (2CH), 127.9 (2CH), 127.8 (2CH), 106.0 (C<sub>e</sub>), 52.9 (C<sub>b</sub>H<sub>2</sub>), 51.8 (C<sub>d</sub>H), 51.0 (C<sub>c</sub>H), 50.2

(C<sub>a</sub>H<sub>2</sub>), 21.8 (2CH<sub>3</sub>), 14.7 (SCH<sub>3</sub>) ppm; one quaternary carbon resonance not observed in <sup>13</sup>C NMR (C<sub>f</sub>); HRMS (ES–TOF): m/z: calcd for C<sub>34</sub>H<sub>33</sub>N<sub>3</sub>O<sub>5</sub>S<sub>3</sub>Na: 682.1475, found 682.1483 [M+Na]<sup>+</sup>.

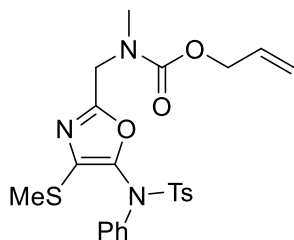
**NOTE:** Stereochemistry of stereogenic centre assigned through <sup>3</sup>J vicinal coupling of J = 3.3 Hz between H<sub>d</sub> and H<sub>c</sub>.

**4-Methyl-N-(4-(methylthio)-2-(pent-4-en-1-yl)oxazol-5-yl)-N-phenylbenzenesulfonamide 141**



Following **GP9** with amide **121b** (76.8 mg, 0.36 mmol), ynamide **44a** (95.3 mg, 0.30 mmol), Cp\*CoI<sub>2</sub>(CO) (3.53 mg, 2.5 mol%) and NaOAc (1.28 mg, 5 mol%) for 4 h at 50 °C followed by 24 h at 101 °C. Purification by flash column chromatography (8:2 hexane/EtOAc) gave **141** as pale yellow oil (88.6 mg, 69%); IR (neat): ν = 3067, 2928, 1691, 1596, 1559, 1488, 1363, 1163 cm<sup>-1</sup>; <sup>1</sup>H NMR (400 MHz, CDCl<sub>3</sub>): δ = 7.62 (d<sub>AA'XX'</sub>, J = 8.4, 2H), 7.31 (s, 5H), 7.27 (d<sub>AA'XX'</sub>, J = 8.4, 2H), 5.79 (ddt, J = 17.0, 10.2, 6.7 Hz, 1H), 5.07 – 4.97 (m, 2H), 2.70 (t, J = 7.3 Hz, 2H), 2.44 (s, 3H), 2.40 (s, 3H), 2.13 (app. qt, J = 7.3, 1.3 Hz, 2H), 1.83 (p, J = 7.4 Hz, 2H) ppm; <sup>13</sup>C NMR (101 MHz, CDCl<sub>3</sub>): δ = 163.4 (C), 144.5 (C), 141.9 (C), 139.2 (C), 137.5 (CH), 135.9 (C), 132.2 (C), 129.7 (2CH), 129.5 (2CH), 128.7 (CH), 128.5 (2CH), 128.5 (2CH), 115.7 (CH<sub>2</sub>), 33.1 (CH<sub>2</sub>), 28.2 (CH<sub>2</sub>), 25.9 (CH<sub>2</sub>), 21.8 (CH<sub>3</sub>), 16.2 (SCH<sub>3</sub>) ppm; HRMS (ES–TOF): m/z: calcd for C<sub>22</sub>H<sub>25</sub>N<sub>2</sub>O<sub>3</sub>S<sub>2</sub>: 429.1301, found 429.1308 [M+H]<sup>+</sup>.

***Allyl methyl((5-((4-methyl-N-phenylphenyl)sulfonamido)-4-(methylthio)oxazol-2-yl)methyl)carbamate 144***

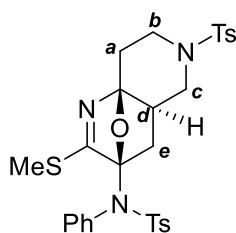


Following **GP9** with amide **133** (98.0 mg, 0.36 mmol), ynamide **44a** (95.2 mg, 0.30 mmol), Cp\*CoI<sub>2</sub>(CO) (3.56 mg, 5 mol%) and NaOAc (1.28 mg, 5 mol%) for 4 h at 50 °C followed by 24 h at 101 °C.

Purification by flash column chromatography (6:4 hexane/EtOAc)

gave **144** as a yellow oil (111 mg, 76%); IR (neat):  $\nu$  = 2928, 1704, 1595, 1488, 1400, 1362, 1223, 1165, 1090 cm<sup>-1</sup>; NMR spectra display a mixture of rotamers in a 1:1 ratio; <sup>1</sup>H NMR (400 MHz, CDCl<sub>3</sub>):  $\delta$  = 7.62 – 7.54 (m, 2H), 7.36 – 7.24 (m, 7H), 5.95 and 5.82 (ddt,  $J$  = 16.3, 10.7, 5.4 Hz, 1H), 5.37 – 5.08 (m, 2H), 4.68 – 4.55 (m, 2H), 4.54 and 4.49 (s, 2H), 3.00 (s, 3H), 2.42 (s, 3H), 2.41 (s, 3H) ppm; <sup>13</sup>C NMR (101 MHz, CDCl<sub>3</sub>):  $\delta$  = 158.6 (C), 156.3 and 155.6 (C), 144.7 and 144.6 (C), 142.5 and 142.3 (C), 138.8 (C), 135.5 (C), 132.8 and 132.7 (CH), 129.7 and 129.6 (2CH), 129.5 (2CH), 128.7 (CH), 128.5 (2CH), 128.4 and 128.3 (2CH), 117.6 (CH<sub>2</sub>), 66.6 and 66.4 (CH<sub>2</sub>), 46.4 (CH<sub>2</sub>), 35.4 and 34.5 (CH<sub>3</sub>), 29.8 (CH<sub>2</sub>), 21.7 (CH<sub>3</sub>), 16.0 and 16.0 (CH<sub>3</sub>) ppm; HRMS (ES-TOF):  $m/z$ : calcd for C<sub>23</sub>H<sub>26</sub>N<sub>3</sub>O<sub>5</sub>S<sub>2</sub>: 488.1308, found 488.1325 [M+H]<sup>+</sup>.

***4-Methyl-N-((3R,4aR,8aS)-2-(methylthio)-6-tosyl-4,4a,5,6,7,8-hexahydro-3H-3,8a-epoxy-1,6-naphthyridin-3-yl)-N-phenylbenzenesulfonamide 150a***



Following **GP9** with amide **149c** (91.8 mg, 0.24 mmol), ynamide **44a** (63.5 mg, 0.20 mmol), Cp\*CoI<sub>2</sub>(CO) (2.4 mg, 2.5 mol%) and NaOAc (0.84 mg, 5 mol%) for 8 h at 50 °C followed by 24 h at 101 °C.

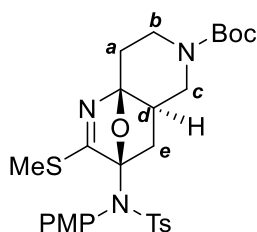
Purification by hot recrystallisation (EtOH) gave **150a** as a white powder

(105 mg, 88%); mp: 218–219 °C; IR (neat):  $\nu$  = 2931, 2864, 1545, 1486, 1357, 1257, 1172, 1152, 1090, 1035 cm<sup>-1</sup>; <sup>1</sup>H NMR (400 MHz, CDCl<sub>3</sub>):  $\delta$  = 7.67 (d<sub>AA'XX'</sub>,  $J$  = 8.3 Hz, 2H), 7.46



(d<sub>AA'XX'</sub>,  $J = 8.3$  Hz, 2H), 7.35 (d,  $J = 7.8$  Hz, 2H), 7.31 (tt,  $J = 7.8, 1.3$  Hz, 1H), 7.23 (t,  $J = 7.8$ , 2H), 7.06 (app. d,  $J = 7.8$  Hz, 4H), 3.91 – 3.86 (m, 1H<sub>b</sub>), 3.82 (ddd,  $J = 11.4, 5.9, 2.1$ , 1H<sub>c</sub>), 2.65 – 2.51 (m, 1H<sub>b</sub>+1H<sub>a</sub>), 2.50 – 2.38 (m, 1H<sub>a</sub>), 2.46 (s, 3H), 2.40 (s, 3H), 2.37 (s, 3H), 2.06 (app. t,  $J = 11.4$  Hz, 1H<sub>c</sub>), 2.00 – 1.92 (m, 1H<sub>d</sub>), 1.44 (dd,  $J = 12.7, 7.2$  Hz, 1H<sub>e</sub>), 1.30 (dd,  $J = 12.7, 2.6$  Hz, 1H<sub>e</sub>) ppm; <sup>13</sup>C NMR (101 MHz, CDCl<sub>3</sub>):  $\delta = 179.8$  (C), 144.2 (C), 143.8 (C), 137.7 (C), 135.8 (C), 134.5 (C), 131.5 (2CH), 129.9 (2CH), 129.3 (CH), 129.2 (2CH), 129.0 (4CH), 127.8 (2CH), 101.9 (C), 98.0 (C), 50.2 (C<sub>c</sub>H<sub>2</sub>), 43.5 (C<sub>b</sub>H<sub>2</sub>), 40.3 (C<sub>d</sub>H), 34.0 (C<sub>e</sub>H<sub>2</sub>), 29.8 (C<sub>a</sub>H<sub>2</sub>), 21.7 (2CH<sub>3</sub>), 14.5 (SCH<sub>3</sub>) ppm; HRMS (ES–TOF):  $m/z$ : calcd for C<sub>29</sub>H<sub>31</sub>N<sub>3</sub>O<sub>5</sub>S<sub>3</sub>Na: 620.1324, found 620.1326 [M+Na]<sup>+</sup>.

***tert*-Butyl (3*R*,4*aR*,8*aS*)–3–((*N*–(4-methoxyphenyl)–4-methylphenyl)sulfonamido)–2–(methylthio)–3,4,4*a*,5,7,8–hexahydro–6*H*–3,8*a*–epoxy–1,6–naphthyridine–6–carboxylate **150b****



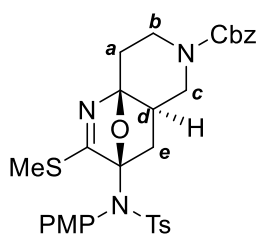
Following **GP9** with amide **149b** (98.5 mg, 0.30 mmol), ynamide **44b** (86.9 mg, 0.25 mmol), Cp\*CoI<sub>2</sub>(CO) (3.0 mg, 2.5 mol%) and NaOAc (1.0 mg, 5 mol%) for 5 h at 50 °C followed by 24 h at 101 °C.

Purification by flash column chromatography (6:4 hexane/EtOAc) and

hot recrystallisation (EtOH) gave **150b** as colourless crystals (90.3 mg, 63%); mp: 195–196 °C; IR (neat):  $\nu = 2971, 2362, 1690, 1507, 1360, 1243, 1163, 1088$  cm<sup>–1</sup>; NMR spectra display a mixture of rotamers; <sup>1</sup>H NMR (400 MHz, CDCl<sub>3</sub>):  $\delta = 7.59$  (d<sub>AA'XX'</sub>,  $J = 8.2$  Hz, 2H), 7.18 (d<sub>AA'XX'</sub>,  $J = 8.2$  Hz, 2H), 7.00 (br. app. s, 2H), 6.75 (d<sub>AA'XX'</sub>,  $J = 8.5$  Hz, 2H), 4.12 (br. s, 2H), 3.79 (s, 3H), 2.86 (br. s, 1H), 2.49 – 2.25 (m, 9H), 1.81 (br. s, 1H), 1.49 – 1.35 (m, 1H), 1.43 (s, 9H), 1.16 (br. s, 1H) ppm; <sup>13</sup>C NMR (101 MHz, CDCl<sub>3</sub>):  $\delta = 179.8$  (C), 160.0 (C), 154.4 (C), 144.1 (C), 135.9 (C), 132.7 (2CH), 130.1 (C), 129.4 (2CH), 129.0 (2CH), 114.1 (2CH), 102.1 (C), 99.1 (C), 79.9 (C), 55.5 (CH<sub>3</sub>), 40.1 (CH), 34.0 (CH<sub>2</sub>), 30.0 (CH<sub>2</sub>), 28.5 (3CH<sub>3</sub>), 21.7

(CH<sub>3</sub>), 14.4 (SCH<sub>3</sub>); *C<sub>b</sub>* and *C<sub>c</sub>* peaks in <sup>13</sup>C NMR broadened at around 42 and 48 ppm respectively; HRMS (ES–TOF): *m/z*: calcd for C<sub>28</sub>H<sub>36</sub>N<sub>3</sub>O<sub>6</sub>S<sub>2</sub>: 574.2040, found 574.2050 [M+H]<sup>+</sup>.

***Benzyl (3R,4aR,8aS)–3–((N–(4–methoxyphenyl)–4–methylphenyl)sulfonamido)–2–(methylthio)–3,4,4a,5,7,8–hexahydro–6H–3,8a–epoxy–1,6–naphthyridine–6–carboxylate 150c***

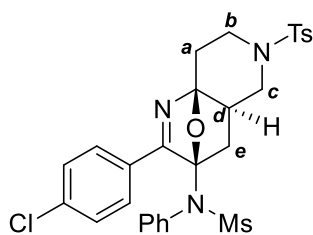


Following **GP9** with amide **149a** (109 mg, 0.30 mmol), ynamide **44b** (86.9 mg, 0.25 mmol), Cp\*CoI<sub>2</sub>(CO) (3.6 mg, 2.5 mol%) and NaOAc (1.0 mg, 5 mol%) for 5 h at 50 °C followed by 24 h at 101 °C.

Purification by flash column chromatography (6:4 hexane/EtOAc) gave

**150c** as a white powder (104 mg, 69%); mp: 166–168 °C; IR (neat):  $\nu$  = 2954, 1697, 1558, 1507, 1430, 1358, 1236, 1164, 1088 cm<sup>–1</sup>; *NMR spectra display a mixture of rotamers*; <sup>1</sup>H NMR (400 MHz, CDCl<sub>3</sub>):  $\delta$  = 7.59 (d<sub>AA'XX'</sub>, *J* = 8.1 Hz, 2H), 7.33 (br. app. s, 5H), 7.19 (d<sub>AA'XX'</sub>, *J* = 8.1 Hz, 2H), 7.00 (br. app. s, 2H), 6.75 (d<sub>AA'XX'</sub>, *J* = 8.4 Hz, 2H), 5.11 (br. s, 2H), 4.37 – 4.10 (m, 2H), 3.81 (s, 3H), 2.97 (br. s, 1H), 2.50 – 2.35 (m, 3H), 2.44 (s, 3H), 2.41 (s, 3H), 1.84 (br. s, 1H), 1.39 (dd, *J* = 12.6, 7.4 Hz, 1H), 1.22 – 1.14 (m, 1H) ppm; <sup>13</sup>C NMR (101 MHz, CDCl<sub>3</sub>):  $\delta$  = 179.9 (C), 160.0 (C), 144.1 (C), 136.7 (C), 135.9 (C), 132.7 (2CH), 130.0 (C), 129.3 (2CH), 129.1 (2CH), 128.7 (CH), 128.2 (CH), 128.0 (2CH), 114.1 (2CH), 102.2 (C), 98.8 (C), 67.4 (CH<sub>2</sub>), 55.5 (CH<sub>3</sub>), 48.5 (CH<sub>2</sub>), 41.5 (CH<sub>2</sub>), 40.0 (CH), 34.0 (CH<sub>2</sub>), 30.1 (CH<sub>2</sub>), 21.7 (CH<sub>3</sub>), 14.4 (SCH<sub>3</sub>) ppm; *one quaternary carbon resonance not observed in <sup>13</sup>C NMR spectra*; HRMS (ES–TOF): *m/z*: calcd for C<sub>31</sub>H<sub>33</sub>N<sub>3</sub>O<sub>6</sub>S<sub>2</sub>Na: 630.1703, found 630.1714 [M+Na]<sup>+</sup>.

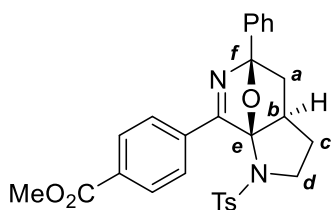
***N*–((3*R*,4*aR*,8*aS*)–2–(4–Chlorophenyl)–6–tosyl–4,4*a*,5,6,7,8–hexahydro–3*H*–3,8*a*–epoxy–1,6–naphthyridin–3–yl)–*N*–phenylmethanesulfonamide 150*d***



Following **GP9** with amide **149c** (115 mg, 0.30 mmol), ynamide **441** (76.4 mg, 0.25 mmol), Cp\*CoI<sub>2</sub>(CO) (3.0 mg, 2.5 mol%) and NaOAc (1.0 mg, 5 mol%) for 12 h at 50 °C followed by 48 h at 101 °C. Purification by flash column chromatography (6:4 hexane/EtOAc) and hot recrystallisation (EtOH) gave **150d** as a white powder (116 mg, 79%); mp: 232–235 °C; IR (neat):  $\nu$  = 2860, 1595, 1562, 1489, 1349, 1278, 1162, 1138, 1090 cm<sup>-1</sup>; <sup>1</sup>H NMR (400 MHz, CDCl<sub>3</sub>):  $\delta$  = 7.84 (d<sub>AA'XX'</sub>,  $J$  = 8.2 Hz, 2H), 7.68 (d<sub>AA'XX'</sub>,  $J$  = 8.3, 2H), 7.50 – 7.33 (m, 9H), 4.00 – 3.87 (m, 1H<sub>b</sub>+1H<sub>c</sub>), 2.91 (s, 3H), 2.85 – 2.62 (m, 1H<sub>b</sub>+1H<sub>a</sub>), 2.53 – 2.46 (m, 1H<sub>a</sub>), 2.48 (s, 3H), 2.16 (app. t,  $J$  = 8.2 Hz, 1H<sub>c</sub>), 2.09 – 2.02 (m, 1H<sub>d</sub>), 1.49 (dd,  $J$  = 12.7, 7.3 Hz, 1H<sub>e</sub>), 1.33 (br. s, 1H<sub>e</sub>) ppm; <sup>13</sup>C NMR (101 MHz, CDCl<sub>3</sub>):  $\delta$  = 173.4 (C), 143.9 (C), 137.6 (C), 137.1 (C), 134.3 (C), 130.2 (C), 129.92 (4CH), 129.87 (CH), 129.0 (4CH), 128.2 (2CH), 127.7 (2CH), 100.7 (C), 96.3 (C), 50.1 (C<sub>c</sub>H<sub>2</sub>), 43.3 (C<sub>b</sub>H<sub>2</sub>), 39.9 (C<sub>d</sub>H), 39.4 (CH<sub>3</sub>), 32.9 (C<sub>e</sub>H<sub>2</sub>), 29.4 (C<sub>a</sub>H<sub>2</sub>), 21.8 (CH<sub>3</sub>) ppm;  $m/z$ : 100% 608.1 [M+Na]<sup>+</sup>, 38% 610.1 [M+Na]<sup>+</sup>, 58% 586.1 [M+H]<sup>+</sup>, 20% 588.1 [M+H]<sup>+</sup>; HRMS (ES–TOF):  $m/z$ : calcd for C<sub>28</sub>H<sub>29</sub>N<sub>3</sub>O<sub>5</sub>S<sub>2</sub>Cl: 586.1232, found 586.1235 [M+H]<sup>+</sup>.

**Products derived from enynamides (Chapter 2.2.5)**

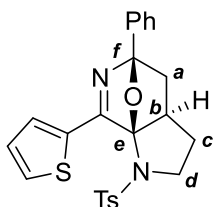
***Methyl 4–((3*aR*,5*R*,7*aR*)–5–phenyl–1–tosyl–1,2,3,3*a*,4,5–hexahydro–5,7*a*–epoxypyrrolo[2,3–*c*]pyridin–7–yl)benzoate 152*a****



Following **GP9** with amide **111a** (48.7 mg, 0.22 mmol), ynamide **151a** (61.5 mg, 0.16 mmol), Cp\*CoI<sub>2</sub>(CO) (2.4 mg, 5 mol%) and NaOAc (0.82 mg, 5 mol%) for 2 h at r.t. followed by 12 h at 110 °C in PhMe (5.0 mL). Purification by flash column chromatography (7:3 hexane/EtOAc) gave

**152a** as a pale beige powder (39.1 mg, 49%); mp: 188–190 °C; IR (neat):  $\nu$  = 2954, 2924, 1721, 1597, 1437, 1347, 1278, 1163  $\text{cm}^{-1}$ ;  $^1\text{H}$  NMR (400 MHz,  $\text{CDCl}_3$ ):  $\delta$  = 8.17 (d<sub>AA'XX'</sub>,  $J$  = 8.7 Hz, 2H), 8.14 (d<sub>AA'XX'</sub>,  $J$  = 8.7 Hz, 2H), 7.89 (d<sub>AA'XX'</sub>,  $J$  = 8.1 Hz, 2H), 7.67 (d,  $J$  = 6.8 Hz, 2H), 7.50 – 7.40 (m, 3H) 7.29 (d<sub>AA'XX'</sub>,  $J$  = 8.1 Hz, 2H), 4.04 (td,  $J$  = 10.6, 6.5 Hz, 1H<sub>d</sub>), 3.94 (s, 3H), 3.71 (app. t,  $J$  = 9.7 Hz, 1H<sub>d</sub>), 2.53 – 2.45 (m, 1H<sub>b</sub>), 2.43 (s, 3H), 2.33 – 2.23 (m, 1H<sub>c</sub>), 2.17 (dd,  $J$  = 11.9, 7.5 Hz, 1H<sub>a</sub>), 1.88 (dd,  $J$  = 11.9, 3.2 Hz, 1H<sub>a</sub>), 1.84 – 1.71 (m, 1H<sub>c</sub>) ppm;  $^{13}\text{C}$  NMR (101 MHz,  $\text{CDCl}_3$ ):  $\delta$  = 171.0 (C), 166.7 (C), 144.2 (C), 137.7 (C), 135.3 (C), 135.0 (C), 132.3 (C), 129.9 (2CH), 129.4 (2CH), 129.1 (2CH), 128.8 (CH), 128.6 (2CH), 127.5 (2CH), 126.1 (2CH), 104.9 (C<sub>e</sub>), 101.8 (C<sub>f</sub>), 52.4 (CH<sub>3</sub>), 52.3 (C<sub>d</sub>H<sub>2</sub>), 45.3 (C<sub>b</sub>H), 40.5 (C<sub>a</sub>H<sub>2</sub>), 29.5 (C<sub>c</sub>H<sub>2</sub>), 21.7 (CH<sub>3</sub>) ppm; HRMS (ES-TOF):  $m/z$ : calcd for  $\text{C}_{28}\text{H}_{27}\text{N}_2\text{O}_5\text{S}$ : 503.1635, found 503.1653  $[\text{M}+\text{H}]^+$ .

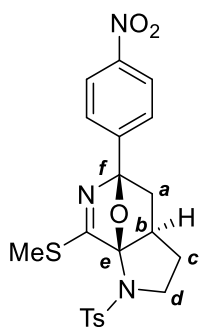
**(3aR,5R,7aR)–5–Phenyl–7–(thiophen–2–yl)–1–tosyl–1,2,3,3a,4,5–hexahydro–5,7a–epoxypyrrolo[2,3–c]pyridine 152b**



Following **GP9** with amide **111a** (66.4 mg, 0.30 mmol), ynamide **151b** (82.9 mg, 0.25 mmol),  $\text{Cp}^*\text{CoI}_2(\text{CO})$  (3.0 mg, 2.5 mol%) and NaOAc (1.0 mg, 5 mol%) for 6 h at r.t. followed by 24 h at 101 °C. Purification by flash column chromatography (3:1 hexane/EtOAc) gave **152b** as a beige powder (78.5 mg, 70%); mp: (dec.) 205–207 °C; IR (neat):  $\nu$  = 2949, 1580, 1432, 1382, 1340, 1251, 1161  $\text{cm}^{-1}$ ;  $^1\text{H}$  NMR (400 MHz,  $\text{CDCl}_3$ ):  $\delta$  = 8.10 (dd,  $J$  = 3.8, 1.1 Hz, 1H), 7.96 (d<sub>AA'XX'</sub>,  $J$  = 8.2 Hz, 2H), 7.68 – 7.63 (m, 2H), 7.54 (dd,  $J$  = 5.1, 1.1 Hz, 1H), 7.49 – 7.38 (m, 3H), 7.30 (d<sub>AA'XX'</sub>,  $J$  = 8.2 Hz, 2H), 7.19 (dd,  $J$  = 5.1, 3.8 Hz, 1H), 3.98 (app. td,  $J$  = 10.9, 6.3 Hz, 1H<sub>d</sub>), 3.69 (app. t,  $J$  = 9.6 Hz, 1H<sub>d</sub>), 2.44 (s, 3H), 2.45 – 2.37 (m, 1H<sub>b</sub>), 2.19 (dd,  $J$  = 11.7, 7.6 Hz, 1H<sub>a</sub>), 2.20 – 2.12 (m, 1H<sub>c</sub>), 1.87 (dd,  $J$  = 11.8, 3.3 Hz, 1H<sub>a</sub>), 1.71 – 1.60 (m, 1H<sub>c</sub>) ppm;  $^{13}\text{C}$  NMR (101 MHz,  $\text{CDCl}_3$ ):  $\delta$  = 166.4 (C), 144.2 (C), 137.9 (C), 135.0 (C), 133.5 (C), 131.7 (CH), 130.8 (CH),

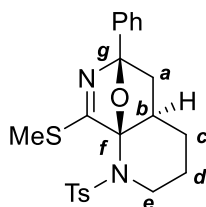
129.4 (2CH), 129.3 (2CH), 128.7 (CH), 128.5 (2CH), 128.3 (CH), 126.3 (2CH), 104.9 (C<sub>f</sub>), 102.0 (C<sub>e</sub>), 52.9 (C<sub>d</sub>H<sub>2</sub>), 45.7 (C<sub>b</sub>H), 40.7 (C<sub>a</sub>H<sub>2</sub>), 29.5 (C<sub>c</sub>H<sub>2</sub>), 21.8 (CH<sub>3</sub>) ppm; HRMS (ES–TOF): m/z: calcd for C<sub>24</sub>H<sub>23</sub>N<sub>2</sub>O<sub>3</sub>S<sub>2</sub>: 451.1145, found 451.1158 [M+H]<sup>+</sup>.

**(3aR,5R,7aR)–7–(Methylthio)–5–(4–nitrophenyl)–1–tosyl–1,2,3,3a,4,5–hexahydro–5,7a–epoxypyrrolo[2,3–c]pyridine 152c**



Following **GP9** with amide **111d** (95.9 mg, 0.36 mmol), ynamide **151c** (88.5 mg, 0.30 mmol), Cp\*CoI<sub>2</sub>(CO) (3.6 mg, 2.5 mol%) and NaOAc (1.2 mg, 5 mol%) for 2 h at r.t. followed by 24 h at 101 °C. Purification by hot recrystallisation (EtOH) gave **152c** as an orange powder (104.3 mg, 76%); mp: 195–195 °C; IR (neat): ν = 2943, 2935, 1595, 1551, 1448, 1342, 1280, 1163 cm<sup>–1</sup>; <sup>1</sup>H NMR (300 MHz, CDCl<sub>3</sub>): δ = 8.28 (d<sub>AA'XX'</sub>, J = 8.8 Hz, 2H), 7.90 (d<sub>AA'XX'</sub>, J = 8.2 Hz, 2H), 7.79 (d<sub>AA'XX'</sub>, J = 8.8 Hz, 1H), 7.31 (d<sub>AA'XX'</sub>, J = 8.2 Hz, 2H), 3.85 (td, J = 10.6, 6.4 Hz, 1H<sub>d</sub>), 3.65 (app. t, J = 9.7, 1H<sub>d</sub>), 2.51 (s, 3H), 2.44 (s, 3H), 2.46 – 2.36 (m, 1H<sub>b</sub>), 2.24 – 2.12 (m, 1H<sub>c</sub>), 2.11 (dd, J = 11.7, 7.5 Hz, 1H<sub>a</sub>), 1.79 (dd, J = 11.7, 3.5 Hz, 1H<sub>a</sub>), 1.73 – 1.59 (m, 1H<sub>c</sub>) ppm; <sup>13</sup>C NMR (101 MHz, CDCl<sub>3</sub>): δ = 177.1 (C), 148.1 (C), 144.9 (C), 144.4 (C), 135.1 (C), 129.5 (2CH), 128.9 (2CH), 127.3 (2CH), 123.8 (2CH), 106.2 (C), 102.4 (C), 53.0 (C<sub>d</sub>H<sub>2</sub>), 46.2 (C<sub>b</sub>H), 41.7 (C<sub>a</sub>H<sub>2</sub>), 29.3 (C<sub>c</sub>H<sub>2</sub>), 21.8 (CH<sub>3</sub>), 14.0 (SCH<sub>3</sub>) ppm; HRMS (ES–TOF): m/z: calcd for C<sub>21</sub>H<sub>22</sub>N<sub>3</sub>O<sub>5</sub>S<sub>2</sub>: 460.0995, found 460.1000 [M+H]<sup>+</sup>.

**(4aR,6R,8aR)–8–(Methylthio)–6–phenyl–1–tosyl–2,3,4,4a,5,6–hexahydro–1H–6,8a–epoxy–1,7–naphthyridine 153**



Following **GP9** with amide **111a** (79.6 mg, 0.360 mmol), ynamide **151d** (93.2 mg, 0.301 mmol), Cp\*CoI<sub>2</sub>(CO) (3.6 mg, 2.5 mol%) and NaOAc (1.2 mg, 5 mol%) for 6 h at r.t. followed by 24 h at 101 °C. Purification by flash column chromatography (3:1 hexane/EtOAc) gave **153** as a white powder (98.4 mg, 77%);

mp: 203–204 °C; IR (neat):  $\nu$  = 2978, 1754, 1698, 1455, 1399, 1367, 1247, 1201, 1167, 1144  $\text{cm}^{-1}$ ;  $^1\text{H}$  NMR (400 MHz,  $\text{CDCl}_3$ ):  $\delta$  = 7.89 ( $d_{\text{AA'XX'}}$ ,  $J$  = 8.2 Hz, 2H), 7.68 – 7.61 (m, 2H), 7.48 – 7.34 (m, 3H), 7.27 ( $d_{\text{AA'XX'}}$ ,  $J$  = 8.2 Hz, 2H), 3.79 – 3.66 (m, 1H<sub>e</sub>), 2.60 (ddd,  $J$  = 12.8, 10.7, 3.2 Hz, 1H<sub>e</sub>), 2.51 (s, 3H), 2.41 (s, 3H), 2.18 (dd,  $J$  = 11.3, 7.6 Hz, 1H<sub>a</sub>), 2.03 – 1.92 (m, 1H<sub>d</sub>), 1.93 – 1.76 (m, 1H<sub>b</sub>+1H<sub>c</sub>), 1.73 – 1.63 (m, 1H<sub>c</sub>), 1.64 (dd,  $J$  = 11.3, 3.8 Hz, 1H<sub>a</sub>), 1.13 (app. qd,  $J$  = 13.0, 3.0 Hz, 1H<sub>d</sub>) ppm;  $^{13}\text{C}$  NMR (101 MHz,  $\text{CDCl}_3$ ):  $\delta$  = 178.3 (C), 144.2 (C), 137.8 (C), 134.3 (C), 129.9 (2CH), 129.2 (2CH), 128.7 (CH), 128.4 (2CH), 126.5 (2CH), 101.3 (C<sub>g</sub>), 97.7 (C<sub>f</sub>), 45.9 (C<sub>e</sub>H<sub>2</sub>), 42.6 (C<sub>a</sub>H<sub>2</sub>), 39.0 (C<sub>b</sub>H), 27.9 (C<sub>d</sub>H<sub>2</sub>), 23.5 (C<sub>c</sub>H<sub>2</sub>), 21.7 (CH<sub>3</sub>), 14.6 (SCH<sub>3</sub>) ppm; HRMS (ES–TOF):  $m/z$ : calcd for  $\text{C}_{22}\text{H}_{25}\text{N}_2\text{O}_3\text{S}_2$ : 429.1301, found 429.1303  $[\text{M}+\text{H}]^+$ .

## Post catalysis transformations

### Formation of aminoalcohol derivatives

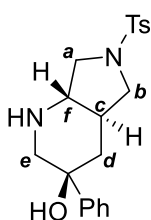
#### General procedure 10: reduction of polycycles with $\text{LiAlH}_4$ (GP10)

*Solid  $\text{LiAlH}_4$ :*  $\text{LiAlH}_4$  (5.0 eq.) was weighed in a glovebox and transferred to a flame dried Schlenk tube. THF (0.1 M wrt polycycle) was added cautiously and the reaction mixture cooled to 0 °C. The relevant polycycle (1.0 eq.) was added and the reaction mixture vigorously stirred at 0 °C for 10 min before the reaction mixture was allowed to warm to r.t. and stirred for the allotted time.

*$\text{LiAlH}_4$  solution:* the relevant polycycle (1.0 eq.) was dissolved in THF (0.1 M wrt polycycle) and cooled to 0 °C. 1 M  $\text{LiAlH}_4$  in THF (5.0 eq.) was added dropwise over 2 min and the resulting mixture vigorously stirred for 10 min at 0 °C before the reaction mixture was allowed to warm to r.t. and stirred for the allotted time.

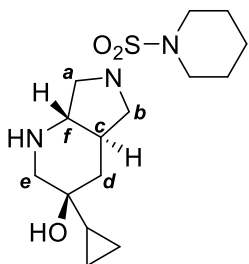
Upon completion of the reaction by TLC, satd Rochelle's salt<sub>(aq)</sub> was added cautiously and the resulting mixture stirred vigorously for 30 min. The resulting mixture was transferred to a separating funnel and extracted with CHCl<sub>3</sub>/IPA (3:1, 3×). The combined organics were washed with H<sub>2</sub>O (1×), brine (1×), dried over Na<sub>2</sub>SO<sub>4</sub>, filtered and concentrated under reduced pressure. Purification by flash column chromatography gave the corresponding amino alcohols.

**(3*S*,4*aR*,7*aS*)-3-Phenyl-6-tosyloctahydro-1*H*-pyrrolo[3,4-*b*]pyridin-3-ol **155****



Following **GP10** with polycycle **154** (82.7 mg, 0.15 mmol), LiAlH<sub>4</sub> (28.5 mg, 0.75 mmol) and THF (1.5 mL) for 1 h. Purification by flash column chromatography (EtOAc) gave amino alcohol **155** as a white foam (53.6 mg, 96%); mp: 80–82 °C; IR (neat):  $\nu$  = 3100 (br.), 2946, 1448, 1338, 1156, 1093, 1016 cm<sup>-1</sup>; <sup>1</sup>H NMR (400 MHz, CDCl<sub>3</sub>):  $\delta$  = 7.67 – 7.58 (m, 4H), 7.36 – 7.20 (m, 5H), 3.61 – 3.51 (m, 1H<sub>a</sub>+1H<sub>e</sub>), 3.35 (dd,  $J$  = 9.3, 7.1 Hz, 1H<sub>b</sub>), 2.88 – 2.77 (m, 1H<sub>a</sub>+1H<sub>b</sub>+1H<sub>e</sub>), 2.52 (app. td,  $J$  = 10.4, 7.0 Hz, 1H<sub>f</sub>), 2.40 (s, 3H), 2.41 – 2.33 (m, 1H<sub>d</sub>), 1.93 (br. s, OH+NH), 1.53 (app. t,  $J$  = 12.5 Hz, 1H<sub>d</sub>), 1.44 – 1.33 (m, 1H<sub>c</sub>) ppm; <sup>13</sup>C NMR (101 MHz, CDCl<sub>3</sub>):  $\delta$  = 145.0 (C), 143.5 (C), 134.6 (C), 129.8 (2CH), 128.5 (2CH), 127.8 (CH), 127.3 (2CH), 126.7 (2CH), 71.2 (C), 61.7 (C<sub>f</sub>H), 57.0 (C<sub>e</sub>H<sub>2</sub>), 51.3 (C<sub>a</sub>H<sub>2</sub>), 50.7 (C<sub>b</sub>H<sub>2</sub>), 41.2 (C<sub>c</sub>H), 41.1 (C<sub>d</sub>H<sub>2</sub>), 21.6 (CH<sub>3</sub>) ppm; HRMS (ES–TOF):  $m/z$ : calcd for C<sub>20</sub>H<sub>25</sub>N<sub>2</sub>O<sub>3</sub>S: 373.1580, found 373.1586 [M+H]<sup>+</sup>.

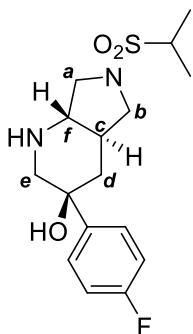
**(3*S*,4*aR*,7*aS*)-3-Cyclopropyl-6-(piperidin-1-ylsulfonyl)octahydro-1*H*-pyrrolo[3,4-*b*]pyridin-3-ol 158a**



Following **GP10** with polycycle **91c** (80.9 mg, 0.15 mmol), LiAlH<sub>4</sub> (34.2 mg, 0.9 mmol) and THF (1.5 mL) for 6 h. Purification by flash column chromatography (94:6 CH<sub>2</sub>Cl<sub>2</sub>/MeOH) gave amino alcohol **158a** as a brown solid (42.3 mg, 86%); mp: 111–113 °C; IR (neat):  $\nu$  = 3509

(br.), 2939, 2854, 1445, 1320, 1276, 1135, 1053, 1004 cm<sup>-1</sup>; <sup>1</sup>H NMR (400 MHz, CDCl<sub>3</sub>):  $\delta$  = 3.58 (dd,  $J$  = 8.7, 7.0 Hz, 1H<sub>a</sub>), 3.50 (dd,  $J$  = 9.1, 6.9 Hz, 1H<sub>b</sub>), 3.19 – 3.14 (m, 4H), 3.03 – 2.97 (m, 1H<sub>a</sub>+1H<sub>e</sub>), 2.93 (dd,  $J$  = 11.4, 9.1 Hz, 1H<sub>b</sub>), 2.73 (app. dt,  $J$  = 10.4, 7.0 Hz, 1H<sub>f</sub>), 2.70 (d,  $J_{AB}$  = 11.4 Hz, 1H<sub>e</sub>), 2.07 – 1.96 (m, 1H<sub>c</sub>+1H<sub>d</sub>), 1.66 – 1.57 (m, 4H+NH+OH), 1.56 – 1.48 (m, 2H), 1.43 – 1.31 (m, 1H<sub>d</sub>+1H), 0.57 – 0.51 (m, 1H), 0.44 – 0.38 (m, 3H) ppm; <sup>13</sup>C NMR (101 MHz, CDCl<sub>3</sub>):  $\delta$  = 68.2 (C), 62.4 (C<sub>f</sub>H), 57.8 (C<sub>e</sub>H<sub>2</sub>), 51.8 (C<sub>b</sub>H<sub>2</sub>), 51.7 (C<sub>a</sub>H<sub>2</sub>), 47.1 (2CH<sub>2</sub>), 41.9 (C<sub>c</sub>H), 40.9 (C<sub>d</sub>H<sub>2</sub>), 25.6 (2CH<sub>2</sub>), 23.9 (CH<sub>2</sub>), 17.5 (CH), 1.2 (CH<sub>2</sub>), 0.6 (CH<sub>2</sub>) ppm; HRMS (ES–TOF):  $m/z$ : calcd for C<sub>15</sub>H<sub>28</sub>N<sub>3</sub>O<sub>3</sub>S: 330.1846, found 330.1852 [M+H]<sup>+</sup>.

**(3*S*,4*aR*,7*aS*)-3-(4-Fluorophenyl)-6-(isopropylsulfonyl)octahydro-1*H*-pyrrolo[3,4-*b*]pyridin-3-ol 158b**

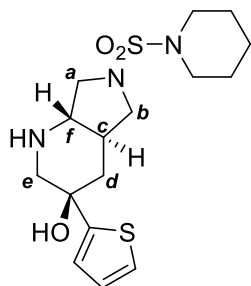


Following **GP10** with polycycle **91d** (89.6 mg, 0.15 mmol), LiAlH<sub>4</sub> (28.5 mg, 0.75 mmol) and THF (1.5 mL) for 2 h. Purification by flash column chromatography (0→5<sub>hold</sub>→10 CH<sub>2</sub>Cl<sub>2</sub>/MeOH) gave amino alcohol **158b** as a pale yellow powder (43.2 mg, 84%); mp: 90–91 °C; IR (neat):  $\nu$  = 3478 (br.), 2939, 2877, 1601, 1507, 1316, 1224, 1130, 1015 cm<sup>-1</sup>; <sup>1</sup>H NMR (400 MHz, CDCl<sub>3</sub>):  $\delta$  = 7.78 – 7.71 (m, 2H), 7.08 – 7.00 (m, 2H), 3.67 (dd,  $J$  = 8.4, 6.7 Hz, 1H<sub>a</sub>), 3.60 (dd,  $J$  = 12.1, 2.2 Hz, 1H<sub>e</sub>), 3.41 (dd,  $J$  = 9.0, 6.9 Hz, 1H<sub>b</sub>), 3.14 (hept,  $J$  = 6.8 Hz, 1H), 3.04 (dd,  $J$  = 11.0, 9.0 Hz, 1H<sub>b</sub>), 2.99 (dd,  $J$  = 10.2, 8.4 Hz, 1H<sub>a</sub>), 2.99 (d,  $J_{AB}$  = 12.1 Hz, 1H<sub>e</sub>), 2.86 (app.



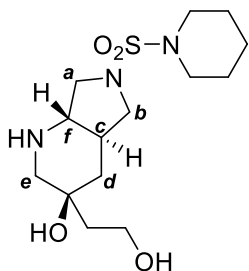
td,  $J = 10.1, 6.7$ , Hz 1H<sub>f</sub>), 2.37 (app. dt,  $J = 11.8, 2.4$  Hz, 1H<sub>d</sub>), 1.99 (s, OH+NH), 1.68 (dd,  $J = 12.7, 11.8$  Hz, 1H<sub>d</sub>), 1.63 – 1.53 (m, 1H<sub>c</sub>), 1.30 (d,  $J = 6.8$  Hz, 3H), 1.28 (d,  $J = 6.8$  Hz, 3H) ppm; <sup>13</sup>C NMR (101 MHz, CDCl<sub>3</sub>):  $\delta = 162.18$  (d,  $J = 246.9$  Hz, C), 141.3 (d,  $J = 3.3$  Hz, C), 128.8 (d,  $J = 7.9$  Hz, 2CH), 115.22 (d,  $J = 21.1$  Hz, 2CH), 71.2 (C), 62.2 (C<sub>f</sub>H), 57.4 (C<sub>e</sub>H<sub>2</sub>), 53.6 (CH), 51.9 (C<sub>a</sub>H<sub>2</sub>), 51.2 (C<sub>b</sub>H<sub>2</sub>), 41.7 (C<sub>d</sub>H<sub>2</sub>), 41.6 (C<sub>c</sub>H), 16.73 (CH<sub>3</sub>), 16.70 (CH<sub>3</sub>) ppm; HRMS (ES–TOF):  $m/z$ : calcd for C<sub>16</sub>H<sub>24</sub>N<sub>2</sub>O<sub>3</sub>FS: 343.1486, found 343.1493 [M+H]<sup>+</sup>.

**(3*R*,4*aR*,7*aS*)–6–(Piperidin–1-ylsulfonyl)–3–(thiophen–2-yl)octahydro–1*H*–pyrrolo[3,4–*b*]pyridin–3–ol 158c**



Following **GP10** with polycycle **91e** (82.0 mg, 0.141 mmol), LiAlH<sub>4</sub> (28.5 mg, 0.50 mmol) and THF (1.5 mL) for 14 h. Purification by flash column chromatography (EtOAc) gave amino alcohol **158c** as a pale brown solid (42.9 mg, 82%); mp: 156–157 °C; IR (neat):  $\nu = 3479$  (br.), 2937, 2854, 1445, 1329, 1158, 1137, 1012, 930 cm<sup>–1</sup>; <sup>1</sup>H NMR (400 MHz, CDCl<sub>3</sub>):  $\delta = 7.31$  (dd,  $J = 5.1, 1.2$  Hz, 1H), 7.24 (dd,  $J = 3.6, 1.2$  Hz, 1H), 7.02 (dd,  $J = 5.1, 3.6$  Hz, 1H), 3.65 – 3.54 (m, 1H<sub>e</sub>+1H<sub>a</sub>), 3.45 (dd,  $J = 9.3, 6.4$  Hz, 1H<sub>b</sub>), 3.15 (app. t,  $J = 5.4$  Hz, 4H), 3.06 (d,  $J_{AB} = 12.8$  Hz, 1H<sub>c</sub>), 2.98 (dd,  $J = 10.9, 9.3$  Hz, 1H<sub>b</sub>), 2.94 – 2.80 (m, 1H<sub>a</sub>+1H<sub>f</sub>), 2.56 – 2.50 (m, 1H<sub>c</sub>), 2.11 (br. s, OH+NH), 1.82 – 1.76 (m, 2H), 1.66 – 1.54 (m, 4H), 1.56 – 1.46 (m, 2H) ppm; <sup>13</sup>C NMR (101 MHz, CDCl<sub>3</sub>):  $\delta = 149.6$  (C), 127.3 (CH), 125.6 (CH), 125.1 (CH), 70.6 (C), 62.4 (C<sub>f</sub>H), 58.4 (C<sub>e</sub>H<sub>2</sub>), 51.44 (C<sub>a</sub>H<sub>2</sub>), 51.36 (C<sub>b</sub>H<sub>2</sub>), 47.1 (2CH<sub>2</sub>), 42.2 (C<sub>c</sub>H), 41.7 (C<sub>d</sub>H<sub>2</sub>), 25.6 (2CH<sub>2</sub>), 23.9 (CH<sub>2</sub>) ppm; HRMS (ES–TOF):  $m/z$ : calcd for C<sub>16</sub>H<sub>26</sub>N<sub>3</sub>O<sub>3</sub>S<sub>2</sub>: 372.1410, found 372.1414 [M+H]<sup>+</sup>.

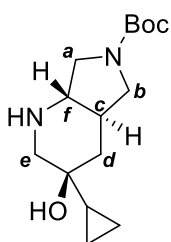
**(3*S*,4*aR*,7*aS*)-3-(2-Hydroxyethyl)-6-(isopropylsulfonyl)octahydro-1*H*-pyrrolo[3,4-*b*]pyridin-3-ol 158d**



Following **GP10** with polycycle **91g** (75.5 mg, 0.13 mmol), 1 M LiAlH<sub>4</sub> in THF (0.65 mL, 0.65 mmol) and THF (1.3 mL) for 17 h. Purification by flash column chromatography (0→5<sub>hold</sub>→10 CH<sub>2</sub>Cl<sub>2</sub>/MeOH) gave amino alcohol **158d** as a light brown powder (29.8 mg, 69%); mp: 146–149 °C;

IR (neat):  $\nu$  = 3325 (br.), 2927, 2868, 1737, 1437, 1337, 1281, 1173, 1158, 1137, 1047, 1034, 1022, 924 cm<sup>-1</sup>; <sup>1</sup>H NMR (400 MHz, CDCl<sub>3</sub>):  $\delta$  = 4.00 – 3.85 (m, 2H), 3.57 (dd,  $J$  = 8.7, 6.9 Hz, 1H<sub>a</sub>), 3.48 (dd,  $J$  = 9.1, 6.9 Hz, 1H<sub>b</sub>), 3.21 – 3.14 (m, 4H+1H<sub>e</sub>), 2.99 (dd,  $J$  = 10.4, 8.7 Hz, 1H<sub>a</sub>), 2.94 (dd,  $J$  = 11.3, 9.1 Hz, 1H<sub>b</sub>), 2.74 (td,  $J$  = 10.5, 6.9 Hz, 1H<sub>f</sub>), 2.68 (d,  $J_{AB}$  = 11.9 Hz, 1H<sub>e</sub>), 2.47 (br. s, NH+2OH), 2.12 (ddd,  $J$  = 12.5, 3.5, 1.9 Hz, 1H<sub>d</sub>), 2.06 – 1.93 (m, 2H), 1.85 – 1.72 (m, 1H), 1.65 – 1.57 (m, 4H), 1.57 – 1.49 (m, 2H), 1.38 (app. t,  $J$  = 12.6 Hz, 1H<sub>d</sub>) ppm; <sup>13</sup>C NMR (101 MHz, CDCl<sub>3</sub>):  $\delta$  = 71.8 (C), 62.5 (C<sub>f</sub>H), 59.7 (CH<sub>2</sub>), 56.9 (C<sub>e</sub>H<sub>2</sub>), 51.7 (C<sub>a</sub>H-<sub>2</sub>+C<sub>b</sub>H<sub>2</sub>), 47.1 (2CH<sub>2</sub>), 42.0 (C<sub>c</sub>H), 39.7 (C<sub>d</sub>H<sub>2</sub>), 38.1 (CH<sub>2</sub>), 25.6 (2CH<sub>2</sub>), 23.9 (CH<sub>2</sub>) ppm; HRMS (ES-TOF):  $m/z$ : calcd for C<sub>14</sub>H<sub>28</sub>N<sub>3</sub>O<sub>4</sub>S: 334.1795, found 334.1802 [M+H]<sup>+</sup>.

***tert*-Butyl (3*S*,4*aR*,7*aS*)-3-cyclopropyl-3-hydroxyoctahydro-6*H*-pyrrolo[3,4-*b*]pyridine-6-carboxylate 158e**

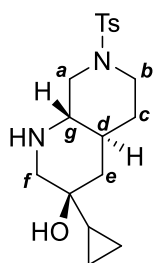


Following **GP10** with polycycle **91h** (148 mg, 0.30 mmol), 1 M LiAlH<sub>4</sub> in THF (1.50 mL, 1.50 mmol) and THF (3.0 mL) for 16 h. Purification by flash column chromatography (95:5 CH<sub>2</sub>Cl<sub>2</sub>/MeOH) gave amino alcohol **158e** as a pale yellow solid (52.6 mg, 62%); mp: 121–125 °C; IR (neat):  $\nu$  = 3281 (br.), 2924,

1674, 1408, 1366, 1150, 1089 cm<sup>-1</sup>; *NMR spectra display a mixture of rotamers*: <sup>1</sup>H NMR (400 MHz, CDCl<sub>3</sub>):  $\delta$  = 3.67 and 3.52 (d,  $J_{AB}$  = 10.0, 7.0 Hz, 1H<sub>a</sub>), 3.58 (app. dt,  $J$  = 10.3, 7.2 Hz, 1H<sub>b</sub>), 3.00 (d,  $J_{AB}$  = 11.8 Hz, 1H<sub>e</sub>), 2.00 – 2.93 (m, 1H<sub>b</sub>), 2.86 (app. t,  $J$  = 10.7 Hz, 1H<sub>a</sub>), 2.71

(dd,  $J = 11.8, 1.7$  Hz,  $1H_e$ ), 2.70 – 2.61 (m,  $1H_f$ ), 2.08 – 1.84 (m,  $1H_c+1H_d+OH+NH$ ), 1.43 (s, 9H), 1.48 – 1.31 (m,  $1H_d+1H$ ), 0.58 – 0.49 (m, 1H), 0.45 – 0.35 (m, 3H) ppm;  $^{13}C$  NMR (101 MHz,  $CDCl_3$ ):  $\delta = 154.8$  and  $154.7$  (C), 79.50 and 79.47 (C), 68.2 (C), 62.4 and 61.8 ( $C_fH$ ), 57.9 ( $C_eH_2$ ), 49.8 and 49.7 ( $C_aH_2$ ), 49.3 and 49.1 ( $C_bH_2$ ), 41.6 and 41.03 ( $C_cH$ ), 41.09 and 40.98 ( $C_dH_2$ ), 28.6 ( $3CH_3$ ), 17.58 and 17.56 (CH), 1.1 ( $CH_2$ ), 0.62 and 0.56 ( $CH_2$ ) ppm; HRMS (ES–TOF):  $m/z$ : calcd for  $C_{15}H_{27}N_2O_3$ : 283.2016, found 283.2025  $[M+H]^+$ .

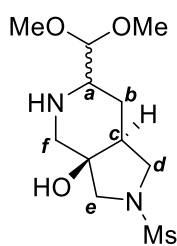
**(3*S*,4*aS*,8*aS*)–3–Cyclopropyl–7–tosyldecahydro–1,7–naphthyridin–3–ol 159**



Following **GP10** with polycycle **93a** (77.3 mg, 0.15 mmol),  $LiAlH_4$  (28.5 mg, 0.75 mmol) and THF (1.5 mL) for 2 h. Purification by flash column chromatography (EtOAc) gave amino alcohol **159** as flakey white crystals (31.1 mg, 60%); mp: 143–144 °C; IR (neat):  $\nu = 3100$  (br.), 2919, 2849, 1597,

1449, 1339, 1162, 1094  $cm^{-1}$ ;  $^1H$  NMR (400 MHz,  $CDCl_3$ ):  $\delta = 7.64$  ( $d_{AA'XX'}$ ,  $J = 8.3$  Hz, 2H), 7.31 ( $d_{AA'XX'}$ ,  $J = 8.3$  Hz, 2H), 3.86 – 3.78 (m,  $1H_a+1H_b$ ), 2.93 (dd,  $J = 11.0, 2.3$  Hz,  $1H_f$ ), 2.64 (d,  $J_{AB} = 11.0$  Hz,  $1H_f$ ), 2.43 (s, 3H), 2.39 (app. td,  $J = 10.0, 3.9$  Hz,  $1H_g$ ), 2.23 (app. td,  $J = 12.1, 2.8$  Hz,  $1H_b$ ), 2.05 (app. t,  $J = 10.7$  Hz,  $1H_a$ ), 1.78 (dd,  $J = 8.5, 2.3$  Hz,  $1H_e$ ), 1.60 (app. dq,  $J = 13.0, 2.3$ ,  $1H_c$ ), 1.52 – 1.38 (m,  $1H_c+OH+NH$ ), 1.34 – 1.21 (m,  $1H_d+1H_e+1H$ ), 0.50 – 0.43 (m, 1H), 0.38 – 0.31 (m, 3H) ppm;  $^{13}C$  NMR (101 MHz,  $CDCl_3$ ):  $\delta = 143.7$  (C), 133.3 (C), 129.8 (2CH), 127.8 (2CH), 68.3 (C), 59.0 ( $C_gH$ ), 57.5 ( $C_fH_2$ ), 51.1 ( $C_aH_2$ ), 46.5 ( $C_bH_2$ ), 44.5 ( $C_eH_2$ ), 38.3 ( $C_dH$ ), 30.7 ( $C_cH_2$ ), 21.7 ( $CH_3$ ), 17.1 (CH), 0.9 ( $CH_2$ ), 0.4 ( $CH_2$ ) ppm; HRMS (ES–TOF):  $m/z$ : calcd for  $C_{18}H_{27}N_2O_3S$ : 351.1737, found 351.1744  $[M+H]^+$ .

**(3aR,7aS)-6-(Dimethoxymethyl)-2-(methylsulfonyl)octahydro-3aH-pyrrolo[3,4-c]pyridin-3a-ol **160a****



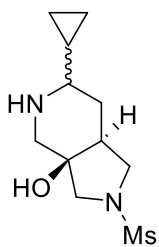
Following **GP10** with polycycle **50b** (237 mg, 0.50 mmol), 1 M LiAlH<sub>4</sub> in THF (2.5 mL, 2.50 mmol) and THF (5.0 mL) for 20 h. Purification by flash column chromatography (9:1 CH<sub>2</sub>Cl<sub>2</sub>/MeOH) gave a 1:1 mixture of diastereomers of **160a** as a white solid (114.4 mg, 78%), which was subjected to further flash column chromatography (95:5 CH<sub>2</sub>Cl<sub>2</sub>/MeOH) to give **160a** (30.6 mg, 34:1 mixture) and **160a'** (11.9 mg, 5.6:1 mixture) – the remainder was isolated as a mixed fraction:

**160a**: mp: 131–133 °C; IR (neat):  $\nu$  = 3099 (br.) 2933, 2876, 1326, 1313, 1171, 1148, 1083, 1065, 1048, 924 cm<sup>-1</sup>; <sup>1</sup>H NMR (400 MHz, CDCl<sub>3</sub>):  $\delta$  = 4.11 (d,  $J$  = 7.2 Hz, 1H), 3.47 (dd,  $J$  = 8.3, 6.9 Hz, 1H<sub>d</sub>), 3.40 (s, 3H), 3.38 (s, 3H), 3.38 (d,  $J_{AB}$  = 11.3 Hz, 1H<sub>e</sub>), 3.21 (d,  $J_{AB}$  = 11.3 Hz, 1H<sub>e</sub>), 3.05 (d,  $J_{AB}$  = 10.8 Hz, 1H<sub>f</sub>), 2.98 (dd,  $J$  = 11.4, 8.3 Hz, 1H<sub>d</sub>), 2.84 (s, 3H), 2.68 (ddd,  $J$  = 10.9, 7.2, 2.8 Hz, 1H<sub>a</sub>), 2.61 (d,  $J_{AB}$  = 10.8 Hz, 1H<sub>f</sub>), 2.00 (br. s, OH+NH), 1.90 – 1.76 (m, 1H<sub>c</sub>+1H<sub>b</sub>), 1.32 – 1.21 (m, 1H<sub>b</sub>) ppm; <sup>13</sup>C NMR (101 MHz, CDCl<sub>3</sub>):  $\delta$  = 106.7 (CH), 73.8 (C), 56.5 (C<sub>a</sub>H), 56.4 (C<sub>e</sub>H<sub>2</sub>), 54.7 (CH<sub>3</sub>), 54.5 (CH<sub>3</sub>), 52.3 (C<sub>f</sub>H<sub>2</sub>), 50.5 (C<sub>d</sub>H<sub>2</sub>), 45.0 (C<sub>c</sub>H), 34.0 (CH<sub>3</sub>), 25.3 (C<sub>b</sub>H<sub>2</sub>) ppm; HRMS (ES–TOF):  $m/z$ : calcd for C<sub>11</sub>H<sub>23</sub>N<sub>2</sub>O<sub>5</sub>S: 295.1322, found 295.1331 [M+H]<sup>+</sup>.

**160a'**: mp: 120–124 °C; IR (neat):  $\nu$  = 3473 (br.), 2923, 2881, 2851, 1324, 1275, 1160, 1143, 1113, 1042 cm<sup>-1</sup>; <sup>1</sup>H NMR (400 MHz, CDCl<sub>3</sub>):  $\delta$  = 4.56 (d,  $J$  = 8.2 Hz, 1H), 3.49 (dd,  $J$  = 8.3, 6.9 Hz, 1H<sub>d</sub>), 3.44 (s, 3H), 3.39 (s, 3H), 3.39 (d,  $J_{AB}$  = 11.3 Hz, 1H<sub>e</sub>), 3.23 (d,  $J_{AB}$  = 11.3 Hz, 1H<sub>e</sub>), 3.00 – 2.93 (m, 1H<sub>a</sub>), 2.96 (dd,  $J$  = 11.3, 8.3 Hz, 1H<sub>d</sub>), 2.86 (s, 3H), 2.86 – 2.82 (m, 2H<sub>f</sub>), 1.98 (dddd,  $J$  = 13.1, 11.3, 6.9, 4.4 Hz, 1H<sub>c</sub>), 1.91 (br. s, OH+NH), 1.87 (ddd,  $J$  = 13.5, 4.5, 1.7 Hz, 1H<sub>b</sub>), 1.76 (app. td,  $J$  = 13.4, 6.0 Hz, 1H<sub>b</sub>) ppm; <sup>13</sup>C NMR (101 MHz, CDCl<sub>3</sub>):  $\delta$  = 101.7

(CH), 73.8 (C), 56.7 (C<sub>e</sub>H<sub>2</sub>), 54.9 (CH<sub>3</sub>), 54.4 (CH<sub>3</sub>), 51.3 (C<sub>a</sub>H), 51.0 (C<sub>d</sub>H<sub>2</sub>), 48.1 (C<sub>f</sub>H<sub>2</sub>), 41.1 (C<sub>c</sub>H), 34.2 (CH<sub>3</sub>), 22.2 (C<sub>b</sub>H<sub>2</sub>) ppm; HRMS (ES–TOF): m/z: calcd for C<sub>11</sub>H<sub>23</sub>N<sub>2</sub>O<sub>5</sub>S: 295.1322, found 295.1331 [M+H]<sup>+</sup>.

**(3aR,7aS)-6-cyclopropyl-2-(methylsulfonyl)octahydro-3aH-pyrrolo[3,4-c]pyridin-3a-ol 160b**

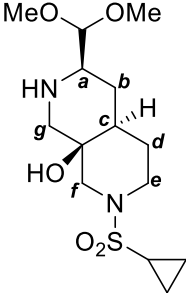


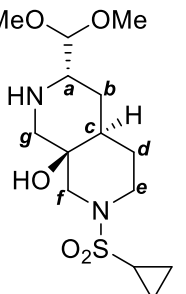
Following **GP10** with polycycle **50d** (220 mg, 0.50 mmol), 1 M LiAlH<sub>4</sub> in THF (2.5 mL, 2.50 mmol) and THF (5.0 mL) for 20 h. Purification by flash column chromatography (9:1 CH<sub>2</sub>Cl<sub>2</sub>) gave a 1:1 mixture of diastereomers of **160b** as a white solid (111 mg, 85%); mp: 134–138 °C; IR (neat): ν = 3239 (br.), 2941, 2885, 1329, 1304, 1145, 1036, 1009 cm<sup>-1</sup>; *due to excessive overlap, both sets of resonances are reported as a mixture, OH and NH resonances not observed in <sup>1</sup>H NMR spectra*: <sup>1</sup>H NMR (400 MHz, MeOD): δ = 3.51 – 3.40 (m, 2H), 3.38 – 3.29 (m, 3H), 3.21 (d, *J*<sub>AB</sub> = 10.9 Hz, 1H), 3.20 (d, *J*<sub>AB</sub> = 12.9 Hz, 1H), 3.13 – 3.06 (m, 3H), 3.00 (d, *J*<sub>AB</sub> = 12.9 Hz, 1H), 2.88 (s, 3H), 2.87 (s, 3H), 2.77 (d, *J*<sub>AB</sub> = 12.7 Hz, 1H), 2.35 (dddd, *J* = 12.8, 11.4, 7.2, 4.0, 1H), 2.26 (ddd, *J* = 10.6, 5.3, 1.5 Hz, 1H), 2.03 – 1.89 (m, 3H), 1.83 – 1.75 (m, 2H), 1.61 – 1.50 (m, 1H), 1.45 – 1.35 (m, 1H), 0.91 – 0.82 (m, 1H), 0.67 – 0.46 (m, 4H), 0.40 – 0.33 (m, 2H), 0.25 – 0.17 (m, 2H) ppm; <sup>13</sup>C NMR (101 MHz, MeOD): δ = 74.0 and 73.9 (C), 62.0 and 58.9 (CH), 58.6 and 58.4 (CH<sub>2</sub>), 52.9 and 51.5 (CH<sub>2</sub>) 51.8 and 48.4 (CH<sub>2</sub>), 46.1 and 41.0 (CH), 34.15 and 34.09 (CH<sub>3</sub>), 29.1 and 27.2 (CH<sub>2</sub>), 16.5 and 12.1 (CH), 5.8 and 4.2 (CH<sub>2</sub>), 4.6 and 2.9 (CH<sub>2</sub>) ppm; HRMS (ES–TOF): m/z: calcd for C<sub>11</sub>H<sub>21</sub>N<sub>2</sub>O<sub>3</sub>S: 261.1267, found 261.1279 [M+H]<sup>+</sup>.

**(4aR,8aR)-2-(Cyclopropylsulfonyl)-6-(dimethoxymethyl)octahydro-2,7-naphthyridin-8a(1H)-ol 161a**

Following **GP10** with polycycle **106d** (80.1 mg, 0.156 mmol), 1 M LiAlH<sub>4</sub> in THF (0.78 mL, 0.78 mmol) and THF (2.0 mL) for 16 h. Purification by flash column chromatography (8:2

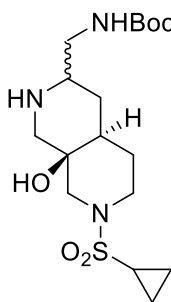
EtOAc/MeOH) gave a 1:1 mixture of diastereomers of **161a** as a white solid (44.2 mg, 85%), which was subjected to further flash column chromatography (95:5 CH<sub>2</sub>Cl<sub>2</sub>/MeOH) to give **161a** (20 mg, 11:1 mixture) and **161a'** (19 mg, 5:1 mixture):


**161a** mp: 169–171 °C; IR (neat):  $\nu$  = 3235 (br.), 2920, 2852, 1455, 1330, 1305, 1150, 1138, 1065, 1039, 940, 890 cm<sup>-1</sup>; <sup>1</sup>H NMR (400 MHz, CDCl<sub>3</sub>):  $\delta$  = 4.11 (d,  $J$  = 6.8 Hz, 1H), 3.83 (app. ddt,  $J$  = 12.8, 4.4, 2.0 Hz, 1H<sub>e</sub>), 3.68 (dd,  $J$  = 12.6, 1.9 Hz, 1H<sub>f</sub>), 3.41 (s, 3H), 3.40 (s, 3H), 2.87 (app. td,  $J$  = 12.8, 2.7 Hz, 1H<sub>e</sub>), 2.79 (d,  $J_{AB}$  = 11.4 Hz, 1H<sub>g</sub>), 2.75 – 2.67 (m, 1H<sub>a</sub>), 2.69 (d,  $J_{AB}$  = 12.6 Hz, 1H<sub>f</sub>), 2.54 (tt,  $J$  = 8.1, 5.0 Hz, 1H), 2.48 (d,  $J_{AB}$  = 11.4 Hz, 1H<sub>g</sub>), 2.60 – 2.05 (br. m, NH+OH), 1.74 (app. dtd,  $J$  = 14.0, 12.6, 4.3 Hz, 1H<sub>d</sub>), 1.52 (app. dt,  $J$  = 12.9, 3.4 Hz, 1H<sub>b</sub>), 1.44 – 1.37 (m, 1H<sub>c</sub>+1H<sub>d</sub>), 1.27 – 1.19 (m, 1H<sub>b</sub>), 1.19 – 1.11 (m, 2H), 1.00 – 0.90 (m, 2H) ppm; <sup>13</sup>C NMR (101 MHz, CDCl<sub>3</sub>):  $\delta$  = 107.2 (CH), 65.9 (C), 58.0 (C<sub>a</sub>H), 55.12 (CH<sub>3</sub>), 55.05 (CH<sub>3</sub>), 54.23 (C<sub>f/g</sub>H<sub>2</sub>), 54.20 (C<sub>f/g</sub>H<sub>2</sub>), 46.6 (C<sub>e</sub>H<sub>2</sub>), 40.6 (C<sub>c</sub>H), 29.0 (C<sub>b</sub>H<sub>2</sub>), 27.6 (CH), 27.3 (C<sub>d</sub>H<sub>2</sub>), 5.1 (CH<sub>2</sub>), 4.7 (CH<sub>2</sub>) ppm; HRMS (ES–TOF):  $m/z$ : calcd for C<sub>14</sub>H<sub>27</sub>N<sub>2</sub>O<sub>5</sub>S: 335.1635, found 335.1640 [M+H]<sup>+</sup>.


**161a'** mp: 135–138 °C; IR (neat):  $\nu$  = 3230 (br.), 2921, 2852, 1458, 1331, 1306, 1150, 1138, 1065, 1040 cm<sup>-1</sup>; <sup>1</sup>H NMR (400 MHz, CDCl<sub>3</sub>):  $\delta$  = 4.63 (d,  $J$  = 7.9 Hz, 1H), 3.84 (app. ddt,  $J$  = 13.0, 4.3, 2.1 Hz, 1H<sub>e</sub>), 3.67 (dd,  $J$  = 12.7, 1.9 Hz, 1H<sub>f</sub>), 3.43 (s, 3H), 3.38 (s, 3H), 3.00 (ddd,  $J$  = 7.9, 5.9, 1.6 Hz, 1H<sub>a</sub>), 2.89 (app. td,  $J$  = 12.7, 2.8 Hz, 1H<sub>e</sub>), 2.77 – 2.67 (m, 1H<sub>f</sub>+1H<sub>g</sub>), 2.60 – 2.53 (m, 1H), 2.56 (d,  $J_{AB}$  = 12.2 Hz, 1H<sub>g</sub>), 2.17 (br. s, OH+NH), 1.73 – 1.62 (m, 1H<sub>d</sub>+1H<sub>b</sub>), 1.61 – 1.51 (m, 1H<sub>c</sub>+1H<sub>b</sub>), 1.37 (app. dq,  $J$  = 12.8, 2.8 Hz, 1H<sub>d</sub>), 1.19 – 1.12 (m, 2H), 1.00 – 0.93 (m, 2H) ppm; <sup>13</sup>C NMR (101 MHz, CDCl<sub>3</sub>):  $\delta$  = 102.0 (CH), 66.0 (C), 54.7 (CH<sub>3</sub>), 54.4

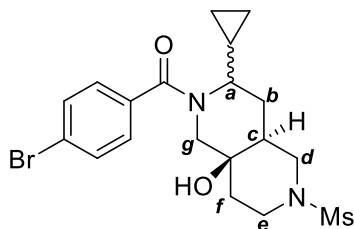
(C<sub>f</sub>H<sub>2</sub>), 54.0 (CH<sub>3</sub>), 52.2 (C<sub>a</sub>H), 49.3 (C<sub>g</sub>H<sub>2</sub>), 46.6 (C<sub>e</sub>H<sub>2</sub>), 36.8 (C<sub>c</sub>H), 27.8 (CH), 27.4 (C<sub>d</sub>H<sub>2</sub>), 26.0 (C<sub>b</sub>H<sub>2</sub>), 5.1 (CH<sub>2</sub>), 4.7 (CH<sub>2</sub>) ppm; HRMS (ES–TOF): m/z: calcd for C<sub>14</sub>H<sub>27</sub>N<sub>2</sub>O<sub>5</sub>S: 335.1635, found 335.1639 [M+H]<sup>+</sup>.

***tert*–Butyl (((4*aR*,8*aR*)–7–(cyclopropylsulfonyl)–8*a*–hydroxydecahydro–2,7–naphthyridin–3–yl)methyl)carbamate **161b****



Following **GP10** with polycycle **106c** (114 mg, 0.20 mmol), LiAlH<sub>4</sub> (38.0 mg, 1.00 mmol) and THF (2.0 mL) for 24 h. Purification by flash column chromatography (9:1 CH<sub>2</sub>Cl<sub>2</sub>/MeOH) gave a 1:1 mixture of diastereomers of **161b** as a white solid (68.1 mg, 87%); IR (neat):  $\nu$  = 3348 (br.), 2926, 1697, 1517, 1332, 1250, 1143, 888 cm<sup>-1</sup>; *due to excessive overlap, both sets of resonances are reported as a mixture*: <sup>1</sup>H NMR (400 MHz, CDCl<sub>3</sub>):  $\delta$  = 5.00 (br. s, 2H), 3.85 – 3.79 (m, 2H), 3.61 (dd, *J* = 12.4, 2.0 Hz, 1H), 3.51 (dd, *J* = 12.0, 1.9 Hz, 1H), 3.32 (ddd, *J* = 14.1, 10.3, 4.2 Hz, 1H), 3.26 – 3.10 (m, 2H), 3.02 (app. dt, *J* = 10.9, 5.6 Hz, 1H), 2.93 (ddd, *J* = 13.7, 7.9, 5.5 Hz, 1H), 2.90 – 2.76 (m, 3H), 2.74 – 2.60 (m, 4H), 2.50 (app. t, *J* = 12.3, 2H), 2.60 – 2.00 (br. m, 2OH+2NH), 2.49 – 2.39 (m, 1H), 2.35 (tt, *J* = 8.1, 4.0 Hz, 1H), 1.79 – 1.55 (m, 4H), 1.48 – 1.33 (m, 20H), 1.30 – 1.20 (m, 4H), 1.19 – 1.10 (m, 4H), 1.01 – 0.92 (m, 4H) ppm; <sup>13</sup>C NMR (101 MHz, CDCl<sub>3</sub>):  $\delta$  = 156.4 and 156.3 (C), 79.5 and 79.4 (C), 66.2 and 66.0 (C), 56.7 and 51.1 (CH), 54.7 and 54.4 (CH<sub>2</sub>), 48.0 and 46.9 (CH<sub>2</sub>), 46.7 and 46.0 (CH<sub>2</sub>), 40.8 and 36.1 (CH), 40.0 (CH<sub>2</sub>), 31.5 and 28.9 (CH<sub>2</sub>), 28.5 (3CH<sub>3</sub>), 27.5 and 27.3 (CH<sub>2</sub>), 27.0 and 26.4 (CH), 4.9 and 4.7 (CH<sub>2</sub>), 4.6 and 4.5 (CH<sub>2</sub>) ppm; HRMS (ES–TOF): m/z: calcd for C<sub>17</sub>H<sub>32</sub>N<sub>3</sub>O<sub>5</sub>S: 390.2057, found 390.2063 [M+H]<sup>+</sup>.

**(3aR,7aS)-6-Cyclopropyl-2-(methylsulfonyl)octahydro-3aH-pyrrolo[3,4-c]pyridin-3a-ol  
(4-Bromophenyl)((4aS,8aR)-3-cyclopropyl-8a-hydroxy-6-(methylsulfonyl)octahydro-  
2,6-naphthyridin-2(1H)-yl)methanone 162**



Following **GP10** with polycycle **107c** (136 mg, 0.30 mmol), 1 M LiAlH<sub>4</sub> in THF (1.5 mL, 1.50 mmol) and THF (3.0 mL) for 18 h. The crude material and NEt<sub>3</sub> (46 µL, 0.33 mmol) were dissolved in CH<sub>2</sub>Cl<sub>2</sub> (3.0 mL) and cooled to 0 °C. 4-Bromobenzoyl

chloride was added in one portion and the reaction was stirred for 5 h. 2 M HCl<sub>(aq)</sub> (10 mL) was added and the organics extracted CH<sub>2</sub>Cl<sub>2</sub> (3×10 mL). The combined organics were washed with brine (20 mL), dried over Na<sub>2</sub>SO<sub>4</sub>, filtered and concentrated under reduced pressure. Purification by flash column chromatography (2:8 hexane/EtOAc) gave amido alcohols **162a** (45 mg, 33%) and **162b** (45 mg, 33%) as pale yellow solids;

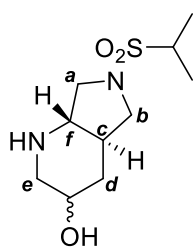
**162a**: mp: 164-166 °C; IR (neat): ν = 3507, 2925, 2863, 1607, 1592, 1321, 1310, 1143, 1126 cm<sup>-1</sup>; <sup>1</sup>H NMR (400 MHz, CDCl<sub>3</sub>): δ = 7.50 (d<sub>AA'XX'</sub>, *J* = 8.5 Hz, 2H), 7.36 (d<sub>AA'XX'</sub>, *J* = 8.5 Hz, 2H), 3.85 (d, *J*<sub>AB</sub> = 13.6 Hz, 1H<sub>g</sub>), 3.60 (ddd, *J* = 11.6, 4.5, 2.1 Hz, 1H<sub>d</sub>), 3.41 (ddd, *J* = 11.2, 3.9, 1.6 Hz, 1H<sub>e</sub>), 3.00 (app. td, *J* = 12.0, 3.1 Hz, 1H<sub>d</sub>), 2.90 (d, *J*<sub>AB</sub> = 13.6 Hz, 1H<sub>g</sub>), 2.75 (s, 3H), 2.77 – 2.71 (m, 1H<sub>e</sub>), 2.48 (br. s, OH), 2.27 (app. td, *J* = 10.6, 2.9 Hz, 1H<sub>a</sub>), 1.94 – 1.74 (m, 1H<sub>b</sub>+1H<sub>c</sub>), 1.64 (app. dt, *J* = 12.1, 3.2 Hz, 1H<sub>b</sub>), 1.56 (ddd, *J* = 13.5, 12.4, 4.9 Hz, 1H<sub>f</sub>), 1.46 (app. dt, *J* = 13.4, 2.7 Hz, 1H<sub>f</sub>), 1.33 – 1.19 (m, 1H), 0.58 (dddd, *J* = 8.7, 7.9, 5.9, 4.4 Hz, 1H), 0.36 – 0.22 (m, 2H), 0.12 – 0.04 (m, 1H) ppm; <sup>13</sup>C NMR (101 MHz, CDCl<sub>3</sub>): δ = 173.0 (C), 136.8 (C), 131.6 (2CH), 129.6 (2CH), 124.4 (C), 68.4 (C), 67.8 (C<sub>a</sub>H), 59.6 (C<sub>g</sub>H<sub>2</sub>), 45.6 (C<sub>e</sub>H<sub>2</sub>), 43.4 (C<sub>c</sub>H), 41.5 (C<sub>d</sub>H<sub>2</sub>), 34.9 (C<sub>f</sub>H<sub>2</sub>), 34.8 (CH<sub>3</sub>), 29.6 (C<sub>b</sub>H<sub>2</sub>), 14.8 (CH), 7.0 (CH<sub>2</sub>), 4.9 (CH<sub>2</sub>) ppm; MS (ES-TOF): *m/z*: 100% 481.1 [M+Na]<sup>+</sup>, 95% 479.1 [M+Na]<sup>+</sup>; HRMS (ES-TOF): *m/z*: calcd for C<sub>19</sub>H<sub>25</sub><sup>79</sup>BrN<sub>2</sub>O<sub>4</sub>SNa: 479.0611, found 479.0623 [M+Na]<sup>+</sup>.



**162b**: mp: 172-175 °C; IR (neat):  $\nu$  = 3508, 2922, 1682, 1609, 1451, 1320, 1310  $\text{cm}^{-1}$ ; MS (ES-TOF):  $m/z$ : 100% 459.1  $[\text{M}+\text{H}]^+$ , 95% 457.1  $[\text{M}+\text{Na}]^+$ ; HRMS (ES-TOF):  $m/z$ : calcd for  $\text{C}_{19}\text{H}_{26}^{79}\text{BrN}_2\text{O}_4\text{S}$ : 457.0792, found 457.0810  $[\text{M}+\text{H}]^+$ .

## Products derived from reduction of thioketals

### (4aR,7aS)-6-(Isopropylsulfonyl)octahydro-1H-pyrrolo[3,4-b]pyridin-3-ol **179**

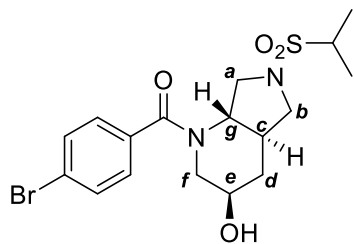


Following **GP10** with polycycle **91b** (270 mg, 0.50 mmol),  $\text{LiAlH}_4$  (94.9 mg, 2.50 mmol) and THF (5.0 mL) for 6 h. Purification by flash column chromatography (9:1  $\text{CH}_2\text{Cl}_2/\text{MeOH}$ ) gave a 4:1 diastereotopic mixture of amino alcohols **179** as white solids (102 mg, 82%); mp: 87–89 °C; IR (neat):

$\nu$  = 3297 (br.), 2934, 1465, 1316, 1130, 1027, 929  $\text{cm}^{-1}$ ; *only the major diastereomer resonances are reported*:  $^1\text{H}$  NMR (400 MHz,  $\text{CDCl}_3$ ):  $\delta$  = 3.76 (app. tt,  $J$  = 10.1, 4.6, 1H), 3.67 (dd,  $J$  = 8.8, 7.0 Hz, 1H), 3.57 (dd,  $J$  = 9.1, 7.2 Hz, 1H), 3.29 (ddd,  $J$  = 11.6, 4.8, 1.6 Hz, 1H), 3.20 (p,  $J$  = 6.8 Hz, 1H), 3.11 – 2.99 (m, 2H), 2.72 (app. td,  $J$  = 10.4, 7.0 Hz, 1H), 2.62 – 2.52 (m, 1H+OH+NH), 2.26 – 2.19 (m, 1H), 1.86 – 1.74 (m, 1H), 1.34 (d,  $J$  = 6.8 Hz, 3H), 1.32 (d,  $J$  = 6.8 Hz, 3H) 1.29 – 1.19 (m, 1H) ppm;  $^{13}\text{C}$  NMR (101 MHz,  $\text{CDCl}_3$ ):  $\delta$  = 67.7, 61.6, 53.7, 53.5, 51.5, 51.3, 43.3, 36.2, 16.7, 16.7 ppm; HRMS (ES-TOF):  $m/z$ : calcd for  $\text{C}_{10}\text{H}_{21}\text{N}_2\text{O}_3\text{S}$ : 249.1267, found 249.1275  $[\text{M}+\text{H}]^+$ .

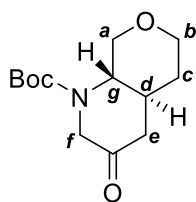
Attempts to crystallise to diastereomeric purity were unsuccessful. Material recrystallised from  $\text{CH}_2\text{Cl}_2/\text{hexane}$  was subsequently used in:

**(4-Bromophenyl)((4a*R*,7a*S*)-3-hydroxy-6-(isopropylsulfonyl)octahydro-1*H*-pyrrolo[3,4-*b*]pyridin-1-yl)methanone **182a****



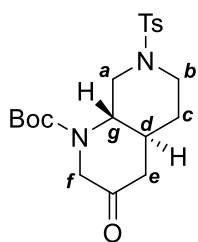
A recrystallised mixture of diastereomers **179** (24.8 mg, 0.10 mmol) and NEt<sub>3</sub> (16  $\mu$ L, 0.11 mmol) was dissolved in CH<sub>2</sub>Cl<sub>2</sub> (1.0 mL) and cooled to 0 °C. 4-Bromobenzoyl chloride (23.1 mg, 0.11 mmol) was added in one portion and the mixture stirred at 0 °C for 2 h. 2 M HCl<sub>(aq)</sub> (10 mL) was added and the organics extracted with CH<sub>2</sub>Cl<sub>2</sub> (3 $\times$ 10 mL). The combined organics were washed with brine (20 mL), dried over Na<sub>2</sub>SO<sub>4</sub>, filtered and concentrated under reduced pressure. Purification by flash column chromatography (2:8 hexane/EtOAc) allowed isolation of the single diastereomer **182a** as a white solid (33.8 mg, 78%) alongside a mixture of diastereomers (9.5 mg, 22%, 2.3:1.0 d.r., **182a:182b**); **182a**: mp: 173–175 °C; IR (neat):  $\nu$  = 3362, 2989, 2902, 1762, 1622, 1590, 1444, 1319, 1133, 1015, 1067, 1049, 1034 cm<sup>-1</sup>; <sup>1</sup>H NMR (400 MHz, CDCl<sub>3</sub>):  $\delta$  = 7.55 (d<sub>AA'</sub>XX',  $J$  = 8.4 Hz, 2H), 7.31 (d<sub>AA'</sub>XX',  $J$  = 8.4 Hz, 2H), 4.41 (dd,  $J$  = 9.7, 6.4 Hz, 1H<sub>a</sub>), 3.97 (app. dq,  $J$  = 9.6, 4.4 Hz, 1H<sub>e</sub>), 3.76 (ddd,  $J$  = 13.2, 3.9, 1.0 Hz, 1H<sub>f</sub>), 3.64 (dd,  $J$  = 9.3, 7.2 Hz, 1H<sub>b</sub>), 3.41 (app. t,  $J$  = 10.0 Hz, 1H<sub>a</sub>), 3.32 (app. td,  $J$  = 10.7, 6.4 Hz, 1H<sub>g</sub>), 3.22 (p,  $J$  = 6.8 Hz, 1H), 3.09 (dd,  $J$  = 11.3, 9.3 Hz, 1H<sub>b</sub>), 2.91 (dd,  $J$  = 13.2, 8.6 Hz, 1H<sub>f</sub>), 2.37 (d,  $J_{AB}$  = 4.5 Hz, OH), 2.31 (app. dt,  $J$  = 12.7, 4.9 Hz, 1H<sub>d</sub>), 2.11 (app. dddd,  $J$  = 18.3, 11.5, 5.8, 3.5 Hz, 1H<sub>c</sub>), 1.35 (d,  $J$  = 6.8 Hz, 3H), 1.34 (d,  $J$  = 6.8 Hz, 3H), 1.31 – 1.23 (m, 1H<sub>d</sub>) ppm; <sup>13</sup>C NMR (101 MHz, CDCl<sub>3</sub>):  $\delta$  = 172.5 (C), 134.2 (C), 132.0 (2CH), 129.4 (2CH), 125.2 (C), 66.2 (C<sub>e</sub>H), 59.6 (C<sub>g</sub>H), 54.3 (C<sub>f</sub>H<sub>2</sub>), 53.6 (CH), 51.6 (C<sub>a</sub>H<sub>2</sub>), 50.0 (C<sub>b</sub>H<sub>2</sub>), 41.2 (C<sub>c</sub>H), 34.9 (C<sub>d</sub>H<sub>2</sub>), 16.8 (CH<sub>3</sub>), 16.7 (CH<sub>3</sub>) ppm; MS (ES–TOF):  $m/z$ : 100% 433.1 [M+H]<sup>+</sup>, 95% 431.1 [M+H]<sup>+</sup>; HRMS (ES–TOF):  $m/z$ : calcd for C<sub>17</sub>H<sub>24</sub>N<sub>2</sub>O<sub>4</sub>S<sup>79</sup>Br: 431.0635, found 431.0641 [M+H]<sup>+</sup>.

***tert*-Butyl (4*aS*,8*aS*)-3-oxooctahydro-1*H*-pyrano[3,4-*b*]pyridine-1-carboxylate **184a****



Following **GP10** with polycycle **97** (133 mg, 0.30 mmol), 1 M LiAlH<sub>4</sub> in THF (1.5 mL, 1.50 mmol) and THF (3.0 mL) and heated to reflux for 18 h. The crude material and NEt<sub>3</sub> (83  $\mu$ L, 0.60 mmol) were dissolved in CH<sub>2</sub>Cl<sub>2</sub> (3.0 mL) and a solution of Boc<sub>2</sub>O in THF (1M, 0.6 mL, 0.60 mmol) was added dropwise over 2 min. The resulting reaction mixture was stirred at r.t for 6 h before satd NaHCO<sub>3(aq)</sub> was added and the organics extracted with CH<sub>2</sub>Cl<sub>2</sub> (3 $\times$ 10 mL). The combined organics were washed with brine (20 mL), dried over Na<sub>2</sub>SO<sub>4</sub>, filtered and concentrated under reduced pressure. The crude material was re-dissolved in CH<sub>2</sub>Cl<sub>2</sub> (3.0 mL) and DMP (127.3 mg, 0.30 mmol) was added in 2 portions 2 min apart. The reaction mixture was stirred for 6 h at r.t. before satd Na<sub>2</sub>CO<sub>3(aq)</sub> (10 mL) was added and the organics extracted with CH<sub>2</sub>Cl<sub>2</sub> (3 $\times$ 10 mL). The combined organics were washed with brine (20 mL), dried over Na<sub>2</sub>SO<sub>4</sub>, filtered and concentrated under reduced pressure. Purification by flash column chromatography (1:1 hexane/EtOAc) gave amino ketone **184a** as a white powder (50.1 mg, 67% over 3 steps); mp: 133–135  $^{\circ}$ C; IR (neat):  $\nu$  = 2981, 2854, 2937, 1722, 1683, 1400, 1366, 1156, 1083 cm<sup>-1</sup>; <sup>1</sup>H NMR (400 MHz, CDCl<sub>3</sub>):  $\delta$  = 4.51 (d,  $J_{AB}$  = 18.4 Hz, 1H<sub>f</sub>), 4.36 (dd,  $J$  = 10.3, 3.8 Hz, 1H<sub>a</sub>), 4.00 (ddd,  $J$  = 11.6, 4.6, 1.5 Hz, 1H<sub>b</sub>), 3.61 (dd,  $J$  = 18.4, 1.0 Hz, 1H<sub>f</sub>), 3.46 (ddd,  $J$  = 11.5, 9.8, 3.0 Hz, 1H<sub>g</sub>), 3.41 (app. td,  $J$  = 11.7, 2.4 Hz, 1H<sub>b</sub>), 3.13 (app. t,  $J$  = 10.1 Hz, 1H<sub>a</sub>), 2.43 (dd,  $J$  = 17.4, 2.6 Hz, 1H<sub>e</sub>), 2.21 (ddd,  $J$  = 17.4, 13.7, 1.0 Hz, 1H<sub>e</sub>), 1.95 (app. dtt,  $J$  = 14.3, 11.5, 3.0 Hz, 1H<sub>d</sub>), 1.75 (app. dddd,  $J$  = 13.2, 3.8, 2.5, 1.5 Hz, 1H<sub>c</sub>), 1.64 (app. td,  $J$  = 11.8, 4.5 Hz, 1H<sub>c</sub>), 1.45 (s, 9H) ppm; <sup>13</sup>C NMR (101 MHz, CDCl<sub>3</sub>):  $\delta$  = 206.7 (C), 154.9 (C), 81.2 (C), 70.4 (C<sub>a</sub>H<sub>2</sub>), 67.8 (C<sub>b</sub>H<sub>2</sub>), 57.2 (C<sub>g</sub>H), 51.1 (C<sub>f</sub>H<sub>2</sub>), 43.9 (C<sub>e</sub>H<sub>2</sub>), 36.1 (C<sub>d</sub>H), 32.1 (C<sub>c</sub>H<sub>2</sub>), 28.4 (3CH<sub>3</sub>) ppm; HRMS (ES–TOF):  $m/z$ : calcd for C<sub>13</sub>H<sub>21</sub>NO<sub>4</sub>Na: 278.1363, found 278.1375 [M+Na]<sup>+</sup>.

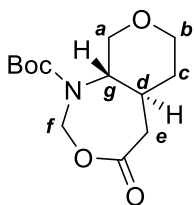
***tert*-Butyl (4*aS*,8*aS*)-3-oxo-7-tosyloctahydro-1,7-naphthyridine-1(2*H*)-carboxylate **184b****



Following **GP10** with polycycle **93b** (88.0 mg, 0.14 mmol), LiAlH<sub>4</sub> (28.5 mg, 0.75 mmol) and THF (1.5 mL) at r.t. for 18 h. Purification by flash column chromatography (9:1 CH<sub>2</sub>Cl<sub>2</sub>/MeOH) gave amino alcohol **183** as a mixture of diastereomers (33.1 mg, 72%). **183** and NEt<sub>3</sub> (28 μL, 0.20 mmol) were dissolved in CH<sub>2</sub>Cl<sub>2</sub> (2.0 mL) and Boc<sub>2</sub>O in THF (1M, 0.15 mL, 0.15 mmol) was added dropwise over 2 min. The resulting reaction mixture was stirred at r.t for 6 h before satd NaHCO<sub>3(aq)</sub> was added and the organics extracted with CH<sub>2</sub>Cl<sub>2</sub> (3×10 mL). The combined organics were washed with brine (20 mL), dried over Na<sub>2</sub>SO<sub>4</sub>, filtered and concentrated under reduced pressure. The crude material was re-dissolved in CH<sub>2</sub>Cl<sub>2</sub> (2.0 mL) and DMP (84.8 mg, 0.20 mmol) was added in 2 portions 2 min apart. The reaction mixture was stirred for 16 h at r.t. before satd Na<sub>2</sub>CO<sub>3(aq)</sub> (10 mL) was added and the organics extracted with CH<sub>2</sub>Cl<sub>2</sub> (3×10 mL). The combined organics were washed with brine (20 mL), dried over Na<sub>2</sub>SO<sub>4</sub>, filtered and concentrated under reduced pressure. Purification by flash column chromatography (1:1 hexane/EtOAc) gave amino ketone **184b** as a white solid (29.2 mg, 51% over 3 steps); mp: 216–219 °C; IR (neat): ν = 2986, 2925, 1729, 1694, 1398, 1365, 1344, 1161 cm<sup>-1</sup>; <sup>1</sup>H NMR (400 MHz, CDCl<sub>3</sub>): δ = 7.65 (d<sub>AA'XX'</sub>, *J* = 8.3 Hz, 2H), 7.33 (d<sub>AA'XX'</sub>, *J* = 8.3 Hz, 2H), 4.55 (d, *J*<sub>AB</sub> = 18.6 Hz, 1H<sub>f</sub>), 4.42 (ddd, *J* = 10.6, 3.8, 1.7 Hz, 1H<sub>a</sub>), 3.89 (app. dp, *J* = 11.9, 2.0 Hz, 1H<sub>b</sub>), 3.53 (app. td, *J* = 10.8, 3.6 Hz, 1H<sub>g</sub>), 3.49 (dd, *J* = 18.6, 1.0 Hz, 1H<sub>f</sub>), 2.43 (s, 3H), 2.43 – 2.36 (m, 1H<sub>e</sub>), 2.31 (app. td, *J* = 11.8, 3.0 Hz, 1H<sub>b</sub>), 2.21 (dd, *J* = 17.4, 13.0 Hz, 1H<sub>e</sub>), 2.08 (app. t, *J* = 10.4 Hz, 1H<sub>a</sub>), 1.82 (app. dt, *J* = 10.1, 2.8 Hz, 1H<sub>c</sub>), 1.69 – 1.56 (m, 1H<sub>c</sub>+1H<sub>d</sub>), 1.53 (s, 9H) ppm; <sup>13</sup>C NMR (101 MHz, CDCl<sub>3</sub>): δ = 206.2 (C), 154.8 (C), 143.9 (C), 133.7 (C), 129.9 (2CH), 127.7 (2CH), 81.9 (C), 57.0 (C<sub>g</sub>H), 50.5 (C<sub>f</sub>H<sub>2</sub>), 50.0 (C<sub>a</sub>H<sub>2</sub>), 46.1 (C<sub>b</sub>H<sub>2</sub>), 43.5 (C<sub>e</sub>H<sub>2</sub>), 36.4

(C<sub>d</sub>H), 30.2 (C<sub>c</sub>H<sub>2</sub>), 28.5 (3CH<sub>3</sub>), 21.7 (CH<sub>3</sub>) ppm; HRMS (ES–TOF): m/z: calcd for C<sub>20</sub>H<sub>28</sub>N<sub>2</sub>O<sub>5</sub>SNa: 431.1611, found 431.1621 [M+Na]<sup>+</sup>.

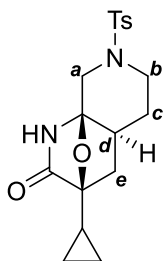
***tert*-Butyl (5*a**S*,9*a**S*)–4–oxohexahydro–4*H*–pyrano[3,4-*d*][1,3]oxazepine–1(2*H*)–carboxylate **185****



Amino ketone **184a** (18.0 mg, 70.5 μmol) and *m*-CPBA (77%, 21.5 mg, 95.9 μmol) were dissolved in CH<sub>2</sub>Cl<sub>2</sub> (0.8 mL) and stirred at r.t. for 2 h. The reaction mixture was diluted with EtOAc (20 mL) and washed with satd Na<sub>2</sub>S<sub>2</sub>O<sub>3(aq)</sub> (2×5 mL), satd NaHCO<sub>3(aq)</sub> (2×5 mL) and brine (10 mL), dried over Na<sub>2</sub>SO<sub>4</sub>, filtered and concentrated under reduced pressure. Purification by flash column chromatography (1:1 hexane/EtOAc) gave lactone **185** as a white powder (19.1 mg, quant.); mp: 150–152 °C; IR (neat): ν = 2971, 2955, 2861, 1713, 1697, 1264, 1170, 1153, 1076, 1002 cm<sup>-1</sup>; <sup>1</sup>H NMR (300 MHz, CDCl<sub>3</sub>): δ = 5.53 (d, *J*<sub>AB</sub> = 12.3 Hz, 1H<sub>f</sub>), 5.27 (d, *J*<sub>AB</sub> = 12.3 Hz, 1H<sub>f</sub>), 4.05 – 3.94 (m, 2H), 3.62 (app. td, *J* = 10.9, 4.5 Hz, 1H), 3.38 (app. td, *J* = 12.0, 2.4 Hz, 1H), 3.17 (app. t, *J* = 10.5 Hz, 1H), 2.80 (dd, *J* = 17.7, 2.4 Hz, 1H<sub>e</sub>), 2.65 (dd, *J* = 17.7, 12.0 Hz, 1H<sub>e</sub>), 2.21 (app. qdd, *J* = 11.5, 3.7, 2.4, 1H), 1.73 (app. ddt, *J* = 13.4, 4.0, 2.0 Hz, 1H), 1.56 (app. td, *J* = 11.8, 4.2 Hz, 1H), 1.49 (s, 9H) ppm; <sup>13</sup>C NMR (101 MHz, CDCl<sub>3</sub>): δ = 170.7 (C), 153.9 (C), 82.7 (C), 72.0 (CH<sub>2</sub>), 69.5 (CH), 67.5 (CH<sub>2</sub>), 59.6 (CH<sub>2</sub>), 42.3 (CH), 34.4 (CH<sub>2</sub>), 33.1 (CH<sub>2</sub>), 28.3 (3CH<sub>3</sub>) ppm; HRMS (ES–TOF): m/z: calcd for C<sub>13</sub>H<sub>21</sub>NO<sub>5</sub>Na: 294.1312, found 294.1312 [M+Na]<sup>+</sup>.

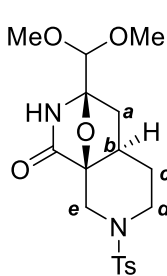
## Products derived from treatment with Brønsted and Lewis acids

### *(3S,4aS,8aR)*-3-Cyclopropyl-7-tosylhexahydro-1*H*-3,8a-epoxy-1,7-naphthyridin-2(3*H*)-one **190**



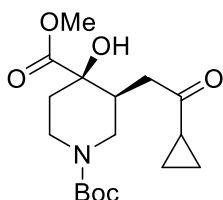
Polycycle **93a** (232 mg, 0.45 mmol) and TsOH•H<sub>2</sub>O (423 mg, 2.25 mmol) were dissolved in THF (2.3 mL) and MeOH (2.3 mL) and the resulting mixture stirred at r.t. for 3 h. The mixture was poured into satd NaHCO<sub>3(aq)</sub> (10 mL) and extracted with CH<sub>2</sub>Cl<sub>2</sub> (3×10 mL). The combined organics were washed with H<sub>2</sub>O (15 mL), brine (20 mL), dried over Na<sub>2</sub>SO<sub>4</sub>, filtered and concentrated under reduced pressure. Purification by flash column chromatography (2:8 hexane/EtOAc) gave lactam **190** as a white solid (161 mg, 98%); mp: 175–178 °C; IR (neat):  $\nu$  = 3234, 2851, 1726, 1341, 1162 cm<sup>-1</sup>; <sup>1</sup>H NMR (400 MHz, CDCl<sub>3</sub>):  $\delta$  = 7.66 (d<sub>AA'XX'</sub>,  $J$  = 8.3 Hz, 2H), 7.32 (d<sub>AA'XX'</sub>,  $J$  = 8.3 Hz, 2H), 7.24 (br. s, NH), 4.21 (dd,  $J$  = 13.3, 1.7 Hz, 1H<sub>a</sub>), 3.80 (app. dq,  $J$  = 12.7, 4.0 Hz, 1H<sub>b</sub>), 2.82 (d,  $J_{AB}$  = 13.3 Hz, 1H<sub>a</sub>), 2.43 (s, 3H), 2.41 (app. td,  $J$  = 12.7, 2.2 Hz, 1H<sub>b</sub>), 2.04 – 1.94 (m, 1H<sub>d</sub>), 1.88 – 1.81 (m, 1H<sub>c</sub>), 1.85 (dd,  $J$  = 12.6, 7.7 Hz, 1H<sub>e</sub>), 1.39 (app. qd,  $J$  = 12.9, 4.0 Hz, 1H<sub>c</sub>), 1.32 – 1.19 (m, 1H), 1.24 (dd,  $J$  = 12.6, 7.7 Hz, 1H<sub>e</sub>), 0.67 – 0.55 (m, 3H), 0.41 – 0.34 (m, 1H) ppm; <sup>13</sup>C NMR (101 MHz, CDCl<sub>3</sub>):  $\delta$  = 178.4 (C), 144.0 (C), 134.0 (C), 129.9 (2CH), 127.8 (2CH), 89.2 (C), 88.3 (C), 46.7 (C<sub>a</sub>H<sub>2</sub>), 45.1 (C<sub>b</sub>H<sub>2</sub>), 42.5 (C<sub>d</sub>H), 35.2 (C<sub>e</sub>H<sub>2</sub>), 30.8 (C<sub>c</sub>H<sub>2</sub>), 21.7 (CH<sub>3</sub>), 9.1 (CH), 1.8 (CH<sub>2</sub>), 1.4 (CH<sub>2</sub>) ppm; HRMS (ES–TOF):  $m/z$ : calcd for C<sub>18</sub>H<sub>23</sub>N<sub>2</sub>O<sub>4</sub>S: 363.1373, found 363.1375 [M+H]<sup>+</sup>.

**(3*R*,4*aR*,8*aS*)-3-(Hydroxy(methoxy)methyl)-7-tosyloctahydro-1*H*-3,8*a*-epoxy-2,7-naphthyridin-1-one **191****



Polycycle **54** (76.1 mg, 0.135 mmol) and TsOH•H<sub>2</sub>O (127 mg, 0.68 mmol) were dissolved in THF (1.0 mL) and MeOH (2.7 mL) and the resulting mixture stirred at r.t. for 4 h. The mixture was poured into satd NaHCO<sub>3(aq)</sub> (10 mL) and extracted with CH<sub>2</sub>Cl<sub>2</sub> (3×10 mL). The combined organics were washed with H<sub>2</sub>O (15 mL), brined (20 mL), dried over Na<sub>2</sub>SO<sub>4</sub>, filtered and concentrated under reduced pressure. Purification by flash column chromatography (3:7 hexane/EtOAc) gave lactam **191** as a white powder (23.3 mg, 44%); mp: 187–188 °C; IR (neat):  $\nu$  = 2926, 2841, 1730, 1341, 1164, 1087 cm<sup>-1</sup>; <sup>1</sup>H NMR (400 MHz, CDCl<sub>3</sub>):  $\delta$  = 7.66 (d<sub>AA'XX'</sub>,  $J$  = 8.3 Hz, 2H), 7.33 (d<sub>AA'XX'</sub>,  $J$  = 8.3 Hz, 2H), 6.24 (br. s, NH), 4.55 (s, 1H), 4.18 (dd,  $J$  = 13.9, 1.7 Hz, 1H<sub>e</sub>), 3.82 (app. dtd,  $J$  = 12.0, 3.4, 1.2 Hz, 1H<sub>d</sub>), 3.56 (s, 3H), 3.52 (s, 3H), 2.99 (d,  $J_{AB}$  = 13.9 Hz, 1H<sub>e</sub>), 2.43 (s, 3H), 2.23 (app. td,  $J$  = 12.4, 2.0 Hz, 1H<sub>d</sub>), 2.06 (dd,  $J$  = 12.2, 7.9 Hz, 1H<sub>a</sub>), 1.98 (app. ddt,  $J$  = 13.5, 5.6, 2.5 Hz, 1H<sub>c</sub>), 1.80 – 1.74 (m, 1H<sub>a</sub>+1H<sub>b</sub>), 1.69 – 1.57 (m, 1H<sub>c</sub>) ppm; <sup>13</sup>C NMR (101 MHz, CDCl<sub>3</sub>):  $\delta$  = 174.7 (C), 143.9 (C), 133.0 (C), 130.0 (2CH), 127.9 (2CH), 103.2 (CH), 95.0 (C), 83.3 (C), 58.0 (CH<sub>3</sub>), 56.9 (CH<sub>3</sub>), 45.0 (C<sub>d</sub>H<sub>2</sub>), 44.1 (C<sub>e</sub>H<sub>2</sub>), 39.3 (C<sub>a</sub>H<sub>2</sub>), 33.4 (C<sub>b</sub>H), 29.5 (C<sub>c</sub>H<sub>2</sub>), 21.7 (CH<sub>3</sub>) ppm; HRMS (ES–TOF):  $m/z$ : calcd for C<sub>18</sub>H<sub>25</sub>N<sub>2</sub>O<sub>6</sub>S: 397.1428 found 397.1420 [M+H]<sup>+</sup>.

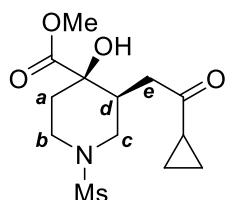
**1-(*tert*-Butyl) 4-methyl (3*S*,4*R*)-3-(2-cyclopropyl-2-oxoethyl)-4-hydroxypiperidine-1,4-dicarboxylate **194a****



Polycycle **107d** (71.4 mg, 0.15 mmol) and TsOH•H<sub>2</sub>O (56.4 mg, 0.30 mmol) were dissolved in THF (0.75 mL) and MeOH (0.75 mL) and the resulting mixture stirred at r.t. for 12 h. The mixture was poured into satd NaHCO<sub>3(aq)</sub> (10 mL) and extracted with CH<sub>2</sub>Cl<sub>2</sub> (3×10 mL). The combined organics were

washed with H<sub>2</sub>O (15 mL), brined (20 mL), dried over Na<sub>2</sub>SO<sub>4</sub>, filtered and concentrated under reduced pressure. Purification by flash column chromatography (3:7 hexane/EtOAc) gave **194a** as a pale yellow oil that solidified upon standing (38.0 mg, 74%); mp: 112–114 °C; IR (neat):  $\nu$  = 3522, 2981, 2924, 1706, 1678, 1431, 1244, 1148, 1066 cm<sup>-1</sup>; <sup>1</sup>H NMR (400 MHz, CDCl<sub>3</sub>):  $\delta$  = 4.08 – 3.85 (br. m, 2H), 3.75 (s, 3H), 3.46 – 3.19 (br. m, 1H), 3.12 – 2.95 (br. m, 1H), 2.85 – 2.68 (m, 1H), 2.56 – 2.47 (br. m, 1H), 2.45 – 2.36 (m, 2H), 1.99 (td,  $J$  = 13.1, 4.9 Hz, 1H), 1.86 (tt,  $J$  = 7.8, 4.6 Hz, 1H), 1.59 (dt,  $J$  = 13.5, 2.7 Hz, 1H), 1.45 (s, 9H), 1.02 – 0.96 (m, 2H), 0.89 – 0.83 (m, 2H) ppm; <sup>13</sup>C NMR (101 MHz, CDCl<sub>3</sub>):  $\delta$  = 208.6 (C), 176.5 (C), 154.6 (C), 79.8 (C), 74.1 (C), 53.3 (CH<sub>3</sub>), 44.4 (CH<sub>2</sub>), 41.7 (CH<sub>2</sub>), 38.7 (CH<sub>2</sub>), 37.4 (CH), 35.3 (CH<sub>2</sub>), 28.5 (3CH<sub>3</sub>), 21.0 (CH), 11.2 (CH<sub>2</sub>), 11.1 (CH<sub>2</sub>) ppm; HRMS (ES–TOF):  $m/z$ : calcd for C<sub>17</sub>H<sub>27</sub>NO<sub>6</sub>Na: 364.1731, found 364.1739 [M+Na]<sup>+</sup>.

***Methyl (3S,4R)-3-(2-cyclopropyl-2-oxoethyl)-4-hydroxy-1-(methylsulfonyl)piperidine-4-carboxylate 194b***

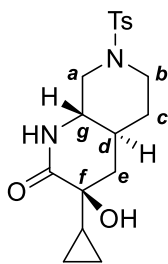


Polycycle **107c** (90.7 mg, 0.20 mmol) and TsOH•H<sub>2</sub>O (188 mg, 1.00 mmol) were dissolved in THF (1.0 mL) and MeOH (1.0 mL) and the resulting mixture stirred at r.t. for 3 h. The mixture was poured into satd NaHCO<sub>3(aq)</sub> (10 mL) and extracted with CH<sub>2</sub>Cl<sub>2</sub> (3×10 mL). The combined organics were washed with H<sub>2</sub>O (15 mL), brined (20 mL), dried over Na<sub>2</sub>SO<sub>4</sub>, filtered and concentrated under reduced pressure. Purification by flash column chromatography (3:7 hexane/EtOAc) gave **194b** as a white solid (38.0 mg, 59%); mp: 152–153 °C; IR (neat):  $\nu$  = 3532, 2984, 2925, 1711, 1435, 1245 cm<sup>-1</sup>; <sup>1</sup>H NMR (400 MHz, CDCl<sub>3</sub>):  $\delta$  = 3.79 (s, 3H), 3.71 (dddd,  $J$  = 12.1, 4.7, 2.6, 1.7 Hz, 1H<sub>b</sub>), 3.64 – 3.61 (m, 1H<sub>c</sub>), 3.40 (s, OH), 3.05 (app. td,  $J$  = 12.1, 2.8 Hz, 1H<sub>b</sub>), 2.80 (s, 3H), 2.75 – 2.71 (m, 1H<sub>d</sub>+1H<sub>c</sub>), 2.49 (dd,  $J$  = 17.6, 4.2 Hz, 1H<sub>e</sub>), 2.41 (ddd,  $J$  = 17.6, 7.1, 1.5 Hz, 1H<sub>e</sub>), 2.18 (app. dt,  $J$  = 13.5, 12.6, 4.8 Hz, 1H<sub>a</sub>), 1.86 (tt,  $J$  = 7.8, 4.6 Hz, 1H), 1.73 (app. dt,  $J$  = 13.5, 2.7 Hz, 1H<sub>a</sub>),



1.03 – 0.98 (m, 2H), 0.91 – 0.86 (m, 2H) ppm;  $^{13}\text{C}$  NMR (101 MHz,  $\text{CDCl}_3$ ):  $\delta$  = 208.1 (C), 176.2 (C), 73.3 (C), 53.6 ( $\text{CH}_3$ ), 45.9 ( $\text{C}_\text{cH}_2$ ), 41.7 ( $\text{C}_\text{eH}_2$ ), 41.1 ( $\text{C}_\text{bH}_2$ ), 37.4 ( $\text{C}_\text{dH}$ ), 35.6 ( $\text{CH}_3$ ), 35.2 ( $\text{C}_\text{aH}_2$ ), 20.9 (CH), 11.4 ( $\text{CH}_2$ ), 11.3 ( $\text{CH}_2$ ) ppm; HRMS (ES–TOF):  $m/z$ : calcd for  $\text{C}_{13}\text{H}_{21}\text{NO}_6\text{SNa}$ : 342.0982, found 342.0976  $[\text{M}+\text{Na}]^+$ .

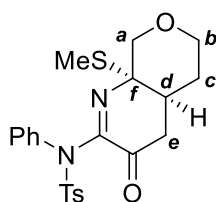
**(3*S*,4*aS*)-3-Cyclopropyl-3-hydroxy-7-tosyloctahydro-1,7-naphthyridin-2(1*H*)-one 209**



Lactam **190** (36.2 mg, 0.10 mmol) and triethylsilane (80  $\mu\text{L}$ , 0.50 mmol) were dissolved in dry  $\text{CH}_2\text{Cl}_2$  (1.0 mL) and cooled to 0  $^\circ\text{C}$ .  $\text{BF}_3\cdot\text{OEt}$  (63  $\mu\text{L}$ , 0.50 mmol) was added in one portion and the resulting mixture stirred for 10 min before the reaction was allowed to warm to r.t. and stirred for 1 h. Satd

$\text{NaHCO}_{3(\text{aq})}$  was added and the organics extracted with  $\text{CH}_2\text{Cl}_2$  (3 $\times$ 10 mL). The combined organics were washed with brine (20 mL), dried over  $\text{Na}_2\text{SO}_4$ , filtered and concentrated under reduced pressure. Purification by flash column chromatography (3:7 hexane/EtOAc) gave **209** as white powder (35.3 mg, 97%); mp: 98–101  $^\circ\text{C}$ ; IR (neat):  $\nu$  = 3316 (br.), 2925, 2855, 1665, 1465, 1337, 1158, 1089  $\text{cm}^{-1}$ ;  $^1\text{H}$  NMR (400 MHz,  $\text{CDCl}_3$ ):  $\delta$  = 7.65 ( $\text{d}_{\text{AA}'\text{XX}'}$ ,  $J$  = 8.3 Hz, 2H), 7.34 ( $\text{d}_{\text{AA}'\text{XX}'}$ ,  $J$  = 8.3 Hz, 2H), 5.83 (br. s, NH), 3.93 – 3.87 (m,  $1\text{H}_\text{a}+1\text{H}_\text{b}$ ), 3.25 (app. td,  $J$  = 10.0, 3.9 Hz,  $1\text{H}_\text{g}$ ), 3.15 (s, OH), 2.44 (s, 3H), 2.36 (app. td,  $J$  = 12.1, 2.8 Hz,  $1\text{H}_\text{b}$ ), 2.16 (app. t,  $J$  = 10.8 Hz,  $1\text{H}_\text{a}$ ), 2.03 (dd,  $J$  = 10.2, 1.7 Hz,  $1\text{H}_\text{e}$ ), 1.84 – 1.70 (m,  $1\text{H}_\text{e}+1\text{H}_\text{d}+1\text{H}_\text{c}$ ), 1.55 (app. tdd,  $J$  = 13.2, 11.2, 4.3 Hz,  $1\text{H}_\text{c}$ ), 1.06 (tt,  $J$  = 8.3, 5.5 Hz, 1H), 0.55 – 0.44 (m, 3H), 0.33 – 0.26 (m, 1H) ppm;  $^{13}\text{C}$  NMR (101 MHz,  $\text{CDCl}_3$ ):  $\delta$  = 176.7 (C), 144.1 (C), 133.4 (C), 130.0 (2CH), 127.7 (2CH), 71.5 ( $\text{C}_\text{f}$ ), 56.5 ( $\text{C}_\text{gH}$ ), 50.4 ( $\text{C}_\text{aH}_2$ ), 46.3 ( $\text{C}_\text{bH}_2$ ), 40.6 ( $\text{C}_\text{eH}_2$ ), 36.2 ( $\text{C}_\text{dH}$ ), 29.5 ( $\text{C}_\text{cH}_2$ ), 21.7 ( $\text{CH}_3$ ), 20.7 (CH), 3.0 ( $\text{CH}_2$ ), 0.0 ( $\text{CH}_2$ ) ppm; HRMS (ES–TOF):  $m/z$ : calcd for  $\text{C}_{18}\text{H}_{25}\text{N}_2\text{O}_4\text{S}$ : 365.1530, found 365.1525  $[\text{M}+\text{H}]^+$ .

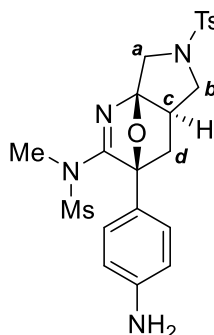
**4-Methyl-N-((4a*S*,8a*S*)-8a-(methylthio)-3-oxo-4,4a,5,6,8,8a-hexahydro-3H-pyrano[3,4-*b*]pyridin-2-yl)-N-phenylbenzenesulfonamide **216****



Polycycle **97** (88.9 mg, 0.20 mmol) was dissolved in dry CH<sub>2</sub>Cl<sub>2</sub> (2.0 mL) in a flame dried Schlenk tube and cooled to 0 °C. BF<sub>3</sub>•OEt<sub>2</sub> (76 µL, 0.60 mmol) was added in one portion and the reaction mixture was stirred for 1 h at 0 °C before allowing to warm to r.t. and stirring for 18 h. The reaction mixture was purified directly by flash column chromatography to give **216** as bright yellow crystals (71.4 mg, 80%); mp: (dec.) 188–189 °C; IR (neat):  $\nu$  = 2970, 2921, 2845, 1712, 1318, 1594, 1485, 1353, 1162, 1153, 1067, 1051 cm<sup>-1</sup>; <sup>1</sup>H NMR (400 MHz, CDCl<sub>3</sub>):  $\delta$  = 7.64 (d<sub>AA'XX'</sub>,  $J$  = 8.4 Hz, 2H), 7.33 – 7.29 (m, 3H), 7.28 – 7.24 (m, 2H), 7.21 (d<sub>AA'XX'</sub>,  $J$  = 8.4 Hz, 2H), 4.26 (d,  $J_{AB}$  = 11.4 Hz, 1H<sub>a</sub>), 3.98 (ddd,  $J$  = 11.8, 4.3, 1.9 Hz, 1H<sub>b</sub>), 3.64 (d,  $J_{AB}$  = 11.4 Hz, 1H<sub>a</sub>), 3.50 (app, td,  $J$  = 11.5, 2.7 Hz, 1H<sub>b</sub>), 3.13 (dd,  $J$  = 18.0, 5.8 Hz, 1H<sub>c</sub>), 2.47 – 2.41 (m, 1H<sub>d</sub>), 2.40 (s, 3H), 2.29 (dd,  $J$  = 18.0, 2.6 Hz, 1H<sub>c</sub>), 2.03 (s, 3H), 1.77 (app. dtd,  $J$  = 13.7, 11.7, 4.7 Hz, 1H<sub>c</sub>), 1.67 – 1.58 (m, 1H<sub>c</sub>) ppm; <sup>13</sup>C NMR (101 MHz, CDCl<sub>3</sub>):  $\delta$  = 186.0 (C), 154.9 (C), 144.0 (C), 137.8 (C), 136.1 (C), 129.8 (2CH), 129.3 (2CH), 129.0 (2CH), 128.9 (2CH), 128.7 (CH), 76.2 (C<sub>a</sub>H<sub>2</sub>), 67.2 (C<sub>b</sub>H<sub>2</sub>), 64.3 (C<sub>f</sub>), 39.9 (C<sub>e</sub>H<sub>2</sub>), 37.4 (C<sub>d</sub>H), 28.9 (C<sub>c</sub>H<sub>2</sub>), 21.7 (CH<sub>3</sub>), 10.4 (SCH<sub>3</sub>) ppm; HRMS (ES–TOF):  $m/z$ : calcd for C<sub>22</sub>H<sub>25</sub>N<sub>2</sub>O<sub>4</sub>S<sub>2</sub>: 445.1250, found 445.1251 [M+H]<sup>+</sup>.

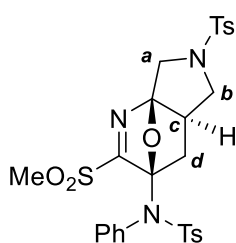
## Products derived from functional group manipulation

### *N*-((3*S*,4*aR*,7*aR*)-3-(4-Aminophenyl)-6-tosyl-3,4,4*a*,5,6,7-hexahydro-3,7*a*-epoxypyrrolo[3,4-*b*]pyridin-2-yl)-*N*-methylmethanesulfonamide **221**



Polycycle **46f** (23.0 mg, 44  $\mu$ mol) was dissolved in degassed EtOH (1.0 mL) under argon and Pd/C (10%, 5.1 mg, 10 mol%) was added. The resulting mixture was sparged with H<sub>2(g)</sub> for 5 min and left to stir under a positive pressure of H<sub>2(g)</sub> via a balloon for 18 h. The H<sub>2(g)</sub> was replaced by sparging the solution with argon for 5 min, and the mixture was filtered through a 3 cm pad of celite (EtOAc) and concentrated under reduced pressure. Purification by flash column chromatography (3:7 hexane/EtOAc) gave aniline **221** as a pale yellow powder (20.0 mg, 85%); mp: 134–135 °C; IR (neat):  $\nu$  = 3481, 2925, 1627, 1583, 1431, 1238, 1158, 1094 cm<sup>-1</sup>; <sup>1</sup>H NMR (400 MHz, CDCl<sub>3</sub>):  $\delta$  = 7.70 (d<sub>AA'XX'</sub>,  $J$  = 8.3 Hz, 2H), 7.28 (d<sub>AA'XX'</sub>,  $J$  = 8.3 Hz, 2H), 7.18 (d<sub>AA'XX'</sub>,  $J$  = 8.5 Hz, 2H), 6.67 (d<sub>AA'XX'</sub>,  $J$  = 8.5 Hz, 2H), 4.10 (d,  $J_{AB}$  = 11.7 Hz, 1H<sub>a</sub>), 3.90 (dd,  $J$  = 9.5, 8.2 Hz, 1H<sub>b</sub>), 3.81 (br. s, NH<sub>2</sub>), 3.71 (d,  $J_{AB}$  = 11.7 Hz, 1H<sub>a</sub>), 2.85 (s, 3H), 2.84 – 2.78 (m, 1H<sub>b</sub>), 2.70 (s, 3H), 2.48 – 2.39 (m, 1H<sub>c</sub>), 2.40 (s, 3H), 2.26 (dd,  $J$  = 12.0, 7.6 Hz, 1H<sub>d</sub>), 1.84 (dd,  $J$  = 12.0, 3.4 Hz, 1H<sub>d</sub>) ppm; <sup>13</sup>C NMR (101 MHz, CDCl<sub>3</sub>):  $\delta$  = 171.3 (C), 147.5 (C), 143.7 (C), 134.2 (C), 129.9 (2CH), 129.2 (2CH), 127.6 (2CH), 124.5 (C), 114.8 (2CH), 107.1 (C), 93.8 (C), 53.0 (CH<sub>2</sub>), 49.6 (CH<sub>2</sub>), 45.7 (C<sub>6</sub>H), 40.1 (CH<sub>3</sub>), 35.5 (CH<sub>3</sub>), 32.5 (C<sub>d</sub>H<sub>2</sub>), 21.7 (CH<sub>3</sub>) ppm; HRMS (ES–TOF):  $m/z$ : calcd for C<sub>22</sub>H<sub>27</sub>N<sub>4</sub>O<sub>5</sub>S<sub>2</sub>: 491.1417, found 491.1424 [M+H]<sup>+</sup>.

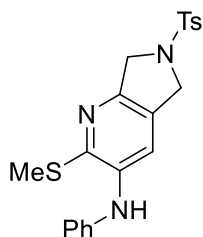
**4-Methyl-N-((3R,4aR,7aR)-2-(methanesulfonyl)-6-tosyl-4a,5,6,7-tetrahydro-3,7a-epoxypyrrolo[3,4-b]pyridin-3(4H)-yl)-N-phenylbenzenesulfonamide 222**



Sulfide **120f** (58.3 mg, 0.10 mmol) was dissolved in CH<sub>2</sub>Cl<sub>2</sub> (1.0 mL) and cooled to 0 °C. *m*-CPBA (55.8 mg, 0.22 mmol) was added in one portion and the ice bath removed after 10 min. After stirring for 4 h at r.t., the reaction was quenched with satd Na<sub>2</sub>SO<sub>3(aq)</sub> (5.0 mL) and the organics

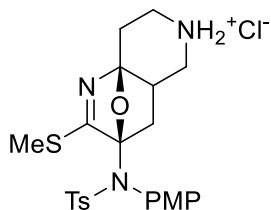
extracted with CH<sub>2</sub>Cl<sub>2</sub> (3×5 mL). The combined organics were washed with brine (10 mL), dried over Na<sub>2</sub>SO<sub>4</sub>, filtered and concentrated under reduced pressure. Purification by flash column chromatography (1:1 hexane/EtOAc) gave sulfone **222** as a white fluffy powder (56.4 mg, 92%); mp: 201–203 °C; IR (neat):  $\nu$  = 1761, 1597, 1329 (SO<sub>2</sub>Me), 1321, 1163, 1089, 1034, 815, 699, 665 cm<sup>-1</sup>; *restricted rotation around the NTsPh sulfonamide results in broadening within the NMR*: <sup>1</sup>H NMR (400 MHz, CDCl<sub>3</sub>):  $\delta$  = 7.71 (d<sub>AA'XX'</sub>, *J* = 8.3 Hz, 2H), 7.52 (d<sub>AA'XX'</sub>, *J* = 8.3 Hz, 2H), 7.40 (br. app. s., 2H), 7.36 (t, *J* = 7.3 Hz, 1H), 7.31 (d<sub>AA'XX'</sub>, *J* = 8.3 Hz, 2H), 7.20 (d<sub>AA'XX'</sub>, *J* = 8.3 Hz, 2H), 7.13 (br. app. s, 1H), 6.41 (br. app. s, 1H), 4.16 (d, *J*<sub>AB</sub> = 12.1 Hz, 1H<sub>a</sub>), 4.07 (d, *J*<sub>AB</sub> = 12.1 Hz, 1H<sub>a</sub>), 3.70 (dd, *J* = 10.0, 8.5 Hz, 1H<sub>b</sub>), 3.43 (s, 3H), 2.72 (app. t, *J* = 10.1 Hz, 1H<sub>b</sub>), 2.45 (s, 3H), 2.44 (s, 3H), 2.15 (dddd, *J* = 10.2, 8.5, 7.4, 3.1 Hz, 1H<sub>c</sub>), 1.50 (dd, *J* = 12.9, 7.4 Hz, 1H<sub>d</sub>), 1.32 (dd, *J* = 12.9, 3.1 Hz, 1H<sub>d</sub>) ppm; *the restricted rotation results in aromatic CH broadening in <sup>13</sup>C NMR and prevents assignment of 2x2CH peaks*: <sup>13</sup>C NMR (101 MHz, CDCl<sub>3</sub>):  $\delta$  = 177.2 (C), 144.8 (C), 144.1 (C), 136.0 (C), 134.7 (C), 134.1 (C), 130.2 (CH), 130.0 (2CH), 129.4 (2CH), 129.4 (2CH), 127.6 (2CH), 106.3 (C), 101.9 (C), 51.9 (C<sub>b</sub>H<sub>2</sub>), 49.4 (C<sub>a</sub>H<sub>2</sub>), 43.9 (CH), 42.8 (CH<sub>3</sub>), 32.8 (C<sub>d</sub>H<sub>2</sub>), 21.8 (CH<sub>3</sub>), 21.7 (CH<sub>3</sub>) ppm; HRMS (ES–TOF): *m/z*: calcd for C<sub>28</sub>H<sub>29</sub>N<sub>3</sub>O<sub>7</sub>S<sub>3</sub>Na: 638.1060, found 638.1069 [M+Na]<sup>+</sup>.

**2-(Methylthio)-N-phenyl-6-tosyl-6,7-dihydro-5H-pyrrolo[3,4-b]pyridin-3-amine 223**



Following a literature procedure,<sup>110</sup> **120f** (117 mg, 0.20 mmol) was added to a dried Schlenk tube and subjected to 3 vacuum/argon cycles. After dissolving in dry DCE (5.0 mL), TfOH (44  $\mu$ L, 0.50 mmol) was added and the resulting mixture heated to 80 °C for 2 h. After allowing to cool to r.t. ethylenediamine (3 drops) was added, followed by 1 M NaOH<sub>(aq)</sub> (10 mL) and the organics extracted with CH<sub>2</sub>Cl<sub>2</sub> (3 $\times$ 10 mL). The combined organics were washed with brine (20 mL), dried over Na<sub>2</sub>SO<sub>4</sub>, filtered and concentrated under reduced pressure. Purification by flash column chromatography (8:2 $\rightarrow$ 6:4 hexane/EtOAc) gave aminopyridine **223** as a brown solid (66.4 mg, 80%); mp: 169–171 °C; IR (neat):  $\nu$  = 3349, 2920, 1712, 1592, 1503, 1442, 1337, 1157, 1093 cm<sup>-1</sup>; <sup>1</sup>H NMR (400 MHz, CDCl<sub>3</sub>):  $\delta$  = 7.76 (d<sub>AA'XX'</sub>,  $J$  = 8.3 Hz, 2H), 7.35 – 7.26 (m, 4H), 7.19 (s, 1H), 7.03 – 6.96 (m, 3H), 5.55 (br. s, NH), 4.57 – 4.51 (m, 4H), 2.55 (s, 3H), 2.41 (s, 3H) ppm; <sup>13</sup>C NMR (101 MHz, CDCl<sub>3</sub>):  $\delta$  = 149.4 (C), 148.2 (C), 143.9 (C), 141.7 (C), 137.2 (C), 133.7 (C), 130.0 (2CH), 129.7 (2CH), 127.7 (2CH), 125.9 (C), 122.6 (CH), 119.4 (2CH), 116.2 (CH), 53.6 (CH<sub>2</sub>), 52.2 (CH<sub>2</sub>), 21.7 (CH<sub>3</sub>), 13.6 (SCH<sub>3</sub>) ppm; HRMS (ES–TOF):  $m/z$ : calcd for C<sub>21</sub>H<sub>22</sub>N<sub>3</sub>O<sub>2</sub>S<sub>2</sub>: 412.1148, found 412.1151 [M+H]<sup>+</sup>.

**(3R,8aS)-3-((N-(4-Methoxyphenyl)-4-methylphenyl)sulfonamido)-2-(methylthio)-4,4a,5,6,7,8-hexahydro-3H-3,8a-epoxy-1,6-naphthyridin-6-ium chloride 224**

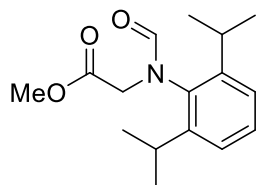


Carbamate **150b** (57.3 mg, 0.10 mmol) was dissolved in CH<sub>2</sub>Cl<sub>2</sub> (1.0 mL) and cooled to 0 °C. TFA (1.0 mL total) was added in 3 portions over 1 min and the reaction stirred for 1 h at 0 °C. The reaction was quenched with satd NaHCO<sub>3</sub> (5.0 mL) and the organics extracted with CH<sub>2</sub>Cl<sub>2</sub> (3 $\times$ 5 mL). The combined organics were washed with brine (10 mL), dried over Na<sub>2</sub>SO<sub>4</sub>, filtered and concentrated under reduced pressure. As the free amine rapidly discoloured in air (from

colourless to orange), the crude material was dissolved in CH<sub>2</sub>Cl<sub>2</sub> (2.0 mL), and 4 M HCl in dioxane (0.10 mL, 4 eq.) was added dropwise over 2 min. After stirring for 5 min at r.t., Et<sub>2</sub>O (2.0 mL) was added and the resulting mixture was cooled on ice. After 10 min, the precipitate was collected via filtration with a positive pressure of argon and dried under high vacuum to yield **224** as a pale yellow hygroscopic solid (48.9 mg, 96%); IR (neat):  $\nu$  = 2829 (br.), 1672, 1561, 1463, 1413, 1273, 1254 cm<sup>-1</sup>; *restricted rotation around the NTsPMP sulfonamide results in broadening within the NMR*: <sup>1</sup>H NMR (400 MHz, acetone-*d*<sub>6</sub>):  $\delta$  = 7.63 (d<sub>AA'XX'</sub>, *J* = 8.3 Hz, 2H), 7.33 (d<sub>AA'XX'</sub>, *J* = 8.3 Hz, 2H), 7.04 (br. app. s, 2H), 6.85 (d<sub>AA'XX'</sub>, *J* = 8.5 Hz, 2H), 3.80 (s, 3H), 3.65 – 3.58 (m, 1H), 3.54 (dd, *J* = 12.5, 5.9 Hz, 1H), 3.09 (app. t, *J* = 12.9 Hz, 1H), 2.98 (td, *J* = 14.3, 4.5 Hz, 1H), 2.66 – 2.51 (m, 2H), 2.42 (s, 3H), 2.41 (s, 3H), 2.38 – 2.30 (m, 1H), 1.54 (dd, *J* = 12.8, 7.5 Hz, 1H), 1.38 (dd, *J* = 12.9, 2.4 Hz, 1H) ppm; <sup>13</sup>C NMR (101 MHz, acetone-*d*<sub>6</sub>):  $\delta$  = 181.0 (C), 161.0 (C), 145.1 (C), 136.9 (C), 133.5 (2CH), 130.8 (C), 130.04 (2CH), 129.96 (2CH), 114.9 (2CH), 103.1 (C), 97.4 (C), 55.8 (CH<sub>3</sub>), 47.7 (CH<sub>2</sub>), 41.6 (CH<sub>2</sub>), 38.5 (CH), 35.7 (CH<sub>2</sub>), 27.4 (CH<sub>2</sub>), 21.5 (CH<sub>3</sub>), 14.4 (SCH<sub>3</sub>) ppm; HRMS (ES–TOF): *m/z*: calcd for C<sub>23</sub>H<sub>28</sub>N<sub>3</sub>O<sub>4</sub>S<sub>2</sub>: 474.1516, found 474.1523 [M–Cl]<sup>+</sup>.

## Formation of oxazole annulated imidazolium salts

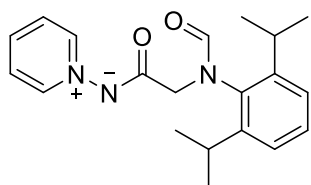
### *Methyl N*–(2,6–diisopropylphenyl)–*N*–formylglycinate **367**



Methyl bromoacetate (2.8 mL, 30.0 mmol) was added to a mixture of 2,6–diisopropylaniline (5.7 mL, 30.0 mmol) and NaOAc (4.92 g, 60.0 mmol) in dry MeOH (4.5 mL) and the reaction mixture was heated at 65 °C for 23 h. After allowing to cool r.t., satd NaHCO<sub>3(aq)</sub> (50 mL) was added and the aqueous phase was extracted with CH<sub>2</sub>Cl<sub>2</sub> (3×25 mL). The combined organic fractions were washed with brine (50 mL), dried over Na<sub>2</sub>SO<sub>4</sub>, filtered and concentrated under reduced pressure to

give a crude amine that was used directly in the next reaction. Formic acid (4.5 mL, 119 mmol) and Ac<sub>2</sub>O (4.0 mL, 42.4 mmol) were mixed for 1.5 h at r.t. and the resulting mixture was added to a solution of the crude amine in CH<sub>2</sub>Cl<sub>2</sub> (15 mL). The resulting reaction mixture was stirred for 21 h at r.t. and 3 h at 40 °C. After allowing to cool to r.t., satd NaHCO<sub>3(aq)</sub> (100 mL) was added, the phases were separated and the aqueous phase was extracted with CH<sub>2</sub>Cl<sub>2</sub> (3×40 mL). The combined organic phases were dried over Na<sub>2</sub>SO<sub>4</sub>, filtered, concentrated under reduced pressure and purified by flash column chromatography (85:15 hexane/EtOAc) to give formamide **367** as a white solid (4.90 g, 59% over 2 steps); IR (neat):  $\nu$  = 2964, 2868, 1762, 1664, 1460, 1323, 1205 cm<sup>-1</sup>; <sup>1</sup>H NMR (400 MHz, CDCl<sub>3</sub>):  $\delta$  = 8.13 (s, 1H), 7.38 (t, *J* = 7.8 Hz, 1H), 7.23 (d, *J* = 7.8 Hz, 2H), 4.21 (s, 2H), 3.77 (s, 3H), 3.23 (hept, *J* = 6.8 Hz, 2H), 1.22 (d, *J* = 6.8 Hz, 6H), 1.17 (d, *J* = 6.8 Hz, 6H); <sup>13</sup>C NMR (101 MHz, CDCl<sub>3</sub>):  $\delta$  = 168.3 (C), 163.8 (CH), 148.0 (2C), 135.7 (C), 129.9 (CH), 124.8 (2CH), 52.4 (CH<sub>3</sub>), 50.0 (CH<sub>2</sub>), 28.2 (2CH), 25.0 (2CH<sub>3</sub>), 24.3 (2CH<sub>3</sub>) ppm; HRMS (ES–TOF): *m/z*: calcd for C<sub>16</sub>H<sub>24</sub>NO<sub>3</sub>: 278.1751, found: 278.1755 [M+H]<sup>+</sup>.

*(N-(2,6-Diisopropylphenyl)-N-formylglycyl)(pyridin-1-ium-1-yl)amide 356a*



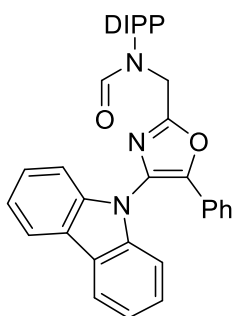
*N*-Aminopyridinium iodide (1.33 g, 6.00 mmol), K<sub>2</sub>CO<sub>3</sub> (1.82 g, 13.2 mmol) and formamide **367** (1.83 g, 6.60 mmol) were stirred in MeOH (30 mL) for 3 days at r.t. before the solvent was removed under reduced pressure. The residue was passed through a pad of basic alumina, eluting with 9:1 CH<sub>2</sub>Cl<sub>2</sub>/MeOH. The crude residue was purified by flash column chromatography (94:6 CH<sub>2</sub>Cl<sub>2</sub>/MeOH) to give ylide **356a** as a brown solid (1.56 g, 77%); mp: 168–172 °C; IR (neat):  $\nu$  = 2961, 2923, 2870, 1666, 1620, 1591, 1470, 1294, 1221 cm<sup>-1</sup>; *restricted rotation around the amide bond results in 2 sets of signals (one major one minor)*: <sup>1</sup>H NMR (300 MHz, CDCl<sub>3</sub>):  $\delta$

= 8.72 – 8.66 (m, 2H), 8.70<sub>min</sub> and 8.18<sub>maJ</sub> (s, 1H), 7.95<sub>min</sub> and 7.88<sub>maJ</sub> (tt,  $J = 7.7, 1.3$  Hz, 1H), 7.68<sub>min</sub> and 7.63<sub>maJ</sub> (t,  $J = 7.3$  Hz, 2H), 7.35<sub>maJ</sub> and 7.30<sub>min</sub> (t,  $J = 7.3$  Hz, 1H) 7.21<sub>maJ</sub> and 7.19<sub>min</sub> (d,  $J = 7.3$  Hz, 2H), 4.26<sub>maJ</sub> and 4.16<sub>min</sub> (s, 2H), 3.48<sub>maJ</sub> and 3.18<sub>min</sub> (hept,  $J = 6.8$  Hz, 2H), 1.25 – 1.15 (m, 12H) ppm;  $^{13}\text{C}$  NMR (101 MHz, CDCl<sub>3</sub>):  $\delta = 171.7$  and  $171.2$  (C),  $164.7$  and  $163.8$  (CH),  $148.3$  and  $146.7$  (2C),  $143.0$  and  $142.8$  (2CH),  $137.6$  and  $137.0$  (CH),  $136.9$  and  $136.2$  (C),  $129.3$  and  $128.8$  (CH),  $126.4$  and  $126.2$  (2CH),  $124.4$  and  $124.3$  (2CH),  $54.9$  and  $52.9$  (CH<sub>2</sub>),  $28.6$  and  $28.0$  (2CH),  $25.2$  and  $24.7$  (2CH<sub>3</sub>),  $24.4$  and  $24.3$  (2CH<sub>3</sub>) ppm; HRMS (ES–TOF):  $m/z$ : calcd for C<sub>20</sub>H<sub>26</sub>N<sub>3</sub>O<sub>2</sub>: 340.2020, found 340.2030 [M+H]<sup>+</sup>.

### General procedure 11: oxazole synthesis (GP11)

Following the method developed within the Davies group,<sup>48,49</sup> the relevant ynamide (1.0 eq.), ylide (1.2–1.5 eq.) Au(Pic)Cl<sub>2</sub> (2–5 mol%) and dry toluene (0.1 M wrt ynamide) were combined in a flame dried flask (typically a Schlenk tube) under argon and heated to 90 °C for 2–6 h. After allowing to cool to r.t., the reaction mixture was flushed through a pad of silica (EtOAc), concentrated under reduced pressure and purified by either recrystallization or flash column chromatography.

#### *N*–((4–(9H–Carbazol–9–yl)–5–phenyloxazol–2–yl)methyl)–*N*–(2,6–diisopropylphenyl)formamide **358a**

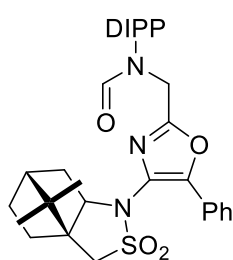


Following **GP11** using ynamine **44s** (95.0 mg, 0.36 mmol), ylide **356a** (148 mg, 0.44 mmol), Au(Pic)Cl<sub>2</sub> (2.77 mg, 5 mol%) and toluene (3.5 mL). Purification by flash column chromatography (9:1 hexane/EtOAc) gave oxazole **358a** as a white foam (167 mg, 85%); mp: 186–188 °C; IR (neat):  $\nu = 2962, 2252, 1691, 1542, 1341, 1232$  cm<sup>–1</sup>; *restricted rotation around the amide bond results in 2 sets of resonances in a 10:1 ratio*:  $^1\text{H}$  NMR (300 MHz, CDCl<sub>3</sub>):  $\delta = 8.83_{\text{min}}$  and



8.28<sub>maJ</sub> (s, 1H), 8.13 – 8.08 (m, 2H), 7.46 – 7.15 (m, 12H), 7.05 – 7.00 (m, 2H), 5.07<sub>maJ</sub> and 4.91<sub>min</sub> (s, 2H), 3.09<sub>maJ</sub> and 2.94<sub>min</sub> (hept,  $J = 6.8$  Hz, 2H), 1.18 (d,  $J = 6.8$  Hz, 6H), 1.13 (d,  $J = 6.8$  Hz, 6H); *only the peaks for the major isomer are reported*:  $^{13}\text{C}$  NMR (101 MHz,  $\text{CDCl}_3$ ):  $\delta = 163.7$  (CH), 156.9 (2C), 148.2 (2C), 146.5 (C), 145.0 (C), 139.9 (C), 134.4 (C), 130.1 (CH), 129.0 (CH), 128.9 (2CH), 126.5 (C), 126.3 (2CH), 125.1 (2CH), 124.8 (2CH), 124.2 (2C), 120.9 (2CH), 120.5 (2CH), 111.0 (CH), 44.1 ( $\text{CH}_2$ ), 28.6 (2CH), 25.4 ( $2\text{CH}_3$ ), 23.8 ( $2\text{CH}_3$ ) ppm; HRMS (ES–TOF):  $m/z$  calcd for  $\text{C}_{35}\text{H}_{33}\text{N}_3\text{O}_2\text{Na}$ : 550.2465, found 550.2478  $[\text{M}+\text{Na}]^+$ . Crystals suitable for single crystal X-ray diffraction were grown by diffusion of hexane into a solution of **358a** in  $\text{CH}_2\text{Cl}_2$ .

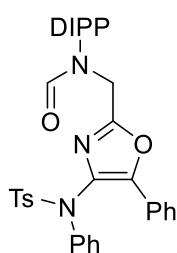
***N*–(2,6–diisopropylphenyl)–N–((4–((3*aS*,6*R*)–8,8–dimethyl–2,2–dioxidotetrahydro–3*H*–3*a*,6–methanobenzo[*c*]isothiazol–1(4*H*)–yl)–5–phenyloxazol–2–yl)methyl)formamide **358b****



Following **GP11** using ynamide **44t** (630 mg, 2.00 mmol), ylide **356a** (814 mg, 2.40 mmol),  $\text{Au}(\text{Pic})\text{Cl}_2$  (15.6 mg, 2 mol%) and toluene (30 mL). Purification by flash column chromatography (1:1 hexane/EtOAc) gave oxazole **358b** as a white solid (1.00 g, 87%); mp: 112–115 °C; IR (neat):  $\nu = 2961, 2872, 1683, 1450, 1326, 1167, 1137\text{ cm}^{-1}$ ; *restricted rotation around the amide bond results in 2 sets of resonances in a 3:1 ratio*:  $^1\text{H}$  NMR (300 MHz,  $\text{CDCl}_3$ ):  $\delta = 8.76_{\text{min}}$  and 8.21<sub>maJ</sub> (s, 1H), 7.93 – 7.86 (m, 2H), 7.41 – 7.33 (m, 4H), 7.20 (td,  $J = 7.3, 1.6$  Hz, 2H), 4.98<sub>maJ</sub> and 4.83<sub>min</sub> (d,  $J_{AB} = 15.3$  Hz, 1H), 4.88<sub>maJ</sub> and 4.74<sub>min</sub> (d,  $J_{AB} = 15.3$  Hz, 1H), 3.97 (dd,  $J = 8.0, 4.7$  Hz, 1H), 3.38<sub>min</sub> and 3.35<sub>maJ</sub> (s, 2H), 2.97<sub>maJ</sub> and 2.87<sub>min</sub> (hept,  $J = 6.8$  Hz, 2H), 1.90 – 1.80 (m, 3H) 1.72 – 1.45 (m, 4H), 1.34 – 1.24 (m, 3H), 1.15 (d,  $J = 6.8$  Hz, 3H), 1.16 – 1.10 (m, 9H), 1.04 (d,  $J = 6.8$  Hz, 2H), 0.95 (s, 3H) ppm; *only the peaks for the major isomer are reported*:  $^{13}\text{C}$  NMR (101 MHz,  $\text{CDCl}_3$ ):  $\delta = 163.6$  (CH), 156.7 (C), 148.9 (C), 148.2 (C), 148.0 (C), 134.7 (C), 130.0 (CH), 129.4 (CH), 128.7 (2CH), 127.6 (C), 126.4 (C), 126.1 (2CH), 124.8 (CH),

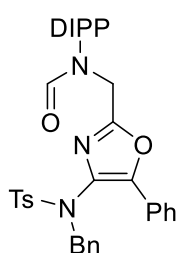
124.6 (CH), 67.0 (CH), 50.4 (CH<sub>2</sub>), 49.8 (C), 48.1 (C), 44.6 (CH), 44.3 (CH<sub>2</sub>), 35.1 (CH<sub>2</sub>), 32.5 (CH<sub>2</sub>), 28.5 (2CH), 27.0 (CH<sub>2</sub>), 25.3 (CH<sub>3</sub>), 25.2 (CH<sub>3</sub>), 23.9 (CH<sub>3</sub>), 23.7 (CH<sub>3</sub>), 20.9 (CH<sub>3</sub>), 20.2 (CH<sub>3</sub>) ppm; HRMS (ES–TOF):  $m/z$ : calcd for C<sub>33</sub>H<sub>41</sub>N<sub>3</sub>O<sub>4</sub>NaS: 598.2710, found 598.2717 [M+Na]<sup>+</sup>.

***N*–(2,6-Diisopropylphenyl)–N–((4–((4-methyl–N-phenylphenyl)sulfonamido)–5-phenyloxazol–2-yl)methyl)formamide 358c**



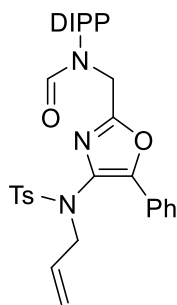
Following **GP11** using ynamide **44f** (350 mg, 1.01 mmol), ylide **356a** (410 mg, 1.21 mmol), Au(Pic)Cl<sub>2</sub> (7.9 mg, 2 mol%) and toluene (10 mL). Purification by flash column chromatography (8:2 hexane/EtOAc) gave oxazole **358c** as a white fluffy solid (607 mg, 88%); mp: 235–238 °C; IR (neat):  $\nu$  = 2964, 2926, 2868, 1681, 1595, 1490, 1450, 1358, 1168 cm<sup>–1</sup>; *restricted rotation around the amide bond results in 2 sets of resonances in a 4:1 ratio*: <sup>1</sup>H NMR (400 MHz, CDCl<sub>3</sub>):  $\delta$  = 8.74<sub>min</sub> and 8.19<sub>maJ</sub> (s, 1H), 7.93 (dt,  $J$  = 7.2, 1.4 Hz, 2H), 7.49 – 7.41 (m, 4H), 7.40 – 7.33 (m, 2H), 7.25 – 7.10 (m, 9H), 4.94<sub>maJ</sub> and 4.74<sub>min</sub> (s, 2H), 2.94 and 2.78 (hept,  $J$  = 6.8 Hz, 2H), 2.41 and 2.39 (s, 3H), 1.13<sub>min</sub> and 1.12<sub>maJ</sub> (d,  $J$  = 6.8 Hz, 6H), 0.98<sub>maJ</sub> and 0.95<sub>min</sub> (d,  $J$  = 6.8 Hz, 6H) ppm; *only the peaks for the major isomer are reported*: <sup>13</sup>C NMR (101 MHz, CDCl<sub>3</sub>):  $\delta$  = 163.4 (CH), 155.2 (C), 148.3 (2C), 148.0 (C), 146.6 (C), 143.9 (C), 139.8 (C), 135.4 (C), 134.0 (C), 133.1 (C), 130.0 (CH), 129.4 (CH), 129.2 (2CH), 129.1 (4CH), 129.0 (2CH), 127.7 (CH), 127.5 (2CH), 126.6 (C), 125.7 (2CH), 124.7 (2CH), 43.4 (CH<sub>2</sub>), 28.4 (2CH), 25.4 (2CH<sub>3</sub>), 23.5 (2CH<sub>3</sub>), 21.8 (CH<sub>3</sub>); HRMS (ES–TOF):  $m/z$ : calcd for C<sub>36</sub>H<sub>38</sub>N<sub>3</sub>O<sub>4</sub>S: 608.2578, found 608.2586 [M+H]<sup>+</sup>.

***N*-((4-((*N*-benzyl-4-methylphenyl)sulfonamido)-5-phenyloxazol-2-yl)methyl)-*N*-(2,6-diisopropylphenyl)formamide **358d****



Following **GP11** using ynamide **44s** (1.08 g, 3.00 mmol), ylide **356a** (1.22 g, 3.59 mmol), Au(Pic)Cl<sub>2</sub> (23.3 mg, 2 mol%) and toluene (30 mL). Purification by flash column chromatography (3:1 hexane/EtOAc) gave oxazole **358d** as a white solid (1.44 g, 77%); mp: 146-149 °C; IR (neat):  $\nu$  = 2965, 2158, 1686, 1450, 1353, 1165 cm<sup>-1</sup>; *restricted rotation around the amide bond results in 2 sets of resonances in a 8:1 ratio*: <sup>1</sup>H NMR (400 MHz, CDCl<sub>3</sub>):  $\delta$  = 8.60<sub>min</sub> and 8.18<sub>maJ</sub> (s, 1H), 7.70 – 7.65 (m, 2H), 7.61 (d<sub>AA'XX'</sub>,  $J$  = 8.3 Hz, 2H), 7.40 (t,  $J$  = 7.8 Hz, 1H), 7.43 – 7.36 (m, 3H), 7.26 – 7.19 (m, 4H), 7.11 – 7.01 (m, 5H), 4.83<sub>maJ</sub> and 4.65<sub>min</sub> (s, 2H), 4.53<sub>min</sub> and 4.47<sub>maJ</sub> (s, 2H), 2.95<sub>maJ</sub> and 2.77<sub>min</sub> (hept,  $J$  = 6.8 Hz, 2H), 2.46<sub>min</sub> and 2.43<sub>maJ</sub> (s, 3H), 1.15<sub>min</sub> and 1.12<sub>maJ</sub> (d,  $J$  = 6.8 Hz, 6H), 1.01 (d,  $J$  = 6.8 Hz, 6H) ppm; *only the peaks for the major isomer are reported*: <sup>13</sup>C NMR (101 MHz, CDCl<sub>3</sub>):  $\delta$  = 163.4(CH), 155.4 (C), 148.2 (2C), 147.8 (C), 144.0 (C), 135.3 (C), 134.8 (C), 134.3 (C), 131.5 (C), 130.0 (CH), 129.6 (2CH), 129.2 (2CH), 129.1 (CH), 128.7 (2CH), 128.4 (2CH), 128.3 (2CH), 128.0 (CH), 126.5 (C), 125.7 (2CH), 124.7 (2CH), 54.1 (CH<sub>2</sub>), 43.9 (CH<sub>2</sub>), 28.4 (2CH), 25.4 (2CH<sub>3</sub>), 23.7 (2CH<sub>3</sub>), 21.8 (CH<sub>3</sub>) ppm; HRMS (ES-TOF):  $m/z$ : calcd for C<sub>37</sub>H<sub>39</sub>N<sub>3</sub>O<sub>4</sub>SNa: 644.2553, found 644.2562 [M+Na]<sup>+</sup>.

***N*-((4-((*N*-allyl-4-methylphenyl)sulfonamido)-5-phenyloxazol-2-yl)methyl)-*N*-(2,6-diisopropylphenyl)formamide **358e****



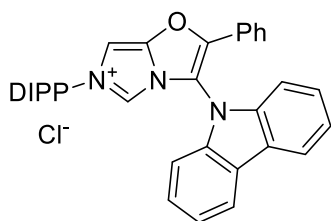
Following **GP11** using ynamide **44t** (311 mg, 1.00 mmol), ylide **356a** (410 mg, 1.21 mmol), Au(Pic)Cl<sub>2</sub> (7.8 mg, 2 mol%) and toluene (5.0 mL). Purification by flash column chromatography (85:15 hexane/EtOAc) and hot recrystallisation (toluene) gave oxazole **358e** as a white solid (479 mg, 83%); mp: 135-137 °C; IR (neat):  $\nu$  = 2922, 2853, 1685, 1462, 1354 cm<sup>-1</sup>; *restricted*

rotation around the amide bond results in 2 sets of resonances in a 9:1 ratio:  $^1\text{H}$  NMR (300 MHz,  $\text{CDCl}_3$ ):  $\delta$  = 8.64<sub>min</sub> and 8.19<sub>maJ</sub> (s, 1H), 7.94 (d,  $J$  = 7.0, 2H), 7.63<sub>min</sub> and 7.57<sub>maJ</sub> (d,  $J$  = 8.3 Hz, 2H), 7.48 – 7.31 (m, 4H), 7.23 – 7.20 (m, 4H), 5.61 (ddt,  $J$  = 16.7, 10.0, 6.6 Hz, 1H), 4.93 (dd,  $J$  = 16.7, 1.2 Hz, 1H), 4.88 (dd,  $J$  = 10.0, 1.3 Hz, 1H), 4.85 (s, 2H), 4.00<sub>min</sub> and 3.96<sub>maJ</sub> (d,  $J$  = 6.6 Hz, 2H), 2.97<sub>maJ</sub> and 2.80<sub>min</sub> (hept,  $J$  = 6.8 Hz, 2H), 2.44<sub>min</sub> and 2.41<sub>maJ</sub> (s, 3H), 1.16<sub>min</sub> and 1.13<sub>maJ</sub> (d,  $J$  = 6.8 Hz, 6H), 1.06 (d,  $J$  = 6.8 Hz, 6H) ppm; *only the peaks for the major isomer are reported*:  $^{13}\text{C}$  NMR (101 MHz,  $\text{CDCl}_3$ ):  $\delta$  = 163.4 (CH), 155.4 (C), 148.6 (C), 148.1 (2C), 146.5 (C), 143.9 (C), 135.3 (C), 134.3 (C), 131.7 (CH), 130.0 (CH), 129.5 (2CH), 129.2 (CH), 128.8 (2CH), 128.7 (2CH), 126.8 (C), 125.6 (2CH), 124.6 (2CH), 119.8 (CH<sub>2</sub>), 53.1 (CH<sub>2</sub>), 43.9 (CH<sub>2</sub>), 28.4 (2CH), 25.4 (2CH<sub>3</sub>), 23.7 (2CH<sub>3</sub>), 21.7 (CH<sub>3</sub>) ppm; HRMS (ES–TOF):  $m/z$ : calcd for  $\text{C}_{33}\text{H}_{38}\text{N}_3\text{O}_4\text{S}$ : 572.2578, found 572.2568  $[\text{M}+\text{H}]^+$ .

#### **General procedure 12: POCl<sub>3</sub> mediated cyclisation to imidazolium salts (GP12)**

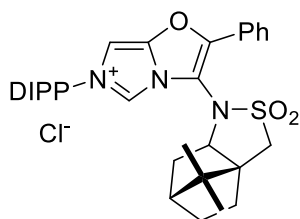
A round bottom flask was equipped with a reflux condenser and 2 M NaOH<sub>(aq)</sub> bubbler (for quenching HCl produced in the reaction) and flame dried under vacuum. Oxazole (1.0 eq.), dry *m*-xylene (0.1 M wrt oxazole) and POCl<sub>3</sub> (3.0 eq.) were added and the reaction mixture heated to 140 °C for 3 days with a positive pressure of argon and active water cooling in the reflux condenser. After allowing to cool to r.t., satd NaHCO<sub>3(aq)</sub> was added and the organics extracted with CH<sub>2</sub>Cl<sub>2</sub> (3×). The combined organics were washed with brine (1×), dried over Na<sub>2</sub>SO<sub>4</sub>, filtered and concentrated under reduced pressure. The residue was taken up in MeOH and stirred with DOWEX 22 Cl<sup>−</sup> resin for 3 h, filtered through cotton, concentrated under reduced pressure and purified by flash column chromatography to give the imidazolium salt.

**3-(9*H*-Carbazol-9-yl)-6-(2,6-diisopropylphenyl)-2-phenylimidazo[5,1-*b*]oxazol-6-ium chloride 353a•HCl**



Following **GP12** using oxazole **358a** (953 mg, 1.81 mmol), POCl<sub>3</sub> (500 μL, 5.35 mmol) and *m*-xylene (18 mL). Purification by flash column chromatography (94:6 CH<sub>2</sub>Cl<sub>2</sub>/MeOH) and trituration with hot EtOAc provided **353a•HCl** as a pale yellow solid (510 mg, 55%); mp: (dec.) 275 °C; IR (neat): ν = 2962, 2921, 2853, 1674, 1622, 1499, 1451, 1222, 1183, 1059 cm<sup>-1</sup>; <sup>1</sup>H NMR (400 MHz, CDCl<sub>3</sub>): δ = 8.41 (br. s, 1H), 8.17 (dd, *J* = 7.3, 1.3 Hz, 2H), 7.86 (br. s, 1H), 7.62 (d, *J* = 7.5 Hz, 2H), 7.54 – 7.40 (m, 8H), 7.34 (t, *J* = 7.5 Hz, 2H), 7.29 (d, *J* = 7.5 Hz, 2H), 2.59 (hept, *J* = 6.6 Hz, 2H), 1.30 (d, *J* = 6.6 Hz, 6H), 1.13 (d, *J* = 6.6 Hz, 6H) ppm; <sup>13</sup>C NMR (101 MHz, CDCl<sub>3</sub>): δ = 151.3 (C), 145.9 (2C), 144.7 (C), 138.5 (C), 132.3 (CH), 132.1 (CH), 131.1 (C), 129.5 (2CH), 127.7 (2CH), 126.8 (2CH), 125.3 (2C), 124.8 (2CH), 124.1 (C), 123.2 (2CH), 121.4 (2CH), 117.1 (CH), 111.1 (2CH), 103.6 (CH), 28.8 (2CH), 24.9 (2CH<sub>3</sub>), 24.6 (2CH<sub>3</sub>) ppm; HRMS (ES-TOF): *m/z*: calcd for C<sub>35</sub>H<sub>32</sub>N<sub>3</sub>O: 510.2540, found 510.2542 [M-Cl]<sup>+</sup>.

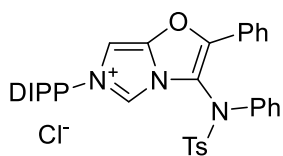
**6-(2,6-Diisopropylphenyl)-3-((3*aS*,6*R*)-8,8-dimethyl-2,2-dioxidotetrahydro-3*H*-3*a*,6-methanobenzo[*c*]isothiazol-1(4*H*)-yl)-2-phenylimidazo[5,1-*b*]oxazol-6-ium chloride 353b•HCl**



Following **GP12** using oxazole **358b** (863 mg, 1.50 mmol), POCl<sub>3</sub> (420 μL, 4.49 mmol) and *m*-xylene (15 mL). Purification by flash column chromatography (95:5 CH<sub>2</sub>Cl<sub>2</sub>/MeOH) provided **353b•HCl** as a pale yellow solid (603 mg, 68%); mp: (dec.) 270 °C; IR (neat): ν = 2963, 2877, 2292, 2686, 1622, 1498, 1459, 1326, 1200, 1168, 1142, 1060 cm<sup>-1</sup>; <sup>1</sup>H NMR (300 MHz, CDCl<sub>3</sub>): δ = 11.12 (br. s, 1H), 8.04 (d, *J* = 7.3 Hz, 2H), 7.66 – 7.44 (m, 4H), 7.38 – 7.23 (m, 2H), 6.95 (br. s, 1H), 4.96 (br. s, 1H), 4.22 (d, *J* = 13.4 Hz, 1H), 3.46 (d, *J* = 13.4 Hz,

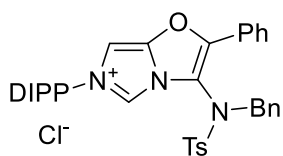
1H), 2.87 – 2.73 (m, 1H), 2.54 – 2.42 (m, 1H), 2.35 – 2.07 (m, 2H), 1.93 – 1.56 (m, 4H), 1.38 (d,  $J = 6.8$  Hz, 3H), 1.27 (d,  $J = 6.8$  Hz, 3H), 1.25 – 1.20 (m, 7H), 1.13 (d,  $J = 6.8$  Hz, 3H), 0.96 (s, 3H) ppm;  $^{13}\text{C}$  NMR (101 MHz,  $\text{CDCl}_3$ )  $\delta = 155.1, 145.9, 145.8, 144.3, 132.5, 132.1, 131.4, 129.2, 128.1, 127.4, 124.9, 124.6, 123.9, 97.7, 67.3, 60.5, 51.6, 51.3, 48.2, 45.8, 35.9, 31.4, 29.0, 28.9, 26.4, 25.1, 24.5, 24.1, 21.5, 21.2, 20.2, 14.3$  ppm; ;HRMS (ES–TOF):  $m/z$ : calcd for  $\text{C}_{33}\text{H}_{40}\text{N}_3\text{O}_3\text{S}$ : 558.2785, found 558.2796  $[\text{M} - \text{Cl}]^+$ .

**6–(2,6-Diisopropylphenyl)–3–((4-methyl-N-phenylphenyl)sulfonamido)–2-phenylimidazo[5,1-b]oxazol–6-ium chloride 353c•HCl**



Following **GP12** using oxazole **358c** (600 mg, 0.99 mmol),  $\text{POCl}_3$  (280  $\mu\text{L}$ , 3.00 mmol) and  $m$ -xylene (10 mL). Purification by flash column chromatography (8:2 EtOAc/MeOH) and trituration with hot EtOAc provided **353c•HCl** as a white solid (210 mg, 34%); mp: 205–208  $^\circ\text{C}$ ; IR (neat):  $\nu = 2965, 1613, 1492, 1367, 1237, 1170$   $\text{cm}^{-1}$ ;  $^1\text{H}$  NMR (400 MHz,  $\text{CDCl}_3$ ):  $\delta = 9.48$  (d,  $J = 1.5$  Hz, 1H), 8.22 (d,  $J = 1.5$  Hz, 1H), 7.84 ( $d_{\text{AA'XX'}}$ ,  $J = 8.1$  Hz, 2H), 7.75 – 7.70 (m, 2H), 7.57 (t,  $J = 7.8$  Hz, 1H), 7.50 (tt,  $J = 7.5, 1.3$  Hz, 1H), 7.47 – 7.44 (m, 2H), 7.40 – 7.25 (m, 9H), 2.48 (hept,  $J = 6.8$  Hz, 2H), 2.38 (s, 3H), 1.27 (d,  $J = 6.8$  Hz, 6H), 1.26 (d,  $J = 6.8$  Hz, 6H) ppm;  $^{13}\text{C}$  NMR (101 MHz,  $\text{CDCl}_3$ ):  $\delta = 153.0$  (C), 146.6 (C), 145.7 (2C), 143.9 (C), 138.5 (C), 133.5 (C), 132.4 (CH), 132.3 (CH), 131.4 (C), 130.7 (2CH), 130.3 (2CH), 129.2 (2CH), 129.0 (CH), 128.7 (2CH), 127.5 (2CH), 126.0 (2CH), 124.8 (2CH), 123.7 (C), 120.8 (C), 117.6 (CH), 102.2 (CH), 31.7 ( $\text{CH}_3$ ), 29.0 (2CH), 24.8 ( $2\text{CH}_3$ ), 24.4 ( $2\text{CH}_3$ ) ppm; HRMS (ES–TOF):  $m/z$ : calcd for  $\text{C}_{36}\text{H}_{36}\text{N}_3\text{O}_3\text{S}$ : 590.2472, found 590.2480  $[\text{M} - \text{Cl}]^+$ .

**3-((*N*-Benzyl-4-methylphenyl)sulfonamido)-6-(2,6-diisopropylphenyl)-2-phenylimidazo[5,1-*b*]oxazol-6-ium chloride **353d•HCl****



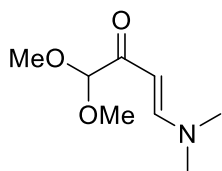
Following **GP12** using oxazole **358d** (933 mg, 1.50 mmol), POCl<sub>3</sub> (420  $\mu$ L, 4.49 mmol) and *m*-xylene (15 mL). Purification by flash column chromatography (95:5 CH<sub>2</sub>Cl<sub>2</sub>/MeOH) provided **353d•HCl** as

a white solid (504 mg, 53%); mp: (dec.) 185 °C; IR (neat):  $\nu$  = 2965, 1664, 1615, 1362, 1166 cm<sup>-1</sup>; <sup>1</sup>H NMR (400 MHz, CDCl<sub>3</sub>):  $\delta$  = 8.63 – 8.53 (m, 1H), 8.22 (br. s, 1H), 7.84 – 7.78 (m, 2H), 7.59 – 7.49 (m, 1H), 7.48 – 7.42 (m, 1H), 7.40 – 7.26 (m, 10H), 7.25 – 7.16 (m, 3H), 5.60 – 5.45 (m, 1H), 4.62 – 4.45 (m, 1H), 2.41 (s, 3H), 2.29 – 2.15 (m, 2H), 1.28 – 1.12 (m, 12H) ppm; <sup>13</sup>C NMR (101 MHz, CDCl<sub>3</sub>):  $\delta$  = 152.7 (C), 146.2 (C), 145.5 (C), 145.4 (C), 143.7 (C), 134.4 (C), 134.3 (C), 132.2 (2CH), 131.1 (C), 130.8 (2CH), 129.7 (2CH), 129.3 (4CH), 129.2 (2CH), 128.0 (2CH), 126.8 (CH), 124.73 (CH), 124.70 (CH), 123.7 (C), 119.8 (CH), 115.8 (C), 103.4 (CH), 54.2 (CH<sub>2</sub>), 28.9 (CH), 28.8 (CH), 25.1 (CH<sub>3</sub>), 24.9 (CH<sub>3</sub>), 24.5 (CH<sub>3</sub>), 24.3 (CH<sub>3</sub>), 21.9 (CH<sub>3</sub>) ppm; HRMS (ES–TOF): *m/z*: calcd for C<sub>37</sub>H<sub>38</sub>N<sub>3</sub>O<sub>3</sub>S: 604.2628, found 604.2635 [M–Cl]<sup>+</sup>.

## Formation of pyrimidines annulated imidazolium salts

### Condensation reactions to access functionalised pyrimidines (Chapter 5.3.1)

**(*E*)-4-(Dimethylamino)-1,1-dimethoxybut-3-en-2-one **380****

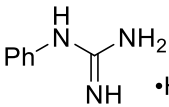


Pyruvaldehyde dimethyl acetal (4.84 mL, 40.0 mmol) and *N,N*-dimethylformamide dimethyl acetal (5.56 mL, 41.9 mmol) were combined in a flame dried round bottom flask equipped with a condenser and refluxed

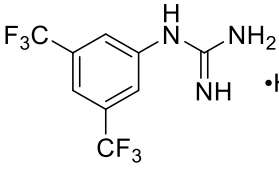
at 110 °C for 18 h under argon. After allowing to cool to r.t., the crude material was purified by flash column chromatography (95:5 EtOAc/MeOH) to give **380** as a dark yellow oil (4.86 g,

70%); IR (neat):  $\nu = 2932, 1651, 1576 \text{ cm}^{-1}$ ;  $^1\text{H}$  NMR (400 MHz,  $\text{CDCl}_3$ ):  $\delta = 7.72$  (d,  $J = 12.6$  Hz, 1H), 5.32 (d,  $J = 12.6$  Hz, 1H), 4.56 (s, 1H), 3.39 (s, 6H), 3.09 (s, 3H), 2.85 (s, 3H) ppm;  $^{13}\text{C}$  NMR (101 MHz,  $\text{CDCl}_3$ ):  $\delta = 191.1$  (C), 154.5 (CH), 104.5 (CH), 91.1 (CH), 54.2 (2CH<sub>3</sub>), 45.1 (CH<sub>3</sub>), 37.3 (CH<sub>3</sub>) ppm; MS (TOF-AP):  $m/z$ : 100% 114.15  $[\text{M}-2(\text{OCH}_3)\text{H}]^+$ , 30% 174.18  $[\text{M}+\text{H}]^+$ . Spectroscopic data matched that reported in the literature.<sup>265</sup>

### ***1-Phenylguanidine bicarbonate 385a***

 Aniline (4.56 mL, 50.0 mmol) and 37% HCl (3.5 mL, 42.0 mmol) were heated to 85 °C and 50% aqueous cyanamide solution was added portion wise (4.35 g, 54.8 mmol) (4 x approx. 1.1 g additions). Before the final portion was added, another portion of 37% HCl<sub>(aq)</sub> (0.7 mL, 8.40 mmol) was added. After complete addition, the reaction was stirred for a further 2 h at 85 °C before lowering the temperature to 60 °C. A solution of Na<sub>2</sub>CO<sub>3</sub> (3.15 g, 30.0 mmol) in H<sub>2</sub>O (12 mL) was added over 10 min and the mixture stirred at 60 °C for 30 min. Upon cooling to 0 °C, the precipitate was collected via filtration, washed with H<sub>2</sub>O (30 mL) and dried under high vacuum (50 °C/0.1 mbar) to give **385a** as a beige solid (7.12 g, 72%); mp: 146–149 °C (lit: 148–150 °C); IR (neat):  $\nu = 3434, 3314, 3114, 2965, 2735, 1674, 1619, 1567, 1344 \text{ cm}^{-1}$ ;  $^{13}\text{C}$  NMR (101 MHz, DMSO-*d*<sub>6</sub>):  $\delta = 161.1$  (C), 155.3 (C), 143.6 (C), 128.6 (2CH), 123.2 (CH), 120.8 (2CH) ppm; Spectroscopic data matched that reported in the literature.<sup>266</sup>

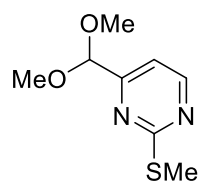
### ***1-(3,5-Bis(trifluoromethyl)phenyl)guanidine bicarbonate 385b***

 3,5-Bis(trifluoromethyl)aniline (4.67 mL, 30.0 mmol) and 37% HCl<sub>(aq)</sub> (2.5 mL, 30 mmol) were heated to 85 °C and 50% aqueous cyanamide solution was added portion wise (2.40 mL, 30.3 mmol) (4 x approx. 0.60 mL additions). Before the final portion was added, another portion



of 37% HCl<sub>(aq)</sub> (0.4 mL, 4.8 mmol) was added. After complete addition, the reaction was stirred for a further 2 h at 85 °C before lowering the temperature to 60 °C. A solution of Na<sub>2</sub>CO<sub>3</sub> (3.15 g, 30.0 mmol) in H<sub>2</sub>O (12 mL) was added over 10 min and the mixture stirred at 60 °C for 30 min. Upon cooling to 0 °C, the precipitate was collected via filtration, washed with H<sub>2</sub>O (30 mL) and Et<sub>2</sub>O (250 mL) and dried under high vacuum (50 °C/0.1 mbar) to give **385b** as a beige solid (6.66 g, 67%); mp: 142-145 °C; IR (neat):  $\nu$  = 3063 (brd.), 2662 (brd.), 1707, 1575, 1379, 1276, 1168, 1108 cm<sup>-1</sup>; <sup>19</sup>F NMR (377 MHz, DMSO-*d*<sub>6</sub>):  $\delta$  = -61.6 ppm; <sup>13</sup>C NMR (101 MHz, DMSO-*d*<sub>6</sub>):  $\delta$  = 162.0 (C), 155.2 (C), 143.8 (C), 131.1 (q, *J* = 32.5 Hz, 2C), 123.8 (q, *J* = 272.7 Hz, 2CF<sub>3</sub>), 120.6 (m, 2CH), 115.2 (m, CH) ppm.

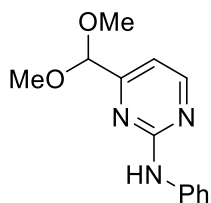
#### 4-(Dimethoxymethyl)-2-(methylthio)pyrimidine **368**



Pyruvaldehyde dimethyl acetal (4.84 mL, 50.0 mmol) and *N,N*-dimethylformamide dimethyl acetal (6.64 mL, 50.0 mmol) were combined in a flame dried round bottom flask with condenser attached and refluxed at 100 °C for 18 h under argon. After allowing to cool to r.t., thiourea (3.81 g, 50.0 mmol) and freshly prepared 5.0 M NaOMe (11 mL, 55.0 mmol) were added sequentially and the reaction heated to 45 °C for 16 h. After cooling to 0 °C, MeI (3.42 mL, 54.9 mmol) was added dropwise over 3 min before heating to 60 °C for 16 h. After allowing to cool to r.t., H<sub>2</sub>O was added (100 mL) and the aqueous layer extracted with EtOAc (3×50 mL). The combined organics were washed with brine (50 mL), dried over Na<sub>2</sub>SO<sub>4</sub>, filtered, concentrated under reduced pressure and purified by flash column chromatography (85:15 hexane/EtOAc) to give **368** as a pale yellow oil (5.96 g, 60%); IR (neat):  $\nu$  = 2929, 2831, 1548, 1429, 1351, 1319, 1205, 1111, 1058 cm<sup>-1</sup>; <sup>1</sup>H NMR (400 MHz, CDCl<sub>3</sub>):  $\delta$  = 8.55 (d, *J* = 5.0 Hz, 1H), 7.18 (d, *J* = 5.0 Hz, 1H), 5.18 (s, 1H), 3.41 (s, 6H), 2.57 (s, 3H) ppm; <sup>13</sup>C NMR (101 MHz, CDCl<sub>3</sub>):  $\delta$  = 172.8 (C), 165.7 (C),

158.0 (CH), 113.4 (CH), 103.2 (CH), 54.2 (2CH<sub>3</sub>), 14.3 (CH<sub>3</sub>) ppm; MS(ES–TOF): *m/z*: 100% 201.06 [M+H]<sup>+</sup>. Spectroscopic data matched that reported in the literature.<sup>267</sup>

**4–(Dimethoxymethyl)–N–phenylpyrimidin–2–amine 372a**



**Conventional heat:**

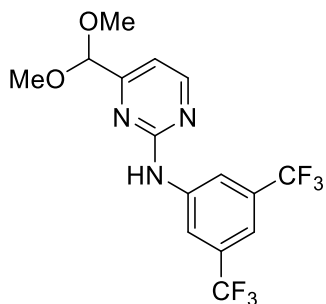
Pruvaldehyde dimethyl acetal (1.20 mL, 9.91 mmol) and *N,N*-dimethylformamide dimethyl acetal (1.33 mL, 10.0 mmol) were combined in a flame dried round bottom flask equipped with a condenser and refluxed at 100 °C for 18 h under argon. After allowing to cool to r.t., **385a** (2.95 g, 15.0 mmol) and dry DMAA (20 mL) were added and the reaction heated to 140 °C for 16 h. After allowing to cool to r.t., most of the DMAA was removed by distillation (25 mbar, 50 °C), 1.0 M HCl was added (20 mL) and the organics extracted with EtOAc (30 mL). The aqueous layer was neutralised with satd NaHCO<sub>3(aq)</sub> and extracted with EtOAc (3×30 mL) before the combined organics washed with brine (30 mL), dried over Na<sub>2</sub>SO<sub>4</sub>, filtered and concentrated under reduced pressure. Purification by flash column chromatography (9:1 hexane/EtOAc) gave **372a** as a yellow oil that solidified upon standing (1.69 g, 69%). Data below

**Microwave synthesis:**

**380** (170 mg, 0.98 mmol), **385a** (295 mg, 1.50 mmol) and MeCN (2.0 mL) were combined in a microwave tube and heated to 150 °C for 4 h. The crude product was concentrated under reduced pressure and purification by flash column chromatography gave **372a** as a yellow oil that solidified upon standing (225 mg, 92%); mp: 56–59 °C; IR (neat):  $\nu$  = 3261, 3197, 3070, 2960, 2937, 1609, 1573, 1537, 1498, 1439, 1411, 1333, 1115 cm<sup>-1</sup>; <sup>1</sup>H NMR (400 MHz, CDCl<sub>3</sub>):  $\delta$  = 8.47 (d, *J* = 5.0 Hz, 1H), 7.64 (dt, *J* = 8.5, 1.0 Hz, 2H), 7.38 – 7.29 (m, 3H), 7.04 (tt, *J* = 7.4, 1.0 Hz, 1H), 6.95 (d, *J* = 5.0 Hz, 1H), 5.20 (s, 1H), 3.43 (s, 6H) ppm; <sup>13</sup>C NMR (101 MHz, CDCl<sub>3</sub>):  $\delta$  = 166.3 (C), 160.1 (C), 158.8 (CH), 139.5 (C), 129.1 (2CH), 122.7 (CH), 119.3

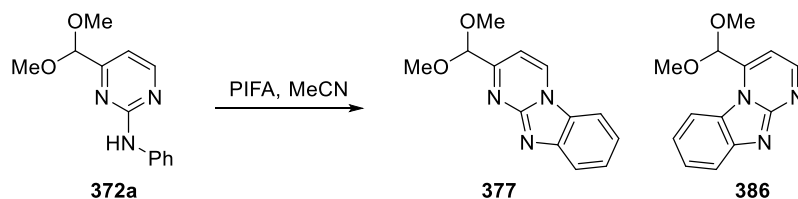
(2CH), 109.8 (CH), 102.8 (CH), 53.8 (2CH<sub>3</sub>) ppm; HRMS (ES–TOF): *m/z*: calcd for C<sub>13</sub>H<sub>16</sub>N<sub>3</sub>O<sub>2</sub>: 246.1237, found 246.1243 [M+H]<sup>+</sup>. Spectroscopic data matched that reported in the literature (incomplete).<sup>268</sup>

***N*–(3,5–Bis(trifluoromethyl)phenyl)–4–(dimethoxymethyl)pyrimidin–2–amine 372b**



Pruvaldehyde dimethyl acetal (1.95 mL, 16.0 mmol) and *N,N*–dimethylformamide dimethyl acetal (2.13 mL, 16.0 mmol) were combined in a flame dried round bottom flask with condenser attached and refluxed at 100 °C for 18 h under argon. After allowing to cool to r.t., guanidinium salt **385b** (6.40 g, 19.2 mmol) and dry DMA (40 mL) were added and the reaction heated to 140 °C for 16 h. After allowing to cool to r.t., the reaction mixture was diluted with EtOAc (120 mL) and washed with H<sub>2</sub>O (2×80 mL) and brine (2×80 mL), dried over Na<sub>2</sub>SO<sub>4</sub>, filtered and concentrated under reduced pressure. Purification by flash column chromatography (9:1→8:2 hexane/EtOAc) gave **372b** as a pale yellow solid (3.83 g, 63%); mp: 55–57 °C; IR (neat):  $\nu$  = 3272, 3104, 2968, 1575, 1376, 1273, 1175, 1111, 1070 cm<sup>–1</sup>; <sup>1</sup>H NMR (300 MHz, CDCl<sub>3</sub>):  $\delta$  = 8.55 (d, *J* = 5.0 Hz, 1H), 8.20 (br. s, 2H), 7.84 (br. s, NH), 7.49 (br. s, 1H), 7.10 (d, *J* = 5.0 Hz, 1H), 5.22 (s, 1H), 3.46 (s, 6H) ppm; <sup>13</sup>C NMR (75 MHz, CDCl<sub>3</sub>):  $\delta$  = 166.8 (C), 159.3 (C), 159.0 (CH), 141.2 (C), 132.3 (q, *J* = 33.1 Hz, 2C), 123.5 (q, *J* = 272.6 Hz, 2CF<sub>3</sub>), 118.4 (q, *J* = 3.9 Hz, 2CH), 115.4 (hept, *J* = 3.9 Hz, CH), 111.2 (CH), 102.8 (CH), 54.1 (2CH<sub>3</sub>) ppm; <sup>19</sup>F NMR (282 MHz, CDCl<sub>3</sub>):  $\delta$  = –63.05 ppm; HRMS (ES–TOF): *m/z*: calcd for C<sub>15</sub>H<sub>14</sub>N<sub>3</sub>O<sub>2</sub>F<sub>6</sub>: 382.0985, found 382.0989 [M+H]<sup>+</sup>.

**Hypervalent iodine mediated ring closure:**



Aminopyrimidine **372a** (210 mg, 0.85 mmol) and PIFA (550 mg, 1.28 mmol) were dissolved in MeCN (4.25 mL) and stirred at r.t. for 20 min. Satd  $\text{NaHCO}_{3(\text{aq})}$  (10 mL) was added and the aqueous layer extracted EtOAc (3×10 mL). The combined organics were washed with brine (10 mL), dried over  $\text{Na}_2\text{SO}_4$ , filtered and concentrated under reduced pressure. Purification by flash column chromatography (100:1 EtOAc/ $\text{NEt}_3$ ) gave **377** (82.7 mg, 40%) and **386** (78.2 mg, 38%) as yellow solids:

**2-(Dimethoxymethyl)benzo[4,5]imidazo[1,2-a]pyrimidine 377**

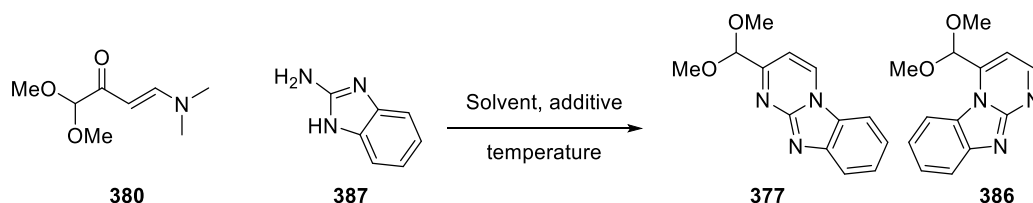
mp: 161–163 °C; IR (neat):  $\nu = 2934, 2832, 1624, 1517, 1441, 1283, 1103, 1062 \text{ cm}^{-1}$ ;  $^1\text{H}$  NMR (400 MHz,  $\text{CDCl}_3$ ):  $\delta = 8.77$  (d,  $J = 7.0$  Hz, 1H), 8.01 (app. dt,  $J = 8.3, 0.9$  Hz, 1H), 7.88 (app. dt,  $J = 8.2, 1.0$  Hz, 1H), 7.57 (ddd,  $J = 8.3, 7.2, 1.1$  Hz, 1H), 7.42 (ddd,  $J = 8.3, 7.2, 1.1$  Hz, 1H), 7.18 (d,  $J = 7.0$  Hz, 1H), 5.27 (s, 1H), 3.53 (s, 6H) ppm;  $^{13}\text{C}$  NMR (101 MHz,  $\text{CDCl}_3$ ):  $\delta = 163.9$  (C), 150.0 (C), 144.7 (C), 133.8 (CH), 127.0 (C), 126.6 (CH), 122.3 (CH), 120.9 (CH), 110.7 (CH), 105.4 (CH), 104.1 (CH), 55.4 (2CH<sub>3</sub>) ppm; HRMS (ES–TOF):  $m/z$ : calcd for  $\text{C}_{13}\text{H}_{14}\text{N}_3\text{O}_2$ : 244.1081, found 244.1085  $[\text{M}+\text{H}]^+$ .

**4-(Dimethoxymethyl)benzo[4,5]imidazo[1,2-a]pyrimidine 386**

mp: 163–165 °C; IR (neat):  $\nu = 3061, 2950, 1600, 1508, 1452, 1425, 1193, 1055, 739 \text{ cm}^{-1}$ ;  $^1\text{H}$  NMR (400 MHz,  $\text{CDCl}_3$ ):  $\delta = 8.79$  (d,  $J = 4.2$  Hz, 1H), 8.21 (app. dt,  $J = 8.5, 0.9$  Hz, 1H), 8.03 (ddd,  $J = 8.3, 1.2, 0.7$  Hz, 1H), 7.58 (ddd,  $J = 8.3, 7.1, 1.1$  Hz, 1H), 7.41 (ddd,  $J = 8.3, 7.1, 1.2$  Hz, 1H), 7.19 (d,  $J = 4.2$ , 1H), 6.05 (s, 1H), 3.44 (s, 6H) ppm;  $^{13}\text{C}$  NMR (101 MHz,  $\text{CDCl}_3$ ):  $\delta$

= 154.6 (CH), 151.5 (C), 145.7 (C), 144.8 (C), 127.0 (C), 126.4 (CH), 122.5 (CH), 120.5 (CH), 116.5 (CH), 105.8 (CH), 97.2 (CH), 53.2 (2CH<sub>3</sub>) ppm; HRMS (ES–TOF): *m/z*: calcd for C<sub>13</sub>H<sub>14</sub>N<sub>3</sub>O<sub>2</sub>: 244.1081, found 244.1088 [M+H]<sup>+</sup>.

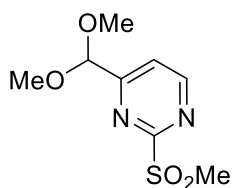
**Procedure for optimisation of condensation with 2-aminobenzimidazole:**



**380** (173 mg, 1.00 mmol), 2-aminobenzimidazole **387** (134 mg, 1.01 mmol) and solvent (2.0 mL) were combined in a microwave tube and heated to the indicated temperature for the indicated time. After the solvent was removed under reduced pressure, ratios were calculated through analysing the <sup>1</sup>H NMR of the crude reaction mixture, in which the acetal CH protons were distinguishable. Data above.

**Products derived from S<sub>N</sub>Ar reactions**

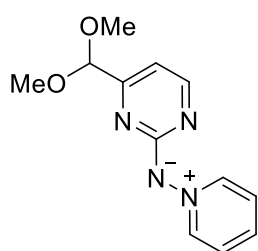
**4-(Dimethoxymethyl)-2-(methylsulfonyl)pyrimidine 381**



Pyrimidine **368** (1.01 g, 5.05 mmol) was dissolved in CH<sub>2</sub>Cl<sub>2</sub> (15 mL) and cooled to 0 °C and *m*-CPBA (70%, 3.00 g, 12.2 mmol) was added in 3 portions with 5 min intervals. The ice bath was removed and the reaction stirred for 2 h at r.t. before satd Na<sub>2</sub>SO<sub>3(aq)</sub> (15 mL) was added. After pouring into a separating funnel, the layers were separated and the aqueous layer extracted with CH<sub>2</sub>Cl<sub>2</sub> (20 mL). The combined organics were then washed satd NaHCO<sub>3(aq)</sub> (3×20 mL) and brine (20 mL), dried over Na<sub>2</sub>SO<sub>4</sub>, filtered and concentrated under reduced pressure to give sulfone **381** as a viscous colourless oil (1.06 g, 92%); IR (neat): ν = <sup>1</sup>H NMR (400 MHz, CDCl<sub>3</sub>): δ = 8.96 (d, *J* = 5.0

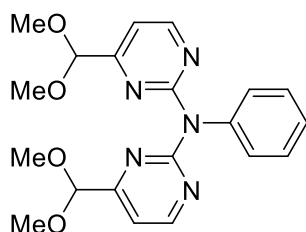
Hz, 1H), 7.78 (d,  $J = 5.0$  Hz, 1H), 5.34 (s, 1H), 3.45 (s, 6H), 3.37 (s, 3H) ppm;  $^{13}\text{C}$  NMR (101 MHz,  $\text{CDCl}_3$ ):  $\delta = 168.1$  (C), 165.9 (C), 159.4 (CH), 121.1 (CH), 102.8 (CH), 54.8 (2CH<sub>3</sub>), 39.3 (CH<sub>3</sub>) ppm; MS (ES–TOF):  $m/z$ : 100% 255.0  $[\text{M}+\text{Na}]^+$ . Spectroscopic data matched that reported in the literature.<sup>269</sup>

**(4-(Dimethoxymethyl)pyrimidin-2-yl)(pyridin-1-ium-1-yl)amide 382**



*N*-Aminopyridinium iodide **90** (444 mg, 2.00 mmol), **381** (497 mg, 2.14 mmol) and  $\text{K}_2\text{CO}_3$  (642 mg, 4.65 mmol) were stirred in MeOH (5.0 mL) for 18 h. The solvent was removed under reduced pressure and the residue flushed through a pad of basic alumina with 10% MeOH in  $\text{CH}_2\text{Cl}_2$ . Purification by flash column chromatography (92:8  $\text{CH}_2\text{Cl}_2/\text{MeOH}$ ) gave **382** as a hygroscopic yellow solid (479 mg, 97%); IR (neat):  $\nu = 3007, 2830, 1570$  (br.), 1471, 1407 (br.), 1109, 1055  $\text{cm}^{-1}$ ;  $^1\text{H}$  NMR (400 MHz,  $\text{CDCl}_3$ ):  $\delta = 9.02$  (app. dt,  $J = 6.9, 1.0$  Hz, 2H), 8.22 (d,  $J = 5.0$  Hz, 1H), 7.83 (tt,  $J = 7.7, 1.2$  Hz, 1H), 7.67 (app. tt,  $J = 7.2, 1.6$  Hz, 2H), 6.64 (d,  $J = 5.0$  Hz, 1H), 5.01 (s, 1H), 3.39 (s, 6H) ppm;  $^{13}\text{C}$  NMR (101 MHz,  $\text{CDCl}_3$ ):  $\delta = 166.6$  (C), 166.1 (C), 158.1 (CH), 142.9 (2CH), 135.6 (CH), 126.5 (2CH), 106.5 (CH), 104.1 (CH), 54.25 (2CH<sub>3</sub>) ppm; HRMS (ES–TOF): calcd for  $\text{C}_{12}\text{H}_{15}\text{N}_4\text{O}_2$ : 247.1190, found 247.1197  $[\text{M}+\text{H}]^+$ .

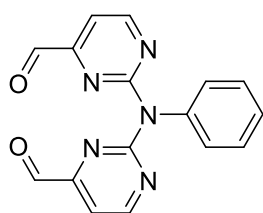
**4-(Dimethoxymethyl)-*N*-(4-(dimethoxymethyl)pyrimidin-2-yl)-*N*-phenylpyrimidin-2-amine 383**



Aniline (370  $\mu\text{L}$ , 4.06 mmol) was dissolved in THF (8.0 mL) in a flame dried Schlenk tube and the mixture cooled to  $-78^\circ\text{C}$  under argon. A solution of *n*-BuLi (2.5 M in hexanes, 1.90 mL, 4.80 mmol) was added dropwise over 2 min and stirred for 1.5 h. A solution of **381** (1.06 g, 4.60 mmol) in THF (4.6 mL) was added over 5 min and stirred at  $-78^\circ\text{C}$  for 10

min before the ice bath was removed. After stirring for 2 h at r.t., satd  $\text{NH}_4\text{Cl}_{(\text{aq})}$  (10 mL) was added and the aqueous layer extracted with EtOAc (3×10 mL). The combined organics were washed with brine (15 mL), dried over  $\text{Na}_2\text{SO}_4$ , filtered and concentrated under reduced pressure. Purification by flash column chromatography (85:15 hexane/EtOAc) gave **383** as yellow solid (531 mg, 58%); mp: 82–85 °C; IR (neat):  $\nu = 2958, 2867, 2358, 1632, 1602, 1514, 1454, 1347, 757, 733 \text{ cm}^{-1}$ ;  $^1\text{H}$  NMR (400 MHz,  $\text{CDCl}_3$ ):  $\delta = 8.58$  (d,  $J = 5.0$  Hz, 2H), 7.38 (app. tt,  $J = 7.7, 2.1$  Hz, 2H), 7.29 – 7.23 (m, 3H), 7.19 (d,  $J = 5.0$  Hz, 2H), 5.08 (s, 2H), 3.38 (s, 12H) ppm;  $^{13}\text{C}$  NMR (101 MHz,  $\text{CDCl}_3$ ):  $\delta = 166.8$  (2C), 162.5 (2C), 159.0 (2CH), 143.3 (C), 129.4 (2CH), 127.6 (2CH), 126.5 (CH), 113.1 (2CH), 103.2 (2CH), 54.2 (4CH<sub>3</sub>) ppm; HRMS (ES–TOF):  $m/z$ : calcd for  $\text{C}_{20}\text{H}_{24}\text{N}_5\text{O}_4$  398.1823, found 398.1824  $[\text{M}+\text{H}]^+$ .

**2,2'–(phenylazanediy)bis(pyrimidine–4–carbaldehyde) 384**

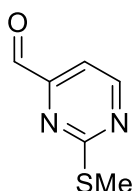


**383** (491 mg, 1.24 mmol) and 3 M HCl (2.0 mL, 6.00 mmol) were heated to 45 °C for 18 h. After allowing to cool to r.t., EtOAc (5.0 mL) was added, followed by  $\text{Na}_2\text{CO}_3$  (735 mg, 7.00 mmol) in  $\text{H}_2\text{O}$  (10 mL). The layers were separated and the aqueous layer extracted with EtOAc (3×10 mL). The combined organic layers were washed with brine (15 mL), dried over  $\text{Na}_2\text{SO}_4$ , filtered and concentrated under reduced pressure. Purification by flash column chromatography (1:9 hexane/EtOAc) gave **384** as a yellow solid (277 mg, 76%); mp: 139–141 °C; IR (neat):  $\nu = 2848, 1716, 1558, 1426, 1368, 1330, 699 \text{ cm}^{-1}$ ;  $^1\text{H}$  NMR (400 MHz,  $\text{CDCl}_3$ ):  $\delta = 9.74$  (d,  $J = 0.9$  Hz, 2H), 8.75 (dd,  $J = 4.8, 0.9$  Hz, 2H), 7.43 (d,  $J = 4.8$  Hz, 2H), 7.41 – 7.36 (m, 2H), 7.34 – 7.28 (tt,  $J = 7.4, 1.2$  Hz, 1H), 7.26 – 7.22 (m, 2H) ppm;  $^{13}\text{C}$  NMR (101 MHz,  $\text{CDCl}_3$ ):  $\delta = 192.8$  (2CH), 163.5 (2C), 160.6 (2CH), 159.3 (2C), 142.4 (C), 129.8 (2CH), 128.0 (2CH), 127.5

(CH), 111.8 (2CH) ppm; HRMS (ES–TOF):  $m/z$ : calcd for  $C_{16}H_{12}N_5O_2$ : 306.0986, found 306.0980  $[M+H]^+$ .

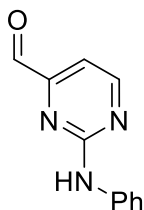
### Products derived from the synthesis of imidazolium salts (Chapter 5.3.3)

#### 2–(Methylthio)pyrimidine–4–carbaldehyde 369



Acetal **368** (2.05 g, 10.3 mmol) was dissolved in 3 M  $HCl_{(aq)}$  (7.5 mL, 22.5 mmol) and stirred at 45 °C for 16 h. After allowing to cool to r.t., the mixture was diluted with  $H_2O$  (15 mL) and  $Na_2CO_3$  (2.36 g, 22.4 mmol) was added in four portions. The organics were extracted with EtOAc (3×30 mL) and the combined organics washed with brine (40 mL), dried over  $Na_2SO_4$ , filtered and concentrated under reduced pressure. Purification by flash column chromatography (85:15:1 hexane/EtOAc/ $NEt_3$ ) gave **369** as a yellow solid (1.33 g, 86%); mp: 68–70 °C (lit. 68 °C); IR (neat):  $\nu$  = 3119, 3063, 2931, 2849, 1707, 1546, 1425, 1322, 1256, 1180, 853  $cm^{-1}$ ;  $^1H$  NMR (400 MHz,  $CDCl_3$ ):  $\delta$  = 9.95 (d,  $J$  = 0.7 Hz, 1H), 8.77 (dd,  $J$  = 4.9, 0.7 Hz, 1H), 7.44 (d,  $J$  = 4.9 Hz, 1H), 2.64 (s, 3H) ppm;  $^{13}C$  NMR (101 MHz,  $CDCl_3$ ):  $\delta$  = 192.8 (CH), 174.7 (C), 159.3 (CH), 157.9 (C), 111.7 (CH), 14.4 (CH<sub>3</sub>) ppm. Spectroscopic data matched that reported in the literature.<sup>267</sup>

#### 2–(Phenylamino)pyrimidine–4–carbaldehyde 373a

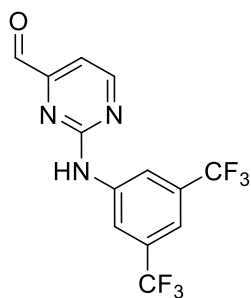


Acetal **372a** (1.23 g, 5.02 mmol) was dissolved in 3 M  $HCl_{(aq)}$  (5.0 mL, 15.0 mmol) and stirred at 50 °C for 16 h. After allowing to cool to r.t., the mixture was diluted with  $H_2O$  (15 mL) and  $Na_2CO_3$  (1.58 g, 15.0 mmol) was added in four portions. The organics were extracted with EtOAc (3×30 mL) and the combined organics washed with brine (40 mL), dried over  $Na_2SO_4$ , filtered and concentrated under reduced pressure. Purification by flash column chromatography (80:20:1 hexane/EtOAc/ $NEt_3$ ) gave **373a** as a yellow solid (906 mg, 91%); mp: 128–130 °C; IR (neat):  $\nu$  = 3250, 2924, 1716, 1606,



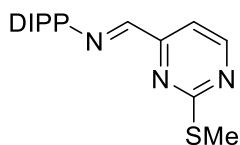
1572, 1539, 1443, 1410  $\text{cm}^{-1}$ ;  $^1\text{H}$  NMR (300 MHz,  $\text{CDCl}_3$ ):  $\delta$  = 9.92 (s, 1H), 8.66 (d,  $J$  = 4.8 Hz, 1H), 7.68 (dd,  $J$  = 9.7, 1.9 Hz, 2H), 7.47 (br. s, 1H, NH), 7.38 (app. tt,  $J$  = 8.0, 1.9 Hz, 2H), 7.22 (d,  $J$  = 4.8 Hz, 1H), 7.11 (tt,  $J$  = 7.4, 1.0 Hz, 1H) ppm; MS (ES–TOF):  $m/z$ : 100% 232.1  $[\text{MH}+\text{MeOH}]^+$ , 45% 200.1  $[\text{M}+\text{H}]^+$ . Spectroscopic data matched that reported in the literature.<sup>268</sup>

**2–((3,5–Bis(trifluoromethyl)phenyl)amino)pyrimidine–4–carbaldehyde **373b****



Acetal **372b** (3.81 g, 10.0 mmol) and 2 M HCl (20 mL, 40 mmol) were dissolved in THF (50 mL) and heated to 65 °C for 44 h. After allowing to cool to r.t., satd  $\text{Na}_2\text{CO}_{3(\text{aq})}$  (60 mL) was added and the organics extracted with EtOAc (3×50 mL). The combined organics were washed with  $\text{H}_2\text{O}$  (60 mL), brine (60 mL), dried over  $\text{Na}_2\text{SO}_4$ , filtered and concentrated under reduced pressure. Purification by flash column chromatography (8:2→7:3 hexane/EtOAc) gave aldehyde **373b** as a pale yellow solid (3.21 g, 96%); mp: 133–135 °C; IR (neat):  $\nu$  = 3351, 1716, 1588, 1574, 1549, 1437, 1381, 1275, 1123, 1113  $\text{cm}^{-1}$ ;  $^1\text{H}$  NMR (400 MHz,  $\text{CDCl}_3$ ):  $\delta$  = 9.94 (s, 1H), 8.76 (d,  $J$  = 4.8 Hz, 1H), 8.24 (br. s, 2H), 7.70 (br. s, NH), 7.57 (br. s, 1H), 7.37 (d,  $J$  = 4.8 Hz, 1H) ppm;  $^{13}\text{C}$  NMR (101 MHz,  $\text{CDCl}_3$ ):  $\delta$  = 192.4 (CH), 160.7 (CH), 160.2 (C), 158.9 (C), 140.5 (C), 132.5 (q,  $J$  = 33.4 Hz, 2C), 123.4 (q,  $J$  = 272.8 Hz, 2 $\text{CF}_3$ ), 118.8 (q,  $J$  = 3.8 Hz, 2CH), 116.2 (hept,  $J$  = 3.8 Hz, CH) 109.8 (CH) ppm;  $^{19}\text{F}$  NMR (377 MHz,  $\text{CDCl}_3$ ):  $\delta$  = –63.05 ppm; HRMS (ES–TOF):  $m/z$ : calcd for  $\text{C}_{13}\text{H}_8\text{N}_3\text{OF}_6$ : 336.0566, found 336.0574  $[\text{M}+\text{H}]^+$ .

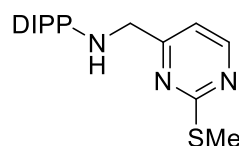
**(E)–N–(2,6–Diisopropylphenyl)–1–(2–(methylthio)pyrimidin–4–yl)methanimine **370****



Adapted from a literature procedure.<sup>270</sup> Aldehyde **369** (308 mg, 2.00 mmol) and 2,6–diisopropylaniline (0.38 mL, 2.01 mmol) were refluxed in

CH<sub>2</sub>Cl<sub>2</sub> (10 mL) for 16 h. After allowing to cool to r.t., the reaction mixture was concentrated under reduced pressure and purified by flash column chromatography (95:5 hexane/EtOAc) to give imine **370** as a yellow solid (600 mg, 96%); mp: 126–128 °C; IR (neat):  $\nu$  = 2964, 2928, 2870, 1639, 1559, 1545, 1426, 1345, 1315, 1219 cm<sup>-1</sup>; <sup>1</sup>H NMR (300 MHz, CDCl<sub>3</sub>):  $\delta$  = 8.69 (dd,  $J$  = 5.0, 0.5 Hz, 1H), 8.16 (s, 1H), 7.82 (d,  $J$  = 5.0 Hz, 1H), 7.20 – 7.13 (m, 3H), 2.88 (hept,  $J$  = 6.8 Hz, 2H), 2.62 (s, 3H), 1.17 (d,  $J$  = 6.9 Hz, 12H) ppm; <sup>13</sup>C NMR (126 MHz, CDCl<sub>3</sub>):  $\delta$  = 173.5 (C), 162.0 (2C), 161.0 (C), 158.2 (CH), 147.9 (C), 137.0 (CH), 125.2 (CH), 123.3 (2CH), 112.2 (CH), 28.1 (2CH), 23.5 (4CH<sub>3</sub>), 14.3 (CH<sub>3</sub>) ppm; HRMS (ES–TOF):  $m/z$ : calcd for C<sub>18</sub>H<sub>24</sub>N<sub>3</sub>S: 314.1685, found 314.1686 [M+H]<sup>+</sup>.

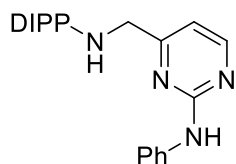
**2,6-Diisopropyl-N-((2-(methylthio)pyrimidin-4-yl)methyl)aniline 406a**



Aldehyde **369** (624 mg, 4.05 mmol), 2,6-diisopropylaniline (750  $\mu$ L, 3.98 mmol), AcOH (80  $\mu$ L, 1.40 mmol) and dry 1,2-DCE (16 mL) were combined in a flame dried Schlenk tube containing 3 Å molecular sieves and stirred for 15 h at 40 °C under argon. After allowing to cool to r.t., NaBH(OAc)<sub>3</sub> (1.02 g, 4.81 mmol) was added in one portion before stirring at 40 °C for 48 h. After cooling to r.t., 1 M NaOH<sub>(aq)</sub> (20 mL) was added and the aqueous layer extracted with Et<sub>2</sub>O (3×30 mL). The combined organic layers were dried over Na<sub>2</sub>SO<sub>4</sub>, filtered, concentrated under reduced pressure and purified by flash column chromatography (90:10:1 hexane/EtOAc/NEt<sub>3</sub>) to give amine **406a** as a yellow oil that solidified upon standing (1.00 g, 79%); mp: 72–74 °C; IR (neat):  $\nu$  = 2960, 2928, 2866, 2375, 2362, 1563, 1545, 1437, 1414, 1348, 1317, 1210 cm<sup>-1</sup>; <sup>1</sup>H NMR (400 MHz, CDCl<sub>3</sub>):  $\delta$  = 8.47 (d,  $J$  = 5.0 Hz, 1H), 7.15 – 7.07 (m, 3H), 7.02 (d,  $J$  = 5.0 Hz, 1H), 4.11 (s, 2H), 3.32 (hept,  $J$  = 6.8 Hz, 2H), 2.61 (s, 3H), 1.25 (d,  $J$  = 6.9 Hz, 12H) ppm; <sup>13</sup>C NMR (101 MHz, CDCl<sub>3</sub>):  $\delta$  = 172.8 (C), 167.8 (C), 157.4 (CH), 142.8 (C), 127.4 (C), 124.4 (CH), 123.8 (2CH), 114.3 (CH),

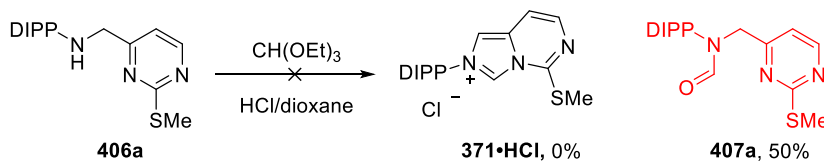
55.8 (CH<sub>2</sub>), 28.0 (2CH), 24.4 (4CH<sub>3</sub>), 14.2 (SCH<sub>3</sub>) ppm; HRMS (ES–TOF): *m/z*: calcd for C<sub>18</sub>H<sub>26</sub>N<sub>3</sub>S: 316.1842, found 316.1840 [M+H]<sup>+</sup>.

**4-(((2,6-Diisopropylphenyl)amino)methyl)-N-phenylpyrimidin-2-amine 406b**



Aldehyde **373a** (420 mg, 2.06 mmol), 2,6-diisopropylaniline (378 μL, 2.01 mmol), AcOH (40 μL, 0.70 mmol) and dry 1,2-DCE (8.0 mL) were combined in a flame dried Schlenk tube containing 3 Å molecular sieves and stirred for 15 h at 40 °C under argon. After allowing to cool to r.t., NaBH(OAc)<sub>3</sub> (510 mg, 2.41 mmol) was added in one portion before stirring at 40 °C for 48 h. After cooling to r.t., 1 M NaOH<sub>(aq)</sub> (20 mL) was added and the aqueous layer extracted with Et<sub>2</sub>O (3×30 mL). The combined organic layers were dried over Na<sub>2</sub>SO<sub>4</sub>, filtered, concentrated under reduced pressure and purified by flash column chromatography (90:10:1 hexane/EtOAc/NEt<sub>3</sub>) to give **406b** as a yellow solid (539 mg, 75%); mp: 126–128 °C; IR (neat): ν = 3304, 3262, 3194, 3120, 3057, 2966, 2961, 2926, 2378, 1606, 1570, 1543, 1460, 1437, 1383 cm<sup>-1</sup>; <sup>1</sup>H NMR (400 MHz, CDCl<sub>3</sub>): δ = 8.38 (d, *J* = 5.0 Hz, 1H), 7.64 (dd, *J* = 8.6, 1.0 Hz, 2H), 7.38 – 7.32 (m, 2H), 7.25 (br. s, 1H), 7.16 – 7.09 (m, 3H), 7.09 – 7.01 (m, 1H), 6.78 (d, *J* = 5.0 Hz, 1H), 4.07 (s, 2H), 3.33 (hept, *J* = 6.8 Hz, 2H), 1.24 (d, *J* = 6.9 Hz, 12H) ppm; <sup>13</sup>C NMR (101 MHz, CDCl<sub>3</sub>): δ = 168.5 (C), 160.2 (C), 158.3 (CH), 142.9 (C), 142.8 (C), 139.5 (C), 129.1 (2CH), 124.3 (CH), 123.8 (2CH), 122.9 (CH), 119.7 (2CH), 110.5 (CH), 56.0 (CH<sub>2</sub>), 27.9 (2CH), 24.4 (2CH<sub>3</sub>) ppm; HRMS (ES–TOF): *m/z*: calcd For C<sub>23</sub>H<sub>29</sub>N<sub>4</sub>: 361.2387, found 361.2388 [M+H]<sup>+</sup>.

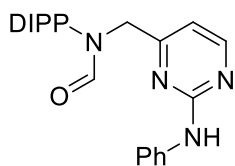
**N-(2,6-Diisopropylphenyl)-N-((2-(methylthio)pyrimidin-4-yl)methyl)formamide 407a**



Amine **406a** (80.1 mg, 0.254 mmol), HCl in 1,4-dioxane (4 M, 250  $\mu$ L, 1.00 mmol) and triethyl orthoformate (1.25 mL) were combined in a flame dried round bottom flask and heated to 130  $^{\circ}$ C for 20 h under argon. After allowing to cool to r.t., most of the triethyl orthoformate was removed under reduced pressure, at which point a pale yellow solid precipitated. The solid was collected by filtration and washed with Et<sub>2</sub>O (2 $\times$ 10 mL) to give formamide **407a** as a yellow solid (42 mg, 50%). Data below.

Formic acid (150  $\mu$ L, 3.98 mmol) and Ac<sub>2</sub>O (132  $\mu$ L, 1.40 mmol) were combined in a flame dried Schlenk tube and stirred for 1.5 h under argon. A solution of amine **406a** (320 mg, 1.02 mmol) in CH<sub>2</sub>Cl<sub>2</sub> (1.5 mL) was added and the reaction mixture stirred for 2 h at r.t. and then for 6 h at 40  $^{\circ}$ C. After allowing to cool to r.t., satd NaHCO<sub>3(aq)</sub> (20 mL) was added and the organics extracted with Et<sub>2</sub>O (3 $\times$ 20 mL). The combined organics were washed with brine (30 mL), dried over Na<sub>2</sub>SO<sub>4</sub>, filtered, concentrated under reduced pressure and purified by flash column chromatography (80:20 hexane/EtOAc) to give formamide **407a** as a yellow solid (256 mg, 75%); mp: 151–152  $^{\circ}$ C; IR (neat):  $\nu$  = 3061, 2962, 2928, 2863, 1669, 1557, 1377, 1344, 1313, 1222 cm<sup>-1</sup>; *restricted rotation around the amide bond results in 2 sets of resonances in a 9:1 ratio*: <sup>1</sup>H NMR (400 MHz, CDCl<sub>3</sub>):  $\delta$  = 8.75<sub>min</sub> and 8.16<sub>maJ</sub> (s, 1H), 8.48<sub>maJ</sub> and 8.41<sub>min</sub> (d,  $J$  = 4.9 Hz, 1H), 7.35<sub>maJ</sub> and 7.31<sub>min</sub> (t,  $J$  = 7.8 Hz, 1H), 7.20 – 7.12 (m, 3H), 6.68<sub>min</sub> (d,  $J$  = 4.9 Hz) – *major peak in multiplet*, 4.74<sub>maJ</sub> and 4.56<sub>min</sub> (s, 2H), 2.83 (hept,  $J$  = 6.8 Hz, 2H), 2.56<sub>min</sub> and 2.42<sub>maJ</sub> (s, 3H), 1.11 (d,  $J$  = 6.8 Hz, 6H), 1.02 (d,  $J$  = 6.8 Hz, 6H) ppm; *only the major rotamer is reported*: <sup>13</sup>C NMR (101 MHz, CDCl<sub>3</sub>):  $\delta$  = 172.8 (C), 164.5 (C), 163.9 (CH), 157.7 (CH), 147.8 (C), 135.3 (C), 129.8 (CH), 124.6 (2CH), 116.4 (CH), 52.8 (CH<sub>2</sub>), 28.5 (2CH), 25.3 (2CH<sub>3</sub>), 23.6 (2CH<sub>3</sub>), 14.1 (CH<sub>3</sub>) ppm; HRMS (ES–TOF):  $m/z$ : calcd for C<sub>19</sub>H<sub>26</sub>N<sub>3</sub>OS: 344.1791, found 344.1799 [M+H]<sup>+</sup>;

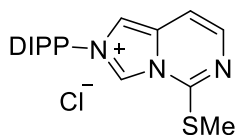
***N*-(2,6-Diisopropylphenyl)-*N*-((2-(phenylamino)pyrimidin-4-yl)methyl)formamide **407b****



Formic acid (76  $\mu$ L, 2.02 mmol) and Ac<sub>2</sub>O (104  $\mu$ L, 1.11 mmol) were combined in a flame dried Schlenk tube and stirred for 1.5 h under argon.

A solution of amine **406b** (360 mg, 1.0 mmol) in CH<sub>2</sub>Cl<sub>2</sub> (5.0 mL) was added and the reaction mixture stirred for 2 h at r.t. then 6 h at 40 °C. After allowing to cool to r.t., satd NaHCO<sub>3(aq)</sub> (20 mL) was added and the organics extracted with Et<sub>2</sub>O (3 $\times$ 20 mL). The combined organics were washed with brine (30 mL), dried over Na<sub>2</sub>SO<sub>4</sub>, filtered, concentrated under reduced pressure and purified by flash column chromatography (80:20 hexane/EtOAc) to give formamide **407b** as a yellow solid (378 mg, 98%); mp: 124–125 °C; IR (neat):  $\nu$  = 3246, 3188, 2969, 2929, 2868, 2361, 1674, 1607, 1572, 1535, 1440, 1417, 1358, 1252 cm<sup>-1</sup>; *restricted rotation around the amide bond results in 2 sets of resonances in a 9:1 ratio*: <sup>1</sup>H NMR (300 MHz, CDCl<sub>3</sub>):  $\delta$  = 8.77<sub>min</sub> and 8.18<sub>maJ</sub> (s, 1H), 8.37<sub>maJ</sub> and 8.32<sub>min</sub> (d,  $J$  = 4.9 Hz, 1H), 7.45 – 7.30 (m, 3H), 7.29 – 7.22 *overlap with CDCl<sub>3</sub>* (m, 1H), 7.21 – 7.14 (m, 2H), 7.06 – 6.96 (m, 3H), 6.87<sub>maJ</sub> and 6.48<sub>min</sub> (d,  $J$  = 4.9 Hz, 1H), 4.73<sub>maJ</sub> and 4.51<sub>min</sub> (s, 2H), 2.89 (hept,  $J$  = 6.8 Hz, 2H), 1.10 *minor peak overlaps* (d,  $J$  = 6.8 Hz, 6H), 1.01<sub>maJ</sub> and 0.95<sub>min</sub> (d,  $J$  = 6.8 Hz, 6H) ppm; *only the major rotamer is reported*: <sup>13</sup>C NMR (101 MHz, CDCl<sub>3</sub>):  $\delta$  = 164.8 (C), 163.7 (CH), 159.9 (C), 158.6 (CH), 147.8 (C), 139.3 (C), 135.0 (C), 129.7 (CH), 129.0 (2CH), 124.6 (2CH), 122.7 (CH), 119.3 (2CH), 112.6 (CH), 52.4 (CH<sub>2</sub>), 28.5 (2CH), 25.4 (2CH<sub>3</sub>), 23.6 (2CH<sub>3</sub>) ppm; HRMS (ES–TOF):  $m/z$ : calcd for C<sub>24</sub>H<sub>29</sub>N<sub>4</sub>O: 389.2336, found 389.2342 [M+H]<sup>+</sup>.

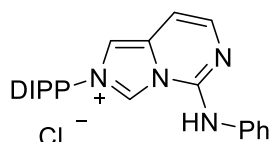
***2*-(2,6-Diisopropylphenyl)-5-(methylthio)imidazo[1,5-*c*]pyrimidin-2-ium chloride **371**•HCl**



95% Paraformaldehyde (38 mg, 1.20 mmol) and dry toluene (3.0 mL) were added to a flame dried Schlenk tube and stirred at 90 °C for 10 min under argon. After allowing to cool to r.t., imine **370** (315 mg, 1.00 mmol) was added followed by

dropwise addition of HCl in 1,4-dioxane (4 M, 380  $\mu$ L, 1.52 mmol) and the reaction mixture stirred at r.t. for 18 h. The solvent was then decanted and the remaining solid dissolved in MeOH (5.0 mL), concentrated under reduced pressure and purified by flash column chromatography (95:5 CH<sub>2</sub>Cl<sub>2</sub>/MeOH) to give **371•HCl** as a white solid (105 mg, 29%); mp: 197–199 °C; IR (neat):  $\nu$  = 3352, 3070, 2962, 2930, 2870, 1654, 1556, 1475, 1382, 1215, 1186, 990, 952 cm<sup>-1</sup>; <sup>1</sup>H NMR (400 MHz, CDCl<sub>3</sub>):  $\delta$  = 10.90 (s, 1H), 8.45 (d,  $J$  = 1.2 Hz, 1H), 7.99 (d,  $J$  = 6.5 Hz, 1H), 7.87 (d,  $J$  = 6.5 Hz, 1H), 7.57 (t,  $J$  = 7.9 Hz, 1H), 7.33 (d,  $J$  = 7.9 Hz, 2H), 2.84 (s, 3H), 2.14 (hept,  $J$  = 6.8 Hz, 2H), 1.23 (d,  $J$  = 6.8 Hz, 6H), 1.15 (d,  $J$  = 6.8 Hz, 6H) ppm; <sup>13</sup>C NMR (101 MHz, CDCl<sub>3</sub>):  $\delta$  = 149.3 (C), 145.0 (CH), 138.0 (CH), 132.4 (CH), 130.7 (C), 130.6 (C), 127.0 (C), 124.8 (2CH), 117.9 (CH), 108.4 (CH), 29.0 (2CH), 24.6 (2CH<sub>3</sub>), 24.5 (2CH<sub>3</sub>), 14.7 (CH<sub>3</sub>) ppm; HRMS (ES–TOF):  $m/z$  calculated for C<sub>19</sub>H<sub>24</sub>N<sub>3</sub>S: 326.1685, found 326.1693 [M–Cl]<sup>+</sup>.

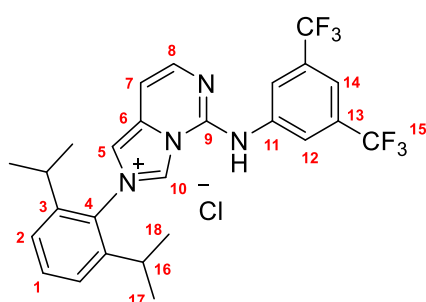
**2–(2,6-Diisopropylphenyl)–5–(phenylamino)imidazo[1,5-c]pyrimidin–2-ium chloride  
354a•HCl**



Formamide **407b** (172 mg, 0.442 mmol), POCl<sub>3</sub> (140  $\mu$ L, 1.50 mmol) and toluene (5.0 mL) were combined in a flame dried Schlenk tube and heated to 80 °C for 12 h under argon. After allowing to cool to r.t. and transferring to a separating funnel, satd NaHCO<sub>3(aq)</sub> (10 mL) was added and the aqueous layer extracted with CH<sub>2</sub>Cl<sub>2</sub> (3×10 mL). The combined organic layers were dried over Na<sub>2</sub>SO<sub>4</sub>, filtered, concentrated under reduced pressure and purified by flash column chromatography (95:5 CH<sub>2</sub>Cl<sub>2</sub>/MeOH) to give **354a•HCl** as a pale brown solid (170 mg, 95%); mp: (dec.) 225 °C; IR (neat):  $\nu$  = 3066, 2966, 2927, 2870, 1642, 1565, 1545, 1447, 1293, 1107 cm<sup>-1</sup>; <sup>1</sup>H NMR (400 MHz, CDCl<sub>3</sub>):  $\delta$  = 11.68 (br. s, 1H), 11.14 (br. s, 1H), 8.05 – 7.99 (m, 2H), 7.76 (d,  $J$  = 6.5 Hz, 1H), 7.60 (t,  $J$  = 7.9 Hz, 1H), 7.41 – 7.36 (m, 5H), 7.18 (tt,  $J$  = 7.4, 1.2 Hz, 1H), 6.97 (dd,  $J$  =

6.5, 0.9 Hz, 1H), 2.22 (hept,  $J = 6.8$  Hz, 2H), 1.31 (d,  $J = 6.8$  Hz, 6H), 1.18 (d,  $J = 6.8$  Hz, 6H) ppm;  $^{13}\text{C}$  NMR (101 MHz,  $\text{CDCl}_3$ ):  $\delta = 145.1$  (C), 140.9 (CH), 137.4 (C), 132.8 (C), 132.5 (CH), 130.6 (C), 129.0 (2CH), 128.4 (C), 125.4 (CH), 124.9 (2CH), 122.6 (2CH), 113.4 (CH), 99.7 (CH), 29.0 (2CH), 24.6 (4CH<sub>3</sub>) ppm; HRMS (ES-TOF):  $m/z$ : calcd for  $\text{C}_{24}\text{H}_{27}\text{N}_4$ : 371.2230, found 371.2235  $[\text{M}-\text{Cl}]^+$ .

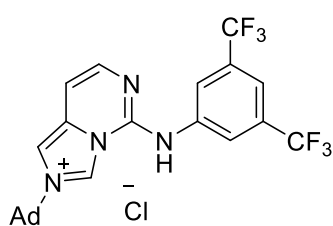
**5-((3,5-bis(trifluoromethyl)phenyl)amino)-2-(2,6-diisopropylphenyl)imidazo[1,5-*c*]pyrimidin-2-ium chloride 354b•HCl**



Aldehyde **373b** (1.68 g, 5.01 mmol) and 2,6-diisopropylaniline (0.94 mL, 4.98 mmol) were dissolved in dry PhMe (25 mL) and heated to reflux for 14 h. After allowing to cool to 80 °C, paraformaldehyde (95%, 226 mg, 7.15 mmol) and HCl in 1,4-dioxane (4 M, 1.88 mL, 7.52 mmol) were added and the mixture stirred vigorously for 2 h. After allowing to cool to r.t., the reaction mixture was diluted with Et<sub>2</sub>O (15 mL) and cooled to 0 °C for 1 h. The precipitate was collected by vacuum filtration and washed with PhMe (20 mL), EtOAc (20 mL) and Et<sub>2</sub>O (50 mL) before being dried under high vacuum to give **354b•HCl** as a white solid containing PhMe. The solid was dissolved in  $\text{CHCl}_3$  and the solvent removed under reduced pressure to give **354b•HCl** as a white solid (2.19 g, 81%); mp: (dec.) 278 °C; IR (neat):  $\nu = 3045, 2932, 2808, 1648, 1591, 1548, 1378, 1276, 1174, 1125\text{ cm}^{-1}$ ;  $^1\text{H}$  NMR (400 MHz,  $\text{CDCl}_3$ ):  $\delta = 12.84$  (br. s, NH), 12.44 (s, 1H<sub>10</sub>), 8.79 (br. s, 2H<sub>12</sub>), 7.79 (d,  $J = 6.5$  Hz, 1H<sub>7/8</sub>), 7.65 (br. s, 1H<sub>14</sub>), 7.61 (t,  $J = 7.9$  Hz, 1H<sub>1</sub>), 7.43 (d,  $J = 1.6$  Hz, 1H<sub>5</sub>), 7.38 (d,  $J = 7.9$  Hz, 2H<sub>2</sub>), 7.08 (d,  $J = 6.5$  Hz, 1H<sub>7/8</sub>), 2.21 (hept,  $J = 6.9$  Hz, 2H<sub>16</sub>), 1.30 (d,  $J = 6.9$  Hz, 6H<sub>17/18</sub>), 1.18 (d,  $J = 6.9$  Hz, 6H<sub>17/18</sub>) ppm;  $^{13}\text{C}$  NMR (101 MHz,  $\text{CDCl}_3$ ):  $\delta = 145.1$  (C<sub>3</sub>), 140.2 (C<sub>7/8</sub>H), 140.1 (C<sub>9</sub>), 139.4 (C<sub>11</sub>), 132.6 (C<sub>1</sub>H), 132.5 (C<sub>6</sub>), 132.0 (q,  $J = 33.4$  Hz, 2C<sub>13</sub>), 130.4 (C<sub>4</sub>) 129.4 (C<sub>10</sub>H), 125.0

(2C<sub>2</sub>H), 122.4 (m, 2C<sub>12</sub>H), 123.4 (q,  $J = 272.8$  Hz, 2C<sub>15</sub>F<sub>3</sub>), 118.2 (m, C<sub>14</sub>H), 113.6 (C<sub>5</sub>H), 101.3 (C<sub>7/8</sub>H), 29.0 (2C<sub>16</sub>H), 24.7 (2C<sub>17/18</sub>H<sub>3</sub>), 24.4 (2C<sub>17/18</sub>H<sub>3</sub>) ppm; <sup>19</sup>F NMR (377 MHz, CDCl<sub>3</sub>):  $\delta = -62.76$  ppm; HRMS (ES–TOF):  $m/z$ : calcd for C<sub>26</sub>H<sub>25</sub>N<sub>4</sub>F<sub>6</sub>: 507.1978, found 507.1980 [M–Cl]<sup>+</sup>. *Note: arbitrary numbering system used in this analysis for full assignment of NMR resonances.*

**2–((3*s*,5*s*,7*s*)–adamantan–1–yl)–5–((3,5–bis(trifluoromethyl)phenyl)amino)imidazo[1,5–*c*]pyrimidin–2–ium chloride **354c•HCl****

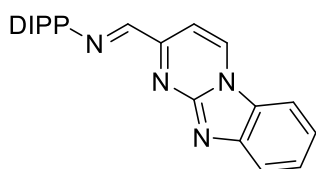


Aldehyde **373b** (335 mg, 1.00 mmol) and adamantylamine (151 mg, 1.00 mmol) were dissolved in dry PhMe (5.0 mL) and heated to reflux for 14 h. After allowing to cool to 80 °C, paraformaldehyde (95%, 45 mg, 1.42 mmol) and HCl in 1,4–dioxane (4 M, 0.38 mL, 1.52 mmol) were added and the mixture stirred vigorously for 2 h. After allowing to cool to r.t., the reaction mixture was diluted with Et<sub>2</sub>O (10 mL) and cooled to 0 °C for 1 h. The precipitate was collected by vacuum filtration and washed with PhMe (10 mL), EtOAc (10 mL) and Et<sub>2</sub>O (20 mL) before being dried under high vacuum to give **354c•HCl** as a white solid containing adamantylamine•HCl. The crude material was purified by flash column chromatography (95:5→9:1 CH<sub>2</sub>Cl<sub>2</sub>/MeOH) to give **354c•HCl** as a yellow solid (346 mg, 67%); mp: (dec.) 220 °C; IR (neat):  $\nu = 3083, 2909, 2852, 1652, 1634, 1595, 1549, 1377, 1275, 1116, 935$  cm<sup>–1</sup>; <sup>1</sup>H NMR (400 MHz, CDCl<sub>3</sub>):  $\delta = 12.30$  (br. s, NH), 11.84, (br. s, 1H), 8.69 (br. s, 2H), 7.60 (d,  $J = 6.4$  Hz, 1H), 7.60 – 7.56 (m, 2H), 6.84 (d, 6.4 Hz, 1H), 2.42 – 2.32 (m, 9H), 1.88 – 1.78 (m, 6H) ppm; <sup>13</sup>C NMR (101 MHz, CDCl<sub>3</sub>):  $\delta = 141.1$  (C), 140.5 (C), 139.6 (CH), 132.4 (C), 131.9 (q,  $J = 33.3$  Hz, 2C), 125.7 (br., NCHN), 123.5 (q,  $J = 272.8$  Hz, 2CF<sub>3</sub>), 122.2 (m, 2CH), 117.3 (m, CH), 107.4 (CH), 100.3 (CH), 62.8 (C), 43.4



(3CH<sub>2</sub>), 35.4 (3CH<sub>2</sub>), 29.6 (3CH) ppm; <sup>19</sup>F NMR (377 MHz, CDCl<sub>3</sub>): δ = -62.8 ppm; HRMS (ES-TOF): *m/z*: calcd for C<sub>24</sub>H<sub>23</sub>N<sub>4</sub>F<sub>6</sub>: 481.1821, found 481.1824 [M-Cl]<sup>+</sup>.

**(*E*)-1-(benzo[4,5]imidazo[1,2-*a*]pyrimidin-2-yl)-*N*-(2,6-diisopropylphenyl)methanimine**  
**409**

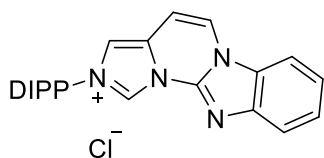


Acetal **377** (1.11 g, 4.53 mmol) and 1 M HCl<sub>(aq)</sub> (13.5 mL, 13.5 mmol) were stirred at 50 °C for 18 h. After cooling to r.t., H<sub>2</sub>O (25 mL) was added and the aqueous layer extracted CH<sub>2</sub>Cl<sub>2</sub> (3×40 mL).

The combined organic phases were washed with brine (25 mL), dried over Na<sub>2</sub>SO<sub>4</sub>, filtered and concentrated under reduced pressure. The crude aldehyde and 2,6-diisopropylaniline (0.85 mL, 4.51 mmol) were refluxed in toluene (35 mL) for 18 h with Dean-Stark apparatus. After allowing to cool to r.t., the solvent was removed under reduced pressure and the crude material purified by flash column chromatography (7:3 hexane/EtOAc) to give imine **409** as a spongy bright yellow solid (968 mg, 65%); mp: (dec.) at 280 °C; IR (neat): ν = 3058, 2690, 2927, 2888, 2868, 2360, 2337, 1632, 1602, 1514, 1454 cm<sup>-1</sup>; <sup>1</sup>H NMR (400 MHz, CDCl<sub>3</sub>): δ = 8.85 (dd, *J* = 7.1, 0.7 Hz, 1H), 8.38 (d, *J* = 0.7 Hz, 1H), 8.08 (app. dt, *J* = 8.3, 0.9 Hz, 1H), 7.96 (app. dt, *J* = 8.2, 0.9 Hz, 1H), 7.92 (d, *J* = 7.1 Hz, 1H), 7.63 (ddd, *J* = 8.4, 7.2, 1.2 Hz, 1H), 7.50 (ddd, *J* = 8.3, 7.2, 1.1 Hz, 1H), 7.24 – 7.15 (m, 3H), 2.96 (hept, *J* = 6.9 Hz, 2H), 1.20 (d, *J* = 6.9 Hz, 12H) ppm; <sup>13</sup>C NMR (101 MHz, CDCl<sub>3</sub>): δ = 162.2 (CH), 158.8 (C), 147.9 (C), 145.5 (C), 137.2 (2C), 133.3 (CH), 127.3 (C), 126.9 (CH), 125.4 (CH), 123.4 (2CH), 123.1 (CH), 121.3 (CH), 110.9 (CH), 103.5 (CH), 28.3 (2CH), 23.6 (4CH<sub>3</sub>) ppm; *one quaternary carbon resonance not observed in <sup>13</sup>C NMR spectra*; HRMS (ES-TOF): *m/z*: calcd for C<sub>23</sub>H<sub>25</sub>N<sub>4</sub>: 357.2074, found 357.2080 [M+H]<sup>+</sup>.

Note: Purification of the aldehyde by flash column chromatography (98:2 EtOAc/MeOH) gave an orange solid that was susceptible to degradation. Therefore, the crude aldehyde was used in the imine formation and not isolated.

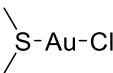
**2-(2,6-Diisopropylphenyl)benzo[4,5]imidazo[1,2-a]imidazo[1,5-c]pyrimidin-2-ium chloride 355•HCl**



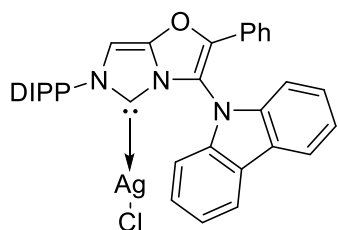
Imine **409** (178 mg, 0.50 mmol), 95% paraformaldehyde (22.5 mg, 0.71 mmol) and toluene (5.0 mL) were combined in a flame dried Schlenk tube and heated to 80 °C under argon. HCl in 1,4-dioxane (4 M, 380  $\mu$ L, 1.52 mmol) added dropwise over 1 min and reaction stirred for 18 h. After allowing to cool to r.t., satd  $\text{NaHCO}_{3(\text{aq})}$  was added and the aqueous layer extracted with  $\text{CH}_2\text{Cl}_2$  (3 $\times$ 25 mL). The combined organics were washed with brine (25 mL), dried over  $\text{Na}_2\text{SO}_4$ , filtered and concentrated under reduced pressure. The crude material was purified by flash column chromatography, first by eluting with EtOAc/MeOH to remove the aldehyde generated in the reaction and then DCM/MeOH (200 mL, 9:1) to give **355•HCl** as a brown solid (104 mg, 51%); mp: (dec.) 275 °C; IR (neat):  $\nu$  = 3443, 3306, 2966, 2932, 2874, 1648, 1625, 1582, 1515, 1456, 1367, 1341  $\text{cm}^{-1}$ ;  $^1\text{H}$  NMR (300 MHz,  $\text{CDCl}_3$ ):  $\delta$  = 9.38 (s, 1H), 9.28 (s, 1H), 8.75 (d,  $J$  = 4.4 Hz, 1H), 8.43 (d,  $J$  = 5.0 Hz, 1H), 8.22 – 7.88 (m, 1H), 7.90 – 7.84 (m, 1H), 7.68 – 7.55 (m, 3H), 7.40 (d,  $J$  = 7.9 Hz, 2H), 2.34 (hept,  $J$  = 6.4 Hz, 2H), 1.27 (d,  $J$  = 6.4 Hz, 6H), 1.21 (d,  $J$  = 6.4 Hz, 6H) ppm;  $^{13}\text{C}$  NMR (101 MHz,  $\text{CDCl}_3$ ):  $\delta$  = 148.1 (C), 145.2 (2C), 140.3 (C), 135.9 (C), 132.8 (CH), 130.1 (C), 129.7 (C), 126.5 (CH), 125.6 (CH), 125.1 (2CH), 124.6 (CH), 122.7 (CH), 120.3 (CH), 112.0 (CH), 102.0 (C), 29.1 (2CH), 24.8 (2 $\text{CH}_3$ ), 24.4 (2 $\text{CH}_3$ ) ppm; *one quaternary carbon resonance not observed in  $^{13}\text{C}$  NMR spectra*; HRMS (ES–TOF):  $m/z$ : calcd for  $\text{C}_{24}\text{H}_{25}\text{N}_4$ : 369.2074, found 369.2080  $[\text{M} - \text{Cl}]^+$ . Crystals suitable for single crystal X-ray diffraction were grown by slow evaporation from a solution **355•HCl** in  $\text{CH}_2\text{Cl}_2$ .

## Formation of transition metal complexes (Chapter 6)

### *Chloro(dimethylsulfide)gold(I) - Au(SMe<sub>2</sub>)Cl*

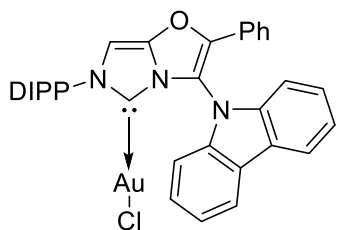
 KAuCl<sub>4</sub> (377 mg, 1.00 mmol) was dissolved in dry MeOH (10 mL) before dropwise addition of dimethyl sulfide (213  $\mu$ L, 2.90 mmol) over 2 min. The reaction was then stirred at r.t. for 30 min in complete darkness, before the solid was collected by filtration and washed with dry MeOH (1 mL), Et<sub>2</sub>O (2 mL) and pentane (4 mL), giving **Au(SMe<sub>2</sub>)Cl** as a white solid (286 mg, 97%); IR (neat):  $\nu$  = 1436, 1421, 1411, 1033, 994, 954 cm<sup>-1</sup>; <sup>1</sup>H NMR (300 MHz, CDCl<sub>3</sub>):  $\delta$  = 2.80 (s, 6H) ppm. Spectroscopic data matched that reported in the literature.<sup>271</sup>

### **353aAgCl**



Imidazolium salt **353a•HCl** (109 mg, 0.20 mmol), Ag<sub>2</sub>O (23.2 mg, 0.10 mmol) and dry CH<sub>2</sub>Cl<sub>2</sub> (5.0 mL) were combined in a flame dried Schlenk tube containing 4 Å molecular sieves. After stirring in darkness overnight, the reaction mixture was filtered through a 2 cm plug of celite (CH<sub>2</sub>Cl<sub>2</sub>) and concentrated under reduced pressure. The crude material was triturated with Et<sub>2</sub>O and hexane to give **353aAgCl** as a white solid (114 mg, 87%) which was characterised by <sup>1</sup>H NMR and used directly in the transmetalation step; <sup>1</sup>H NMR (400 MHz, CDCl<sub>3</sub>):  $\delta$  = 8.26 – 8.22 (m, 2H), 7.56 (app. dt,  $J$  = 3.6, 2.5 Hz, 2H), 7.47 – 7.37 (m, 6H), 7.37 – 7.32 (m, 2H), 7.24 – 7.19 (m, 4H), 6.91 (dd,  $J$  = 5.1, 1.7 Hz, 1H), 2.38 (hept,  $J$  = 6.8 Hz, 2H), 1.18 (d,  $J$  = 6.8 Hz, 6H), 1.15 (d,  $J$  = 6.8 Hz, 6H) ppm; Crystals suitable for single crystal X-ray diffraction were grown by diffusion of hexane into a solution of silver complex **353aAgCl** in CDCl<sub>3</sub>.

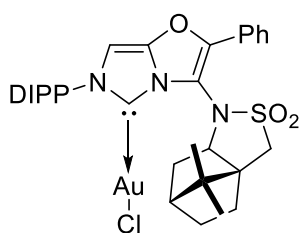
### 353aAuCl



Silver complex **353aAgCl** (65.0 mg, 99.4  $\mu\text{mol}$ ), Au(SMe<sub>2</sub>)Cl (29.5 mg, 100  $\mu\text{mol}$ ) and CH<sub>2</sub>Cl<sub>2</sub> (2.0 mL) were combined in a flame dried Schlenk tube under argon. After stirring in darkness for 3 h, the reaction mixture was filtered through a 2 cm plug of

celite (CH<sub>2</sub>Cl<sub>2</sub>) and concentrated under reduced pressure to give **353aAuCl** as a colourless solid (74.0 mg, 99%); mp: (colourless to opaque) 190 °C; IR (neat):  $\nu$  = 2964, 2926, 1681, 1625, 1450, 1422, 1388, 1059 cm<sup>-1</sup>; <sup>1</sup>H NMR (400 MHz, CDCl<sub>3</sub>):  $\delta$  = 8.25 – 8.19 (m, 2H), 7.58 – 7.53 (m, 2H), 7.46 – 7.37 (m, 6H), 7.36 – 7.30 (m, 2H), 7.25 – 7.21 (m, 2H), 7.20 (d,  $J$  = 7.8 Hz, 2H), 6.87 (s, 1H), 2.39 (hept,  $J$  = 6.8 Hz, 2H), 1.20 (d,  $J$  = 6.8 Hz, 6H), 1.17 (d,  $J$  = 6.8 Hz, 6H) ppm; <sup>13</sup>C NMR (101 MHz, CDCl<sub>3</sub>):  $\delta$  = 156.8 (C), 148.6 (C), 145.7 (2C), 144.7 (C), 139.5 (2C), 135.3 (C), 131.1 (CH), 130.9 (CH), 129.4 (2CH), 126.7 (2CH), 125.64 (2CH), 125.60 (2C), 125.3 (C), 124.3 (2CH), 122.7 (2CH), 121.7 (2CH), 115.4 (C), 110.7 (2CH), 97.2 (CH), 28.6 (2CH), 24.6 (2CH<sub>3</sub>), 24.5 (2CH<sub>3</sub>) ppm; Elemental analysis calcd for C<sub>35</sub>H<sub>31</sub>AuClN<sub>3</sub>O C: 56.65, H: 4.21, N: 5.66. Found C: 56.63, H: 4.37, N: 5.51. Crystals suitable for single crystal X-ray diffraction were grown by diffusion of hexane into a solution of **353aAuCl** in CDCl<sub>3</sub>.

### 353bAuCl

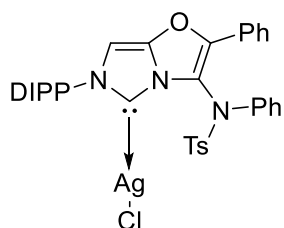


Imidazolium salt **353b•HCl** (178 mg, 0.30 mmol), Ag<sub>2</sub>O (34.8 mg, 0.15 mmol) and dry CH<sub>2</sub>Cl<sub>2</sub> (6.0 mL) were added to a screw thread capped vial containing 4 Å molecular sieves and stirred for 4 h in complete darkness. DMSAuCl (94.2 mg, 0.32 mol) was then added

and the reaction stirred at r.t. for a further 4 h. The crude was passed through 1 cm pads of celite and silica (CH<sub>2</sub>Cl<sub>2</sub>) before the solvent was removed under reduced pressure. Purification by

flash column chromatography ( $\text{CH}_2\text{Cl}_2$ ) provided **353bAuCl** as a white crystalline solid (200 mg, 84%); mp: (colourless to opaque) 185 °C; IR (neat):  $\nu = 3102, 2967, 1673, 1618, 1470, 1387, 1364, 1355, 1168 \text{ cm}^{-1}$ ;  $^1\text{H}$  NMR (400 MHz,  $\text{CDCl}_3$ ):  $\delta = 8.17 - 8.12$  (m, 2H), 7.54 – 7.44 (m, 4H), 7.27 (d,  $J = 7.8$  Hz, 2H), 6.79 (s, 1H), 5.34 (dd,  $J = 7.9, 4.3$  Hz, 1H), 4.28 (d,  $J_{AB} = 13.7$  Hz, 1H), 3.55 (d,  $J_{AB} = 13.7$  Hz, 1H), 2.56 (hept,  $J = 6.8$  Hz, 1H), 2.35 (hept,  $J = 6.8$  Hz, 1H), 2.17 (ddd,  $J = 12.9, 9.7, 3.3$  Hz, 1H), 2.05 – 1.95 (m, 1H), 1.86 – 1.72 (m, 3H), 1.61 (dd,  $J = 12.6, 7.9$  Hz, 1H), 1.35 (d,  $J = 6.8$  Hz, 3H), 1.34 (d,  $J = 6.8$  Hz, 3H), 1.32 (s, 3H), 1.31 – 1.24 (m, 1H), 1.21 (d,  $J = 6.8$  Hz, 3H), 1.11 (d,  $J = 6.8$  Hz, 3H), 1.02 (s, 3H) ppm;  $^{13}\text{C}$  NMR (101 MHz,  $\text{CDCl}_3$ ):  $\delta = 158.2$  (C), 153.3 (C), 146.6 (C), 145.5 (C), 145.3 (C), 135.3 (C), 131.6 (CH), 131.0 (CH), 129.1 (2CH), 127.5 (2CH), 125.0 (C), 124.6 (CH), 124.2 (CH), 114.8 (C), 96.7 (CH), 67.9 (CH), 51.6 ( $\text{CH}_2$ ), 51.4 (C), 47.8 (C), 46.1 (CH), 36.9 ( $\text{CH}_2$ ), 32.4 ( $\text{CH}_2$ ), 28.6 (CH), 28.5 (CH), 26.6 ( $\text{CH}_2$ ), 24.70 ( $\text{CH}_3$ ), 24.66 ( $\text{CH}_3$ ), 24.63 ( $\text{CH}_3$ ), 24.56 ( $\text{CH}_3$ ), 21.9 ( $\text{CH}_3$ ), 20.3 ( $\text{CH}_3$ ) ppm; Elemental analysis calcd for  $\text{C}_{33}\text{H}_{39}\text{AuClN}_3\text{O}_3\text{S}$  C: 50.16, H: 4.98, N: 5.32. Found C: 50.13, H: 5.17, N: 5.40. Crystals suitable for single crystal X-ray diffraction were grown by diffusion of hexane into a solution of **353bAuCl** in  $\text{CH}_2\text{Cl}_2$ .

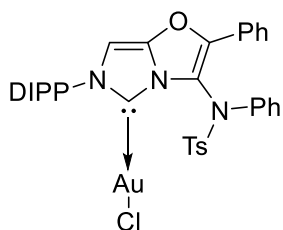
### **353cAgCl**



Imidazolium salt **353c•HCl** (62 mg, 99.2  $\mu\text{mol}$ ),  $\text{Ag}_2\text{O}$  (11.6 mg, 50.1  $\mu\text{mol}$ ) and dry  $\text{CH}_2\text{Cl}_2$  (1.0 mL) were combined in a flame dried Schlenk tube containing 4 Å molecular sieves. After stirring in darkness overnight, the reaction mixture was filtered through a 2 cm plug of celite ( $\text{CH}_2\text{Cl}_2$ ). Concentration under reduced pressure afforded **353cAgCl** as a white solid (53.4 mg, 73%) which was characterised by  $^1\text{H}$  NMR and used directly in the transmetalation step;  $^1\text{H}$  NMR (300 MHz,  $\text{CDCl}_3$ ):  $\delta = 8.20 - 8.15$  (m, 2H), 7.79 (d,  $J = 8.3$  Hz, 2H), 7.62 – 7.56 (m, 5H), 7.45

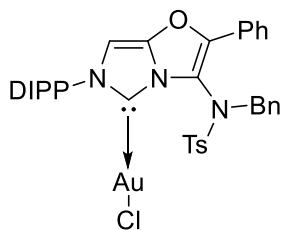
(t,  $J = 7.8$  Hz, 1H), 7.39 – 7.25 (m, 6H), 7.19 (app. dd,  $J = 7.8, 1.4$  Hz, 1H), 6.79 (d,  $J = 1.6, 1$  H), 2.47 (hept,  $J = 6.9$  Hz, 1H), 2.44 (s, 3H) 2.12 (hept,  $J = 6.9$  Hz, 1H), 1.35 (d,  $J = 6.9, 3$  H), 1.23 (d,  $J = 6.9$  Hz, 3H), 1.05 (d,  $J = 6.9$  Hz, 3H), 1.04 (d,  $J = 6.9$  Hz, 3H) ppm. Crystals suitable for single crystal X-ray diffraction were grown by diffusion of hexane into a solution of **353cAgCl** in  $\text{CDCl}_3$ .

### **353cAuCl**



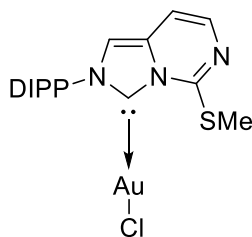
Silver complex **353cAgCl** (40.0 mg, 54.6  $\mu\text{mol}$ ),  $\text{Au}(\text{SMe}_2)\text{Cl}$  (16.7 mg, 100  $\mu\text{mol}$ ) and  $\text{CH}_2\text{Cl}_2$  (1.0 mL) were combined in a round bottom flask under air. After stirring in darkness for 4 h, the reaction mixture was filtered through a 2 cm plug of celite ( $\text{CH}_2\text{Cl}_2$ ) and concentrated under reduced pressure to give **353cAuCl** as a white solid (43.7 mg, 99%); mp: (colourless to opaque) 192  $^\circ\text{C}$ , (dec.) 275  $^\circ\text{C}$ ; IR (neat):  $\nu = 2966, 1670, 1615, 1386, 1366, 1170, 1060$   $\text{cm}^{-1}$ ;  $^1\text{H}$  NMR (400 MHz,  $\text{CDCl}_3$ ):  $\delta = 8.22 - 8.17$  (m, 2H), 7.82 (d,  $J = 8.0$  Hz, 2H), 7.69 (d,  $J = 7.2$  Hz, 2H), 7.61 – 7.56 (m, 3H), 7.45 (t,  $J = 7.8$  Hz, 1H), 7.35 – 7.24 (m, 6H), 7.19 (app. dd,  $J = 7.9, 1.4$  Hz, 1H), 6.74 (s, 1H), 2.46 (hept,  $J = 6.9$  Hz, 1H), 2.41 (s, 3H), 2.22 (hept,  $J = 6.9$  Hz, 1H), 1.42 (d,  $J = 6.9$  Hz, 3H), 1.22 (d,  $J = 6.9$  Hz, 3H), 1.11 (d,  $J = 6.9$  Hz, 3H), 1.06 (d,  $J = 6.9$  Hz, 3H) ppm;  $^{13}\text{C}$  NMR (101 MHz,  $\text{CDCl}_3$ ):  $\delta = 156.5$  (C), 156.4 (C), 151.9 (C), 146.4 (C), 145.8 (C), 145.5 (C), 144.6 (C), 138.9 (C), 136.1 (C), 135.5 (C), 131.6 (CH), 130.9 (CH), 130.7 (2CH), 129.8 (2CH), 129.4 (2CH), 128.7 (2CH), 128.2 (CH), 126.9 (2CH), 125.7 (2CH), 124.4 (CH), 124.3 (CH), 118.7 (C), 96.8 (CH), 28.8 (CH), 28.5 (CH), 24.7 ( $\text{CH}_3$ ), 24.59 ( $\text{CH}_3$ ), 24.57 ( $\text{CH}_3$ ), 24.3 ( $\text{CH}_3$ ), 22.0 ( $\text{CH}_3$ ) ppm; Elemental analysis calcd for  $\text{C}_{36}\text{H}_{35}\text{AuClN}_3\text{O}_3\text{S}$  C: 52.59, H: 4.29, N: 5.11. Found C: 52.33, H: 4.17, N: 4.71. Crystals suitable for single crystal X-ray diffraction were grown by diffusion of hexane into a solution of **353cAuCl** in  $\text{CH}_2\text{Cl}_2$ .

### 353dAuCl



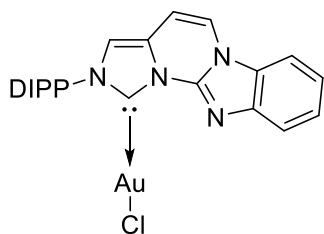
Imidazolium salt **353d•HCl** (64.0 mg, 100  $\mu$ mol), Ag<sub>2</sub>O (11.6 mg, 50.1  $\mu$ mol) and dry CH<sub>2</sub>Cl<sub>2</sub> (1.0 mL) were added to a screw thread capped vial containing 4 Å molecular sieves and stirred for 4 h in complete darkness. DMSAuCl (29.4 mg, 99.8  $\mu$ mol) was then added and the reaction stirred at r.t. for a further 4 h. The crude was passed through 1 cm pads of celite and silica (CH<sub>2</sub>Cl<sub>2</sub>) before the solvent was removed under reduced pressure to provide pure **353dAuCl** as a white crystalline solid (53.7 mg, 64%); mp: (colourless to opaque) 196 °C; IR (neat):  $\nu$  = 2965, 1664, 1615, 1362, 1166 cm<sup>-1</sup>; <sup>1</sup>H NMR (300 MHz, CDCl<sub>3</sub>):  $\delta$  = 7.89 (dd,  $J$  = 7.4, 2.2 Hz, 2H), 7.83 (d,  $J$  = 8.1 Hz, 2H), 7.51 – 7.42 (m, 4H), 7.37 – 7.31 (m, 4H), 7.27 – 7.19 (m, 2H), 7.15 (t,  $J$  = 7.1 Hz, 1H), 7.07 (t,  $J$  = 7.4 Hz, 2H), 6.65 (s, 1H), 5.59 (d,  $J_{AB}$  = 12.7 Hz, 1H), 5.27 (d,  $J_{AB}$  = 12.7 Hz, 1H), 2.42 (hept,  $J$  = 6.8 Hz, 1H), 2.42 (s, 3H), 2.19 (hept,  $J$  = 6.8 Hz, 1H), 1.35 (d,  $J$  = 6.8 Hz, 3H), 1.34 (d,  $J$  = 6.8 Hz, 3H) 1.20 (d,  $J$  = 6.8 Hz, 3H), 1.10 (d,  $J$  = 6.8 Hz, 3H) ppm; <sup>13</sup>C NMR (101 MHz, CDCl<sub>3</sub>):  $\delta$  = 156.4 (C), 152.2 (C), 146.2 (C), 145.8 (C), 145.3 (C), 144.5 (C), 135.15 (C), 135.12 (C), 133.15 (C), 131.08 (2CH), 131.0 (CH), 130.1 (4CH), 128.9 (CH), 128.8 (2CH), 128.4 (2CH), 128.3 (CH), 126.6 (2CH), 125.5 (C), 124.5 (CH), 124.3 (CH), 116.6 (C), 96.6 (CH), 53.7 (CH<sub>2</sub>), 28.7 (CH), 28.6 (CH), 24.8 (CH<sub>3</sub>), 24.7 (CH<sub>3</sub>), 24.6 (CH<sub>3</sub>), 24.4 (CH<sub>3</sub>), 22.0 (CH<sub>3</sub>) ppm; Elemental analysis calcd for C<sub>37</sub>H<sub>37</sub>AuClN<sub>3</sub>O<sub>3</sub>S C: 53.15, H: 4.46, N: 5.03. Found C: 53.04, H: 4.44, N: 4.98. Crystals suitable for single crystal X-ray diffraction were grown by diffusion of hexane into a solution of **353dAuCl** in CH<sub>2</sub>Cl<sub>2</sub>.

### 371AuCl



Imidazolium salt **371•HCl** (17.5 mg, 48.5  $\mu\text{mol}$ ),  $\text{Ag}_2\text{O}$  (5.61 mg, 24.1  $\mu\text{mol}$ ) and  $\text{CH}_2\text{Cl}_2$  (1.0 mL) were added to a flame dried Schlenk tube containing 4 Å molecular sieves and stirred for 18 h in complete darkness under argon. After filtering through a plug of cotton wool, the solvent was removed under reduced pressure to give crude **371AgCl** which was dissolved in dry  $\text{CH}_2\text{Cl}_2$  (1 mL).  $\text{DMSAuCl}$  (14.2 mg, 48.3  $\mu\text{mol}$ ) was added and the reaction stirred at r.t. for 4 h. The crude was passed through 1 cm pads of celite and silica ( $\text{CH}_2\text{Cl}_2$ ) before the solvent was removed under reduced pressure to provide **371AuCl** as a pale yellow powder (20.2 mg, 75% over 2 steps); mp: (dec.) 180 °C (white to black solid); IR (neat):  $\nu = 3144, 2961, 2927, 2866, 2362, 2334, 1632, 1486, 1412, 1317, 1254, 1033 \text{ cm}^{-1}$ ;  $^1\text{H}$  NMR (400 MHz,  $\text{CDCl}_3$ ):  $\delta = 7.59$  (d,  $J = 6.5 \text{ Hz}$ , 1H), 7.45 (t,  $J = 7.8 \text{ Hz}$ , 1H), 7.28 (s, 1H), 7.26 – 7.18 (m, 2H), 7.11 (d,  $J = 6.5 \text{ Hz}$ , 1H), 2.69 (s, 3H), 2.09 (hept,  $J = 6.8 \text{ Hz}$ , 2H), 1.17 (d,  $J = 6.8 \text{ Hz}$ , 6H), 1.04 (d,  $J = 6.8 \text{ Hz}$ , 6H) ppm;  $^{13}\text{C}$  NMR (101 MHz,  $\text{CDCl}_3$ ):  $\delta = 153.2$  (C), 145.2 (C), 136.1 (CH), 135.1 (C), 131.2 (CH), 130.7 (C), 124.5 (2CH), 114.6 (CH), 106.9 (CH), 28.5 (2CH), 24.7 (2CH<sub>3</sub>), 24.5 (2CH<sub>3</sub>), 15.5 (SCH<sub>3</sub>) ppm; MS (ES-TOF):  $m/z$ : 100% 326.17 [M-AuCl+H]<sup>+</sup>.

### 355AuCl

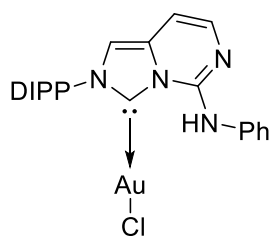


Imidazolium salt **355•HCl** (36.0 mg, 90.0  $\mu\text{mol}$ ),  $\text{Ag}_2\text{O}$  (11.5 mg, 49.6  $\mu\text{mol}$ ) and  $\text{CH}_2\text{Cl}_2$  (1.0 mL) were added to a flame dried Schlenk tube containing 4 Å molecular sieves and stirred for 18 h in complete darkness under argon. After filtering through a plug of cotton, the filtrate was concentrated under reduced pressure and redissolved in dry  $\text{CH}_2\text{Cl}_2$  (1 mL).  $\text{DMSAuCl}$  (21.6 mg, 73.3  $\mu\text{mol}$ ) was added and the reaction stirred at r.t. for 6 h. The



reaction mixture was passed through 1 cm pads of celite and silica (CH<sub>2</sub>Cl<sub>2</sub>) and the solvent was concentrated under reduced pressure to give **355AuCl** as a yellow solid (35.1 mg, 65% over two-steps); mp: (dec.) 238 °C; IR (neat):  $\nu$  = 3092, 2962, 2923, 2865, 1646, 1625, 1585, 1555, 1456, 1381 cm<sup>-1</sup>; <sup>1</sup>H NMR (400 MHz, CDCl<sub>3</sub>):  $\delta$  = 8.01 (dd,  $J$  = 7.1, 1.3 Hz, 1H), 7.87 (d,  $J$  = 7.7 Hz, 1H), 7.66 (dd,  $J$  = 7.1, 1.3 Hz, 1H), 7.53 (t,  $J$  = 7.8 Hz, 1H), 7.51 – 7.42 (m, 2H), 7.33 – 7.29 (m, 3H), 6.86 (d,  $J$  = 7.7 Hz, 1H), 2.39 (hept,  $J$  = 6.8 Hz, 2H), 1.33 (d,  $J$  = 6.8 Hz, 6H), 1.14 (d,  $J$  = 6.8 Hz, 6H) ppm; <sup>13</sup>C NMR (101 MHz, CDCl<sub>3</sub>):  $\delta$  = 169.7 (C), 145.4 (C), 141.1 (C), 134.6 (C), 131.3 (CH), 129.8 (C), 127.2 (C), 125.5 (CH), 124.6 (2CH), 124.2 (CH), 121.7 (CH), 121.2 (CH), 117.3 (CH), 109.1 (CH), 99.4 (CH), 28.7 (2CH), 24.53 (CH<sub>3</sub>), 24.51 (CH<sub>3</sub>) ppm; Elemental analysis calcd for C<sub>24</sub>H<sub>24</sub>AuClN<sub>4</sub> C: 47.97, H: 4.03, N: 9.32. Found C: 48.05, H: 4.10, N: 9.30. Crystals suitable for single crystal X-ray diffraction were grown by diffusion of hexane into a solution of **355AuCl** in CH<sub>2</sub>Cl<sub>2</sub>.

### **354aAuCl**

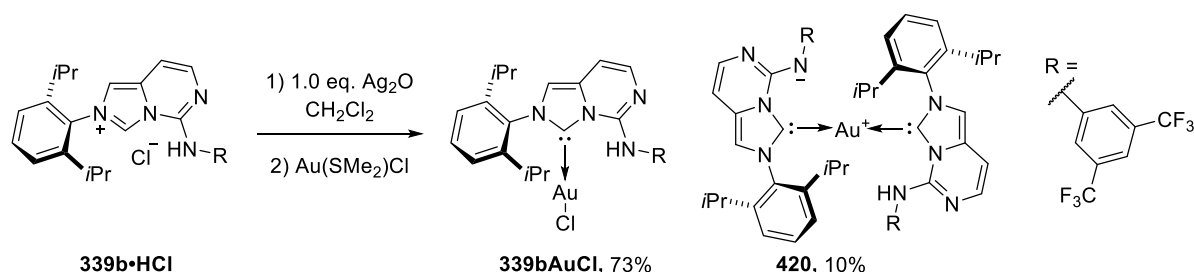


Imidazolium salt **354a•HCl** (40.6 mg, 0.10 mmol), DMSAuCl (29.4 mg, 0.10 mmol), K<sub>2</sub>CO<sub>3</sub> (13.8 mg, 0.10 mmol) and acetone (1.0 mL) were combined in a 8 mL screw thread capped vial and heated to 60 °C for 18 h. After allowing to cool to r.t., the reaction mixture was concentrated

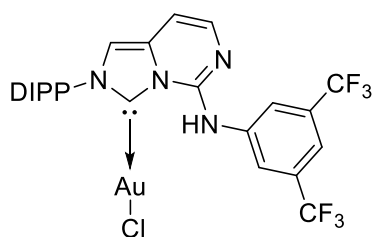
under reduced pressure and the residue taken up in CH<sub>2</sub>Cl<sub>2</sub> (2 mL), passed through a 1 cm pad of celite (CH<sub>2</sub>Cl<sub>2</sub>) and concentrated under reduced pressure. Purification by flash column chromatography (CH<sub>2</sub>Cl<sub>2</sub>) gave **354aAuCl** as a pale yellow solid (14.5 mg, 24%); mp: 273-275 °C; IR (neat):  $\nu$  = 3245, 3149, 2692, 2926, 2866, 1646, 1602, 1559, 1530, 1470, 1448, 1217 cm<sup>-1</sup>; <sup>1</sup>H NMR (400 MHz, CDCl<sub>3</sub>):  $\delta$  = 10.24 (br. s, 1H, NH), 7.90 (dd,  $J$  = 8.6, 1.0 Hz, 2H), 7.59 – 7.53 (m, 2H), 7.44 – 7.39 (m, 2H), 7.33 (d,  $J$  = 7.8 Hz, 2H), 7.22 – 7.14 (m, 2H), 6.85

(d,  $J = 6.5$  Hz, 1H), 2.27 (hept,  $J = 6.8$  Hz, 2H), 1.33 (d,  $J = 6.8$  Hz, 6H), 1.14 (d,  $J = 6.8$  Hz, 6H) ppm;  $^{13}\text{C}$  NMR (101 MHz,  $\text{CDCl}_3$ ):  $\delta = 159.9$  (C), 145.4 (2C), 141.4 (C), 138.8 (C), 137.3 (CH), 134.8 (C), 132.3 (2C), 131.4 (CH), 129.3 (2CH), 124.9 (CH), 124.7 (2CH), 120.9 (2CH), 113.9 (CH), 101.8 (CH), 28.7 (2CH), 24.7 (2CH<sub>3</sub>), 24.6 (2CH<sub>3</sub>) ppm; Elemental analysis calcd for  $\text{C}_{24}\text{H}_{26}\text{AuClN}_4$  C: 47.81, H: 4.35, N: 9.29. Found C: 47.00, H: 4.36, N: 8.95. Crystals suitable for single crystal X-ray diffraction were grown by diffusion of hexane into a solution of **354aAuCl** in  $\text{CDCl}_3$ .

### **354bAuCl and 420**

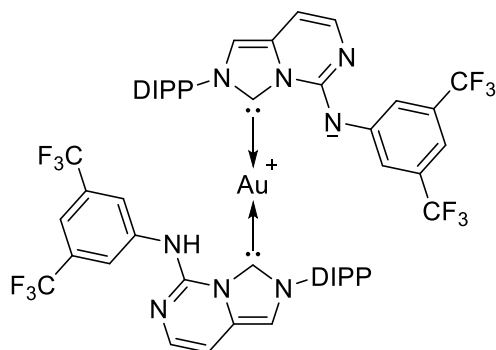


Imidazolium salt **354b•HCl** (54.3 mg, 0.10 mmol),  $\text{Ag}_2\text{O}$  (23.2 mg, 0.10 mmol) and  $\text{CH}_2\text{Cl}_2$  (1.0 mL) were combined in an 8 mL screw thread capped vial and stirred in complete darkness for 24 h. The reaction mixture was filtered through a 2 cm pad of celite ( $\text{CH}_2\text{Cl}_2$ ) and concentrated under reduced pressure. The crude material was redissolved in  $\text{CH}_2\text{Cl}_2$  (1.0 mL) and  $\text{DMSAuCl}$  (29.5 mg, 0.10 mmol) was added. After stirring at r.t. for 1 h, the reaction mixture was filtered through a 2 cm pad of celite ( $\text{CH}_2\text{Cl}_2$ ) and the filtrate concentrated under reduced pressure. Purification by flash column chromatography (0→5% MeOH in  $\text{CH}_2\text{Cl}_2$ ) yielded **354bAuCl** as a white solid (54.0 mg, 73%) and **420** as a beige powder (12.1 mg, 10%):

**354bAuCl**

mp: 150-152 °C; IR (neat):  $\nu = \text{cm}^{-1}$ ;  $^1\text{H}$  NMR (400 MHz,  $\text{CDCl}_3$ ):  $\delta = 10.69$  (s, 1H), 8.47 (br. s, 2H), 7.66 (br. s, 1H), 7.63 (d,  $J = 6.5$  Hz, 1H), 7.57 (t,  $J = 7.8$  Hz, 1H), 7.34 (d,  $J = 7.8$  Hz, 2H), 7.26 (s, 1H), 6.98 (d,  $J = 6.5$  Hz, 1H), 2.24 (hept,  $J = 6.8$

Hz, 2H), 1.33 (d,  $J = 6.8$  Hz, 6H), 1.15 (d,  $J = 6.9$  Hz, 6H) ppm;  $^{13}\text{C}$  NMR (101 MHz,  $\text{CDCl}_3$ ):  $\delta = 160.2$  (C), 145.3 (2C), 140.6 (C), 138.9 (C), 136.6 (CH), 134.5 (C), 132.6 (q,  $J = 33.6$  Hz, 2C), 132.0 (C), 131.6 (CH), 124.8 (2CH), 123.2 (q,  $J = 272.9$  Hz, 2 $\text{CF}_3$ ), 120.1 (m, 2CH), 117.9 (m, CH), 114.4 (CH), 103.6 (CH), 28.7 (2CH), 24.7 (2 $\text{CH}_3$ ), 24.6 (2 $\text{CH}_3$ ) ppm;  $^{19}\text{F}$  NMR (282 MHz,  $\text{CDCl}_3$ ):  $\delta = -62.9$  ppm; Elemental analysis calcd for  $\text{C}_{26}\text{H}_{24}\text{AuClF}_6\text{N}_4$ : C: 42.26, H: 3.27, N: 7.58. Found C: 42.26, H: 3.45, N: 7.36.

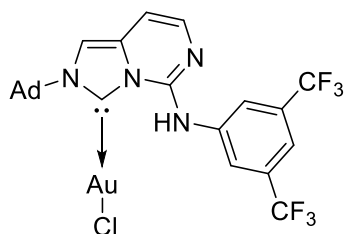
**420**

mp: (dec.) 229 °C; IR (neat):  $\nu = 2966, 1652, 1629, 1574, 1511, 1273, 1167, 1123 \text{ cm}^{-1}$ ;  $^1\text{H}$  NMR (500 MHz,  $\text{CDCl}_3$ ):  $\delta = 11.11$  (br. s, 1H), 7.74 (br. s, 4H), 7.50 (d,  $J = 6.5$  Hz, 2H), 7.40 (t,  $J = 7.7$  Hz, 2H), 7.24 (br. s, 2H), 7.16 (d,  $J = 7.7$  Hz, 2H), 7.12 (d,  $J = 7.7$  Hz, 2H), 6.98 (s, 2H), 6.60 (d,  $J = 6.5$  Hz, 2H), 2.25

(hept,  $J = 6.8$  Hz, 2H), 2.08 (hept,  $J = 6.8$  Hz, 2H), 1.15 (d,  $J = 6.8$  Hz, 6H), 1.07 (d,  $J = 6.8$  Hz, 12H), 0.43 (d,  $J = 6.8$  Hz, 6H) ppm;  $^{13}\text{C}$  NMR (126 MHz,  $\text{CDCl}_3$ ):  $\delta = 170.4$  (2C), 145.8 (2C), 145.2 (2C), 143.8 (2C), 138.9 (2CH), 135.3 (2C), 133.7 (2C), 131.4 (4C), 130.7 (2CH), 124.8 (2C), 124.1 (2CH), 123.9 (2CH), 123.5 (q,  $J = 278.8$  Hz, 4 $\text{CF}_3$ ), 120.5 (m, 4CH), 114.2 (m, 2CH), 113.0 (2CH), 98.1 (2CH), 28.6 (2CH), 28.3 (2CH), 24.9 (2 $\text{CH}_3$ ), 24.7 (2 $\text{CH}_3$ ), 24.3

(2CH<sub>3</sub>), 23.5 (2CH<sub>3</sub>) ppm; Elemental analysis calcd for C<sub>52</sub>H<sub>57</sub>AuF<sub>6</sub>N<sub>8</sub> C: 51.66, H: 3.92, N: 9.27. Found C: 51.69, H: 4.05, N: 9.25.

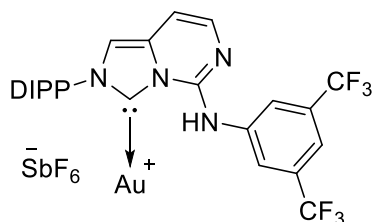
### 354cAuCl



Imidazolium salt **354c•HCl** (51.5 mg, 0.10 mmol), Ag<sub>2</sub>O (23.1 mg, 0.10 mmol) and CH<sub>2</sub>Cl<sub>2</sub> (1.0 mL) were combined in an 8 mL screw thread capped vial and stirred in complete darkness for 24 h. The reaction mixture was filtered through a 2 cm pad of celite

(CH<sub>2</sub>Cl<sub>2</sub>) and concentrated under reduced pressure. The crude material was redissolved in CH<sub>2</sub>Cl<sub>2</sub> (1.0 mL) and DMSAuCl (29.4 mg, 0.10 mmol) was added. After stirring at r.t. for 1 h, the reaction mixture was filtered through a 2 cm pad of celite (CH<sub>2</sub>Cl<sub>2</sub>) and the filtrate concentrated under reduced pressure. Purification by flash column chromatography yielded **354cAuCl** as a white solid (49.7 mg, 70%); mp: (dec.) 235 °C; IR (neat):  $\nu = \text{cm}^{-1}$ ; <sup>1</sup>H NMR (400 MHz, CDCl<sub>3</sub>):  $\delta$  = 10.92 (s, 1H), 8.47 (br. s, 2H), 7.62 (br. s, 1H), 7.50 (s, 1H), 7.45 (d,  $J$  = 6.5 Hz, 1H), 6.87 (d,  $J$  = 6.5 Hz, 1H), 2.69 (d,  $J$  = 2.9 Hz, 6H), 2.45 – 2.35 (m, 3H), 1.86 – 1.82 (m, 6H) ppm; <sup>13</sup>C NMR (101 MHz, CDCl<sub>3</sub>):  $\delta$  = 156.1 (C), 139.9 (C), 139.3 (C), 135.2 (CH), 132.5 (q,  $J$  = 33.4 Hz, 2C), 130.7 (C), 123.3 (q,  $J$  = 272.8 Hz, 2CF<sub>3</sub>), 119.8 (m, 2CH), 117.4 (m, CH), 109.5 (CH), 103.8 (CH), 62.2 (C), 45.1 (3CH<sub>2</sub>), 35.7 (3CH<sub>2</sub>), 30.1 (3CH) ppm; <sup>19</sup>F NMR (377 MHz, CDCl<sub>3</sub>):  $\delta$  = –62.9 ppm; Elemental analysis calcd for C<sub>24</sub>H<sub>22</sub>AuClF<sub>6</sub>N<sub>4</sub> C: 40.44, H: 3.11, N: 7.86. Found C: 40.36, H: 3.14, N: 7.60.

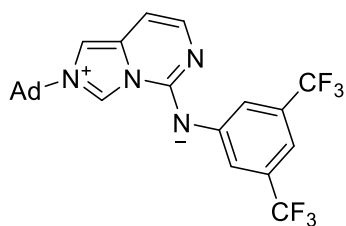
### 354bAuSbF<sub>6</sub>



**354bAuCl** (42.0 mg, 56.8  $\mu\text{mol}$ ) and AgSbF<sub>6</sub> (23.5 mg, 68.3  $\mu\text{mol}$ ) and dry MeCN (2.5 mL) were combined in a heat-gun dried Schlenk tube and stirred for 20 min. The reaction mixture

was filtered through a 2 cm pad of celite (CH<sub>2</sub>Cl<sub>2</sub>) and concentrated under reduced pressure. Recrystallisation from acetone/Et<sub>2</sub>O provided **354bAuSbF<sub>6</sub>** as a beige solid (39.5 mg, 71%); mp: 267-269 °C; IR (neat):  $\nu = \text{cm}^{-1}$ ; <sup>1</sup>H NMR (400 MHz, Acetone-*d*<sub>6</sub>):  $\delta = 8.19$  (s, 1H), 8.12 (br. s, 1H), 7.75 (br. s, 2H), 7.58 (t, *J* = 7.8 Hz, 1H), 7.30 (d, *J* = 7.8 Hz, 2H), 7.01 (d, *J* = 7.4 Hz, 1H), 6.98 (d, *J* = 7.4 Hz, 1H), 2.28 (hept, *J* = 6.9 Hz, 2H), 1.08 (d, *J* = 6.9 Hz, 6H), 0.99 (d, *J* = 6.9 Hz, 6H) ppm; <sup>13</sup>C NMR (101 MHz, Acetone-*d*<sub>6</sub>):  $\delta = 163.3$  (C), 151.3 (C), 145.5 (2C), 136.1 (C), 135.3 (q, *J* = 33.8 Hz, 2C), 134.6 (C), 132.6 (CH), 127.1 (m, 2CH), 126.7 (CH), 125.4 (2CH), 123.8 (q, *J* = 272.9 Hz, 2CF<sub>3</sub>), 123.5 (m, CH), 119.2 (CH), 100.6 (CH), 29.3 (2CH), 24.6 (2CH<sub>3</sub>), 24.2 (2CH<sub>3</sub>) ppm; *one quaternary carbon resonance not observed in <sup>13</sup>C NMR spectra*; <sup>19</sup>F NMR (377 MHz, CDCl<sub>3</sub>):  $\delta = -57.8$  ppm; Elemental analysis calcd for C<sub>26</sub>H<sub>24</sub>AuF<sub>12</sub>N<sub>4</sub>Sb C: 33.25, H: 2.58, N: 5.97. Found C: 32.46, H: 2.42, N: 5.66. *Note: 354bAuSbF<sub>6</sub> was unstable in solution, quickly discolouring and providing a gold mirror on the NMR tube within 4 h.*

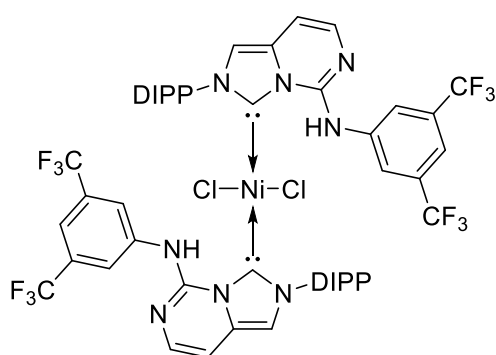
**(2-((3*s*,5*s*,7*s*)-adamantan-1-yl)imidazo[1,5-*c*]pyrimidin-2-ium-5-yl)(3,5-bis(trifluoromethyl)phenyl)amide 425**



Imidazolium salt **354c•HCl** (25.9 mg, 50  $\mu$ mol) was dissolved in MeOH and cooled to 0 °C. A solution of KOH in MeOH (0.5 M, 0.12 mL, 60  $\mu$ mol) was added dropwise and the reaction mixture stirred for 5 minutes before H<sub>2</sub>O (10 mL) was added. The reaction mixture was transferred to a separating funnel and extracted with CH<sub>2</sub>Cl<sub>2</sub> (3 $\times$ 10 mL). The combined organic phases were washed with brine (15 mL), dried over Na<sub>2</sub>SO<sub>4</sub>, filtered and concentrated under reduced pressure to give zwitterion **425** as a yellow crystalline solid (20.4 mg, 85%); mp: 215-217 °C; IR (neat):  $\nu = 2911, 1856, 1632, 1595, 1548, 1378, 1245, 1116 \text{ cm}^{-1}$ ; <sup>1</sup>H NMR (400 MHz, CDCl<sub>3</sub>):  $\delta = 10.11$  (br. s, 1H), 8.31 (br. s, 2H), 7.58 (d, *J* = 6.4 Hz,

1H), 7.43 (s, 1H), 7.29 (d,  $J = 1.9$  Hz, 1H), 6.44 (d,  $J = 6.4$  Hz, 1H), 2.42 – 2.35 (m, 3H), 2.30 – 2.25 (m, 6H), 1.92 – 1.77 (m, 6H) ppm;  $^{19}\text{F}$  NMR (377 MHz,  $\text{CDCl}_3$ ):  $\delta = -62.7$  ppm;  $^{13}\text{C}$  NMR (101 MHz,  $\text{CDCl}_3$ ):  $\delta = 143.2$  (C), 142.3 (CH), 133.5 (C), 131.5 (q,  $J = 32.6$  Hz, 2C) 123.8 (q,  $J = 272.2$  Hz,  $2\text{CF}_3$ ), 123.0 (m, 2CH), 122.3 (C), 114.9 (m, CH), 105.7 (CH), 94.5 (CH), 61.1 (C), 43.3 ( $3\text{CH}_2$ ), 35.4 ( $3\text{CH}_2$ ), 29.5 ( $3\text{CH}$ ) ppm; Elemental analysis calcd for  $\text{C}_{24}\text{H}_{22}\text{F}_6\text{N}_4$  C: 60.00, H: 4.62, N: 11.66. Found C: 59.90, H: 4.59, N: 11.60.

### Nickel complex **427**

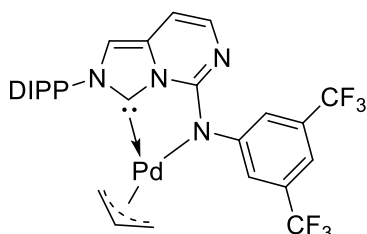


Imidazolium salt **354b**•HCl (54.3mg, 0.10 mmol),  $\text{NiCl}_2 \cdot \text{H}_2\text{O}$  (23.7 mg, 0.10  $\mu\text{mol}$ )  $\text{K}_2\text{CO}_3$  (42.0 mg, 0.30 mmol) and MeCN (5.0 mL) were combined and heated to reflux for 24 h. After allowing to cool to r.t., the reaction mixture was concentrated under reduced

pressure and the residue taken up in  $\text{CH}_2\text{Cl}_2$  (20 mL). The organic phase was washed with  $\text{H}_2\text{O}$  ( $2 \times 20$  mL) and brine (15 mL), dried over  $\text{Na}_2\text{SO}_4$ , filtered and concentrated under reduced pressure. Purification by flash column chromatography (97:3  $\text{CH}_2\text{Cl}_2/\text{MeOH}$ ) provided **427** as a brown solid (45.0 mg, 79%); mp: 109-111  $^\circ\text{C}$ ; IR (neat):  $\nu = \text{cm}^{-1}$ ;  $^1\text{H}$  NMR (400 MHz,  $\text{CDCl}_3$ ):  $\delta = 8.97$  (br. s, 2H), 8.09 (br. s, 4H), 7.66 (d,  $J = 6.4$  Hz, 2H), 7.59 (t,  $J = 7.8$  Hz, 2H), 7.37 (d,  $J = 7.8$  Hz, 4H), 7.35 (br. s, 2H), 6.98 (s, 2H), 6.29 (d,  $J = 6.4$  Hz, 2H), 2.34 (hept,  $J = 6.8$  Hz, 4H), 1.24 (d,  $J = 6.8$  Hz, 12H), 1.20 (d,  $J = 6.8$  Hz, 12H) ppm;  $^{13}\text{C}$  NMR (101 MHz,  $\text{CDCl}_3$ ):  $\delta = 151.0$  (2C), 145.5 (2CH), 145.2 (2C), 144.9 (2C), 134.8 (2C), 132.0 (2CH), 131.4 (q,  $J = 32.4$  Hz, 4C), 131.1 (2C), 124.7 (4CH), 124.25 (4C), 124.20 (q,  $J = 272.5$  Hz,  $4\text{CF}_3$ ), 123.9 (m, 4CH), 113.6 (m, 2CH), 111.1 (2CH), 90.1 (2CH), 28.7 (4CH), 24.8 ( $4\text{CH}_3$ ), 24.6

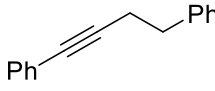
(4CH<sub>3</sub>) ppm; <sup>19</sup>F NMR (377 MHz, CDCl<sub>3</sub>): δ = −62.7 ppm; Elemental analysis calcd for C<sub>52</sub>H<sub>48</sub>NiCl<sub>2</sub>F<sub>12</sub>N<sub>8</sub> C: 58.28, H: 4.51, N: 5.48. Found C: 58.33, H: 4.56, N: 10.17.

### ***Palladium complex 428***

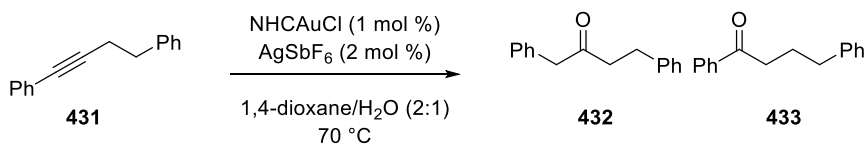


Imidazolium salt **354b•HCl** (27.2 mg, 50 μmol), Ag<sub>2</sub>O (11.6 mg, 50 μmol) and CH<sub>2</sub>Cl<sub>2</sub> (0.5 mL) were combined in an 8 mL screw thread capped vial and stirred in complete darkness for 4 h. [Pd(allyl)Cl]<sub>2</sub> (9.20 mg, 25 μmol) was then added and the reaction mixture stirred for 18 h. The crude material was passed through a 2 cm pad of silica (CH<sub>2</sub>Cl<sub>2</sub>) and the filtrate concentrated under reduced pressure to provide **428** as a dark green waxy solid (32.2 mg, 99%); mp: 104-106 °C; IR (neat): ν = 2966, 2929, 2971, 1619, 1495, 1468, 1366, 1352, 1273, 1168, 1123 cm<sup>−1</sup>; <sup>1</sup>H NMR (400 MHz, CDCl<sub>3</sub>): δ = 8.09 (br. s, 2H), 7.54 (t, *J* = 7.8 Hz, 1H), 7.50 (d, *J* = 6.5 Hz, 1H), 7.43 (br. s, 1H), 7.35 – 7.30 (m, 2H), 6.96 (s, 1H), 6.44 (d, *J* = 6.5 Hz, 1H), 5.11 (app. tt, *J* = 12.8, 6.4 Hz, 1H), 3.55 (dd, *J* = 7.4, 2.3 Hz, 1H), 3.14 (d, *J* = 13.3 Hz, 1H), 2.57 – 2.46 (m, 2H), 2.30 (hept, *J* = 6.9 Hz, 1H), 2.02 (d, *J* = 12.1 Hz, 1H), 1.19 (d, *J* = 6.9 Hz, 3H), 1.17 (d, *J* = 6.9 Hz, 3H), 1.14 (d, *J* = 6.9 Hz, 3H), 1.09 (d, *J* = 6.9 Hz, 3H) ppm; <sup>13</sup>C NMR (101 MHz, CDCl<sub>3</sub>): δ = 168.4 (C), 153.1 (C), 152.7 (C), 145.8 (C), 145.6 (C), 142.1 (CH), 136.2 (C), 131.8 (C), 131.0 (q, *J* = 32.7 Hz, 2C), 130.5 (CH), 126.2 (2CH), 124.0 (q, *J* = 272.6 Hz, 2CF<sub>3</sub>), 123.9 (2CH), 115.4 (m, CH), 115.3 (CH), 110.4 (CH), 95.5 (CH), 69.7 (CH<sub>2</sub>), 47.3 (CH<sub>2</sub>), 28.5 (CH), 28.3 (CH), 24.9 (CH<sub>3</sub>), 24.6 (CH<sub>3</sub>), 24.2 (CH<sub>3</sub>), 24.0 (CH<sub>3</sub>) ppm; <sup>19</sup>F NMR (282 MHz, CDCl<sub>3</sub>): δ = −62.7 ppm; HRMS (ES-TOF): *m/z*: calcd for C<sub>29</sub>H<sub>29</sub>N<sub>4</sub>F<sub>6</sub><sup>104</sup>Pd: 651.1337, found 651.1343 [M+H]<sup>+</sup>.

### ***But-1-yne-1,4-diyl*dibenzene **431****

 A flame dried Schlenk tube was charged with bis(triphenylphosphine)palladium(II) dichloride (84.0 mg, 0.02 mmol), copper(I) iodide (45.0 mg, 0.24 mmol), tetrahydrofuran (30 mL, degassed), iodobenzene (0.67 mL, 6.01 mmol), triethylamine (5.8 mL, 41.6 mmol, degassed) and 4-phenyl-1-butyne (0.93 mL, 6.61 mmol) sequentially and stirred at room temperature for 20 h. The reaction mixture was concentrated under reduced pressure and the resulting slurry was filtered through a 3 cm pad of silica (Et<sub>2</sub>O). The filtrate was concentrated under reduced pressure and purified by flash column chromatography (hexane) to give alkyne **431** as a colourless oil (1.23 g, 99%); IR (neat):  $\nu = 3027, 2927, 1599, 1490 \text{ cm}^{-1}$ ; <sup>1</sup>H NMR (400 MHz, CDCl<sub>3</sub>):  $\delta = 7.39\text{--}7.19$  (m, 10H), 2.92 (t,  $J = 7.5$  Hz, 2H), 2.69 (t,  $J = 7.5$  Hz, 2H) ppm; <sup>13</sup>C NMR (101 MHz, CDCl<sub>3</sub>):  $\delta = 140.9, 131.7, 128.7, 128.5, 128.3, 127.8, 126.5, 124.0, 89.6, 81.5, 35.3, 21.8$  ppm. Spectroscopic data matched that reported in the literature.<sup>272</sup>

### ***Hydration of alkyne **431*****



Adapting a literature procedure, AgSbF<sub>6</sub> (2 mol%), (NHC)AuCl (1 mol%), degassed 1,4-dioxane (0.67 M), alkyne **431** (1.0 eq.) and degassed H<sub>2</sub>O (0.33 M) were added to a screw thread capped vial under an argon atmosphere and the reaction mixture was heated at 70 °C for 18 h. After allowing to cool to r.t., the reaction mixture was diluted with CH<sub>2</sub>Cl<sub>2</sub>, dried over Na<sub>2</sub>SO<sub>4</sub> and concentrated under reduced pressure. Purification by flash column chromatography (95:5 hexane/EtOAc) provided a mixture of ketones **432** and **433**. Product ratios were determined by <sup>1</sup>H-NMR spectroscopy with an internal standard.



***1,4-Diphenylbutan-1-one 432***

White solid; IR (neat):  $\nu = 3062, 3027, 2936, 1683, 1598, 1448 \text{ cm}^{-1}$ ;  $^1\text{H}$  NMR (300 MHz,  $\text{CDCl}_3$ ):  $\delta = 7.97\text{--}7.89$  (m, 2H),  $7.59\text{--}7.52$  (m, 1H),  $7.49\text{--}7.41$  (m, 2H),  $7.34\text{--}7.26$  (m, 2H),  $7.25\text{--}7.17$  (m, 3H),  $2.99$  (t,  $J = 7.3 \text{ Hz}$ , 2H),  $2.73$  (t,  $J = 7.5 \text{ Hz}$ , 2H),  $2.09$  (app. quint,  $J = 7.4 \text{ Hz}$ , 2H) ppm;  $^{13}\text{C}$  NMR (101 MHz,  $\text{CDCl}_3$ ):  $\delta$  200.3, 141.8, 137.1, 133.1, 128.7, 128.7, 128.5, 128.2, 126.1, 37.8, 35.3, 25.8 ppm. Spectroscopic data matched that reported in the literature.<sup>273</sup>

***1,4-Diphenylbutan-2-one 433***

Pale yellow oil; IR (neat):  $\nu = 3063, 3028, 2926, 1710, 1496, 1454 \text{ cm}^{-1}$ ;  $^1\text{H}$  NMR (300 MHz,  $\text{CDCl}_3$ ):  $\delta = 7.37\text{--}7.22$  (m, 5H),  $7.22\text{--}7.08$  (m, 5H),  $3.67$  (s, 2H),  $2.87$  (m, 2H),  $2.77$  (m, 2H);  $^{13}\text{C}$  NMR (101 MHz,  $\text{CDCl}_3$ ):  $\delta$  207.6, 141.0, 134.2, 129.5, 128.9, 128.6, 128.5, 127.2, 126.2, 50.5, 43.6, 29.9. Spectroscopic data matched that reported in the literature.<sup>274</sup>

## Chapter 8: X-Ray data

### 8.1 Macrocycle 109

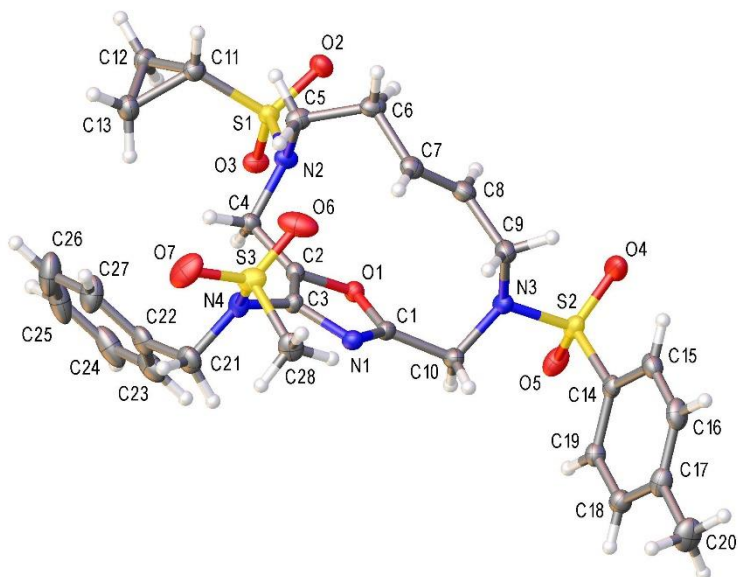
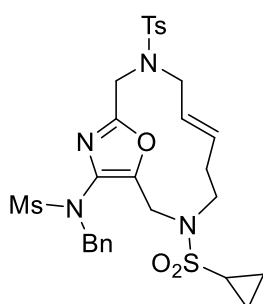


**Table 1** Crystal data and structure refinement for 109.

Identification code	109
Empirical formula	C <sub>28</sub> H <sub>34</sub> N <sub>4</sub> O <sub>7</sub> S <sub>3</sub>
Formula weight	634.77
Temperature/K	100.00(10)
Crystal system	monoclinic
Space group	P2 <sub>1</sub> /c
a/Å	9.9996(3)
b/Å	30.7693(10)
c/Å	10.3178(4)
α/°	90
β/°	109.715(4)
γ/°	90
Volume/Å <sup>3</sup>	2988.50(19)
Z	4
ρ <sub>calc</sub> /cm <sup>3</sup>	1.411
μ/mm <sup>-1</sup>	2.713
F(000)	1336.0
Crystal size/mm <sup>3</sup>	0.2 × 0.108 × 0.052
Radiation	CuKα (λ = 1.54184)
2θ range for data collection/°	9.396 to 149.206
Index ranges	-12 ≤ h ≤ 12, -37 ≤ k ≤ 37, -12 ≤ l ≤ 10
Reflections collected	12495
Independent reflections	5922 [R <sub>int</sub> = 0.0235, R <sub>sigma</sub> = 0.0297]
Data/restraints/parameters	5922/0/381
Goodness-of-fit on F <sup>2</sup>	1.081
Final R indexes [I ≥ 2σ (I)]	R <sub>1</sub> = 0.0384, wR <sub>2</sub> = 0.0890
Final R indexes [all data]	R <sub>1</sub> = 0.0433, wR <sub>2</sub> = 0.0917
Largest diff. peak/hole / e Å <sup>-3</sup>	0.31/-0.42

**Table 2 Fractional Atomic Coordinates ( $\times 10^4$ ) and Equivalent Isotropic Displacement Parameters ( $\text{\AA}^2 \times 10^3$ ) for MGW\_823.  $U_{\text{eq}}$  is defined as 1/3 of of the trace of the orthogonalised  $U_{\text{IJ}}$  tensor.**

Atom	x	y	z	$U(\text{eq})$
C1	4019.6(19)	3294.3(6)	3569.4(18)	18.6(4)
C2	2329.0(19)	3705.7(6)	3727.7(18)	18.4(3)
C3	3439.8(19)	3713.1(6)	4906.9(18)	18.4(3)
C4	967.9(19)	3944.4(6)	3223.0(18)	20.2(4)
C5	1926(2)	4614.0(6)	2422(2)	23.6(4)
C6	3018(2)	4613.5(6)	1689(2)	25.2(4)
C7	4157(2)	4278.6(6)	2198(2)	23.0(4)
C8	4392(2)	3971.2(7)	1412(2)	25.4(4)
C9	5556(2)	3636.8(6)	1870(2)	24.8(4)
C10	4738(2)	2993.7(6)	2893.4(19)	22.6(4)
C11	-1476(2)	4708.3(6)	1420.3(19)	22.6(4)
C12	-3071(2)	4667.0(7)	1035(2)	26.1(4)
C13	-2139(2)	4590.6(7)	2490(2)	28.6(4)
C14	7023(2)	2629.4(6)	1634.9(18)	20.4(4)
C15	8289(2)	2839.6(7)	1739(2)	26.0(4)
C16	9560(2)	2664.0(7)	2593(2)	29.2(4)
C17	9590(2)	2287.3(7)	3354(2)	26.9(4)
C18	8314(2)	2084.8(7)	3229.1(19)	24.2(4)
C19	7028(2)	2251.5(6)	2375.5(19)	21.6(4)
C20	10971(2)	2098.1(9)	4297(2)	38.1(5)
C21	2940(2)	3647.3(8)	7064(2)	29.6(4)
C22	1344(2)	3658.1(8)	6561.8(19)	29.3(4)
C23	549(3)	3312.2(8)	5824(2)	36.5(5)
C24	-920(3)	3333.9(10)	5320(2)	47.7(7)
C25	-1604(3)	3698.4(12)	5547(2)	52.1(8)
C26	-831(3)	4043.4(11)	6283(3)	51.5(7)
C27	641(2)	4024.7(9)	6790(2)	38.9(5)
C28	6282(2)	3952.4(8)	7714(2)	28.9(4)
N1	4529.7(16)	3450.4(5)	4799.4(15)	19.5(3)
N2	958.9(16)	4230.6(5)	2070.1(15)	20.0(3)
N3	4929.4(18)	3195.4(5)	1673.4(16)	22.2(3)
N4	3485.8(17)	3916.2(5)	6149.1(15)	22.2(3)
O1	2670.1(13)	3423.3(4)	2853.8(12)	18.2(3)
O2	-291.3(14)	4473.4(5)	-324.2(13)	24.0(3)
O3	-1350.2(14)	3903.7(4)	720.2(13)	22.2(3)
O4	5558.3(17)	3115.0(5)	-427.9(14)	34.4(4)
O5	4338.3(15)	2517.1(5)	339.3(15)	29.3(3)
O6	5023(2)	4490.9(5)	5752.5(16)	41.9(4)
O7	4377.7(19)	4494.1(6)	7874.8(16)	43.1(4)
S1	-572.7(4)	4304.6(2)	852.5(4)	17.85(10)
S2	5373.6(5)	2858.0(2)	656.9(4)	23.19(11)
S3	4775.9(5)	4262.7(2)	6858.9(5)	26.94(12)

**Table 3 Anisotropic Displacement Parameters ( $\text{\AA}^2 \times 10^3$ ) for MGW\_823. The Anisotropic displacement factor exponent takes the form:  $-2\pi^2[h^2a^{*2}U_{11}+2hka^*b^*U_{12}+\dots]$ .**

Atom	U <sub>11</sub>	U <sub>22</sub>	U <sub>33</sub>	U <sub>23</sub>	U <sub>13</sub>	U <sub>12</sub>
C1	19.7(8)	18.8(9)	18.0(8)	2.9(7)	7.3(7)	3.4(7)
C2	19.8(9)	19.7(9)	17.0(8)	-0.1(7)	8.0(7)	0.1(7)
C3	20.1(8)	19.5(9)	15.8(8)	0.5(7)	6.5(7)	3.2(7)
C4	19.8(9)	23.3(9)	17.3(8)	2.8(7)	6.1(7)	2.2(7)
C5	20.7(9)	20.4(9)	26.4(9)	-0.4(7)	3.8(8)	-0.8(7)
C6	22.8(9)	20.7(9)	31.2(10)	4.7(8)	7.7(8)	-1.3(8)
C7	20.9(9)	24.0(10)	24.4(9)	2.0(7)	7.9(7)	-2.7(7)
C8	30.3(10)	24.2(10)	23.2(9)	4.7(8)	11.0(8)	-0.4(8)
C9	29.4(10)	23.6(10)	25.5(9)	1.1(8)	14.6(8)	0.5(8)
C10	28.4(10)	19.9(9)	21.4(9)	2.7(7)	11.2(8)	4.4(8)
C11	21.8(9)	22.5(9)	23.3(9)	1.4(7)	7.5(7)	0.6(7)
C12	21.8(9)	30.5(10)	27.0(10)	4.4(8)	9.8(8)	4.4(8)
C13	30.2(10)	33.9(11)	25.0(10)	1.2(8)	13.4(8)	3.6(9)
C14	23.1(9)	23.0(9)	16.6(8)	-3.4(7)	8.8(7)	3.0(7)
C15	32.2(10)	25.4(10)	25.5(9)	-2.5(8)	16.6(8)	-3.1(8)
C16	22.5(10)	36.4(12)	31.8(10)	-9.7(9)	13.2(8)	-7.9(8)
C17	21.3(9)	35.6(11)	21.8(9)	-7.1(8)	4.9(8)	1.6(8)
C18	24.7(9)	26.5(10)	20.9(9)	0.0(8)	7.1(8)	2.5(8)
C19	19.7(9)	24.1(9)	22.1(9)	-2.3(7)	8.4(7)	-1.2(7)
C20	24.1(10)	51.0(15)	34.2(11)	-5.1(10)	3.2(9)	3.8(10)
C21	34.5(11)	38.3(12)	16.5(9)	0.4(8)	9.3(8)	1.4(9)
C22	33.1(11)	42.0(12)	15.2(8)	-1.8(8)	11.5(8)	-3.7(9)
C23	47.6(13)	42.7(13)	23.0(10)	-1.1(9)	16.7(10)	-10.8(11)
C24	47.6(14)	75(2)	24.3(11)	-8.2(11)	16.7(10)	-28.2(14)
C25	30.3(12)	104(3)	25.6(11)	-10.0(13)	14.6(10)	-11.8(14)
C26	35.3(13)	83(2)	41.5(13)	-14.3(14)	20.4(11)	5.2(13)
C27	32.5(11)	53.2(15)	33.7(11)	-16.0(11)	14.5(10)	-2.3(11)
C28	22.8(9)	40.8(12)	19.5(9)	-0.9(8)	2.3(8)	0.5(9)
N1	22.3(7)	18.7(8)	17.0(7)	1.4(6)	6.2(6)	2.9(6)
N2	17.4(7)	21.1(8)	19.1(7)	3.6(6)	2.8(6)	-0.2(6)
N3	30.0(8)	19.8(8)	19.0(7)	1.1(6)	11.2(6)	4.8(7)
N4	22.8(8)	27.6(9)	15.2(7)	-4.1(6)	5.2(6)	2.0(7)
O1	19.6(6)	19.8(6)	15.2(5)	-0.7(5)	5.7(5)	0.9(5)
O2	26.4(7)	28.1(7)	17.1(6)	3.2(5)	7.0(5)	1.1(6)
O3	20.6(6)	19.6(7)	22.6(6)	0.9(5)	2.2(5)	-2.3(5)
O4	45.7(9)	40.4(9)	20.6(7)	6.7(6)	16.0(6)	17.1(7)
O5	23.3(7)	31.5(8)	27.7(7)	-10.2(6)	1.3(6)	4.8(6)
O6	57.6(11)	29.3(8)	28.1(8)	3.2(6)	0.3(7)	-14.6(8)
O7	47.6(10)	40.7(10)	31.3(8)	-19.0(7)	0.6(7)	9.6(8)
S1	17.7(2)	18.8(2)	15.54(19)	1.26(15)	3.71(16)	0.62(16)
S2	26.9(2)	26.2(2)	16.0(2)	-1.13(17)	6.60(17)	8.01(18)
S3	32.5(3)	23.1(2)	19.0(2)	-3.98(17)	0.50(18)	0.31(19)

**Table 4 Bond Lengths for 109.**

Atom Atom	Length/ $\text{\AA}$	Atom Atom	Length/ $\text{\AA}$
C1 C10	1.482(2)	C15 C16	1.389(3)
C1 N1	1.290(2)	C16 C17	1.395(3)
C1 O1	1.361(2)	C17 C18	1.386(3)
C2 C3	1.343(3)	C17 C20	1.512(3)

C2	C4	1.478(2)	C18	C19	1.388(3)
C2	O1	1.375(2)	C21	C22	1.503(3)
C3	N1	1.391(2)	C21	N4	1.490(3)
C3	N4	1.413(2)	C22	C23	1.391(3)
C4	N2	1.478(2)	C22	C27	1.391(3)
C5	C6	1.523(3)	C23	C24	1.385(4)
C5	N2	1.491(2)	C24	C25	1.374(4)
C6	C7	1.494(3)	C25	C26	1.380(4)
C7	C8	1.317(3)	C26	C27	1.387(3)
C8	C9	1.505(3)	C28	S3	1.750(2)
C9	N3	1.481(3)	N2	S1	1.6363(15)
C10	N3	1.473(2)	N3	S2	1.6398(16)
C11	C12	1.514(3)	N4	S3	1.6431(17)
C11	C13	1.511(3)	O2	S1	1.4330(13)
C11	S1	1.749(2)	O3	S1	1.4398(14)
C12	C13	1.494(3)	O4	S2	1.4323(15)
C14	C15	1.393(3)	O5	S2	1.4319(16)
C14	C19	1.391(3)	O6	S3	1.4311(17)
C14	S2	1.7639(19)	O7	S3	1.4303(16)

**Table 5 Bond Angles for 109.**

Atom	Atom	Atom	Angle/°	Atom	Atom	Atom	Angle/°
N1	C1	C10	127.00(17)	C24	C23	C22	120.5(2)
N1	C1	O1	114.57(16)	C25	C24	C23	120.0(2)
O1	C1	C10	118.42(16)	C24	C25	C26	120.2(2)
C3	C2	C4	133.84(17)	C25	C26	C27	120.1(3)
C3	C2	O1	107.01(15)	C26	C27	C22	120.2(2)
O1	C2	C4	119.05(15)	C1	N1	C3	103.55(15)
C2	C3	N1	110.41(16)	C4	N2	C5	116.64(15)
C2	C3	N4	126.41(16)	C4	N2	S1	116.80(12)
N1	C3	N4	122.87(16)	C5	N2	S1	116.06(12)
N2	C4	C2	109.55(14)	C9	N3	S2	118.33(13)
N2	C5	C6	113.16(16)	C10	N3	C9	116.14(15)
C7	C6	C5	114.58(16)	C10	N3	S2	114.93(13)
C8	C7	C6	123.55(18)	C3	N4	C21	114.97(16)
C7	C8	C9	125.28(18)	C3	N4	S3	118.15(13)
N3	C9	C8	109.70(16)	C21	N4	S3	118.56(13)
N3	C10	C1	111.27(15)	C1	O1	C2	104.38(13)
C12	C11	S1	118.03(15)	N2	S1	C11	107.27(9)
C13	C11	C12	59.20(13)	O2	S1	C11	107.31(9)
C13	C11	S1	118.55(15)	O2	S1	N2	107.48(8)
C13	C12	C11	60.30(13)	O2	S1	O3	118.97(8)
C12	C13	C11	60.49(13)	O3	S1	C11	108.48(9)
C15	C14	S2	120.60(15)	O3	S1	N2	106.81(8)
C19	C14	C15	120.77(18)	N3	S2	C14	106.82(8)
C19	C14	S2	118.48(14)	O4	S2	C14	108.96(9)
C16	C15	C14	118.79(19)	O4	S2	N3	106.53(9)
C15	C16	C17	121.43(19)	O5	S2	C14	107.65(9)
C16	C17	C20	121.6(2)	O5	S2	N3	106.21(9)
C18	C17	C16	118.51(19)	O5	S2	O4	119.96(10)
C18	C17	C20	119.9(2)	N4	S3	C28	106.47(10)
C17	C18	C19	121.28(19)	O6	S3	C28	108.61(11)

C18	C19	C14	119.23(18)	O6	S3	N4	106.48(9)
N4	C21	C22	110.03(16)	O7	S3	C28	107.89(10)
C23	C22	C21	121.1(2)	O7	S3	N4	106.20(10)
C27	C22	C21	119.9(2)	O7	S3	O6	120.40(11)
C27	C22	C23	119.0(2)				

**Table 6 Hydrogen Atom Coordinates ( $\text{\AA} \times 10^4$ ) and Isotropic Displacement Parameters ( $\text{\AA}^2 \times 10^3$ ) for 109.**

Atom	x	y	z	U(eq)
H4A	185.54	3740.01	2915.74	24
H4B	848.59	4117.15	3962.93	24
H5A	2419.69	4618.2	3408.51	28
H5B	1362.24	4877.14	2179.8	28
H6A	2528	4566.35	714.22	30
H6B	3459	4898.13	1793.85	30
H7	4731.91	4287.71	3118.14	28
H8	3790.46	3959.81	501.52	30
H9A	6186.78	3667.44	1337.79	30
H9B	6108.25	3681.22	2833.01	30
H10A	5657.53	2913	3542.83	27
H10B	4175.84	2731.15	2619.8	27
H11	-1100.4	5004.26	1465.74	27
H12A	-3629.74	4931.89	834.77	31
H12B	-3525.77	4416.58	494.13	31
H13A	-2031.59	4293.99	2827.8	34
H13B	-2135.54	4809.24	3168.4	34
H15	8282.64	3092.87	1244.76	31
H16	10410.56	2800.62	2659.28	35
H18	8318.94	1832.36	3726.69	29
H19	6179.81	2112.05	2299.94	26
H20A	11750.17	2224.06	4084.2	57
H20B	10967.84	1789	4168.68	57
H20C	11070.46	2160.99	5236.23	57
H21A	3307.02	3758.46	7997.35	36
H21B	3263.94	3349.8	7071.19	36
H23	1007.08	3064.81	5668.63	44
H24	-1444.57	3101.51	4826.78	57
H25	-2590.25	3712.6	5203.91	63
H26	-1298.33	4288.68	6440.13	62
H27	1158.68	4257.95	7283.25	47
H28A	6111.94	3785.83	8429.86	43
H28B	7079.06	4141.64	8110.36	43
H28C	6481.67	3759.35	7071.37	43

## Experimental

A suitable crystal was selected on a **SuperNova, Dual, Cu at zero, Atlas** diffractometer. The crystal was kept at 100.00(10) K during data collection. Using Olex2,<sup>275</sup> the structure was solved with the ShelXT<sup>276</sup> structure solution program using Intrinsic Phasing and refined with the ShelXL<sup>277</sup> refinement package using Least Squares minimisation.

## Crystal structure determination of [109]

**Crystal Data** for  $\text{C}_{28}\text{H}_{34}\text{N}_4\text{O}_7\text{S}_3$  ( $M = 634.77$  g/mol): monoclinic, space group  $P2_1/c$  (no. 14),  $a = 9.9996(3)$   $\text{\AA}$ ,  $b = 30.7693(10)$   $\text{\AA}$ ,  $c = 10.3178(4)$   $\text{\AA}$ ,  $\beta = 109.715(4)^\circ$ ,  $V = 2988.50(19)$   $\text{\AA}^3$ ,  $Z = 4$ ,  $T = 100.00(10)$  K,  $\mu(\text{CuK}\alpha) = 2.713$   $\text{mm}^{-1}$ ,  $D_{\text{calc}} = 1.411$   $\text{g/cm}^3$ , 12495 reflections measured ( $9.396^\circ \leq 2\theta \leq 149.206^\circ$ ), 5922 unique ( $R_{\text{int}} = 0.0235$ ,  $R_{\text{sigma}} = 0.0297$ ) which were used in all calculations. The final  $R_1$  was 0.0384 ( $I > 2\sigma(I)$ ) and  $wR_2$  was 0.0917 (all data).

## Refinement model description

Number of restraints - 0, number of constraints - unknown.

Details:

1. Fixed Uiso

At 1.2 times of:

All C(H) groups, All C(H,H) groups

At 1.5 times of:

All C(H,H,H) groups

2.a Ternary CH refined with riding coordinates:

C11(H11)

2.b Secondary CH2 refined with riding coordinates:

C4(H4A,H4B), C5(H5A,H5B), C6(H6A,H6B), C9(H9A,H9B), C10(H10A,H10B), C12(H12A,H12B), C13(H13A,H13B), C21(H21A,H21B)

2.c Aromatic/amide H refined with riding coordinates:

C7(H7), C8(H8), C15(H15), C16(H16), C18(H18), C19(H19), C23(H23), C24(H24), C25(H25), C26(H26), C27(H27)

2.d Idealised Me refined as rotating group:

C20(H20A,H20B,H20C), C28(H28A,H28B,H28C)

## 8.2 Polycycle 120a

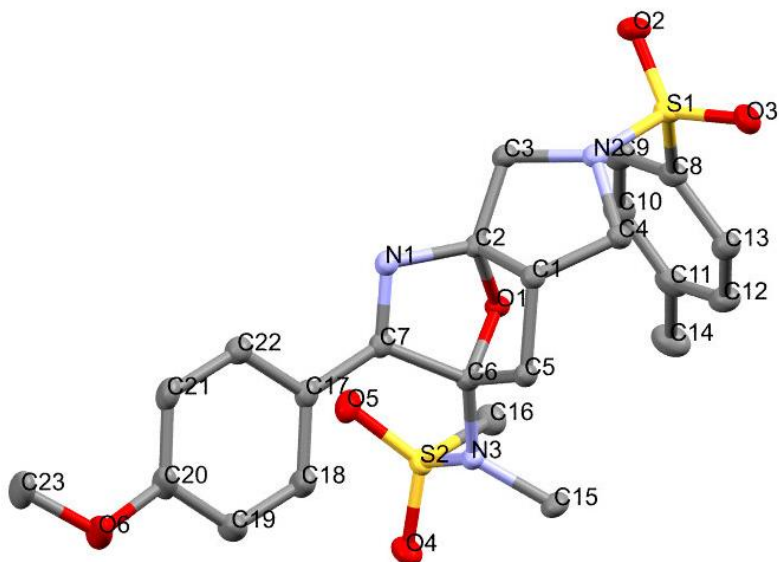
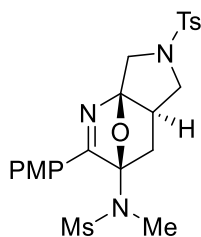


Table 1 Crystal data and structure refinement for 120a.

Identification code	120a
Empirical formula	C <sub>9.2</sub> H <sub>11.2</sub> N <sub>1.2</sub> O <sub>2.4</sub> S <sub>0.8</sub>
Formula weight	202.64
Temperature/K	100.00(10)
Crystal system	monoclinic
Space group	P2 <sub>1</sub> /c
a/Å	8.3705(2)
b/Å	43.5771(12)
c/Å	6.6468(2)
α/°	90
β/°	104.585(3)
γ/°	90
Volume/Å <sup>3</sup>	2346.37(12)
Z	10
ρ <sub>calc</sub> /cm <sup>3</sup>	1.434

$\mu/\text{mm}^{-1}$	2.450
F(000)	1068.0
Crystal size/ $\text{mm}^3$	$0.111 \times 0.099 \times 0.049$
Radiation	$\text{CuK}\alpha$ ( $\lambda = 1.54184$ )
2 $\Theta$ range for data collection/ $^\circ$	8.116 to 140.1
Index ranges	$-10 \leq h \leq 8, -52 \leq k \leq 52, -8 \leq l \leq 8$
Reflections collected	15878
Independent reflections	4444 [ $R_{\text{int}} = 0.0402, R_{\text{sigma}} = 0.0369$ ]
Data/restraints/parameters	4444/0/311
Goodness-of-fit on $F^2$	1.050
Final R indexes [ $I \geq 2\sigma(I)$ ]	$R_1 = 0.0369, wR_2 = 0.0895$
Final R indexes [all data]	$R_1 = 0.0433, wR_2 = 0.0941$
Largest diff. peak/hole / $e \text{ \AA}^{-3}$	0.46/-0.77

**Table 2 Fractional Atomic Coordinates ( $\times 10^4$ ) and Equivalent Isotropic Displacement Parameters ( $\text{\AA}^2 \times 10^3$ ) for 120a.  $U_{\text{eq}}$  is defined as 1/3 of the trace of the orthogonalised  $U_{ij}$  tensor.**

Atom	x	y	z	U(eq)
S2	6125.0(5)	3874.8(2)	5906.8(7)	17.19(12)
S1	550.3(5)	3128.8(2)	-1966.1(7)	17.32(12)
O1	3052.0(14)	3709.0(3)	2458.5(19)	14.6(2)
O2	-686.5(16)	2945.7(3)	-1380(2)	23.6(3)
O4	7663.1(16)	4022.8(3)	6831(2)	24.7(3)
O5	4847.5(16)	3878.7(3)	7002(2)	23.2(3)
O3	570.1(17)	3159.9(3)	-4110(2)	22.9(3)
O6	2933(2)	5228.1(3)	8698(3)	31.3(3)
N1	1010.8(18)	4002.5(3)	3286(2)	16.5(3)
N3	5369.5(18)	4043.8(3)	3635(2)	15.9(3)
N2	342.3(18)	3475.0(3)	-1140(2)	16.2(3)
C7	2382(2)	4149.8(4)	3904(3)	15.6(3)
C6	3624(2)	4022.4(4)	2738(3)	15.1(3)
C2	1339(2)	3789.7(4)	1738(3)	15.4(3)
C1	1348(2)	3977.6(4)	-237(3)	15.7(3)
C5	2984(2)	4156.0(4)	494(3)	16.0(3)
C13	3893(2)	3066.6(4)	-1265(3)	21.0(4)
C17	2542(2)	4428.5(4)	5190(3)	17.3(4)
C4	1303(2)	3724.0(4)	-1833(3)	17.2(4)
C8	2503(2)	2996.4(4)	-557(3)	18.8(4)
C3	255(2)	3515.8(4)	1047(3)	17.8(4)
C20	2717(3)	4963.8(4)	7559(3)	23.4(4)
C12	5441(2)	2986.0(4)	-55(3)	22.1(4)
C11	5632(2)	2836.0(4)	1846(3)	23.1(4)
C22	1174(2)	4532.2(4)	5841(3)	20.5(4)
C9	2660(2)	2844.6(4)	1323(3)	22.7(4)
C10	4216(3)	2765.9(4)	2509(3)	24.2(4)
C21	1256(2)	4797.7(4)	7017(3)	23.2(4)
C18	3995(2)	4599.0(5)	5741(3)	24.8(4)
C14	7319(3)	2747.9(5)	3134(4)	30.2(5)
C19	4089(3)	4864.6(5)	6915(3)	26.9(4)
C16	6519(2)	3491.3(4)	5351(3)	23.4(4)
C15	6475(2)	4030.5(5)	2221(3)	21.6(4)
C23	1684(3)	5308.0(5)	9720(4)	35.4(5)

**Table 3 Anisotropic Displacement Parameters ( $\text{\AA}^2 \times 10^3$ ) for 120a. The Anisotropic displacement factor exponent takes the form:  $-2\pi^2[h^2a^{*2}U_{11}+2hka^*b^*U_{12}+\dots]$ .**

Atom	$U_{11}$	$U_{22}$	$U_{33}$	$U_{23}$	$U_{13}$	$U_{12}$
------	----------	----------	----------	----------	----------	----------



S2	13.2(2)	21.2(2)	15.6(2)	-2.88(16)	0.90(16)	2.57(15)
S1	13.6(2)	17.3(2)	19.6(2)	-1.62(16)	1.46(16)	-1.33(15)
O1	11.8(6)	15.0(6)	16.7(6)	0.4(5)	2.8(5)	-0.1(4)
O2	17.7(6)	21.9(7)	30.3(7)	-0.5(5)	4.7(5)	-4.7(5)
O4	16.3(6)	28.9(7)	25.0(7)	-6.9(6)	-2.2(5)	1.4(5)
O5	19.6(7)	33.7(8)	16.3(6)	1.3(5)	4.5(5)	5.5(5)
O3	22.8(7)	24.9(7)	19.3(7)	-4.8(5)	1.9(5)	-0.2(5)
O6	41.6(9)	20.9(7)	39.0(9)	-11.4(6)	23.9(7)	-5.6(6)
N1	14.8(7)	19.6(7)	15.0(7)	0.6(6)	3.9(6)	1.5(6)
N3	11.8(7)	19.8(7)	16.3(7)	-1.5(6)	3.8(6)	0.2(5)
N2	12.8(7)	17.9(7)	17.4(7)	0.3(6)	2.7(6)	0.3(6)
C7	14.9(8)	17.5(8)	14.4(8)	2.3(7)	3.7(6)	2.8(6)
C6	13.2(8)	14.8(8)	17.3(8)	-0.4(6)	3.9(7)	-0.4(6)
C2	11.1(8)	19.3(8)	15.9(8)	0.4(7)	3.5(6)	1.3(6)
C1	14.1(8)	16.9(8)	15.6(8)	1.2(7)	3.1(7)	1.0(6)
C5	15.4(8)	17.3(8)	15.6(8)	0.0(7)	4.6(7)	-0.6(6)
C13	20.6(9)	19.2(9)	23.7(10)	1.4(7)	6.7(8)	1.4(7)
C17	18.9(9)	18.0(8)	15.6(8)	2.1(7)	5.6(7)	3.9(7)
C4	15.9(8)	18.7(8)	16.8(9)	-0.1(7)	3.7(7)	-1.4(7)
C8	16.5(8)	14.9(8)	24.0(9)	-0.8(7)	3.1(7)	1.1(7)
C3	15.3(8)	20.0(8)	19.2(9)	-0.4(7)	6.3(7)	-1.2(7)
C20	33.9(11)	15.5(9)	23.8(10)	-1.8(7)	13.1(8)	0.3(7)
C12	16.0(9)	19.3(9)	31.2(11)	-0.3(8)	6.2(8)	1.0(7)
C11	21.5(9)	14.8(8)	29.5(10)	-4.0(7)	0.0(8)	2.0(7)
C22	18.3(9)	21.4(9)	22.3(9)	0.0(7)	6.0(7)	1.6(7)
C9	21.7(9)	18.8(9)	28.5(10)	1.9(8)	8.1(8)	1.1(7)
C10	28.4(10)	19.0(9)	23.5(10)	3.9(7)	3.3(8)	2.7(7)
C21	25.8(10)	23.4(9)	24.1(10)	-1.0(8)	13.1(8)	4.5(7)
C18	22.8(10)	24.4(10)	30.3(11)	-6.2(8)	12.6(8)	-0.8(8)
C14	23.8(10)	24.8(10)	35.7(12)	-1.2(9)	-4.2(9)	3.9(8)
C19	26.8(10)	23.3(10)	33.0(11)	-7.5(8)	12.0(9)	-5.1(8)
C16	21.7(9)	21.4(9)	25.1(10)	-0.3(7)	2.3(8)	4.4(7)
C15	14.3(9)	28.0(10)	23.6(10)	-1.1(7)	6.6(7)	-1.0(7)
C23	45.3(13)	28.1(11)	41.4(13)	-12.1(9)	26.7(11)	-2.2(9)

**Table 4 Bond Lengths for 120a.**

Atom	Atom	Length/Å	Atom	Atom	Length/Å
S2	O4	1.4325(14)	C7	C17	1.472(3)
S2	O5	1.4372(14)	C6	C5	1.564(2)
S2	N3	1.6555(16)	C2	C1	1.549(2)
S2	C16	1.7604(19)	C2	C3	1.500(2)
S1	O2	1.4366(14)	C1	C5	1.543(2)
S1	O3	1.4359(15)	C1	C4	1.526(2)
S1	N2	1.6296(15)	C13	C8	1.394(3)
S1	C8	1.7639(18)	C13	C12	1.388(3)
O1	C6	1.443(2)	C17	C22	1.397(3)
O1	C2	1.436(2)	C17	C18	1.392(3)
O6	C20	1.365(2)	C8	C9	1.391(3)
O6	C23	1.426(3)	C20	C21	1.388(3)
N1	C7	1.289(2)	C20	C19	1.392(3)
N1	C2	1.462(2)	C12	C11	1.395(3)
N3	C6	1.436(2)	C11	C10	1.399(3)

N3	C15	1.477(2)	C11	C14	1.505(3)
N2	C4	1.491(2)	C22	C21	1.388(3)
N2	C3	1.484(2)	C9	C10	1.385(3)
C7	C6	1.548(2)	C18	C19	1.387(3)

**Table 5 Bond Angles for 120a.**

Atom	Atom	Atom	Angle/°	Atom	Atom	Atom	Angle/°
O4	S2	O5	118.72(9)	O1	C2	C1	101.23(13)
O4	S2	N3	106.65(8)	O1	C2	C3	112.56(14)
O4	S2	C16	108.76(9)	N1	C2	C1	107.64(14)
O5	S2	N3	107.13(8)	N1	C2	C3	120.92(15)
O5	S2	C16	108.65(9)	C3	C2	C1	107.03(14)
N3	S2	C16	106.24(9)	C5	C1	C2	101.09(13)
O2	S1	N2	106.09(8)	C4	C1	C2	101.63(14)
O2	S1	C8	108.01(9)	C4	C1	C5	116.65(15)
O3	S1	O2	120.73(8)	C1	C5	C6	100.17(13)
O3	S1	N2	106.03(8)	C12	C13	C8	119.04(18)
O3	S1	C8	108.49(9)	C22	C17	C7	119.00(17)
N2	S1	C8	106.69(8)	C18	C17	C7	122.59(17)
C2	O1	C6	94.71(12)	C18	C17	C22	118.39(17)
C20	O6	C23	117.33(17)	N2	C4	C1	103.47(14)
C7	N1	C2	103.29(14)	C13	C8	S1	119.29(15)
C6	N3	S2	117.72(12)	C9	C8	S1	119.84(14)
C6	N3	C15	117.92(15)	C9	C8	C13	120.68(17)
C15	N3	S2	113.96(12)	N2	C3	C2	102.71(14)
C4	N2	S1	117.24(12)	O6	C20	C21	124.69(18)
C3	N2	S1	118.47(12)	O6	C20	C19	115.35(18)
C3	N2	C4	112.27(14)	C21	C20	C19	119.96(18)
N1	C7	C6	108.56(15)	C13	C12	C11	121.39(18)
N1	C7	C17	122.65(16)	C12	C11	C10	118.34(18)
C17	C7	C6	127.78(15)	C12	C11	C14	120.78(19)
O1	C6	C7	99.27(13)	C10	C11	C14	120.88(19)
O1	C6	C5	101.93(13)	C21	C22	C17	121.02(18)
N3	C6	O1	112.64(14)	C10	C9	C8	119.42(18)
N3	C6	C7	120.66(15)	C9	C10	C11	121.13(19)
N3	C6	C5	116.13(14)	C20	C21	C22	119.76(18)
C7	C6	C5	103.41(13)	C19	C18	C17	121.02(18)
O1	C2	N1	105.63(13)	C18	C19	C20	119.84(19)

**Table 6 Torsion Angles for 120a.**

A	B	C	D	Angle/°	A	B	C	D	Angle/°
S2	N3	C6	O1	-57.04(18)	C6	C7	C17	C22	169.74(17)
S2	N3	C6	C7	59.72(19)	C6	C7	C17	C18	-8.5(3)
S2	N3	C6	C5	-174.04(12)	C2	O1	C6	N3	175.66(15)
S1	N2	C4	C1	-159.95(12)	C2	O1	C6	C7	46.76(14)
S1	N2	C3	C2	137.01(12)	C2	O1	C6	C5	-59.19(14)
S1	C8	C9	C10	-174.23(15)	C2	N1	C7	C6	-0.96(18)
O1	C6	C5	C1	34.58(15)	C2	N1	C7	C17	168.35(16)
O1	C2	C1	C5	-38.67(16)	C2	C1	C5	C6	2.23(16)
O1	C2	C1	C4	81.80(15)	C2	C1	C4	N2	31.54(16)

O1 C2 C3 N2	-85.01(16)	C1 C2 C3 N2	25.34(17)
O2 S1 N2 C4	-170.62(12)	C5 C1 C4 N2	140.40(15)
O2 S1 N2 C3	49.55(14)	C13 C8 C9 C10	0.7(3)
O2 S1 C8 C13	160.49(15)	C13 C12 C11 C10	0.4(3)
O2 S1 C8 C9	-24.48(18)	C13 C12 C11 C14	179.53(18)
O4 S2 N3 C6	-157.77(13)	C17 C7 C6 O1	160.54(16)
O4 S2 N3 C15	57.90(14)	C17 C7 C6 N3	37.2(3)
O5 S2 N3 C6	-29.67(15)	C17 C7 C6 C5	-94.73(19)
O5 S2 N3 C15	-174.00(13)	C17 C22 C21 C20	0.0(3)
O3 S1 N2 C4	-41.11(14)	C17 C18 C19 C20	0.0(3)
O3 S1 N2 C3	179.06(12)	C4 N2 C3 C2	-4.69(18)
O3 S1 C8 C13	28.01(17)	C4 C1 C5 C6	-106.94(16)
O3 S1 C8 C9	-156.96(15)	C8 S1 N2 C4	74.39(14)
O6 C20 C21 C22	179.66(19)	C8 S1 N2 C3	-65.44(14)
O6 C20 C19 C18	-179.73(19)	C8 C13 C12 C11	0.2(3)
N1 C7 C6 O1	-30.85(17)	C8 C9 C10 C11	-0.1(3)
N1 C7 C6 N3	-154.23(16)	C3 N2 C4 C1	-17.74(18)
N1 C7 C6 C5	73.88(17)	C3 C2 C1 C5	-156.69(14)
N1 C7 C17 C22	2.6(3)	C3 C2 C1 C4	-36.23(17)
N1 C7 C17 C18	-175.60(18)	C12 C13 C8 S1	174.24(14)
N1 C2 C1 C5	71.90(16)	C12 C13 C8 C9	-0.7(3)
N1 C2 C1 C4	-167.63(13)	C12 C11 C10 C9	-0.4(3)
N1 C2 C3 N2	148.91(15)	C22 C17 C18 C19	0.3(3)
N3 C6 C5 C1	157.38(15)	C21 C20 C19 C18	-0.3(3)
N2 S1 C8 C13	-85.83(16)	C18 C17 C22 C21	-0.3(3)
N2 S1 C8 C9	89.20(16)	C14 C11 C10 C9	-179.55(18)
C7 N1 C2 O1	33.59(17)	C19 C20 C21 C22	0.3(3)
C7 N1 C2 C1	-73.94(17)	C16 S2 N3 C6	86.33(14)
C7 N1 C2 C3	162.79(16)	C16 S2 N3 C15	-58.00(15)
C7 C6 C5 C1	-68.11(15)	C15 N3 C6 O1	85.88(19)
C7 C17 C22 C21	-178.57(17)	C15 N3 C6 C7	-157.37(16)
C7 C17 C18 C19	178.49(19)	C15 N3 C6 C5	-31.1(2)
C6 O1 C2 N1	-51.48(15)	C23 O6 C20 C21	12.1(3)
C6 O1 C2 C1	60.63(14)	C23 O6 C20 C19	-168.5(2)
C6 O1 C2 C3	174.57(15)		

**Table 7 Hydrogen Atom Coordinates ( $\text{\AA}\times 10^4$ ) and Isotropic Displacement Parameters ( $\text{\AA}^2\times 10^3$ ) for 120a.**

Atom	x	y	z	U(eq)
H2	-788.56	3525.13	-1905.63	19
H1	393.06	4114.89	-639.96	19
H5A	2800	4375.64	516.58	19
H5B	3735.65	4111.85	-365.34	19
H13	3783.29	3166.08	-2530.98	25
H4A	756.82	3793.31	-3222.93	21
H4B	2408.62	3655.31	-1817.27	21
H3A	673.84	3336.57	1878.95	21
H3B	-868	3555.25	1126.35	21
H12	6371.34	3032.94	-520.4	27
H22	192.96	4421.59	5481	25
H9	1727.36	2796.29	1779.98	27
H10	4320.98	2664.79	3767.61	29
H21	336.18	4864.03	7439.81	28

H18	4915.23	4533.68	5315	30
H14A	7479.07	2531.21	3010.28	45
H14B	7410.02	2798.66	4563.57	45
H14C	8144.52	2857.54	2648.85	45
H19	5067.24	4976.09	7271.22	32
H16A	7354.7	3485.9	4592.96	35
H16B	5524.54	3399.6	4529.76	35
H16C	6891.8	3379.41	6627.22	35
H15A	7602.46	4025.82	3023.23	32
H15B	6300.55	4208.23	1339.54	32
H15C	6241.11	3848.77	1382.13	32
H23A	680	5355.77	8699.95	53
H23B	2033.43	5483.51	10592.19	53
H23C	1496.14	5138.49	10553.83	53

## Experimental

A suitable crystal was selected on a **SuperNova, Dual, Cu at zero, Atlas** diffractometer. The crystal was kept at 100.00(10) K during data collection. Using Olex2,<sup>275</sup> the structure was solved with the ShelXT<sup>276</sup> structure solution program using Intrinsic Phasing and refined with the ShelXL<sup>277</sup> refinement package using Least Squares minimisation.

## Crystal structure determination of [120a]

**Crystal Data** for  $C_{9.2}H_{11.2}N_{1.2}O_{2.4}S_{0.8}$  ( $M = 202.64$  g/mol): monoclinic, space group  $P2_1/c$  (no. 14),  $a = 8.3705(2)$  Å,  $b = 43.5771(12)$  Å,  $c = 6.6468(2)$  Å,  $\beta = 104.585(3)^\circ$ ,  $V = 2346.37(12)$  Å<sup>3</sup>,  $Z = 10$ ,  $T = 100.00(10)$  K,  $\mu(\text{CuK}\alpha) = 2.450$  mm<sup>-1</sup>,  $D_{\text{calc}} = 1.434$  g/cm<sup>3</sup>, 15878 reflections measured ( $8.116^\circ \leq 2\theta \leq 140.1^\circ$ ), 4444 unique ( $R_{\text{int}} = 0.0402$ ,  $R_{\text{sigma}} = 0.0369$ ) which were used in all calculations. The final  $R_1$  was 0.0369 ( $I > 2\sigma(I)$ ) and  $wR_2$  was 0.0941 (all data).

## Refinement model description

Number of restraints - 0, number of constraints - unknown.

Details:

1. Fixed Uiso

At 1.2 times of:

All C(H) groups, All C(H,H) groups, All N(H) groups

At 1.5 times of:

All C(H,H,H) groups

2.a Ternary CH refined with riding coordinates:

N2(H2), C1(H1)

2.b Secondary CH2 refined with riding coordinates:

C5(H5A,H5B), C4(H4A,H4B), C3(H3A,H3B)

2.c Aromatic/amide H refined with riding coordinates:

C13(H13), C12(H12), C22(H22), C9(H9), C10(H10), C21(H21), C18(H18), C19(H19)

2.d Idealised Me refined as rotating group:

C14(H14A,H14B,H14C), C16(H16A,H16B,H16C), C15(H15A,H15B,H15C), C23(H23A,H23B,H23C)

### 8.3 Formamide 358a

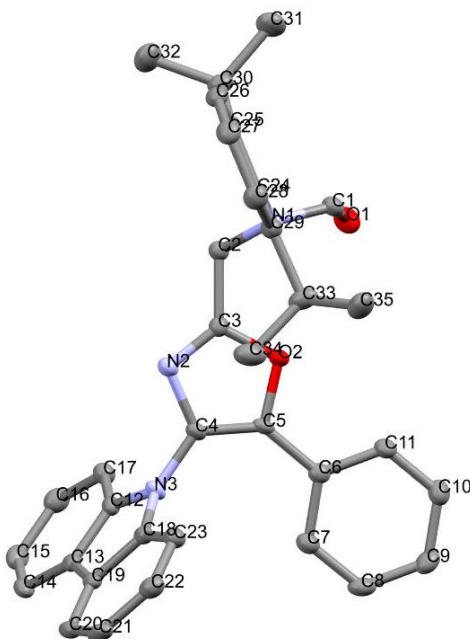
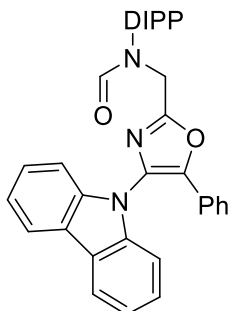


**Table 1** Crystal data and structure refinement for 358A.

Identification code	358A
Empirical formula	C <sub>35</sub> H <sub>33</sub> N <sub>3</sub> O <sub>2</sub>
Formula weight	527.64
Temperature/K	100.00(10)
Crystal system	monoclinic
Space group	P2 <sub>1</sub> /n
a/Å	15.1958(6)
b/Å	8.6814(4)
c/Å	21.6384(8)
α/°	90
β/°	98.134(4)
γ/°	90
Volume/Å <sup>3</sup>	2825.85(19)
Z	4
ρ <sub>calc</sub> /cm <sup>3</sup>	1.240
μ/mm <sup>-1</sup>	0.077
F(000)	1120.0
Crystal size/mm <sup>3</sup>	0.389 × 0.331 × 0.163
Radiation	MoKα (λ = 0.71073)
2θ range for data collection/°	6.654 to 52.044
Index ranges	-13 ≤ h ≤ 18, -10 ≤ k ≤ 8, -26 ≤ l ≤ 22
Reflections collected	12655
Independent reflections	5563 [R <sub>int</sub> = 0.0227, R <sub>sigma</sub> = 0.0349]
Data/restraints/parameters	5563/0/365
Goodness-of-fit on F <sup>2</sup>	1.076
Final R indexes [I ≥ 2σ (I)]	R <sub>1</sub> = 0.0435, wR <sub>2</sub> = 0.0995
Final R indexes [all data]	R <sub>1</sub> = 0.0530, wR <sub>2</sub> = 0.1057
Largest diff. peak/hole / e Å <sup>-3</sup>	0.21/-0.22

**Table 2 Fractional Atomic Coordinates ( $\times 10^4$ ) and Equivalent Isotropic Displacement Parameters ( $\text{\AA}^2 \times 10^3$ ) for 358A.**  
 **$U_{eq}$  is defined as 1/3 of of the trace of the orthogonalised  $U_{ij}$  tensor.**

Atom	x	y	z	$U(eq)$
C1	10179.6(10)	7590.2(19)	-718.2(7)	19.7(3)
C2	9009.6(10)	5687.6(17)	-794.2(7)	16.9(3)
C3	8466.6(9)	5859.1(17)	-277.8(7)	15.8(3)
C4	7556.5(9)	5673.2(17)	368.2(7)	15.6(3)
C5	8228.8(9)	6557.7(17)	648.5(7)	15.8(3)
C6	8451.6(9)	7338.6(17)	1246.6(7)	17.3(3)
C7	7911.7(10)	7198.1(18)	1717.6(7)	20.5(3)
C8	8127.8(10)	7975.5(19)	2276.4(7)	23.8(4)
C9	8875.4(11)	8905.8(19)	2376.4(7)	24.2(4)
C10	9418.0(11)	9033.6(19)	1916.2(7)	24.8(4)
C11	9210.4(10)	8257.9(18)	1355.7(7)	20.4(3)
C12	6723.5(9)	3622.8(17)	816.9(6)	17.1(3)
C13	5857.9(10)	3417.3(18)	962.6(6)	18.1(3)
C14	5626.4(11)	1979.1(19)	1180.1(7)	23.1(4)
C15	6249.7(11)	819.7(19)	1248.5(7)	26.7(4)
C16	7102.7(11)	1054.3(19)	1093.3(7)	25.3(4)
C17	7351(1)	2462.8(18)	872.0(7)	21.3(3)
C18	5997.6(9)	5894.4(18)	620.5(6)	16.9(3)
C19	5395.6(9)	4861.0(18)	834.1(6)	17.7(3)
C20	4524.6(10)	5342(2)	858.2(7)	22.0(3)
C21	4285.6(10)	6830(2)	680.9(7)	24.0(4)
C22	4899.6(10)	7843(2)	483.4(7)	23.4(4)
C23	5768.5(10)	7391.7(18)	449.4(7)	20.9(3)
C24	8971.6(9)	7861.0(17)	-1567.8(7)	15.8(3)
C25	9220.6(9)	7295.7(17)	-2125.2(7)	17.7(3)
C26	8848.4(10)	7991.0(19)	-2680.8(7)	21.5(3)
C27	8253.8(10)	9191.3(19)	-2682.7(7)	23.3(4)
C28	8026.8(10)	9740.8(19)	-2125.9(7)	23.0(3)
C29	8383.7(10)	9096.5(18)	-1555.0(7)	18.9(3)
C30	9902.5(10)	6014.8(19)	-2136.3(7)	22.0(3)
C31	10762.4(11)	6646(2)	-2333.3(9)	32.4(4)
C32	9543.1(12)	4691(2)	-2558.8(9)	33.0(4)
C33	8139.5(11)	9754(2)	-948.8(7)	24.7(4)
C34	7217.4(12)	9221(2)	-831.9(8)	33.1(4)
C35	8185.5(12)	11509(2)	-937.6(9)	32.8(4)
N1	9365.9(8)	7146.7(14)	-990.3(5)	15.5(3)
N2	7710.5(8)	5244.4(14)	-227.8(6)	17.2(3)
N3	6810.1(8)	5138.6(14)	619.0(6)	17.3(3)
O1	10621.3(7)	6930.5(14)	-286.7(5)	26.4(3)
O2	8826.4(6)	6697.2(12)	226.3(4)	16.8(2)

**Table 3 Anisotropic Displacement Parameters ( $\text{\AA}^2 \times 10^3$ ) for 358A. The Anisotropic displacement factor exponent takes the form:  $-2\pi^2[h^2a^{*2}U_{11}+2hka^*b^*U_{12}+\dots]$ .**

Atom	$U_{11}$	$U_{22}$	$U_{33}$	$U_{23}$	$U_{13}$	$U_{12}$
C1	16.9(7)	23.0(8)	20.0(8)	0.6(6)	5.1(6)	-1.4(6)
C2	17.1(7)	16.4(7)	17.6(7)	0.8(6)	3.7(6)	0.2(6)
C3	17.6(7)	14.6(7)	15.1(7)	1.8(6)	1.2(6)	0.9(6)
C4	13.3(7)	16.1(7)	18.3(7)	1.9(6)	5.2(5)	1.0(6)
C5	13.8(7)	17.3(7)	17.8(7)	4.1(6)	7.6(5)	1.7(6)

C6	18.1(7)	16.0(7)	18.0(7)	3.3(6)	3.3(6)	2.5(6)
C7	18.4(7)	22.3(8)	21.2(8)	3.4(6)	4.7(6)	0.2(7)
C8	26.4(8)	27.8(9)	19.1(8)	3.8(7)	9.7(6)	5.3(7)
C9	33.6(9)	22.3(8)	16.0(7)	-0.4(6)	1.3(6)	1.7(7)
C10	26.8(8)	23.9(8)	23.1(8)	1.7(7)	1.5(7)	-5.8(7)
C11	21.2(8)	22.3(8)	18.6(7)	1.9(6)	6.3(6)	-2.2(7)
C12	19.4(7)	18.1(8)	14.1(7)	-0.4(6)	3.0(6)	-4.8(6)
C13	19.2(7)	23.4(8)	12.1(7)	-3.6(6)	3.3(6)	-4.8(6)
C14	25.6(8)	27.9(9)	17.1(7)	-0.8(7)	7.3(6)	-10.2(7)
C15	39.1(10)	20.5(8)	21.1(8)	1.9(7)	6.6(7)	-8.1(8)
C16	32.6(9)	20.4(8)	23.1(8)	1.4(7)	4.0(7)	3.5(7)
C17	20.0(7)	22.9(8)	21.3(8)	0.7(7)	4.1(6)	-1.1(7)
C18	14.4(7)	22.3(8)	14.0(7)	-2.7(6)	2.0(5)	-1.0(6)
C19	17.2(7)	24.2(8)	12.2(7)	-2.7(6)	4.0(5)	-4.6(6)
C20	16.6(7)	34.3(9)	16.2(7)	-4.5(7)	5.8(6)	-4.2(7)
C21	16.9(7)	38(1)	17.8(8)	-6.6(7)	4.4(6)	4.6(7)
C22	24.0(8)	26.1(9)	20.0(8)	-2.8(7)	2.6(6)	5.1(7)
C23	19.6(7)	23.1(8)	20.5(8)	-1.1(7)	5.0(6)	-1.7(7)
C24	13.6(7)	18.1(7)	15.7(7)	1.6(6)	2.4(5)	-1.8(6)
C25	16.5(7)	18.7(8)	18.4(7)	-1.0(6)	3.8(6)	-2.2(6)
C26	23.0(8)	25.9(8)	15.6(7)	-2.0(6)	3.5(6)	-1.8(7)
C27	24.6(8)	26.2(9)	18.2(8)	3.9(7)	-0.3(6)	0.5(7)
C28	20.0(8)	23.0(8)	25.4(8)	0.6(7)	0.8(6)	5.3(7)
C29	17.1(7)	20.7(8)	19.2(7)	-0.1(6)	3.0(6)	0.6(6)
C30	24.0(8)	25.1(8)	17.7(7)	-0.5(6)	5.7(6)	5.3(7)
C31	24.6(9)	34.6(10)	40.2(10)	-3.5(8)	12.1(7)	5.9(8)
C32	33.3(10)	27.1(9)	38.6(10)	-8.5(8)	4.7(8)	6.0(8)
C33	25.8(8)	30.5(9)	17.5(8)	-0.3(7)	2.4(6)	12.1(7)
C34	37.1(10)	33.3(10)	32.4(10)	4.3(8)	16.5(8)	6.2(8)
C35	28.6(9)	34.2(10)	35.8(10)	-12.8(8)	5.2(7)	3.5(8)
N1	14.1(6)	18.0(6)	14.5(6)	1.0(5)	2.9(5)	-0.6(5)
N2	15.6(6)	18.1(6)	18.4(6)	1.1(5)	4.2(5)	-0.4(5)
N3	12.6(6)	17.3(6)	23.0(6)	1.3(5)	6.1(5)	-1.2(5)
O1	20.1(5)	34.0(7)	23.7(6)	7.6(5)	-1.9(5)	0.1(5)
O2	15.7(5)	19.5(5)	16.2(5)	-0.8(4)	5.6(4)	-1.9(4)

**Table 4 Bond Lengths for 358A.**

Atom	Atom	Length/Å	Atom	Atom	Length/Å
C1	N1	1.3483(18)	C15	C16	1.399(2)
C1	O1	1.2136(18)	C16	C17	1.385(2)
C2	C3	1.487(2)	C18	C19	1.405(2)
C2	N1	1.4638(19)	C18	C23	1.383(2)
C3	N2	1.2853(18)	C18	N3	1.3986(19)
C3	O2	1.3599(17)	C19	C20	1.396(2)
C4	C5	1.351(2)	C20	C21	1.382(2)
C4	N2	1.3935(19)	C21	C22	1.393(2)
C4	N3	1.4038(18)	C22	C23	1.389(2)
C5	C6	1.458(2)	C24	C25	1.403(2)
C5	O2	1.3816(17)	C24	C29	1.399(2)
C6	C7	1.401(2)	C24	N1	1.4468(18)
C6	C11	1.395(2)	C25	C26	1.392(2)
C7	C8	1.383(2)	C25	C30	1.523(2)

C8	C9	1.386(2)	C26	C27	1.379(2)
C9	C10	1.384(2)	C27	C28	1.384(2)
C10	C11	1.384(2)	C28	C29	1.394(2)
C12	C13	1.407(2)	C29	C33	1.524(2)
C12	C17	1.380(2)	C30	C31	1.532(2)
C12	N3	1.3959(19)	C30	C32	1.521(2)
C13	C14	1.397(2)	C33	C34	1.531(2)
C13	C19	1.444(2)	C33	C35	1.525(2)
C14	C15	1.376(2)			

**Table 5 Bond Angles for 358A.**

Atom	Atom	Atom	Angle/°	Atom	Atom	Atom	Angle/°
O1	C1	N1	125.06(15)	C20	C19	C13	133.63(15)
N1	C2	C3	113.48(12)	C20	C19	C18	119.10(14)
N2	C3	C2	128.26(13)	C21	C20	C19	118.85(15)
N2	C3	O2	114.67(13)	C20	C21	C22	120.97(14)
O2	C3	C2	116.95(12)	C23	C22	C21	121.40(15)
C5	C4	N2	110.61(13)	C18	C23	C22	117.16(15)
C5	C4	N3	127.97(14)	C25	C24	N1	117.62(13)
N2	C4	N3	121.34(13)	C29	C24	C25	122.42(13)
C4	C5	C6	136.78(14)	C29	C24	N1	119.94(13)
C4	C5	O2	106.20(12)	C24	C25	C30	122.42(13)
O2	C5	C6	117.02(12)	C26	C25	C24	117.70(14)
C7	C6	C5	121.25(13)	C26	C25	C30	119.83(13)
C11	C6	C5	119.94(13)	C27	C26	C25	121.08(14)
C11	C6	C7	118.80(14)	C26	C27	C28	120.13(14)
C8	C7	C6	120.16(14)	C27	C28	C29	121.29(15)
C7	C8	C9	120.59(15)	C24	C29	C33	122.58(13)
C10	C9	C8	119.54(14)	C28	C29	C24	117.36(14)
C11	C10	C9	120.42(15)	C28	C29	C33	120.05(14)
C10	C11	C6	120.48(14)	C25	C30	C31	110.65(13)
C17	C12	C13	123.00(14)	C32	C30	C25	111.96(13)
C17	C12	N3	128.33(13)	C32	C30	C31	110.53(14)
N3	C12	C13	108.67(13)	C29	C33	C34	111.65(14)
C12	C13	C19	106.95(13)	C29	C33	C35	111.83(14)
C14	C13	C12	118.49(14)	C35	C33	C34	109.93(14)
C14	C13	C19	134.56(14)	C1	N1	C2	118.32(12)
C15	C14	C13	119.19(14)	C1	N1	C24	119.80(12)
C14	C15	C16	120.99(15)	C24	N1	C2	119.76(11)
C17	C16	C15	121.23(15)	C3	N2	C4	103.66(12)
C12	C17	C16	117.08(14)	C12	N3	C4	123.14(12)
C23	C18	C19	122.50(14)	C12	N3	C18	108.66(12)
C23	C18	N3	129.00(14)	C18	N3	C4	127.42(12)
N3	C18	C19	108.50(13)	C3	O2	C5	104.85(11)
C18	C19	C13	107.21(13)				

**Table 6 Torsion Angles for 358A.**

A	B	C	D	Angle/°	A	B	C	D	Angle/°
C2	C3	N2	C4	174.40(14)	C24	C25	C26	C27	-0.2(2)
C2	C3	O2	C5	-174.93(12)	C24	C25	C30	C31	-109.96(16)



C3 C2 N1 C1	91.86(16)	C24 C25 C30 C32	126.26(16)
C3 C2 N1 C24	-104.71(14)	C24 C29 C33 C34	-102.89(17)
C4 C5 C6 C7	3.5(3)	C24 C29 C33 C35	133.46(15)
C4 C5 C6 C11	-175.91(17)	C25 C24 C29 C28	1.6(2)
C4 C5 O2 C3	-0.73(15)	C25 C24 C29 C33	-177.56(14)
C5 C4 N2 C3	1.00(16)	C25 C24 N1 C1	82.74(18)
C5 C4 N3 C12	-104.01(18)	C25 C24 N1 C2	-80.44(17)
C5 C4 N3 C18	87.3(2)	C25 C26 C27 C28	0.9(2)
C5 C6 C7 C8	-178.69(14)	C26 C25 C30 C31	67.36(18)
C5 C6 C11 C10	178.50(14)	C26 C25 C30 C32	-56.41(19)
C6 C5 O2 C3	179.30(12)	C26 C27 C28 C29	-0.5(2)
C6 C7 C8 C9	0.3(2)	C27 C28 C29 C24	-0.8(2)
C7 C6 C11 C10	-0.9(2)	C27 C28 C29 C33	178.39(15)
C7 C8 C9 C10	-1.2(2)	C28 C29 C33 C34	78.00(19)
C8 C9 C10 C11	1.0(2)	C28 C29 C33 C35	-45.6(2)
C9 C10 C11 C6	0.1(2)	C29 C24 C25 C26	-1.1(2)
C11 C6 C7 C8	0.7(2)	C29 C24 C25 C30	176.25(14)
C12 C13 C14 C15	0.4(2)	C29 C24 N1 C1	-95.58(17)
C12 C13 C19 C18	-0.51(16)	C29 C24 N1 C2	101.24(16)
C12 C13 C19 C20	176.54(15)	C30 C25 C26 C27	-177.61(14)
C13 C12 C17 C16	-1.3(2)	N1 C2 C3 N2	134.94(15)
C13 C12 N3 C4	-172.18(13)	N1 C2 C3 O2	-49.20(17)
C13 C12 N3 C18	-1.60(16)	N1 C24 C25 C26	-179.41(13)
C13 C14 C15 C16	-1.1(2)	N1 C24 C25 C30	-2.0(2)
C13 C19 C20 C21	-177.85(15)	N1 C24 C29 C28	179.82(13)
C14 C13 C19 C18	-179.93(16)	N1 C24 C29 C33	0.7(2)
C14 C13 C19 C20	-2.9(3)	N2 C3 O2 C5	1.49(16)
C14 C15 C16 C17	0.6(2)	N2 C4 C5 C6	179.81(16)
C15 C16 C17 C12	0.5(2)	N2 C4 C5 O2	-0.14(16)
C17 C12 C13 C14	0.8(2)	N2 C4 N3 C12	72.35(18)
C17 C12 C13 C19	-178.73(13)	N2 C4 N3 C18	-96.38(18)
C17 C12 N3 C4	7.8(2)	N3 C4 C5 C6	-3.5(3)
C17 C12 N3 C18	178.42(14)	N3 C4 C5 O2	176.53(13)
C18 C19 C20 C21	-1.1(2)	N3 C4 N2 C3	-175.93(13)
C19 C13 C14 C15	179.79(15)	N3 C12 C13 C14	-179.17(12)
C19 C18 C23 C22	-1.3(2)	N3 C12 C13 C19	1.29(16)
C19 C18 N3 C4	171.34(13)	N3 C12 C17 C16	178.71(14)
C19 C18 N3 C12	1.28(15)	N3 C18 C19 C13	-0.46(16)
C19 C20 C21 C22	-0.3(2)	N3 C18 C19 C20	-178.02(12)
C20 C21 C22 C23	0.9(2)	N3 C18 C23 C22	178.60(14)
C21 C22 C23 C18	-0.1(2)	O1 C1 N1 C2	-5.7(2)
C23 C18 C19 C13	179.49(13)	O1 C1 N1 C24	-169.15(15)
C23 C18 C19 C20	1.9(2)	O2 C3 N2 C4	-1.54(16)
C23 C18 N3 C4	-8.6(2)	O2 C5 C6 C7	-176.57(13)
C23 C18 N3 C12	-178.68(14)	O2 C5 C6 C11	4.0(2)

**Table 7 Hydrogen Atom Coordinates ( $\text{\AA} \times 10^4$ ) and Isotropic Displacement Parameters ( $\text{\AA}^2 \times 10^3$ ) for 358A.**

Atom	x	y	z	U(eq)
H1	10421.05	8469.83	-873.06	24
H2A	9500.11	4993.65	-660.94	20
H2B	8646	5221.58	-1149.87	20
H7	7406.82	6580.71	1654.28	25

H8	7768.13	7872.95	2587.79	29
H9	9011.7	9440.56	2750.13	29
H10	9925.28	9644.48	1984.1	30
H11	9579.63	8350.35	1049.69	24
H14	5057.76	1807.45	1277.65	28
H15	6101.94	-134.39	1400.05	32
H16	7510.61	249.42	1139.61	30
H17	7915.85	2620.32	765.19	26
H20	4112.27	4671.63	991.26	26
H21	3706.25	7160.48	693.7	29
H22	4724.29	8843.56	371.82	28
H23	6178.62	8067.56	317.19	25
H26	9003.26	7640.24	-3057.02	26
H27	8004.84	9632.43	-3058.75	28
H28	7628.37	10555.83	-2132.8	28
H30	10044.36	5610.56	-1710.99	26
H31A	10638.36	7070.37	-2746.1	49
H31B	11187.49	5826.78	-2330.69	49
H31C	11000.23	7435.09	-2046.68	49
H32A	9006.46	4306.61	-2428.13	50
H32B	9976.89	3881.27	-2533.24	50
H32C	9418.99	5049.99	-2981.85	50
H33	8573.47	9368.68	-605.4	30
H34A	6779.17	9571.79	-1165.5	50
H34B	7089.61	9638.9	-443.59	50
H34C	7204.96	8116.04	-813.13	50
H35A	8760.35	11835.82	-1021.53	49
H35B	8089.67	11875.63	-533.89	49
H35C	7735.46	11919.52	-1250.21	49

## Experimental

A suitable crystal was selected on a **SuperNova, Dual, Cu at zero, Atlas** diffractometer. The crystal was kept at 100.00(10) K during data collection. Using Olex2,<sup>275</sup> the structure was solved with the ShelXS<sup>278</sup> structure solution program using Intrinsic Phasing and refined with the ShelXL<sup>277</sup> refinement package using Least Squares minimisation.

### Crystal structure determination of [358A]

**Crystal Data** for  $C_{35}H_{33}N_3O_2$  ( $M = 527.64$  g/mol): monoclinic, space group  $P2_1/n$  (no. 14),  $a = 15.1958(6)$  Å,  $b = 8.6814(4)$  Å,  $c = 21.6384(8)$  Å,  $\beta = 98.134(4)^\circ$ ,  $V = 2825.85(19)$  Å<sup>3</sup>,  $Z = 4$ ,  $T = 100.00(10)$  K,  $\mu(\text{MoK}\alpha) = 0.077$  mm<sup>-1</sup>,  $D_{\text{calc}} = 1.240$  g/cm<sup>3</sup>, 12655 reflections measured ( $6.654^\circ \leq 2\theta \leq 52.044^\circ$ ), 5563 unique ( $R_{\text{int}} = 0.0227$ ,  $R_{\text{sigma}} = 0.0349$ ) which were used in all calculations. The final  $R_1$  was 0.0435 ( $I > 2\sigma(I)$ ) and  $wR_2$  was 0.1057 (all data).

### Refinement model description

Number of restraints - 0, number of constraints - unknown.

Details:

1. Fixed Uiso

At 1.2 times of:

All C(H) groups, All C(H,H) groups

At 1.5 times of:

All C(H,H,H) groups

2.a Ternary CH refined with riding coordinates:

C30(H30), C33(H33)

2.b Secondary CH2 refined with riding coordinates:

C2(H2A,H2B)

2.c Aromatic/amide H refined with riding coordinates:

C1(H1), C7(H7), C8(H8), C9(H9), C10(H10), C11(H11), C14(H14), C15(H15),

C16(H16), C17(H17), C20(H20), C21(H21), C22(H22), C23(H23), C26(H26), C27(H27),

C28(H28)

2.d Idealised Me refined as rotating group:

C31(H31A,H31B,H31C), C32(H32A,H32B,H32C), C34(H34A,H34B,H34C), C35(H35A,H35B,H35C)

## 8.4 Imidazolium 355•HCl

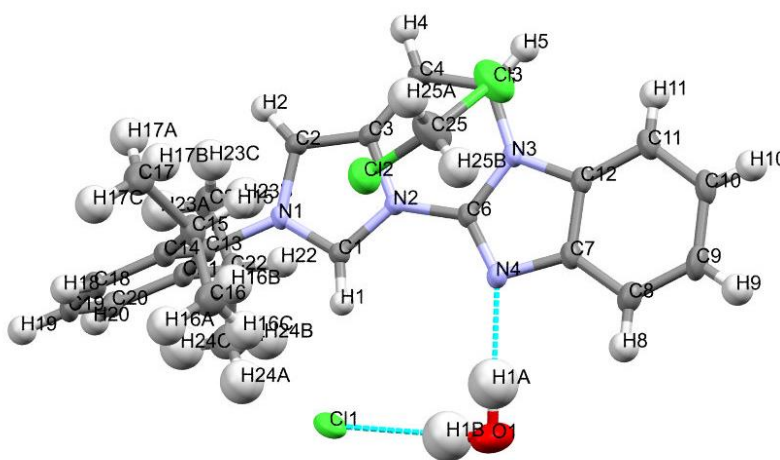
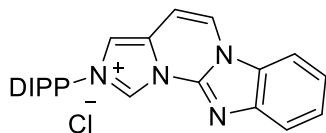


**Table 1** Crystal data and structure refinement for 355•HCl.

Identification code	355•HCL
Empirical formula	C <sub>25</sub> H <sub>29</sub> Cl <sub>3</sub> N <sub>4</sub> O
Formula weight	507.87
Temperature/K	100.01(10)
Crystal system	monoclinic
Space group	P2 <sub>1</sub> /n
a/Å	9.5894(2)
b/Å	23.6439(6)
c/Å	11.3564(3)
α/°	90
β/°	90.075(2)
γ/°	90
Volume/Å <sup>3</sup>	2574.84(10)
Z	4
ρ <sub>calc</sub> /cm <sup>3</sup>	1.310
μ/mm <sup>-1</sup>	3.415
F(000)	1064.0
Crystal size/mm <sup>3</sup>	0.237 × 0.127 × 0.078
Radiation	CuKα (λ = 1.54184)
2θ range for data collection/°	7.478 to 140.066
Index ranges	-11 ≤ h ≤ 7, -28 ≤ k ≤ 27, -13 ≤ l ≤ 13
Reflections collected	10643
Independent reflections	4853 [R <sub>int</sub> = 0.0269, R <sub>sigma</sub> = 0.0325]
Data/restraints/parameters	4853/1/308
Goodness-of-fit on F <sup>2</sup>	1.087
Final R indexes [I ≥ 2σ (I)]	R <sub>1</sub> = 0.0527, wR <sub>2</sub> = 0.1368
Final R indexes [all data]	R <sub>1</sub> = 0.0582, wR <sub>2</sub> = 0.1412
Largest diff. peak/hole / e Å <sup>-3</sup>	0.65/-0.37

**Table 2** Fractional Atomic Coordinates (×10<sup>4</sup>) and Equivalent Isotropic Displacement Parameters (Å<sup>2</sup>×10<sup>3</sup>) for 355•HCl. U<sub>eq</sub> is defined as 1/3 of the trace of the orthogonalised U<sub>ij</sub> tensor.

Atom	x	y	z	U(eq)
------	---	---	---	-------

C1	-636(2)	6756.9(9)	4285.0(19)	17.6(4)
C2	593(2)	7345.3(10)	5422.9(19)	19.6(4)
C3	1530(2)	7015.1(10)	4839.3(19)	19.1(4)
C4	3016(2)	6977.3(11)	4786(2)	24.1(5)
C5	3617(2)	6597.0(11)	4071(2)	24.5(5)
C6	1346(2)	6242.7(10)	3416.2(18)	17.9(4)
C7	1852(2)	5584.3(10)	2226(2)	20.9(5)
C8	1835(3)	5147.1(11)	1409(2)	26.5(5)
C9	3108(3)	4931.0(11)	1050(2)	29.7(5)
C10	4369(3)	5141.1(11)	1501(2)	28.9(5)
C11	4418(3)	5581.4(11)	2296(2)	26.4(5)
C12	3126(2)	5797.4(10)	2638.2(19)	21.1(5)
C13	-2026(2)	7410.9(10)	5513.0(19)	18.1(4)
C14	-2671(2)	7117.2(10)	6426(2)	22.0(5)
C15	-2123(3)	6563.4(11)	6912(2)	27.3(5)
C16	-3035(3)	6074.0(12)	6470(3)	36.1(6)
C17	-2010(3)	6571.6(13)	8258(2)	34.6(6)
C18	-3913(2)	7347.4(11)	6847(2)	25.2(5)
C19	-4461(2)	7840.5(11)	6386(2)	24.6(5)
C20	-3780(3)	8120.5(11)	5480(2)	24.5(5)
C21	-2539(2)	7907.5(10)	5011.7(19)	21.1(5)
C22	-1803(3)	8206.9(11)	4014(2)	27.2(5)
C23	-965(3)	8702.3(13)	4475(3)	40.1(7)
C24	-2815(4)	8390.8(15)	3048(3)	45.7(8)
N1	-721.4(19)	7179.7(8)	5060.2(16)	17.9(4)
N2	727.9(18)	6648.1(8)	4136.1(15)	16.6(4)
N3	2779.3(19)	6235.2(9)	3410.9(16)	19.5(4)
N4	731(2)	5876.3(8)	2745.5(16)	20.0(4)
Cl1	-3261.5(6)	6760.5(3)	2540.1(5)	32.85(18)
C25	1840(3)	5017.7(15)	6277(3)	48.6(8)
Cl2	496.0(8)	5524.4(3)	6189.4(7)	43.9(2)
Cl3	3383.0(8)	5252.8(4)	5635.3(8)	55.8(2)
O1	-1726(3)	5772.6(12)	1166(2)	60.2(7)

**Table 3 Anisotropic Displacement Parameters ( $\text{\AA}^2 \times 10^3$ ) for 355•HCl. The Anisotropic displacement factor exponent takes the form:  $-2\pi^2[h^2a^{*2}U_{11}+2hka^{*}b^{*}U_{12}+\dots]$ .**

Atom	U <sub>11</sub>	U <sub>22</sub>	U <sub>33</sub>	U <sub>23</sub>	U <sub>13</sub>	U <sub>12</sub>
C1	16(1)	18.8(10)	18(1)	-0.7(8)	0.6(8)	0.5(8)
C2	18.6(10)	21.6(11)	18.8(10)	-2.3(8)	-0.1(8)	-1.5(9)
C3	20.5(11)	21.0(11)	15.9(10)	-1.3(8)	0.2(8)	-2.3(9)
C4	17.5(11)	31.1(13)	23.8(11)	-6.2(10)	-2.8(9)	-0.8(9)
C5	15.9(10)	31.5(13)	26.1(12)	-2(1)	-1.7(9)	-0.2(9)
C6	17.8(10)	20.1(11)	15.9(10)	0.8(8)	2.9(8)	2.4(8)
C7	22.7(11)	20.5(11)	19.5(10)	2.2(9)	5.0(8)	3.1(9)
C8	34.2(13)	22.2(12)	23.1(11)	-1.3(9)	5.6(10)	-1(1)
C9	41.7(14)	21.5(12)	25.8(12)	-1.5(10)	11.2(10)	4.8(10)
C10	32.0(13)	26.0(12)	28.9(12)	0.7(10)	11.2(10)	9(1)
C11	23.7(12)	29.1(13)	26.5(12)	3(1)	5.8(9)	6.2(10)
C12	22.9(11)	22.0(11)	18.4(10)	0.3(9)	3.4(8)	3.9(9)
C13	14.7(10)	21.2(11)	18.4(10)	-5.0(8)	4.0(8)	1.5(8)
C14	20.9(11)	24.0(12)	21.2(11)	-3.0(9)	2.8(9)	-1.5(9)
C15	29.5(12)	26.6(13)	25.8(12)	4.5(10)	7.4(9)	1.3(10)

C16	45.7(16)	27.6(14)	35.0(14)	2.7(11)	3.2(12)	-3.3(12)
C17	40.4(15)	35.3(15)	28.1(13)	6.1(11)	2.5(11)	0.9(12)
C18	20.1(11)	33.0(13)	22.4(11)	-2.7(10)	7.2(9)	-3.5(9)
C19	17.6(11)	31.1(13)	25.1(11)	-11.8(10)	3.1(9)	1.0(9)
C20	24.7(12)	25.9(12)	22.8(11)	-6.0(9)	-1.5(9)	6.9(10)
C21	21.8(11)	23.0(11)	18.5(10)	-4.3(9)	1.4(8)	1.4(9)
C22	34.1(13)	25.0(12)	22.6(12)	0.5(9)	8.4(10)	5.3(10)
C23	40.2(15)	39.0(16)	41.1(15)	2.2(13)	11.5(12)	-9.3(13)
C24	60(2)	49.7(19)	27.2(14)	13.6(13)	-3.3(13)	-4.9(15)
N1	14.9(9)	21.0(9)	17.7(9)	-1.3(7)	3.7(7)	1.2(7)
N2	15.0(8)	20.0(9)	14.9(8)	-0.9(7)	0.8(7)	-0.4(7)
N3	16.6(9)	24.4(10)	17.5(9)	-1.1(7)	2.2(7)	2.1(7)
N4	21.1(9)	19.9(9)	18.9(9)	-1.9(7)	3.2(7)	0.8(7)
Cl1	22.5(3)	45.1(4)	30.9(3)	8.8(3)	-4.4(2)	-0.1(2)
C25	38.1(16)	41.1(17)	67(2)	14.6(16)	4.7(14)	1.9(13)
Cl2	43.2(4)	37.5(4)	51.0(4)	-3.2(3)	1.5(3)	6.8(3)
Cl3	40.9(4)	62.9(5)	63.7(5)	22.7(4)	11.1(4)	2.7(4)
O1	58.7(15)	56.6(16)	65.4(16)	-18.9(13)	-29.2(13)	10.3(12)

**Table 4 Bond Lengths for 355•HCl.**

Atom	Atom	Length/Å	Atom	Atom	Length/Å
C1	N1	1.335(3)	C11	C12	1.395(3)
C1	N2	1.344(3)	C12	N3	1.398(3)
C2	C3	1.363(3)	C13	C14	1.394(3)
C2	N1	1.382(3)	C13	C21	1.394(3)
C3	C4	1.429(3)	C13	N1	1.459(3)
C3	N2	1.408(3)	C14	C15	1.515(3)
C4	C5	1.342(3)	C14	C18	1.395(3)
C5	N3	1.392(3)	C15	C16	1.535(4)
C6	N2	1.393(3)	C15	C17	1.532(4)
C6	N3	1.374(3)	C18	C19	1.382(4)
C6	N4	1.295(3)	C19	C20	1.388(4)
C7	C8	1.390(3)	C20	C21	1.398(3)
C7	C12	1.401(3)	C21	C22	1.511(3)
C7	N4	1.408(3)	C22	C23	1.513(4)
C8	C9	1.385(4)	C22	C24	1.527(4)
C9	C10	1.403(4)	C25	Cl2	1.762(3)
C10	C11	1.379(4)	C25	Cl3	1.741(3)

**Table 5 Bond Angles for 355•HCl.**

Atom	Atom	Atom	Angle/°	Atom	Atom	Atom	Angle/°
N1	C1	N2	106.68(19)	C18	C14	C15	120.6(2)
C3	C2	N1	107.12(19)	C14	C15	C16	109.6(2)
C2	C3	C4	135.6(2)	C14	C15	C17	112.1(2)
C2	C3	N2	105.59(19)	C17	C15	C16	112.0(2)
N2	C3	C4	118.8(2)	C19	C18	C14	121.6(2)
C5	C4	C3	119.8(2)	C18	C19	C20	120.3(2)
C4	C5	N3	119.3(2)	C19	C20	C21	120.8(2)
N3	C6	N2	115.97(19)	C13	C21	C20	116.6(2)
N4	C6	N2	127.7(2)	C13	C21	C22	122.4(2)

N4	C6	N3	116.3(2)	C20	C21	C22	121.0(2)
C8	C7	C12	120.0(2)	C21	C22	C23	110.6(2)
C8	C7	N4	129.5(2)	C21	C22	C24	112.0(2)
C12	C7	N4	110.5(2)	C23	C22	C24	111.4(2)
C9	C8	C7	117.5(2)	C1	N1	C2	110.62(18)
C8	C9	C10	121.4(2)	C1	N1	C13	124.50(18)
C11	C10	C9	122.3(2)	C2	N1	C13	124.79(18)
C10	C11	C12	115.4(2)	C1	N2	C3	109.99(18)
C11	C12	C7	123.3(2)	C1	N2	C6	128.38(19)
C11	C12	N3	131.1(2)	C6	N2	C3	121.63(18)
N3	C12	C7	105.52(19)	C5	N3	C12	130.98(19)
C14	C13	C21	124.5(2)	C6	N3	C5	124.47(19)
C14	C13	N1	117.2(2)	C6	N3	C12	104.54(18)
C21	C13	N1	118.27(19)	C6	N4	C7	103.11(18)
C13	C14	C15	123.2(2)	C13	C25	C12	112.41(19)
C13	C14	C18	116.2(2)				

**Table 6 Hydrogen Bonds for 355•HCl.**

D	H	A	d(D-H)/Å	d(H-A)/Å	d(D-A)/Å	D-H-A/°
C1	H1	Cl1	0.93	2.43	3.202(2)	140.3
C2	H2	Cl1 <sup>1</sup>	0.93	2.47	3.384(2)	167.7
C5	H5	Cl1 <sup>2</sup>	0.93	2.70	3.485(2)	142.7
C11	H11	Cl1 <sup>2</sup>	0.93	2.83	3.578(3)	137.8
C25	H25A	O1 <sup>3</sup>	0.97	2.59	3.455(5)	148.6
O1	H1A	N4	0.99(5)	1.98(5)	2.969(3)	177(5)
O1	H1B	Cl1	0.916(19)	2.26(2)	3.173(3)	172(5)

<sup>1</sup>1/2+X,3/2-Y,1/2+Z; <sup>2</sup>1+X,+Y,+Z; <sup>3</sup>-X,1-Y,1-Z

**Table 7 Torsion Angles for 355•HCl.**

A	B	C	D	Angle/°	A	B	C	D	Angle/°
C2	C3	C4	C5	-178.4(3)	C18	C14	C15	C16	72.0(3)
C2	C3	N2	C1	0.5(2)	C18	C14	C15	C17	-53.1(3)
C2	C3	N2	C6	-179.49(19)	C18	C19	C20	C21	0.6(4)
C3	C2	N1	C1	0.6(3)	C19	C20	C21	C13	-0.9(3)
C3	C2	N1	C13	177.2(2)	C19	C20	C21	C22	179.2(2)
C3	C4	C5	N3	-1.4(4)	C20	C21	C22	C23	80.0(3)
C4	C3	N2	C1	-178.5(2)	C20	C21	C22	C24	-44.9(3)
C4	C3	N2	C6	1.6(3)	C21	C13	C14	C15	177.0(2)
C4	C5	N3	C6	1.2(4)	C21	C13	C14	C18	0.0(3)
C4	C5	N3	C12	-177.9(2)	C21	C13	N1	C1	-99.1(3)
C7	C8	C9	C10	0.5(4)	C21	C13	N1	C2	84.8(3)
C7	C12	N3	C5	-179.7(2)	N1	C1	N2	C3	-0.1(2)
C7	C12	N3	C6	1.0(2)	N1	C1	N2	C6	179.9(2)
C8	C7	C12	C11	-2.0(4)	N1	C2	C3	C4	178.0(3)
C8	C7	C12	N3	178.5(2)	N1	C2	C3	N2	-0.6(2)
C8	C7	N4	C6	-178.9(2)	N1	C13	C14	C15	-3.2(3)
C8	C9	C10	C11	-1.8(4)	N1	C13	C14	C18	179.8(2)
C9	C10	C11	C12	1.1(4)	N1	C13	C21	C20	-179.1(2)
C10	C11	C12	C7	0.8(4)	N1	C13	C21	C22	0.8(3)

C10C11C12N3	-179.8(2)	N2 C1 N1 C2	-0.3(2)
C11C12N3 C5	0.8(4)	N2 C1 N1 C13	-176.91(19)
C11C12N3 C6	-178.4(2)	N2 C3 C4 C5	0.1(3)
C12C7 C8 C9	1.3(3)	N2 C6 N3 C5	0.4(3)
C12C7 N4 C6	0.5(2)	N2 C6 N3 C12	179.75(18)
C13C14C15C16	-104.9(3)	N2 C6 N4 C7	179.6(2)
C13C14C15C17	130.1(2)	N3 C6 N2 C1	178.2(2)
C13C14C18C19	-0.4(3)	N3 C6 N2 C3	-1.8(3)
C13C21C22C23	-99.9(3)	N3 C6 N4 C7	0.2(3)
C13C21C22C24	135.2(3)	N4 C6 N2 C1	-1.1(4)
C14C13C21C20	0.7(3)	N4 C6 N2 C3	178.8(2)
C14C13C21C22	-179.5(2)	N4 C6 N3 C5	179.9(2)
C14C13N1 C1	81.1(3)	N4 C6 N3 C12	-0.8(3)
C14C13N1 C2	-95.0(3)	N4 C7 C8 C9	-179.4(2)
C14C18C19C20	0.2(4)	N4 C7 C12C11	178.5(2)
C15C14C18C19	-177.5(2)	N4 C7 C12N3	-1.0(3)

**Table 8 Hydrogen Atom Coordinates ( $\text{\AA} \times 10^4$ ) and Isotropic Displacement Parameters ( $\text{\AA}^2 \times 10^3$ ) for 355•HCl.**

Atom	x	y	z	U(eq)
H1	-1377	6573	3919	21
H2	799	7629	5964	24
H4	3565	7216	5244	29
H5	4583	6575	4018	29
H8	1000	5005	1113	32
H9	3127	4640	499	36
H10	5201	4978	1255	35
H11	5254	5724	2585	32
H15	-1182	6507	6597	33
H16A	-3958	6111	6788	54
H16B	-2638	5721	6720	54
H16C	-3080	6084	5626	54
H17A	-1439	6885	8499	52
H17B	-1596	6225	8525	52
H17C	-2923	6610	8593	52
H18	-4384	7165	7453	30
H19	-5291	7985	6684	30
H20	-4153	8454	5180	29
H22	-1146	7938	3664	33
H23A	-1587	8985	4779	60
H23B	-422	8861	3847	60
H23C	-355	8576	5092	60
H24A	-3355	8071	2795	69
H24B	-2299	8539	2393	69
H24C	-3427	8678	3349	69
H25A	2013	4928	7098	58
H25B	1540	4674	5886	58
H1A	-910(50)	5820(20)	1690(50)	90
H1B	-2170(50)	6077(16)	1490(40)	90

## Experimental

A suitable crystal was selected on a **SuperNova, Dual, Cu at zero, Atlas** diffractometer. The crystal was kept at 100.01(10) K during data collection. Using Olex2,<sup>275</sup> the structure was solved with the olex2.solve<sup>279</sup> structure solution program using Charge Flipping and refined with the ShelXL<sup>276</sup> refinement package using Least Squares minimisation.

### Crystal structure determination of [355•HCl]

**Crystal Data** for  $C_{25}H_{29}Cl_3N_4O$  ( $M = 507.87$  g/mol): monoclinic, space group  $P2_1/n$  (no. 14),  $a = 9.5894(2)$  Å,  $b = 23.6439(6)$  Å,  $c = 11.3564(3)$  Å,  $\beta = 90.075(2)^\circ$ ,  $V = 2574.84(10)$  Å<sup>3</sup>,  $Z = 4$ ,  $T = 100.01(10)$  K,  $\mu(\text{CuK}\alpha) = 3.415$  mm<sup>-1</sup>,  $D_{\text{calc}} = 1.310$  g/cm<sup>3</sup>, 10643 reflections measured ( $7.478^\circ \leq 2\theta \leq 140.066^\circ$ ), 4853 unique ( $R_{\text{int}} = 0.0269$ ,  $R_{\text{sigma}} = 0.0325$ ) which were used in all calculations. The final  $R_1$  was 0.0527 ( $I > 2\sigma(I)$ ) and  $wR_2$  was 0.1412 (all data).

### Refinement model description

Number of restraints - 1, number of constraints - unknown.

Details:

1. Fixed Uiso

At 1.2 times of:

All C(H) groups, All C(H,H) groups

At 1.5 times of:

All C(H,H,H) groups, All O(H,H) groups

2. Restrained distances

O1-H1B

0.9 with sigma of 0.02

3.a Ternary CH refined with riding coordinates:

C15(H15), C22(H22)

3.b Secondary CH2 refined with riding coordinates:

C25(H25A,H25B)

3.c Aromatic/amide H refined with riding coordinates:

C1(H1), C2(H2), C4(H4), C5(H5), C8(H8), C9(H9), C10(H10), C11(H11), C18(H18), C19(H19), C20(H20)

3.d Idealised Me refined as rotating group:

C16(H16A,H16B,H16C), C17(H17A,H17B,H17C), C23(H23A,H23B,H23C), C24(H24A,H24B,H24C)

## 8.5 353aAgCl

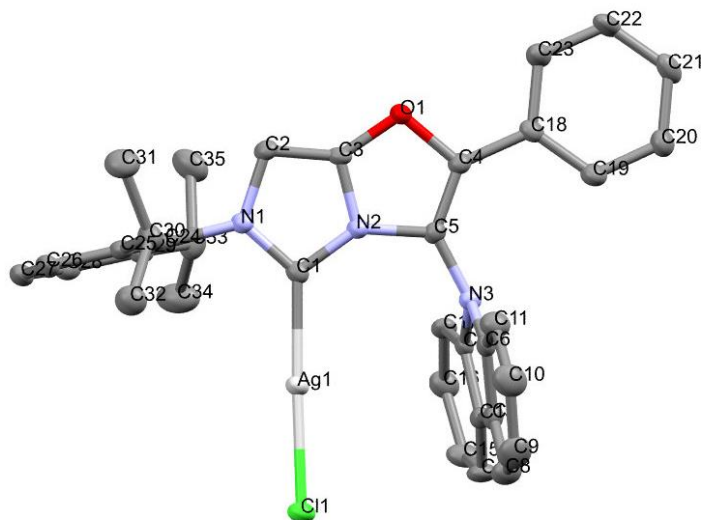
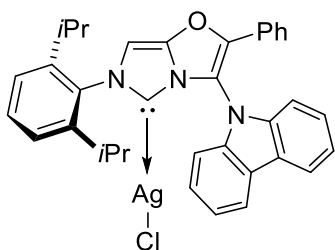


**Table 1** Crystal data and structure refinement for 353aAgCl.

Identification code	<b>353aAgCl</b>
Empirical formula	$C_{35}H_{31}AgClN_3O$
Formula weight	652.95
Temperature/K	100.01(10)
Crystal system	orthorhombic
Space group	$P2_12_12_1$
$a/\text{\AA}$	9.42364(19)
$b/\text{\AA}$	14.5288(3)
$c/\text{\AA}$	22.0648(4)



$\alpha/^\circ$	90
$\beta/^\circ$	90
$\gamma/^\circ$	90
Volume/ $\text{\AA}^3$	3020.98(10)
Z	4
$\rho_{\text{calc}}/\text{g}/\text{cm}^3$	1.436
$\mu/\text{mm}^{-1}$	0.788
F(000)	1336.0
Crystal size/ $\text{mm}^3$	$0.238 \times 0.144 \times 0.096$
Radiation	MoK $\alpha$ ( $\lambda = 0.71073$ )
2 $\Theta$ range for data collection/ $^\circ$	6.34 to 52.744
Index ranges	$-11 \leq h \leq 11, -17 \leq k \leq 18, -27 \leq l \leq 27$
Reflections collected	32364
Independent reflections	6167 [ $R_{\text{int}} = 0.0420, R_{\text{sigma}} = 0.0323$ ]
Data/restraints/parameters	6167/0/374
Goodness-of-fit on $F^2$	1.054
Final R indexes [ $I \geq 2\sigma(I)$ ]	$R_1 = 0.0253, wR_2 = 0.0617$
Final R indexes [all data]	$R_1 = 0.0278, wR_2 = 0.0634$
Largest diff. peak/hole / $e \text{ \AA}^{-3}$	0.64/-0.44
Flack parameter	-0.044(10)

**Table 2 Fractional Atomic Coordinates ( $\times 10^4$ ) and Equivalent Isotropic Displacement Parameters ( $\text{\AA}^2 \times 10^3$ ) for 353aAgCl.  $U_{\text{eq}}$  is defined as 1/3 of the trace of the orthogonalised  $U_{ij}$  tensor.**

Atom	x	y	z	U(eq)
Ag1	7755.5(3)	3700.0(2)	2402.3(2)	18.28(8)
Cl2	6231.0(9)	2455.9(5)	2496.6(4)	22.8(2)
O2	10600(2)	6360.2(17)	1282.1(11)	17.9(5)
N3	7806(3)	4713.0(18)	948.9(13)	16.4(6)
C5	9153(4)	4789(2)	2280.8(16)	16.7(7)
N6	10057(3)	5211.9(18)	2663.8(14)	16.9(6)
C7	9527(4)	6404(2)	283.3(16)	18.5(7)
C8	8035(4)	3792(2)	753.3(15)	18.4(7)
C9	9051(4)	5535(2)	3658.8(18)	20.8(8)
C10	12216(5)	2928(3)	3290(2)	31.3(9)
C11	10853(3)	5914(2)	2394.1(18)	17.5(7)
C12	4301(4)	3821(3)	1216.7(18)	24.7(8)
C14	7968(4)	6182(3)	3363.5(18)	27.3(8)
N15	9410(3)	5236(2)	1749.5(14)	16.4(6)
C16	9096(4)	5404(3)	4283.0(19)	25.0(9)
C17	10055(4)	5052(2)	3312.7(16)	17.0(7)
C18	3602(5)	4552(3)	1476(2)	29.1(10)
C19	7986(5)	1968(3)	450(2)	33.7(10)
C20	9267(5)	3411(3)	522.5(19)	26.6(9)
C21	10324(5)	7190(3)	160.4(19)	27.1(9)
C22	11055(4)	4464(2)	3558.6(18)	18.7(8)
C23	13612(5)	4425(3)	3257(2)	34.2(10)
C24	5737(4)	3917(2)	1068.5(16)	18.6(8)
C26	5718(4)	5501(2)	1440.4(18)	19.9(8)
C27	11045(4)	4358(2)	4191.6(19)	23.3(8)
C28	6391(4)	4772(2)	1164.9(16)	16.9(7)

C29	10410(4)	5908(2)	1814.8(17)	16.5(7)
C30	8498(4)	6504(3)	-714.7(18)	25.0(9)
C31	10199(5)	7613(3)	-395.8(19)	30(1)
C32	8896(4)	5289(2)	1148.0(17)	16.6(7)
C33	6777(4)	3303(3)	819.6(17)	19.1(8)
C34	9612(4)	5975(2)	879.0(17)	17.5(7)
C35	9281(5)	7284(3)	-832.3(18)	26.2(9)
C36	6767(4)	2360(3)	674.0(19)	27.1(9)
C37	12162(4)	3976(2)	3168.6(17)	22.3(8)
C38	8507(5)	7179(3)	3358(2)	37.6(11)
C39	10081(4)	4820(3)	4539.3(18)	25.8(9)
C41	8616(4)	6060(3)	-155.6(18)	25.0(9)
C44	4299(4)	5381(3)	1598(2)	25.9(9)
C51	9210(5)	2479(3)	370(2)	34.2(10)
C0AA	6521(5)	6134(3)	3652(3)	44.2(12)

**Table 3 Anisotropic Displacement Parameters ( $\text{\AA}^2 \times 10^3$ ) for 353aAgCl. The Anisotropic displacement factor exponent takes the form:  $-2\pi^2[h^2a^{*2}U_{11}+2hka^*b^*U_{12}+\dots]$ .**

Atom	U <sub>11</sub>	U <sub>22</sub>	U <sub>33</sub>	U <sub>23</sub>	U <sub>13</sub>	U <sub>12</sub>
Ag1	19.69(13)	15.77(12)	19.39(13)	2.17(10)	0.34(11)	-2.7(1)
Cl2	23.7(4)	17.6(4)	27.1(5)	2.0(4)	2.3(4)	-4.2(3)
O2	17.7(12)	18.8(11)	17.3(12)	2.4(11)	0.3(10)	-2.9(11)
N3	17.4(14)	14.3(13)	17.5(14)	-0.3(11)	1.3(14)	-1.1(12)
C5	14.7(17)	16.4(15)	19.0(19)	2.9(14)	2.5(15)	3.4(13)
N6	14.2(14)	15.6(13)	20.9(15)	2.8(12)	-1.7(14)	0.8(10)
C7	17.9(17)	18.0(17)	19.7(17)	1.7(15)	5.4(14)	1.5(15)
C8	24.3(19)	17.5(16)	13.4(15)	-0.3(14)	-1.1(14)	-0.9(15)
C9	17.2(19)	19.8(18)	25(2)	1.8(15)	-0.4(17)	-0.3(15)
C10	32(2)	24.6(19)	37(2)	1.2(16)	0(2)	4.9(19)
C11	13.0(16)	16.6(14)	22.9(17)	0.6(15)	-3.0(16)	-0.2(12)
C12	22.4(19)	17.9(18)	34(2)	-0.5(16)	1.8(17)	-7.6(16)
C14	24(2)	31(2)	27.5(19)	-3.8(17)	-2.7(16)	9.2(18)
N15	14.7(15)	15.8(14)	18.8(16)	1.7(12)	-1.7(13)	-0.7(12)
C16	24(2)	25.3(19)	25(2)	-2.4(16)	5.1(18)	-3.9(16)
C17	18.3(19)	17.1(17)	15.8(17)	1.2(14)	-2.7(15)	-4.4(14)
C18	21(2)	23(2)	43(3)	0.9(18)	11(2)	-0.3(16)
C19	41(3)	18.6(18)	41(3)	-8.8(17)	-1(2)	7.5(18)
C20	25(2)	24.1(19)	31(2)	-0.8(16)	5.0(19)	-0.2(16)
C21	37(2)	22.4(19)	22(2)	-0.8(16)	0.2(19)	-7.9(18)
C22	16.2(18)	15.4(16)	25(2)	2.5(14)	-2.1(16)	-2.9(14)
C23	23(2)	34(2)	46(3)	2(2)	3(2)	1.5(18)
C24	21.5(19)	16.3(17)	18.0(17)	0.9(13)	-2.7(15)	-2.0(14)
C26	24(2)	11.7(16)	24(2)	-0.9(14)	-0.3(17)	-1.9(14)
C27	27(2)	19.2(17)	24(2)	6.9(15)	-5.0(18)	-3.3(15)
C28	20.8(19)	16.7(16)	13.1(17)	2.2(14)	-1.3(15)	-1.8(14)
C29	12.1(17)	13.6(15)	23.9(19)	3.5(14)	0.8(15)	-1.0(14)
C30	27(2)	27(2)	20.2(19)	0.8(15)	0.9(17)	0.6(16)
C31	46(3)	19.7(19)	24(2)	2.8(16)	6(2)	-9.8(18)
C32	16.2(17)	15.1(17)	18.5(18)	-1.6(14)	-1.1(15)	1.4(14)
C33	22(2)	19.0(16)	15.9(18)	-1.0(14)	-3.1(15)	1.6(14)
C34	14.9(17)	17.5(16)	20.2(18)	-0.1(14)	-0.5(15)	-0.2(14)
C35	39(2)	20.9(18)	18.9(19)	3.0(15)	7.4(19)	6.1(17)

C36	31(2)	19.4(18)	31(2)	-5.6(16)	3.0(18)	-2.8(16)
C37	20.4(18)	23.6(18)	22.9(18)	4.2(14)	-0.5(18)	3.7(16)
C38	34(3)	33(2)	46(3)	15(2)	5(2)	9(2)
C39	34(2)	22.9(19)	20.6(19)	3.1(16)	-0.5(19)	-9.8(17)
C41	24(2)	26(2)	25(2)	3.6(15)	1.7(17)	-6.0(16)
C44	26(2)	20.5(18)	31(2)	1.0(17)	5.1(18)	6.2(16)
C51	37(3)	27(2)	38(3)	-5.1(19)	10(2)	8.1(19)
C0AA	28(2)	33(2)	71(4)	8(2)	0(2)	2(2)

**Table 4 Bond Lengths for 353aAgCl.**

Atom Atom	Length/Å	Atom Atom	Length/Å
Ag1 Cl2	2.3182(8)	C14 C0AA	1.507(6)
Ag1 C5	2.076(3)	N15 C29	1.365(5)
O2 C29	1.358(4)	N15 C32	1.415(5)
O2 C34	1.404(4)	C16 C39	1.379(6)
N3 C8	1.422(4)	C17 C22	1.384(5)
N3 C28	1.419(5)	C18 C44	1.399(6)
N3 C32	1.396(5)	C19 C36	1.374(6)
C5 N6	1.348(4)	C19 C51	1.384(6)
C5 N15	1.361(4)	C20 C51	1.396(6)
N6 C11	1.399(4)	C21 C31	1.378(6)
N6 C17	1.450(5)	C22 C27	1.405(6)
C7 C21	1.394(5)	C22 C37	1.527(5)
C7 C34	1.457(5)	C23 C37	1.526(6)
C7 C41	1.387(5)	C24 C28	1.402(5)
C8 C20	1.384(5)	C24 C33	1.434(5)
C8 C33	1.390(5)	C26 C28	1.377(5)
C9 C14	1.533(5)	C26 C44	1.393(6)
C9 C16	1.391(6)	C27 C39	1.366(6)
C9 C17	1.403(5)	C30 C35	1.378(6)
C10 C37	1.547(5)	C30 C41	1.396(5)
C11 C29	1.345(5)	C31 C35	1.380(6)
C12 C18	1.375(6)	C32 C34	1.342(5)
C12 C24	1.398(6)	C33 C36	1.408(5)
C14 C38	1.535(6)		

**Table 5 Bond Angles for 353aAgCl.**

Atom Atom Atom	Angle/°	Atom Atom Atom	Angle/°
C5 Ag1 Cl2	177.39(10)	C31 C21 C7	119.5(4)
C29 O2 C34	105.5(3)	C17 C22 C27	117.0(4)
C28 N3 C8	107.5(3)	C17 C22 C37	122.1(3)
C32 N3 C8	123.2(3)	C27 C22 C37	120.9(3)
C32 N3 C28	123.4(3)	C12 C24 C28	118.6(3)
N6 C5 Ag1	131.8(2)	C12 C24 C33	133.5(3)
N6 C5 N15	102.2(3)	C28 C24 C33	107.9(3)
N15 C5 Ag1	125.9(3)	C28 C26 C44	117.2(3)
C5 N6 C11	113.9(3)	C39 C27 C22	120.6(4)
C5 N6 C17	123.1(3)	C24 C28 N3	108.0(3)
C11 N6 C17	122.5(3)	C26 C28 N3	128.9(3)
C21 C7 C34	119.8(3)	C26 C28 C24	123.1(3)

C41	C7	C21	119.5(3)	O2	C29	N15	110.2(3)
C41	C7	C34	120.7(3)	C11	C29	O2	141.1(3)
C20	C8	N3	128.0(3)	C11	C29	N15	108.6(3)
C20	C8	C33	123.4(3)	C35	C30	C41	120.2(4)
C33	C8	N3	108.6(3)	C21	C31	C35	121.4(4)
C16	C9	C14	121.6(4)	N3	C32	N15	120.9(3)
C16	C9	C17	116.8(3)	C34	C32	N3	132.5(3)
C17	C9	C14	121.6(4)	C34	C32	N15	106.5(3)
C29	C11	N6	103.5(3)	C8	C33	C24	107.8(3)
C18	C12	C24	119.0(4)	C8	C33	C36	118.6(4)
C9	C14	C38	111.2(3)	C36	C33	C24	133.5(4)
C0AA	C14	C9	113.2(3)	O2	C34	C7	116.0(3)
C0AA	C14	C38	110.3(3)	C32	C34	O2	110.4(3)
C5	N15	C29	111.9(3)	C32	C34	C7	133.6(3)
C5	N15	C32	140.6(3)	C30	C35	C31	119.3(4)
C29	N15	C32	107.2(3)	C19	C36	C33	118.7(4)
C39	C16	C9	120.7(4)	C22	C37	C10	112.5(3)
C9	C17	N6	117.3(3)	C23	C37	C10	111.7(3)
C22	C17	N6	119.0(3)	C23	C37	C22	110.0(3)
C22	C17	C9	123.7(3)	C27	C39	C16	121.4(4)
C12	C18	C44	121.4(4)	C7	C41	C30	120.0(4)
C36	C19	C51	121.4(4)	C26	C44	C18	120.7(4)
C8	C20	C51	116.4(4)	C19	C51	C20	121.4(4)

**Table 6 Torsion Angles for 353aAgCl.**

A	B	C	D	Angle/°	A	B	C	D	Angle/°
Ag1	C5	N6	C11	178.3(2)	C17	C9	C14	C0AA	141.3(4)
Ag1	C5	N6	C17	-10.5(5)	C17	C9	C16	C39	-0.5(6)
Ag1	C5	N15	C29	-178.6(2)	C17	C22	C27	C39	0.2(5)
Ag1	C5	N15	C32	8.6(6)	C17	C22	C37	C10	-129.3(4)
N3	C8	C20	C51	179.3(4)	C17	C22	C37	C23	105.6(4)
N3	C8	C33	C24	-0.8(4)	C18	C12	C24	C28	-2.9(6)
N3	C8	C33	C36	-177.7(3)	C18	C12	C24	C33	177.4(4)
N3	C32	C34	O2	178.6(3)	C20	C8	C33	C24	-179.8(3)
N3	C32	C34	C7	1.5(7)	C20	C8	C33	C36	3.3(6)
C5	N6	C11	C29	-0.5(4)	C21	C7	C34	O2	-4.6(5)
C5	N6	C17	C9	-81.7(4)	C21	C7	C34	C32	172.4(4)
C5	N6	C17	C22	100.2(4)	C21	C7	C41	C30	-0.3(6)
C5	N15	C29	O2	-177.7(3)	C21	C31	C35	C30	-1.6(7)
C5	N15	C29	C11	0.8(4)	C22	C27	C39	C16	-0.3(6)
C5	N15	C32	N3	-4.0(7)	C24	C12	C18	C44	-0.5(6)
C5	N15	C32	C34	173.8(4)	C24	C33	C36	C19	-178.4(4)
N6	C5	N15	C29	-1.0(4)	C27	C22	C37	C10	53.1(5)
N6	C5	N15	C32	-173.8(4)	C27	C22	C37	C23	-72.0(4)
N6	C11	C29	O2	177.6(4)	C28	N3	C8	C20	-178.4(4)
N6	C11	C29	N15	-0.2(4)	C28	N3	C8	C33	2.7(4)
N6	C17	C22	C27	177.7(3)	C28	N3	C32	N15	67.7(5)
N6	C17	C22	C37	0.0(5)	C28	N3	C32	C34	-109.5(5)
C7	C21	C31	C35	1.1(7)	C28	C24	C33	C8	-1.5(4)
C8	N3	C28	C24	-3.6(4)	C28	C24	C33	C36	174.8(4)
C8	N3	C28	C26	174.7(4)	C28	C26	C44	C18	-0.2(6)
C8	N3	C32	N15	-81.9(4)	C29	O2	C34	C7	175.0(3)

C8 N3 C32 C34	101.0(5)	C29 O2 C34 C32	-2.7(4)
C8 C20 C51 C19	-0.5(7)	C29 N15 C32 N3	-177.0(3)
C8 C33 C36 C19	-2.4(6)	C29 N15 C32 C34	0.7(4)
C9 C16 C39 C27	0.4(6)	C32 N3 C8 C20	-24.7(5)
C9 C17 C22 C27	-0.2(5)	C32 N3 C8 C33	156.3(3)
C9 C17 C22 C37	-177.9(3)	C32 N3 C28 C24	-157.2(3)
C11 N6 C17 C9	88.7(4)	C32 N3 C28 C26	21.1(6)
C11 N6 C17 C22	-89.4(4)	C32 N15 C29 O2	-2.5(4)
C12 C18 C44 C26	2.1(7)	C32 N15 C29 C11	176.0(3)
C12 C24 C28 N3	-176.6(3)	C33 C8 C20 C51	-1.8(6)
C12 C24 C28 C26	5.0(6)	C33 C24 C28 N3	3.1(4)
C12 C24 C33 C8	178.2(4)	C33 C24 C28 C26	-175.3(3)
C12 C24 C33 C36	-5.5(8)	C34 O2 C29 C11	-174.6(5)
C14 C9 C16 C39	-179.9(4)	C34 O2 C29 N15	3.1(4)
C14 C9 C17 N6	1.8(5)	C34 C7 C21 C31	-177.5(4)
C14 C9 C17 C22	179.8(3)	C34 C7 C41 C30	177.1(4)
N15 C5 N6 C11	0.9(4)	C35 C30 C41 C7	-0.2(6)
N15 C5 N6 C17	172.1(3)	C36 C19 C51 C20	1.2(7)
N15 C32 C34 O2	1.2(4)	C37 C22 C27 C39	177.8(3)
N15 C32 C34 C7	-176.0(4)	C41 C7 C21 C31	-0.2(6)
C16 C9 C14 C38	85.5(5)	C41 C7 C34 O2	178.1(3)
C16 C9 C14 C0AA	-39.4(5)	C41 C7 C34 C32	-4.9(6)
C16 C9 C17 N6	-177.5(3)	C41 C30 C35 C31	1.1(6)
C16 C9 C17 C22	0.4(5)	C44 C26 C28 N3	178.6(4)
C17 N6 C11 C29	-171.7(3)	C44 C26 C28 C24	-3.4(6)
C17 C9 C14 C38	-93.9(4)	C51 C19 C36 C33	0.3(7)

**Table 7 Hydrogen Atom Coordinates ( $\text{\AA} \times 10^4$ ) and Isotropic Displacement Parameters ( $\text{\AA}^2 \times 10^3$ ) for 353aAgCl.**

Atom	x	y	z	U(eq)
H10A	12488	2820	3703	47
H10B	12897	2648	3024	47
H10C	11297	2665	3218	47
H11	11528	6294	2573	21
H12	3828	3272	1141	30
H14	7862	5988	2940	33
H16	8454	5714	4530	30
H18	2645	4493	1573	35
H19	7988	1346	351	40
H20	10089	3757	472	32
H21	10936	7428	452	33
H23A	13883	4382	3675	51
H23B	13562	5060	3140	51
H23C	14302	4114	3011	51
H26	6190	6051	1518	24
H27	11702	3970	4375	28
H30	7889	6271	-1009	30
H31	10745	8132	-479	36
H35	9192	7587	-1202	31
H36	5951	2009	728	33
H37	11890	4063	2744	27
H38A	8629	7390	3767	56
H38B	7830	7563	3154	56

H38C	9400	7206	3149	56
H39	10089	4739	4957	31
H41	8084	5534	-77	30
H44	3809	5858	1786	31
H51	10013	2196	210	41
H0AA	6153	5521	3614	66
H0AB	5895	6559	3453	66
H0AC	6594	6293	4073	66

## Experimental

A suitable crystal was selected on a **SuperNova, Dual, Cu at zero, Atlas** diffractometer. The crystal was kept at 100.01(10) K during data collection. Using Olex2,<sup>275</sup> the structure was solved with the ShelXS<sup>278</sup> structure solution program using Direct Methods and refined with the ShelXL<sup>277</sup> refinement package using Least Squares minimisation.

## Crystal structure determination of [353aAgCl]

**Crystal Data** for  $C_{35}H_{31}AgClN_3O$  ( $M = 652.95$  g/mol): orthorhombic, space group  $P2_12_12_1$  (no. 19),  $a = 9.42364(19)$  Å,  $b = 14.5288(3)$  Å,  $c = 22.0648(4)$  Å,  $V = 3020.98(10)$  Å<sup>3</sup>,  $Z = 4$ ,  $T = 100.01(10)$  K,  $\mu(\text{MoK}\alpha) = 0.788$  mm<sup>-1</sup>,  $D_{\text{calc}} = 1.436$  g/cm<sup>3</sup>, 32364 reflections measured ( $6.34^\circ \leq 2\theta \leq 52.744^\circ$ ), 6167 unique ( $R_{\text{int}} = 0.0420$ ,  $R_{\text{sigma}} = 0.0323$ ) which were used in all calculations. The final  $R_1$  was 0.0253 ( $I > 2\sigma(I)$ ) and  $wR_2$  was 0.0634 (all data).

## Refinement model description

Number of restraints - 0, number of constraints - unknown.

Details:

1. Fixed Uiso

At 1.2 times of:

All C(H) groups

At 1.5 times of:

All C(H,H,H) groups

2.a Ternary CH refined with riding coordinates:

C33(H14), C30(H37)

2.b Aromatic/amide H refined with riding coordinates:

C2(H11), C10(H12), C28(H16), C9(H18), C14(H19), C16(H20), C23(H21), C7(H26), C26(H27), C20(H30), C22(H31), C21(H35), C13(H36), C27(H39), C19(H41), C8(H44), C15(H51)

2.c Idealised Me refined as rotating group:

C31(H10A,H10B,H10C), C32(H23A,H23B,H23C), C34(H38A,H38B,H38C), C35(H0AA,H0AB,H0AC)

## 8.6 353cAgCl

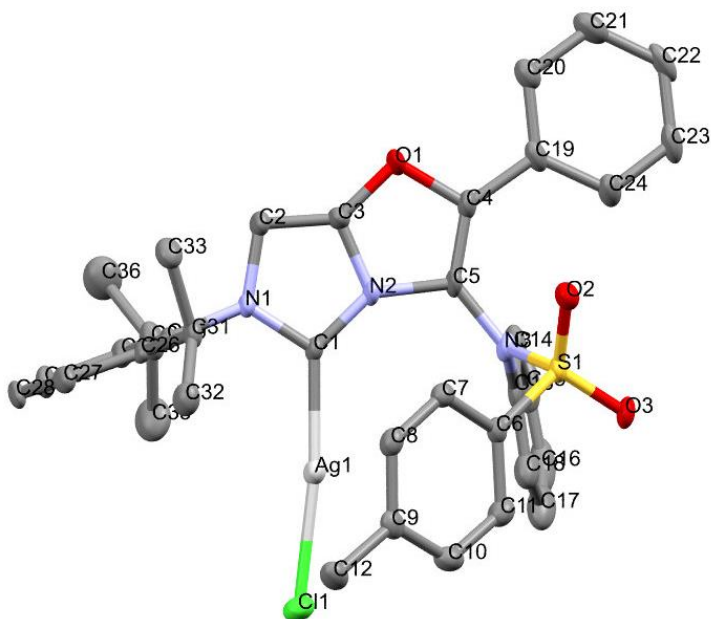
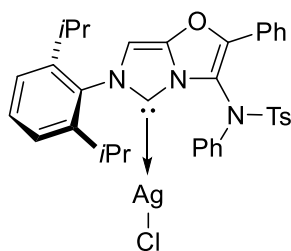


**Table 1 Crystal data and structure refinement for 353cAgCl.**

Identification code	353cAgCl
Empirical formula	C <sub>36</sub> H <sub>35</sub> AgClN <sub>3</sub> O <sub>3</sub> S
Formula weight	687.02
Temperature/K	100.00(10)
Crystal system	triclinic
Space group	P-1
a/Å	9.5159(3)
b/Å	12.5311(3)
c/Å	14.9148(3)
$\alpha$ /°	92.727(2)
$\beta$ /°	101.710(2)
$\gamma$ /°	104.879(2)
Volume/Å <sup>3</sup>	1673.74(8)
Z	2
$\rho_{\text{calc}}/\text{cm}^3$	1.363
$\mu/\text{mm}^{-1}$	0.775
F(000)	704.0
Crystal size/mm <sup>3</sup>	0.172 × 0.104 × 0.075
Radiation	MoK $\alpha$ ( $\lambda$ = 0.71073)
2 $\theta$ range for data collection/°	6.766 to 52.744
Index ranges	-11 ≤ h ≤ 11, -15 ≤ k ≤ 15, -18 ≤ l ≤ 18
Reflections collected	26113
Independent reflections	6824 [R <sub>int</sub> = 0.0304, R <sub>sigma</sub> = 0.0304]
Data/restraints/parameters	6824/0/411
Goodness-of-fit on F <sup>2</sup>	1.054
Final R indexes [I ≥ 2 $\sigma$ (I)]	R <sub>1</sub> = 0.0324, wR <sub>2</sub> = 0.0813
Final R indexes [all data]	R <sub>1</sub> = 0.0366, wR <sub>2</sub> = 0.0838
Largest diff. peak/hole / e Å <sup>-3</sup>	0.55/-0.48

**Table 2 Fractional Atomic Coordinates (×10<sup>4</sup>) and Equivalent Isotropic Displacement Parameters (Å<sup>2</sup>×10<sup>3</sup>) for 353cAgCl. U<sub>eq</sub> is defined as 1/3 of the trace of the orthogonalised U<sub>ij</sub> tensor.**

Atom	x	y	z	U(eq)
Ag01	9097.3(2)	7276.5(2)	2846.2(2)	19.39(7)
S002	7105.8(7)	3825.3(5)	1266.1(4)	18.06(14)
Cl03	11661.7(7)	8050.4(6)	3159.3(5)	29.84(16)
O004	3349(2)	4839.1(14)	2316.0(14)	24.6(4)
O005	7987(2)	3054.0(15)	1402.2(13)	23.4(4)
O006	5654(2)	3512.5(15)	671.9(13)	22.7(4)
N007	5952(2)	7462.6(16)	2759.4(14)	16.0(4)
N008	5770(2)	5750.6(16)	2489.6(15)	17.4(4)
N009	6848(2)	4180.1(17)	2309.3(15)	18.8(4)
C00A	8127(3)	5048(2)	916.6(17)	17.5(5)
C00B	6799(3)	6754.3(19)	2669.6(17)	15.4(5)
C00C	9675(3)	5326(2)	1092.1(19)	23.3(6)
C00D	5627(3)	4595(2)	2338.2(18)	19.0(5)
C00E	7348(3)	5746(2)	476.7(17)	19.2(5)
C00F	8134(3)	6736(2)	232.0(18)	20.3(5)
C00G	9689(3)	7057(2)	432.4(17)	20.6(5)
C00H	4433(3)	6931(2)	2640.7(19)	20.6(5)

C00I	4368(3)	5854(2)	2474.2(19)	21.0(5)
C00J	7793(3)	4030(2)	3161.5(18)	23.6(6)
C00K	6536(3)	8659.0(19)	2944.3(18)	17.1(5)
C00L	6627(3)	9277(2)	2193.6(18)	17.3(5)
C00M	10441(3)	6327(2)	852.2(19)	24.3(6)
C00N	3323(3)	2904(2)	2179.7(18)	21.9(6)
C00O	7109(3)	10429(2)	2384.2(19)	21.7(6)
C00P	4178(3)	4069(2)	2252.5(19)	21.9(6)
C00Q	1695(4)	712(2)	2186.2(19)	30.3(7)
C00R	6936(3)	9133(2)	3853.5(19)	21.9(6)
C00S	7427(3)	10288(2)	4007(2)	25.4(6)
C00T	4018(3)	2041(2)	2197(2)	27.2(6)
C00V	3197(4)	957(2)	2206(2)	30.4(7)
C00W	1799(3)	2650(2)	2146.9(19)	25.5(6)
C00X	7512(3)	10928(2)	3281(2)	24.3(6)
C00Y	6147(3)	8740(2)	1204.9(18)	20.6(5)
C00Z	10543(3)	8159(2)	205(2)	26.0(6)
C010	4569(3)	8801(2)	786(2)	27.6(6)
C011	7243(3)	9280(2)	623(2)	27.7(6)
C012	7127(4)	3656(2)	3875(2)	33.7(7)
C013	997(4)	1558(3)	2150(2)	33.1(7)
C014	6875(4)	8453(2)	4666.8(19)	29.7(7)
C015	9314(4)	4221(2)	3263(2)	32.7(7)
C016	5777(4)	8708(3)	5207(2)	45.5(9)
C017	10155(4)	3987(3)	4062(2)	44.6(9)
C018	8007(5)	3454(3)	4683(2)	47.1(10)
C019	8439(4)	8648(3)	5285(2)	43.3(8)
C01A	9507(5)	3599(3)	4763(2)	50.5(11)

**Table 3 Anisotropic Displacement Parameters ( $\text{\AA}^2 \times 10^3$ ) for 353cAgCl. The Anisotropic displacement factor exponent takes the form:  $-2\pi^2[h^2a^{*2}U_{11}+2hka^*b^*U_{12}+\dots]$ .**

Atom	U <sub>11</sub>	U <sub>22</sub>	U <sub>33</sub>	U <sub>23</sub>	U <sub>13</sub>	U <sub>12</sub>
Ag01	20.75(11)	16.22(11)	23.16(11)	3.26(7)	5.86(8)	7.54(8)
S002	22.7(3)	11.7(3)	20.9(3)	0.1(2)	5.7(3)	6.5(2)
Cl03	20.0(3)	32.8(4)	38.5(4)	2.4(3)	7.3(3)	10.0(3)
O004	22.2(10)	9.8(8)	41.8(12)	-1.2(8)	11.4(9)	1.7(7)
O005	31.2(10)	15.1(9)	27.2(10)	0.0(7)	6.9(8)	12.5(8)
O006	23.9(10)	17.0(9)	25.7(10)	0.3(7)	5.3(8)	3.6(8)
N007	17.8(10)	10.8(10)	20.2(11)	1.2(8)	3.6(9)	5.7(8)
N008	21.3(11)	9.2(10)	24.0(11)	2.5(8)	7.9(9)	6.0(8)
N009	26.9(12)	13.5(10)	19.7(11)	3.6(8)	7.7(9)	9.9(9)
C00A	23.0(13)	13.2(12)	17.3(12)	1.1(9)	5.9(10)	5.6(10)
C00B	19.8(12)	10.9(11)	18.0(12)	3.2(9)	5.8(10)	7.1(10)
C00C	24.2(14)	25.8(14)	22.4(13)	3.6(11)	4.5(11)	11.4(12)
C00D	26.5(14)	8.9(11)	24.7(13)	3.3(10)	10.4(11)	6.4(10)
C00E	17.9(12)	19.6(13)	19.7(13)	-0.7(10)	3.3(10)	5.6(10)
C00F	25.3(14)	19.9(13)	18.8(13)	4.6(10)	6.1(11)	10.3(11)
C00G	26.5(14)	19.3(13)	15.6(12)	-2.3(10)	7.5(11)	3.8(11)
C00H	19.2(13)	13.0(12)	30.6(15)	2.2(10)	5.5(11)	6.4(10)
C00I	16.1(12)	14.6(12)	31.8(15)	0.1(11)	6.5(11)	2.7(10)
C00J	41.1(17)	11.2(12)	20.0(13)	-1.3(10)	3.0(12)	13.2(12)
C00K	15.6(12)	8.9(11)	26.6(13)	-0.2(10)	3.5(10)	4.5(9)



C00L	16.0(12)	12.0(12)	24.8(13)	1.9(10)	2.9(10)	6.6(10)
C00M	19.3(13)	27.5(15)	24.8(14)	0.6(11)	5.1(11)	4.2(11)
C00N	30.5(15)	13.4(12)	20.1(13)	-0.5(10)	8.7(11)	0.7(11)
C00O	22.7(13)	14.0(12)	29.3(14)	6.5(11)	4.8(11)	6.7(11)
C00P	28.3(14)	12.8(12)	27.8(14)	1.1(10)	10.6(12)	7.8(11)
C00Q	45.9(18)	14.6(13)	21.8(14)	0.3(11)	8.6(13)	-7.3(13)
C00R	25.3(14)	17.0(13)	24.5(14)	1.6(10)	4.1(11)	9.0(11)
C00S	31.0(15)	15.8(13)	27.3(14)	-5.9(11)	1.1(12)	8.2(11)
C00T	34.9(16)	16.0(13)	33.3(16)	1.6(11)	17.0(13)	4.6(12)
C00V	51.0(19)	13.4(13)	27.3(15)	-0.3(11)	14.1(14)	5.9(13)
C00W	29.4(15)	18.0(13)	26.3(14)	1.6(11)	6.0(12)	1.7(11)
C00X	23.2(14)	8.8(12)	37.4(16)	-2.1(11)	0.3(12)	4.1(10)
C00Y	26.9(14)	11.8(12)	23.7(13)	2.5(10)	4.2(11)	7.2(11)
C00Z	26.4(14)	22.9(14)	29.1(15)	1.8(11)	12.9(12)	2.3(12)
C010	28.1(15)	22.6(14)	27.8(15)	-1.0(11)	-1.2(12)	6.2(12)
C011	36.1(16)	22.8(14)	27.9(15)	6.9(12)	10.4(13)	11.4(13)
C012	59(2)	17.4(14)	28.4(15)	4.4(12)	12.2(15)	13.8(14)
C013	31.6(16)	27.8(16)	32.9(16)	4.3(13)	7.9(13)	-4.8(13)
C014	46.6(18)	18.2(14)	22.5(14)	1.2(11)	5.9(13)	7.5(13)
C015	39.9(18)	24.6(15)	31.5(16)	-4.4(12)	-0.3(14)	13.0(13)
C016	61(2)	46(2)	33.9(18)	9.7(15)	20.8(17)	13.4(18)
C017	56(2)	35.3(18)	36.3(19)	-11.0(15)	-12.2(17)	21.6(17)
C018	99(3)	22.0(16)	22.4(16)	4.7(12)	11.0(18)	22.0(18)
C019	57(2)	40.7(19)	33.9(18)	11.4(15)	0.1(16)	23.3(17)
C01A	88(3)	28.6(17)	28.0(18)	-6.9(14)	-17.2(19)	28.1(19)

**Table 4 Bond Lengths for 353cAgCl.**

Atom Atom	Length/Å	Atom Atom	Length/Å
Ag01 Cl03	2.3221(7)	C00J C012	1.386(4)
Ag01 C00B	2.073(2)	C00J C015	1.380(4)
S002 O005	1.4295(18)	C00K C00L	1.396(4)
S002 O006	1.428(2)	C00K C00R	1.391(4)
S002 N009	1.680(2)	C00L C00O	1.394(3)
S002 C00A	1.756(3)	C00L C00Y	1.520(4)
O004 C00I	1.364(3)	C00N C00P	1.464(4)
O004 C00P	1.406(3)	C00N C00T	1.404(4)
N007 C00B	1.362(3)	C00N C00W	1.393(4)
N007 C00H	1.398(3)	C00O C00X	1.384(4)
N007 C00K	1.450(3)	C00Q C00V	1.377(5)
N008 C00B	1.357(3)	C00Q C013	1.385(5)
N008 C00D	1.422(3)	C00R C00S	1.394(4)
N008 C00I	1.369(3)	C00R C014	1.518(4)
N009 C00D	1.397(3)	C00S C00X	1.381(4)
N009 C00J	1.451(3)	C00T C00V	1.385(4)
C00A C00C	1.389(4)	C00W C013	1.386(4)
C00A C00E	1.391(4)	C00Y C010	1.528(4)
C00C C00M	1.383(4)	C00Y C011	1.536(4)
C00D C00P	1.343(4)	C012 C018	1.395(5)
C00E C00F	1.382(4)	C014 C016	1.527(5)
C00F C00G	1.395(4)	C014 C019	1.536(5)
C00G C00M	1.395(4)	C015 C017	1.384(4)
C00G C00Z	1.504(4)	C017 C01A	1.367(6)

C00H C00I 1.343(4) C018 C01A 1.371(6)

**Table 5 Bond Angles for 353cAgCl.**

Atom Atom Atom	Angle/°	Atom Atom Atom	Angle/°
C00B Ag01 Cl03	172.85(7)	C015 C00J N009	121.6(3)
O005 S002 N009	106.03(11)	C015 C00J C012	120.0(3)
O005 S002 C00A	109.83(12)	C00L C00K N007	117.9(2)
O006 S002 O005	120.84(11)	C00R C00K N007	118.6(2)
O006 S002 N009	105.51(11)	C00R C00K C00L	123.4(2)
O006 S002 C00A	107.56(12)	C00K C00L C00Y	122.4(2)
N009 S002 C00A	106.09(11)	C00O C00L C00K	117.0(2)
C00I O004 C00P	105.3(2)	C00O C00L C00Y	120.6(2)
C00B N007 C00H	113.6(2)	C00C C00M C00G	121.3(3)
C00B N007 C00K	124.2(2)	C00T C00N C00P	121.5(3)
C00H N007 C00K	122.1(2)	C00W C00N C00P	119.2(2)
C00B N008 C00D	142.1(2)	C00W C00N C00T	119.1(2)
C00B N008 C00I	111.3(2)	C00X C00O C00L	121.1(2)
C00I N008 C00D	106.6(2)	O004 C00P C00N	114.7(2)
C00D N009 S002	117.35(18)	C00D C00P O004	110.5(2)
C00D N009 C00J	119.7(2)	C00D C00P C00N	134.5(2)
C00J N009 S002	122.93(17)	C00V C00Q C013	119.7(3)
C00C C00A S002	121.0(2)	C00K C00R C00S	117.3(2)
C00C C00A C00E	120.8(2)	C00K C00R C014	123.0(2)
C00E C00A S002	118.2(2)	C00S C00R C014	119.6(2)
N007 C00B Ag01	123.09(17)	C00X C00S C00R	120.9(3)
N008 C00B Ag01	134.41(17)	C00V C00T C00N	120.0(3)
N008 C00B N007	102.5(2)	C00Q C00V C00T	120.6(3)
C00M C00C C00A	119.1(2)	C013 C00W C00N	119.9(3)
N009 C00D N008	122.3(2)	C00S C00X C00O	120.3(2)
C00P C00D N008	106.8(2)	C00L C00Y C010	109.7(2)
C00P C00D N009	130.8(2)	C00L C00Y C011	111.6(2)
C00F C00E C00A	119.2(2)	C010 C00Y C011	111.0(2)
C00E C00F C00G	121.3(2)	C00J C012 C018	119.2(3)
C00F C00G C00M	118.3(2)	C00Q C013 C00W	120.7(3)
C00F C00G C00Z	121.2(2)	C00R C014 C016	110.8(3)
C00M C00G C00Z	120.5(2)	C00R C014 C019	110.6(3)
C00I C00H N007	103.1(2)	C016 C014 C019	111.6(3)
O004 C00I N008	110.8(2)	C00J C015 C017	119.6(3)
C00H C00I O004	139.7(2)	C01A C017 C015	120.9(4)
C00H C00I N008	109.5(2)	C01A C018 C012	120.4(3)
C012 C00J N009	118.3(3)	C017 C01A C018	119.8(3)

**Table 6 Hydrogen Atom Coordinates ( $\text{\AA} \times 10^4$ ) and Isotropic Displacement Parameters ( $\text{\AA}^2 \times 10^3$ ) for 353cAgCl.**

Atom	x	y	z	U(eq)
H00C	10189	4845	1367	28
H00E	6311	5548	349	23
H00F	7615	7198	-72	24
H00H	3657	7246	2670	25
H00M	11477	6518	973	29
H00O	7160	10870	1901	26

H00Q	1152	-17	2197	36
H00S	7701	10633	4607	31
H00T	5029	2197	2201	33
H00V	3665	389	2227	36
H00W	1321	3212	2123	31
H00X	7841	11698	3395	29
H00Y	6131	7955	1211	25
H00A	9856	8533	-110	39
H00B	11192	8042	-183	39
H00D	11125	8604	763	39
H01A	3893	8414	1136	41
H01B	4271	8464	161	41
H01C	4551	9564	798	41
H01D	7255	10046	594	41
H01E	6935	8900	12	41
H01F	8225	9232	900	41
H012	6106	3541	3815	40
H013	-21	1391	2128	40
H014	6515	7666	4426	36
H015	9770	4504	2796	39
H01G	6131	9467	5475	68
H01H	5692	8227	5687	68
H01I	4817	8592	4800	68
H017	11176	4096	4123	53
H018	7574	3220	5170	57
H01J	9111	8515	4919	65
H01K	8399	8151	5755	65
H01L	8784	9402	5566	65
H01M	10081	3433	5293	61

**Table 7 Solvent masks information for 353cAgCl.**

Number	X	Y	Z	Volume	Electron count	Content
1	0.500	0.500	0.500	92	14	

#### Experimental

A suitable crystal was selected on a **SuperNova, Dual, Cu at zero, Atlas** diffractometer. The crystal was kept at 100.00(10) K during data collection. Using Olex2,<sup>275</sup> the structure was solved with the ShelXT<sup>276</sup> structure solution program using Intrinsic Phasing and refined with the ShelXL<sup>277</sup> refinement package using Least Squares minimisation.

#### Crystal structure determination of [353cAgCl]

**Crystal Data** for  $C_{36}H_{35}AgClN_3O_3S$  ( $M = 687.02$  g/mol): triclinic, space group P-1 (no. 2),  $a = 9.5159(3)$  Å,  $b = 12.5311(3)$  Å,  $c = 14.9148(3)$  Å,  $\alpha = 92.727(2)^\circ$ ,  $\beta = 101.710(2)^\circ$ ,  $\gamma = 104.879(2)^\circ$ ,  $V = 1673.74(8)$  Å<sup>3</sup>,  $Z = 2$ ,  $T = 100.00(10)$  K,  $\mu(\text{MoK}\alpha) = 0.775$  mm<sup>-1</sup>,  $D_{\text{calc}} = 1.363$  g/cm<sup>3</sup>, 26113 reflections measured ( $6.766^\circ \leq 2\theta \leq 52.744^\circ$ ), 6824 unique ( $R_{\text{int}} = 0.0304$ ,  $R_{\text{sigma}} = 0.0304$ ) which were used in all calculations. The final  $R_1$  was 0.0324 ( $I > 2\sigma(I)$ ) and  $wR_2$  was 0.0838 (all data).

#### Refinement model description

Number of restraints - 0, number of constraints - unknown.

Details:

1. Fixed Uiso

At 1.2 times of:

All C(H) groups

At 1.5 times of:

All C(H,H,H) groups

2.a Ternary CH refined with riding coordinates:

C00Y(H00Y), C014(H014)

2.b Aromatic/amide H refined with riding coordinates:

C00C(H00C), C00E(H00E), C00F(H00F), C00H(H00H), C00M(H00M), C00O(H00O), C00Q(H00Q), C00S(H00S), C00T(H00T), C00V(H00V), C00W(H00W), C00X(H00X), C012(H012), C013(H013), C015(H015), C017(H017), C018(H018), C01A(H01M)

2.c Idealised Me refined as rotating group:

C00Z(H00A,H00B,H00D), C010(H01A,H01B,H01C), C011(H01D,H01E,H01F), C016(H01G,H01H,H01I), C019(H01J,H01K,H01L)

## 8.7 353aAuCl

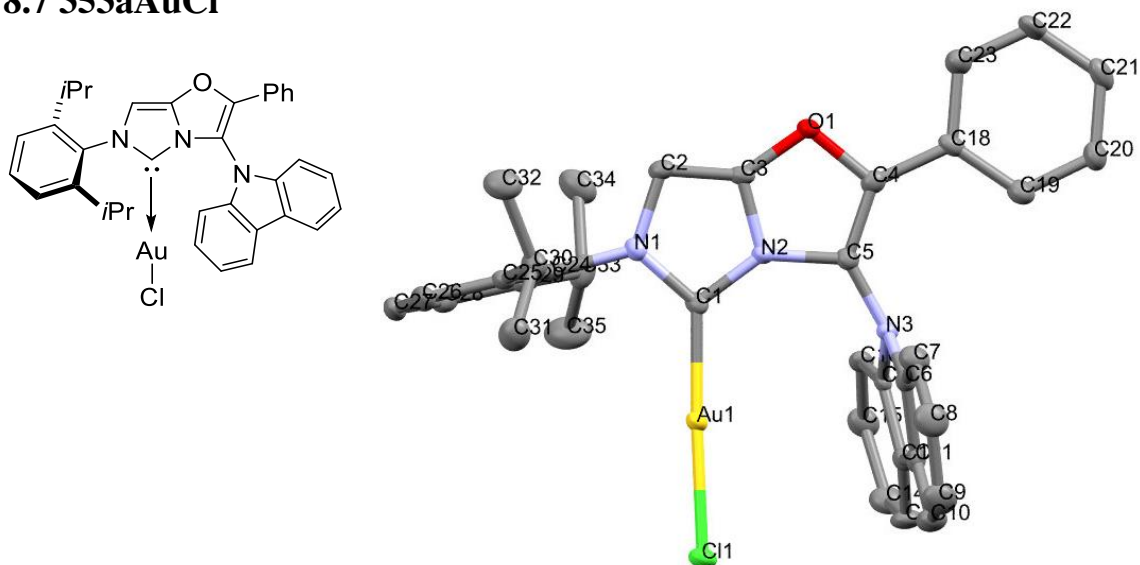


**Table 1** Crystal data and structure refinement for 353aAuCl.

Identification code	353aAuCl
Empirical formula	C <sub>35</sub> H <sub>31</sub> N <sub>3</sub> OAuCl
Formula weight	742.04
Temperature/K	100.01(10)
Crystal system	orthorhombic
Space group	P2 <sub>1</sub> 2 <sub>1</sub> 2 <sub>1</sub>
a/Å	9.45860(10)
b/Å	14.4467(2)
c/Å	22.1038(3)
α/°	90
β/°	90
γ/°	90
Volume/Å <sup>3</sup>	3020.39(7)
Z	4
ρ <sub>calc</sub> /cm <sup>3</sup>	1.632
μ/mm <sup>-1</sup>	4.992
F(000)	1464.0
Crystal size/mm <sup>3</sup>	0.269 × 0.163 × 0.094
Radiation	MoKα (λ = 0.71073)
2θ range for data collection/°	6.738 to 52.744
Index ranges	-11 ≤ h ≤ 11, -18 ≤ k ≤ 18, -27 ≤ l ≤ 27

Reflections collected	31104
Independent reflections	6167 [ $R_{\text{int}} = 0.0338$ , $R_{\text{sigma}} = 0.0268$ ]
Data/restraints/parameters	6167/0/374
Goodness-of-fit on $F^2$	1.038
Final R indexes [ $I > 2\sigma(I)$ ]	$R_1 = 0.0177$ , $wR_2 = 0.0348$
Final R indexes [all data]	$R_1 = 0.0190$ , $wR_2 = 0.0352$
Largest diff. peak/hole / $e \text{ \AA}^{-3}$	0.65/-0.42
Flack parameter	-0.019(3)

**Table 2 Fractional Atomic Coordinates ( $\times 10^4$ ) and Equivalent Isotropic Displacement Parameters ( $\text{\AA}^2 \times 10^3$ ) for 353aAuCl.  $U_{\text{eq}}$  is defined as 1/3 of the trace of the orthogonalised  $U_{\text{ij}}$  tensor.**

Atom	x	y	z	U(eq)
Au1	7161.1(2)	6277.5(2)	7410.2(2)	13.87(4)
Cl1	8682.9(10)	7491.1(6)	7510.8(5)	19.9(2)
N2	5610(4)	4777(2)	6753.1(15)	13.5(7)
O1	4441(3)	3642(2)	6284.9(11)	16.5(6)
N3	7224(4)	5296(2)	5952.5(14)	13.7(7)
N1	4946(3)	4798(2)	7665.6(16)	15.5(7)
C6	7000(4)	6222(3)	5752.0(15)	15.9(8)
C1	5848(4)	5234(3)	7283.1(18)	14.4(9)
C5	6147(4)	4727(3)	6153.1(18)	14.8(9)
C11	8264(4)	6708(3)	5810.0(18)	16.7(10)
C24	4940(4)	4956(3)	8311.9(18)	14.9(9)
C17	8634(4)	5235(3)	6161.7(18)	14.3(9)
C7	5781(5)	6614(3)	5527(2)	23.9(11)
C20	6521(5)	3500(3)	4294.0(19)	22.6(11)
C12	9302(4)	6080(3)	6059.6(17)	15.9(9)
C29	5941(5)	4473(3)	8659(2)	18.6(10)
C2	4174(4)	4091(2)	7392.5(19)	15.4(8)
C25	3932(4)	5548(3)	8556.3(19)	16.2(9)
C13	10730(4)	6174(3)	6200.2(19)	22.9(9)
C10	8287(5)	7651(3)	5662(2)	24.0(11)
C16	9304(5)	4497(3)	6432.9(19)	17.8(9)
C9	7075(5)	8055(3)	5443(2)	28.9(11)
C3	4621(4)	4098(3)	6818.0(19)	15.2(9)
C26	3945(5)	5651(3)	9185(2)	21.5(10)
C30	2831(5)	6031(3)	8167.6(18)	20.8(9)
C15	10712(5)	4611(3)	6583(2)	23.3(10)
C28	5884(5)	4600(3)	9281(2)	21.1(10)
C21	5728(5)	2729(3)	4172(2)	24.8(10)
C31	2771(6)	7077(3)	8283(2)	29.4(10)
C33	7006(4)	3826(3)	8362.5(18)	24.3(9)
C34	6478(5)	2822(3)	8367(2)	33.5(12)
C32	1384(5)	5576(3)	8253(2)	32.0(12)
C14	11428(5)	5435(3)	6460(2)	27.1(11)
C18	5508(4)	3601(3)	5290.6(18)	17.3(9)
C4	5424(4)	4030(3)	5883.2(19)	16.0(9)
C23	4697(5)	2818(3)	5164(2)	25.0(11)
C8	5841(5)	7547(3)	5374(2)	28.9(12)
C19	6419(5)	3941(3)	4849.4(19)	22.7(10)

C35	8461(5)	3883(4)	8652(3)	42.2(14)
C27	4901(5)	5188(3)	9538(2)	23.6(11)
C22	4818(5)	2393(3)	4608(2)	28.1(12)

**Table 3 Anisotropic Displacement Parameters ( $\text{\AA}^2 \times 10^3$ ) for 353aAuCl. The Anisotropic displacement factor exponent takes the form:  $-2\pi^2[h^2a^{*2}U_{11}+2hka^*b^*U_{12}+\dots]$ .**

Atom	U <sub>11</sub>	U <sub>22</sub>	U <sub>33</sub>	U <sub>23</sub>	U <sub>13</sub>	U <sub>12</sub>
Au1	15.50(7)	12.31(7)	13.80(7)	-2.10(6)	-0.36(6)	-0.98(7)
Cl1	21.7(5)	15.0(4)	23.0(6)	-2.6(4)	-2.6(5)	-3.8(4)
N2	13.6(18)	12.2(17)	14.7(18)	-1.7(14)	0.1(15)	-2.0(16)
O1	16.4(14)	17.1(15)	16.1(14)	-2.7(13)	-0.3(11)	-4.8(14)
N3	15.3(16)	11.7(15)	14.3(16)	-0.7(12)	-0.6(17)	-3.0(16)
N1	14.5(17)	16.0(17)	16.0(18)	-3.1(15)	-0.2(15)	1.6(13)
C6	21(2)	14.5(18)	12.6(18)	-0.1(18)	1.6(17)	-2(2)
C1	8.7(18)	16.3(19)	18(2)	-4.5(17)	0.1(17)	3.0(16)
C5	14(2)	16(2)	15(2)	-0.8(17)	-2.4(17)	0.6(18)
C11	20(2)	19(2)	12(2)	1.5(17)	1.9(17)	1.4(18)
C24	15(2)	14(2)	16(2)	-2.5(17)	1.3(17)	-5.5(17)
C17	15(2)	18(2)	10(2)	-3.0(16)	0.3(17)	-2.0(19)
C7	23(2)	22(2)	26(3)	0.3(19)	-6(2)	0(2)
C20	26(2)	26(3)	16(2)	-0.9(17)	-0.1(19)	0(2)
C12	20(2)	15(2)	13(2)	-2.6(16)	1.1(17)	-0.4(18)
C29	15(2)	15(2)	25(3)	1.8(19)	1.1(19)	-3.8(18)
C2	11.3(17)	13.0(17)	22(2)	0.0(18)	0.9(19)	-0.5(15)
C25	15(2)	14(2)	19(2)	-2.2(17)	0.5(18)	-2.8(17)
C13	21(2)	17(2)	31(2)	1(2)	-1.6(19)	-8(2)
C10	26(3)	18(2)	28(3)	2.6(19)	-1(2)	-4.5(19)
C16	24(2)	11(2)	18(2)	0.1(17)	0(2)	-2.3(19)
C9	34(3)	16(2)	36(3)	5.1(18)	-4(3)	5(2)
C3	11(2)	11(2)	23(2)	-3.1(17)	-0.7(18)	0.1(17)
C26	24(2)	19(2)	22(2)	-6.3(19)	6(2)	-1.8(19)
C30	19(2)	22(2)	22(2)	-3.1(16)	2(2)	4(2)
C15	26(2)	17(2)	28(3)	1.1(19)	-6(2)	7(2)
C28	18(2)	23(2)	22(3)	3.9(19)	-2(2)	-3(2)
C21	39(3)	21(2)	14(2)	-2.1(19)	-6(2)	5(2)
C31	35(3)	22(2)	32(3)	1.8(19)	3(3)	6(2)
C33	20(2)	29(2)	23(2)	6(2)	2.9(18)	9(2)
C34	30(3)	29(3)	41(3)	-12(2)	-7(3)	10(2)
C32	22(3)	28(3)	45(3)	-3(2)	-6(2)	3(2)
C14	19(2)	26(3)	36(3)	-1(2)	-7(2)	1(2)
C18	19(2)	14(2)	18(2)	-1.8(18)	-7.3(17)	0.8(19)
C4	15(2)	14(2)	19(2)	2.4(16)	0.0(18)	1.7(17)
C23	32(3)	23(3)	20(2)	1.5(19)	-1(2)	-7(2)
C8	29(3)	25(3)	33(3)	4(2)	-9(2)	9(2)
C19	21(2)	24(3)	23(2)	-4.4(18)	-2.1(19)	-3(2)
C35	21(2)	33(3)	72(4)	-6(3)	0(3)	5(2)
C27	33(3)	23(3)	15(2)	-2.8(19)	1(2)	-10(2)
C22	45(3)	18(2)	21(3)	-4(2)	-6(2)	-9(2)

**Table 4 Bond Lengths for 353aAuCl.**

Atom	Atom	Length/Å	Atom	Atom	Length/Å
Au1	Cl1	2.2793(9)	C20	C19	1.387(6)
Au1	C1	1.973(4)	C12	C13	1.393(6)
N2	C1	1.364(5)	C29	C28	1.387(6)
N2	C5	1.422(5)	C29	C33	1.523(6)
N2	C3	1.363(5)	C2	C3	1.338(6)
O1	C3	1.361(5)	C25	C26	1.398(6)
O1	C4	1.403(5)	C25	C30	1.520(6)
N3	C6	1.425(5)	C13	C14	1.380(6)
N3	C5	1.382(5)	C10	C9	1.373(6)
N3	C17	1.414(5)	C16	C15	1.383(7)
N1	C1	1.356(5)	C9	C8	1.387(7)
N1	C24	1.447(5)	C26	C27	1.369(6)
N1	C2	1.393(5)	C30	C31	1.533(6)
C6	C11	1.392(6)	C30	C32	1.531(6)
C6	C7	1.377(6)	C15	C14	1.395(6)
C5	C4	1.355(6)	C28	C27	1.382(6)
C11	C12	1.446(6)	C21	C22	1.380(7)
C11	C10	1.402(6)	C33	C34	1.533(7)
C24	C29	1.405(6)	C33	C35	1.520(6)
C24	C25	1.390(6)	C18	C4	1.451(6)
C17	C12	1.393(5)	C18	C23	1.395(6)
C17	C16	1.377(6)	C18	C19	1.391(6)
C7	C8	1.391(6)	C23	C22	1.379(6)
C20	C21	1.370(6)			

**Table 5 Bond Angles for 353aAuCl.**

Atom	Atom	Atom	Angle/°	Atom	Atom	Atom	Angle/°
C1	Au1	Cl1	177.41(12)	C28	C29	C24	116.7(4)
C1	N2	C5	140.1(4)	C28	C29	C33	122.3(4)
C3	N2	C1	111.8(3)	C3	C2	N1	103.9(3)
C3	N2	C5	107.9(3)	C24	C25	C26	116.5(4)
C3	O1	C4	105.7(3)	C24	C25	C30	122.2(4)
C5	N3	C6	123.3(4)	C26	C25	C30	121.3(4)
C5	N3	C17	123.6(3)	C14	C13	C12	118.8(4)
C17	N3	C6	107.5(3)	C9	C10	C11	118.8(4)
C1	N1	C24	123.0(3)	C17	C16	C15	117.1(4)
C1	N1	C2	113.6(3)	C10	C9	C8	121.1(4)
C2	N1	C24	122.8(3)	O1	C3	N2	110.1(3)
C11	C6	N3	108.5(3)	C2	C3	N2	108.8(4)
C7	C6	N3	128.5(4)	C2	C3	O1	141.1(4)
C7	C6	C11	123.0(4)	C27	C26	C25	121.3(4)
N2	C1	Au1	126.6(3)	C25	C30	C31	112.6(4)
N1	C1	Au1	131.4(3)	C25	C30	C32	110.2(3)
N1	C1	N2	101.9(3)	C32	C30	C31	111.7(4)
N3	C5	N2	122.1(3)	C16	C15	C14	121.5(4)
C4	C5	N2	105.6(4)	C27	C28	C29	121.0(4)
C4	C5	N3	132.3(4)	C20	C21	C22	119.3(4)
C6	C11	C12	107.6(4)	C29	C33	C34	111.2(4)
C6	C11	C10	118.8(4)	C35	C33	C29	112.6(4)
C10	C11	C12	133.5(4)	C35	C33	C34	110.1(4)
C29	C24	N1	117.3(4)	C13	C14	C15	120.6(4)

C25	C24	N1	118.9(4)	C23	C18	C4	119.8(4)
C25	C24	C29	123.7(4)	C19	C18	C4	121.1(4)
C12	C17	N3	108.6(3)	C19	C18	C23	119.1(4)
C16	C17	N3	128.7(4)	O1	C4	C18	115.9(3)
C16	C17	C12	122.7(4)	C5	C4	O1	110.7(4)
C6	C7	C8	116.9(5)	C5	C4	C18	133.4(4)
C21	C20	C19	120.7(4)	C22	C23	C18	119.6(4)
C17	C12	C11	107.7(4)	C9	C8	C7	121.3(5)
C17	C12	C13	119.3(4)	C20	C19	C18	120.1(4)
C13	C12	C11	133.1(4)	C26	C27	C28	120.7(4)
C24	C29	C33	121.0(4)	C23	C22	C21	121.2(4)

**Table 6 Torsion Angles for 353aAuCl.**

A	B	C	D	Angle/°	A	B	C	D	Angle/°
N2	C5	C4	O1	0.6(4)	C17	N3	C6	C7	-178.1(4)
N2	C5	C4	C18	-176.5(4)	C17	N3	C5	N2	68.4(5)
N3	C6	C11	C12	-0.8(4)	C17	N3	C5	C4	-109.0(5)
N3	C6	C11	C10	-177.5(4)	C17	C12	C13	C14	-2.6(6)
N3	C6	C7	C8	178.7(4)	C17	C16	C15	C14	-0.6(7)
N3	C5	C4	O1	178.4(4)	C7	C6	C11	C12	180.0(4)
N3	C5	C4	C18	1.3(8)	C7	C6	C11	C10	3.2(6)
N3	C17	C12	C11	3.2(4)	C20	C21	C22	C23	-0.2(7)
N3	C17	C12	C13	-176.7(3)	C12	C11	C10	C9	-178.0(5)
N3	C17	C16	C15	178.5(4)	C12	C17	C16	C15	-2.6(6)
N1	C24	C29	C28	-177.3(4)	C12	C13	C14	C15	-0.4(7)
N1	C24	C29	C33	1.3(6)	C29	C24	C25	C26	0.0(6)
N1	C24	C25	C26	177.9(4)	C29	C24	C25	C30	-177.6(4)
N1	C24	C25	C30	0.3(6)	C29	C28	C27	C26	0.8(7)
N1	C2	C3	N2	-0.1(4)	C2	N1	C1	Au1	178.9(3)
N1	C2	C3	O1	177.9(5)	C2	N1	C1	N2	0.3(4)
C6	N3	C5	N2	-81.7(5)	C2	N1	C24	C29	88.3(4)
C6	N3	C5	C4	100.8(5)	C2	N1	C24	C25	-89.8(5)
C6	N3	C17	C12	-3.7(4)	C25	C24	C29	C28	0.6(6)
C6	N3	C17	C16	175.4(4)	C25	C24	C29	C33	179.3(4)
C6	C11	C12	C17	-1.5(4)	C25	C26	C27	C28	-0.1(7)
C6	C11	C12	C13	178.3(4)	C10	C11	C12	C17	174.5(5)
C6	C11	C10	C9	-2.3(6)	C10	C11	C12	C13	-5.6(8)
C6	C7	C8	C9	0.2(7)	C10	C9	C8	C7	0.6(8)
C1	N2	C5	N3	-3.3(8)	C16	C17	C12	C11	-176.0(4)
C1	N2	C5	C4	174.8(5)	C16	C17	C12	C13	4.2(6)
C1	N2	C3	O1	-178.4(3)	C16	C15	C14	C13	2.1(7)
C1	N2	C3	C2	0.3(5)	C3	N2	C1	Au1	-179.1(3)
C1	N1	C24	C29	-82.2(5)	C3	N2	C1	N1	-0.3(4)
C1	N1	C24	C25	99.8(4)	C3	N2	C5	N3	-176.7(4)
C1	N1	C2	C3	-0.2(4)	C3	N2	C5	C4	1.4(4)
C5	N2	C1	Au1	7.7(7)	C3	O1	C4	C5	-2.3(4)
C5	N2	C1	N1	-173.6(5)	C3	O1	C4	C18	175.3(3)
C5	N2	C3	O1	-2.9(4)	C26	C25	C30	C31	53.5(5)
C5	N2	C3	C2	175.7(3)	C26	C25	C30	C32	-72.0(5)
C5	N3	C6	C11	156.9(4)	C30	C25	C26	C27	177.4(4)
C5	N3	C6	C7	-23.9(6)	C28	C29	C33	C34	83.7(5)
C5	N3	C17	C12	-157.8(4)	C28	C29	C33	C35	-40.4(6)



C5 N3 C17C16	21.3(6)	C21 C20 C19 C18	0.2(7)
C11 C6 C7 C8	-2.1(7)	C33 C29 C28 C27	-179.6(4)
C11 C12 C13 C14	177.6(4)	C18 C23 C22 C21	-0.1(7)
C11 C10 C9 C8	0.5(7)	C4 O1 C3 N2	3.2(4)
C24 N1 C1 Au1	-9.9(6)	C4 O1 C3 C2	-174.7(5)
C24 N1 C1 N2	171.5(3)	C4 C18 C23 C22	-177.7(4)
C24 N1 C2 C3	-171.4(3)	C4 C18 C19 C20	177.6(4)
C24 C29 C28 C27	-1.0(6)	C23 C18 C4 O1	-3.6(6)
C24 C29 C33 C34	-94.9(5)	C23 C18 C4 C5	173.4(5)
C24 C29 C33 C35	141.0(4)	C23 C18 C19 C20	-0.5(6)
C24 C25 C26 C27	-0.2(6)	C19 C20 C21 C22	0.1(7)
C24 C25 C30 C31	-129.0(4)	C19 C18 C4 O1	178.4(4)
C24 C25 C30 C32	105.5(5)	C19 C18 C4 C5	-4.6(7)
C17 N3 C6 C11	2.7(4)	C19 C18 C23 C22	0.4(7)

**Table 7 Hydrogen Atom Coordinates ( $\text{\AA}\times 10^4$ ) and Isotropic Displacement Parameters ( $\text{\AA}^2\times 10^3$ ) for 353aAuCl.**

Atom	x	y	z	U(eq)
H7	4956.75	6271.33	5479.97	29
H20	7134.65	3730.11	4001.53	27
H2	3503.49	3704.58	7568.42	19
H13	11205.19	6723.94	6120.57	27
H10	9107.76	7997.41	5709.96	29
H16	8829.52	3946.05	6511.66	21
H9	7082.47	8678.84	5340.5	35
H26	3290.57	6042.71	9367.67	26
H30	3105.81	5942.1	7744.08	25
H15	11193.78	4128.33	6769.83	28
H28	6517.64	4285.3	9528.07	25
H21	5801.29	2435.39	3798.83	30
H31A	2544.12	7188.43	8699.73	44
H31B	2058.04	7349.06	8029.87	44
H31C	3672.27	7347.66	8190.69	44
H33	7103.14	4015.71	7938.94	29
H34A	6421.25	2605.27	8776.99	50
H34B	7123.3	2440.04	8143.67	50
H34C	5558.96	2793.23	8183.89	50
H32A	1445.55	4931.19	8150.36	48
H32B	704.45	5872.23	7994.94	48
H32C	1093.16	5637.68	8667.13	48
H14	12383.24	5485.99	6553.79	33
H23	4079.2	2584.03	5453.48	30
H8	5038.01	7836.41	5221.52	35
H19	6960.22	4465.56	4927.12	27
H35A	8792.56	4510.53	8637.73	63
H35B	9105.74	3490.9	8435.39	63
H35C	8403.77	3683.21	9065.46	63
H27	4888.59	5269.64	9955.2	28
H22	4276.99	1870.71	4525.08	34

## Experimental

A suitable crystal was selected on a **SuperNova, Dual, Cu at zero, Atlas** diffractometer. The crystal was kept at 100.01(10) K during data collection. Using Olex2<sup>275</sup>, the structure was solved with the ShelXS<sup>278</sup> structure solution program using Direct Methods and refined with the ShelXL<sup>277</sup> refinement package using Least Squares minimisation.

**Crystal Data** for  $\text{C}_{35}\text{H}_{31}\text{N}_3\text{OAUCl}$  ( $M = 742.04$  g/mol): orthorhombic, space group  $\text{P2}_1\text{2}_1\text{2}_1$  (no. 19),  $a = 9.45860(10)$  Å,  $b = 14.4467(2)$  Å,  $c = 22.1038(3)$  Å,  $V = 3020.39(7)$  Å<sup>3</sup>,  $Z = 4$ ,  $T = 100.01(10)$  K,  $\mu(\text{MoK}\alpha) = 4.992$  mm<sup>-1</sup>,  $D_{\text{calc}} = 1.632$  g/cm<sup>3</sup>, 31104 reflections measured ( $6.738^\circ \leq 2\theta \leq 52.744^\circ$ ), 6167 unique ( $R_{\text{int}} = 0.0338$ ,  $R_{\text{sigma}} = 0.0268$ ) which were used in all calculations. The final  $R_1$  was 0.0177 ( $I > 2\sigma(I)$ ) and  $wR_2$  was 0.0352 (all data).

Number of restraints - 0, number of constraints - unknown.

## 1. Fixed Uiso

At 1.2 times of:

All C(H) groups

At 1.5 times of:

All C(H,H,H) groups

### 2.a Ternary CH refined with riding coordinates:

C30(H30), C33(H33)

2.b Aromatic/amide H refined with riding coordinates:

C7(H7), C20(H20), C2(H2), C13(H13), C10(H10), C16(H16), C9(H9), C26(H26),

C15(H15), C28(H28), C21(H21), C14(H14), C23(H23), C8(H8), C19(H19), C27(H27),

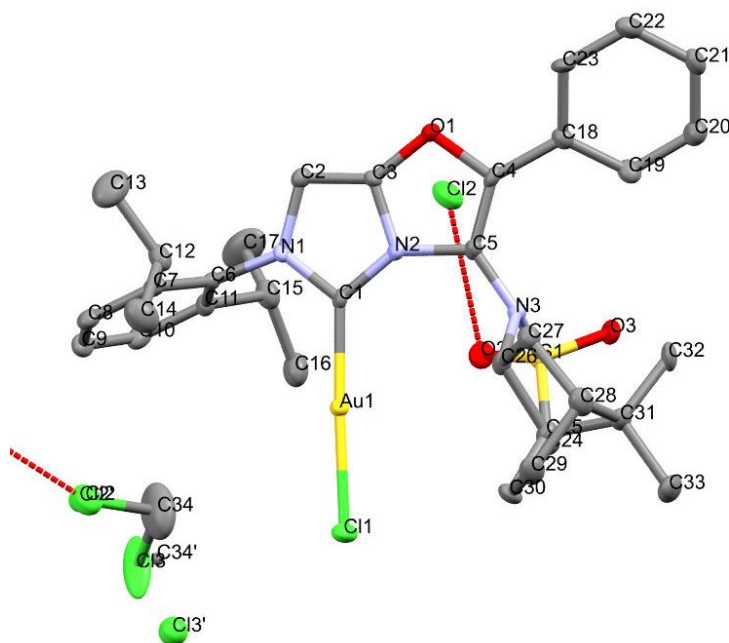
C22(H22)

### 2.c Idealised Me refined as rotating group:

C31(H31A,H31B,H31C), C34(H34A,H34B,H34C), C32(H32A,H32B,H32C), C35(H35A,H35B,

H35C)

Chemical reaction scheme showing the synthesis of a gold complex. A ligand with a benzimidazole core, a phenyl group, and two isopropyl groups reacts with AuCl to form a gold complex where the ligand is coordinated to the gold atom.



Identification code	353bAuCl
Empirical formula	C <sub>34</sub> H <sub>41</sub> AuCl <sub>3</sub> N <sub>3</sub> O <sub>3</sub> S
Formula weight	875.07
Temperature/K	100.00(10)
Crystal system	orthorhombic
Space group	P2 <sub>1</sub> 2 <sub>1</sub> 2
a/Å	18.1161(4)
b/Å	16.9788(4)
c/Å	11.4699(3)

$\alpha/^\circ$	90
$\beta/^\circ$	90
$\gamma/^\circ$	90
Volume/ $\text{\AA}^3$	3528.03(14)
Z	4
$\rho_{\text{calc}}/\text{g}/\text{cm}^3$	1.647
$\mu/\text{mm}^{-1}$	10.783
F(000)	1744.0
Crystal size/ $\text{mm}^3$	$0.201 \times 0.137 \times 0.103$
Radiation	CuK $\alpha$ ( $\lambda = 1.54184$ )
2 $\Theta$ range for data collection/ $^\circ$	7.136 to 140.14
Index ranges	$-22 \leq h \leq 21, -12 \leq k \leq 20, -13 \leq l \leq 12$
Reflections collected	13141
Independent reflections	6659 [ $R_{\text{int}} = 0.0413, R_{\text{sigma}} = 0.0523$ ]
Data/restraints/parameters	6659/7/425
Goodness-of-fit on $F^2$	1.033
Final R indexes [ $I \geq 2\sigma(I)$ ]	$R_1 = 0.0349, wR_2 = 0.0903$
Final R indexes [all data]	$R_1 = 0.0357, wR_2 = 0.0911$
Largest diff. peak/hole / $e \text{ \AA}^{-3}$	1.57/-1.71
Flack parameter	-0.032(8)

**Table 2 Fractional Atomic Coordinates ( $\times 10^4$ ) and Equivalent Isotropic Displacement Parameters ( $\text{\AA}^2 \times 10^3$ ) for 353bAuCl.  $U_{\text{eq}}$  is defined as 1/3 of the trace of the orthogonalised  $U_{ij}$  tensor.**

Atom	$x$	$y$	$z$	$U(\text{eq})$
C1	2868(4)	2319(4)	3473(7)	12.9(15)
C2	3174(4)	998(4)	3587(7)	14.6(16)
C3	3520(4)	1323(4)	2664(7)	13.0(15)
C4	4175(4)	1844(4)	1246(7)	15.0(15)
C5	3761(4)	2445(5)	1678(7)	14.0(16)
C6	2360(4)	1591(4)	5139(6)	13.1(14)
C7	1635(5)	1322(5)	5131(8)	17.7(17)
C8	1239(5)	1349(4)	6170(8)	19.7(16)
C9	1562(5)	1646(6)	7171(7)	21.9(17)
C10	2291(6)	1885(5)	7164(7)	23.2(19)
C11	2714(4)	1867(4)	6164(7)	16.9(15)
C12	1277(5)	988(5)	4045(8)	22.0(18)
C13	1173(7)	91(7)	4178(10)	44(3)
C14	554(5)	1394(7)	3742(10)	37(2)
C15	3513(5)	2119(5)	6170(9)	24.1(18)
C16	3570(6)	3003(6)	6459(9)	33(2)
C17	3963(6)	1635(8)	7006(13)	53(3)
C18	4728(4)	1794(5)	320(7)	16.4(16)
C19	5155(5)	2439(5)	0(8)	20.4(17)
C20	5673(5)	2374(5)	-895(8)	25(2)
C21	5767(4)	1666(6)	-1477(7)	21.7(17)
C22	5361(5)	1013(5)	-1157(9)	24.5(18)
C23	4842(5)	1071(5)	-263(8)	19.3(18)
C24	3646(5)	4705(5)	1950(7)	16.5(16)
C25	3152(5)	4487(5)	931(7)	17.6(17)
C26	3035(4)	3583(4)	945(7)	15.0(16)

C27	2811(4)	3386(5)	-319(7)	19.2(16)
C28	2742(5)	4219(5)	-889(7)	24.1(19)
C29	2079(5)	4631(5)	-307(8)	23.4(19)
C30	2369(5)	4842(5)	942(7)	21.1(17)
C31	3414(5)	4652(5)	-351(7)	18.6(17)
C32	4151(5)	4311(5)	-722(8)	22.8(19)
C33	3451(6)	5545(5)	-608(9)	30(2)
Au1	2409.1(2)	3350.4(2)	3803.6(2)	13.84(10)
Cl1	1908.3(13)	4565.9(12)	4115.0(19)	25.7(5)
N1	2770(3)	1626(4)	4058(5)	13.6(12)
N2	3340(4)	2110(4)	2599(6)	13.4(14)
N3	3744(3)	3240(4)	1368(6)	12.1(12)
O1	4021(3)	1140(3)	1835(5)	16.2(12)
O2	4192(3)	3622(3)	3410(5)	20.7(13)
O3	4948(3)	3980(3)	1735(5)	19.3(12)
S1	4223.2(11)	3870.5(11)	2221.2(18)	14.6(4)
C101	904(9)	3483(11)	6084(17)	49(4)
Cl11	64.9(13)	2984.9(13)	6048(2)	32.7(5)
Cl12	1020(3)	4019(3)	7364(4)	69(2)
C11'	540(20)	3940(30)	5960(40)	49(4)
Cl1'	64.9(13)	2984.9(13)	6048(2)	32.7(5)
Cl2'	-40(5)	4629(4)	5345(9)	42(3)

**Table 3 Anisotropic Displacement Parameters ( $\text{\AA}^2 \times 10^3$ ) for 353bAuCl. The Anisotropic displacement factor exponent takes the form:  $-2\pi^2[h^2a^{*2}U_{11}+2hka^*b^*U_{12}+\dots]$ .**

Atom	$U_{11}$	$U_{22}$	$U_{33}$	$U_{23}$	$U_{13}$	$U_{12}$
C1	12(3)	13(3)	14(4)	2(3)	2(3)	-4(3)
C2	19(4)	13(3)	11(4)	1(3)	-1(3)	-2(3)
C3	15(4)	11(3)	13(4)	-2(3)	4(3)	0(3)
C4	19(3)	12(3)	14(4)	4(3)	-1(3)	-4(3)
C5	12(4)	14(4)	16(4)	2(3)	1(3)	0(3)
C6	17(4)	11(3)	11(3)	1(3)	3(3)	1(4)
C7	16(4)	13(4)	24(4)	-1(3)	-2(3)	-3(3)
C8	27(4)	13(3)	19(4)	0(3)	2(4)	-3(3)
C9	33(5)	21(4)	12(4)	-3(4)	7(3)	0(4)
C10	38(5)	18(4)	14(4)	-1(3)	-1(4)	-6(4)
C11	17(3)	17(3)	16(4)	1(3)	0(3)	-2(3)
C12	19(4)	28(4)	19(5)	-5(3)	3(3)	-4(3)
C13	66(8)	37(6)	30(6)	-5(5)	-12(5)	-14(6)
C14	33(5)	50(6)	27(5)	-2(5)	-4(5)	7(4)
C15	19(4)	32(5)	21(4)	-3(4)	0(4)	-4(3)
C16	32(5)	34(5)	31(6)	-1(4)	4(4)	-8(4)
C17	36(6)	44(6)	80(9)	19(7)	-34(6)	-5(6)
C18	14(3)	20(4)	16(4)	-3(3)	0(3)	2(3)
C19	24(4)	21(4)	17(4)	-5(3)	2(3)	-2(3)
C20	25(5)	21(4)	30(5)	1(4)	4(4)	-4(4)
C21	19(4)	29(4)	18(4)	3(4)	5(3)	7(4)
C22	32(5)	22(4)	19(4)	-2(4)	1(4)	9(3)
C23	24(4)	9(4)	25(4)	-3(3)	5(3)	5(3)
C24	18(4)	10(4)	21(4)	1(3)	-3(3)	2(3)
C25	19(4)	16(4)	17(4)	4(3)	-2(3)	-3(3)
C26	10(3)	19(4)	16(4)	5(3)	-3(3)	-1(3)

C27	19(4)	21(4)	18(4)	0(4)	1(3)	-2(4)
C28	24(4)	30(5)	18(4)	4(3)	-2(3)	2(4)
C29	19(4)	29(5)	22(5)	9(4)	-5(4)	3(4)
C30	23(4)	20(4)	20(4)	-4(3)	7(4)	6(3)
C31	22(4)	20(4)	14(4)	5(3)	3(3)	2(3)
C32	20(4)	30(5)	18(4)	6(4)	8(3)	-5(4)
C33	38(6)	23(5)	29(5)	12(4)	8(4)	3(4)
Au1	16.85(15)	11.79(15)	12.90(16)	-1.08(11)	2.25(11)	0.23(11)
Cl1	35.6(12)	17.0(9)	24.6(11)	-1.7(8)	9.2(9)	5.7(8)
N1	17(3)	13(3)	10(3)	-1(2)	2(2)	-1(3)
N2	14(3)	11(3)	15(3)	0(3)	0(3)	-2(3)
N3	12(3)	14(3)	10(3)	0(3)	-2(2)	0(2)
O1	18(3)	12(3)	19(3)	1(2)	3(2)	0(2)
O2	25(3)	23(3)	14(3)	-3(2)	-5(2)	-5(2)
O3	12(3)	19(3)	27(3)	0(2)	1(2)	-6(2)
S1	13.6(9)	13.3(9)	16.9(10)	-0.1(7)	-2.1(7)	-2.0(7)
C101	35(8)	51(10)	60(10)	8(9)	-3(8)	-11(6)
Cl11	24.1(10)	32.0(11)	42.1(14)	-8.4(10)	2.3(11)	-2.0(9)
Cl12	78(3)	103(4)	28(2)	-27(2)	11(2)	-75(3)
C11'	35(8)	51(10)	60(10)	8(9)	-3(8)	-11(6)
Cl1'	24.1(10)	32.0(11)	42.1(14)	-8.4(10)	2.3(11)	-2.0(9)
Cl2'	27(4)	10(3)	87(6)	24(4)	24(4)	5(3)

**Table 4 Bond Lengths for 353bAuCl.**

Atom	Atom	Length/Å	Atom	Atom	Length/Å
C1	Au1	1.976(8)	C19	C20	1.395(13)
C1	N1	1.365(10)	C20	C21	1.386(13)
C1	N2	1.364(10)	C21	C22	1.379(13)
C2	C3	1.348(11)	C22	C23	1.395(12)
C2	N1	1.402(10)	C24	C25	1.518(11)
C3	N2	1.379(10)	C24	S1	1.789(8)
C3	O1	1.351(10)	C25	C26	1.550(11)
C4	C5	1.360(11)	C25	C30	1.541(12)
C4	C18	1.463(11)	C25	C31	1.570(11)
C4	O1	1.400(9)	C26	C27	1.543(11)
C5	N2	1.422(10)	C26	N3	1.490(9)
C5	N3	1.397(10)	C27	C28	1.563(12)
C6	C7	1.390(11)	C28	C29	1.542(12)
C6	C11	1.418(11)	C28	C31	1.551(12)
C6	N1	1.447(9)	C29	C30	1.567(12)
C7	C8	1.392(13)	C31	C32	1.515(12)
C7	C12	1.515(12)	C31	C33	1.546(12)
C8	C9	1.385(12)	Au1	Cl1	2.282(2)
C9	C10	1.381(13)	N3	S1	1.690(6)
C10	C11	1.380(12)	O2	S1	1.429(6)
C11	C15	1.511(11)	O3	S1	1.439(6)
C12	C13	1.542(14)	C101	Cl11	1.741(15)
C12	C14	1.520(12)	C101	Cl12	1.74(2)
C15	C16	1.540(13)	C11'	Cl1'	1.84(4)
C15	C17	1.504(14)	C11'	Cl2'	1.73(5)
C18	C19	1.390(12)	Cl2'	Cl2' <sup>1</sup>	1.268(15)
C18	C23	1.412(11)			

<sup>1</sup>-X,1-Y,+Z

**Table 5 Bond Angles for 353bAuCl.**

Atom Atom Atom	Angle/°	Atom Atom Atom	Angle/°
N1 C1 Au1	127.9(6)	C24 C25 C30	116.1(7)
N2 C1 Au1	129.4(6)	C24 C25 C31	120.0(7)
N2 C1 N1	102.7(6)	C26 C25 C31	103.2(7)
C3 C2 N1	103.5(6)	C30 C25 C26	105.1(6)
C2 C3 N2	109.2(7)	C30 C25 C31	102.5(6)
C2 C3 O1	140.5(7)	C27 C26 C25	103.9(6)
O1 C3 N2	110.1(7)	N3 C26 C25	105.8(6)
C5 C4 C18	133.3(7)	N3 C26 C27	116.7(7)
C5 C4 O1	110.8(7)	C26 C27 C28	102.6(7)
O1 C4 C18	115.9(7)	C29 C28 C27	106.9(7)
C4 C5 N2	105.5(7)	C29 C28 C31	103.0(7)
C4 C5 N3	130.2(7)	C31 C28 C27	101.5(7)
N3 C5 N2	124.3(7)	C28 C29 C30	103.8(7)
C7 C6 C11	122.7(7)	C25 C30 C29	102.2(6)
C7 C6 N1	119.5(7)	C28 C31 C25	92.9(6)
C11 C6 N1	117.7(7)	C32 C31 C25	117.5(7)
C6 C7 C8	118.1(8)	C32 C31 C28	113.5(7)
C6 C7 C12	122.2(8)	C32 C31 C33	106.4(8)
C8 C7 C12	119.7(8)	C33 C31 C25	111.5(7)
C9 C8 C7	120.2(8)	C33 C31 C28	115.0(8)
C10 C9 C8	120.4(8)	C1 Au1 Cl1	177.4(2)
C11 C10 C9	122.0(8)	C1 N1 C2	113.5(6)
C6 C11 C15	122.0(8)	C1 N1 C6	121.6(6)
C10 C11 C6	116.4(7)	C2 N1 C6	124.5(6)
C10 C11 C15	121.5(8)	C1 N2 C3	111.1(7)
C7 C12 C13	109.9(8)	C1 N2 C5	141.2(7)
C7 C12 C14	112.8(8)	C3 N2 C5	107.5(6)
C14 C12 C13	111.4(8)	C5 N3 C26	118.6(6)
C11 C15 C16	109.9(7)	C5 N3 S1	117.0(5)
C17 C15 C11	111.5(8)	C26 N3 S1	112.6(5)
C17 C15 C16	111.1(9)	C3 O1 C4	106.2(6)
C19 C18 C4	121.8(7)	N3 S1 C24	95.8(4)
C19 C18 C23	118.6(8)	O2 S1 C24	112.1(4)
C23 C18 C4	119.6(8)	O2 S1 N3	110.2(3)
C18 C19 C20	120.5(8)	O2 S1 O3	116.4(4)
C21 C20 C19	120.3(8)	O3 S1 C24	111.4(4)
C22 C21 C20	120.3(8)	O3 S1 N3	109.0(3)
C21 C22 C23	119.9(8)	Cl12 C101 Cl11	112.3(10)
C22 C23 C18	120.5(8)	Cl2' C11' Cl1'	109(2)
C25 C24 S1	106.6(5)	Cl2' <sup>1</sup> Cl2' C11'	127.4(17)
C24 C25 C26	108.3(6)		

<sup>1</sup>-X,1-Y,+Z

**Table 6 Torsion Angles for 353bAuCl.**

A B C D	Angle/°	A B C D	Angle/°
---------	---------	---------	---------

C2 C3 N2 C1	-0.4(9)	C25 C26 N3 S1	26.4(7)
C2 C3 N2 C5	175.3(7)	C26 C25 C30 C29	-70.4(8)
C2 C3 O1 C4	-172.4(11)	C26 C25 C31 C28	53.1(7)
C3 C2 N1 C1	-1.3(9)	C26 C25 C31 C32	-65.4(9)
C3 C2 N1 C6	-173.6(7)	C26 C25 C31 C33	171.4(7)
C4 C5 N2 C1	173.0(10)	C26 C27 C28 C29	-67.1(8)
C4 C5 N2 C3	-0.5(9)	C26 C27 C28 C31	40.4(8)
C4 C5 N3 C26	120.5(9)	C26 N3 S1 C24	-8.7(6)
C4 C5 N3 S1	-99.2(9)	C26 N3 S1 O2	107.4(6)
C4 C18 C19 C20	-179.4(8)	C26 N3 S1 O3	-123.7(5)
C4 C18 C23 C22	179.4(8)	C27 C26 N3 C5	-76.8(9)
C5 C4 C18 C19	27.3(14)	C27 C26 N3 S1	141.3(6)
C5 C4 C18 C23	-153.4(9)	C27 C28 C29 C30	73.0(8)
C5 C4 O1 C3	-1.9(9)	C27 C28 C31 C25	-56.6(7)
C5 N3 S1 C24	-151.3(6)	C27 C28 C31 C32	65.1(8)
C5 N3 S1 O2	-35.1(7)	C27 C28 C31 C33	-171.9(7)
C5 N3 S1 O3	93.8(6)	C28 C29 C30 C25	-2.5(8)
C6 C7 C8 C9	0.8(13)	C29 C28 C31 C25	54.0(7)
C6 C7 C12 C13	109.0(10)	C29 C28 C31 C32	175.7(7)
C6 C7 C12 C14	-126.1(9)	C29 C28 C31 C33	-61.4(9)
C6 C11 C15 C16	115.9(9)	C30 C25 C26 C27	76.9(7)
C6 C11 C15 C17	-120.4(10)	C30 C25 C26 N3	-159.7(6)
C7 C6 C11 C10	-2.5(11)	C30 C25 C31 C28	-56.0(7)
C7 C6 C11 C15	176.9(8)	C30 C25 C31 C32	-174.4(7)
C7 C6 N1 C1	101.3(9)	C30 C25 C31 C33	62.4(9)
C7 C6 N1 C2	-86.9(9)	C31 C25 C26 C27	-30.2(8)
C7 C8 C9 C10	-3.1(14)	C31 C25 C26 N3	93.2(7)
C8 C7 C12 C13	-69.6(11)	C31 C25 C30 C29	37.2(8)
C8 C7 C12 C14	55.3(11)	C31 C28 C29 C30	-33.5(8)
C8 C9 C10 C11	2.6(13)	Au1 C1 N1 C2	179.3(5)
C9 C10 C11 C6	0.1(12)	Au1 C1 N1 C6	-8.1(11)
C9 C10 C11 C15	-179.2(8)	Au1 C1 N2 C3	-178.6(6)
C10 C11 C15 C16	-64.7(11)	Au1 C1 N2 C5	8.0(15)
C10 C11 C15 C17	59.0(12)	N1 C1 N2 C3	-0.4(9)
C11 C6 C7 C8	2.0(12)	N1 C1 N2 C5	-173.8(9)
C11 C6 C7 C12	-176.6(8)	N1 C2 C3 N2	0.9(9)
C11 C6 N1 C1	-76.2(9)	N1 C2 C3 O1	174.9(10)
C11 C6 N1 C2	95.5(9)	N1 C6 C7 C8	-175.4(7)
C12 C7 C8 C9	179.4(8)	N1 C6 C7 C12	6.0(12)
C18 C4 C5 N2	-178.7(8)	N1 C6 C11 C10	175.0(7)
C18 C4 C5 N3	-1.3(16)	N1 C6 C11 C15	-5.6(11)
C18 C4 O1 C3	178.2(7)	N2 C1 N1 C2	1.0(9)
C18 C19 C20 C21	0.1(14)	N2 C1 N1 C6	173.6(6)
C19 C18 C23 C22	-1.3(13)	N2 C3 O1 C4	1.5(9)
C19 C20 C21 C22	-1.6(14)	N2 C5 N3 C26	-62.6(10)
C20 C21 C22 C23	1.6(14)	N2 C5 N3 S1	77.7(9)
C21 C22 C23 C18	-0.2(13)	N3 C5 N2 C1	-4.5(16)
C23 C18 C19 C20	1.3(13)	N3 C5 N2 C3	-178.0(7)
C24 C25 C26 C27	-158.4(7)	N3 C26 C27 C28	-121.8(7)
C24 C25 C26 N3	-35.0(8)	O1 C3 N2 C1	-176.3(6)
C24 C25 C30 C29	170.0(7)	O1 C3 N2 C5	-0.7(9)
C24 C25 C31 C28	173.6(7)	O1 C4 C5 N2	1.5(9)
C24 C25 C31 C32	55.1(11)	O1 C4 C5 N3	178.8(7)
C24 C25 C31 C33	-68.1(10)	O1 C4 C18 C19	-152.8(8)

C25 C24 S1 N3	-12.3(6)	O1 C4 C18 C23	26.5(11)
C25 C24 S1 O2	-126.9(6)	S1 C24 C25 C26	29.0(8)
C25 C24 S1 O3	100.7(6)	S1 C24 C25 C30	146.9(6)
C25 C26 C27 C28	-5.8(8)	S1 C24 C25 C31	-88.9(8)
C25 C26 N3 C5	168.3(7)	Cl1' C11' Cl2' Cl2 <sup>1</sup>	165.4(12)

<sup>1</sup>-X,1-Y,+Z

**Table 7 Hydrogen Atom Coordinates ( $\text{\AA}\times 10^4$ ) and Isotropic Displacement Parameters ( $\text{\AA}^2\times 10^3$ ) for 353bAuCl.**

Atom	x	y	z	U(eq)
H2	3198.18	480.58	3850.13	18
H8	754.78	1166.25	6191.57	24
H9	1286.9	1686.11	7853.07	26
H10	2503.02	2062.43	7853.83	28
H12	1617.84	1074.02	3393.72	26
H13A	1639.43	-150.64	4349.25	66
H13B	979.93	-123.07	3465.3	66
H13C	833.28	-13.01	4802.41	66
H14A	202.21	1304.15	4353.96	55
H14B	366.04	1183.79	3023.79	55
H14C	637.11	1949.01	3657.54	55
H15	3712.82	2038.62	5384.5	29
H16A	3321.48	3302.46	5867.22	49
H16B	4079.65	3154.75	6488.7	49
H16C	3342.74	3101.74	7200.88	49
H17A	3809.13	1744.2	7789.88	79
H17B	4476.3	1764.64	6919.99	79
H17C	3892.27	1085.4	6841.32	79
H19	5094.9	2916.36	385.09	25
H20	5957.02	2808.7	-1102.04	30
H21	6104.16	1630.01	-2085.11	26
H22	5433.85	534.86	-1535.65	29
H23	4567.72	630.81	-50	23
H24A	3350.26	4825.04	2633.23	20
H24B	3942.64	5162.62	1760.31	20
H26	2633.86	3445.92	1481.25	18
H27A	2343.99	3106.6	-343.41	23
H27B	3185.47	3072.56	-704.86	23
H28	2729.99	4217.67	-1743.37	29
H29A	1656.47	4281.24	-264.31	28
H29B	1939.78	5102.34	-731.69	28
H30A	2383.11	5407.06	1061.94	25
H30B	2065.94	4602.41	1542.87	25
H32A	4153.77	3753.96	-578.77	34
H32B	4539.52	4556.16	-284.31	34
H32C	4225.3	4406.92	-1538.48	34
H33A	3523.44	5626.18	-1427.97	45
H33B	3855.03	5773.79	-184.58	45
H33C	2997.78	5789.72	-369.61	45
H10A	1303.5	3104.78	6012.15	58
H10B	931.79	3837.8	5422.82	58
H11A	691.08	4105.27	6729.9	58



H11B	983.78	3882.82	5482.58	58
------	--------	---------	---------	----

**Table 8 Atomic Occupancy for 353bAuCl.**

Atom	Occupancy	Atom	Occupancy	Atom	Occupancy
C101	0.706(7)	H10A	0.706(7)	H10B	0.706(7)
Cl11	0.706(7)	Cl12	0.706(7)	C11'	0.294(7)
H11A	0.294(7)	H11B	0.294(7)	Cl1'	0.294(7)
Cl2'	0.294(7)				

## Experimental

A suitable crystal was selected on a **SuperNova, Dual, Cu at zero, Atlas** diffractometer. The crystal was kept at 100.00(10) K during data collection. Using Olex2,<sup>275</sup> the structure was solved with the ShelXS<sup>278</sup> structure solution program using Direct Methods and refined with the ShelXL<sup>277</sup> refinement package using Least Squares minimisation.

## Crystal structure determination of [353bAuCl]

**Crystal Data** for  $C_{34}H_{41}AuCl_3N_3O_3S$  ( $M = 875.07$  g/mol): orthorhombic, space group  $P2_12_12$  (no. 18),  $a = 18.1161(4)$  Å,  $b = 16.9788(4)$  Å,  $c = 11.4699(3)$  Å,  $V = 3528.03(14)$  Å<sup>3</sup>,  $Z = 4$ ,  $T = 100.00(10)$  K,  $\mu(\text{CuK}\alpha) = 10.783$  mm<sup>-1</sup>,  $D_{\text{calc}} = 1.647$  g/cm<sup>3</sup>, 13141 reflections measured ( $7.136^\circ \leq 2\theta \leq 140.14^\circ$ ), 6659 unique ( $R_{\text{int}} = 0.0413$ ,  $R_{\text{sigma}} = 0.0523$ ) which were used in all calculations. The final  $R_1$  was 0.0349 ( $I > 2\sigma(I)$ ) and  $wR_2$  was 0.0911 (all data).

## Refinement model description

Number of restraints - 7, number of constraints - unknown.

Details:

1. Fixed Uiso

At 1.2 times of:

All C(H) groups, All C(H,H) groups

At 1.5 times of:

All C(H,H,H) groups

2. Shared sites

{Cl11, Cl1'}

3. Rigid bond restraints

Cl11', Cl2'

with sigma for 1-2 distances of 0.01 and sigma for 1-3 distances of 0.01

4. Uiso/Uanis restraints and constraints

Cl2'  $\approx$  Cl11: within 3Å with sigma of 0.01 and sigma for terminal atoms of 0.01

Uanis(Cl11) = Uanis(Cl1')

Uanis(Cl101) = Uanis(Cl11')

5. Others

Sof(Cl11')=Sof(H11A)=Sof(H11B)=Sof(Cl1')=Sof(Cl2')=1-FVAR(1)

Sof(C101)=Sof(H10A)=Sof(H10B)=Sof(Cl11)=Sof(Cl12)=FVAR(1)

6.a Ternary CH refined with riding coordinates:

C12(H12), C15(H15), C26(H26), C28(H28)

6.b Secondary CH2 refined with riding coordinates:

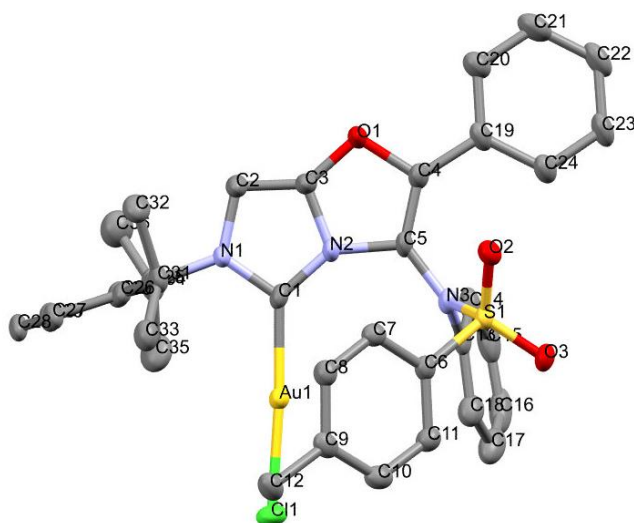
C24(H24A,H24B), C27(H27A,H27B), C29(H29A,H29B), C30(H30A,H30B), C101(H10A, H10B), C11'(H11A,H11B)

6.c Aromatic/amide H refined with riding coordinates:

C2(H2), C8(H8), C9(H9), C10(H10), C19(H19), C20(H20), C21(H21), C22(H22), C23(H23)

6.d Idealised Me refined as rotating group:

C13(H13A,H13B,H13C), C14(H14A,H14B,H14C), C16(H16A,H16B,H16C), C17(H17A,H17B, H17C), C32(H32A,H32B,H32C), C33(H33A,H33B,H33C)



Identification code	353cAuCl
Empirical formula	C <sub>36</sub> H <sub>35</sub> AuClN <sub>3</sub> O <sub>3</sub> S
Formula weight	822.14
Temperature/K	104(5)
Crystal system	triclinic
Space group	P-1
a/Å	9.4707(4)
b/Å	12.5573(5)
c/Å	15.1065(6)
α/°	92.503(3)
β/°	102.852(3)
γ/°	105.513(4)
Volume/Å <sup>3</sup>	1677.54(12)
Z	2
ρ <sub>calc</sub> /g/cm <sup>3</sup>	1.628
μ/mm <sup>-1</sup>	9.872
F(000)	816.0
Crystal size/mm <sup>3</sup>	0.124 × 0.115 × 0.094
Radiation	CuKα (λ = 1.54184)
2θ range for data collection/°	7.35 to 136.484
Index ranges	-8 ≤ h ≤ 11, -15 ≤ k ≤ 15, -18 ≤ l ≤ 18
Reflections collected	11539
Independent reflections	6138 [R <sub>int</sub> = 0.0260, R <sub>sigma</sub> = 0.0351]
Data/restraints/parameters	6138/0/411
Goodness-of-fit on F <sup>2</sup>	1.029
Final R indexes [I ≥ 2σ (I)]	R <sub>1</sub> = 0.0237, wR <sub>2</sub> = 0.0564
Final R indexes [all data]	R <sub>1</sub> = 0.0269, wR <sub>2</sub> = 0.0584
Largest diff. peak/hole / e Å <sup>-3</sup>	1.52/-0.83

**Table 2 Fractional Atomic Coordinates ( $\times 10^4$ ) and Equivalent Isotropic Displacement Parameters ( $\text{\AA}^2 \times 10^3$ ) for 353cAuCl.  $U_{eq}$  is defined as 1/3 of the trace of the orthogonalised  $U_{ij}$  tensor.**

Atom	$x$	$y$	$z$	U(eq)
------	-----	-----	-----	-------

Au1	9066.1(2)	7260.4(2)	2869.3(2)	20.26(5)
C1	6839(4)	6773(3)	2669(2)	21.9(7)
C2	4439(4)	6893(3)	2593(3)	34.0(9)
C3	4390(4)	5818(3)	2445(3)	32.0(9)
C4	4237(4)	4040(3)	2262(3)	26.5(7)
C5	5713(4)	4596(3)	2353(2)	22.9(7)
C6	8141(4)	5062(3)	917(2)	21.5(7)
C7	7336(4)	5748(3)	485(2)	23.7(7)
C8	8097(4)	6729(3)	221(2)	24.6(7)
C9	9672(4)	7063(3)	392(2)	24.4(7)
C10	10455(4)	6350(3)	808(2)	27.0(7)
C11	9706(4)	5351(3)	1071(2)	25.8(7)
C12	10503(4)	8162(3)	144(3)	30.7(8)
C13	7938(4)	4071(3)	3157(2)	25.7(7)
C14	7304(5)	3687(3)	3876(3)	33.6(9)
C15	8214(6)	3482(3)	4669(3)	44.4(11)
C16	9730(6)	3639(3)	4742(3)	47.5(12)
C17	10368(5)	4034(4)	4038(3)	44.7(11)
C18	9468(4)	4280(3)	3249(3)	33.2(8)
C19	3398(4)	2873(3)	2203(2)	26.3(7)
C20	1861(4)	2583(3)	2187(3)	32.1(8)
C21	1074(5)	1491(3)	2201(3)	39.4(10)
C22	1794(5)	661(3)	2233(3)	35.6(9)
C23	3308(5)	935(3)	2239(3)	32.9(8)
C24	4121(4)	2032(3)	2220(3)	30.9(8)
C25	6545(4)	8667(3)	2922(3)	25.5(7)
C26	6637(4)	9279(3)	2183(3)	24.8(7)
C27	7126(4)	10435(3)	2373(3)	28.4(8)
C28	7510(4)	10935(3)	3261(3)	32.5(9)
C29	7415(4)	10297(3)	3979(3)	32.2(8)
C30	6927(4)	9132(3)	3824(3)	28.6(8)
C31	6169(4)	8749(3)	1195(3)	28.8(8)
C32	4575(4)	8793(3)	752(3)	36.1(9)
C33	7287(5)	9287(3)	647(3)	35.7(9)
C34	6863(5)	8453(3)	4627(3)	36.6(9)
C35	8445(5)	8668(4)	5261(3)	46.9(11)
C36	5737(5)	8675(4)	5146(3)	48.2(11)
Cl1	11631.6(9)	7930.0(8)	3157.7(7)	33.9(2)
N1	5971(3)	7459(2)	2733(2)	23.5(6)
N2	5827(3)	5751(2)	2479(2)	24.9(6)
N3	6944(3)	4208(2)	2321.3(19)	21.5(6)
O1	3384(3)	4792(2)	2300(2)	35.9(7)
O2	5653(3)	3502.6(19)	699.1(17)	26.2(5)
O3	8046(3)	3081.5(19)	1413.8(16)	25.6(5)
S1	7147.0(9)	3840.9(6)	1280.4(5)	20.37(16)

**Table 3 Anisotropic Displacement Parameters ( $\text{\AA}^2 \times 10^3$ ) for 353cAuCl. The Anisotropic displacement factor exponent takes the form:  $-2\pi^2[h^2a^{*2}U_{11}+2hka^*b^*U_{12}+\dots]$ .**

Atom	U <sub>11</sub>	U <sub>22</sub>	U <sub>33</sub>	U <sub>23</sub>	U <sub>13</sub>	U <sub>12</sub>
Au1	20.49(8)	18.29(7)	23.01(8)	1.57(5)	5.40(5)	7.23(5)
C1	26.3(17)	18.4(15)	23.6(17)	1.1(13)	5.2(13)	11.6(13)
C2	20.4(17)	21.5(17)	57(3)	-5.9(17)	3.9(17)	6.3(14)

C3	18.4(16)	20.5(17)	55(2)	-3.8(16)	7.9(16)	4.9(13)
C4	28.2(18)	19.3(16)	34(2)	-2.4(14)	11.6(15)	7.9(14)
C5	27.6(17)	13.9(15)	28.6(18)	-0.9(13)	9.7(14)	6.7(13)
C6	25.9(17)	18.6(15)	20.9(16)	0.5(13)	7.4(13)	6.8(13)
C7	21.5(16)	25.4(17)	23.0(17)	-1.6(14)	4.7(13)	5.8(13)
C8	28.0(18)	23.1(17)	23.3(17)	3.7(14)	5.9(14)	8.1(14)
C9	28.3(18)	24.2(17)	19.0(16)	-2.8(13)	9.2(14)	2.6(14)
C10	22.7(17)	33.1(19)	22.7(17)	-1.9(14)	5.5(14)	4.8(14)
C11	24.3(17)	28.0(18)	26.3(18)	1.9(14)	6.1(14)	9.9(14)
C12	33.1(19)	24.5(18)	34(2)	0.3(15)	14.4(16)	2.7(15)
C13	34.3(19)	15.1(15)	25.5(18)	-2.5(13)	1.3(15)	9.2(14)
C14	52(2)	18.7(17)	28.8(19)	0.2(15)	9.8(17)	8.9(16)
C15	80(3)	22.6(19)	27(2)	1.2(16)	6(2)	14(2)
C16	79(3)	30(2)	27(2)	-7.6(17)	-11(2)	27(2)
C17	49(3)	41(2)	39(2)	-12.9(19)	-9(2)	23(2)
C18	39(2)	32(2)	26.6(19)	-3.2(16)	1.1(16)	14.0(17)
C19	34.1(19)	18.4(16)	24.3(18)	-1.1(13)	11.0(15)	1.6(14)
C20	30.3(19)	28.1(19)	35(2)	0.7(16)	10.4(16)	1.3(15)
C21	33(2)	37(2)	41(2)	6.5(18)	10.2(18)	-4.5(17)
C22	48(2)	22.4(18)	28(2)	3.9(15)	11.0(17)	-5.4(16)
C23	47(2)	17.2(17)	33(2)	2.7(15)	14.4(17)	3.1(15)
C24	35(2)	20.6(17)	36(2)	-3.2(15)	14.1(16)	3.5(15)
C25	19.4(16)	13.7(15)	41(2)	-2.2(14)	1.1(14)	6.9(12)
C26	21.2(16)	18.8(16)	34.6(19)	-0.2(14)	3.6(14)	9.0(13)
C27	26.1(18)	16.1(16)	39(2)	-0.4(15)	1.6(15)	5.3(13)
C28	28.9(19)	16.2(16)	48(2)	-5.0(16)	0.1(17)	8.1(14)
C29	32.2(19)	22.9(18)	36(2)	-6.9(16)	-2.9(16)	9.8(15)
C30	26.6(18)	23.0(17)	34(2)	-3.4(15)	2.0(15)	9.5(14)
C31	31.0(19)	15.5(15)	38(2)	0.9(15)	5.6(16)	6.4(14)
C32	31(2)	32(2)	39(2)	-4.5(17)	-1.5(17)	8.3(16)
C33	40(2)	26.1(19)	41(2)	2.5(17)	7.1(18)	11.5(16)
C34	45(2)	24.9(18)	36(2)	-5.2(16)	3.0(18)	10.9(17)
C35	54(3)	46(2)	42(2)	9(2)	-1(2)	25(2)
C36	56(3)	47(3)	45(3)	2(2)	15(2)	18(2)
Cl1	19.7(4)	40.8(5)	41.2(5)	1.4(4)	7.8(4)	9.0(3)
N1	18.5(13)	14.1(13)	35.8(16)	-2.1(12)	3.6(12)	4.7(11)
N2	23.5(14)	14.7(13)	37.2(17)	-2.3(12)	7.8(12)	6.8(11)
N3	27.2(14)	15.5(13)	23.9(14)	2.4(11)	8.4(12)	8.1(11)
O1	21.8(12)	17.1(12)	67.4(19)	-8.7(12)	14.2(12)	2.6(10)
O2	25.4(12)	21.4(12)	28.5(13)	-1.9(10)	4.8(10)	3.5(10)
O3	31.6(13)	20.7(11)	27.7(13)	-1.3(10)	8.1(10)	12.6(10)
S1	23.2(4)	16.1(3)	22.1(4)	-0.8(3)	5.5(3)	6.6(3)

**Table 4 Bond Lengths for 353cAuCl.**

Atom	Atom	Length/Å	Atom	Atom	Length/Å
Au1	C1	1.981(3)	C15	C16	1.374(7)
Au1	Cl1	2.2814(8)	C16	C17	1.383(7)
C1	N1	1.355(4)	C17	C18	1.401(6)
C1	N2	1.355(4)	C19	C20	1.397(5)
C2	C3	1.345(5)	C19	C24	1.402(5)
C2	N1	1.398(4)	C20	C21	1.378(5)
C3	N2	1.376(4)	C21	C22	1.387(6)

C3	O1	1.358(4)	C22	C23	1.380(6)
C4	C5	1.358(5)	C23	C24	1.392(5)
C4	C19	1.456(5)	C25	C26	1.387(5)
C4	O1	1.404(4)	C25	C30	1.389(5)
C5	N2	1.426(4)	C25	N1	1.460(4)
C5	N3	1.388(4)	C26	C27	1.395(5)
C6	C7	1.389(5)	C26	C31	1.526(5)
C6	C11	1.390(5)	C27	C28	1.382(5)
C6	S1	1.752(3)	C28	C29	1.382(6)
C7	C8	1.376(5)	C29	C30	1.403(5)
C8	C9	1.396(5)	C30	C34	1.515(6)
C9	C10	1.394(5)	C31	C32	1.526(5)
C9	C12	1.503(5)	C31	C33	1.522(6)
C10	C11	1.388(5)	C34	C35	1.536(6)
C13	C14	1.397(5)	C34	C36	1.530(6)
C13	C18	1.375(5)	N3	S1	1.685(3)
C13	N3	1.445(4)	O2	S1	1.431(2)
C14	C15	1.390(6)	O3	S1	1.432(2)

**Table 5 Bond Angles for 353cAuCl.**

Atom	Atom	Atom	Angle/°	Atom	Atom	Atom	Angle/°
C1	Au1	Cl1	176.04(10)	C23	C22	C21	119.4(3)
N1	C1	Au1	124.8(2)	C22	C23	C24	120.9(4)
N1	C1	N2	103.3(3)	C23	C24	C19	119.7(4)
N2	C1	Au1	131.8(2)	C26	C25	C30	124.2(3)
C3	C2	N1	103.8(3)	C26	C25	N1	117.7(3)
C2	C3	N2	108.9(3)	C30	C25	N1	118.1(3)
C2	C3	O1	139.9(3)	C25	C26	C27	116.9(3)
O1	C3	N2	111.1(3)	C25	C26	C31	123.2(3)
C5	C4	C19	134.5(3)	C27	C26	C31	119.9(3)
C5	C4	O1	110.4(3)	C28	C27	C26	120.9(4)
O1	C4	C19	114.9(3)	C29	C28	C27	120.5(3)
C4	C5	N2	106.5(3)	C28	C29	C30	120.8(4)
C4	C5	N3	130.8(3)	C25	C30	C29	116.7(4)
N3	C5	N2	122.7(3)	C25	C30	C34	123.7(3)
C7	C6	C11	120.5(3)	C29	C30	C34	119.7(3)
C7	C6	S1	118.6(3)	C32	C31	C26	109.7(3)
C11	C6	S1	120.9(3)	C33	C31	C26	112.1(3)
C8	C7	C6	119.6(3)	C33	C31	C32	111.5(3)
C7	C8	C9	121.4(3)	C30	C34	C35	110.6(4)
C8	C9	C12	121.2(3)	C30	C34	C36	111.6(3)
C10	C9	C8	118.1(3)	C36	C34	C35	111.5(4)
C10	C9	C12	120.8(3)	C1	N1	C2	113.1(3)
C11	C10	C9	121.4(3)	C1	N1	C25	124.5(3)
C10	C11	C6	119.0(3)	C2	N1	C25	122.4(3)
C14	C13	N3	118.3(3)	C1	N2	C3	110.9(3)
C18	C13	C14	119.9(3)	C1	N2	C5	142.5(3)
C18	C13	N3	121.8(3)	C3	N2	C5	106.4(3)
C15	C14	C13	119.8(4)	C5	N3	C13	120.1(3)
C16	C15	C14	120.2(4)	C5	N3	S1	117.2(2)
C15	C16	C17	120.3(4)	C13	N3	S1	122.6(2)
C16	C17	C18	119.9(4)	C3	O1	C4	105.6(3)

C13	C18	C17	119.8(4)	N3	S1	C6	106.16(14)
C20	C19	C4	119.7(3)	O2	S1	C6	107.52(15)
C20	C19	C24	118.9(3)	O2	S1	N3	105.59(15)
C24	C19	C4	121.3(3)	O2	S1	O3	120.64(14)
C21	C20	C19	120.6(4)	O3	S1	C6	109.92(15)
C20	C21	C22	120.6(4)	O3	S1	N3	106.06(14)

**Table 6 Torsion Angles for 353cAuCl.**

A	B	C	D	Angle/°	A	B	C	D	Angle/°
Au1	C1	N1	C2	-177.6(3)	C20	C19	C24	C23	-1.3(6)
Au1	C1	N1	C25	2.7(5)	C20	C21	C22	C23	-0.8(6)
Au1	C1	N2	C3	176.8(3)	C21	C22	C23	C24	0.4(6)
Au1	C1	N2	C5	2.3(7)	C22	C23	C24	C19	0.6(6)
C2	C3	N2	C1	1.3(5)	C24	C19	C20	C21	0.9(6)
C2	C3	N2	C5	177.8(4)	C25	C26	C27	C28	0.6(5)
C2	C3	O1	C4	-176.1(6)	C25	C26	C31	C32	98.2(4)
C3	C2	N1	C1	0.4(5)	C25	C26	C31	C33	-137.4(3)
C3	C2	N1	C25	-179.9(4)	C25	C30	C34	C35	117.2(4)
C4	C5	N2	C1	174.0(5)	C25	C30	C34	C36	-118.2(4)
C4	C5	N2	C3	-0.7(4)	C26	C25	C30	C29	0.8(5)
C4	C5	N3	C13	-97.0(5)	C26	C25	C30	C34	-178.2(3)
C4	C5	N3	S1	79.5(5)	C26	C25	N1	C1	88.7(4)
C4	C19	C20	C21	-175.1(4)	C26	C25	N1	C2	-90.9(4)
C4	C19	C24	C23	174.6(4)	C26	C27	C28	C29	-0.1(6)
C5	C4	C19	C20	174.6(4)	C27	C26	C31	C32	-79.0(4)
C5	C4	C19	C24	-1.3(7)	C27	C26	C31	C33	45.4(4)
C5	C4	O1	C3	-1.9(4)	C27	C28	C29	C30	-0.1(6)
C5	N3	S1	C6	86.0(3)	C28	C29	C30	C25	-0.3(5)
C5	N3	S1	O2	-27.9(3)	C28	C29	C30	C34	178.8(4)
C5	N3	S1	O3	-157.1(2)	C29	C30	C34	C35	-61.8(5)
C6	C7	C8	C9	-1.1(5)	C29	C30	C34	C36	62.8(5)
C7	C6	C11	C10	1.7(5)	C30	C25	C26	C27	-1.0(5)
C7	C6	S1	N3	-85.4(3)	C30	C25	C26	C31	-178.3(3)
C7	C6	S1	O2	27.3(3)	C30	C25	N1	C1	-92.9(4)
C7	C6	S1	O3	160.3(3)	C30	C25	N1	C2	87.5(4)
C7	C8	C9	C10	2.6(5)	C31	C26	C27	C28	178.0(3)
C7	C8	C9	C12	-177.0(3)	N1	C1	N2	C3	-1.0(4)
C8	C9	C10	C11	-1.9(5)	N1	C1	N2	C5	-175.5(4)
C9	C10	C11	C6	-0.2(5)	N1	C2	C3	N2	-1.0(5)
C11	C6	C7	C8	-1.1(5)	N1	C2	C3	O1	176.6(5)
C11	C6	S1	N3	93.5(3)	N1	C25	C26	C27	177.3(3)
C11	C6	S1	O2	-153.8(3)	N1	C25	C26	C31	0.0(5)
C11	C6	S1	O3	-20.8(3)	N1	C25	C30	C29	-177.5(3)
C12	C9	C10	C11	177.6(3)	N1	C25	C30	C34	3.5(5)
C13	C14	C15	C16	-1.0(6)	N2	C1	N1	C2	0.3(4)
C13	N3	S1	C6	-97.6(3)	N2	C1	N1	C25	-179.3(3)
C13	N3	S1	O2	148.4(3)	N2	C3	O1	C4	1.4(5)
C13	N3	S1	O3	19.3(3)	N2	C5	N3	C13	84.5(4)
C14	C13	C18	C17	4.4(5)	N2	C5	N3	S1	-99.0(3)
C14	C13	N3	C5	37.4(4)	N3	C5	N2	C1	-7.2(7)
C14	C13	N3	S1	-138.9(3)	N3	C5	N2	C3	178.1(3)
C14	C15	C16	C17	1.9(6)	N3	C13	C14	C15	176.1(3)

C15 C16 C17 C18	0.3(6)	N3 C13 C18 C17	-173.8(3)
C16 C17 C18 C13	-3.5(6)	O1 C3 N2 C1	-177.0(3)
C18 C13 C14 C15	-2.2(5)	O1 C3 N2 C5	-0.5(4)
C18 C13 N3 C5	-144.3(3)	O1 C4 C5 N2	1.6(4)
C18 C13 N3 S1	39.4(4)	O1 C4 C5 N3	-177.1(3)
C19 C4 C5 N2	-173.1(4)	O1 C4 C19 C20	0.0(5)
C19 C4 C5 N3	8.2(7)	O1 C4 C19 C24	-175.8(3)
C19 C4 O1 C3	174.0(3)	S1 C6 C7 C8	177.8(3)
C19 C20 C21 C22	0.1(6)	S1 C6 C11 C10	-177.2(3)

**Table 7 Hydrogen Atom Coordinates ( $\text{\AA}\times 10^4$ ) and Isotropic Displacement Parameters ( $\text{\AA}^2\times 10^3$ ) for 353cAuCl.**

Atom	x	y	z	U(eq)
H2	3640.61	7189.89	2600.81	41
H7	6288.16	5544.67	374.24	28
H8	7552.36	7179.76	-77.79	30
H10	11501.65	6547.3	910.74	32
H11	10242.32	4882.4	1345.53	31
H12A	11087.37	8636.9	690.87	46
H12B	9788.99	8504.85	-191.13	46
H12C	11162.51	8045.12	-225.92	46
H14	6275.13	3569.91	3823.36	40
H15	7796.64	3237.15	5151.37	53
H16	10328.44	3478.57	5266.21	57
H17	11393.88	4136.42	4088.71	54
H18	9903.91	4583.76	2789.53	40
H20	1365	3131.36	2166.56	38
H21	51.22	1308.65	2189.06	47
H22	1261.49	-73.69	2249.88	43
H23	3791.51	378.89	2256.59	40
H24	5138.72	2206.5	2218.94	37
H27	7193.95	10874.54	1896.44	34
H28	7835.71	11705.86	3374.56	39
H29	7678.39	10644.17	4572.96	39
H31	6148.51	7965.14	1202.85	35
H32A	3880.93	8379.77	1075.09	54
H32B	4293.79	8473.57	126.93	54
H32C	4548.21	9551.94	776.01	54
H33A	7335.95	10059.3	633.6	53
H33B	6961.94	8921.86	34.88	53
H33C	8268.62	9218.61	928.11	53
H34	6512.32	7665.99	4384.4	44
H35A	9133.92	8554.07	4911.46	70
H35B	8406.99	8165.17	5721.64	70
H35C	8784.48	9420.18	5547.26	70
H36A	6077.7	9433.95	5414.74	72
H36B	5663.42	8189.58	5618.1	72
H36C	4763.5	8538.85	4731.06	72

**Table 8 Solvent masks information for 353cAuCl.**

Number	X	Y	Z	Volume	Electron count	Content
--------	---	---	---	--------	----------------	---------

## Experimental

A suitable crystal was selected on a **SuperNova, Dual, Cu at zero, Atlas** diffractometer. The crystal was kept at 104(5) K during data collection. Using Olex2<sup>275</sup>, the structure was solved with the ShelXT<sup>276</sup> structure solution program using Intrinsic Phasing and refined with the ShelXL<sup>277</sup> refinement package using Least Squares minimisation.

## Crystal structure determination of [353cAuCl]

**Crystal Data** for  $C_{36}H_{35}AuClN_3O_3S$  ( $M = 822.14$  g/mol): triclinic, space group P-1 (no. 2),  $a = 9.4707(4)$  Å,  $b = 12.5573(5)$  Å,  $c = 15.1065(6)$  Å,  $\alpha = 92.503(3)^\circ$ ,  $\beta = 102.852(3)^\circ$ ,  $\gamma = 105.513(4)^\circ$ ,  $V = 1677.54(12)$  Å<sup>3</sup>,  $Z = 2$ ,  $T = 104(5)$  K,  $\mu(\text{CuK}\alpha) = 9.872$  mm<sup>-1</sup>,  $D_{\text{calc}} = 1.628$  g/cm<sup>3</sup>, 11539 reflections measured ( $7.35^\circ \leq 2\theta \leq 136.484^\circ$ ), 6138 unique ( $R_{\text{int}} = 0.0260$ ,  $R_{\text{sigma}} = 0.0351$ ) which were used in all calculations. The final  $R_1$  was 0.0237 ( $I > 2\sigma(I)$ ) and  $wR_2$  was 0.0584 (all data).

## Refinement model description

Number of restraints - 0, number of constraints - unknown.

Details:

1. Fixed Uiso

At 1.2 times of:

All C(H) groups

At 1.5 times of:

All C(H,H,H) groups

2.a Ternary CH refined with riding coordinates:

C31(H31), C34(H34)

2.b Aromatic/amide H refined with riding coordinates:

C2(H2), C7(H7), C8(H8), C10(H10), C11(H11), C14(H14), C15(H15), C16(H16), C17(H17), C18(H18), C20(H20), C21(H21), C22(H22), C23(H23), C24(H24), C27(H27), C28(H28), C29(H29)

2.c Idealised Me refined as rotating group:

C12(H12A,H12B,H12C), C32(H32A,H32B,H32C), C33(H33A,H33B,H33C), C35(H35A,H35B,H35C), C36(H36A,H36B,H36C)

## 8.10 353dAuCl

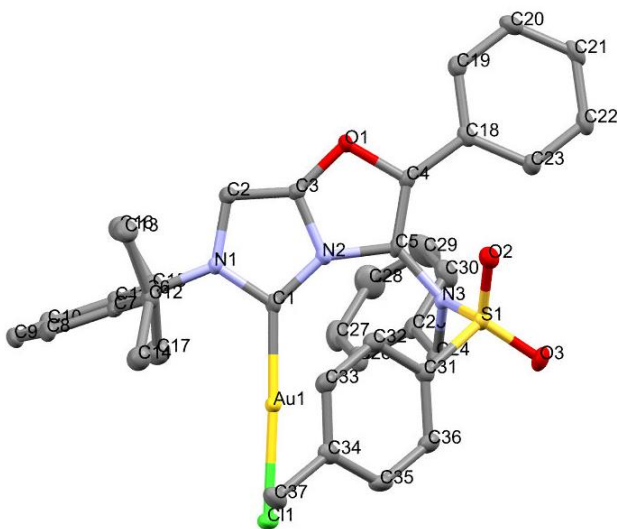
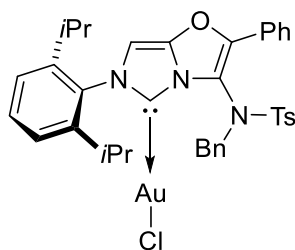


**Table 1** Crystal data and structure refinement for 353dAuCl.

Identification code	353dAuCl
Empirical formula	$C_{37}H_{37}AuClN_3O_3S$
Formula weight	836.17
Temperature/K	100.01(10)
Crystal system	triclinic
Space group	P-1
$a/\text{\AA}$	9.4226(4)



b/Å	12.6393(5)
c/Å	15.0477(4)
$\alpha/^\circ$	96.410(3)
$\beta/^\circ$	103.863(3)
$\gamma/^\circ$	105.149(3)
Volume/Å <sup>3</sup>	1650.15(11)
Z	2
$\rho_{\text{calc}}/\text{cm}^3$	1.683
$\mu/\text{mm}^{-1}$	10.047
F(000)	832.0
Crystal size/mm <sup>3</sup>	0.209 × 0.115 × 0.013
Radiation	CuK $\alpha$ ( $\lambda$ = 1.54184)
2 $\Theta$ range for data collection/ $^\circ$	7.374 to 149.07
Index ranges	-11 ≤ h ≤ 11, -14 ≤ k ≤ 15, -14 ≤ l ≤ 18
Reflections collected	11914
Independent reflections	6522 [R <sub>int</sub> = 0.0261, R <sub>sigma</sub> = 0.0359]
Data/restraints/parameters	6522/0/420
Goodness-of-fit on F <sup>2</sup>	1.032
Final R indexes [I ≥ 2 $\sigma$ (I)]	R <sub>1</sub> = 0.0223, wR <sub>2</sub> = 0.0542
Final R indexes [all data]	R <sub>1</sub> = 0.0246, wR <sub>2</sub> = 0.0555
Largest diff. peak/hole / e Å <sup>-3</sup>	0.80/-0.94

**Table 2 Fractional Atomic Coordinates (×10<sup>4</sup>) and Equivalent Isotropic Displacement Parameters (Å<sup>2</sup>×10<sup>3</sup>) for 353dAuCl. U<sub>eq</sub> is defined as 1/3 of the trace of the orthogonalised U<sub>ij</sub> tensor.**

Atom	x	y	z	U(eq)
C1	6954(3)	6984(2)	2646.1(19)	13.8(5)
C2	4516(3)	7075(2)	2573.8(19)	14.3(5)
C3	4483(3)	6000(2)	2382.4(19)	13.4(5)
C4	4328(3)	4221(2)	2182.7(18)	12.8(5)
C5	5811(3)	4775(2)	2293.7(19)	13.0(5)
C6	6626(3)	8857(2)	2989(2)	13.3(5)
C7	6736(3)	9488(2)	2290(2)	14.0(5)
C8	7197(3)	10645(2)	2557(2)	17.3(6)
C9	7528(3)	11135(2)	3487(2)	19.5(6)
C10	7428(3)	10493(2)	4163(2)	19.2(6)
C11	6976(3)	9329(2)	3937(2)	16.1(6)
C12	6291(3)	8938(2)	1269(2)	16.7(6)
C13	4673(4)	8955(3)	787(2)	23.6(7)
C14	7447(4)	9477(3)	766(2)	23.6(7)
C15	6929(4)	8631(2)	4692(2)	18.9(6)
C16	5762(4)	8785(3)	5206(2)	23.6(6)
C17	8535(4)	8903(3)	5377(2)	25.4(7)
C18	3465(3)	3060(2)	2130.4(19)	15.0(5)
C19	1938(3)	2803(2)	2126(2)	18.0(6)
C20	1129(4)	1729(3)	2155(2)	21.2(6)
C21	1836(4)	895(2)	2199(2)	21.5(6)
C22	3354(4)	1140(2)	2187(2)	20.4(6)
C23	4179(4)	2210(2)	2145(2)	18.2(6)
C24	8425(3)	4711(3)	3100(2)	17.3(6)
C25	8030(3)	4877(2)	4011(2)	16.9(6)
C26	8793(4)	5872(2)	4645(2)	20.5(6)
C27	8480(4)	6023(3)	5499(2)	26.9(7)
C28	7418(5)	5196(3)	5715(2)	35.8(9)
C29	6662(5)	4204(3)	5094(3)	37.8(9)

C30	6964(4)	4045(3)	4240(2)	25.0(7)
C31	8220(3)	5122(2)	914.2(19)	15.4(6)
C32	7361(3)	5757(2)	464(2)	18.0(6)
C33	8110(3)	6740(2)	237(2)	17.8(6)
C34	9704(4)	7096(2)	444(2)	17.9(6)
C35	10535(3)	6431(3)	875(2)	18.6(6)
C36	9801(3)	5448(3)	1111(2)	18.2(6)
C37	10529(4)	8188(3)	229(2)	22.6(6)
Au1	9188.3(2)	7547.8(2)	2837.2(2)	12.97(4)
Cl1	11772.5(8)	8274.2(6)	3119.5(5)	22.20(15)
N1	6057(3)	7654.9(19)	2726.8(16)	12.6(4)
N2	5934(3)	5941.8(19)	2425.4(16)	12.9(5)
N3	7022(3)	4340.5(19)	2290.6(16)	14.0(5)
O1	3463(2)	4972.5(15)	2200.6(14)	14.8(4)
O2	5739(2)	3480.5(17)	626.7(14)	19.8(4)
O3	8221(3)	3217.2(17)	1431.4(15)	21.7(5)
S1	7247.8(8)	3918.8(5)	1251.1(5)	15.39(13)

**Table 3 Anisotropic Displacement Parameters ( $\text{\AA}^2 \times 10^3$ ) for 353dAuCl. The Anisotropic displacement factor exponent takes the form:  $-2\pi^2[h^2a^{*2}U_{11}+2hka^*b^*U_{12}+\dots]$ .**

Atom	$U_{11}$	$U_{22}$	$U_{33}$	$U_{23}$	$U_{13}$	$U_{12}$
C1	19.0(14)	10.5(12)	14.2(13)	5.4(10)	6.4(11)	5.6(11)
C2	13.2(13)	13.0(12)	17.3(13)	3.3(10)	4.2(11)	4.6(11)
C3	11.8(13)	14.3(13)	15.2(13)	4.8(10)	4.3(11)	4.4(10)
C4	16.7(14)	12.8(13)	11.2(12)	3.0(10)	5.9(11)	6.4(11)
C5	18.1(14)	10.5(12)	14.1(13)	3.9(10)	6.7(11)	7.5(11)
C6	10.8(13)	9.5(12)	19.9(14)	1.4(10)	4.7(11)	3.9(10)
C7	11.3(13)	14.6(13)	17.3(14)	4.4(11)	3.5(11)	5.5(10)
C8	17.2(14)	12.4(13)	23.8(15)	6.2(11)	5.6(12)	5.6(11)
C9	16.7(14)	12.1(13)	27.2(16)	1.4(11)	3.6(12)	3.2(11)
C10	20.3(15)	15.1(13)	21.0(15)	-0.6(11)	5.5(12)	5.5(12)
C11	14.7(14)	13.9(13)	19.9(14)	3.0(11)	5.0(11)	4.3(11)
C12	21.0(15)	14.8(13)	16.3(14)	4.9(11)	6.3(12)	6.7(11)
C13	21.1(16)	25.0(15)	22.0(15)	2.9(12)	2.7(13)	5.8(13)
C14	25.4(17)	25.5(16)	22.5(15)	6.2(13)	8.9(13)	9.2(13)
C15	23.7(16)	15.1(13)	17.4(14)	1.1(11)	5.8(12)	5.9(12)
C16	25.1(17)	24.3(15)	22.7(15)	6.0(12)	8.5(13)	7.4(13)
C17	27.8(18)	27.8(16)	22.6(16)	9.6(13)	6.7(14)	10.0(14)
C18	18.7(14)	12.6(13)	12.3(13)	2.4(10)	4.1(11)	2.3(11)
C19	19.8(15)	15.6(13)	18.4(14)	1.3(11)	5.6(12)	5.7(11)
C20	17.4(15)	19.5(14)	22.8(15)	2.8(12)	6.2(12)	-1.4(12)
C21	27.5(17)	12.0(13)	20.3(15)	3.0(11)	6.7(13)	-1.6(12)
C22	27.1(16)	12.6(13)	20.4(14)	1.8(11)	5.8(13)	5.3(12)
C23	19.3(15)	14.6(13)	22.1(15)	4.0(11)	8.3(12)	5.0(11)
C24	15.5(14)	21.4(14)	16.4(14)	3.8(11)	3.4(11)	8.5(11)
C25	19.0(15)	16.9(13)	15.8(14)	4.0(11)	1.7(12)	9.6(12)
C26	24.7(16)	17.0(14)	19.3(15)	7.3(12)	1.7(12)	7.8(12)
C27	39(2)	22.2(15)	18.3(15)	0.3(12)	4.5(14)	11.7(14)
C28	51(2)	38(2)	19.7(16)	1.4(15)	16.7(16)	9.2(18)
C29	48(2)	34.2(19)	26.7(18)	6.5(15)	16.0(17)	-0.4(17)
C30	34.0(19)	19.1(15)	19.1(15)	2.1(12)	8.4(14)	3.0(13)
C31	16.9(14)	15.5(13)	13.3(13)	1.9(10)	5.3(11)	3.3(11)

C32	16.4(14)	20.7(14)	16.4(14)	2.1(11)	4.6(11)	5.2(12)
C33	20.0(15)	21.2(14)	15.2(13)	4.7(11)	7.0(12)	8.7(12)
C34	19.9(15)	18.4(14)	14.4(13)	0.0(11)	7.2(11)	3.4(12)
C35	11.6(14)	24.8(15)	18.0(14)	-0.2(12)	5.8(11)	3.3(11)
C36	16.4(14)	22.8(14)	17.5(14)	2.7(11)	6.6(12)	8.1(12)
C37	22.9(16)	19.7(14)	22.7(15)	0.6(12)	10.0(13)	0.2(12)
Au1	12.00(7)	11.28(6)	16.00(7)	1.61(4)	4.73(4)	3.72(4)
Cl1	13.3(3)	19.5(3)	30.9(4)	-3.3(3)	6.4(3)	3.2(3)
N1	13.5(11)	11.2(11)	14.1(11)	2.4(9)	5.1(9)	4.4(9)
N2	13.0(11)	11.0(11)	15.3(11)	3.7(9)	4.6(9)	3.5(9)
N3	14.6(12)	14.9(11)	13.7(11)	1.6(9)	4.8(9)	6.3(9)
O1	13.7(10)	8.9(9)	21.8(10)	1.4(7)	5.7(8)	3.3(7)
O2	20.7(11)	16.6(10)	20.1(10)	-0.7(8)	6.1(9)	3.7(8)
O3	25.4(12)	18.8(10)	27.1(11)	3.6(9)	11.9(10)	13.0(9)
S1	17.5(3)	13.5(3)	16.9(3)	1.2(2)	7.5(3)	5.9(3)

**Table 4 Bond Lengths for 353dAuCl.**

Atom	Atom	Length/Å	Atom	Atom	Length/Å
C1	Au1	1.976(3)	C18	C23	1.409(4)
C1	N1	1.360(4)	C19	C20	1.383(4)
C1	N2	1.363(4)	C20	C21	1.387(5)
C2	C3	1.347(4)	C21	C22	1.387(5)
C2	N1	1.394(4)	C22	C23	1.389(4)
C3	N2	1.376(4)	C24	C25	1.511(4)
C3	O1	1.352(3)	C24	N3	1.493(4)
C4	C5	1.350(4)	C25	C26	1.392(4)
C4	C18	1.463(4)	C25	C30	1.389(4)
C4	O1	1.406(3)	C26	C27	1.391(4)
C5	N2	1.435(3)	C27	C28	1.372(5)
C5	N3	1.390(4)	C28	C29	1.379(5)
C6	C7	1.396(4)	C29	C30	1.387(5)
C6	Cl1	1.407(4)	C31	C32	1.398(4)
C6	N1	1.446(3)	C31	C36	1.385(4)
C7	C8	1.393(4)	C31	S1	1.754(3)
C7	C12	1.523(4)	C32	C33	1.383(4)
C8	C9	1.392(4)	C33	C34	1.395(4)
C9	C10	1.375(4)	C34	C35	1.402(4)
C10	C11	1.398(4)	C34	C37	1.508(4)
C11	C15	1.517(4)	C35	C36	1.384(4)
C12	C13	1.530(4)	Au1	Cl1	2.2806(7)
C12	C14	1.531(4)	N3	S1	1.676(2)
C15	C16	1.527(4)	O2	S1	1.429(2)
C15	C17	1.540(4)	O3	S1	1.435(2)
C18	C19	1.388(4)			

**Table 5 Bond Angles for 353dAuCl.**

Atom	Atom	Atom	Angle/°	Atom	Atom	Atom	Angle/°
N1	C1	Au1	123.7(2)	C22	C23	C18	119.3(3)
N1	C1	N2	102.9(2)	N3	C24	C25	111.4(2)
N2	C1	Au1	133.4(2)	C26	C25	C24	119.0(3)

C3	C2	N1	103.1(2)	C30	C25	C24	121.3(3)
C2	C3	N2	109.7(2)	C30	C25	C26	119.6(3)
C2	C3	O1	138.8(3)	C27	C26	C25	119.7(3)
O1	C3	N2	111.4(2)	C28	C27	C26	120.1(3)
C5	C4	C18	135.2(3)	C27	C28	C29	120.7(3)
C5	C4	O1	110.4(2)	C28	C29	C30	119.8(3)
O1	C4	C18	114.1(2)	C29	C30	C25	120.1(3)
C4	C5	N2	106.6(2)	C32	C31	S1	118.3(2)
C4	C5	N3	128.4(2)	C36	C31	C32	121.0(3)
N3	C5	N2	124.9(2)	C36	C31	S1	120.7(2)
C7	C6	C11	123.5(2)	C33	C32	C31	119.3(3)
C7	C6	N1	118.7(2)	C32	C33	C34	120.7(3)
C11	C6	N1	117.8(2)	C33	C34	C35	118.8(3)
C6	C7	C12	121.5(2)	C33	C34	C37	121.0(3)
C8	C7	C6	117.4(3)	C35	C34	C37	120.2(3)
C8	C7	C12	121.0(3)	C36	C35	C34	121.0(3)
C9	C8	C7	120.4(3)	C35	C36	C31	119.1(3)
C10	C9	C8	121.0(3)	C1	Au1	Cl1	176.88(8)
C9	C10	C11	121.1(3)	C1	N1	C2	113.8(2)
C6	C11	C15	122.8(2)	C1	N1	C6	124.2(2)
C10	C11	C6	116.6(3)	C2	N1	C6	121.9(2)
C10	C11	C15	120.6(3)	C1	N2	C3	110.5(2)
C7	C12	C13	109.5(2)	C1	N2	C5	143.4(2)
C7	C12	C14	112.4(2)	C3	N2	C5	105.8(2)
C13	C12	C14	111.6(3)	C5	N3	C24	120.0(2)
C11	C15	C16	111.9(3)	C5	N3	S1	117.18(19)
C11	C15	C17	110.3(3)	C24	N3	S1	116.79(18)
C16	C15	C17	110.9(3)	C3	O1	C4	105.6(2)
C19	C18	C4	119.3(3)	N3	S1	C31	106.30(12)
C19	C18	C23	119.3(3)	O2	S1	C31	108.82(14)
C23	C18	C4	121.2(3)	O2	S1	N3	105.92(12)
C20	C19	C18	120.6(3)	O2	S1	O3	120.51(13)
C19	C20	C21	120.5(3)	O3	S1	C31	109.56(14)
C20	C21	C22	119.3(3)	O3	S1	N3	104.74(13)
C21	C22	C23	121.0(3)				

**Table 6 Torsion Angles for 353dAuCl.**

A	B	C	D	Angle/°	A	B	C	D	Angle/°
C2	C3	N2	C1	-0.1(3)	C24	N3	S1	O3	44.5(2)
C2	C3	N2	C5	175.1(2)	C25	C24	N3	C5	37.8(4)
C2	C3	O1	C4	-172.8(4)	C25	C24	N3	S1	-170.16(19)
C3	C2	N1	C1	-0.6(3)	C25	C26	C27	C28	-0.3(5)
C3	C2	N1	C6	-177.9(2)	C26	C25	C30	C29	0.1(5)
C4	C5	N2	C1	172.5(3)	C26	C27	C28	C29	0.7(6)
C4	C5	N2	C3	0.0(3)	C27	C28	C29	C30	-0.7(7)
C4	C5	N3	C24	-124.5(3)	C28	C29	C30	C25	0.3(6)
C4	C5	N3	S1	83.6(3)	C30	C25	C26	C27	-0.1(5)
C4	C18	C19	C20	-174.7(3)	C31	C32	C33	C34	0.6(4)
C4	C18	C23	C22	173.7(3)	C32	C31	C36	C35	1.5(4)
C5	C4	C18	C19	171.9(3)	C32	C31	S1	N3	-84.8(2)
C5	C4	C18	C23	-3.9(5)	C32	C31	S1	O2	28.9(3)
C5	C4	O1	C3	-3.6(3)	C32	C31	S1	O3	162.5(2)

C5 N3 S1 C31	81.3(2)	C32 C33 C34 C35	0.9(4)
C5 N3 S1 O2	-34.3(2)	C32 C33 C34 C37	-177.7(3)
C5 N3 S1 O3	-162.7(2)	C33 C34 C35 C36	-1.3(4)
C6 C7 C8 C9	-0.1(4)	C34 C35 C36 C31	0.1(4)
C6 C7 C12 C13	99.0(3)	C36 C31 C32 C33	-1.8(4)
C6 C7 C12 C14	-136.5(3)	C36 C31 S1 N3	93.6(2)
C6 C11 C15 C16	-118.8(3)	C36 C31 S1 O2	-152.7(2)
C6 C11 C15 C17	117.2(3)	C36 C31 S1 O3	-19.1(3)
C7 C6 C11 C10	1.2(4)	C37 C34 C35 C36	177.4(3)
C7 C6 C11 C15	-176.7(3)	Au1 C1 N1 C2	-179.18(19)
C7 C6 N1 C1	89.0(3)	Au1 C1 N1 C6	-2.0(4)
C7 C6 N1 C2	-94.1(3)	Au1 C1 N2 C3	179.4(2)
C7 C8 C9 C10	0.9(5)	Au1 C1 N2 C5	7.2(6)
C8 C7 C12 C13	-77.8(3)	N1 C1 N2 C3	-0.3(3)
C8 C7 C12 C14	46.8(4)	N1 C1 N2 C5	-172.5(3)
C8 C9 C10 C11	-0.7(5)	N1 C2 C3 N2	0.4(3)
C9 C10 C11 C6	-0.3(4)	N1 C2 C3 O1	176.8(3)
C9 C10 C11 C15	177.6(3)	N1 C6 C7 C8	176.1(2)
C10 C11 C15 C16	63.3(4)	N1 C6 C7 C12	-0.8(4)
C10 C11 C15 C17	-60.7(4)	N1 C6 C11 C10	-175.9(3)
C11 C6 C7 C8	-1.0(4)	N1 C6 C11 C15	6.1(4)
C11 C6 C7 C12	-177.9(3)	N2 C1 N1 C2	0.6(3)
C11 C6 N1 C1	-93.8(3)	N2 C1 N1 C6	177.8(2)
C11 C6 N1 C2	83.2(3)	N2 C3 O1 C4	3.7(3)
C12 C7 C8 C9	176.8(3)	N2 C5 N3 C24	55.2(4)
C18 C4 C5 N2	-171.4(3)	N2 C5 N3 S1	-96.7(3)
C18 C4 C5 N3	8.3(5)	N3 C5 N2 C1	-7.3(6)
C18 C4 O1 C3	171.5(2)	N3 C5 N2 C3	-179.8(3)
C18 C19 C20 C21	0.8(5)	N3 C24 C25 C26	-129.6(3)
C19 C18 C23 C22	-2.1(4)	N3 C24 C25 C30	52.7(4)
C19 C20 C21 C22	-1.9(5)	O1 C3 N2 C1	-177.6(2)
C20 C21 C22 C23	1.0(5)	O1 C3 N2 C5	-2.4(3)
C21 C22 C23 C18	1.1(5)	O1 C4 C5 N2	2.2(3)
C23 C18 C19 C20	1.2(4)	O1 C4 C5 N3	-178.0(2)
C24 C25 C26 C27	-177.8(3)	O1 C4 C18 C19	-1.6(4)
C24 C25 C30 C29	177.8(3)	O1 C4 C18 C23	-177.4(2)
C24 N3 S1 C31	-71.5(2)	S1 C31 C32 C33	176.6(2)
C24 N3 S1 O2	172.8(2)	S1 C31 C36 C35	-176.9(2)

**Table 7 Hydrogen Atom Coordinates ( $\text{\AA}\times 10^4$ ) and Isotropic Displacement Parameters ( $\text{\AA}^2\times 10^3$ ) for 353dAuCl.**

Atom	x	y	z	U(eq)
H2	3708.17	7360.24	2597.88	17
H8	7283.8	11092.94	2110.27	21
H9	7820.48	11907.87	3654.18	23
H10	7665.22	10839.77	4780.95	23
H12	6271.02	8156.14	1245.68	20
H13A	3982.35	8626.41	1126.34	35
H13B	4348.99	8536.71	162.94	35
H13C	4671.81	9711.36	769.19	35
H14A	7506.8	10250.12	791.68	35
H14B	7121.98	9103.87	127.58	35
H14C	8435.44	9414.23	1063.79	35

H15	6617.95	7844.51	4393.51	23
H16A	6052.47	9548.15	5515	35
H16B	5732.64	8307.17	5658.62	35
H16C	4768.02	8597.85	4768.1	35
H17A	9238.05	8764.54	5043.14	38
H17B	8496.29	8440.92	5840.53	38
H17C	8872.55	9673.48	5673.28	38
H19	1455	3357.99	2104.74	22
H20	102.95	1565.5	2143.51	25
H21	1298.57	178.46	2237.11	26
H22	3826.95	578.96	2207.71	24
H23	5191.36	2362.49	2127.34	22
H24A	9097.12	5405.58	3034.22	21
H24B	8967.97	4156.14	3104.33	21
H26	9508.91	6433.28	4496.79	25
H27	8991.02	6684.7	5925.52	32
H28	7205.69	5304.82	6284.64	43
H29	5952.2	3645.14	5248.75	45
H30	6452.56	3378.22	3819.28	30
H32	6297.25	5520.04	319.64	22
H33	7544.42	7169.26	-57.05	21
H35	11596.85	6653.71	1004.52	22
H36	10361.8	5012.5	1397.48	22
H37A	9794.03	8509.21	-104.18	34
H37B	11183.68	8060.92	-144.67	34
H37C	11134.84	8690.72	800.82	34

## Experimental

A suitable crystal was selected on a **SuperNova, Dual, Cu at home/near, Atlas** diffractometer. The crystal was kept at 100.00(10) K during data collection. Using Olex2,<sup>275</sup> the structure was solved with the ShelXT<sup>276</sup> structure solution program using Intrinsic Phasing and refined with the ShelXL<sup>277</sup> refinement package using Least Squares minimisation.

## Crystal structure determination of [353dAuCl]

**Crystal Data** for  $C_{37}H_{37}AuClN_3O_3S$  ( $M = 836.17$  g/mol): triclinic, space group P-1 (no. 2),  $a = 9.4226(4)$  Å,  $b = 12.6393(5)$  Å,  $c = 15.0477(4)$  Å,  $\alpha = 96.410(3)^\circ$ ,  $\beta = 103.863(3)^\circ$ ,  $\gamma = 105.149(3)^\circ$ ,  $V = 1650.15(11)$  Å<sup>3</sup>,  $Z = 2$ ,  $T = 100.01(10)$  K,  $\mu(\text{CuK}\alpha) = 10.047$  mm<sup>-1</sup>,  $D_{\text{calc}} = 1.683$  g/cm<sup>3</sup>, 11914 reflections measured ( $7.374^\circ \leq 2\theta \leq 149.07^\circ$ ), 6522 unique ( $R_{\text{int}} = 0.0261$ ,  $R_{\text{sigma}} = 0.0359$ ) which were used in all calculations. The final  $R_1$  was 0.0223 ( $I > 2\sigma(I)$ ) and  $wR_2$  was 0.0555 (all data).

## Refinement model description

Number of restraints - 0, number of constraints - unknown.

Details:

1. Fixed Uiso

At 1.2 times of:

All C(H) groups, All C(H,H) groups

At 1.5 times of:

All C(H,H,H) groups

2.a Ternary CH refined with riding coordinates:

C12(H12), C15(H15)

2.b Secondary CH2 refined with riding coordinates:

C24(H24A,H24B)

2.c Aromatic/amide H refined with riding coordinates:

C2(H2), C8(H8), C9(H9), C10(H10), C19(H19), C20(H20), C21(H21), C22(H22),  
C23(H23), C26(H26), C27(H27), C28(H28), C29(H29), C30(H30), C32(H32), C33(H33),  
C35(H35), C36(H36)

2.d Idealised Me refined as rotating group:

C13(H13A,H13B,H13C), C14(H14A,H14B,H14C), C16(H16A,H16B,H16C), C17(H17A,H17B,  
H17C), C37(H37A,H37B,H37C)

### 3.11 354aAuCl

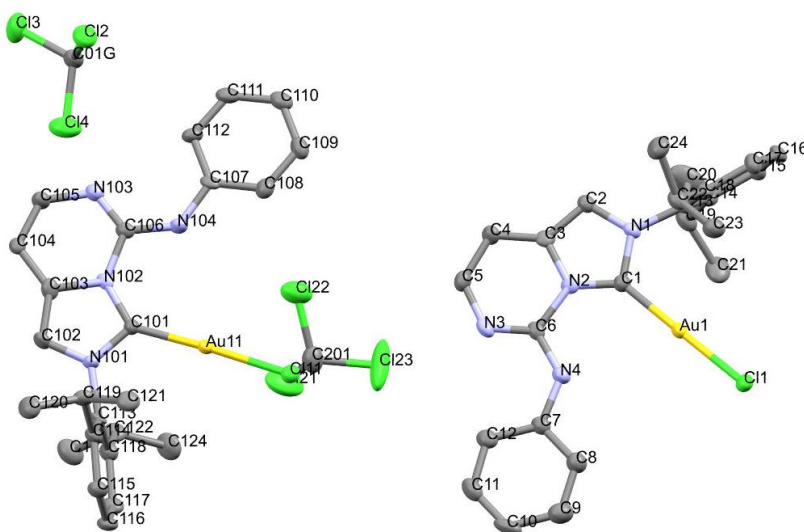
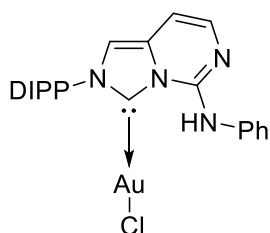


**Table 1 Crystal data and structure refinement for 354aAuCl.**

Identification code	354aAuCl
Empirical formula	C <sub>50</sub> H <sub>54</sub> Au <sub>2</sub> Cl <sub>8</sub> N <sub>8</sub>
Formula weight	1444.54
Temperature/K	100.01(10)
Crystal system	triclinic
Space group	P-1
a/Å	11.7878(5)
b/Å	13.2010(5)
c/Å	17.4519(4)
α/°	91.301(2)
β/°	92.211(3)
γ/°	90.879(3)
Volume/Å <sup>3</sup>	2712.62(17)
Z	2
ρ <sub>calc</sub> /cm <sup>3</sup>	1.769
μ/mm <sup>-1</sup>	13.982
F(000)	1408.0
Crystal size/mm <sup>3</sup>	0.154 × 0.09 × 0.042
Radiation	CuKα (λ = 1.54184)
2θ range for data collection/°	7.506 to 136.496
Index ranges	-14 ≤ h ≤ 14, -15 ≤ k ≤ 15, -18 ≤ l ≤ 21
Reflections collected	21843
Independent reflections	9905 [R <sub>int</sub> = 0.0366, R <sub>sigma</sub> = 0.0438]
Data/restraints/parameters	9905/12/611
Goodness-of-fit on F <sup>2</sup>	1.037
Final R indexes [I ≥ 2σ (I)]	R <sub>1</sub> = 0.0495, wR <sub>2</sub> = 0.1346
Final R indexes [all data]	R <sub>1</sub> = 0.0552, wR <sub>2</sub> = 0.1411
Largest diff. peak/hole / e Å <sup>-3</sup>	6.90/-2.17

**Table 2 Fractional Atomic Coordinates (×10<sup>4</sup>) and Equivalent Isotropic Displacement Parameters (Å<sup>2</sup>×10<sup>3</sup>) for 354aAuCl. U<sub>eq</sub> is defined as 1/3 of the trace of the orthogonalised U<sub>ij</sub> tensor.**

Atom	<i>x</i>	<i>y</i>	<i>z</i>	U(eq)
Au11	-1223.5(2)	2505.6(2)	3480.3(2)	16.47(10)
Au1	6202.6(2)	2424.2(2)	-1698.2(2)	17.79(10)
Cl11	-882.8(15)	2396.7(13)	2210(1)	24.4(4)
Cl1	5711.6(16)	2466.4(14)	-2970(1)	26.4(4)
Cl2	2595.2(19)	-79.4(15)	7369.4(12)	36.3(4)
Cl3	3499.7(18)	1219(2)	8598.7(12)	43.0(5)
Cl4	2476(2)	2090.0(17)	7251.3(15)	45.4(5)
Cl22	2044(2)	2775.9(18)	3108.2(15)	47.5(6)
Cl21	2043(3)	4948(2)	2909(2)	69.5(9)
Cl23	2254(6)	3602(3)	1639(2)	128(2)
N2	6107(5)	2614(4)	59(3)	16.7(11)
N102	-1105(5)	2304(4)	5241(3)	16.0(11)
N101	-2420(5)	3252(4)	4823(3)	16.9(11)
C101	-1553(6)	2664(5)	4568(4)	17.0(13)
N1	7432(5)	1687(4)	-320(3)	17.5(12)
N104	346(5)	1336(5)	4725(3)	20.8(12)
N3	4798(5)	3521(5)	825(4)	22.9(13)
N103	208(5)	1449(5)	6050(4)	23.6(13)
C1	6550(6)	2301(6)	-590(4)	20.7(14)
N4	4659(5)	3596(5)	-508(4)	23.4(13)
C4	6249(6)	2502(6)	1451(4)	22.0(15)
C3	6622(6)	2241(5)	726(4)	20.4(14)
C106	-151(6)	1666(5)	5370(4)	19.2(14)
C2	7474(6)	1648(5)	461(4)	21.0(14)
C5	5350(7)	3159(6)	1470(4)	24.8(16)
C113	-3133(6)	3863(5)	4317(4)	16.8(13)
C104	-1275(6)	2388(5)	6626(4)	18.2(14)
C107	1326(6)	750(5)	4656(4)	19.7(14)
C102	-2504(6)	3263(6)	5601(4)	19.9(14)
C6	5150(6)	3276(5)	152(4)	18.7(14)
C119	-4607(6)	2431(6)	4296(4)	23.5(15)
C105	-354(6)	1808(6)	6675(4)	22.6(15)
C108	1600(7)	467(6)	3901(4)	25.9(16)
C13	8179(6)	1127(5)	-807(4)	19.1(14)
C109	2540(7)	-112(6)	3771(5)	28.8(17)
C122	-1557(7)	5217(6)	4374(5)	27.2(16)
C15	10019(6)	921(6)	-1313(4)	25.4(16)
C103	-1670(6)	2668(6)	5887(4)	21.7(15)
C18	7776(6)	215(5)	-1145(4)	20.8(14)
C112	2020(6)	443(6)	5268(4)	22.7(15)
C115	-4889(6)	4100(6)	3648(4)	23.7(15)
C14	9276(6)	1511(5)	-891(4)	20.3(14)
C121	-4880(7)	1781(6)	3576(5)	29.9(17)
C114	-4206(6)	3472(5)	4082(4)	20.3(14)
C118	-2731(6)	4811(6)	4121(4)	23.8(15)
C16	9654(7)	2(6)	-1640(4)	25.7(16)
C116	-4521(7)	5047(6)	3445(5)	26.6(16)
C12	3137(7)	4700(6)	-30(5)	26.7(16)
C22	6581(7)	-196(6)	-1050(4)	25.8(16)
C110	3231(7)	-421(6)	4388(5)	29.1(17)
C19	9651(7)	2546(6)	-579(5)	28.7(17)
C01G	3291(7)	1093(6)	7596(4)	26.4(16)
C123	-1621(8)	6122(7)	4924(6)	40(2)



C8	3355(7)	4365(6)	-1381(5)	29.3(17)
C117	-3455(7)	5404(6)	3679(5)	26.8(16)
C7	3714(6)	4227(6)	-627(4)	22.2(15)
C120	-5640(7)	2477(7)	4812(5)	32.7(18)
C23	5978(7)	-439(7)	-1824(5)	31.3(18)
C111	2955(7)	-138(6)	5123(5)	29.6(17)
C124	-838(8)	5465(8)	3691(6)	42(2)
C24	6599(8)	-1117(7)	-549(5)	35.6(19)
C10	1867(7)	5442(6)	-973(6)	33.3(19)
C17	8546(7)	-350(6)	-1560(4)	26.7(16)
C11	2217(7)	5292(6)	-227(5)	32.2(18)
C9	2451(8)	4979(7)	-1558(5)	38(2)
C201	1633(8)	3772(7)	2505(5)	35.2(19)
C21	9659(10)	3304(7)	-1242(6)	45(2)
C20	10808(9)	2531(9)	-168(8)	61(3)

**Table 3 Anisotropic Displacement Parameters ( $\text{\AA}^2 \times 10^3$ ) for 354aAuCl. The Anisotropic displacement factor exponent takes the form:  $-2\pi^2[h^2a^{*2}U_{11}+2hka^*b^*U_{12}+\dots]$ .**

Atom	$U_{11}$	$U_{22}$	$U_{33}$	$U_{23}$	$U_{13}$	$U_{12}$
Au11	14.89(16)	14.78(16)	19.74(17)	0.85(11)	-0.16(11)	1.35(11)
Au1	16.39(16)	16.24(16)	21.05(17)	1.61(11)	3.60(11)	1.36(11)
Cl11	26.5(9)	23.9(8)	22.5(8)	0.4(6)	-1.5(6)	-0.3(7)
Cl1	30.0(9)	27.6(9)	22.3(8)	6.3(7)	5.6(7)	5.5(7)
Cl2	40.1(11)	26.3(10)	42.6(11)	-0.8(8)	2.0(9)	-1.6(8)
Cl3	31.3(11)	68.9(16)	28.5(10)	-5.1(10)	2.2(8)	-8.9(10)
Cl4	35.6(11)	30.1(11)	69.9(15)	12.6(10)	-9.3(10)	-2.9(9)
Cl22	39.1(12)	39.8(12)	61.8(14)	-2.1(10)	-17.7(10)	2.9(10)
Cl21	83(2)	32.8(13)	90(2)	-22.1(13)	-30.2(17)	13.5(13)
Cl23	257(7)	65(2)	69(2)	-13.0(17)	102(3)	-17(3)
N2	10(3)	16(3)	24(3)	3(2)	0(2)	-5(2)
N102	10(3)	12(3)	26(3)	0(2)	4(2)	-4(2)
N101	13(3)	19(3)	20(3)	4(2)	0(2)	3(2)
N1	15(3)	13(3)	24(3)	-3(2)	-1(2)	1(2)
N104	15(3)	25(3)	23(3)	5(2)	-1(2)	4(2)
N3	22(3)	16(3)	31(3)	-4(2)	6(3)	1(2)
N103	22(3)	22(3)	27(3)	2(2)	1(2)	3(3)
N4	23(3)	20(3)	27(3)	1(2)	3(2)	4(3)
C4	14(3)	28(4)	24(4)	1(3)	2(3)	-2(3)
C3	25(4)	10(3)	26(4)	1(3)	-1(3)	-5(3)
C106	13(3)	17(3)	27(4)	3(3)	0(3)	-3(3)
C2	21(4)	18(3)	25(4)	-1(3)	2(3)	0(3)
C5	28(4)	26(4)	20(4)	-1(3)	3(3)	-4(3)
C113	16(3)	11(3)	25(3)	2(3)	4(3)	9(3)
C104	19(3)	14(3)	21(3)	1(3)	3(3)	-2(3)
C107	19(3)	9(3)	32(4)	4(3)	0(3)	1(3)
C102	12(3)	23(4)	25(4)	-1(3)	1(3)	3(3)
C6	14(3)	15(3)	27(4)	-2(3)	4(3)	-5(3)
C119	20(4)	23(4)	27(4)	5(3)	-6(3)	0(3)
C105	17(3)	27(4)	24(4)	1(3)	-1(3)	2(3)
C108	27(4)	26(4)	24(4)	3(3)	3(3)	-4(3)
C13	18(3)	15(3)	25(4)	3(3)	2(3)	4(3)
C109	29(4)	24(4)	34(4)	-2(3)	11(3)	-1(3)

C122	29(4)	13(3)	40(4)	4(3)	3(3)	-5(3)
C15	18(4)	27(4)	32(4)	3(3)	5(3)	4(3)
C103	17(3)	24(4)	24(4)	-6(3)	1(3)	-8(3)
C18	25(4)	15(3)	23(3)	1(3)	5(3)	5(3)
C112	23(4)	20(4)	25(4)	5(3)	-6(3)	1(3)
C115	19(4)	23(4)	29(4)	3(3)	-1(3)	2(3)
C14	21(4)	14(3)	25(4)	2(3)	-1(3)	-1(3)
C121	33(4)	19(4)	38(4)	2(3)	-1(3)	-5(3)
C114	18(3)	18(4)	25(4)	1(3)	2(3)	4(3)
C118	18(4)	24(4)	29(4)	2(3)	4(3)	-1(3)
C16	26(4)	23(4)	29(4)	1(3)	8(3)	10(3)
C116	27(4)	21(4)	32(4)	9(3)	2(3)	9(3)
C12	25(4)	21(4)	35(4)	4(3)	3(3)	-1(3)
C22	24(4)	19(4)	34(4)	-2(3)	3(3)	-3(3)
C110	24(4)	20(4)	44(5)	4(3)	4(3)	1(3)
C19	21(4)	24(4)	42(5)	-7(3)	5(3)	-2(3)
C01G	20(4)	30(4)	30(4)	2(3)	1(3)	3(3)
C123	32(5)	30(5)	58(6)	-9(4)	3(4)	-5(4)
C8	28(4)	29(4)	31(4)	0(3)	2(3)	1(3)
C117	30(4)	15(4)	37(4)	7(3)	5(3)	2(3)
C7	17(3)	20(4)	30(4)	2(3)	3(3)	-1(3)
C120	30(4)	30(4)	39(5)	7(3)	8(3)	-5(3)
C23	29(4)	31(4)	34(4)	3(3)	-2(3)	3(3)
C111	31(4)	19(4)	38(4)	6(3)	-5(3)	4(3)
C124	22(4)	45(6)	59(6)	4(4)	14(4)	-7(4)
C24	40(5)	35(5)	33(4)	8(4)	6(4)	-4(4)
C10	19(4)	19(4)	62(6)	8(4)	-1(4)	5(3)
C17	30(4)	22(4)	28(4)	-2(3)	8(3)	1(3)
C11	25(4)	26(4)	46(5)	-1(3)	13(4)	0(3)
C9	39(5)	34(5)	40(5)	5(4)	-5(4)	2(4)
C201	28(4)	43(5)	34(4)	-7(4)	2(3)	-8(4)
C21	62(7)	20(4)	53(6)	0(4)	15(5)	-5(4)
C20	31(5)	51(7)	98(9)	-20(6)	-20(5)	-3(5)

**Table 4 Bond Lengths for 354aAuCl.**

Atom Atom	Length/Å	Atom Atom	Length/Å
Au11 Cl11	2.2700(17)	C104 C103	1.413(10)
Au11 Cl101	1.960(7)	C107 C108	1.413(11)
Au1 Cl1	2.2742(17)	C107 C112	1.391(10)
Au1 C1	1.971(7)	C102 C103	1.356(11)
Cl2 C01G	1.771(8)	C119 C121	1.526(11)
Cl3 C01G	1.761(8)	C119 C114	1.507(10)
Cl4 C01G	1.745(8)	C119 C120	1.543(11)
Cl22 C201	1.765(10)	C108 C109	1.379(12)
Cl21 C201	1.744(9)	C13 C18	1.398(10)
Cl23 C201	1.716(9)	C13 C14	1.396(10)
N2 C1	1.325(9)	C109 C110	1.397(12)
N2 C3	1.395(9)	C122 C118	1.522(10)
N2 C6	1.449(9)	C122 C123	1.519(11)
N102 C101	1.367(9)	C122 C124	1.528(12)
N102 C106	1.430(9)	C15 C14	1.400(10)
N102 C103	1.410(9)	C15 C16	1.384(11)

N101 C101	1.375(9)	C18 C22	1.518(10)
N101 C113	1.460(9)	C18 C17	1.397(10)
N101 C102	1.364(9)	C112 C111	1.380(11)
N1 C1	1.402(9)	C115 C114	1.383(10)
N1 C2	1.365(9)	C115 C116	1.375(11)
N1 C13	1.446(9)	C14 C19	1.512(10)
N104 C106	1.355(10)	C118 C117	1.390(11)
N104 C107	1.408(9)	C16 C17	1.393(11)
N3 C5	1.377(10)	C116 C117	1.378(12)
N3 C6	1.298(9)	C12 C7	1.406(11)
N103 C106	1.283(10)	C12 C11	1.384(12)
N103 C105	1.377(10)	C22 C23	1.527(11)
N4 C6	1.349(10)	C22 C24	1.513(11)
N4 C7	1.413(10)	C110 C111	1.382(12)
C4 C3	1.393(10)	C19 C21	1.547(13)
C4 C5	1.380(11)	C19 C20	1.518(12)
C3 C2	1.371(11)	C8 C7	1.382(11)
C113 C114	1.401(10)	C8 C9	1.379(13)
C113 C118	1.386(10)	C10 C11	1.370(13)
C104 C105	1.339(10)	C10 C9	1.388(13)

**Table 5 Bond Angles for 354aAuCl.**

Atom Atom Atom	Angle/°	Atom Atom Atom	Angle/°
C101 Au11 C111	177.2(2)	C14 C13 N1	118.2(6)
C1 Au1 C11	175.8(2)	C14 C13 C18	123.6(7)
C1 N2 C3	115.3(6)	C108 C109 C110	120.1(7)
C1 N2 C6	127.8(6)	C118 C122 C124	111.9(7)
C3 N2 C6	116.9(6)	C123 C122 C118	111.9(7)
C101 N102 C106	129.5(6)	C123 C122 C124	111.3(7)
C101 N102 C103	112.7(6)	C16 C15 C14	120.3(7)
C103 N102 C106	117.8(6)	N102 C103 C104	119.0(7)
C101 N101 C113	123.3(6)	C102 C103 N102	105.1(6)
C102 N101 C101	113.5(6)	C102 C103 C104	135.8(7)
C102 N101 C113	123.0(6)	C13 C18 C22	123.2(6)
N102 C101 Au11	135.7(5)	C17 C18 C13	116.9(7)
N102 C101 N101	101.6(5)	C17 C18 C22	119.8(7)
N101 C101 Au11	122.7(5)	C111 C112 C107	119.3(7)
C1 N1 C13	124.5(6)	C116 C115 C114	121.5(7)
C2 N1 C1	111.7(6)	C13 C14 C15	117.5(7)
C2 N1 C13	123.8(6)	C13 C14 C19	122.2(7)
C106 N104 C107	128.8(6)	C15 C14 C19	120.2(7)
C6 N3 C5	119.7(7)	C113 C114 C119	122.2(6)
C106 N103 C105	119.9(7)	C115 C114 C113	116.4(7)
N2 C1 Au1	137.0(6)	C115 C114 C119	121.4(7)
N2 C1 N1	101.7(6)	C113 C118 C122	122.9(7)
N1 C1 Au1	121.1(5)	C113 C118 C117	117.1(7)
C6 N4 C7	129.8(6)	C117 C118 C122	119.9(7)
C5 C4 C3	116.1(7)	C15 C16 C17	120.9(7)
C4 C3 N2	121.8(7)	C115 C116 C117	120.6(7)
C2 C3 N2	103.7(6)	C11 C12 C7	117.8(8)
C2 C3 C4	134.5(7)	C18 C22 C23	111.6(6)
N104 C106 N102	114.7(6)	C24 C22 C18	110.7(7)

N103 C106 N102	121.7(7) C24 C22 C23	110.9(7)
N103 C106 N104	123.6(7) C111 C110 C109	118.9(8)
N1 C2 C3	107.6(6) C14 C19 C21	109.4(7)
N3 C5 C4	123.8(7) C14 C19 C20	112.4(7)
C114 C113 N101	117.9(6) C20 C19 C21	110.3(8)
C118 C113 N101	118.3(6) C13 C01G C12	109.1(4)
C118 C113 C114	123.7(7) C14 C01G C12	110.1(4)
C105 C104 C103	117.7(7) C14 C01G C13	110.0(4)
N104 C107 C108	115.8(7) C9 C8 C7	120.9(8)
C112 C107 N104	124.9(7) C116 C117 C118	120.6(7)
C112 C107 C108	119.2(7) C12 C7 N4	123.7(7)
C103 C102 N101	107.1(6) C8 C7 N4	116.5(7)
N3 C6 N2	121.5(7) C8 C7 C12	119.8(7)
N3 C6 N4	123.5(7) C112 C111 C110	122.1(8)
N4 C6 N2	115.0(6) C11 C10 C9	119.0(8)
C121 C119 C120	110.8(6) C16 C17 C18	120.7(7)
C114 C119 C121	110.3(6) C10 C11 C12	122.6(8)
C114 C119 C120	111.8(6) C8 C9 C10	119.8(8)
C104 C105 N103	123.9(7) C121 C201 C122	111.2(5)
C109 C108 C107	120.4(7) C123 C201 C122	108.6(6)
C18 C13 N1	118.2(6) C123 C201 C121	109.7(5)

**Table 6 Torsion Angles for 354aAuCl.**

A B C D	Angle/°	A B C D	Angle/°
N2 C3 C2 N1	-0.3(7)	C6 N3 C5 C4	-2.7(11)
N101 C113 C114 C119	-3.5(10)	C6 N4 C7 C12	4.0(12)
N101 C113 C114 C115	175.6(6)	C6 N4 C7 C8	-175.5(7)
N101 C113 C118 C122	3.3(10)	C105 N103 C106 N102	2.2(10)
N101 C113 C118 C117	-176.0(6)	C105 N103 C106 N104	-179.4(7)
N101 C102 C103 N102	-0.5(7)	C105 C104 C103 N102	1.9(10)
N101 C102 C103 C104	177.7(8)	C105 C104 C103 C102	-176.2(8)
C101 N102 C106 N104	-3.2(10)	C108 C107 C112 C111	-0.6(11)
C101 N102 C106 N103	175.3(7)	C108 C109 C110 C111	0.1(12)
C101 N102 C103 C104	-177.9(6)	C13 N1 C1 Au1	2.3(9)
C101 N102 C103 C102	0.7(8)	C13 N1 C1 N2	178.3(6)
C101 N101 C113 C114	99.6(8)	C13 N1 C2 C3	-177.9(6)
C101 N101 C113 C118	-82.7(8)	C13 C18 C22 C23	126.8(8)
C101 N101 C102 C103	0.1(8)	C13 C18 C22 C24	-109.2(8)
N1 C13 C18 C22	2.2(10)	C13 C18 C17 C16	-1.3(11)
N1 C13 C18 C17	-174.9(6)	C13 C14 C19 C21	-102.1(9)
N1 C13 C14 C15	175.0(6)	C13 C14 C19 C20	135.0(9)
N1 C13 C14 C19	-8.1(10)	C109 C110 C111 C112	-0.2(12)
N104 C107 C108 C109	-179.6(7)	C122 C118 C117 C116	-180.0(7)
N104 C107 C112 C111	179.6(7)	C15 C14 C19 C21	74.7(9)
C1 N2 C3 C4	-180.0(6)	C15 C14 C19 C20	-48.2(11)
C1 N2 C3 C2	0.7(8)	C15 C16 C17 C18	-0.2(12)
C1 N2 C6 N3	179.8(7)	C103 N102 C101 Au11	179.5(5)
C1 N2 C6 N4	0.6(10)	C103 N102 C101 N101	-0.7(7)
C1 N1 C2 C3	-0.2(8)	C103 N102 C106 N104	179.5(6)
C1 N1 C13 C18	-79.0(9)	C103 N102 C106 N103	-2.0(9)
C1 N1 C13 C14	103.1(8)	C103 C104 C105 N103	-1.8(11)
C4 C3 C2 N1	-179.5(7)	C18 C13 C14 C15	-2.8(11)

C3	N2	C1	Au1	174.2(6)	C18	C13	C14	C19	174.1(7)
C3	N2	C1	N1	-0.8(8)	C112	C107	C108	C109	0.5(11)
C3	N2	C6	N3	0.9(9)	C115	C116	C117	C118	0.3(12)
C3	N2	C6	N4	-178.2(6)	C14	C13	C18	C22	180.0(7)
C3	C4	C5	N3	2.6(11)	C14	C13	C18	C17	2.9(11)
C106	N102	C101	Au11	2.1(11)	C14	C15	C16	C17	0.3(12)
C106	N102	C101	N101	-178.1(6)	C121	C119	C114	C113	-120.5(7)
C106	N102	C103	C104	-0.1(9)	C121	C119	C114	C115	60.4(9)
C106	N102	C103	C102	178.5(6)	C114	C113	C118	C122	-179.2(7)
C106	N104	C107	C108	176.1(7)	C114	C113	C118	C117	1.5(11)
C106	N104	C107	C112	-4.1(12)	C114	C115	C116	C117	-0.8(12)
C106	N103	C105	C104	-0.3(11)	C118	C113	C114	C119	179.0(7)
C2	N1	C1	Au1	-175.4(5)	C118	C113	C114	C115	-1.9(11)
C2	N1	C1	N2	0.6(7)	C16	C15	C14	C13	1.1(11)
C2	N1	C13	C18	98.4(8)	C16	C15	C14	C19	-175.8(7)
C2	N1	C13	C14	-79.5(9)	C116	C115	C114	C113	1.5(11)
C5	N3	C6	N2	0.9(10)	C116	C115	C114	C119	-179.4(7)
C5	N3	C6	N4	179.9(7)	C22	C18	C17	C16	-178.5(7)
C5	C4	C3	N2	-0.6(10)	C123	C122	C118	C113	-113.6(9)
C5	C4	C3	C2	178.4(8)	C123	C122	C118	C117	65.7(10)
C113	N101	C101	Au11	-3.9(9)	C7	N4	C6	N2	179.1(6)
C113	N101	C101	N102	176.2(6)	C7	N4	C6	N3	0.0(12)
C113	N101	C102	C103	-175.8(6)	C7	C12	C11	C10	-1.0(12)
C113	C118	C117	C116	-0.6(11)	C7	C8	C9	C10	-2.1(13)
C107	N104	C106	N102	176.2(6)	C120	C119	C114	C113	115.7(8)
C107	N104	C106	N103	-2.2(12)	C120	C119	C114	C115	-63.4(9)
C107	C108	C109	C110	-0.2(12)	C124	C122	C118	C113	120.7(8)
C107	C112	C111	C110	0.5(12)	C124	C122	C118	C117	-60.0(10)
C102	N101	C101	Au11	-179.8(5)	C17	C18	C22	C23	-56.2(10)
C102	N101	C101	N102	0.3(7)	C17	C18	C22	C24	67.8(9)
C102	N101	C113	C114	-84.9(8)	C11	C12	C7	N4	-179.4(7)
C102	N101	C113	C118	92.8(8)	C11	C12	C7	C8	0.1(11)
C6	N2	C1	Au1	-4.7(12)	C11	C10	C9	C8	1.2(13)
C6	N2	C1	N1	-179.6(6)	C9	C8	C7	N4	-179.0(8)
C6	N2	C3	C4	-1.0(9)	C9	C8	C7	C12	1.4(12)
C6	N2	C3	C2	179.7(6)	C9	C10	C11	C12	0.4(13)

**Table 7 Hydrogen Atom Coordinates ( $\text{\AA}\times 10^4$ ) and Isotropic Displacement Parameters ( $\text{\AA}^2\times 10^3$ ) for 354aAuCl.**

Atom	x	y	z	U(eq)
H104	18.24	1509.02	4300.46	25
H4	4968.19	3383.54	-919.21	28
H4A	6585.87	2249.02	1895.68	26
H2	7988.88	1285.12	760.22	25
H5	5101.79	3368.54	1946.86	30
H10A	-1641.36	2598.37	7063.03	22
H102	-3033.12	3613.04	5881.42	24
H119	-3986.15	2110.14	4585.41	28
H105	-76.85	1637.05	7161.03	27
H108	1143.71	673.71	3488.22	31
H109	2713.85	-297.21	3272.01	35
H122	-1172	4677.54	4654.02	33
H15	10760.45	1146.59	-1373.15	30

H112	1856.52	627.41	5768.51	27
H115	-5614.99	3876.84	3489.64	28
H12A	-5472.29	2090.84	3274.84	45
H12B	-5126.43	1117.96	3720.53	45
H12C	-4213	1725.27	3280.32	45
H16	10155.43	-385.47	-1917.14	31
H116	-4995.2	5450.12	3147.91	32
H12	3365.98	4617.45	480.26	32
H22	6149.84	330.48	-790.1	31
H110	3867.09	-811.58	4304.12	35
H19	9095.86	2774.09	-211.65	34
H01G	4029.95	1106.91	7357.34	32
H12D	-1896.68	6696.49	4650.72	60
H12E	-879.25	6275.64	5146.41	60
H12F	-2128.98	5963.68	5323.48	60
H8	3728.62	4038.24	-1773.53	35
H117	-3218.5	6046.63	3539.91	32
H12G	-6262.28	2785.41	4539.01	49
H12H	-5443.62	2870.96	5267.91	49
H12I	-5856.58	1802.82	4948.86	49
H23A	5997.73	148.62	-2137.38	47
H23B	5203.32	-631.99	-1745.78	47
H23C	6354.51	-986.54	-2074.8	47
H111	3413.85	-345.56	5534.18	36
H12J	-875.46	4905.7	3328.64	63
H12K	-63.77	5582.94	3865.01	63
H12L	-1122.95	6060.58	3449.38	63
H24A	6907.55	-1678.79	-825.63	53
H24B	5839.21	-1283.29	-410.2	53
H24C	7060.81	-972.69	-93.36	53
H10	1247.99	5847.76	-1086.23	40
H17	8315.77	-968.6	-1785.51	32
H11	1820.3	5600.92	162.71	39
H9	2233.13	5082.93	-2067.45	45
H201	805.65	3749.76	2423.39	42
H21A	10156.93	3067.09	-1627.67	67
H21B	9920.05	3956.05	-1047.67	67
H21C	8904.17	3359.4	-1462.85	67
H20A	10783.21	2078.45	254.76	91
H20B	11009.77	3200.97	20.82	91
H20C	11364.19	2303.12	-517.73	91

## Experimental

A suitable crystal was selected on a **SuperNova, Dual, Cu at zero, Atlas** diffractometer. The crystal was kept at 100.01(10) K during data collection. Using Olex2<sup>275</sup>, the structure was solved with the ShelXT<sup>276</sup> structure solution program using Intrinsic Phasing and refined with the ShelXL<sup>277</sup> refinement package using Least Squares minimisation.

## Crystal structure determination of [354aAuCl]

**Crystal Data** for C<sub>50</sub>H<sub>54</sub>Au<sub>2</sub>Cl<sub>8</sub>N<sub>8</sub> (*M* = 1444.54 g/mol): triclinic, space group P-1 (no. 2), *a* = 11.7878(5) Å, *b* = 13.2010(5) Å, *c* = 17.4519(4) Å,  $\alpha$  = 91.301(2)°,  $\beta$  = 92.211(3)°,  $\gamma$  = 90.879(3)°, *V* = 2712.62(17) Å<sup>3</sup>, *Z* = 2, *T* = 100.01(10) K,  $\mu$ (CuK $\alpha$ ) = 13.982 mm<sup>-1</sup>, *D*<sub>calc</sub> = 1.769 g/cm<sup>3</sup>, 21843 reflections measured (7.506° ≤ 2 $\theta$  ≤ 136.496°), 9905 unique (*R*<sub>int</sub> = 0.0366, *R*<sub>sigma</sub> = 0.0438) which were used in all calculations. The final *R*<sub>1</sub> was 0.0495 (*I* > 2 $\sigma$ (*I*)) and *wR*<sub>2</sub> was 0.1411 (all data).

## Refinement model description

Number of restraints - 12, number of constraints - unknown.  
Details:

1. Fixed Uiso  
At 1.2 times of:  
All C(H) groups, All N(H) groups  
At 1.5 times of:  
All C(H,H,H) groups
2. Rigid bond restraints  
C1, N1, N2  
with sigma for 1-2 distances of 0.01 and sigma for 1-3 distances of 0.01  
C101, N102, N101  
with sigma for 1-2 distances of 0.01 and sigma for 1-3 distances of 0.01
3. Uiso/Uaniso restraints and constraints  
C1  $\approx$  N2  $\approx$  N1: within 1.7Å with sigma of 0.02 and sigma for terminal atoms of 0.04  
: with sigma of 0.01 and sigma for terminal atoms of 0.1
- 4.a Ternary CH refined with riding coordinates:  
C119(H119), C122(H122), C22(H22), C19(H19), C01G(H01G), C201(H201)
- 4.b Aromatic/amide H refined with riding coordinates:  
N104(H104), N4(H4), C4(H4A), C2(H2), C5(H5), C104(H10A), C102(H102), C105(H105), C108(H108), C109(H109), C15(H15), C112(H112), C115(H115), C16(H16), C116(H116), C12(H12), C110(H110), C8(H8), C117(H117), C111(H111), C10(H10), C17(H17), C11(H11), C9(H9)
- 4.c Idealised Me refined as rotating group:  
C121(H12A,H12B,H12C), C123(H12D,H12E,H12F), C120(H12G,H12H,H12I), C23(H23A,H23B,H23C), C124(H12J,H12K,H12L), C24(H24A,H24B,H24C), C21(H21A,H21B,H21C), C20(H20A,H20B,H20C)

### 3.12 355AuCl

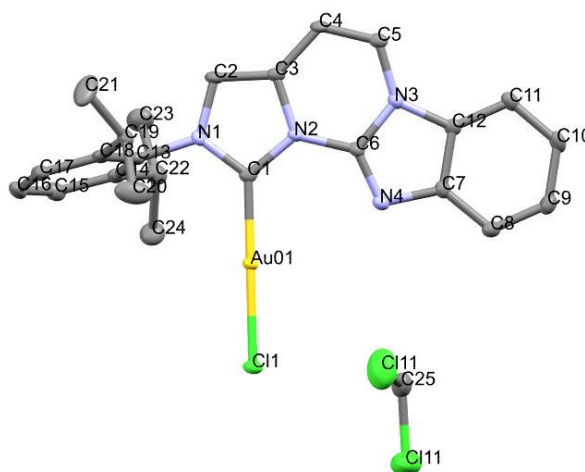
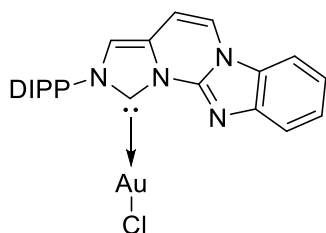


**Table 1 Crystal data and structure refinement for 355AuCl.**

Identification code	355AuCl
Empirical formula	C <sub>24.5</sub> H <sub>25</sub> AuCl <sub>2</sub> N <sub>4</sub>
Formula weight	643.35
Temperature/K	100.01(10)
Crystal system	monoclinic
Space group	C2/c
a/Å	21.9728(4)
b/Å	13.1676(2)
c/Å	17.1097(3)
$\alpha/^\circ$	90
$\beta/^\circ$	107.476(2)
$\gamma/^\circ$	90
Volume/Å <sup>3</sup>	4721.84(15)
Z	8

$\rho_{\text{calc}}/\text{cm}^3$	1.810
$\mu/\text{mm}^{-1}$	13.942
F(000)	2504.0
Crystal size/ $\text{mm}^3$	$0.159 \times 0.15 \times 0.055$
Radiation	$\text{CuK}\alpha$ ( $\lambda = 1.54184$ )
2 $\theta$ range for data collection/ $^\circ$	7.93 to 144.258
Index ranges	$-27 \leq h \leq 24, -16 \leq k \leq 11, -21 \leq l \leq 17$
Reflections collected	9262
Independent reflections	4594 [ $R_{\text{int}} = 0.0307, R_{\text{sigma}} = 0.0314$ ]
Data/restraints/parameters	4594/0/289
Goodness-of-fit on $F^2$	1.055
Final R indexes [ $I \geq 2\sigma(I)$ ]	$R_1 = 0.0239, wR_2 = 0.0628$
Final R indexes [all data]	$R_1 = 0.0254, wR_2 = 0.0640$
Largest diff. peak/hole / $e \text{ \AA}^{-3}$	1.48/-1.65

**Table 2 Fractional Atomic Coordinates ( $\times 10^4$ ) and Equivalent Isotropic Displacement Parameters ( $\text{\AA}^2 \times 10^3$ ) for 355AuCl.  $U_{\text{eq}}$  is defined as 1/3 of the trace of the orthogonalised  $U_{ij}$  tensor.**

Atom	$x$	$y$	$z$	$U(\text{eq})$
Au01	6869.8(2)	3468.5(2)	3140.0(2)	10.82(6)
Cl1	6524.3(3)	2340.4(6)	3930.7(4)	14.78(15)
Cl11	5292.4(6)	1130.4(11)	1838.4(9)	56.7(3)
N1	7772.6(12)	4761(2)	2553.5(15)	13.2(5)
N2	6809.6(12)	5052(2)	1841.3(15)	11.9(5)
N3	5896.8(12)	5835(2)	960.1(16)	13.6(5)
N4	5734.4(12)	4617(2)	1815.0(15)	14.2(5)
C4	6896.4(16)	6391(2)	878(2)	14.1(6)
C8	4532.8(15)	4784(3)	1365.8(19)	16.4(6)
C5	6261.9(16)	6442(2)	604(2)	14.4(6)
C25	5000	1886(4)	2500	29.4(12)
C10	4127.7(15)	6039(2)	294(2)	17.9(7)
C3	7194.3(15)	5709(2)	1542.5(18)	13.1(6)
C2	7801.1(15)	5516(2)	2001.9(19)	14.8(6)
C7	5148.7(14)	5027(2)	1351.6(19)	14.1(6)
C11	4734.5(16)	6296(3)	269(2)	16.7(6)
C6	6147.2(14)	5117(2)	1561.0(18)	12.4(6)
C14	8457.4(15)	4814(2)	3970(2)	15.7(6)
C13	8332.9(14)	4406(2)	3180.8(18)	13.6(6)
C1	7165.0(15)	4466(2)	2473.8(18)	12.8(6)
C18	8737.7(15)	3720(3)	2958(2)	15.3(6)
C12	5237.7(14)	5777(2)	817.7(19)	13.2(6)
C9	4032.3(15)	5301(3)	830(2)	18.0(7)
C17	9291.0(17)	3438(2)	3567(2)	17.7(7)
C15	9021.2(16)	4505(3)	4554(2)	20.8(7)
C22	8028.3(17)	5597(3)	4184(2)	20.6(7)
C16	9433.5(16)	3828(3)	4354(2)	21.6(7)
C19	8580.2(16)	3291(3)	2099(2)	16.7(7)
C24	7861.9(19)	5306(3)	4965(2)	28.5(8)
C20	8356(3)	2189(3)	2066(3)	41.0(11)
C23	8332(2)	6652(3)	4255(3)	31.3(9)
C21	9141(2)	3369(4)	1752(3)	43.7(13)



**Table 3 Anisotropic Displacement Parameters ( $\text{\AA}^2 \times 10^3$ ) for 355AuCl. The Anisotropic displacement factor exponent takes the form:  $-2\pi^2[h^2a^{*2}U_{11}+2hka^*b^*U_{12}+\dots]$ .**

Atom	U <sub>11</sub>	U <sub>22</sub>	U <sub>33</sub>	U <sub>23</sub>	U <sub>13</sub>	U <sub>12</sub>
Au01	13.44(8)	9.84(9)	9.54(8)	1.17(4)	3.98(6)	-0.07(4)
Cl1	20.3(3)	12.1(3)	14.4(3)	2.0(3)	9.0(3)	0.4(3)
Cl11	49.1(7)	62.3(8)	56.8(7)	-21.8(7)	12.8(6)	11.0(6)
N1	15.4(12)	14.9(13)	8.3(11)	0.9(10)	2(1)	-0.1(10)
N2	14.7(12)	11.5(12)	10.1(11)	1.9(10)	4.6(10)	-0.9(10)
N3	15.3(12)	13.6(13)	11.8(12)	0.8(11)	3.7(10)	0.6(10)
N4	16.7(12)	14.7(13)	10.6(11)	0.5(11)	3.4(10)	-1.5(10)
C4	19.6(16)	14.0(15)	11.1(14)	1.9(12)	8.0(13)	-2.9(12)
C8	18.6(15)	17.2(16)	12.9(14)	-0.5(13)	4.1(12)	-4.6(12)
C5	19.9(16)	13.4(16)	11.1(14)	-0.2(12)	6.5(13)	-0.9(12)
C25	22(2)	28(3)	36(3)	0	4(2)	0
C10	18.4(15)	13.7(16)	18.2(15)	-1.8(13)	0.5(12)	4.2(12)
C3	19.1(15)	10.2(14)	11.5(13)	-0.6(12)	6.9(12)	-2.3(12)
C2	20.1(15)	13.1(15)	13.1(14)	2.5(12)	8.0(12)	-2.3(12)
C7	15.3(14)	14.2(15)	11.6(13)	-1.5(12)	2.2(11)	0.2(12)
C11	21.0(16)	13.0(15)	13.4(15)	-1.0(13)	1.1(12)	1.0(13)
C6	16.1(14)	12.8(15)	8.1(13)	0.6(12)	3.2(11)	0.2(12)
C14	18.2(15)	12.4(15)	16.3(15)	0.2(13)	4.8(12)	-4.6(12)
C13	13.5(14)	14.3(15)	11.4(14)	3.4(12)	1.3(11)	-4.1(12)
C1	17.6(14)	11.9(15)	10.4(13)	-2.6(12)	6.4(11)	-1.5(12)
C18	16.8(15)	12.3(14)	16.6(15)	3.0(13)	4.7(12)	-3.7(12)
C12	16.4(14)	10.1(14)	13.1(14)	-3.6(12)	4.4(11)	-0.5(12)
C9	14.6(14)	21.1(17)	18.5(15)	-4.8(14)	5.3(12)	-2.0(13)
C17	17.8(16)	17.9(17)	18.8(17)	4.5(13)	7.5(14)	0.2(12)
C15	25.8(17)	20.1(17)	13.2(14)	-0.7(13)	0.8(13)	-5.6(14)
C22	27.0(17)	18.5(17)	14.8(15)	-3.6(13)	3.9(13)	-1.2(14)
C16	20.1(16)	19.9(17)	20.1(16)	7.7(14)	-1.2(13)	-2.4(14)
C19	16.2(15)	18.9(16)	15.5(15)	2.3(13)	5.4(13)	4.7(12)
C24	33(2)	35(2)	20.6(17)	-4.5(17)	12.6(15)	-2.5(17)
C20	78(3)	26(2)	21.6(18)	-10.1(17)	20(2)	-14(2)
C23	38(2)	23(2)	34(2)	-3.4(17)	13.3(18)	-3.1(16)
C21	26(2)	88(4)	20(2)	-8(2)	12.6(17)	-8(2)

**Table 4 Bond Lengths for 355AuCl.**

Atom	Atom	Length/ $\text{\AA}$	Atom	Atom	Length/ $\text{\AA}$
Au01	Cl1	2.2869(7)	C10	C11	1.388(5)
Au01	C1	1.972(3)	C10	C9	1.396(5)
Cl11	C25	1.767(4)	C3	C2	1.353(4)
N1	C2	1.385(4)	C7	C12	1.398(5)
N1	C13	1.447(4)	C11	C12	1.396(4)
N1	C1	1.358(4)	C14	C13	1.401(4)
N2	C3	1.408(4)	C14	C15	1.398(5)
N2	C6	1.392(4)	C14	C22	1.515(5)
N2	C1	1.367(4)	C13	C18	1.398(5)
N3	C5	1.396(4)	C18	C17	1.393(5)
N3	C6	1.383(4)	C18	C19	1.514(5)
N3	C12	1.397(4)	C17	C16	1.386(5)

N4	C7	1.402(4)	C15	C16	1.385(5)
N4	C6	1.297(4)	C22	C24	1.535(5)
C4	C5	1.333(5)	C22	C23	1.531(5)
C4	C3	1.442(4)	C19	C20	1.528(5)
C8	C7	1.398(4)	C19	C21	1.522(5)
C8	C9	1.381(5)			

**Table 5 Bond Angles for 355AuCl.**

Atom	Atom	Atom	Angle/°	Atom	Atom	Atom	Angle/°
C1	Au01	C11	178.74(9)	N4	C6	N3	115.7(3)
C2	N1	C13	122.3(3)	C13	C14	C22	122.5(3)
C1	N1	C2	112.4(3)	C15	C14	C13	116.9(3)
C1	N1	C13	125.0(3)	C15	C14	C22	120.5(3)
C6	N2	C3	121.1(3)	C14	C13	N1	117.9(3)
C1	N2	C3	111.8(2)	C18	C13	N1	118.4(3)
C1	N2	C6	126.7(3)	C18	C13	C14	123.6(3)
C5	N3	C12	131.1(3)	N1	C1	Au01	128.1(2)
C6	N3	C5	124.3(3)	N1	C1	N2	103.2(3)
C6	N3	C12	104.6(2)	N2	C1	Au01	128.7(2)
C6	N4	C7	103.3(3)	C13	C18	C19	121.8(3)
C5	C4	C3	119.2(3)	C17	C18	C13	116.9(3)
C9	C8	C7	117.2(3)	C17	C18	C19	121.4(3)
C4	C5	N3	119.6(3)	N3	C12	C7	105.4(3)
Cl11	C25	Cl11 <sup>1</sup>	111.4(3)	C11	C12	N3	131.4(3)
C11	C10	C9	121.6(3)	C11	C12	C7	123.2(3)
N2	C3	C4	119.3(3)	C8	C9	C10	122.2(3)
C2	C3	N2	105.5(3)	C16	C17	C18	121.3(3)
C2	C3	C4	135.2(3)	C16	C15	C14	121.0(3)
C3	C2	N1	107.0(3)	C14	C22	C24	111.7(3)
C8	C7	N4	129.1(3)	C14	C22	C23	110.4(3)
C12	C7	N4	110.9(3)	C23	C22	C24	111.7(3)
C12	C7	C8	120.0(3)	C15	C16	C17	120.3(3)
C10	C11	C12	115.8(3)	C18	C19	C20	111.6(3)
N3	C6	N2	116.1(3)	C18	C19	C21	112.2(3)
N4	C6	N2	128.1(3)	C21	C19	C20	109.8(4)

<sup>1</sup>1-X,+Y,1/2-Z

**Table 6 Torsion Angles for 355AuCl.**

A	B	C	D	Angle/°	A	B	C	D	Angle/°
N1	C13	C18	C17	176.5(3)	C6	N4	C7	C12	0.4(3)
N1	C13	C18	C19	-4.2(5)	C14	C13	C18	C17	0.1(5)
N2	C3	C2	N1	0.3(3)	C14	C13	C18	C19	179.4(3)
N4	C7	C12	N3	-0.4(3)	C14	C15	C16	C17	-0.3(5)
N4	C7	C12	C11	178.4(3)	C13	N1	C2	C3	-176.0(3)
C4	C3	C2	N1	179.9(3)	C13	N1	C1	Au01	-2.0(4)
C8	C7	C12	N3	179.6(3)	C13	N1	C1	N2	176.0(3)
C8	C7	C12	C11	-1.5(5)	C13	C14	C15	C16	0.0(5)
C5	N3	C6	N2	3.2(4)	C13	C14	C22	C24	131.2(3)
C5	N3	C6	N4	-179.4(3)	C13	C14	C22	C23	-103.9(4)

C5 N3 C12C7	179.6(3)	C13C18C17C16	-0.5(5)
C5 N3 C12C11	0.9(6)	C13C18C19C20	-105.1(4)
C5 C4 C3 N2	5.2(5)	C13C18C19C21	131.3(4)
C5 C4 C3 C2	-174.4(4)	C1 N1 C2 C3	-0.7(4)
C10C11C12N3	179.9(3)	C1 N1 C13C14	-77.2(4)
C10C11C12C7	1.4(5)	C1 N1 C13C18	106.2(4)
C3 N2 C6 N3	2.0(4)	C1 N2 C3 C4	-179.4(3)
C3 N2 C6 N4	-175.0(3)	C1 N2 C3 C2	0.3(3)
C3 N2 C1 Au01	177.2(2)	C1 N2 C6 N3	174.2(3)
C3 N2 C1 N1	-0.7(3)	C1 N2 C6 N4	-2.8(5)
C3 C4 C5 N3	-0.2(5)	C18C17C16C15	0.6(5)
C2 N1 C13C14	97.4(4)	C12N3 C5 C4	176.6(3)
C2 N1 C13C18	-79.2(4)	C12N3 C6 N2	-177.4(3)
C2 N1 C1 Au01	-177.1(2)	C12N3 C6 N4	0.0(4)
C2 N1 C1 N2	0.9(3)	C9 C8 C7 N4	-179.1(3)
C7 N4 C6 N2	176.8(3)	C9 C8 C7 C12	0.9(5)
C7 N4 C6 N3	-0.2(4)	C9 C10C11C12	-0.6(5)
C7 C8 C9 C10	-0.1(5)	C17C18C19C20	74.1(4)
C11C10C9 C8	0.0(5)	C17C18C19C21	-49.5(5)
C6 N2 C3 C4	-6.2(4)	C15C14C13N1	-176.3(3)
C6 N2 C3 C2	173.5(3)	C15C14C13C18	0.1(5)
C6 N2 C1 Au01	4.5(5)	C15C14C22C24	-52.3(4)
C6 N2 C1 N1	-173.5(3)	C15C14C22C23	72.6(4)
C6 N3 C5 C4	-4.2(5)	C22C14C13N1	0.4(5)
C6 N3 C12C7	0.3(3)	C22C14C13C18	176.8(3)
C6 N3 C12C11	-178.4(3)	C22C14C15C16	-176.7(3)
C6 N4 C7 C8	-179.7(3)	C19C18C17C16	-179.7(3)

**Table 7 Hydrogen Atom Coordinates ( $\text{\AA}\times 10^4$ ) and Isotropic Displacement Parameters ( $\text{\AA}^2\times 10^3$ ) for 355AuCl.**

Atom	x	y	z	U(eq)
H4	7144.34	6790.07	643.73	17
H8	4463.01	4293.83	1721.14	20
H5	6063.25	6880.15	176.81	17
H25A	4660.21	2319.34	2176.44	35
H25B	5339.8	2319.31	2823.57	35
H10	3775.91	6368.09	-56.01	21
H2	8167.73	5830.27	1955.81	18
H11	4801.42	6782.6	-90.32	20
H9	3617.81	5151.4	826.56	22
H17	9570.27	2979.29	3443.56	21
H15	9121.01	4758.88	5084.76	25
H22	7629.22	5617.47	3732.36	25
H16	9807.6	3634.03	4749.77	26
H19	8228.79	3693.19	1746.68	20
H24A	7665.46	4647.92	4895.35	43
H24B	7571.85	5798.25	5065.69	43
H24C	8244.24	5291.77	5420.78	43
H20A	8699.2	1770.89	2382.94	62
H20B	8223.71	1959.91	1507.4	62
H20C	8002.94	2144.34	2286.09	62
H23A	8731.37	6649.59	4684.22	47
H23B	8051.39	7142.45	4379.18	47

H23C	8404.86	6827.1	3745.35	47
H21A	9291.66	4056.53	1796.4	66
H21B	9005.36	3168.61	1186.42	66
H21C	9477.88	2929.18	2054.61	66

**Table 8 Atomic Occupancy for 355AuCl.**

Atom	Occupancy	Atom	Occupancy	Atom	Occupancy
H25A	0.5	H25B	0.5		

## Experimental

A suitable crystal was selected on a **SuperNova, Dual, Cu at zero, Atlas** diffractometer. The crystal was kept at 100.01(10) K during data collection. Using Olex2,<sup>275</sup> the structure was solved with the ShelXS<sup>278</sup> structure solution program using Direct Methods and refined with the ShelXL<sup>277</sup> refinement package using Least Squares minimisation.

## Crystal structure determination of [355AuCl]

**Crystal Data** for  $C_{24.5}H_{25}AuCl_2N_4$  ( $M = 643.35$  g/mol): monoclinic, space group C2/c (no. 15),  $a = 21.9728(4)$  Å,  $b = 13.1676(2)$  Å,  $c = 17.1097(3)$  Å,  $\beta = 107.476(2)^\circ$ ,  $V = 4721.84(15)$  Å<sup>3</sup>,  $Z = 8$ ,  $T = 100.01(10)$  K,  $\mu(\text{CuK}\alpha) = 13.942$  mm<sup>-1</sup>,  $D_{\text{calc}} = 1.810$  g/cm<sup>3</sup>, 9262 reflections measured ( $7.93^\circ \leq 2\theta \leq 144.258^\circ$ ), 4594 unique ( $R_{\text{int}} = 0.0307$ ,  $R_{\text{sigma}} = 0.0314$ ) which were used in all calculations. The final  $R_1$  was 0.0239 ( $I > 2\sigma(I)$ ) and  $wR_2$  was 0.0640 (all data).

## Refinement model description

Number of restraints - 0, number of constraints - unknown.

Details:

1. Fixed Uiso

At 1.2 times of:

All C(H) groups, All C(H,H) groups

At 1.5 times of:

All C(H,H,H) groups

2. Others

Fixed Sof: H25A(0.5) H25B(0.5)

3.a Ternary CH refined with riding coordinates:

C22(H22), C19(H19)

3.b Secondary CH2 refined with riding coordinates:

C25(H25A,H25B)

3.c Aromatic/amide H refined with riding coordinates:

C4(H4), C8(H8), C5(H5), C10(H10), C2(H2), C11(H11), C9(H9), C17(H17),

C15(H15), C16(H16)

3.d Idealised Me refined as rotating group:

C24(H24A,H24B,H24C), C20(H20A,H20B,H20C), C23(H23A,H23B,H23C), C21(H21A,H21B,H21C)

## Chapter 9: References

### References

- 1 D. J. Newman and G. M. Cragg, *J. Nat. Prod.*, 2016, **79**, 629–661.
- 2 D. J. Newman and G. M. Cragg, *J. Nat. Prod.*, 2012, **75**, 311–335.
- 3 H. Lachance, S. Wetzel, K. Kumar and H. Waldmann, *J. Med. Chem.*, 2012, **55**, 5989–6001.
- 4 E. Vitaku, D. T. Smith and J. T. Njardarson, *J. Med. Chem.*, 2014, **57**, 10257–10274.
- 5 R. Vardanyan, in *Piperidine-Based Drug Discovery*, ed. R. Vardanyan, Elsevier, 2017, pp. 1–82.
- 6 M. Freifelder, R. M. Robinson and G. R. Stone, *J. Org. Chem.*, 1962, **27**, 284–286.
- 7 H. Adkins, L. F. Kuick, M. Farlow and B. Wojcik, *J. Am. Chem. Soc.*, 1934, **56**, 2425–2428.
- 8 M. Freifelder and G. R. Stone, *J. Org. Chem.*, 1961, **26**, 3805–3808.
- 9 E. R. Lavagnino, R. R. Chauvette, W. N. Cannon and E. C. Kornfeld, *J. Am. Chem. Soc.*, 1960, **82**, 2609–2613.
- 10 T. S. Hamilton and R. Adams, *J. Am. Chem. Soc.*, 1928, **50**, 2260–2263.
- 11 F. Glorius, N. Spielkamp, S. Holle, R. Goddard and C. W. Lehmann, *Angew. Chem. Int. Ed.*, 2004, **43**, 2850–2852.
- 12 D.-S. Wang, Q.-A. Chen, S.-M. Lu and Y.-G. Zhou, *Chem. Rev.*, 2012, **112**, 2557–2590.
- 13 Yoshiro. Hirai, Takashi. Terada and Takao. Yamazaki, *J. Am. Chem. Soc.*, 1988, **110**, 958–960.
- 14 A. Barco, S. Benetti, A. Casolari, G. Piero Pollini and G. Spalluto, *Tetrahedron Lett.*, 1990, **31**, 3039–3042.
- 15 D. L. Boger and S. N. Weinreb, *Hetero Diels-Alder Methodology in Organic Synthesis*, Elsevier, 2012.
- 16 F. P. J. T. Rutjes and H. E. Schoemaker, *Tetrahedron Lett.*, 1997, **38**, 677–680.
- 17 R. Stragies and S. Blechert, *Tetrahedron*, 1999, **55**, 8179–8188.
- 18 C. Schneider and U. Kazmaier, *Eur. J. Org. Chem.*, 1998, 1155–1159.
- 19 F. Xu, B. Simmons, R. A. Reamer, E. Corley, J. Murry and D. Tschaen, *J. Org. Chem.*, 2008, **73**, 312–315.
- 20 C. A. Lipinski, F. Lombardo, B. W. Dominy and P. J. Feeney, *Adv. Drug Deliv. Rev.*, 1997, **23**, 3–25.
- 21 G. W. Bemis and M. A. Murcko, *J. Med. Chem.*, 1996, **39**, 2887–2893.
- 22 P. Ertl, B. Rohde and P. Selzer, *J. Med. Chem.*, 2000, **43**, 3714–3717.
- 23 S. A. Hitchcock and L. D. Pennington, *J. Med. Chem.*, 2006, **49**, 7559–7583.
- 24 H. Pajouhesh and G. R. Lenz, *NeuroRX*, 2005, **2**, 541–553.
- 25 K. Palm, P. Stenberg, K. Luthman and P. Artursson, *Pharm. Res.*, 1997, **14**, 568–571.
- 26 Y. C. Martin, *J. Med. Chem.*, 2005, **48**, 3164–3170.
- 27 D. F. Veber, S. R. Johnson, H.-Y. Cheng, B. R. Smith, K. W. Ward and K. D. Kopple, *J. Med. Chem.*, 2002, **45**, 2615–2623.
- 28 F. Lovering, J. Bikker and C. Humblet, *J. Med. Chem.*, 2009, **52**, 6752–6756.
- 29 F. Lovering, *MedChemComm*, 2013, **4**, 515–519.
- 30 I. Colomer, C. J. Empson, P. Craven, Z. Owen, R. G. Doveston, I. Churcher, S. P. Marsden and A. Nelson, *Chem. Commun.*, 2016, **52**, 7209–7212.

- 31 S. L. Schreiber, *Science*, 2000, **287**, 1964–1969.
- 32 S. J. Teague, A. M. Davis, P. D. Leeson and T. Oprea, *Angew. Chem. Int. Ed.*, 1999, **38**, 3743–3748.
- 33 B. Raymer and S. K. Bhattacharya, *J. Med. Chem.*, 2018, **61**, 10375–10384.
- 34 M. C. McLeod, G. Singh, J. N. Plampin, D. Rane, J. L. Wang, V. W. Day and J. Aubé, *Nat. Chem.*, 2014, **6**, 133–140.
- 35 H. Mizoguchi, H. Oikawa and H. Oguri, *Nat. Chem.*, 2014, **6**, 57–64.
- 36 In *Comprehensive Organic Name Reactions and Reagents*, American Cancer Society, 2010, pp. 1668–1671.
- 37 D. C. Palmer, *Oxazoles: Synthesis, Reactions, and Spectroscopy, Part A*, John Wiley & Sons, 2003.
- 38 I. J. Turchi, *Ind. Eng. Chem. Prod. Res. Dev.*, 1981, **20**, 32–76.
- 39 M. P. Ball-Jones, PhD, University of Birmingham, 2017.
- 40 A. D. Gillie, PhD, University of Birmingham, 2015.
- 41 S. Shimada and T. Tojo, *Chem. Pharm. Bull. (Tokyo)*, 1983, **31**, 4247–4258.
- 42 M. Chughtai, J. M. Eagan and A. Padwa, *Synlett*, 2011, 215–218.
- 43 A. Padwa, M. A. Brodney, B. Liu, K. Satake and T. Wu, *J. Org. Chem.*, 1999, **64**, 3595–3607.
- 44 P. Janvier, X. Sun, H. Bienaymé and J. Zhu, *J. Am. Chem. Soc.*, 2002, **124**, 2560–2567.
- 45 C. Lalli, M. J. Bouma, D. Bonne, G. Masson and J. Zhu, *Chem. – Eur. J.*, 2011, **17**, 880–889.
- 46 Y. Su, M. J. Bouma, L. Alcaraz, M. Stocks, M. Furber, G. Masson and J. Zhu, *Chem. – Eur. J.*, 2012, **18**, 12624–12627.
- 47 A. Fayol and J. Zhu, *Org. Lett.*, 2004, **6**, 115–118.
- 48 P. W. Davies, A. Cremonesi and L. Dumitrescu, *Angew. Chem. Int. Ed.*, 2011, **50**, 8931–8935.
- 49 A. D. Gillie, R. Jannapu Reddy and P. W. Davies, *Adv. Synth. Catal.*, 2016, **358**, 226–239.
- 50 M. Ball-Jones, *Org. Synth.*, 2018, **95**, 112–126.
- 51 X. Tian, L. Song, C. Han, C. Zhang, Y. Wu, M. Rudolph, F. Rominger and A. S. K. Hashmi, *Org. Lett.*, 2019, **21**, 2937–2940.
- 52 M. Chen, N. Sun, H. Chen and Y. Liu, *Chem. Commun.*, 2016, **52**, 6324–6327.
- 53 Y. Zhao, Y. Hu, C. Wang, X. Li and B. Wan, *J. Org. Chem.*, 2017, **82**, 3935–3942.
- 54 Y. Zhang, R. P. Hsung, M. R. Tracey, K. C. M. Kurtz and E. L. Vera, *Org. Lett.*, 2004, **6**, 1151–1154.
- 55 T. Hamada, X. Ye and S. S. Stahl, *J. Am. Chem. Soc.*, 2008, **130**, 833–835.
- 56 S. J. Mansfield, C. D. Campbell, M. W. Jones and E. A. Anderson, *Chem. Commun.*, 2015, **51**, 3316–3319.
- 57 M. M. Pompeo, J. H. Cheah and M. Movassaghi, *J. Am. Chem. Soc.*, 2019, **141**, 14411–14420.
- 58 J. J. Dotson, J. L. Bachman, M. A. Garcia-Garibay and N. K. Garg, *J. Am. Chem. Soc.*, 2020, **142**, 11685–11690.
- 59 F. G. Bordwell and H. E. Fried, *J. Org. Chem.*, 1991, **56**, 4218–4223.
- 60 F. G. Bordwell and Donald. Algrim, *J. Org. Chem.*, 1976, **41**, 2507–2508.
- 61 F. G. Bordwell, H. E. Fried, D. L. Hughes, T. Y. Lynch, A. V. Satish and Y. E. Whang, *J. Org. Chem.*, 1990, **55**, 3330–3336.
- 62 R. Dorel and A. M. Echavarren, *Chem. Rev.*, 2015, **115**, 9028–9072.

- 63 M.-H. Shen, Y.-M. Zhang, C. Jiang, H.-D. Xu and D. Xu, *Org. Chem. Front.*, 2020, **7**, 73–75.
- 64 P. R. Walker, C. D. Campbell, A. Suleman, G. Carr and E. A. Anderson, *Angew. Chem. Int. Ed.*, 2013, **52**, 9139–9143.
- 65 C. Fernández-Rivas, M. Méndez and A. M. Echavarren, *J. Am. Chem. Soc.*, 2000, **122**, 1221–1222.
- 66 C. Nieto-Oberhuber, S. López, M. P. Muñoz, D. J. Cárdenas, E. Buñuel, C. Nevado and A. M. Echavarren, *Angew. Chem. Int. Ed.*, 2005, **44**, 6146–6148.
- 67 N. Chatani, N. Furukawa, H. Sakurai and S. Murai, *Organometallics*, 1996, **15**, 901–903.
- 68 C.-Z. Zhong, P.-T. Tung, T.-H. Chao and M.-C. P. Yeh, *J. Org. Chem.*, 2017, **82**, 481–501.
- 69 A. Mekareeya, P. R. Walker, A. Couce-Rios, C. D. Campbell, A. Steven, R. S. Paton and E. A. Anderson, *J. Am. Chem. Soc.*, 2017, **139**, 10104–10114.
- 70 S. J. Mansfield, K. E. Christensen, A. L. Thompson, K. Ma, M. W. Jones, A. Mekareeya and E. A. Anderson, *Angew. Chem. Int. Ed.*, 2017, **56**, 14428–14432.
- 71 V. Chintalapudi, E. A. Galvin, R. L. Greenaway and E. A. Anderson, *Chem. Commun.*, 2015, **52**, 693–696.
- 72 S. Couty, C. Meyer and J. Cossy, *Tetrahedron*, 2009, **65**, 1809–1832.
- 73 X.-L. Han, C.-J. Zhou, X.-G. Liu, S.-S. Zhang, H. Wang and Q. Li, *Org. Lett.*, 2017, **19**, 6108–6111.
- 74 X. Yu, K. Chen, Q. Wang, W. Zhang and J. Zhu, *Chem. Commun.*, 2018, **54**, 1197–1200.
- 75 M. Presset, D. Oehlrich, F. Rombouts and G. A. Molander, *Org. Lett.*, 2013, **15**, 1528–1531.
- 76 H. Wang and F. Glorius, *Angew. Chem. Int. Ed.*, 2012, **51**, 7318–7322.
- 77 S. Rakshit, C. Grohmann, T. Besset and F. Glorius, *J. Am. Chem. Soc.*, 2011, **133**, 2350–2353.
- 78 C. Grohmann, H. Wang and F. Glorius, *Org. Lett.*, 2012, **14**, 656–659.
- 79 N. J. Webb, S. P. Marsden and S. A. Raw, *Org. Lett.*, 2014, **16**, 4718–4721.
- 80 N. Guimond, S. I. Gorelsky and K. Fagnou, *J. Am. Chem. Soc.*, 2011, **133**, 6449–6457.
- 81 Y. Fukui, P. Liu, Q. Liu, Z.-T. He, N.-Y. Wu, P. Tian and G.-Q. Lin, *J. Am. Chem. Soc.*, 2014, **136**, 15607–15614.
- 82 A. Coste, G. Karthikeyan, F. Couty and G. Evano, *Angew. Chem. Int. Ed.*, 2009, **48**, 4381–4385.
- 83 Y. Tu, X. Zeng, H. Wang and J. Zhao, *Org. Lett.*, 2018, **20**, 280–283.
- 84 R. Haraguchi, Z. Ikeda, A. Ooguri and S. Matsubara, *Tetrahedron*, 2015, **71**, 8830–8837.
- 85 L. Melzig, A. Metzger and P. Knochel, *Chem. – Eur. J.*, 2011, **17**, 2948–2956.
- 86 R. K. Chaturvedi and G. L. Schmir, *J. Am. Chem. Soc.*, 1969, **91**, 737–746.
- 87 R. K. Chaturvedi, A. E. MacMahon and G. L. Schmir, *J. Am. Chem. Soc.*, 1967, **89**, 6984–6993.
- 88 D. Belmessieri, D. B. Cordes, A. M. Z. Slawin and A. D. Smith, *Org. Lett.*, 2013, **15**, 3472–3475.
- 89 A. Mukherjee, R. B. Dateer, R. Chaudhuri, S. Bhunia, S. N. Karad and R.-S. Liu, *J. Am. Chem. Soc.*, 2011, **133**, 15372–15375.
- 90 R. R. Singh and R.-S. Liu, *Adv. Synth. Catal.*, 2016, **358**, 1421–1427.
- 91 X. Tian, L. Song, K. Farshadfar, M. Rudolph, F. Rominger, T. Oeser, A. Ariafield and A. S. K. Hashmi, *Angew. Chem. Int. Ed.*, 2020, **59**, 471–478.
- 92 N. J. Leonard, L. A. Miller and P. D. Thomas, *J. Am. Chem. Soc.*, 1956, **78**, 3463–3468.

- 93 A. A. El-Barbary, S. Carlsson and S.-O. Lawesson, *Tetrahedron*, 1982, **38**, 405–412.
- 94 E. Toromanoff, *Tetrahedron*, 1980, **36**, 2809–2931.
- 95 B. W. Gung, *Chem. Rev.*, 1999, **99**, 1377–1386.
- 96 G. Burtin, P.-J. Corringer, P. B. Hitchcock and D. W. Young, *Tetrahedron Lett.*, 1999, **40**, 4275–4278.
- 97 P.-P. Ruan, H.-H. Li, X. Liu, T. Zhang, S.-X. Zuo, C. Zhu and L.-W. Ye, *J. Org. Chem.*, 2017, **82**, 9119–9125.
- 98 M. Ono, I. Araya and S. Tamura, *Chem. Pharm. Bull. (Tokyo)*, 1990, **38**, 1373–1378.
- 99 M. Ono, K. Aoki and S. Tamura, *Chem. Pharm. Bull. (Tokyo)*, 1990, **38**, 1379–1388.
- 100 M. Ono, R. Todoriki and S. Tamura, *Chem. Pharm. Bull. (Tokyo)*, 1991, **39**, 558–565.
- 101 W. N. Speckamp and M. J. Moolenaar, *Tetrahedron*, 2000, **56**, 3817–3856.
- 102 P. Wu and T. E. Nielsen, *Chem. Rev.*, 2017, **117**, 7811–7856.
- 103 W. N. Speckamp and H. Hiemstra, *Tetrahedron*, 1985, **41**, 4367–4416.
- 104 D. Russowsky, R. Z. Petersen, M. N. Godoi and R. A. Pilli, *Tetrahedron Lett.*, 2000, **41**, 9939–9942.
- 105 A. S. Vieira, F. P. Ferreira, P. F. Fiorante, R. C. Guadagnin and H. A. Stefani, *Tetrahedron*, 2008, **64**, 3306–3314.
- 106 S. Mizuta and O. Onomura, *RSC Adv.*, 2012, **2**, 2266–2269.
- 107 G. R. LENZ, *Synthesis*, 1978, **1978**, 489–518.
- 108 L. Djakovitch, J. Eames, R. V. H. Jones, S. McIntyre and S. Warren, *Tetrahedron Lett.*, 1995, **36**, 1723–1726.
- 109 D. House and S. Warren, *Phosphorus Sulfur Silicon Relat. Elem.*, 1999, **153**, 59–78.
- 110 T. Javorskis and E. Orentas, *J. Org. Chem.*, 2017, **82**, 13423–13439.
- 111 S. Otsuka, K. Nogi and H. Yorimitsu, *Angew. Chem. Int. Ed.*, 2018, **57**, 6653–6657.
- 112 M. Tobisu, S. Ito, A. Kitajima and N. Chatani, *Org. Lett.*, 2008, **10**, 5223–5225.
- 113 U. Leutenegger, G. Umbricht, C. Fahrni, P. von Matt and A. Pfaltz, *Tetrahedron*, 1992, **48**, 2143–2156.
- 114 G. Bergnes and R. Kaddurah-Daouk, *Bioorg. Med. Chem. Lett.*, 1997, **7**, 1021–1026.
- 115 I. Ghosh and P. A. Jacobi, *J. Org. Chem.*, 2002, **67**, 9304–9309.
- 116 J. Schleiss, P. Rollin and A. Tatibouët, *Angew. Chem. Int. Ed.*, 2010, **49**, 577–580.
- 117 Molinspiration Cheminformatics, *Molinspiration property calculation service*, .
- 118 A. Nadin, C. Hattotuwigama and I. Churcher, *Angew. Chem. Int. Ed.*, 2012, **51**, 1114–1122.
- 119 Alain. Igau, Hansjorg. Grutzmacher, Antoine. Baceiredo and Guy. Bertrand, *J. Am. Chem. Soc.*, 1988, **110**, 6463–6466.
- 120 A. J. Arduengo, R. L. Harlow and M. Kline, *J. Am. Chem. Soc.*, 1991, **113**, 361–363.
- 121 D. Bourissou, O. Guerret, F. P. Gabbaï and G. Bertrand, *Chem. Rev.*, 2000, **100**, 39–92.
- 122 D. J. Nelson and S. P. Nolan, *Chem. Soc. Rev.*, 2013, **42**, 6723–6753.
- 123 N. M. Scott and S. P. Nolan, *Eur. J. Inorg. Chem.*, 2005, 1815–1828.
- 124 D. S. McGuinness and K. J. Cavell, *Organometallics*, 2000, **19**, 741–748.
- 125 M. Alcarazo, S. J. Roseblade, A. R. Cowley, R. Fernández, J. M. Brown and J. M. Lassaletta, *J. Am. Chem. Soc.*, 2005, **127**, 3290–3291.
- 126 S. Saba, A. Brescia and M. K. Kaloustian, *Tetrahedron Lett.*, 1991, **32**, 5031–5034.
- 127 A. J. Arduengo, R. Krafczyk, R. Schmutzler, H. A. Craig, J. R. Goerlich, W. J. Marshall and M. Unverzagt, *Tetrahedron*, 1999, **55**, 14523–14534.
- 128 F. Glorius, G. Altenhoff, R. Goddard and C. Lehmann, *Chem. Commun.*, 2002, 2704–2705.



- 129 L. Jafarpour, E. D. Stevens and S. P. Nolan, *J. Organomet. Chem.*, 2000, **606**, 49–54.
- 130 United States, US7109348B1, 2006.
- 131 L. Hintermann, *Beilstein J. Org. Chem.*, 2007, **3**, 22.
- 132 C.-H. Chien, S. Fujita, S. Yamoto, T. Hara, T. Yamagata, M. Watanabe and K. Mashima, *Dalton Trans.*, 2008, 916–923.
- 133 S. J. Roseblade, A. Ros, D. Monge, M. Alcarazo, E. Álvarez, J. M. Lassaletta and R. Fernández, *Organometallics*, 2007, **26**, 2570–2578.
- 134 M. Espina, I. Rivilla, A. Conde, M. M. Díaz-Requejo, P. J. Pérez, E. Álvarez, R. Fernández and J. M. Lassaletta, *Organometallics*, 2015, **34**, 1328–1338.
- 135 M. Tsimmerman, D. Mallik, T. Matsuo, T. Otani, K. Tamao and M. G. Organ, *Chem. Commun.*, 2012, **48**, 10352–10354.
- 136 L. Benhamou, E. Chardon, G. Lavigne, S. Bellemin-Lapponnaz and V. César, *Chem. Rev.*, 2011, **111**, 2705–2733.
- 137 N. Kuhn and T. Kratz, *Synthesis*, 1993, 561–562.
- 138 H. M. J. Wang and I. J. B. Lin, *Organometallics*, 1998, **17**, 972–975.
- 139 I. J. B. Lin and C. S. Vasam, *Coord. Chem. Rev.*, 2007, **251**, 642–670.
- 140 M. R. L. Furst and C. S. J. Cazin, *Chem. Commun.*, 2010, **46**, 6924–6925.
- 141 C. J. O'Brien, E. A. B. Kantchev, C. Valente, N. Hadei, G. A. Chass, A. Lough, A. C. Hopkinson and M. G. Organ, *Chem. – Eur. J.*, 2006, **12**, 4743–4748.
- 142 O. Santoro, A. Collado, A. M. Z. Slawin, S. P. Nolan and C. S. J. Cazin, *Chem. Commun.*, 2013, **49**, 10483–10485.
- 143 A. Collado, A. Gómez-Suárez, A. R. Martin, A. M. Z. Slawin and S. P. Nolan, *Chem. Commun.*, 2013, **49**, 5541–5543.
- 144 S. Ray, M. M. Shaikh and P. Ghosh, *Eur. J. Inorg. Chem.*, 2009, 1932–1941.
- 145 C.-Y. Liao, K.-T. Chan, Y.-C. Chang, C.-Y. Chen, C.-Y. Tu, C.-H. Hu and H. M. Lee, *Organometallics*, 2007, **26**, 5826–5833.
- 146 A. Doddi, M. Peters and M. Tamm, *Chem. Rev.*, 2019, **119**, 6994–7112.
- 147 A. A. Danopoulos, T. Simler and P. Braunstein, *Chem. Rev.*, 2019, **119**, 3730–3961.
- 148 H. V. Huynh, *Chem. Rev.*, 2018, **118**, 9457–9492.
- 149 Y.-J. Kim and A. Streitwieser, *J. Am. Chem. Soc.*, 2002, **124**, 5757–5761.
- 150 Y. Chu, H. Deng and J.-P. Cheng, *J. Org. Chem.*, 2007, **72**, 7790–7793.
- 151 E. M. Higgins, J. A. Sherwood, A. G. Lindsay, J. Armstrong, R. S. Massey, R. W. Alder and A. C. O'Donoghue, *Chem. Commun.*, 2011, **47**, 1559–1561.
- 152 T. L. Amyes, S. T. Diver, J. P. Richard, F. M. Rivas and K. Toth, *J. Am. Chem. Soc.*, 2004, **126**, 4366–4374.
- 153 R. S. Massey, C. J. Collett, A. G. Lindsay, A. D. Smith and A. C. O'Donoghue, *J. Am. Chem. Soc.*, 2012, **134**, 20421–20432.
- 154 M. K. Denk and J. M. Rodezno, *J. Organomet. Chem.*, 2001, **618**, 737–740.
- 155 A. J. Arduengo, F. Davidson, H. V. R. Dias, J. R. Goerlich, D. Khasnis, W. J. Marshall and T. K. Prakasha, *J. Am. Chem. Soc.*, 1997, **119**, 12742–12749.
- 156 M. K. Denk and J. M. Rodezno, *J. Organomet. Chem.*, 2000, **608**, 122–125.
- 157 C. A. Tolman, *Chem. Rev.*, 1977, **77**, 313–348.
- 158 A. R. Chianese, X. Li, M. C. Janzen, J. W. Faller and R. H. Crabtree, *Organometallics*, 2003, **22**, 1663–1667.
- 159 R. A. Kelly III, H. Clavier, S. Giudice, N. M. Scott, E. D. Stevens, J. Bordner, I. Samardjiev, C. D. Hoff, L. Cavallo and S. P. Nolan, *Organometallics*, 2008, **27**, 202–210.

- 160 D. A. Valyaev, R. Brousses, N. Lugan, I. Fernández and M. A. Sierra, *Chem. – Eur. J.*, 2011, **17**, 6602–6605.
- 161 D. G. Gusev, *Organometallics*, 2009, **28**, 763–770.
- 162 R. Tonner and G. Frenking, *Organometallics*, 2009, **28**, 3901–3905.
- 163 D. G. Gusev, *Organometallics*, 2009, **28**, 6458–6461.
- 164 H. V. Huynh, Y. Han, R. Jothibasu and J. A. Yang, *Organometallics*, 2009, **28**, 5395–5404.
- 165 D. Marchione, M. A. Izquierdo, G. Bistoni, R. W. A. Havenith, A. Macchioni, D. Zuccaccia, F. Tarantelli and L. Belpassi, *Chem. – Eur. J.*, 2017, **23**, 2722–2728.
- 166 C. A. Tolman, *J. Am. Chem. Soc.*, 1970, **92**, 2956–2965.
- 167 A. C. Hillier, W. J. Sommer, B. S. Yong, J. L. Petersen, L. Cavallo and S. P. Nolan, *Organometallics*, 2003, **22**, 4322–4326.
- 168 A. Poater, B. Cosenza, A. Correa, S. Giudice, F. Ragone, V. Scarano and L. Cavallo, *Eur. J. Inorg. Chem.*, 2009, **2009**, 1759–1766.
- 169 M. Brill, A. Collado, D. B. Cordes, A. M. Z. Slawin, M. Vogt, H. Grützmacher and S. P. Nolan, *Organometallics*, 2015, **34**, 263–274.
- 170 L. Falivene, R. Credendino, A. Poater, A. Petta, L. Serra, R. Oliva, V. Scarano and L. Cavallo, *Organometallics*, 2016, **35**, 2286–2293.
- 171 P. Wucher, L. Caporaso, P. Roesle, F. Ragone, L. Cavallo, S. Mecking and I. Göttker-Schnetmann, *Proc. Natl. Acad. Sci.*, 2011, **108**, 8955–8959.
- 172 C. Di Giovanni, A. Poater, J. Benet-Buchholz, L. Cavallo, M. Solà and A. Llobet, *Chem. – Eur. J.*, 2014, **20**, 3898–3902.
- 173 A. Lattanzi, C. D. Fusco, A. Russo, A. Poater and L. Cavallo, *Chem. Commun.*, 2012, **48**, 1650–1652.
- 174 G. Berthon-Gelloz, M. A. Siegler, A. L. Spek, B. Tinant, J. N. H. Reek and I. E. Markó, *Dalton Trans.*, 2010, **39**, 1444–1446.
- 175 A. Gómez-Suárez, R. S. Ramón, O. Songis, A. M. Z. Slawin, C. S. J. Cazin and S. P. Nolan, *Organometallics*, 2011, **30**, 5463–5470.
- 176 A. R. Martin, Y. Makida, S. Meiries, A. M. Z. Slawin and S. P. Nolan, *Organometallics*, 2013, **32**, 6265–6270.
- 177 M. G. Organ, S. Çalimsiz, M. Sayah, K. H. Hoi and A. J. Lough, *Angew. Chem. Int. Ed.*, 2009, **48**, 2383–2387.
- 178 A. Chartoire, M. Lesieur, L. Falivene, A. M. Z. Slawin, L. Cavallo, C. S. J. Cazin and S. P. Nolan, *Chem. – Eur. J.*, 2012, **18**, 4517–4521.
- 179 G. Bastug and S. P. Nolan, *Organometallics*, 2014, **33**, 1253–1258.
- 180 Y. Makida, E. Marelli, A. M. Z. Slawin and S. P. Nolan, *Chem. Commun.*, 2014, **50**, 8010–8013.
- 181 C. A. Urbina-Blanco, A. Leitgeb, C. Slugovc, X. Bantreil, H. Clavier, A. M. Z. Slawin and S. P. Nolan, *Chem. – Eur. J.*, 2011, **17**, 5045–5053.
- 182 S. Manzini, C. A. Urbina Blanco, A. M. Z. Slawin and S. P. Nolan, *Organometallics*, 2012, **31**, 6514–6517.
- 183 A. Gómez-Suárez, Y. Oonishi, S. Meiries and S. P. Nolan, *Organometallics*, 2013, **32**, 1106–1111.
- 184 F. Izquierdo, S. Manzini and S. P. Nolan, *Chem. Commun.*, 2014, **50**, 14926–14937.
- 185 G. Altenhoff, R. Goddard, C. W. Lehmann and F. Glorius, *J. Am. Chem. Soc.*, 2004, **126**, 15195–15201.

- 186 G. Altenhoff, R. Goddard, C. W. Lehmann and F. Glorius, *Angew. Chem. Int. Ed.*, 2003, **42**, 3690–3693.
- 187 S. Würtz, C. Lohre, R. Fröhlich, K. Bergander and F. Glorius, *J. Am. Chem. Soc.*, 2009, **131**, 8344–8345.
- 188 C. Burstein, C. W. Lehmann and F. Glorius, *Tetrahedron*, 2005, **61**, 6207–6217.
- 189 Y. Koto, F. Shibahara and T. Murai, *Org. Biomol. Chem.*, 2017, **15**, 1810–1820.
- 190 Y. Koto, F. Shibahara and T. Murai, *Chem. Lett.*, 2016, **45**, 1327–1329.
- 191 S. Hameury, P. de Frémont and P. Braunstein, *Chem. Soc. Rev.*, 2017, **46**, 632–733.
- 192 D. Janssen-Müller, C. Schlepphorst and F. Glorius, *Chem. Soc. Rev.*, 2017, **46**, 4845–4854.
- 193 C. Fliedel and P. Braunstein, *J. Organomet. Chem.*, 2014, **751**, 286–300.
- 194 W. A. Herrmann, *Angew. Chem. Int. Ed.*, 2002, **41**, 1290–1309.
- 195 E. Peris, *Chem. Rev.*, , DOI:10.1021/acs.chemrev.6b00695.
- 196 S. L. Balof, S. J. P’Pool, N. J. Berger, E. J. Valente, A. M. Shiller and H.-J. Schanz, *Dalton Trans.*, 2008, 5791–5799.
- 197 L. H. Peeck, S. Leuthäusser and H. Plenio, *Organometallics*, 2010, **29**, 4339–4345.
- 198 M. Mondal, T. K. Ranjeesh, S. K. Gupta and J. Choudhury, *Dalton Trans.*, 2014, **43**, 9356–9362.
- 199 V. Leigh, W. Ghattas, H. Mueller-Bunz and M. Albrecht, *J. Organomet. Chem.*, 2014, **771**, 33–39.
- 200 L. Benhamou, V. César, H. Gornitzka, N. Lugan and G. Lavigne, *Chem. Commun.*, 2009, 4720–4722.
- 201 L. Benhamou, N. Vujkovic, V. César, H. Gornitzka, N. Lugan and G. Lavigne, *Organometallics*, 2010, **29**, 2616–2630.
- 202 V. César, J.-C. Tourneux, N. Vujkovic, R. Brousses, N. Lugan and G. Lavigne, *Chem. Commun.*, 2012, **48**, 2349–2351.
- 203 D. Gnanamgari, E. L. O. Sauer, N. D. Schley, C. Butler, C. D. Incarvito and R. H. Crabtree, *Organometallics*, 2009, **28**, 321–325.
- 204 A. Bartoszewicz, R. Marcos, S. Sahoo, A. K. Inge, X. Zou and B. Martín-Matute, *Chem. – Eur. J.*, 2012, **18**, 14510–14519.
- 205 A. Bartoszewicz, G. González Miera, R. Marcos, P.-O. Norrby and B. Martín-Matute, *ACS Catal.*, 2015, **5**, 3704–3716.
- 206 A. V. Zhukhovitskiy, M. J. MacLeod and J. A. Johnson, *Chem. Rev.*, 2015, **115**, 11503–11532.
- 207 C. A. Smith, M. R. Narouz, P. A. Lummis, I. Singh, A. Nazemi, C.-H. Li and C. M. Crudden, *Chem. Rev.*, 2019, **119**, 4986–5056.
- 208 S. Engel, E.-C. Fritz and B. J. Ravoo, *Chem. Soc. Rev.*, 2017, **46**, 2057–2075.
- 209 D. Meyer, M. A. Taige, A. Zeller, K. Hohlfeld, S. Ahrens and T. Strassner, *Organometallics*, 2009, **28**, 2142–2149.
- 210 M. Guerria, L. Sekhri, C. Olivier and P. Jean-Luc, *Orient. J. Chem.*, 2014, **30**, 427–434.
- 211 T. Samanta, S. K. Seth, S. K. Chattopadhyay, P. Mitra, V. Kushwah and J. Dinda, *Inorganica Chim. Acta*, 2014, **411**, 165–171.
- 212 G. Qian, B. Liu, Q. Tan, S. Zhang and B. Xu, *Eur. J. Org. Chem.*, 2014, **2014**, 4837–4843.
- 213 J. L. Adams, J. C. Boehm, S. Kassis, P. D. Gorycki, E. F. Webb, R. Hall, M. Sorenson, J. C. Lee, A. Ayrton, D. E. Griswold and T. F. Gallagher, *Bioorg. Med. Chem. Lett.*, 1998, **8**, 3111–3116.

- 214J. Y. Wu, B. Moreau and T. Ritter, *J. Am. Chem. Soc.*, 2009, **131**, 12915–12917.
- 215J. T. Hutt and Z. D. Aron, *Org. Lett.*, 2011, **13**, 5256–5259.
- 216R. Jazzar, M. Soleilhavoup and G. Bertrand, *Chem. Rev.*, 2020, **120**, 4141–4168.
- 217Q. Zhao, G. Meng, S. P. Nolan and M. Szostak, *Chem. Rev.*, 2020, **120**, 1981–2048.
- 218K. Endo and R. H. Grubbs, *J. Am. Chem. Soc.*, 2011, **133**, 8525–8527.
- 219J. Hartung, P. K. Dornan and R. H. Grubbs, *J. Am. Chem. Soc.*, 2014, **136**, 13029–13037.
- 220Z. Lu, J. Han, O. E. Okoromoba, N. Shimizu, H. Amii, C. F. Tormena, G. B. Hammond and B. Xu, *Org. Lett.*, 2017, **19**, 5848–5851.
- 221A. Linden, T. de Haro and C. Nevado, *Acta Crystallogr. C*, 2012, **68**, m1–m3.
- 222V. Michelet, Y. Tang, I. Benaissa, M. Huynh, L. Vendier, N. Lugan, S. Bastin, P. Belmont and V. César, *Angew. Chem. Int. Ed.*, , DOI:10.1002/anie.201901090.
- 223N. Marion, R. S. Ramón and S. P. Nolan, *J. Am. Chem. Soc.*, 2009, **131**, 448–449.
- 224Y. Xu, X. Hu, J. Shao, G. Yang, Y. Wu and Z. Zhang, *Green Chem.*, 2014, **17**, 532–537.
- 225V. K. Aggarwal, P. W. Davies and W. O. Moss, *Chem. Commun.*, 2002, **0**, 972–973.
- 226S. Alazet, L. Zimmer and T. Billard, *Chem. – Eur. J.*, 2014, **20**, 8589–8593.
- 227N. Bischofberger, H. Waldmann, T. Saito, E. S. Simon, W. Lees, M. D. Bednarski and G. M. Whitesides, *J. Org. Chem.*, 1988, **53**, 3457–3465.
- 228E. Alonso, D. J. Ramón and M. Yus, *Tetrahedron*, 1997, **53**, 14355–14368.
- 229P. R. Sultane, T. B. Mete and R. G. Bhat, *Org. Biomol. Chem.*, 2013, **12**, 261–264.
- 230I. K. Khanna, R. M. Weier, Y. Yu, P. W. Collins, J. M. Miyashiro, C. M. Koboldt, A. W. Veenhuizen, J. L. Currie, K. Seibert and P. C. Isakson, *J. Med. Chem.*, 1997, **40**, 1619–1633.
- 231A. Millet and O. Baudoin, *Org. Lett.*, 2014, **16**, 3998–4000.
- 232D. Campolo, T. Arif, C. Borie, D. Mouysset, N. Vanthuyne, J.-V. Naubron, M. P. Bertrand and M. Nechab, *Angew. Chem. Int. Ed.*, 2014, **53**, 3227–3231.
- 233V. Durel, C. Lalli, T. Roisnel and P. van de Weghe, *J. Org. Chem.*, 2016, **81**, 849–859.
- 234C. Taillier, T. Hameury, V. Bellosta and J. Cossy, *Tetrahedron*, 2007, **63**, 4472–4490.
- 235A. Rosiak, W. Frey and J. Christoffers, *Eur. J. Org. Chem.*, 2006, 4044–4054.
- 236V. Girijavallabhan, C. Alvarez and F. G. Njoroge, *J. Org. Chem.*, 2011, **76**, 6442–6446.
- 237F. Yan, H. Liang, J. Song, J. Cui, Q. Liu, S. Liu, P. Wang, Y. Dong and H. Liu, *Org. Lett.*, 2017, **19**, 86–89.
- 238H. Teller, M. Corbet, L. Mantilli, G. Gopakumar, R. Goddard, W. Thiel and A. Fürstner, *J. Am. Chem. Soc.*, 2012, **134**, 15331–15342.
- 239T. H. Jepsen, E. Glibstrup, F. Crestey, A. A. Jensen and J. L. Kristensen, *Beilstein J. Org. Chem.*, 2017, **13**, 988–994.
- 240D. Chouikhi, S. Barluenga and N. Winssinger, *Chem. Commun.*, 2010, **46**, 5476–5478.
- 241F. Kramm, J. Teske, F. Ullwer, W. Frey and B. Plietker, *Angew. Chem. Int. Ed.*, 2018, **57**, 13335–13338.
- 242A. Sagadevan, A. Ragupathi, C.-C. Lin, J. R. Hwu and K. C. Hwang, *Green Chem.*, 2015, **17**, 1113–1119.
- 243X. Tian, L. Song, M. Rudolph, F. Rominger, T. Oeser and A. S. K. Hashmi, *Angew. Chem. Int. Ed.*, 2019, **58**, 3589–3593.
- 244N. Riddell, K. Villeneuve and W. Tam, *Org. Lett.*, 2005, **7**, 3681–3684.
- 245H. Huang, G. He, G. Zhu, X. Zhu, S. Qiu and H. Zhu, *J. Org. Chem.*, 2015, **80**, 3480–3487.
- 246H. Wen, W. Cao, Y. Liu, L. Wang, P. Chen and Y. Tang, *J. Org. Chem.*, 2018, **83**, 13308–13324.

- 247 L. Zhu, Y. Yu, Z. Mao and X. Huang, *Org. Lett.*, 2015, **17**, 30–33.
- 248 A. Williams, E. C. Lucas, A. R. Rimmer and H. C. Hawkins, *J. Chem. Soc. Perkin Trans. 2*, 1972, 627–633.
- 249 N. B. Palakurthy and B. Mandal, *Tetrahedron Lett.*, 2011, **52**, 7132–7134.
- 250 S. Kotha and K. Singh, *Eur. J. Org. Chem.*, 2007, **2007**, 5909–5916.
- 251 W. Cocker, *J. Chem. Soc. Resumed*, 1943, 373–378.
- 252 C. Olier, N. Azzi, G. Gil, S. Gastaldi and M. P. Bertrand, *J. Org. Chem.*, 2008, **73**, 8469–8473.
- 253 W. R. McKay and G. R. Proctor, *J. Chem. Soc. Perkin 1*, 1981, **0**, 2443–2450.
- 254 D. Belmessieri, A. de la Houpliere, E. D. D. Calder, J. E. Taylor and A. D. Smith, *Chem. – Eur. J.*, 2014, **20**, 9762–9769.
- 255 R. K. Everett and J. P. Wolfe, *J. Org. Chem.*, 2015, **80**, 9041–9056.
- 256 J. W. Robinson and H. Schlaad, *Chem. Commun.*, 2012, **48**, 7835–7837.
- 257 B. Seashore-Ludlow, P. Villo and P. Somfai, *Chem. – Eur. J.*, 2012, **18**, 7219–7223.
- 258 D. Sikriwal and D. K. Dikshit, *Tetrahedron*, 2011, **67**, 210–215.
- 259 M. Mori, A. Somada and S. Oida, *Chem. Pharm. Bull. (Tokyo)*, 2000, **48**, 716–728.
- 260 K. Yamamoto, Y. Yoshikawa, M. Ohue, S. Inuki, H. Ohno and S. Oishi, *Org. Lett.*, 2019, **21**, 373–377.
- 261 A. G. Cameron and A. T. Hewson, *J. Chem. Soc. Perkin 1*, 1983, 2979–2982.
- 262 S. Brass, H.-D. Gerber, S. Dörr and W. E. Diederich, *Tetrahedron*, 2006, **62**, 1777–1786.
- 263 R. Mendoza-Sanchez, V. B. Corless, Q. N. N. Nguyen, M. Bergeron-Brlek, J. Frost, S. Adachi, D. J. Tantillo and A. K. Yudin, *Chem. – Eur. J.*, 2017, **23**, 13319–13322.
- 264 J. J. Mousseau, J. A. Bull, C. L. Ladd, A. Fortier, D. Sustac Roman and A. B. Charette, *J. Org. Chem.*, 2011, **76**, 8243–8261.
- 265 S. M. Allin, W. R. S. Barton, W. Russell Bowman, E. Bridge (née Mann), M. R. J. Elsegood, T. McInally and V. McKee, *Tetrahedron*, 2008, **64**, 7745–7758.
- 266 US5276186 (A), 1994.
- 267 P. Mukherjee, H. Li, I. Sevrioukova, G. Chreifi, P. Martásek, L. J. Roman, T. L. Poulos and R. B. Silverman, *J. Med. Chem.*, 2015, **58**, 1067–1088.
- 268 WO2004101564 (A1), 2004.
- 269 WO2007143456 (A2), 2007.
- 270 J. Y. Wu, B. Moreau and T. Ritter, Iron-Catalyzed 1,4-Hydroboration of 1,3-Dienes, <http://pubs.acs.org/doi/suppl/10.1021/ja9048493>, (accessed 14 November 2016).
- 271 T. E. Müller, J. C. Green, D. M. P. Mingos, C. M. McPartlin, C. Whittingham, D. J. Williams and T. M. Woodroffe, *J. Organomet. Chem.*, 1998, **551**, 313–330.
- 272 S. Ma and L. Wang, *J. Org. Chem.*, 1998, **63**, 3497–3498.
- 273 J.-C. Hsieh, Y.-C. Chen, A.-Y. Cheng and H.-C. Tseng, *Org. Lett.*, 2012, **14**, 1282–1285.
- 274 C. Zhao, X. Jia, X. Wang and H. Gong, *J. Am. Chem. Soc.*, 2014, **136**, 17645–17651.
- 275 O. V. Dolomanov, L. J. Bourhis, R. J. Gildea, J. a. K. Howard and H. Puschmann, *J. Appl. Crystallogr.*, 2009, **42**, 339–341.
- 276 G. M. Sheldrick, *Acta Crystallogr. Sect. Found. Adv.*, 2015, **71**, 3–8.
- 277 G. M. Sheldrick, *Acta Crystallogr. Sect. C Struct. Chem.*, 2015, **71**, 3–8.
- 278 G. M. Sheldrick, *Acta Crystallogr. A*, 2008, **64**, 112–122.
- 279 L. J. Bourhis, O. V. Dolomanov, R. J. Gildea, J. a. K. Howard and H. Puschmann, *Acta Crystallogr. Sect. Found. Adv.*, 2015, **71**, 59–75.

